

















## **ELECTRIC LINES AND NETS**





# ELECTRIC LINES AND NETS

## THEIR THEORY AND ELECTRICAL BEHAVIOR

FORMERLY PUBLISHED UNDER THE TITLE OF  
ARTIFICIAL ELECTRIC LINES

BY

A. E. KENNELLY, A. M., Sc. D.

*Professor of Electrical Engineering, Harvard University; Past  
President, Am. Inst. Elec. Engrs.; Past President, Illum.*

*Eng. Soc.; Past President, Inst. Radio Engrs.;*

*Genl. Secy., Int. Elec. Congress, St. Louis;*

*Hon. Member of Inst. Elec. Engrs.,*

*London, and of Société*

*Française des*

*Électriciens,*

*Paris*

SECOND EDITION  
REVISED AND ENLARGED

McGRAW-HILL BOOK COMPANY, INC.

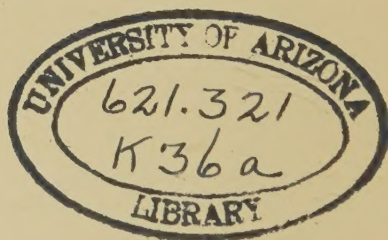
NEW YORK: 370 SEVENTH AVENUE

LONDON: 6 & 8 BOUVERIE ST., E. C. 4

1928

COPYRIGHT, 1917, 1928, BY THE  
MCGRAW-HILL BOOK COMPANY, INC.

PRINTED IN THE UNITED STATES OF AMERICA



THE MAPLE PRESS COMPANY, YORK, PA.



## PREFACE

This book is offered to students of electrical engineering as a revision of the author's earlier book, "Artificial Electric Lines," issued by the same publisher, in 1917, and which is now out of print. Some of the material in that earlier book has undergone abridgment and condensation here, where that has seemed advantageous from the textbook point of view. On the other hand, new material has here been added to bring the subject up to date. Since the new book deals with real lines, as well as artificial lines and nets, the title has been correspondingly altered.

At the date of appearance of the earlier book, the theory of general alternating-current networks was in an undeveloped state, by comparison with that of simple artificial, real, and composite lines. It is now clear that any electric conducting network, connecting selected pairs of terminals, subtends a complex angle  $\theta$ , the numerical value of which, at any given frequency, indicates immediately the nature and extent of the connection. Instead, however, of the network becoming a branch of the general knowledge of artificial and real lines, the network has taken a fundamental position in the general theory of the subject, leaving artificial and real lines to be regarded as subordinate elements, or special cases of nets. Continuous-current lines still form the natural entrance to the subject, by reason of the simplicity of their trigonometrical relations; but after they have provided access to the interior of the subject, they cease to retain the principal attention of the student. The theory is very useful, comprehensive and beautiful.

The author is under many obligations to his former colleague, Prof. C. E. Tucker, for assistance in collecting new material and in preparing this book for the press. He has contributed especially the problems and new demonstrations appearing in the appendices.

A. E. K.

CAMBRIDGE, MASS.,  
*August, 1928.*



# CONTENTS

	PAGE
PREFACE. . . . .	v
 CHAPTER	
I. INTRODUCTION . . . . .	1
II. ELEMENTARY TRIGONOMETRICAL RELATIONS APPLYING TO REAL AND ARTIFICIAL LINES . . . . .	4
III. TRIGONOMETRICAL PROPERTIES OF REAL CONTINUOUS-CUR- RENT LINES . . . . .	17
IV. THE STEADY-STATE DIFFERENTIAL EQUATION OF A UNIFORM REAL LINE. . . . .	26
V. IMPEDANCE, ADMITTANCE, AND POWER OF A SMOOTH LINE AT ANY POINT. . . . .	51
VI. EQUIVALENT CIRCUITS OF A SMOOTH LINE. . . . .	59
VII. LUMPY ARTIFICIAL LINES. . . . .	71
VIII. THE DESIGN, CONSTRUCTION, AND TESTS OF CONTINUOUS- CURRENT ARTIFICIAL LINES. . . . .	93
IX. COMPLEX QUANTITIES AND ALTERNATING-CURRENT QUANTITIES	105
X. FUNDAMENTAL PROPERTIES OF ALTERNATING-CURRENT REAL LINES . . . . .	134
XI. OUTLINE THEORY OF THE INITIAL TRANSIENT STATE IN SIMPLE ALTERNATING-CURRENT LINES. . . . .	165
XII. QUARTER-WAVE AND HALF-WAVE REAL LINES IN THE STEADY STATE . . . . .	181
XIII. REGULARLY LOADED LINES AND ATTENUATION MEASURE. . . . .	193
XIV. DESCRIPTIVE OUTLINE OF ALTERNATING-CURRENT ARTIFICIAL LINES, THEIR HISTORY AND USES . . . . .	207
XV. FUNDAMENTAL PROPERTIES OF ALTERNATING-CURRENT ARTIFI- CIAL LINES. . . . .	229
XVI. TESTS OF ALTERNATING-CURRENT ARTIFICIAL LINES . . . . .	278
XVII. COMPOSITE LINES . . . . .	292
XVIII. ELECTRIC NETWORKS IN THE STEADY STATE. . . . .	323



CHAPTER	PAGE
XIX. THE USE OF AN ARTIFICIAL LINE AS A FILTER FOR ALTERNATING-CURRENT FREQUENCIES. . . . .	358
APPENDIX A. LIST OF IMPORTANT TRIGONOMETRICAL FORMULAS WITH CIRCULAR AND HYPERBOLIC EQUIVALENTS . . . . .	385
APPENDIX B. AN ALTERNATIVE METHOD OF DEALING WITH CONTINUOUS-CURRENT LINES IN TERMS OF POSITION ANGLES IN CASES OF SUPER-SURGE-RESISTANCE LOADS . . . . .	390
APPENDIX C. DERIVATION OF THE ELEMENTS OF THE EQUIVALENT T AND II STRUCTURES . . . . .	394
APPENDIX D. DEVELOPMENT OF VECTOR TRANSMISSION AND REFLECTION COEFFICIENTS OF VOLTAGE AND CURRENT . . . . .	398
APPENDIX E. DERIVATION OF THE ARCHITRAVE IMPEDANCE OF A COMPOSITE LINE . . . . .	401
APPENDIX F. PROBLEMS FOR SOLUTION. . . . .	403
APPENDIX G. CONSTANTS OF TELEPHONE LINES . . . . .	409
LIST OF SYMBOLS EMPLOYED . . . . .	411
INDEX. . . . .	419

# ELECTRIC LINES AND NETS

## CHAPTER I

### INTRODUCTION

**Electric Lines.**—An electric line is a conductor, or group of parallel conductors, connecting two or more stations, or points of circuit discontinuity. A typically simple line may connect a generator with a motor, or a source with a consumption point. A line serves to convey electric impulses or currents between the stations it connects.

Electric lines are either *real* or *artificial*. A real line is a physical conductor or group of conductors, bridging the distance between two stations, and especially mutually remote stations. An artificial line is a localized, and especially a small localized aggregation of electric conductors, simulating the behavior of a real line.

Real lines differ in the number of their conductors, length, nature of current carried, mechanical construction, physical constants, and degree of uniformity.

**Number of Conductors.**—The simplest standard type of line consists of two similar and uniform parallel conductors, such as are commonly used in electric telephony. A metallic-circuit line employs at least two conductors. Groups of three, four, five, and even six conductors are used for electric power transmission or distribution in polyphase systems. On the other hand, ground-return circuits employ single-wire lines, such as aerial telegraph lines. Multiple-wire lines may be reduced, for the purposes of comparison and analysis, to the case of single-wire lines.

**Length.**—Real lines manifestly differ in regard to physical length. They may also be considered as differing in *electrical length*. An electrically long line transmits energy with relatively large loss, or electric current with relatively large attenuation. The amount of loss consistent with “shortness” is not a fixed quantity but depends upon the purpose of the line. An elec-

trically long power-transmission line might be an electrically short telegraph or telephone line. Artificial lines of small actual dimensions may, in their behavior, simulate real lines that are long both mechanically and electrically. The subject will be discussed in detail in a later chapter.

**Current-carrying Properties.**—Real and artificial lines are designed, in general, to carry either discontinuous or alternating currents. Telegraph lines carry discontinuous signalling currents. Telephone lines carry alternating currents fluctuating in frequency and amplitude. Power lines carry either alternating or continuous currents. In general, all these types of current may be reduced, for the purpose of analysis, to the basis of simple alternating currents, *i.e.*, to alternating currents of constant amplitude and frequency. Thus, the continuous current may be treated as the limiting case of alternating current having zero frequency.

**Mechanical Construction.**—Real lines are characterized by definite structural properties. Thus, they may be aerial open wire, aerial cables, subterranean, or submarine cable. When designed to carry heavy currents, they have correspondingly large conductor cross-section and cooling surface. When designed to operate at high voltages, they are given appropriate insulation and mechanical separation. In uniform lines, these mechanical conditions remain substantially constant throughout their length. A line composed of successive sections in series differing in mechanical construction, but each uniform throughout its section length, is often described as a *composite line*.

**Line Constants and Linear Constants.**—A given length of any real uniform line possesses certain corresponding total values of conductor resistance (ohms), and inductance (henrys) as well as of dielectric capacitance (farads) and leakance (mhos). The corresponding *linear constants* are these referred to unit line length. Thus the linear conductor resistance would be expressible in ohms per kilometer or per mile. Uniform lines in normal condition have uniform linear constants.

Artificial lines possess line constants, but not linear constants, except as a consequence of the assumption that they represent a certain definite length of real line.

**Electrical Networks.**—An electrical network or *net* is any fixed group connection of conducting elements, each of which obeys Ohm's law, extended to alternating currents. A local-



ised artificial net is, in general, designed to offer a certain electric behavior, between defined pairs of terminals.

Artificial lines are particular cases and ordinarily fairly simple cases of general nets.

**Scope and Purpose of the Discussion.**—It is the purpose of this book to discuss the electrical-engineering behavior of lines both real and artificial, including general nets, in the steady state, *i.e.*, in the condition of electric equilibrium which tends to be established in them after the application of fixed terminal states. Incidentally, however, an elementary discussion of the initial transient state will be given in Chapter XI.

## CHAPTER II

### ELEMENTARY TRIGONOMETRICAL RELATIONS APPLYING TO REAL AND ARTIFICIAL LINES

Before commencing the study of the electrical properties of real and artificial lines, it is important to define certain fundamental trigonometrical relations.

**Real Circular Angles.**—Let a radius-vector  $OP$ , Fig. 1, start, with center fixed at  $O$ , from an initial position  $OA$ , of unit length, on the reference line  $OX$ , and with its free end  $P$  on the circle  $APB$  defined by

$$x^2 + y^2 = 1 \quad (\text{units of length})^2 \quad (1)$$

and sweep over or describe the circular sector  $AOP$ , in the positive or counter-clockwise direction. Then the circular angle of the sector  $AOP$  is determined by the area of the sector  $AOP$ , and may be expressed in circular radians. We may, for convenience, construct a negative sector  $AOp$ , equal in area but opposite in direction, to the sector  $AOP$ . Then the magnitude of the circular angle  $AOP$ , in circular radians, will be numerically equal to the area of the double sector  $POp$ . In the case represented in Fig. 1, the radius  $OA$  of the circle being, say 1 in., the shaded double sector is drawn to enclose an area of 1 sq. in., and the angle of the circular sector  $AOP$  is, therefore, 1 circ. radian. A positive circular angle is one which is described from the initial line  $OA$  in the positive or counter-clockwise direction of rotation. A negative circular angle, on the other hand, is described in the negative or clockwise direction. Circular angles may be reckoned from 0 to either  $+$  or  $-$  infinity; but for practical purposes they are usually limited to  $360^\circ$  ( $2\pi$  radians or 4 quadrants), excess revolutions being ignored.

**Real Hyperbolic Angles.**—Let a radius-vector  $OP$ , Fig. 2, start with center fixed at  $O$ , from an initial position  $OA$ , of unit length, on the reference axis  $OX$ , and with its free end  $P$  on the rectangular hyperbola  $pAP$  defined by

$$x^2 - y^2 = 1 \quad (\text{units of length})^2 \quad (2)$$

sweep over or describe the hyperbolic sector  $AOP$ , in the positive or counter-clockwise direction. Then the hyperbolic angle of the sector  $AOP$  is determined by the area of the sector  $AOP$ , and may be expressed in *hyperbolic radians*. We may, for convenience, construct a negative sector  $AOp$ , equal in area but opposite in direction, to the sector  $AOP$ . Then the magnitude of the hyperbolic angle  $AOP$ , in hyperbolic radians, will be numerically equal to the area of the double sector  $POp$ . In the case represented in Fig. 2, the radius  $OA$  of the hyperbola being, say 1 in., the shaded double area is drawn to enclose an area of 1

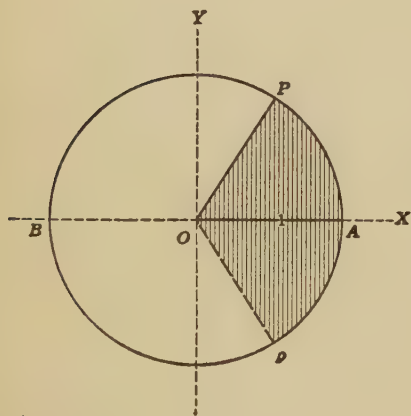


FIG. 1.—Circular angle.

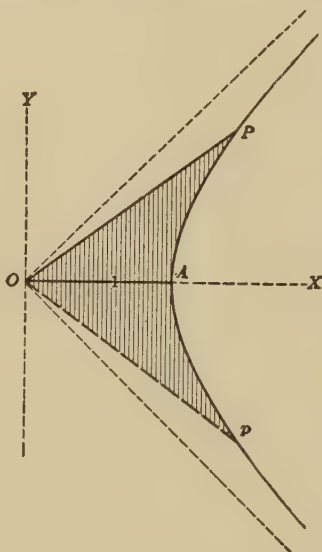


FIG. 2.—Hyperbolic angle.

sq. in., and the angle of the hyperbolic sector  $AOP$  is therefore 1 hyp. radian, or 1 *hyp.*

A positive hyperbolic angle is one which is described from the initial line  $OA$  in the positive or counter-clockwise direction of rotation. A negative hyperbolic angle, on the other hand, is described in the negative or clockwise direction. Hyperbolic angles extend from zero to either  $+$  or  $-$  infinity.

#### Common Properties of Real Circular and Hyperbolic Angles.—

It will be evident from the foregoing that, in radian measure, the magnitudes of circular and hyperbolic angles are similarly defined with reference to the area of circular and hyperbolic sectors. A number of such geometrical analogies may be presented

between circular and hyperbolic angles. One only may be noticed here; namely, that if the free end  $P$  of the radius-vector  $OP$ , Fig. 1, describes a very small circular arc  $ds$ , the magnitude of the very small circular angle thereby described is

$$d\beta = \frac{ds}{\rho} = \frac{ds}{1} = ds \quad \text{circ. radians} \quad (3)$$

where  $\rho$  is the unit length of the constant circular radius-vector  $OP$ . Similarly, if the free end  $P$  of the radius vector  $OP$ , Fig. 2, describes a very small hyperbolic arc  $ds$ , the magnitude of the very small hyperbolic angle thereby described is

$$d\theta = \frac{ds}{\rho} \quad \text{hyp. radians} \quad (4)$$

where  $\rho$  is the instantaneous length of the hyperbolic radius-vector  $OP$ .\* The total circular or hyperbolic angle described in passing from one position to another of the radius-vector is, therefore,

$$\beta = \theta = \int \frac{ds}{\rho} \quad \text{radians} \quad (5)$$

but whereas  $\rho$  is constant in the circular case, it is variable in the hyperbolic case. In fact, if  $\beta$  is the circular angle and  $\theta$  the hyperbolic angle of the hyperbolic segment  $AOP$  in Fig. 2,

$$\rho = \sqrt{\sec 2\beta} = \sqrt{\cosh 2\theta} \quad \text{units of length} \quad (6)$$

Thus, if we consider the case represented in Fig. 2, of a hyperbolic angle of 1 radian, the circular angle  $\beta$  of the aperture  $AOP$  is 0.65088 circ. radian, or  $37^\circ 17' 33.67''$ . The secant of  $74^\circ 35' 07''$  ( $74^\circ.585$ ) is 3.762196, which is also the cosine of 2 hyperbolic radians. The radius-vector  $\rho$  in Fig. 2, therefore has a length of

$$\sqrt{3.762196} = 1.93964$$

units, the unit being represented by the length  $OA$ .

The area  $S$ , of a circle of radius  $r$  is

$$S = \pi r^2 = 2\pi \frac{r^2}{2} = \frac{r^2}{2} \quad (\text{total radians}) \quad (7)$$

The area  $S'$  of a circular sector of arc  $\beta$  radians is  $\beta \frac{r^2}{2}$

$$S' = \frac{r^2}{2} \beta \quad (8)$$

\* For a demonstration of (4), see Appendix L of "The Application of Hyperbolic Functions to Electrical Engineering Problems," by A. E. Kennelly.

or, in Fig. 3, page 8,

$$\beta = \frac{2(\text{area } POA)}{r^2} \quad (9)$$

Similarly, considering the hyperbola of Fig. 4, whose radius  $oa$  is taken as  $r_1$  the area  $poa$  is

$$S' = \theta \frac{r_1^2}{2} \quad (10)$$

or

$$\theta = \frac{2(\text{area } poa)}{r_1^2} \quad (11)$$

where the radius  $r_1$  is a constant.

**Numerical Values of the Sines, Cosines, and Tangents of Real Circular and Hyperbolic Angles.**—Figures 3 and 4 represent, respectively, a certain positive circular angle  $AOP$ , and a certain positive hyperbolic angle  $aop$ . The radii  $OA$  of the circle, and  $oa$  of the hyperbola are each equal to unit length. In Fig. 4,  $os$  and  $os'$  are the asymptotes of the hyperbola, or the two straight lines, each inclined  $45^\circ$  with the radius  $oa$ , which the hyperbola continually approaches but never meets. Then, if we consider only numerical magnitudes, and ignore directions in the plane, we may find the sine, cosine, and tangent of the two angles compared,  $\beta$  and  $\theta$ , respectively, by following the same construction in each case.

**To Find the Numerical Value of the Sine.**—From the free end of the radius-vector, drop a perpendicular on the initial radius. The length of this perpendicular measures the sine of the circular or hyperbolic angle. In Fig. 3, it is  $\sin \beta = PQ$ . In Fig. 4, it is  $\sinh \theta = pq$ . The sine of a real circular angle cannot exceed unity, and changes sign twice per revolution. The sine of a positive real hyperbolic angle is always positive, and may range from 0 to  $+\infty$ .

**To Find the Numerical Value of the Cosine.**—The intercept on the initial line  $OA$ , between the origin and the perpendicular, let fall from the free end of the radius-vector, measures the cosine of the circular or hyperbolic angle. Thus, in Fig. 3, it is  $\cos \beta = OQ$ . In Fig. 4, it is  $\cosh \theta = oq$ . The cosine of a real circular angle cannot exceed unity, and changes sign twice per revolution. The cosine of a real hyperbolic angle cannot be less than unity, and is always positive. It ranges between  $+1$  and  $+\infty$ .



**To Find the Numerical Value of the Tangent.**—Carry a perpendicular from the end of the initial radius (reversed for circular angles between  $\pi/2$  and  $3\pi/2$ ) up to the radius-vector or its production. The length of this perpendicular measures the tangent of the circular or hyperbolic angle. In Fig. 3, it is  $\tan \beta = AT$ . In Fig. 4, it is  $\tanh \theta = at$ . The tangent of a real circular angle may range between 0 and  $\pm\infty$ . It changes sign four times per revolution. The tangent of a positive real hyperbolic angle varies between 0 and  $+1$

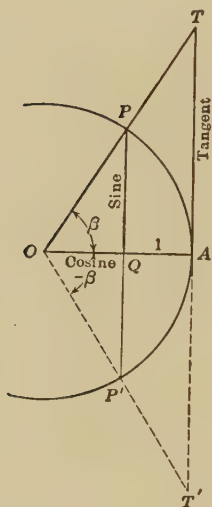


FIG. 3.—Constructions for the sine, cosine, and tangent of a circular angle.

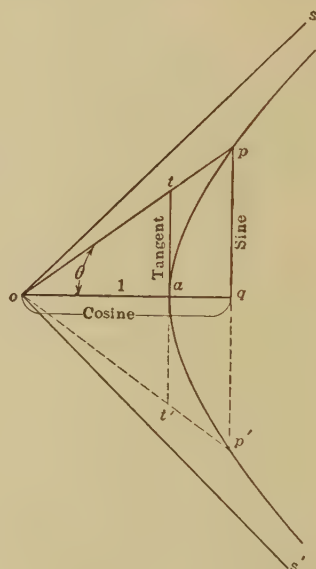


FIG. 4.—Constructions for the sine, cosine, and tangent of a hyperbolic angle.

The rules for finding the numerical values of the same trigonometrical functions of negative angles are identical. Thus taking  $AOP'$  and  $aop'$  as the negative circular and hyperbolic angles,  $QP'$  and  $qp'$  are their respective sines,  $OQ$  and  $oq$  their respective cosines, and  $AT'$  and  $at'$  their respective tangents. In either case, the sine of a negative angle is the negative of the sine of the same angle positive; the cosine of a negative angle is the same as the cosine of the same angle positive; the tangent of a negative angle is the negative of the tangent of the same angle positive.

Figure 5 shows the graphs of the sines, cosines and tangents of positive real circular and hyperbolic angles. The circular angles are expressed in *quadrant measure* and the hyperbolic angles in hyperbolic radian measure.



FIG. 5.—Graphs of circular and hyperbolic functions.

### Geometrical Interpretation of the Exponentials $e^{j\beta}$ and $e^{-j\beta}$ .—

If we expand  $e^{j\beta}$  by Maclaurin's theorem, we obtain

$$\begin{aligned}
 e^{j\beta} &= 1 + j\beta + \frac{(j\beta)^2}{2!} + \frac{(j\beta)^3}{3!} + \frac{(j\beta)^4}{4!} + \cdots \text{numeric} \quad (12) \\
 &= 1 + j\beta - \frac{\beta^2}{2!} - \frac{j\beta^3}{3!} + \frac{\beta^4}{4!} + \frac{j\beta^5}{5!} - \cdots \text{numeric} \\
 &= \left(1 - \frac{\beta^2}{2!} + \frac{\beta^4}{4!} - \cdots\right) + j\left(\beta - \frac{\beta^3}{3!} + \frac{\beta^5}{5!} - \cdots\right) \\
 &= \cos \beta + j \sin \beta \quad \text{numeric} \quad (13)
 \end{aligned}$$

Thus if we construct, as in Fig. 6,  $\cos \beta + j \sin \beta$ , we obtain a plane vector or complex quantity  $OP$ , of unit length, making a circular angle  $\beta$  radians with the initial radius  $OA$ . The exponential  $\epsilon^{j\beta}$ , applied to any numerical quantity, thus leaves the numerical value of that quantity unchanged, but rotates it about the origin through a positive angle of  $\beta$  radians. Similarly,  $\epsilon^{-j\beta} = \cos \beta - j \sin \beta$ ; so that  $OP'$ , Fig. 6, would represent such a quantity. The coefficients  $\epsilon^{j\beta}$  and  $\epsilon^{-j\beta}$  therefore modify only the polar circular angle, or *slope* of the quantity to which they are applied, and may be regarded as twisting

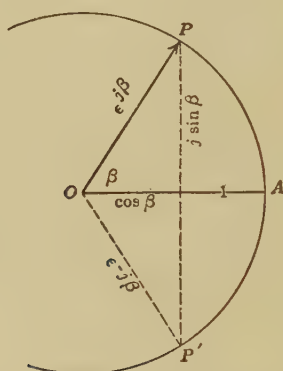


FIG. 6.—Graphical representation of the exponential  $e^{\pm j\beta}$  in relation to an angle of  $\pm \beta$  circular radians.

operators. If  $\beta$  is taken large enough, the operator  $\epsilon^{\pm j\beta}$  may cause the operand to be rotated many times about the origin in the plane of reference.

An exponential of the form  $\epsilon^{j\omega t}$ , where  $t$  is an elapsed time in seconds, is a *rotor* which causes the operand to rotate positively about the origin in the plane of reference at the velocity of  $\omega$  radians per sec. Similarly,  $\epsilon^{-j\omega t}$  is a rotor in the clockwise or negative direction.

**Evaluation of Sin  $\beta$ , Cos  $\beta$ , and Tan  $\beta$  in Terms of Exponentials.** If we subtract  $\epsilon^{-j\beta}$  from  $\epsilon^{j\beta}$  we obtain, using (13),

$$\begin{aligned} \epsilon^{j\beta} - \epsilon^{-j\beta} &= \cos \beta + j \sin \beta - (\cos \beta - j \sin \beta) \\ &= 2j \sin \beta \\ \therefore \sin \beta &= \frac{\epsilon^{j\beta} - \epsilon^{-j\beta}}{2j} \end{aligned} \tag{14}$$

Adding, we obtain

$$\begin{aligned} e^{j\beta} + e^{-j\beta} &= \cos \beta + j \sin \beta + \cos \beta - j \sin \beta \\ &= 2 \cos \beta \\ \cos \beta &= \frac{e^{j\beta} + e^{-j\beta}}{2} \end{aligned} \quad (15)$$

Dividing (14) by (15), we obtain;

$$\tan \beta = \frac{e^{j\beta} - e^{-j\beta}}{j(e^{j\beta} + e^{-j\beta})} \quad (16)$$

**Evaluation of a Hyperbolic Angle  $\theta$  in Terms of Exponentials.**—Consider the hyperbola  $xy = 1$  of Fig. 7. Lay off any hyperbolic

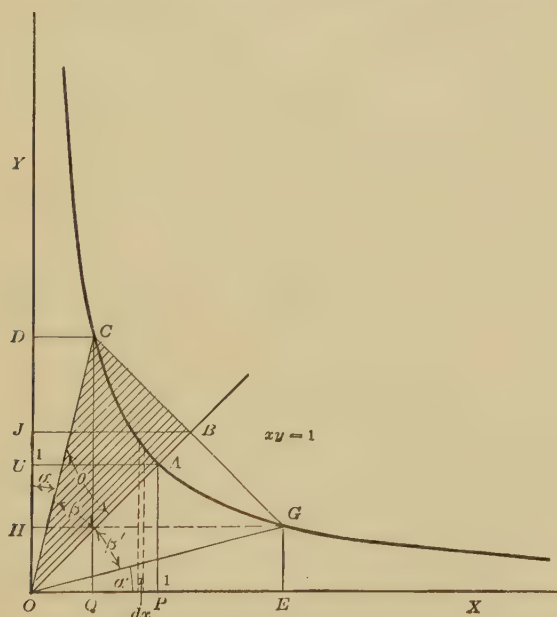


FIG. 7.—Equilateral hyperbola referred to asymptotes as axes.

angle  $\theta$  covering the sector  $AOC$ , and the corresponding negative angle  $-\theta$  covering the sector  $AOG$ . The circular angle between  $OA$  and  $OC$  is  $\beta$ . From  $C$ ,  $B$ ,  $A$  and  $G$ , project the lines  $CD$ ,  $BJ$ ,  $AU$ , and  $GH$  parallel to the  $X$ -axis. Also from  $C$ ,  $A$ , and  $G$  drop perpendiculars  $CQ$ ,  $AP$ , and  $GE$  onto the  $X$ -axis. In order to find the functions of  $\theta$  in terms of exponentials we must first show that

$$\cosh \theta = \frac{OD + OH}{2}$$

By definition,  $\cosh \theta = OB/OA$  and since

$$OA = \sqrt{2}, \quad \cosh \theta = \frac{OB}{\sqrt{2}}$$

and

$$\begin{aligned} \cos \beta &= \frac{OB}{OC} \\ \cos \alpha &= \frac{OD}{OC} = \cos (45^\circ - \beta) \\ &= 0.707(\cos \beta + \sin \beta) \end{aligned}$$

Also

$$\begin{aligned} \cos (\alpha + 2\beta) &= \cos (45^\circ + \beta) \\ &= 0.707(\cos \beta - \sin \beta) = \frac{OH}{OG} = \frac{OH}{OC} \\ OG &= OC \text{ because } \beta = \beta' \\ OD &= OC \times 0.707(\cos \beta + \sin \beta) \\ OH &= OC \times 0.707(\cos \beta - \sin \beta) \end{aligned}$$

Adding

$$\begin{aligned} OD + OH &= \sqrt{2} \times OC \cos \beta = \sqrt{2} \times OC \times \frac{OB}{OC} \\ &= \sqrt{2} \times OB \\ \therefore \frac{OD + OH}{2} &= \frac{OB}{\sqrt{2}} = \cosh \theta \end{aligned} \quad (17)$$

Subtracting

$$\begin{aligned} OD - OH &= \sqrt{2} \times OC \sin \beta = \sqrt{2} \times OC \times \frac{CB}{OC} \\ \frac{OD - OH}{2} &= \frac{CB}{\sqrt{2}} = \sinh \theta \end{aligned} \quad (18)$$

If we can now show that the equation of the curve is  $y = e^\theta$ , we can write the functions of  $\theta$  in terms of exponentials.

By definition, (11)

$$\begin{aligned} \frac{\theta}{2} &= \frac{\text{area } COA}{r_1^2} = \frac{\text{area } COA}{2} \\ \theta &= \text{area } COA = \text{area } CQOD + \text{area } QCAP - \text{area } AOP \\ &\quad - \text{area } OCD \\ &= xy + \text{area } QCAP - \frac{xy}{2} - \frac{xy}{2} \end{aligned}$$



= area  $QCAP$

= area enclosed between the curve  $CA$  and the perpendiculars drawn to the  $X$ -axis.

$$\theta = \int_x^1 y dx = \int_x^1 \frac{dx}{x} = \log_h x \Big|_x^1 \text{ or } \log_e x \Big|_x^1$$

Substituting in the limits,

$$\theta = \log_h 1 - \log_h x = \log_h \frac{1}{x} = \log_h y$$

$$\theta = \log_h y$$

$\epsilon^\theta = y$ . Therefore, taking  $OD$  as a particular value of  $y$ ,  
 $OD = \epsilon^\theta$

$OH = \epsilon^{-\theta}$  being the  $y$ -coördinate of a negative  $\theta$ .

Hence

$$\frac{OD + OH}{2} = \frac{\epsilon^\theta + \epsilon^{-\theta}}{2} = \cosh \theta \quad (19)$$

and

$$\frac{OD - OH}{2} = \frac{\epsilon^\theta - \epsilon^{-\theta}}{2} = \sinh \theta \quad (20)$$

Dividing, (19) by (20), we obtain,

$$\tanh \theta = \frac{\epsilon^\theta - \epsilon^{-\theta}}{\epsilon^\theta + \epsilon^{-\theta}} \quad (21)$$

### Geometrical Interpretation of the Exponentials $\epsilon^\theta$ and $\epsilon^{-\theta}$ .—

If (Fig. 8) we draw the Cartesian axes  $OX$  and  $OY$  through the origin  $O$ , in the plane of reference  $XOY$ , and draw through a point  $A$ , whose coördinates are  $x = 1$ ,  $y = 1$ , a rectangular hyperbola of radius  $OA$ , having  $OX$  and  $OY$  as asymptotes, then a radius-vector  $OP$ , starting from the initial position  $OA$ , with one end fixed at  $O$ , sweeping with its free end  $P$  in the positive direction over the hyperbola, will describe a *hyperbolic angle*  $\theta$ , measured by the area through which it has swept. The projection  $p$  of  $P$ , on the  $Y$ -axis, will then measure  $\epsilon^\theta$  units of length from  $O$ . In Fig. 8, the successive positions of  $P$  for hyperbolic angles, differing by 0.1 hyp. radian, are indicated on the curve up to  $\theta = 1.2$  hyps., with the corresponding scale of exponentials  $\epsilon^\theta$  indicated on  $OY$ .

Similarly, if the radius-vector, starting from  $OA$  moves clockwise or negatively along the curve  $AP'Q'$ , describing an angle

$-\theta$  hyp. radians, the corresponding projection  $p'$  on  $OY$  will be  $Op' = \epsilon^{-\theta}$  units from  $O$ .

An exponential  $\epsilon^{\pm\theta}$ , may thus be interpreted as the *orthogonal\** projection on a positive asymptote of a radius-vector which has described a hyperbolic angle  $\pm\theta$  radians.

Again, an exponential  $\epsilon^{\pm at}$ , where  $t$  is an elapsed time in seconds, may be interpreted as the asymptotic orthogonal projection

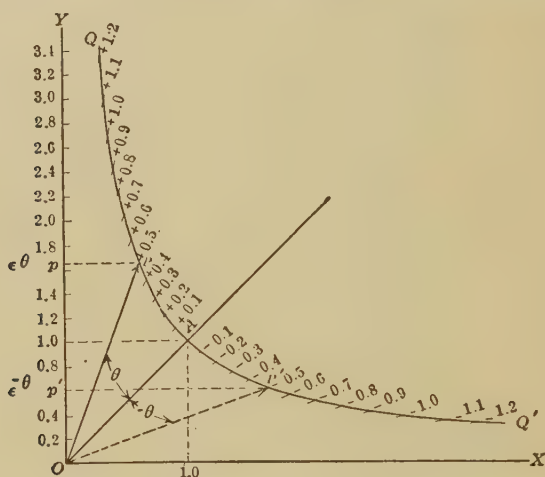


FIG. 8.—Rectangular hyperbola drawn with asymptotes as axes.

of a radius-vector moving over a rectangular hyperbola, with uniform angular velocity  $a$  hyp. radians per sec. describing equal areas in equal times.

**Determination of Hyperbolic Trigonometric Identities.**—If we expand  $\epsilon^{\theta}$  by MacLaurin's theorem, we obtain,

$$\epsilon^{\theta} = 1 + \theta + \frac{\theta^2}{2!} + \frac{\theta^3}{3!} + \frac{\theta^4}{4!} + \frac{\theta^5}{5!} + \dots$$

and

$$\epsilon^{-\theta} = 1 - \theta + \frac{\theta^2}{2!} - \frac{\theta^3}{3!} + \frac{\theta^4}{4!} - \frac{\theta^5}{5!} + \dots$$

so

$$\frac{\epsilon^{\theta} - \epsilon^{-\theta}}{2} = \sinh \theta = \theta + \frac{\theta^3}{3!} + \frac{\theta^5}{5!} + \dots \quad (22)$$

\* An orthogonal projection is defined as a projection made perpendicularly on to the line or plane of projection.

and

$$\frac{\epsilon^\theta + \epsilon^{-\theta}}{2} = \cosh \theta = 1 + \frac{\theta^2}{2!} + \frac{\theta^4}{4!} + \dots \quad (23)$$

If we add (22) and (23), we obtain

$$\cosh \theta + \sinh \theta = \frac{\epsilon^\theta + \epsilon^{-\theta} + \epsilon^\theta - \epsilon^{-\theta}}{2} = \epsilon^\theta \quad (24)$$

and if we subtract,

$$\cosh \theta - \sinh \theta = \frac{\epsilon^\theta + \epsilon^{-\theta} - \epsilon^\theta + \epsilon^{-\theta}}{2} = \epsilon^{-\theta} \quad (25)$$

Multiplying (24) by (25), we obtain

$$\cosh^2 \theta - \sinh^2 \theta = 1 \quad (26)$$

Squaring (24) we obtain

$$\begin{aligned} \cosh^2 \theta + 2 \cosh \theta \sinh \theta + \sinh^2 \theta &= \epsilon^{2\theta} \\ \cosh^2 \theta + \sinh^2 \theta &= \epsilon^{2\theta} - 2 \frac{(\epsilon^\theta + \epsilon^{-\theta})}{2} \frac{(\epsilon^\theta - \epsilon^{-\theta})}{2} \\ &= \frac{\epsilon^{2\theta} + \epsilon^{-2\theta}}{2} \\ \cosh^2 \theta + \sinh^2 \theta &= \cosh 2\theta \end{aligned} \quad (27)$$

Now suppose we have the equation

$$\sinh \theta \cosh \phi + \cosh \theta \sinh \phi$$

and wish to determine its equivalents. If we substitute values as in (19) and (20) and cross multiply, we obtain

$$\begin{aligned} \sinh \theta \cosh \phi + \cosh \theta \sinh \phi &= \frac{\epsilon^{(\theta+\phi)} - \epsilon^{-(\theta+\phi)}}{2} \\ &= \sinh (\theta + \phi) \end{aligned} \quad (28)$$

**Functions of Imaginary Circular Angles.**—From (14),

$$\sin \beta = \frac{\epsilon^{i\beta} - \epsilon^{-i\beta}}{2j}$$

If we replace  $\beta$  by  $j\alpha$ , we have

$$\begin{aligned} \sin j\alpha &= \frac{\epsilon^{j^2\alpha} - \epsilon^{-j^2\alpha}}{2j} = - \frac{\epsilon^\alpha - \epsilon^{-\alpha}}{2j} \\ &= j^2 \frac{\epsilon^\alpha - \epsilon^{-\alpha}}{2j} = j \frac{\epsilon^\alpha - \epsilon^{-\alpha}}{2} = j \sinh \alpha \end{aligned} \quad (29)$$

Similarly,

$$\cos j\alpha = \cosh \alpha \quad (30)$$

$$\tan j\alpha = j \tanh \alpha \quad (31)$$

**Reduction of Formulas from Circular to Hyperbolic Trigonometric Identities.**—By means of formulas (29), (30), and (31), we may convert any known circular identity to the corresponding identity of hyperbolic trigonometry.

For example, let it be given that

$$\cos^2 \beta + \sin^2 \beta = 1$$

and let

$$\beta \text{ have any value } j\theta$$

Then,

$$\begin{aligned} \cos^2 j\theta + \sin^2 j\theta &= 1 && \text{By (29) and (30)} \\ \cosh^2 \theta + j^2 \sinh^2 \theta &= 1 \\ \cosh^2 \theta - \sinh^2 \theta &= 1 && (32) \end{aligned}$$

which is the corresponding hyperbolic identity.

Again,

$$\cos \alpha \cos \beta - \sin \alpha \sin \beta = \cos (\alpha + \beta)$$

let

$$\begin{aligned} \alpha &= j\theta \text{ and } \beta = j\phi \\ &= \cos j\theta \cos j\phi - \sin j\theta \sin j\phi = \cos j(\theta + \phi) \\ &= \cosh \theta \cosh \phi - j^2 \sinh \theta \sinh \phi = \cosh (\theta + \phi) \\ &= \cosh \theta \cosh \phi + \sinh \theta \sinh \phi = \cosh (\theta + \phi) && (33) \end{aligned}$$

As a final example, let us take

$$\tan (\alpha + \beta) = \frac{\tan \alpha + \tan \beta}{1 - \tan \alpha \tan \beta}$$

and let

$$\alpha = j\theta \text{ and } \beta = j\phi, \text{ as before,}$$

then

$$\begin{aligned} \tan j(\theta + \phi) &= \frac{\tan j\theta + \tan j\phi}{1 - \tan j\theta \tan j\phi} \\ j \tanh (\theta + \phi) &= \frac{j \tanh \theta + j \tanh \phi}{1 - j^2 \tanh \theta \tanh \phi} \\ \tanh (\theta + \phi) &= \frac{\tanh \theta + \tanh \phi}{1 + \tanh \theta \tanh \phi} && (34) \end{aligned}$$

Appendix A sets forth in parallel columns the values of a number of corresponding circular and hyperbolic identities.

## CHAPTER III

### TRIGONOMETRICAL PROPERTIES OF REAL CONTINUOUS-CURRENT LINES

Every c.c.\* line, operated in the steady state, possesses two essential electrical properties, namely, (1) conductor resistance, and (2) dielectric leakance. *Smooth* c.c. lines have constant *linear resistance*, i.e., constant conductor resistance in ohms per mile, or per kilometer, or other selected linear unit; and also constant *linear leakance*; i.e., constant insulation leakance in mhos per mile, per kilometer, etc. Strictly speaking, in no actual line are these *linear constants* ever completely uniform. The resistance of equal lengths of conductor are never precisely equal, if only owing to accidental variations of temperature; or of conductor diameter; or of material quality. The dielectric leakance is still more liable to vary, over a certain range, along a line, if only owing to variations of temperature, humidity, dimensions, and quality of the insulator. Nevertheless, if we consider any section of actual line having uniform dimensions and structure, we may, if the line is not defective or faulty, regard it as though it possessed a certain average linear resistance and average linear leakance. The more nearly the line conforms to these average values, the more nearly should its actual electric behavior conform to the behavior computed on the basis of the said averages. Unless we are entitled to assume some average linear constants from statistical knowledge of the line, we are debarred from making any logical quantitative estimate of the line's behavior. If the line is *composite*, i.e., if it consists of a plurality of successive sections, each having its own linear constants, the behavior of the line can be predicated by taking each section into separate account (see Chapter XVII). If the line is discontinuous, in the sense of having a uniform section or sections, except at particular points where definite deviations or loads occur, such as an

\* The contraction c.c. stands for continuous current and a.c. for alternating current.

inserted resistance, or a known applied leak, then the effects of these loads can also be taken into separate account.\*

**Hyperbolic Angle of a Line.**—Consider the case of a single uniform line of length  $L$  km., such as is represented in Fig. 9, having a total actual aggregate conductor resistance of  $R = Lr$  ohms, where  $r$  is the linear resistance in ohms per wire kilometer, also a total actual aggregate dielectric leakance of  $G = Lg$  mhos, where  $g$  is the linear leakance. The number of leaks may be regarded as very great, and sufficiently nearly uniform, so that

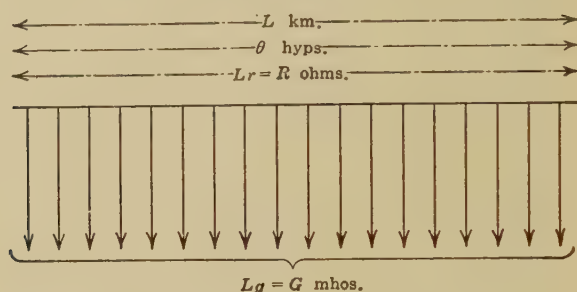


FIG. 9.—Diagram of a smooth or uniform single-wire line.

the leakance of each or any particular kilometer of line is substantially constant at  $g$  mhos. Then *the line will subtend or contain a hyperbolic angle,  $\theta$* , as is demonstrated in the next chapter, and which is defined by the relation

$$\theta = L\sqrt{rg} = L\alpha = \sqrt{RG} \quad \text{hyp. radians}^\dagger \angle \quad (35)$$

Here the *linear hyperbolic angle* of the line is

$$\alpha = \sqrt{rg} \quad \frac{\text{hyp. radians}}{\text{km.}} \angle \quad (36)$$

$\alpha$  is also called the *attenuation constant* of the line. It should be noted that the unit of length does not affect the value of  $\theta$ .

\* KENNELLY, A. E., "Artificial Electric Lines" Chap. XIV, McGraw-Hill Book Company, Inc., 1917.

† The angle sign  $\angle$  is appended to the unit of this and other following formulas to indicate that although, in the c.c. case, the units are essentially real, yet they may be regarded as complex or plane vector units in the general a.c. case. The use of this vectorial sign with the unit of an equation signifies that each and every separate term in the equation is a plane vector; so that no "dots" or other special indices are needed, in the symbols of the equation, to announce vectorial significance. The unit hyp. radians  $\angle$  may be read "vector hyperbolic radians."



In other words, the angle subtended by any uniform line is independent of the unit of length; but the attenuation constant  $\alpha$  is directly dependent on the unit of length, so that if  $r$  and  $g$  are, respectively, the resistance and leakance of the line per wire mile, then  $\alpha$  will be 1.609 times larger than if  $r$  and  $g$  are taken with reference to the wire kilometer. On the other hand, the angle  $\theta$  of a line increases directly as its length, whereas the linear hyperbolic angle  $\alpha$  is a characteristic of a given type of uniform line and has the same value whether the line is long or short.

As an example, let us take the case of a line of  $L = 200$  km. (124.3 miles),  $r = 4$  ohms per wire km. ( $6.437 \Omega/\text{w.m.}$ ) and  $g = 10^{-6}$  mho per wire km. ( $1.609 \times 10^{-6} \Omega/\text{w.m.}$ ). Then  $\alpha = \sqrt{4 \times 10^{-6}} = 0.002$  hyp. per km. This is the linear hyperbolic angle, or the attenuation constant. The angle subtended by the whole line ( $R = 800$  ohms,  $G = 2 \times 10^{-4}$  mho) is  $\theta = \sqrt{800 \times 2 \times 10^{-4}} = 0.4$  hyp. radian, which is also equal to the length multiplied by the linear hyperbolic angle.

**Significance of the Term Linear Hyperbolic Angle or Attenuation Constant.**—A physical interpretation which may be placed upon  $\alpha$ , the linear hyperbolic angle of the line, is that when the line is very long, either the current or the voltage, at the end of any selected kilometer length, is  $\epsilon^{-\alpha}$  of that existing at the beginning of that kilometer length. In other words, the linear attenuation factor is the numeric  $\epsilon^{-\alpha}$ . If  $V$  is the potential in volts at any point on the line, in the steady state, then the potential 1 km. further along the line in the direction of flow of energy is  $V_1 = V\epsilon^{-\alpha}$  volts. Similarly, the current being  $I$  amp. at the same point, the current 1 km. further on is  $I_1 = I\epsilon^{-\alpha}$  amp. This exponential type of linear attenuation is called *normal attenuation*. If, as is necessarily the case in practice, the value of  $\alpha$  is small with respect to unity, since

$$\epsilon^{-\alpha} = 1 - \alpha + \frac{\alpha^2}{2!} - \frac{\alpha^3}{3!} + \dots \quad \text{numeric } \angle \quad (37)$$

we may, for most practical purposes, neglect the term  $\alpha^2/2!$  and all its successors, so that

$$V_1 = V(1 - \alpha) \quad \text{volts } \angle \quad (38)$$

and

$$I_1 = I(1 - \alpha) \quad \text{amp. } \angle \quad (39)$$

Thus, in the case considered,  $\alpha = 0.002$  and

$$V_1 = V(1 - 0.002) = 0.998V \text{ volts,}$$

or the voltage falls by 0.2 per cent, or 0.002 per unit, in each kilometer of line length. The linear hyperbolic angle is thus the *perunitage of attenuation* of either voltage or current in a line that is so long that there is no appreciable reflection from the distant end. If the line is short, the steady-state linear attenuation factor will, in general, differ from  $\alpha$ . In such a case the *actual linear attenuation factor* differs from the *normal linear attenuation factor*  $\epsilon^{-\alpha}$ .

**Normal Attenuation Factor.**—A line of large real hyperbolic angle  $\theta$  is necessarily a line of large attenuation, or one in which the current received at the distant delivery end is very weak with respect to the current at the generator end. If the line is grounded at the receiving end through a resistance equal to the “surge resistance” (see page 48), then the attenuation of voltage and of current will be  $\epsilon^{-L\alpha} = \epsilon^{-\theta}$ ; so that if the potential and current at the generating end  $A$  are respectively  $V_A$  and  $I_A$ , the values at the receiving end,  $B$ , will be

$$V_B = V_A \epsilon^{-\theta} \quad \text{volts } \angle \quad (40)$$

and

$$I_B = I_A \epsilon^{-\theta} \quad \text{amp. } \angle \quad (41)$$

The ratio  $\epsilon^{-\theta} = \epsilon^{-L\alpha}$  of received to generated voltage or current is called the *normal attenuation factor* of the line. In the case considered, this normal attenuation factor is  $\epsilon^{-0.4} = 0.6703$ ; so that the percentage value of the generated current and voltage received at the distant end is 67.03; or the perunitage value 0.6703. The normal attenuation factor of a single line may, therefore, be defined as equal to the perunitage value of the generated voltage or current received at the distant end of the line, when the line is grounded through its surge resistance. If the line is actually grounded through a resistance other than the surge resistance, the *actual attenuation factors* of voltage and current  $V_B/V_A$  and  $I_B/I_A$ , respectively, will, in general, differ from each other and from the normal attenuation factor  $\epsilon^{-\theta}$ .

**Surge Resistance.**—A uniform line of linear conductor resistance  $r$  ohms per wire km., and linear dielectric leakance  $g$  mhos

per wire km., possesses a *surge resistance*  $r_0$  which is the square root of their ratio

$$r_0 = \sqrt{\frac{r}{g}} \quad \text{ohms } \angle \quad (42)$$

This resistance is not affected by the length of the uniform line. If we consider a length  $L$  km. of the line, having a total conductor resistance  $R = Lr$  ohms, and a total dielectric leakance  $G = Lg$  mhos, the square root of their ratio will still be the surge resistance

$$r_0 = \sqrt{\frac{R}{G}} = \sqrt{\frac{Lr}{Lg}} = \sqrt{\frac{r}{g}} \quad \text{ohms } \angle \quad (43)$$

This resistance has been called various names by various writers, such as the *characteristic resistance*, the *natural resistance*, or the *iterative resistance*. Any of these terms may be used. The term *surge resistance* has the advantages of brevity and distinctiveness. It was first applied\* as meaning that resistance which a line automatically offers to its surges or free oscillations at the high-frequency limit (see formula (331)). A physical meaning may be given to the term by noticing that, as will be shown later, the resistance which a uniform wire of indefinitely great length offers, between the home end and ground, is always equal to the surge resistance  $r_0$ , whether the distant end is free, grounded, or in any intermediate condition, assuming that the line is devoid of e.m.f. before applying the measuring apparatus. But although the surge resistance may conveniently be defined as the resistance offered by an infinite length of the uniform line considered, it should be remembered that any finite length of the line possesses a surge resistance, and the same surge resistance in all parts. Another way of presenting the same fact is that if for any length of the uniform line considered, we take the conductor resistance  $R = Lr$ , and the resistance corresponding to the total leakance  $G = Lg$ , then calling this equivalent leak resistance

$$R' = \frac{1}{G} \quad \text{ohms } \angle \quad (44)$$

the surge resistance will always be the geometrical mean of  $R$  and  $R'$ ,  
or

$$r_0 = \sqrt{R \cdot R'} \quad \text{ohms } \angle \quad (45)$$

\* KENNELLY, A. E., "Surges in Transmission Circuits," *Electrical World*, Nov. 23, 1901, vol. xxxviii, No. 21, pp. 847-849.

If the length  $L$  is great, the value of  $R$  will be large and that of  $R'$  small; while, on the contrary, if the length is short,  $R'$  will be large and  $R$  small; but their geometrical mean  $r_0$  will not change.

Moreover, if the uniform line of any length  $L$  km. be successively freed and grounded at the distant end, its resistance to ground as measured at the home end will be, say,  $R_f$  and  $R_g$  ohms, respectively. Then, as we shall see later, the geometrical mean of these two resistances, if correctly measured, will always be equal to the surge resistance  $r_0$  ohms, no matter what the length of line; or, by definition,

$$r_0 = \sqrt{R_f \cdot R_g} \quad \text{ohms} \quad (46)$$

We therefore define the surge resistance of a line as the geometrical mean of its resistances at one end, when the other end is first freed or opened and then grounded or shorted.

**Single-wire and Two-wire Lines in Relation to  $\alpha$ ,  $\theta$ , and  $r_0$ .**—We have hitherto considered only single-wire d.c. real lines using

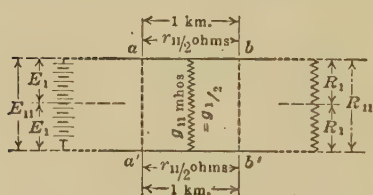


FIG. 10.—Two-wire line with metallic circuit.

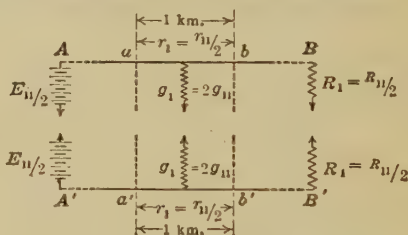


FIG. 11.—Two-wire line divided into two single-wire lines, each with perfect ground return circuit.

ground return, such as those used in ordinary wire telegraphy. We shall now examine two-wire lines forming a metallic circuit, such as are used in ordinary wire telephony.

In Fig. 10 a two-wire or metallic circuit is indicated as being voltage at one end with an e.m.f.  $E_{11}$  volts at battery terminals, and being loaded at the other end with a resistance  $R_{11}$  ohms. A single kilometer length of this circuit  $ab\ b'a'$  is selected from this pair of wires be  $r_{11}$  ohms per loop km., and let the linear leakance be  $g_{11}$  mhos per loop km. Then, if the system is completely symmetrical, it is clear that there will be zero potential at the middle of the battery, and also at the middle of the load resistance. No electrical change can be made in the system by connecting either or both of these zero-potential points to ground. If they

are both perfectly grounded, the system may properly be divided, as in Fig. 11, into two entirely separate and equal parts,  $AB$  and  $A'B'$ , each employing perfect ground-return circuit. The terminal voltage at  $A$  and also at  $A'$  will be  $E_t = E_{t,}/2$ ; while the terminal receiving-end load resistance at  $B$  and also at  $B'$ , Fig. 11, will be  $R_t = R_{t,}/2$ . In the selected kilometer of Fig. 11 there will be in each circuit a conductor resistance of  $r_t = r_{t,}/2$  ohms; while the leakance to ground will be  $g_t = 2g_{t,}$  mhos, since two equal conductances in series produce a total conductance one-half of either taken singly.

The linear hyperbolic angle of either  $AB$  or  $A'B'$  in Fig. 11 will be  $\sqrt{r_t g_t}$ , hyps. per km.; while that of the loop kilometer  $abb'a'$  in Fig. 10 will be

$$\alpha_{t,} = \sqrt{r_{t,} g_{t,}} = \sqrt{2r_t \cdot \frac{g_t}{2}} = \sqrt{r_t g_t} = \alpha, \text{ hyps. per km. } \angle \quad (47)$$

It is evident that the linear hyperbolic angle will be the same, whether reckoned on a loop-kilometer or on a wire-kilometer basis.

As an example, a two-wire line may be considered having a linear resistance  $r_{t,} = 10$  ohms per loop km., and a linear leakance  $g_{t,} = 4 \times 10^{-7}$  mho per loop km. Then, if the system were split into halves as in Fig. 11, we should have two ground-return systems, in each of which the linear resistance was  $r_t = 5$  ohms per wire km., and a linear leakance  $g_t = 8 \times 10^{-7}$  mhos per wire km. The linear hyperbolic angle on the two-wire basis would then be  $\alpha_{t,} = \sqrt{10 \times 4 \times 10^{-7}} = 0.002$  hyp. per loop km.; while on the single-wire basis it would be  $\alpha_t = \sqrt{5 \times 8 \times 10^{-7}} = 0.002$  hyp. per wire km. It is evident that the linear hyperbolic angle would be the same for either case.

It, therefore, follows that since

$$\theta_{t,} = L\alpha_{t,} = L\alpha_t = \theta, \quad \text{hyp. radians or hyps. } \angle \quad (48)$$

the total hyperbolic angle  $\theta$  subtended by a uniform two-wire line is the same as that subtended by either of the two single-wire lines into which it might be resolved.

If we form the surge resistance of the two-wire line based on formula (43) with the data for 1 loop km. we have

$$r_{0,t,} = \sqrt{\frac{r_{t,}}{g_{t,}}} = \sqrt{\frac{2r_t}{(g_t/2)}} = 2\sqrt{\frac{r_t}{g_t}} = 2r_{0,t}, \text{ ohms } \angle \quad (49)$$



from which it appears that the surge resistance of a two-wire line is just double that of either of its single-wire components. This simple relation is easily borne in mind if we notice that the two-wire circuit of Fig. 10 has twice the terminal e.m.f. of either component single-wire circuit of Fig. 11; so that with twice the terminal voltage the same current would flow through the doubled surge resistance of Fig. 10 as with the single voltage and single surge resistance of Fig. 11.

In the case considered, the two-wire surge resistance would be

$$r_{0,,} = \sqrt{\frac{10}{4 \times 10^{-7}}} = 5,000 \quad \text{ohms}$$

while the single-wire surge resistance of each component circuit in Fig. 11 would be

$$r_0 = \sqrt{\frac{5}{8 \times 10^{-7}}} = 2,500 \quad \text{ohms}$$

We, therefore, conclude that when a two-wire circuit is under consideration, it is a matter of indifference whether we form the angle  $\theta$  and surge resistance  $r_0$  of the line from either loop-kilometer or from wire-kilometer constants, provided we adhere to one or the other set throughout. The values of  $\theta$  and of  $\alpha$  for the line will be the same in either case. The value of  $r_0$  will bear a simple and self-evident 2 to 1 relation. Since, however, single wires are easier to represent and to carry in the mind than double wires, we shall continue to discuss only single-wire lines with perfect-ground or zero-potential return circuit, on the understanding that the results obtained are immediately applicable to two-wire or metallic-circuit lines. As for three-wire three-phase circuits, they are very commonly treated in single-wire star-branch single-phase components for general analysis; so that the single-wire mode of representation conveniently applies to them also. Since there is no numerical distinction between  $\theta$ , and  $\theta_{,,}$  or between  $\alpha$ , and  $\alpha_{,,}$  we shall drop these subscripts, and employ only the symbols  $\theta$  and  $\alpha$ . Similarly, we shall continue to use  $r_0$  in preference to  $r_{0,}$  for the surge resistance of a single-wire uniform line.

**Fundamental Constants of a Real Line.**—In the theory of electric lines, the line angle  $\theta$  with its linear value  $\theta/L = \alpha$ , and the surge resistance  $r_0$  are to be regarded as the *fundamental constants*; while the resistance and leakance of the line, together



with their linear values, are *secondary constants* which readily follow. Thus

$$r = \alpha r_0 \quad \text{ohms per wire km. } \angle \quad (50)$$

$$g = \frac{\alpha}{r_0} = \alpha g_0 \quad \text{mhos per wire km. } \angle \quad (51)$$

also

$$R = \theta r_0 \quad \text{ohms } \angle \quad (52)$$

$$G = \frac{\theta}{r_0} = \theta g_0 \quad \text{mhos } \angle \quad (53)$$

where  $g_0 = 1/r_0$  is the *surge admittance* of the line in vector mhos, or in a c.c. case, the *surge conductance* of the line in mhos.

Having postulated the relations between these fundamental constants of a real line, we shall proceed in the next chapter to demonstrate these relations in the theory of real lines, and also as a preliminary step to demonstrating their corresponding relations to the theory of artificial lines.

## CHAPTER IV

### THE STEADY-STATE DIFFERENTIAL EQUATION OF A UNIFORM REAL LINE

**The Fundamental Differential Equations.**—The differential equations of potential and current on a real uniform line, in the steady a.c. state, were given by Heaviside, with their algebraic solutions, in 1887, although the solutions offered were scalar, lengthy and unserviceable.\* The following presentation relates to the c.c. case, but applies also to the a.c. case when the mathematical reasoning is extended from real to complex quantities in a manner to be considered later.

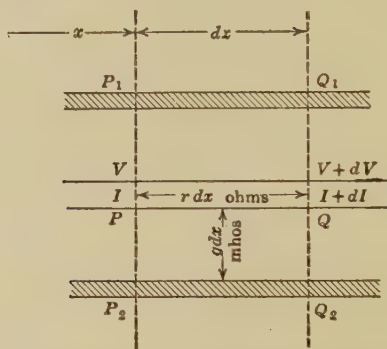


FIG. 12.—Longitudinal section of an element of leaky conductor.

Figure 12 represents the longitudinal section of a short length of single-wire uniform cable conductor, with a metallic conductor  $PQ$  insulated from the grounded metallic sheath  $P_1Q_1$ ,  $P_2Q_2$ . Two neighboring parallel planes  $P_1P_2$ ,  $Q_1Q_2$ ,  $dx$  km., apart, cutting across the cable perpendicularly, are indicated by the dotted lines. The plane  $P_1P_2$  is at a distance  $x$  km. from the origin of the line on the left hand, not shown on the drawing. The plane  $Q_1Q_2$  is therefore at a distance of  $x + dx$  km. from the origin. The electrical conditions at the origin, and at the distant right-hand end of the line are not known, but the potential of the con-

\* *The Electrician*, London, January-February, 1887. Reprinted in "Electrical Papers" by Oliver Heaviside, London, 1892, vol. ii, pp. 247-250.

ductor  $PQ$  is  $V$  volts, at the point  $P$ , with respect to ground. The current in the conductor is also  $I$  amp. at the point  $P$ . This current is flowing from  $P$  to  $Q$ , or in the direction of increasing  $x$ .

Then the potential at  $Q$  will be  $V + dV$  volts. The reason for the change of voltage in  $dx$  is the drop of potential in the conductor impedance. If  $r$  be the linear conductor impedance (linear resistance in the d.c. case), in ohms per kilometer, the resistance of the element of conductor is  $r \cdot dx$  ohms  $\angle$ , and the change in potential from  $P$  to  $Q$  will be:

$$dV = -Ir \cdot dx \quad \text{volts } \angle \quad (54)$$

or

$$\frac{dV}{dx} = -Ir \quad \frac{\text{volts}}{\text{km.}} \angle \quad (55)$$

The current at  $P$ , or at  $x$  km. from the origin, being given as  $I$  amp., the current at  $Q$ , or  $x + dx$ , will be  $I + dI$  amp. The current will change between  $P$  and  $Q$ , owing to dielectric leakance. If  $g$  be the linear admittance of the dielectric in mhos per kilometer (a real leakance in the d.c. case), the total leakance of the element  $PQ$  will be  $g \cdot dx$  mhos  $\angle$ , and the change of current in  $dx$  is

$$dI = -Vg \cdot dx \quad \text{amp. } \angle \quad (56)$$

$$\frac{dI}{dx} = -Vg \quad \frac{\text{amp.}}{\text{km.}} \angle \quad (57)$$

If we differentiate (55) and (57), each with respect to  $x$ , we obtain

$$\frac{d^2V}{dx^2} = -r \frac{dI}{dx} \quad \frac{\text{volts}}{\text{km.}^2} \angle \quad (58)$$

and

$$\frac{d^2I}{dx^2} = -g \frac{dV}{dx} \quad \frac{\text{amp.}}{\text{km.}^2} \angle \quad (59)$$

Substituting (57) in (58), and (55) in (59), we find

$$\frac{d^2V}{dx^2} = gr \cdot V \quad \frac{\text{volts}}{\text{km.}^2} \angle \quad (60)$$

and

$$\frac{d^2I}{dx^2} = gr \cdot I \quad \frac{\text{amp.}}{\text{km.}^2} \angle \quad (61)$$

**Solution of the Fundamental Differential Equation.**—Formulas (60) and (61) are of the general type of the standard linear second-order differential equation:

$$a_0 \frac{d^2 y}{dx^2} + a_1 \frac{dy}{dx} + a_2 y = 0$$

the general solution of which is:

$$y = C_1 \epsilon^{m_1 x} + C_2 \epsilon^{m_2 x}$$

where  $m_1$  and  $m_2$  are the two roots of the auxiliary equation:

$$a_0 m^2 + a_1 m + a_2 = 0$$

In this case,

$$a_0 = 1; a_1 = 0, a_2 = -rg$$

which leads to

$$m^2 - rg = 0$$

or

$$m_1 = +\sqrt{rg} \text{ and } m_2 = -\sqrt{rg}$$

Hence, the general solution of formula (60) is

$$V = C_1 \epsilon^{+\sqrt{rg}x} + C_2 \epsilon^{-\sqrt{rg}x} \quad \text{volts } \angle \quad (62)$$

with a similar expression for  $I$ .

If we substitute the attenuation constant  $\alpha$  for  $\sqrt{rg}$  by (36), the solution can be written:

$$V = C_1 \epsilon^{\alpha x} + C_2 \epsilon^{-\alpha x} \quad \text{volts } \angle \quad (63)$$

and by the use of (581) in Appendix A, substituting hyperbolic functions for exponentials, the solution becomes

$$V = (C_1 + C_2) \cosh \alpha x + (C_1 - C_2) \sinh \alpha x \quad \text{volts } \angle \quad (64)$$

We may now write

$$A_v \text{ for } (C_1 + C_2) \text{ and } B_v \text{ for } (C_1 - C_2),$$

thus obtaining the general solutions in the hyperbolic-function form

$$V = A_v \cosh \alpha x + B_v \sinh \alpha x \quad \text{volts } \angle \quad (65)$$

and likewise

$$I = A_i \cosh \alpha x + B_i \sinh \alpha x \quad \text{amperes } \angle \quad (66)$$

We shall see that in dealing with lines of indefinitely great length, or lines that are grounded at the receiving end through a surge-impedance load, formula (63) is the more convenient general solution, using exponentials; but, in the general case, formula (65) is the more convenient general solution, using hyperbolic functions. From this point of view, the hyperbolic

form (formula (65)) is the general solution, and the exponential form (63) a particular solution.

**Graphical Relations.**—Formulas (55) and (57) show that if we plot, for any d.c. case, the voltage and the current as ordinates, against the distance  $x$  as abscissas, in the manner indicated in Fig. 13, where  $V, V$  is the curve of potential and  $I, I$  the curve of current along the line, then if the gradients of these curves

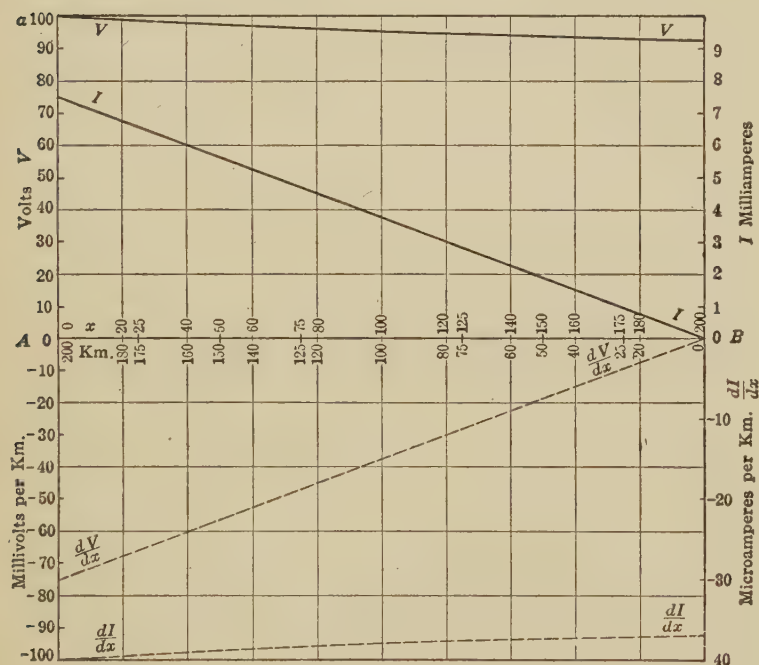


FIG. 13.—Graphs of potential and current and their gradients.

are plotted, as in the broken curves, the gradient of  $V$ , or  $dV/dx$ , is the same, when taken to a suitable scale of ordinates, as the  $I, I$  curve negatived, and similarly for the gradient of  $I$ . These relations must hold, in view of (55) and (57), whatever may be the terminal conditions of the line considered. Moreover, if we plot the gradient of the  $dV/dx$  curve, or  $d^2V/dx^2$ , we reproduce the  $V$  curve to a suitably selected scale, and if we plot the gradient of the  $dI/dx$  curve, or  $d^2I/dx^2$ , we reproduce the  $I$  curve to another particular scale.

In the case represented by Fig. 13, a single-wire uniform line of length  $L = 200$  km. (124.3 miles), is freed at the distant end, and connected at the home end  $x = 0$ , to a potential  $V_A = +100$  volts, supplied by a storage battery, whose negative pole is grounded. The linear constants of the line are  $r = 10$  ohms per wire km. (16.09 ohms per wire mile), and  $g = 0.4 \times 10^{-6}$  mho per wire km. ( $0.6436 \times 10^{-6}$  mho per wire mile). The total resistance of the conductor is thus 2,000 ohms, and the total leakance  $0.08 \times 10^{-3}$  mho, corresponding to a line angle  $\theta = 0.4$  hyp. radian, an attenuation constant  $\alpha = 0.002$  hyp. radian per km., and a surge resistance  $r_0 = 5,000$  ohms.

TABLE I

Particulars relating to a line of  $\theta = 0.4$  hyp. and  $r_0 = 5,000$  ohms freed at far end

$x$ km.	$L_2$ km.	$\theta_2$ hyps.	cosh $\theta_2$	sinh $\theta_2$	$V$ volts	$I$ amp.	$-\frac{dV}{dx}$ volts km.	$-\frac{dI}{dx}$ amp. km.	$\frac{d^2V}{dx^2}$ volts km. <sup>2</sup>	$\frac{d^2I}{dx^2}$ amp. km. <sup>2</sup>
0	200	0.40	1.08107	0.41075	100.000	$\times 10^{-3}$ 7.5990	$\times 10^{-3}$ 75.990	$\times 10^{-6}$ 40.000	$\times 10^{-6}$ 400.00	$\times 10^{-9}$ 30.396
25	175	0.35	1.06188	0.35719	98.225	6.6081	66.081	39.290	392.90	26.432
50	150	0.30	1.04534	0.30452	96.695	5.6337	56.337	38.678	386.78	22.535
75	125	0.25	1.03141	0.25261	95.406	4.6734	46.734	38.163	381.63	18.693
100	100	0.20	1.02007	0.20134	94.357	3.7247	37.247	37.743	377.43	14.899
125	75	0.15	1.01127	0.15056	93.543	2.7854	27.854	37.417	374.17	11.142
150	50	0.10	1.00500	0.10017	92.964	1.8531	18.531	37.185	371.85	7.412
175	25	0.05	1.00125	0.05002	92.616	0.9254	9.254	37.047	370.47	3.702
200	0	0.00	1.00000	0.00000	92.501	0.0000	0.000	37.000	370.00	0.000

The preceding table shows the values of the voltage, current, and their respective gradients, at various distances along the line. Distances  $x$  km. from the home end appear in the first column, with corresponding distances  $L_2$  from the far end, in the second column.

Figure 13 gives the graphs of the values contained in the last six columns. The voltage curve, or catenary  $VV$ , falls from 100 at  $A$ , to 92.501 at  $B$ . The descending or negative gradient,  $dV/dx$ , of  $V$ , is given by the broken ascending line marked  $dV/dx$ , which commences at  $-75.99$  millivolts per km. at  $A$ , and ends in zero at  $B$ . This curve is the image, or negative counterpart, of the



$I, I$  curve of current, which falls from 7.599 milliamp. at  $A$ , to zero at the open end  $B$ . The lowest and broken curve, marked  $dI/dx$ , is the graph of the gradient of  $I$  and is the image or negative counterpart of the  $V$  curve.

If we plot the values of  $d^2I/dx^2$  from the last column of Table I, in Fig. 13, *i.e.*, the gradient of  $dI/dx$ , we should reproduce the  $I, I$  current curve, provided that we take the full ordinate  $Aa$ , as  $40 \times 10^{-9}$  amp. per km.<sup>2</sup> Similarly, if we plot  $d^2V/dx^2$  from the preceding column of the table, or the gradient of  $dV/dx$ , we should reproduce the potential curve, provided that we take the full ordinate as 400 microvolts per km.<sup>2</sup>. The change of scale is represented by the factor  $gr$  in (60) and (61).

Expressing (55) and (57) in words, we may say that on any uniform c.c. line, in the steady state, whatever the terminal conditions may be, *the voltage and current at any point are always so related that the local gradient of the one is proportional to the local value of the other*. Moreover, including the disclosures of (60) and (61), at any point, the gradient of the gradient, or curvature, of the potential or the current, either one, is always proportional to the local value of the same. If the current  $I$ , say, falls in a certain distance to one-half, the gradient of the potential falls likewise to one-half, and the gradient of the gradient of  $I$  also falls to one-half, in the same distance. We shall see that corresponding conditions apply in the a.c. case.

**Overhead Aerial Lines with Their Multiple Segregated Leaks.** The type of cable conductor indicated in Fig. 12 may be regarded as having continuously distributed leakance, such as is contemplated and required in the reasoning of formulas (54) to (66). In the case of an overhead aerial-line conductor, such as a telegraph wire, supported on insulators, spaced say 25 to the kilometer, or 40 to the statute mile, it is evident that the leakance is no longer strictly continuous, but occurs in little lumps 40 m. apart, and that these individual leaks are usually far from being all alike. Actual tests, however, show that, except where faults or localized leak disturbances interfere with the law of averages, an aerial-line conductor normally behaves substantially as though it had strictly continuous leakance. In other words, the deviation from theory in the observed properties of a not very short line, due to *lumpiness*, is ordinarily insignificant, when the lumps of leakance are only a few dekameters apart.

**Primitive Equations, or Complete Solutions of the Fundamental Differential Equations.**—Formulas (65) and (66) are the general solutions of the essential and fundamental differential equations for  $V$  and  $I$  on a uniform line in the steady state. Taking (65),\*

$$V = A_v \cosh \alpha x + B_v \sinh \alpha x \quad \text{volts } \angle \quad (65)$$

$V$  is the potential at point  $x$ ; while  $A_v$  and  $B_v$  are the two arbitrary voltage constants.

We may also use the transformation of (580), Appendix A, and put

$$V = A'_v \cosh (\alpha x + \Delta') = A''_v \sinh (\alpha x + \Delta'') \quad \text{volts } \angle \quad (65a)$$

Either (65) or (65a) may be regarded as the complete solution of the fundamental differential formula (60), and, by differentiating either twice, we can obtain (60). In (65), we have  $V$  expressed as the sum of two hyperbolic functions, each involving an arbitrary or condition-satisfying coefficient. In (65a), we have  $V$  expressed as a single hyperbolic function with one arbitrary coefficient; but the hyperbolic angle includes another arbitrary constant, which is a condition-satisfying hyperbolic angle. In c.c. cases, there is usually but little choice between these two forms of the primitives (65) and (65a); but in a.c. cases, we shall see that (65a) is ordinarily the easier to compute with.

From the type identity of (60) and (61), we may infer that there is a corresponding pair of equivalent solutions of (61), namely,

$$I = A_i \cosh \alpha x + B_i \sinh \alpha x \quad \text{amp. } \angle \quad (67)$$

or

$$I = A'_i \cosh (\alpha x + \Delta_i) = A''_i \sinh (\alpha x + \Delta_{i'}) \quad \text{amp. } \angle \quad (68)$$

where  $I$  is the current at any point  $x$  along the line  $A_i$ ,  $B_i$ ,  $A'_i$ , and  $A''_i$  are condition-satisfying currents in amperes; while  $\Delta_i$  and  $\Delta_{i'}$  are condition-satisfying hyperbolic angles.

**Evaluation of the Arbitrary Constants in the Primitive Equations.**—The assignment of particular values to the arbitrary constants in the primitive formulas (65) and (66), in order to meet a given set of terminal conditions, ordinarily requires that both the current and the potential shall be given at one end of the line. If we consider a line  $AB$ , Fig. 14, we may suppose that  $A$  is the *generator end*, and  $B$  the *motor end* of the line; so that, in

\* O. HEAVISIDE, "Electromagnetic Theory," 1893, vol. i, p. 451.

the steady state, electrical energy shall flow from  $A$  to  $B$ . In order, therefore, to reduce the primitive formulas (65) and (66) to a definite arithmetical basis, we need, in general, to know either  $V_A$  and  $I_A$ , the potential and current at  $A$ ; or else  $V_B$  and  $I_B$ , the potential and current at  $B$ . While, theoretically, it would suffice to have one of these data from the  $A$  end, and the other from the  $B$  end, yet, from a practical standpoint, this would be an unlikely condition. Although two terminal data from one end, therefore, are sufficient for the evaluation of the two arbitrary constants, yet we shall see that if we know the terminal motor load, *i.e.*, the impedance at the receiving end  $B$ , only one other datum, say the potential or current at either  $A$  or  $B$ , is needed for the complete solution of the case.

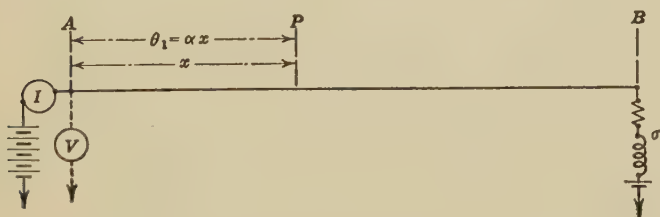


FIG. 14.—Line loaded at the motor end. The potential and current at the generator end are given.

**Evaluation from Data at the Generator End.**—Taking first the case where the  $A$ -end potential and entering current  $I_A$  are given, let  $AB$ , Fig. 14, be any uniform single-wire line, with an impressed potential of  $V_A$  volts at  $A$ , as observed by voltmeter  $V$ , and with any load whatever of  $\sigma$  ohms at  $B$ . By changing  $\sigma$ , this load may also contain any steady counter-e.m.f. Let the steady current entering the line at  $A$  observed on the ammeter  $I$  be  $I_A$  amp., then let the voltage be required at the point  $P$ , distant  $x$  km. from  $A$ . The uniform linear constants  $r$  and  $g$  of the line are supposed to be known; so that the linear angle  $\alpha$  hyp. radians per km. is found by (36). Then the angular distance of the position  $P$  from  $A$  is  $\theta_1 = \alpha x$  hyp. radians. We may therefore, write the primitive equation (65) in the form

$$V_P = A_v \cosh \theta_1 + B_v \sinh \theta_1 \quad \text{volts } \angle \quad (69)$$

Since the distance  $x$  is here quite arbitrary, we may assign to it the particular value  $x = 0$ , which means moving the point  $P$

up to the end  $A$ , where the potential is  $V_A$  volts by hypothesis, and the distance angle  $\theta_1 = 0$ ; so that we have

$$V_A = A_v \cosh 0 + B_v \sinh 0 \quad \text{volts } \angle \quad (70)$$

But  $\cosh 0 = 1$ , and  $\sinh 0 = 0$ ; so that  $A_v = V_A$ , and if this happens when  $x = 0$ , it is evident that it must happen in (69) for any value of  $x$ . Hence, rewriting (69),

$$\begin{aligned} V_P &= V_A \cosh \theta_1 + B_v \sinh \theta_1 \\ &= V_A \cosh \alpha x + B_v \sinh \alpha x \quad \text{volts } \angle \quad (71) \end{aligned}$$

If we differentiate (71) with respect to  $x$ , we have

$$\begin{aligned} \frac{dV_P}{dx} &= \alpha V_A \sinh \alpha x + \alpha B_v \cosh \alpha x \\ &= \alpha V_A \sinh \theta_1 + \alpha B_v \cosh \theta_1 \quad \frac{\text{volts}}{\text{km.}} \angle \quad (72) \end{aligned}$$

and substituting (55)

$$-I_P r = \alpha V_A \sinh \theta_1 + \alpha B_v \cosh \theta_1 \quad \frac{\text{volts}}{\text{km.}} \angle \quad (73)$$

where  $I_P$  is the current strength at the selected point  $P$ . If, as before, we move  $P$  up to  $A$ , so as to make  $x = 0$ , and  $\theta_1 = 0$ ,  $I_P$  becomes  $I_A$  and

$$\begin{aligned} -I_A r &= \alpha V_A \sinh 0 + \alpha B_v \cosh 0 \quad \frac{\text{volts}}{\text{km.}} \angle \quad (74) \\ -I_A r &= 0 + \alpha B_v \end{aligned}$$

whence

$$B_v = -I_A \frac{r}{\alpha} \quad \text{volts } \angle \quad (75)$$

or by (50)

$$= -I_A r_0 \quad \text{volts } \angle \quad (76)$$

or  $B_v$  is the drop in potential produced by the entering current in resistance equal to  $r_0$ ; so that rewriting (69), we have:

$$\begin{aligned} V_P &= V_A \cosh \theta_1 - I_A r_0 \sinh \theta_1 \\ &= V_A \cosh \alpha x - I_A r_0 \sinh \alpha x \quad \text{volts } \angle \quad (77) \end{aligned}$$

This formula expresses the potential  $V_P$  at any point  $P$ , along the line, distant  $\theta_1$  hyp. radians from the generator end, in terms of  $V_A$ ,  $I_A$ , and line constants.

Similarly, from (67), we have for the current in the line at the point  $P$ :

$$I_P = A_i \cosh \alpha x + B_i \sinh \alpha x = A_i \cosh \theta_1 + B_i \sinh \theta_1 \quad \text{amp. } \angle \quad (78)$$

Taking  $x = 0$ , and  $\theta_1 = 0$ , this places  $P$  at  $A$  and makes  $I_P = I_A$ ; so that

$$I_A = A_i \cosh 0 + B_i \sinh 0 \quad \text{amp. } \angle \quad (79)$$

whence

$$A_i = I_A \quad \text{amp. } \angle \quad (80)$$

a condition which must hold for all values of  $x$ , and rewriting (78), we obtain

$$I_P = I_A \cosh \alpha x + B_i \sinh \alpha x = I_A \cosh \theta_1 + B_i \sinh \theta_1 \quad \text{amp. } \angle \quad (81)$$

Differentiating with respect to  $x$ , it follows that:

$$\begin{aligned} \frac{dI_P}{dx} &= \alpha I_A \sinh \alpha x + \alpha B_i \cosh \alpha x \\ &= \alpha I_A \sinh \theta_1 + \alpha B_i \cosh \theta_1 \quad \frac{\text{amp.}}{\text{km.}} \angle \quad (82) \end{aligned}$$

and by (57)

$$-gV_P = \alpha I_A \sinh \theta_1 + \alpha B_i \cosh \theta_1 \quad \text{amp. } \angle \quad (83)$$

where  $V_P$  is the potential at the selected point  $P$ . If we move  $P$  to  $A$  so that  $x = 0$  and  $\theta_1 = 0$ ,  $V_P = V_A$ , and

$$\begin{aligned} -gV_A &= \alpha I_A \sinh 0 + \alpha B_i \cosh 0 \quad \text{amp. } \angle \quad (84) \\ &= 0 + \alpha B_i \end{aligned}$$

or

$$B_i = -\frac{g}{\alpha} V_A \quad \text{amp. } \angle \quad (85)$$

Substituting (51),

$$B_i = -\frac{V_A}{r_0} \quad \text{amp. } \angle \quad (86)$$

so that rewriting (78) and (81)

$$\begin{aligned} I_P &= I_A \cosh \alpha x - \frac{V_A}{r_0} \sinh \alpha x = I_A \cosh \alpha x - V_A g_0 \sinh \alpha x \\ &= I_A \cosh \theta_1 - \frac{V_A}{r_0} \sinh \theta_1 = I_A \cosh \theta_1 - V_A g_0 \sinh \theta_1 \\ &\quad \text{amp. } \angle \quad (87) \end{aligned}$$

This formula expresses the current strength  $I_P$  at any point  $P$  along the line, distant  $\theta_1$  hyp. radians from the generator end, in terms of  $V_A$ ,  $I_A$ , and line constants.

As an example, let us take the case of the line referred to in Table I and Fig. 14. Here the observed impressed terminal potential is  $V_A = 100$  volts, and the terminal entering current  $I_A = 7.599 \times 10^{-3}$  amp. The surge resistance of the line is

$r_0 = 5,000$  ohms. Then the potential at a point  $P$ , 50 km. from  $A$ , and, therefore, removed from  $A$  by an angular distance of 0.1 hyp. radian, is, by (77),

$$\begin{aligned} V_P &= 100 \cosh 0.1 - 7.599 \times 10^{-3} \times 5 \times 10^3 \times \sinh 0.1 \\ &= 100 \times 1.00500 - 37.995 \times 0.10017 \\ &= 100.500 - 3.806 = 96.694 \text{ volts.} \end{aligned}$$

The current strength at the same point is also, by (87)

$$\begin{aligned} I_P &= 7.599 \times 10^{-3} \cosh 0.1 - \frac{100}{5,000} \sinh 0.1 \\ &= 7.599 \times 10^{-3} \times 1.00500 - 0.020 \times 0.10017 \\ &= 7.637 \times 10^{-3} - 2.0034 \times 10^{-3} = 5.6336 \times 10^{-3} \text{ amp} \end{aligned}$$

The above values are in close conformity with those given in Table I, which were computed in a somewhat different way.

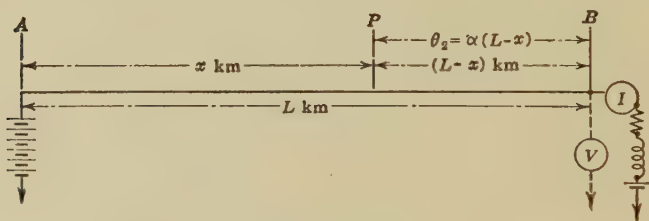


FIG. 15.—Line voltaged at  $A$  and loaded at  $B$ . The potential and current at the  $B$  end are observed.

**Evaluation from Data at the Motor End.**—If the potential and current are observed at the  $B$  end of the line,  $V_B$  and  $I_B$  respectively, as indicated in Fig. 15, then we may reckon the distance  $(L - x)$  km. from  $B$  toward  $A$ , and take

$$\theta_2 = (L - x)\alpha \quad \text{hyp. radians } \angle \quad (88)$$

as the hyperbolic angular distance of the point  $P$  from  $B$ .

We may then rewrite (65):

$$\begin{aligned} V_P &= A_v \cosh \alpha(L - x) + B_v \sinh \alpha(L - x) \\ &= A_v \cosh \theta_2 + B_v \sinh \theta_2 \quad \text{volts } \angle \quad (89) \end{aligned}$$

If now we bring the point  $P$  into coincidence with  $B$ , so that

$$x = L \text{ and } \theta_2 = 0, \quad V_P = V_B$$



and

$$\begin{aligned} V_B &= A_v \cosh 0 + B_v \sinh 0 && \text{volts } \angle \quad (90) \\ &= A_v + 0 \end{aligned}$$

or

$$A_v = V_B$$

We therefore rewrite (89):

$$\begin{aligned} V_P &= V_B \cosh \alpha(L - x) + B_v \sinh \alpha(L - x) \\ &= V_B \cosh \theta_2 + B_v \sinh \theta_2 && \text{volts } \angle \quad (91) \end{aligned}$$

If we differentiate this with respect to increasing  $x$ , we have, by (55),

$$\begin{aligned} \frac{dV_P}{dx} &= -V_B \alpha \sinh \alpha(L - x) - B_v \alpha \cosh \alpha(L - x) \\ &= -V_B \alpha \sinh \theta_2 - B_v \alpha \cosh \theta_2 = -I_P r \frac{\text{volts}}{\text{km.}} \angle \quad (92) \end{aligned}$$

Bringing  $P$  up to  $B$  once more, with  $\theta_2 = 0$ ,  $I_P = I_B$

$$\begin{aligned} V_B \alpha \sinh 0 + B_v \alpha \cosh 0 &= I_B r \frac{\text{volts}}{\text{km.}} \angle \quad (93) \\ 0 + B_v \alpha &= I_B r \end{aligned}$$

whence

$$B_v = I_B \frac{r}{\alpha} = I_B r_0 \quad \text{volts } \angle \quad (94)$$

Consequently, (65) becomes, in the general  $B$ -end case,

$$\begin{aligned} V_P &= V_B \cosh \alpha(L - x) + I_B r_0 \sinh \alpha(L - x) \\ &= V_B \cosh \theta_2 + I_B r_0 \sinh \theta_2 && \text{volts } \angle \quad (95) \end{aligned}$$

In particular, the sending-end voltage is

$$V_A = V_B \cosh \theta + I_B r_0 \sinh \theta \quad \text{volts } \angle \quad (95a)$$

Here the cosh term assigns the vector component of  $V_A$  necessary to maintain  $V_B$  at no load when  $I_B = 0$ ; while the sinh term assigns the additional vector component of  $V_A$  necessary to maintain the current  $I_B$  under the delivered e.m.f.  $V_B$ . Hence, at no load we have, on any line,

$$V_B = V_A / \cosh \theta = V_A \operatorname{sech} \theta \quad \text{volts } \angle \quad (95b)$$

Similarly, to find the current  $I_P$  we may rewrite (67), and, in the same way as before, obtain:

$$\begin{aligned} I_P &= I_B \cosh \theta_2 + \frac{V_B}{r_0} \sinh \theta_2 = I_B \cosh \theta_2 + V_B g_0 \sinh \theta_2 \\ &= I_B \cosh \alpha(L - x) + \frac{V_B}{r_0} \sinh \alpha(L - x) \quad \text{amp. } \angle \quad (96) \end{aligned}$$

As an example, we may consider the case represented in Fig. 16, of a line  $AB$ , 150 km. in length, with 100 volts impressed at  $A$ , and the  $B$  end grounded through a resistance  $\sigma = 1,000$  ohms. The linear constants are  $r = 4$  ohms per wire km. and  $g = 10^{-6}$  mho per wire km. To these correspond the values  $\alpha = 0.002$  hyp. per wire km.,  $\theta = 0.3$  hyp., and  $r_0 = 2,000$  ohms. In this case, the receiving-end potential  $V_B$  is 60.446 volts, and the receiving-end current  $I_B$  is 60.446 milliamp. Starting with these

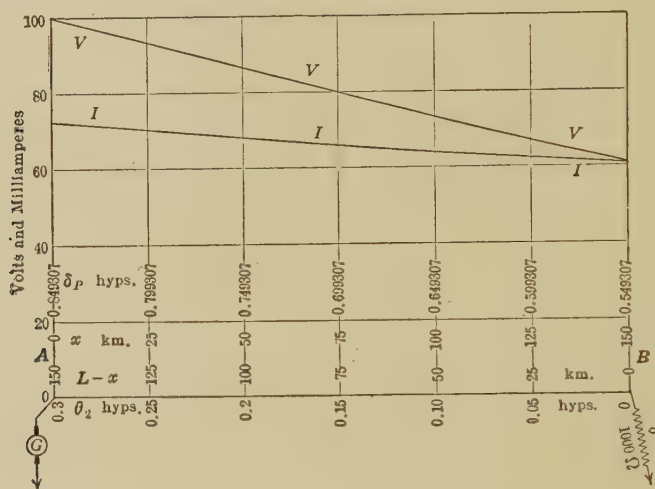


FIG. 16.—Case of a line with  $\theta = 0.3$  hyp. and  $r_0 = 2,000$  ohms, grounded at  $B$  through a resistance  $\sigma$  of 1,000 ohms and with an impressed potential of 100 volts at  $A$ .

data, and taking a point  $P$ , 50 km. from  $B$ ,  $\theta_2 = 0.1$  hyp. radian, we have by (95)

$$\begin{aligned} V_P &= 60.446 \cosh 0.1 + 60.446 \times 10^{-3} \times 2 \times 10^3 \sinh 0.1 \\ &= 60.446 \times 1.00500 + 120.892 \times 0.10017 \\ &= 60.748 + 12.109 = 72.857 \text{ volts} \end{aligned}$$

Similarly, by (96)

$$\begin{aligned} I_P &= 60.446 \times 10^{-3} \cosh 0.1 + \frac{60.446}{2,000} \sinh 0.1 \\ &= 60.446 \times 10^{-3} \times 1.00500 + 30.223 \times 10^{-3} \times 0.10017 \\ &= (60.748 + 3.027)10^{-3} = 63.775 \times 10^{-3} \text{ amp.} \end{aligned}$$

The distributions of potential and current over the line are given in Table II.

TABLE II

Particulars relating to a line  $AB$  of  $\theta = 0.3$  hyp. and  $r_0 = 2,000$  ohms grounded at  $B$  through  $\sigma = 1,000$  ohms, and with an impressed potential at  $A$  of 100 volts

I	II	III	IV	V	VI	VII	VIII	IX	X
$x$ km.	$L - x$ km.	$\theta_2$ hyps.	$\cosh \theta_2$	$\sinh \theta_2$	$V_P$ volts	$I_P$ amp.	$\delta_P =$ $\theta_2 + \theta'$ hyps.	$\cosh \delta_P$	$\sinh \delta_P$
						$\times 10^{-3}$			
0	150	0.30	1.04534	0.30452	100.000	72.390	0.84931	1.38287	0.95516
25	125	0.25	1.03141	0.25261	92.884	69.980	0.79931	1.33683	0.88719
50	100	0.20	1.02007	0.20134	85.998	67.743	0.74931	1.29411	0.82142
75	75	0.15	1.01127	0.15056	79.329	65.677	0.69931	1.25464	0.75771
100	50	0.10	1.00500	0.10017	72.857	63.775	0.64931	1.21831	0.69590
125	25	0.05	1.00125	0.05002	66.568	62.033	0.59931	1.18502	0.63583
150	0	0.00	1.00000	0.00000	60.446	60.446	0.54931	1.15470	0.57735

**Degradation to Ohm's Law in the Case of Negligible Leakage.**—If we take formulas (71), and (77) with (75), we have for the potential  $V_P$  at any point  $P$ ,

$$V_P = V_A \cosh L_1 \alpha - I_A r \frac{\sinh L_1 \alpha}{\alpha} \quad \text{volts } \angle \quad (97)$$

where  $\alpha = \sqrt{rg}$ , according to (36).

If, now, the linear leakage becomes extremely small, so that we may virtually take  $g = 0$ , it follows that  $\alpha = 0$ , and that  $L_1 \alpha = 0$ . Hence,

$$V_P = V_A \cosh 0 - I_A r \frac{\sinh L_1 \alpha}{\alpha} \quad \text{volts } \angle \quad (98)$$

We know from tables, or from elementary hyperbolic trigonometry, that  $\cosh 0 = 1$ , and it is evident from (545) of Appendix A, that

$$\sinh L_1 \alpha = L_1 \alpha + \frac{(L_1 \alpha)^3}{3!} + \frac{(L_1 \alpha)^5}{5!} + \dots \text{numeric } \angle \quad (99)$$

so that, when  $L_1 \alpha$  becomes indefinitely small,  $\sinh L_1 \alpha / \alpha$  tends to the limit  $L_1$ .

Formula (97) thus becomes, when

$$V_P = V_A - I_A L_1 r \quad \text{volts } \angle \quad (100)$$

which is the ordinary Ohm's law value of  $V_P$ , in terms of the terminal potential  $V_A$  and the  $IR$  drop from  $A$  to  $P$ .

Again, taking (87) and remembering that  $r_0 = \infty$  when  $g = 0$ , we obtain for the leakanceless condition:

$$I_P = I_A \cosh 0 - \frac{V_A}{\alpha} \sinh 0 \quad \text{amp. } \angle \quad (101)$$

$$= I_A \quad \text{amp. } \angle \quad (102)$$

which expresses the constancy of current along the line.

Similarly, taking (95) with (93), we have, when  $g = 0$ ,

$$V_P = V_B \cosh 0 + I_B r \frac{\sinh \alpha(L-x)}{\alpha} \quad \text{volts } \angle \quad (103)$$

$$= V_B + I_B r (L-x) \quad \text{volts } \angle \quad (104)$$

which is the corresponding Ohm's law value of  $V_P$  in terms of  $V_B$  and the  $IR$  drop from  $P$  to  $B$ . Formula (96) for current similarly degrades to

$$I_P = I_B \quad \text{amp. } \angle \quad (105)$$

**General Solution in Terms of Position Angles.**—If a line  $AB$ , having a surge resistance  $r_0$  (formula (43)), and subtending  $\theta$  hyp. radians in accordance with (35), is grounded at  $B$ , through a terminal impedance of  $\sigma$  ohms, and receives an impressed voltage at  $A$ , so that electrical energy flows in the steady state from  $A$  to  $B$ , then the series load, being devoid of lateral leakance, has no hyperbolic angle in itself, but the end  $B$  of the line, immediately connected thereto, acquires a hyperbolic *position angle*  $\delta_B$  of  $\theta'$  hyp. radians, defined by the condition:

$$\tanh \delta_B = \tanh \theta' = \frac{\sigma}{r_0} \quad \text{numeric } \angle \quad (106)$$

Having assigned the position angle  $\delta_B$  of the end  $B$  in this way, the position angle\* of the end  $A$  is:

$$\delta_A = \theta + \theta' = \theta + \delta_B \quad \text{hyps. } \angle \quad (107)$$

and at any intermediate point  $P$ , distant  $\theta_2$  hyps. from  $B$ , by (88), the position angle is:

$$\delta_P = \theta_2 + \theta' = \theta_2 + \delta_B \quad \text{hyps. } \angle \quad (108)$$

In words, *the position angle of a point  $P$ , distant  $\theta_2$  hyp. radians from the energy-receiving end  $B$ , is always found by adding to  $\theta_2$  the angle  $\delta_B$ , subtended at  $B$  by the terminal load  $\sigma$ . Position angles are of great importance in the electrical computations of steady-state lines, either with alternating or continuous currents.*

\* "On Electric Conducting Lines of Uniform Conductor and Insulation Resistance in the Steady State," by A. E. Kennelly, *Harvard Engineering Journal*, May, 1903, vol. ii, pp. 135-168.

**Formula for Potential in Terms of the Position Angle.**—The formula which expresses the potential at any point  $P$  of a line in terms of the position angle of  $P$ , belongs to the type of formula (65a), and may be derived by direct transformation either from (77) or from (95). We may proceed to obtain it from the latter.

$$V_P = V_B \cosh \theta_2 + I_B r_0 \sinh \theta_2 \quad \text{volts } \angle \quad (109)$$

$$= V_B \cosh \theta_2 + \frac{V_B}{\sigma} r_0 \sinh \theta_2 \quad \text{volts } \angle \quad (110)$$

$$= V_B \left( \cosh \theta_2 + \frac{r_0}{\sigma} \sinh \theta_2 \right) \quad \text{volts } \angle \quad (111)$$

and from (106) this is

$$V_P = V_B (\cosh \theta_2 + \coth \theta' \sinh \theta_2) \quad \text{volts } \angle \quad (112)$$

using (580) and (549), Appendix A,

$$= V_B \sqrt{\coth^2 \theta' - 1} \cdot \sinh (\theta_2 + \tanh^{-1} \tanh \theta') \quad \text{volts } \angle \quad (113)$$

$$= V_B \frac{1}{\sinh \theta'} \cdot \sinh (\theta_2 + \theta') \quad \text{volts } \angle \quad (114)$$

$$= V_B \frac{\sinh \delta_P}{\sinh \theta'} \quad \text{volts } \angle \quad (115)$$

and

$$\frac{V_P}{V_B} = \frac{\sinh \delta_P}{\sinh \delta_B} \quad \text{numeric } \angle \quad (116)$$

If we take  $P$  at  $A$ , where  $\delta_P = \delta_A = \theta + \theta'$

$$\frac{V_A}{V_B} = \frac{\sinh \delta_A}{\sinh \delta_B} \quad \text{numeric } \angle \quad (117)$$

and dividing (116) by (117),

$$\frac{V_P}{V_A} = \frac{\sinh \delta_P}{\sinh \delta_A} \quad \text{numeric } \angle \quad (118)$$

In general, if at any reference point  $C$  on the line, which may or may not be a terminal, we happen to know the potential  $V_C$ , and the position angle  $\delta_C$ , then the potential  $V_P$  at any other point  $P$  of the line having a position angle  $\delta_P$  is obtainable from

$$\frac{V_P}{V_C} = \frac{\sinh \delta_P}{\sinh \delta_C} \quad \text{numeric } \angle \quad (119)$$

which we can express in language, by saying that *the potentials of any and all points of a line are as the sines of the corresponding position angles*; so that, knowing the distribution of position

angle, and single observed potential surfaces for the determination of the correct potential distribution.

In the case where the line is grounded directly at  $E$ , or  $x = 0$ ,  $\delta_x = 0$ ,  $\delta_1 = \theta$ , and  $\delta_r = \theta_r$

In the case of a line fixed at  $E$ ,  $x = a$ ,  $I_s = \frac{V_s}{Z}$ , and (117) becomes by (576), Appendix A,

$$V_x = V_s \cosh \theta_x \quad \text{volts } \angle \quad (120)$$

and

$$V_x = \frac{V_s}{\cosh \theta} = V_s \operatorname{sech} \theta \quad \text{volts } \angle \quad (121)$$

As an example of (118), we may take the case presented in Fig. 16 and Table II, where  $r = 1,000$  ohms,  $a = 2,000$  ohms, and  $\tanh \theta = 0.5$ ; whence by tables,  $\theta = \theta_s = 1.1071487$  hyp. At a position  $P$ , 50 km. from  $E$ ,  $\theta_1 = 0.1$  hyp., and  $\theta_r = \theta_s + \theta_1 = 1.2071487$  hyp. The position angle at  $E$  where  $V_s = 100$  volts is  $I_s = s + \theta = 1.2071487$  hyp. Consequently,

$$\frac{V_x}{100} = \frac{\sinh 1.2071487}{\sinh 1.2071487} = \frac{0.86340}{0.93345} = 0.92477$$

or

$$V_x = 72.657 \text{ volts}$$

which checks with the solution obtained on page 36, using (85).

**Formula for Current in Terms of the Position Angle.** The formula which expresses the current strength in the line at any assigned point  $P$ , in terms of the position angle  $\theta$ , belongs to the type of formula (82), and may be derived by direct integration from either (57) or (56). We may select the latter,

$$I_x = I_s \cosh \theta_s + \int_{\theta_s}^{\theta} e^{\theta} \sinh \theta_s \quad \text{amp. } \angle \quad (122)$$

$$= I_s \left( \cosh \theta_s + \int_{\theta_s}^{\theta} \sinh \theta_s \right) \quad \text{amp. } \angle \quad (123)$$

$$= I_s \left( \cosh \theta_s + \tanh \theta \sinh \theta_s \right) \text{ by (106)} \quad \text{amp. } \angle \quad (124)$$

$$= I_s \sqrt{1 + \tanh^2 \theta} \cosh (\theta_s + \tanh^{-1} \tanh \theta) \text{ by (56)} \quad \text{amp. } \angle \quad (125)$$

$$= I_s \frac{1}{\cosh \theta} \cosh (\theta_s + \theta) \text{ by (56)} \quad \text{amp. } \angle \quad (126)$$

$$= I_s \frac{\cosh \delta_r}{\cosh \delta_s} \quad \text{amp. } \angle \quad (127)$$

$$\frac{I_x}{I_s} = \frac{\cosh \delta_r}{\cosh \delta_s} \quad \text{amplitude } \angle \quad (128)$$



If we move the point  $P$  up to  $A$ , where  $\delta_P = \delta_A = \theta + \theta'$ , and  $I_P = I_A$ ,

$$\frac{I_A}{I_B} = \frac{\cosh \delta_A}{\cosh \delta_B} \quad \text{numeric } \angle \quad (129)$$

Dividing (128) by (129)

$$\frac{I_P}{I_A} = \frac{\cosh \delta_P}{\cosh \delta_A} \quad \text{numeric } \angle \quad (130)$$

Finally, if at any datum point, say  $C$ , on the line, where the position angle is  $\delta_C$  and the current  $I_C$  are known, we obtain:

$$\frac{I_P}{I_C} = \frac{\cosh \delta_P}{\cosh \delta_C} \quad \text{numeric } \angle \quad (131)$$

In language, *the current strengths at any and all points along a line are as the cosines of the corresponding position angles.*

As an example, we may find the current at the point selected in the last case 50 km. from  $B$ , in the line shown at Fig. 16, where  $\delta_P = 0.649307$  hyp., the current at  $A$  being given as  $I_A = 72.3896 \times 10^{-3}$  amp.

Here

$$\frac{I_P}{72.3896 \times 10^{-3}} = \frac{\cosh 0.649307}{\cosh 0.849307} = \frac{1.21831}{1.38287} = 0.881003$$

or

$$I_P = 63.7754 \times 10^{-3} \text{ amp.}$$

In the particular case when the line is grounded at  $B$ , or  $\sigma = 0$ ,  $\theta' = 0$ , and  $\delta_B = 0$ , so that  $\delta_A = \theta$ , and  $\delta_P = \theta_2$ ; whence

$$\frac{I_P}{I_A} = \frac{\cosh \theta_2}{\cosh \theta} \quad \text{numeric } \angle \quad (130a)$$

**Case When  $\sigma > r_0$ .**—In the c.c. case, there is no difficulty in applying the position-angle formulas (119) and (131), so long as  $\sigma$  is distinctly less than  $r_0$ ; but in the opposite case, when the terminal load  $\sigma$  is distinctly greater than  $r_0$ , we are faced with the condition  $\theta' = \tanh^{-1} (\sigma/r_0)$ , or

$$\tanh \theta' = \frac{\sigma}{r_0} = k \quad \text{numeric } (132)$$

a number greater than unity, which is an impossible condition, so long as  $\theta'$ ,  $\sigma$ , and  $r_0$ , are all real quantities.

Table III gives the value of  $\tanh \theta$  and  $\coth \theta$  for various hyperbolic angles. Referring to columns I and II, it is clear that as  $\theta$  increases from 0 to  $\infty$ ,  $\tanh \theta$  increases from 0 to 1. If, however,

TABLE III  
Tangents and antitangents

I $\theta$	II $\tanh \theta$	III $\coth \theta$	IV $\theta$	V $\tanh \theta$	VI $\coth \theta$
0	0	$\infty$	$0 + j\frac{\pi}{2}$	$\infty$	0
0.5	0.4621	2.1640	$0.5 + j\frac{\pi}{2}$	2.1640	0.4621
1.0	0.7616	1.3130	$1.0 + j\frac{\pi}{2}$	1.3130	0.7616
1.5	0.9052	1.1048	$1.5 + j\frac{\pi}{2}$	1.1048	0.9052
2.0	0.9640	1.0373	$2.0 + j\frac{\pi}{2}$	1.0373	0.9640
2.5	0.9866	1.0136	$2.5 + j\frac{\pi}{2}$	1.0136	0.9866
3.0	0.9951	1.0050	$3.0 + j\frac{\pi}{2}$	1.0050	0.9951
...	.....	.....	.....	.....	.....
$\infty$	1.0000	1.0000	$\infty + j\frac{\pi}{2}$	1.0000	1.0000

we use formula (578), Appendix A, we obtain the entries in columns IV and V. That is, if we add  $j\frac{\pi}{2}$  to any real number its tangent is greater than unity, and is equal to the cotangent of that real number. Thus  $\tanh \left( 1.0 + j\frac{\pi}{2} \right) = 1.313 = \coth 1.0$ .

In fact, as we increase  $\theta$  from  $\left( 0 + j\frac{\pi}{2} \right)$  to  $\left( \infty + j\frac{\pi}{2} \right)$ , the tangent decreases from  $\infty$  to 1. The same conditions are indicated graphically in Fig. 17. In order to solve (106) for  $\theta'$  when  $\sigma/r_0$  exceeds unity, we have only to find in tables the real angle whose cotangent is equal to  $\sigma/r_0$ , and then add  $j\frac{\pi}{2}$  to that angle. Since  $\pi/2$ , in circular radians, is the same as  $90^\circ$ , or 1 circ. quadrant, it follows that any receiving-end load  $\sigma$  greater than the surge impedance  $r_0$  of the line involves position angles having an imaginary circular quadrant, of the type  $\delta_P = \delta'_P + j\frac{\pi}{2}$  hyps.

When we come to apply (119) to a line having a *super-surge-impedance load*, we must use formula (576), Appendix A, thus:

$$\frac{V_P}{V_C} = \frac{\sinh \delta_P}{\sinh \delta_C} = \frac{\sinh \left( \delta'_P + j\frac{\pi}{2} \right)}{\sinh \left( \delta'_C + j\frac{\pi}{2} \right)} = \frac{j \cosh \delta'_P}{j \cosh \delta'_C} = \frac{\cosh \delta'_P}{\cosh \delta'_C}$$

numeric (133)

Similarly (131) becomes by (577), Appendix A,

$$\frac{I_P}{I_C} = \frac{\cosh \delta_P}{\cosh \delta_C} = \frac{\cosh \left( \delta'_P + j\frac{\pi}{2} \right)}{\cosh \left( \delta'_C + j\frac{\pi}{2} \right)} = \frac{j \sinh \delta'_P}{j \sinh \delta'_C} = \frac{\sinh \delta'_P}{\sinh \delta'_C}$$

numeric (134)

TABLE IV

Particulars relating to a line  $AB$  of  $\theta = 0.3$  hyp., and  $r_0 = 2,000$  ohms, grounded at  $B$  through  $\sigma = 4,000$  ohms, and with an impressed potential at  $A$  of 100 volts

I $x$ km.	II $L - x$ km.	III $\theta_2$ hyp.	IV $\cosh \theta_2$	V $\sinh \theta_2$	VI $V_P$ volts	VII $I_P$ amp.	VIII $\delta_P = \theta_2 + \theta'$ hyp.	IX $\cosh \delta_P$	X $\sinh \delta_P$
						$\times 10^{-3}$		$\times j$	$\times j$
0	150	0.30	1.04534	0.30452	100.000	34.535	$0.849307 + j\frac{\pi}{2}$	0.95516	1.38287
25	125	0.25	1.03141	0.25261	96.671	32.078	$0.799307 + j\frac{\pi}{2}$	0.88719	1.33683
50	100	0.20	1.02007	0.20134	93.582	29.700	$0.749307 + j\frac{\pi}{2}$	0.82142	1.29411
75	75	0.15	1.01127	0.15056	90.727	27.396	$0.699307 + j\frac{\pi}{2}$	0.75771	1.25464
100	50	0.10	1.00500	0.10017	88.100	25.162	$0.649307 + j\frac{\pi}{2}$	0.69590	1.21831
125	25	0.05	1.00125	0.05002	85.693	22.990	$0.599307 + j\frac{\pi}{2}$	0.63583	1.18502
150	0	0.00	1.00000	0.00000	83.500	20.875	$0.549307 + j\frac{\pi}{2}$	0.57735	1.15470

The effect, therefore, of a super-surge-impedance load at  $B$  is to introduce imaginary quadrants into the position angles along the line, and to interchange the use of sines and cosines in the general formulas for potential and current, so far as relates to the real components of the position angles.

As an example, we may take the case of the line  $AB$  last considered (Table II and Fig. 16) with 100 volts at  $A$ , but grounded at  $B$ , Fig. 17, through  $\sigma = 4,000$  ohms. The numerical particulars of this case are represented in Table IV. Here  $\tanh \theta' = 4,000/2,000 = 2.0$ ; whence  $\theta' = 0.549307 + j\frac{\pi}{2}$  hyp. The posi-

tion angle at any point  $P$  is found by adding  $\theta_2$  for that point to  $\theta'$ . Such values are given in column VIII. The currents are then as the cosines and the potentials as the sines of these complex position angles, and are respectively as the sines and cosines of their real parts, as will be seen by comparing Tables II and IV. The values of  $V_P$  and  $I_P$  appear in columns VI and VII, respectively. They may also be computed from formulas (95) and (96), using the data of columns IV and V.

At the point  $x = 25$  km., or  $\theta_2 = 0.25$  hyp., the position angle  $\delta_P = 0.799307 + j\frac{\pi}{2}$ , and the potential, by (133), is

$$\begin{aligned} V_P &= 100 \times \frac{\sinh \left( 0.799307 + j\frac{\pi}{2} \right)}{\sinh \left( 0.849307 + j\frac{\pi}{2} \right)} \\ &= 100 \times \frac{\cosh 0.799307}{\cosh 0.849307} = 100 \times \frac{1.33683}{1.38287} \\ &= 96.671 \text{ volts} \end{aligned}$$

Again, since the current  $I_B$  at  $B$  is  $V_B/\sigma$  amp., the current at  $x = 25$  km. becomes, by formula (134)

$$\begin{aligned} I_P &= I_B \frac{\cosh \left( 0.799307 + j\frac{\pi}{2} \right)}{\cosh \left( 0.549307 + j\frac{\pi}{2} \right)} \\ &= 0.020875 \times \frac{j0.88719}{j0.57735} = 0.032078 \text{ amp.} \end{aligned}$$

It is remarkable that in a.c. cases, the question as to whether the terminal-load impedance is greater or less than the surge impedance, has no significance and, as we shall see, has never to be considered. In this respect, the a.c. case is easier to deal with than the c.c. case.

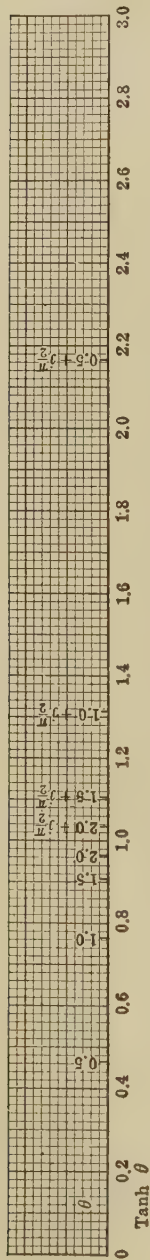


Fig. 17.—Value of real hyperbolic angles  $\theta$  and their corresponding tangents.

An alternative method for dealing with c.e. lines having super-surge-resistance loads, and without using complex position angles, is given in Appendix B.

**Case of  $\sigma = r_0$ . The Virtually Infinite Line.**—In the particular case when the load at the motor end has a resistance equal to the surge resistance of the line, the hyperbolic functions expressing the potential and current distributions reduce, as we shall see, to exponentials.

The position angle at  $B$  is then defined, by (106),

$$\tanh \theta' = \frac{r_0}{r_0} = 1 \quad \text{numeric} \quad (135)$$

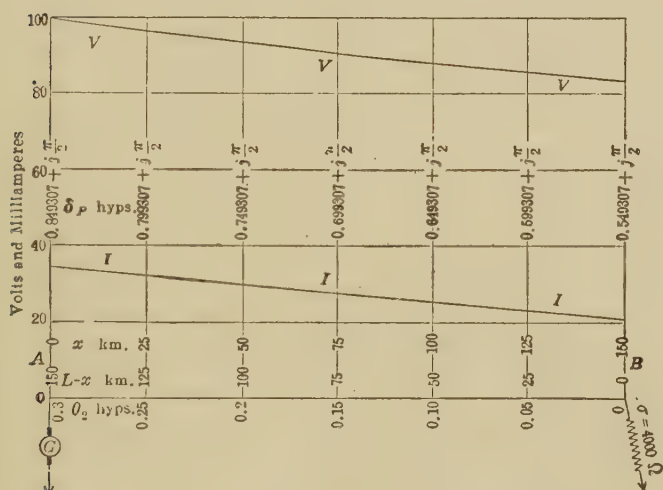


FIG. 18.—Case of a line with  $\theta = 0.3$  hyp. and  $r_0 = 2,000$  ohms grounded at  $B$  through a resistance  $\sigma$  of 4,000 ohms, and with an impressed potential of 100 volts at  $A$ .

the solution of which is  $\theta' = \alpha$ . Entering (118) with this value of  $\theta'$ , we have

$$\frac{V_P}{V_A} = \frac{\sinh \delta_P}{\sinh \delta_A} = \frac{\sinh (\theta_2 + \alpha)}{\sinh (\theta + \alpha)} \quad \text{numeric} \quad (136)$$

$$= \frac{\sinh \theta_2 \cosh \alpha + \cosh \theta_2 \sinh \alpha}{\sinh \theta \cosh \alpha + \cosh \theta \sinh \alpha} \quad \text{numeric} \quad (137)$$

But  $\sinh \alpha = \cosh \alpha$ , and we may assume that since the same infinity occurs in both numerator and denominator, we may divide throughout by  $\sinh \alpha$ ; so that

$$\frac{V_P}{V_A} = \frac{\sinh \theta_2 + \cosh \theta_2}{\sinh \theta + \cosh \theta} = \frac{\epsilon^{\theta_2}}{\epsilon^{\theta}} = \epsilon^{-(\theta - \theta_2)} = \epsilon^{-\theta_1} \text{ numeric } \angle \quad (138)$$

$$V_P = V_A \epsilon^{-\theta_1} = V_A \epsilon^{-L_1 \alpha} = V_A (\cosh \theta_1 - \sinh \theta_1) \text{ volts } \angle \quad (139)$$

It is evident that the potential falls from  $A$  toward  $B$  according to a simple exponential law. It also follows immediately from (117), that

$$V_P = V_B \epsilon^{\theta_2} = V_B \epsilon^{L_2 \alpha} = V_B (\cosh \theta_2 + \sinh \theta_2) \text{ volts } \angle \quad (140)$$

In particular,

$$V_B = V_A \epsilon^{-\theta} \text{ volts } \angle \quad (140a)$$

Similarly, the fundamental equation for current strength (130) becomes

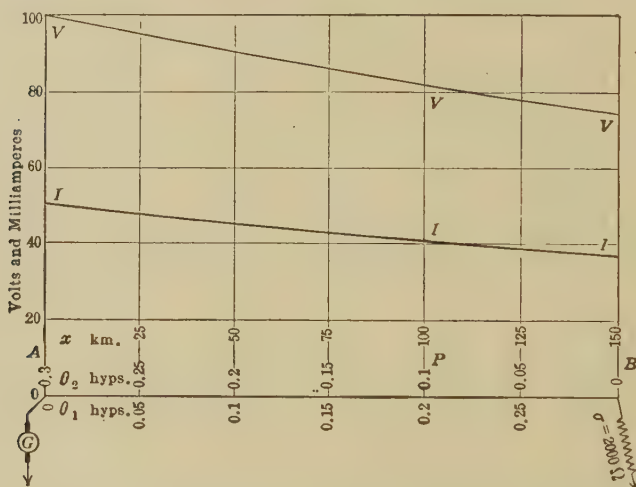


FIG. 19.—Case of a line with  $\theta = 0.3$  hyp. and  $r_0 = 2,000$  ohms grounded at  $B$  through a resistance  $\sigma = 2,000$  ohms and with an impressed potential of 100 volts at  $A$ . Exponential case.

$$I_P = I_A \epsilon^{-\theta_1} = I_A \epsilon^{-L_1 \alpha} = I_A (\cosh \theta_1 - \sinh \theta_1) \text{ amp. } \angle \quad (141)$$

$$= I_B \epsilon^{\theta_2} = I_B \epsilon^{L_2 \alpha} = I_B (\cosh \theta_2 + \sinh \theta_2) \text{ amp. } \angle \quad (142)$$

also

$$I_B = I_A \epsilon^{-\theta} \text{ amp. } \angle \quad (142a)$$

This type of simple exponential attenuation, peculiar either to an infinitely long line, or to a finite line which has been made virtually infinite, *i.e.*, to behave like a portion of an infinite line by surge-impedance loading at  $B$ , is called *normal attenuation*. The



normal attenuation factor of a line  $L$  km. long is  $\epsilon^{-L\alpha}$ . Both the potential and current on such a line undergo normal attenuation.

The power  $P_P$  delivered at an angular distance of  $\theta_1$  hyps. from  $A$  is  $P_A\epsilon^{-2\theta_1}$  watts. In particular, the power delivered at  $B$  is

$$P_B = P_A\epsilon^{-2\theta} \quad \text{watts} \quad (142b)$$

and the efficiency of the line is

$$\eta = \frac{P_B}{P_A} = \epsilon^{-2\theta} \quad \text{numeric} \quad (142c)$$

As an example, we may take the case of the line already considered ( $L = 150$  km.,  $\alpha = 0.002$  hyp./km.,  $\theta = 0.3$  hyp.,  $r_0 = 2,000$  ohms), and with an impressed potential of 100 volts at  $A$ . If this line is grounded at  $B$  through a surge-impedance load  $\sigma = r_0 = 2,000$  ohms, we find the conditions set forth in Table V and Fig. 19.

If we seek the potential at  $P$ , 100 km. from  $A$ , we have  $\theta_1 = 0.2$ ,  $\epsilon^{-\theta_1} = 0.818731$ , and  $V_P = 81.8731$  volts. The current at  $P$  is similarly  $50 \times 10^{-3} \times 0.818731 = 40.9866 \times 10^{-3}$  amps.

TABLE V

Particulars Relating to a Line  $AB$  of  $\theta = 0.3$  Hyp. and  $r_0 = 2,000$  Ohms Grounded at  $B$  Through  $\sigma = 2,000$  Ohms, and with an Impressed Potential at  $A$  of 100 Volts. Exponential Case. Virtually Infinite Line

$x$ km.	$\theta_1$ hyps.	$\theta_2$ hyps.	$\epsilon^{-\theta_1}$	$V_P$ volts	$I_P$ milliamp.	$\epsilon^{-2\theta_1}$	$P_P$ milliwatts
0	0.00	0.30	1.000000	100.0000	50.0000	1.000000	5.000000
25	0.05	0.25	0.951229	95.1229	47.5615	0.904837	4.524185
50	0.10	0.20	0.904837	90.4837	45.2419	0.818731	4.093655
75	0.15	0.15	0.860708	86.0708	43.0354	0.740818	3.704091
100	0.20	0.10	0.818731	81.8731	40.9866	0.670320	3.351600
125	0.25	0.05	0.778801	77.8801	38.9400	0.606531	3.032654
150	0.30	0.00	0.740818	74.0818	37.0409	0.548812	2.744058

**Single Values of Either Potential or Current Needed in Certain Cases.**—It has already been pointed out, in connection with formulas (65) to (69), that since the fundamental differential formula (60) for potential is of the second order, two condition-satisfying or arbitrary constants must be forthcoming, if a numerical solution is to be obtained. Similar conditions apply also

to solutions for current strength. In certain cases, however, only one such arbitrary constant is needed, when the conditions are such as to imply the second arbitrary constant. Thus, if a line  $AB$  is known to be grounded at  $B$ , this condition is equivalent to establishing one arbitrary constant; so that only one other arbitrary constant, such as a potential, or a current, needs to be given, in order to determine the complete distributions of voltage and current over the line, using (119) and (131), with  $\theta' = 0$ . The single necessary quantity to obtain the complete solutions may be either a potential or a current, at some particular point on the line. The potential at  $B$  is, however, in this case, an insufficient datum, because we know that this potential must be zero, and no new datum is provided by offering the gratuitous information that  $V_B = 0$ .

Similarly, if the line is freed at  $B$ , the same formulas (119) and (131) will serve to evaluate the complete distribution, if we remember that  $\theta' = j\frac{\pi}{2}$  hyps., and have one independent datum given, of a potential or a current at an assigned position.

Moreover, if the terminal load at  $B$  is given in the form of an actual or equivalent resistance  $\sigma$ , we know the terminal position angle  $\delta_B = \theta'$ , by (106), and can then evaluate the entire potential-current system from a single independent datum.

The transition from the potential to the current distribution, or *vice versa*, usually requires a knowledge of the impedance offered by the line, and this will be considered in the next chapter.

## CHAPTER V

### IMPEDANCE, ADMITTANCE, AND POWER OF A SMOOTH LINE AT ANY POINT

It is evident that, if we consider any line, having a steady-state distribution of potential and current, the ratio, at every point, of the potential to the current is equal, in the general case, to the impedance (in the d.c. case, to the resistance) of the line at and beyond that point, in the direction of the flow of energy. In other words, if at any point  $P$ , of a single line,  $AB$ , the potential with respect to ground is  $V_P$  volts, and the current is  $I_P$  amp., then their ratio  $V_P/I_P = R_P$  ohms. If the line were cut at the point  $P$ , and the end toward  $B$  were connected to a Wheatstone bridge or other resistance-measuring apparatus,  $R_P$  would be the resistance measured to ground, including the effects of the distributed conductor resistance, the distributed dielectric leakance, and the terminal load, if any, at  $B$ . Similarly, and reciprocally, the ratio  $I_P/V_P$  would be the admittance  $G_P$  in the general case (the conductance in the c.c. case) of the line, at and beyond  $P$ , as measured from  $P$  to ground.

If we divide (119) by (131), we obtain

$$\frac{R_P}{R_C} = \frac{\tanh \delta_P}{\tanh \delta_C} \quad \text{numeric } \angle \quad (143)$$

or, in words, *the impedance at and beyond any point of a line varies as the hyperbolic tangent of the position angle*. If we know the distribution of position angles and the impedance at any point  $C$ , such as the home end or the far end, then we can find at once the impedance offered at and beyond any or all other points of the line. Similarly, dividing (131) by (119) we have

$$\frac{G_P}{G_C} = \frac{\coth \delta_P}{\coth \delta_C} \quad \text{numeric } \angle \quad (144)$$

or *the line admittances are as the cotangents of the position angles*. Formulas (143) and (144) express general laws of smooth lines.

For example, consider the line of hyperbolic angle  $\delta = 0.3$  hyp. and  $r_0 = 2,000$  ohms, grounded at  $B$ , through 1,000 ohms,

as represented in Fig. 16. Table VI shows, in connection with Fig. 20, the values of  $x$ ,  $(L - x)$ ,  $\theta_2$ ,  $\delta_P$ ,  $\tanh \delta_P$ ,  $\coth \delta_P$ ,  $R_P$ , and  $G_P$ .

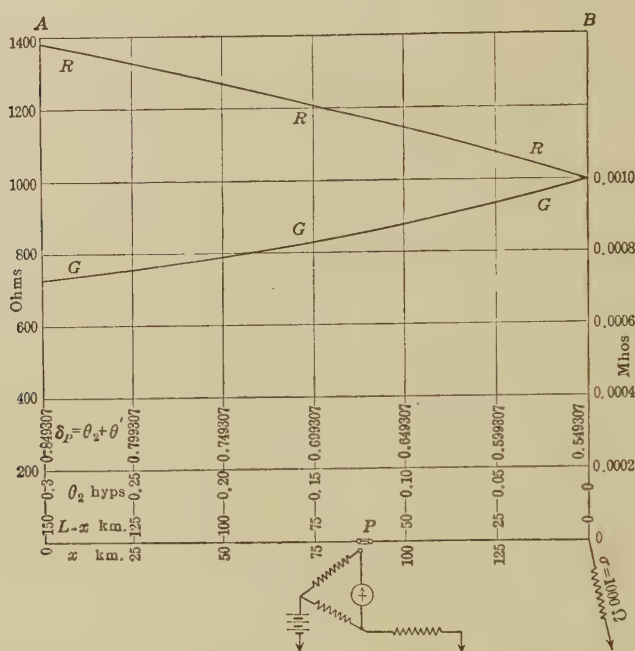


FIG. 20.—Diagram showing changes of resistance and conductance along the line  $AB$  of  $\theta = 0.3$  hyps. and  $r_0 = 2,000$  ohms, grounded at  $B$  through  $1,000$  ohms. A Wheatstone bridge is indicated as ready to connect to the section  $PB$  at  $P$ .

TABLE VI

Values of line resistance and conductance at various points along a line of  $\theta = 0.3$  hyps., and  $r_0 = 2,000$  ohms, grounded at  $B$  through  $\sigma = 1,000$  ohms

I $x$ km.	II $L - x$ km.	III $\theta_2$ hyps.	IV $\theta'$ hyps.	V $\delta_P =$ $\theta_2 + \theta'$ hyps.	VI $\tanh \delta_P$	VII $\coth \delta_P$	VIII $R_P$ ohms	IX $G_P$ mhos
0	150	0.30	0.549307	0.849307	0.69071	1.4478	1,381.4	$\times 10^{-3}$ 0.7239
25	125	0.25	.....	0.799307	0.66368	1.5068	1,327.4	0.7534
50	100	0.20	.....	0.749307	0.63473	1.5754	1,269.5	0.7877
75	75	0.15	.....	0.699307	0.60393	1.6559	1,207.9	0.8280
100	50	0.10	.....	0.649307	0.57121	1.7507	1,142.4	0.8754
125	25	0.05	.....	0.599307	0.53656	1.8637	1,073.1	0.9319
150	0	0.00	.....	0.549307	0.50000	2.0000	1,000.0	1.0000

Here the line resistance is 1,000 ohms at  $B$ , where  $\delta_B = 0.549307$  hyp.; so that entering (143) with these values of  $R_C$  and  $\delta_C$  respectively, we obtain the values recorded in column VIII. Similarly, entering (144) with  $G_C = 1.0 \times 10^{-3}$ , and  $\delta_C = 0.549307$  hyp., we obtain the values of line conductance recorded in column IX. Manifestly, the numerical values of  $R_P$  and  $G_P$ , at any point  $x$ , should be mutually reciprocal.

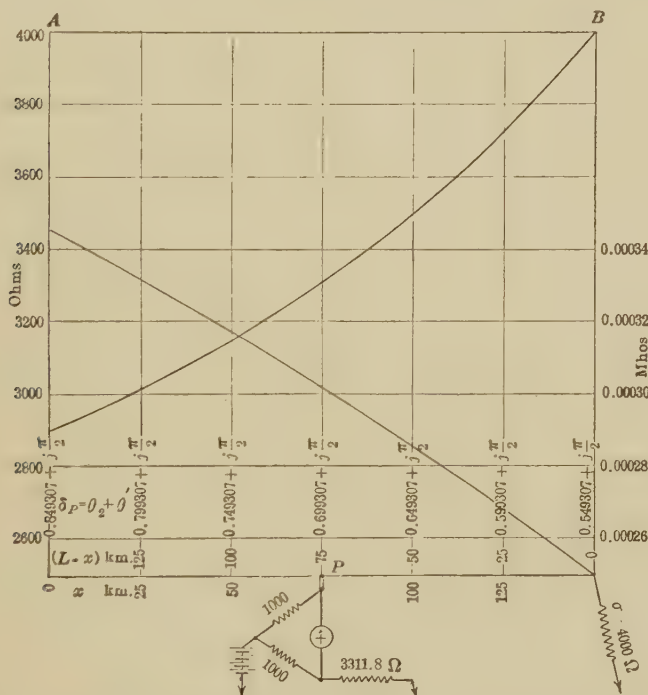


FIG. 21.—Diagram showing change of resistance and conductance along the line  $AB$  of  $\theta = 0.3$  hyp. and  $r_0 = 2,000$  ohms, grounded at  $B$  through 4,000 ohms. A Wheatstone bridge is indicated as connected to the section  $PB$  at  $P$ . Rising curve for resistance, falling curve conductance.

As another example, consider the same line grounded at  $B$  through the super-surge impedance of 4,000 ohms. In this case, as we have already seen, the position angles from  $B$  to  $A$  all contain one imaginary quadrant, or  $j_2^{\pi}$  radians. Referring to formula (578), Appendix A, it is to be observed that this extra imaginary quadrant virtually exchanges the tangent and cotangent of the real component. We thus obtain the values contained in Table VII and Fig. 21.

TABLE VII

Values of line resistance and conductance at various points along a line of  $\theta = 0.3$  hyp. and  $r_0 = 2,000$  ohms, grounded at  $B$  through  $\sigma = 4,000$  ohms

I $x$ km.	II $L - x$ km.	III $\theta_2$ hyps.	IV $\theta'$ hyps.	V $\delta_P = \theta_2 + \theta'$ hyps.	VI $\tanh \delta_P$	VII $\coth \delta_P$	VIII $R_P$ ohms	IX $G_P$ mhos $\times 10^{-3}$
0	150	0.30	$0.549307 + j\frac{\pi}{2}$	$0.849307 + j\frac{\pi}{2}$	1.4478	0.69071	2,895.6	0.34536
25	125	0.25	.....	$0.799307 + j\frac{\pi}{2}$	1.5068	0.66368	3,013.6	0.33184
50	100	0.20	.....	$0.749307 + j\frac{\pi}{2}$	1.5754	0.63473	3,150.8	0.31737
75	75	0.15	.....	$0.699307 + j\frac{\pi}{2}$	1.6559	0.60393	3,311.8	0.30196
100	50	0.10	.....	$0.649307 + j\frac{\pi}{2}$	1.7507	0.57121	3,501.4	0.28560
125	25	0.05	.....	$0.599307 + j\frac{\pi}{2}$	1.8637	0.53656	3,727.4	0.26828
150	0	0.00	.....	$0.549307 + j\frac{\pi}{2}$	2.0000	0.50000	4,000.0	0.25000

Taking Tables VI and VII together, as well as Figs. 20 and 21, we may safely conclude that when a line is grounded through an *infra-surge-resistance load* at the far end, the line resistance falls as we approach that end, while the line conductance reciprocally rises. On the other hand, when the line is grounded at the far end through a *super-surge-resistance load*, the line resistance rises as we approach that end; while the line conductance reciprocally falls. A glance at Table V will likewise show that in the intermediate case, when a line is grounded at the distant end through a *surge-resistance load*, the line resistance neither rises nor falls, but remains constant all along the line.

**Line Resistance in the Transient and Steady States.**—If we consider, as in Chapter XI, the transient building up of potential and current along a line prior to the establishment of the steady state, we find that any line having a surge impedance of  $r_0$  ohms, offers this resistance at any point to each single advancing electric wave in the unsteady state; so that if  $V_P$  is the instantaneous potential at point  $P$ , the instantaneous current in that wave is

$$I_P = \frac{V_P}{r_0} = V_P g_0 \quad \text{amp. } \angle \quad (145)$$

where  $g_0$  is the surge admittance, the reciprocal of the surge impedance. But any outgoing wave tends to be reflected, when



reaching the end of the line toward which it moves. After as many of these successive reflections have taken place as need to be taken into consideration when watching for the establishment of the steady state, the effect on the outgoing stream, of all the superposed reflections of current, is to change the resistance at any point of the line to

$$R_P = r_0 \tanh \delta_P \quad \text{ohms } \angle \quad (146)$$

or

$$G_P = g_0 \coth \delta_P \quad \text{mhos } \angle \quad (147)$$

so that the final current strength becomes

$$I_P = V_P G_P = V_P \cdot g_0 \cdot \coth \delta_P = \frac{V_P}{r_0 \tanh \delta_P} \text{ amp. } \angle \quad (148)$$

Here the factor  $\tanh \delta_P$  covers all the effects of reflected waves to infinity in number and time. If the line is so long that no reflected waves ever come back from the distant end, then the initial surge resistance  $r_0$  remains the final line resistance at any and every point, as in the case presented in Table V and Fig. 19.

**Sending-end Impedance.**—The line impedance at  $A$  the sending or generator end, in the steady state, whatever load there may be at the receiving or motor end, is called the sending-end impedance  $R_a^*$  and by (146), it is

$$R_A = r_0 \tanh \delta_A \quad \text{ohms } \angle \quad (149)$$

In the particular case when the line is grounded at the motor end, so that

$$\sigma = 0, \text{ and } \theta' = 0, \delta_A = \theta,$$

and

$$R_{ag} = r_0 \tanh \theta \quad \text{ohms } \angle \quad (150)$$

In the particular case when the line is freed at the motor end, so that

$$\sigma = \alpha, \text{ and } \theta' = j\frac{\pi}{2}, \quad \delta_A = \theta + j\frac{\pi}{2},$$

and

$$R_{af} = r_0 \coth \theta \quad \text{ohms } \angle \quad (151)$$

\* In a.c. cases, the sending-end impedances  $R_a$ ,  $R_{ag}$  and  $R_{af}$  become vector quantities logically denoted by the symbols  $Z_a$ ,  $Z_{ag}$ , and  $Z_{af}$ . We shall, however, continue to use the resistance symbols  $R_{ag}$  and  $R_{af}$  to denote the measured or measurable values from which the characteristic line- or net-constants  $\theta$  and  $z_0$  are derived.

**Receiving-end Impedance.**—The ratio of the potential  $V_A$  at the generator end to the current  $I_B$  at the motor end, is defined as the *receiving-end impedance*  $R_l$  (in the a.c. case  $Z_l$ )

$$R_l = \frac{V_A}{I_B} \quad \text{ohms } \angle \quad (152)$$

The receiving-end impedance is, therefore, the impedance which the line appears to offer to an observer of the current at the receiving end, who is informed of the voltage at the sending end.

Using formula (146), if the line is loaded at  $B$  with an impedance  $\sigma$ , such that  $\delta_B = \theta' = \tanh^{-1} (\sigma/r_0)$ ,

$$I_B = \frac{V_B}{r_0 \tanh \delta_B} = \frac{V_A}{\sinh \delta_A} \cdot \frac{\sinh \delta_B}{r_0 \tanh \delta_B} = \frac{V_A}{\sinh \delta_A} \cdot \frac{\cosh \delta_B}{r_0} \quad \text{amp. } \angle \quad (153)$$

and

$$R_l = \frac{V_A}{I_B} = \frac{r_0 \sinh \delta_A}{\cosh \delta_B} = \frac{r_0 \sinh (\theta + \theta')}{\cosh \theta'} \quad \text{ohms } \angle \quad (154)$$

$$= r_0 \sinh \theta + \sigma \cosh \theta \quad \text{ohms } \angle \quad (155)$$

In the particular case when the line is grounded directly at  $B$ ,  $\sigma = 0$ ,

$$R_l = r_0 \sinh \theta \quad \text{ohms } \angle \quad (156)$$

which is a simple but important formula. As an example, a line of  $\theta = 1.2$  hyps. and  $r_0 = 1,500$  ohms, is grounded at  $B$  through  $\sigma = 1,000$  ohms. The angle subtended by this load is  $\theta' = \tanh^{-1} (1,000/1,500) = 0.80472 = \delta_B$ . The receiving-end impedance, by (154), is then  $1,500 \sinh 2.00472 / \cosh 0.80472 = 1,500 \times 3.6446 / 1.34164 = 4,074.8$  ohms. By (155), it would be  $1,500 \sinh 1.2 + 1,000 \cosh 1.2 = 1,500 \times 1.50946 + 1,000 \times 1.81066 = 4,074.8$  ohms. The current strength at the receiving end from say 100 volts impressed at the sending end, would then be  $100/4,074.8 = 0.02454$  amp.

In the case where  $\sigma = r_0$ ,

$$R_l = r_0 e^{\theta} \quad \text{ohms } \angle \quad (156a)$$

**Sending-end Impedance in Terms  $\theta$ ,  $r_0$ , and  $\sigma$ .**—A useful expression for  $R_A$  when any load  $\sigma$  is connected at the distant end is obtained as follows:

$$V_B = I_B \sigma$$

by (77)

$$V_P = V_A \cosh \theta_1 - I_A r_0 \sinh \theta_1$$

If we let  $P$  move to  $B$ , we have

$$V_B = I_B \sigma = V_A \cosh \theta - I_A r_0 \sinh \theta \quad \text{volts } \angle \quad (157)$$

We also have, by (87),

$$I_B = I_A \cosh \theta - \frac{V_A}{r_0} \sinh \theta \quad \text{amperes } \angle \quad (158)$$

Multiplying formula (158) by  $\sigma$  and equating to formula (157)

$$I_A \sigma \cosh \theta - \frac{V_A \sigma}{r_0} \sinh \theta = V_A \cosh \theta - I_A r_0 \sinh \theta$$

Rearranging,

$$\begin{aligned} I_A (\sigma \cosh \theta + r_0 \sinh \theta) &= \frac{V_A}{r_0} (\sigma \sinh \theta + r_0 \cosh \theta) \\ R_A = \frac{V_A}{I_A} &= \frac{r_0 (\sigma \cosh \theta + r_0 \sinh \theta)}{\sigma \sinh \theta + r_0 \cosh \theta} \quad \text{ohms } \angle \quad (159) \end{aligned}$$

**Power in the Steady State at Any Point along the Line.**—If we know the potential  $V_P$  and current  $I_P$  at a point  $P$  on the line in the steady state, the power at the point, *i.e.*, the rate at which electrical energy is carried past  $P$  to the rest of the line beyond, is

$$P_P = V_P I_P \quad \text{volt-amp.} \quad (160)$$

and this is ordinarily the most convenient method of determining the power at  $P$ . We may, nevertheless, ascertain the power as a function of the position angle of a point on the line as follows: By (119) and (131)

$$\frac{P_P}{P_C} = \frac{V_P I_P}{V_C I_C} = \frac{\sinh \delta_P}{\sinh \delta_C} \cdot \frac{\cosh \delta_P}{\cosh \delta_C} = \frac{\sinh 2\delta_P}{\sinh 2\delta_C} \quad \text{numeric} \quad (161)$$

so that, in language, *the volt-amperes at any point vary as the sine of twice the position angle* (see formula (408) and (409)).

As an example, we may consider the line represented in Fig. 38, of  $\theta = 1.75868$  hyps. and  $r_0 = 1,436.1$  ohms, 100 km. long, and grounded at the far end through 750 ohms resistance. Having given that the distant-end potential is  $V_B = 11.931$  volts, and the distant-end current  $11.931/750 = 0.015908$  amp., with a delivered power of  $11.931 \times 0.015908 = 0.1898$  watt; also

that the distant-end position angle is  $\delta_c = 0.57941$  hyp., required the power at a point  $P$ , 20 km. from the distant end, where the position angle is 0.93114 hyp.

Here

$$\frac{P_P}{0.1898} = \frac{\sinh (2 \times 0.93114)}{\sinh (2 \times 0.57941)} = \frac{\sinh 1.86228}{\sinh 1.15882} = \frac{3.1416}{1.43615} = 2.1875$$

so that

$$P_P = 2.1875 \times 0.1898 = 0.4152 \text{ watt} \quad (162)$$

## CHAPTER VI

### EQUIVALENT CIRCUITS OF A SMOOTH LINE

A smooth real line, in the normal steady state, is assumed to have uniform linear leakance, such as might correspond to continuous leakance, *i.e.*, to an infinite number of uniformly distributed leaks, each indefinitely small; or to have some large number of uniformly distributed leaks, simulating the behavior of continuous leakance.

It can be shown\* that any such single c.c. real line may be replaced electrically, at its terminals, in any system of conductors, by a certain single *T-network*, consisting of a series or line resistance with a single resistance leak at its center, or by a certain single *II-network*, having two equal resistance leaks at the ends of the series resistance. The distributions of voltage, current, and power at and outside of the terminals of the smooth line will be the same as when the line is replaced by its equivalent *T* or *II*.

In the same way, any smooth a.c. line may be replaced by a certain single *T-network*, or by a certain corresponding single *II-network* of impedances; but the equivalence in this case is only complete at one particular frequency.

The equivalent *T*- and *II*-networks of a smooth line are *equivalent circuits* of that line, and reciprocally, the line is the *conjugate smooth line* of the *T*- and *II*-circuits.

Both the *T* and the *II* equivalent circuits of a smooth line have three elements of impedance. The *T* has two in series and one leak in shunt. The *II* has one in series and two leaks in shunt. It appears that no combination of less than three elements can, in general, be the equivalent of a smooth line. Combinations of more than three elements may, however, be assembled in indefinitely great numbers to form the equivalent circuits. For example, either the equivalent *T* or the equivalent *II* of the

\* "Artificial Lines for Continuous Currents in the Steady State," A. E. Kennelly, *Proc. Am. Acad. Arts Sciences*, November, 1908, vol. xlv, No. 4, pp. 97-130.

"The Application of Hyperbolic Functions to Electrical Engineering Problems," by A. E. Kennelly, Appendix D.

smooth line represented in Fig. 22 may be converted into a four-element equivalent circuit, in an infinity of different ways. Any one of such four-element equivalent circuits might again be converted into an equivalent five-element circuit, in an infinite variety of ways.

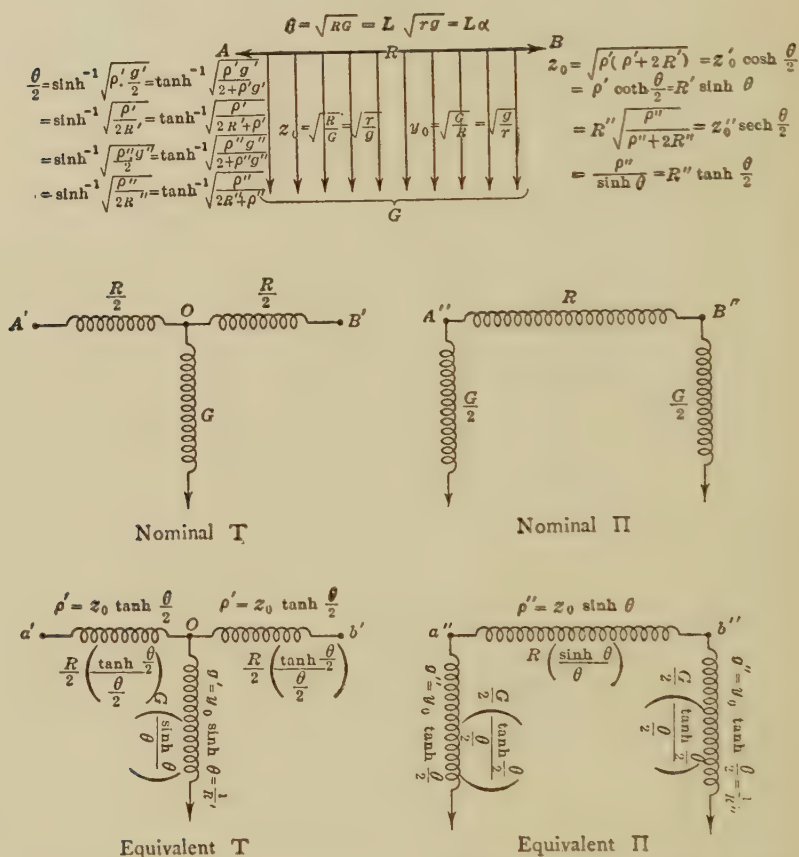


FIG. 22.—Relations between equivalent circuits and their conjugate smooth line.

**The Equivalent T.**—Figure 22 shows diagrammatically, at  $AB$ , a smooth line of conductor impedance  $R$  ohms  $\angle$ , and total leakage  $G$  mhos  $\angle$ . This line, therefore, possesses an angle of  $\theta$  hyps.  $\angle$ , and a surge impedance  $z_0$  ohms  $\angle$ , as well as its reciprocal, a surge admittance  $y_0$  mhos  $\angle$  (see formulas (35) and (43)).



At  $A'OB'$ , is the *nominal*  $T$  of the smooth line  $AB$ , i.e., a  $T$  section of impedances having in its elements the nominal values  $R$  and  $G$ . Thus, the impedance in the line section is  $R$  ohms  $\angle$ , and the leakance in the single central leak,  $G$  mhos  $\angle$ . This nominal  $T$  has a *lumpiness error*, and cannot correctly replace the smooth line. It is only a stepping stone to the "equivalent  $T$ ,"  $a'ob'$ , which can correctly replace the smooth line.\* The *correcting factor* for the line branches is

$$k_{\rho'} = \frac{\tanh \frac{\theta}{2}}{\theta/2} \quad \text{numeric } \angle \quad (163)$$

while the correcting factor for the staff leak is

$$k_{g'} = \frac{\sinh \theta}{\theta} \quad \text{numeric } \angle \quad (164)$$

Applying these factors to the respective elements of the nominal  $T$ , we find that each branch of the equivalent  $T$  has an impedance

$$\rho' = z_0 \tanh \frac{\theta}{2} \quad \text{ohms } \angle \quad (165)$$

while the staff of the equivalent  $T$  has an admittance

$$g' = y_0 \sinh \theta \quad \text{mhos } \angle \quad (166)$$

the impedance of the staff  $1/g'$  may be denoted by  $R'$ .

**The Equivalent II.**—The *nominal*  $\Pi$  of the smooth line  $AB$ , Fig. 22, is indicated at  $A''B''$ , the line element having the conductor impedance  $R$ , and each leak having half the line leakance  $G$ . *Lumpiness correction factors* must now be applied to these elements in order to produce the *equivalent*  $\Pi$ ,  $a''b''$ , which is capable of completely replacing, or of being substituted for, the smooth line  $AB$ , in any single-frequency steady state. The *correcting factor* for the line element is

$$k_{\rho''} = \frac{\sinh \theta}{\theta} \quad \text{numeric } \angle \quad (167)$$

and the correcting factor for each semi-leak is

$$k_{g''} = \frac{\tanh \frac{\theta}{2}}{\theta/2} \quad \text{numeric } \angle \quad (168)$$

\* For a demonstration of this proposition, see Appendix C.

It is evident that the correcting factors which convert the nominal  $\Pi$  into the equivalent  $\Pi$  of the conjugate smooth line, are the same as those which convert the nominal  $T$  into the equivalent  $T$ , but in inverse order, so that  $k_{p,,} = k_{g,,}$  and  $k_{g,,} = k_{p,,}$ .

The corrected elements in the equivalent  $\Pi$  are then found to be

$$\rho'' = z_0 \sinh \theta \quad \text{ohms } \angle \quad (169)$$

and

$$g'' = y_0 \tanh \frac{\theta}{2} \quad \text{mhos } \angle \quad (170)$$

The impedance of each leak  $1/g''$  may be denoted by  $R''$ .

**Relations between the Equivalent  $T$  and  $\Pi$ .**—It can be shown that having derived one of these two equivalent circuits of a smooth line, the other can be derived by direct computation.\* Thus, if the equivalent  $T$  is given, the equivalent  $\Pi$  can be directly computed, and will be found in agreement with the values given in (169) and (170). This is from the known equivalence and general substitutibility of a star and a delta of impedances,† so that one can be replaced by the other in any single-frequency steady electrical system, without disturbing the potentials, currents, or powers in the rest of the system.‡

When  $\theta$  becomes indefinitely small, both the correcting factors  $\frac{\sinh \theta}{\theta}$  and  $\frac{\tanh (\theta/2)}{(\theta/2)}$  become unity. This means that when a smooth line is extremely short, its nominal  $T$  or  $\Pi$  is also its equivalent  $T$  or  $\Pi$ , which is indeed an almost self-evident proposition.

When  $\theta$  is large and real,  $\frac{\sinh \theta}{\theta}$  becomes large with respect to unity; while  $\frac{\tanh (\theta/2)}{(\theta/2)}$  becomes small with respect to unity.

In a.c. cases, with  $\theta$  complex, both these correcting factors are capable of rapid oscillations in value, as  $\theta$  changes.

In all c.c. cases, the equivalent  $T$  and  $\Pi$  are always physically realizable. That is, their elements are always resistances, which

\* "The Application of Hyperbolic Functions to Electrical Engineering Problems," by A. E. Kennelly, London University Press, 1912, Appendix E.

† "The Equivalence of Triangles and Three-pointed Stars in Conducting Networks," by A. E. Kennelly, *Electrical World and Engineer* N. Y., Sept. 16 1899, vol. xxxiv, No. 12, pp. 413-414.

‡ "The Distribution of Voltage and Current in Closed Conducting Networks," by Feldmann and Herzog, *Proc. Intern. Elec. Cong.*, St. Louis, 1904, vol. ii, section E, pp. 689-709.

are capable of being designed and constructed. In a.c. cases, however, it frequently happens that either the equivalent  $T$ , or the equivalent  $\Pi$ , is physically unrealizable, and sometimes both. That is to say, the values of impedance called for in the respective elements may have slopes greater than  $90^\circ$ , and therefore cannot be reproduced in simple series groups of resistors, reactors, and condensers. Such cases may be regarded as *arithmetical equivalent circuits*, but not as *physical equivalent circuits*.

A smooth line, its equivalent  $T$ , and its equivalent  $\Pi$ , all possess the same angle  $\theta$  hyps.  $\angle$ , and the same characteristic or surge impedance  $z_0$  ohms  $\angle$ . Thus, in Fig. 24, each of the three conductors  $AB$ ,  $a'b'$ , and  $a''b''$  possesses or subtends between those terminals an angle of  $\theta = 0.6$  hyp., and a characteristic or surge resistance  $r_0 = 2,000$  ohms.

**Reversion from a T or  $\Pi$  Section to Its Conjugate Smooth Line.**—Having given a  $T$ -section or a  $\Pi$ -section, there must be some conjugate smooth-line equivalent thereto, and it becomes requisite to know the angle  $\theta$  subtended by the section as well as its surge impedance  $z_0$  or admittance  $y_0$ . This is the problem that presents itself in the use of any given artificial line. It is called the *reversion to the conjugate smooth line*.

Reversion, as the name implies, calls for the reversal of the procedure which determines an equivalent circuit from its conjugate smooth line.

Considering the equivalent  $T$   $a'Ob'$  of Fig. 22, each arm  $\rho'$  is defined by (165); while the staff leak  $g'$  is defined by (166). Multiplying together (165) and (166), we obtain

$$\rho'g' = \tanh \frac{\theta}{2} \sinh \theta \quad \text{numeric } \angle \quad (171)$$

Substituting for  $\tanh (\theta/2)$  its value  $\frac{(\cosh \theta - 1)}{\sinh \theta}$ , as in

Appendix A (formula (564)), we obtain the *versed-sine product*

$$\rho'g' = \cosh \theta - 1 = \text{versh } \theta \quad \text{numeric } \angle \quad (172)$$

and

$$\cosh \theta = 1 + \rho'g' \quad \text{numeric } \angle \quad (173)$$

$$= 1 + \frac{\rho'}{R'} = \frac{R' + \rho'}{R'} \quad \text{numeric } \angle \quad (174)$$

Again, from (171), using (558), Appendix A, we have

$$\rho'g' = 2 \sinh^2 \left( \frac{\theta}{2} \right) \quad \text{numeric } \angle \quad (175)$$

or

$$\sinh \left( \frac{\theta}{2} \right) = \pm \sqrt{\frac{\rho'g'}{2}} = \pm \sqrt{\frac{2\rho'g'}{4}} \quad \text{numeric } \angle \quad (176)$$

$$= \pm \sqrt{\frac{2\rho'}{4R'}} = \pm \frac{1}{2} \sqrt{\frac{2\rho'}{R'}} \quad \text{numeric } \angle \quad (177)$$

In all these expressions, the upper or positive sign of the radical presents itself for adoption.

Also, from (177) using (173) and (564) Appendix A, we obtain:

$$\tanh \left( \frac{\theta}{2} \right) = \pm \sqrt{\frac{\rho'g'}{2 + \rho'g'}} = \pm \sqrt{\frac{\rho'}{2R' + \rho'}} \quad \text{numeric } \angle \quad (178)$$

Finally, from (176) and (178)

$$\cosh \left( \frac{\theta}{2} \right) = \pm \sqrt{\frac{2 + \rho'g'}{2}} = \pm \sqrt{\frac{\rho' + 2R'}{2R'}} \quad \text{numeric } \angle \quad (179)$$

Thus knowing  $\rho'$  and  $R'$  for any equivalent  $T$ , the value of its line angle  $\theta$  can be determined.

From the fundamental definition of  $z_0$  in formula (46)

$$Z_f = \rho' + R', \quad Z_o = \rho' + \frac{R'\rho'}{R' + \rho'}, \quad z_0 = \sqrt{\rho'(\rho' + 2R')}$$

Using (178), (171) and (179),

$$z_0 = \rho' \coth \frac{\theta}{2} = R' \sinh \theta = \sqrt{\frac{2\rho'}{g'}} \cdot \cosh \frac{\theta}{2} \quad \text{ohms } \angle \quad (180)$$

These values of  $\theta$  and  $z_0$  pertain alike to the conjugate smooth line, the equivalent  $T$ , and the corresponding equivalent II.

**Reversion from a II to Its Conjugate Smooth Line.**—If we multiply formula (169) and (170), we obtain:

$$\rho''g'' = \frac{\rho''}{R''} = \sinh \theta \cdot \tanh \frac{\theta}{2} \quad \text{numeric } \angle \quad (181)$$

where  $\rho''$  is the architrave impedance of the II and  $g''$  the admittance of either of the two pillar leaks. Substituting for  $\tanh (\theta/2)$  from formula (564), Appendix A, we have:

$$\rho''g'' = \frac{\rho''}{R''} = \cosh \theta - 1 = \text{versh } \theta \quad \text{numeric } \angle \quad (182)$$

or

$$\cosh \theta = 1 + \rho'' g'' = \frac{R'' + \rho''}{R''} = \frac{\nu + g''}{\nu} \quad \text{numeric } \angle \quad (183)$$

where  $\nu$  is the architrave admittance or  $1/\rho''$  mhos  $\angle$ .

Again, from (182), using formula (562), Appendix A,

$$\rho'' g'' = \frac{\rho''}{R''} = 2 \sinh^2 \left( \frac{\theta}{2} \right) \quad \text{numeric } \angle \quad (184)$$

and

$$\sinh \left( \frac{\theta}{2} \right) = \pm \sqrt{\frac{\rho'' g''}{2}} = \pm \sqrt{\frac{\rho''}{2R''}} = \pm \sqrt{\frac{g''}{2\nu}} \quad \text{numeric } \angle \quad (185)$$

also from (563)

$$\cosh \left( \frac{\theta}{2} \right) = \pm \sqrt{\frac{2 + \rho'' g''}{2}} = \pm \sqrt{\frac{2R'' + \rho''}{2R''}} = \pm \sqrt{\frac{g'' + 2\nu}{2\nu}} \quad \text{numeric } \angle \quad (186)$$

or by (564),

$$\tanh \left( \frac{\theta}{2} \right) = \pm \sqrt{\frac{\rho'' g''}{2 + \rho'' g''}} = \pm \sqrt{\frac{\rho''}{2R'' + \rho''}} = \pm \sqrt{\frac{g''}{g'' + 2\nu}} \quad \text{numeric } \angle \quad (187)$$

The positive signs of these radicals claim adoption.

From the fundamental definition of  $z_0$  in formula (46) and from (187), (181), and, (186),

$$\begin{aligned} z_0 &= R'' \sqrt{\frac{\rho''}{\rho'' + 2R''}} = R'' \tanh \frac{\theta}{2} = \frac{\rho''}{\sinh \theta} \\ &= \sqrt{\frac{\rho''}{2g''}} \cdot \operatorname{sech} \frac{\theta}{2} = z_0'' \operatorname{sech} \frac{\theta}{2} \quad \text{ohms } \angle \quad (188) \end{aligned}$$

**General Relations in Reversion.**—It can be shown that just as there is one and only one  $T$  and  $\Pi$  which can replace a given smooth line at any one frequency, so, conversely, for the c.c. case, there is one and only one smooth line which can replace a given  $T$  or a given  $\Pi$ . It frequently happens, however, that the conjugate smooth line so determined cannot be physically realized. In other words, the conjugate smooth lines of some  $T$ 's and  $\Pi$ 's are only arithmetically realizable.

**Example of Equivalent Circuits.**—A convincing numerical example of the substitutibility of an equivalent  $T$  or  $\Pi$  for its

conjugate smooth line, is furnished by the case of a d.c. line voltaged at both ends.

Figure 23 represents the case of a line  $AB$ , 200 km. long, having a linear resistance  $r = 6$ , and a linear leakance  $g = 1.5 \times 10^{-6}$ ; so that its total conductor resistance is 1,200 ohms and its total dielectric leakance  $0.3 \times 10^{-3}$  mho; hence its line angle  $\theta = 0.6$  hyp., its linear angle  $\alpha = 0.003$  hyp. per km., and its surge impedance  $r_0 = 2,000$  ohms. The line has a potential of +100 volts applied at  $A$ , and a potential of +90 volts applied at  $B$ , so that the two batteries oppose each other. In such a case,

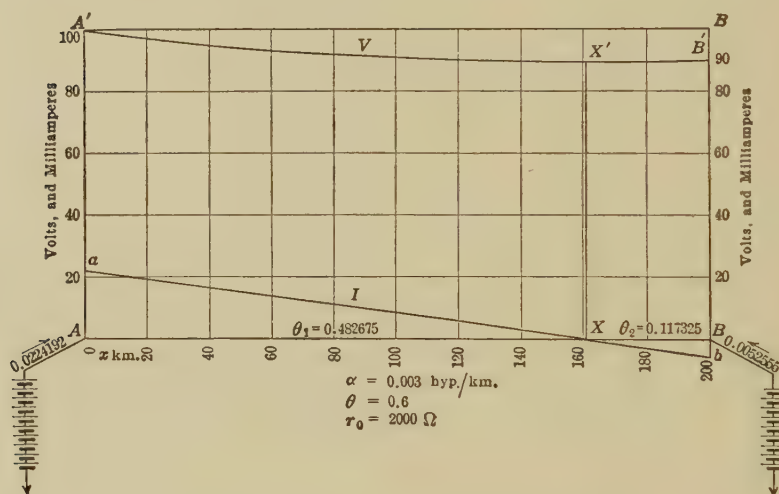


FIG. 23.—Smooth line voltaged at both ends.

provided that the two impressed terminal potentials are not too far apart, there will be a point of minimum potential somewhere on the line. Let  $x$  be the distance of this point in kilometers from  $A$ , and  $\theta_1$  the corresponding distance in angle. Since there can be no current at the point of minimum voltage, by (95b) the potential at this minimum point  $X$  will be:

$$V_X = \frac{V_A}{\cosh \theta_1} = \frac{V_A}{\cosh \alpha x} \quad \text{volts} \quad (189)$$

This will be the same potential as is established over  $L - x$  kilometers from  $B$ , or

$$V_X = \frac{V_B}{\cosh \theta_2} = \frac{V_B}{\cosh \alpha(L - x)} \quad \text{volts} \quad (190)$$



Solving formulas (189) and (190) for  $x$  and  $V_x$ , we obtain:

$x = 160.892$  km.,  $L - x = 39.108$  km.,  $\theta_1 = 0.482675$  hyp.,  $\theta_2 = 0.117325$  hyp., and  $V_x = 89.384$  volts. The fall of potential is indicated in Fig. 23 by the catenary curve  $A'VX'B'$ , with its minimum at  $X'$ . For electrical purposes, the line may

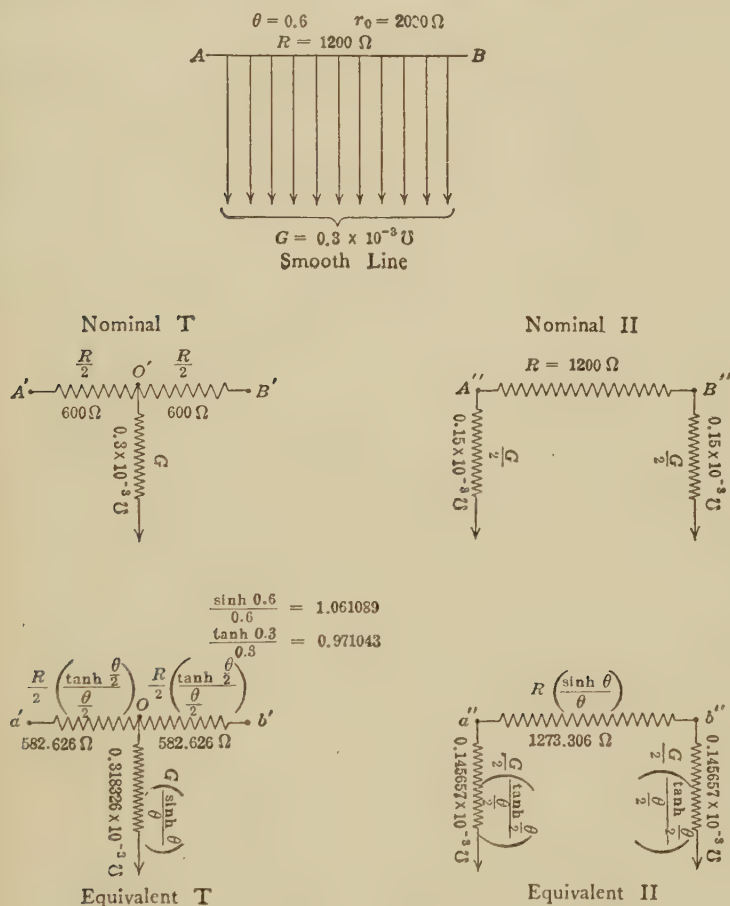


FIG. 24.—Equivalent circuits of a line with  $\theta = 0.6$ ,  $r_0 = 2,000$  ohms.

now be regarded as cut at  $X$ , because no current can flow at this point. The entering current at  $A$ , using (151), with  $\theta = \theta_1$ , is then found to be  $0.0224192$  amp, and at  $B$ ,  $0.0052555$  amp. The curve  $aIXb$  indicates the strength of current along the line, current flowing toward  $B$  being taken as plus.

Incidentally, it may be pointed out that if we know the potential and current at  $B$ , the case may be readily worked out by the use of position angles, as described in Chapter IV. Thus with  $V_B = 90$ , and  $I_B = -0.005\ 2555$ , the line is virtually grounded at  $B$  through a negative resistance  $\sigma = 90/-0.005\ 2555 =$

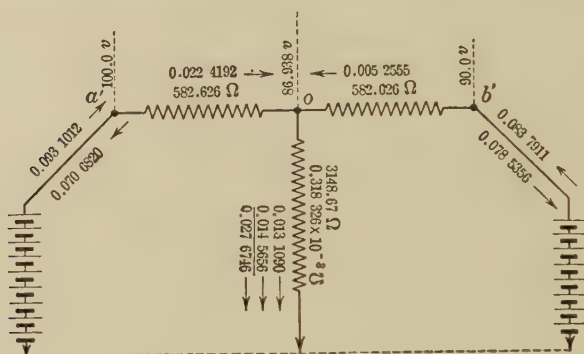


FIG. 25.

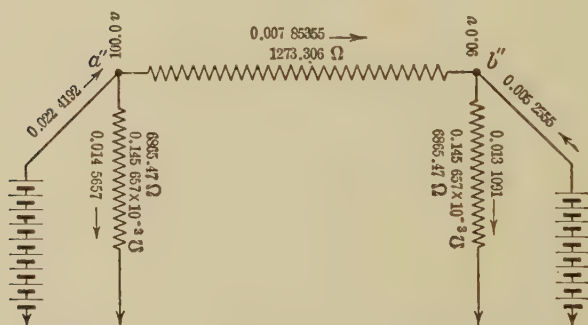


FIG. 26.

FIGS. 25 and 26.—Equivalent circuits of smooth line in Fig. 24, voltage at both ends.

— 17,125 ohms. This *virtual resistance* subtends an angle  $\tanh^{-1}$   $(-17,125/2,000) = \tanh^{-1} (-8.5625) = -0.117325 + j\frac{\pi}{2}$ ; so that  $\delta_x = j\frac{\pi}{2}$ , and  $\delta_A = 0.482675 + j\frac{\pi}{2}$ . The potentials, currents, impedances, and admittances now follow respectively the sines, cosines, tangents, and cotangents of the position angles all along the line, as already described.

Figure 24 shows at  $AB$  a diagram of the smooth line considered. At  $A'OB'$  is its nominal  $T$ , and at  $A''B''$ , its nominal  $\Pi$ . The lumpiness correcting factors are seen to be 1.061089 and 0.971043. Using these factors, the equivalent  $T$  is indicated at  $a'ob'$ , and the equivalent  $\Pi$  at  $a''b''$ . In the equivalent  $T$ , the total line resistance and leakance are 1,165.252 ohms and 0.318326 millimho. In the equivalent  $\Pi$ , the corresponding values are 1,273.306 ohms and 0.291314 millimho.

These equivalent circuits are shown, in Figs. 25 and 26, connected to 100 volts at the  $A$  end, and 90 volts at the  $B$  end. The equivalent  $T$  line is at  $a'ob'$ , in Fig. 25, and the equivalent  $\Pi$  line is at  $a''b''$ , in Fig. 26. Considering the equivalent  $T$ , if the  $A$  battery acted alone, with the  $B$  end grounded, the current entering at  $A$  would, by Ohm's law computation, be 0.093, 1012 amp., splitting at  $O$  into 0.078 5356 and 0.014 5656 amp. Similarly, if the  $B$  battery acted alone, with the  $A$  end grounded, the current entering at  $B$  would be 0.083 7911 amp., splitting at  $O$  into 0.070 6820 and 0.013 1090 amp. Now applying both batteries as shown, the summation current distribution gives 0.022 4192 amp. preponderating at  $a'$ , 0.005 2555 amp. at  $b'$ , and 0.027 6746 amp. through the leak to ground. The two entering line currents agree with those indicated in Fig. 23, as obtained by smooth-line formulas.

Turning to the equivalent  $\Pi$ ,  $a''b''$ , it is evident that 100 volts acting at  $a''$ , through the leak of 0.145 657 millimho, produces a leak current of 14.5657 milliamp. Similarly, 90 volts acting at  $b''$ , through the leak of 0.145 657 millimho, produces a leak current of 13.109 milliamp. The potential difference of 10 volts, between  $a''$  and  $b''$ , acting through 1,273.306 ohms, produces a current in the *architrave* of 7.853 55 milliamp. The total entering current at  $a''$  is thus 22.4192 milliamp., and at  $b''$ , 5.2555 milliamp., again in agreement with the values obtained in Fig. 23.

It is thus evident that although the distributions of potentials and currents are very different inside the  $\Pi$  and the  $T$  of Figs. 25 and 26 and in either from those in the smooth line of Fig. 23, yet at and outside the terminals of these equivalent circuits, all three systems have identical distributions, and any one may be replaced by either of the other two.

We shall see that the same principles apply in any single-frequency a.c. case.

**Multiple-section Equivalent Circuits of a Smooth Line.**—We have thus far considered single-section equivalent circuits, *i.e.*, the equivalent  $T$  and the equivalent  $\Pi$  of a smooth line. These may be sufficient to represent the behavior of the smooth line under any assigned terminal conditions in the steady state. If, however, we desire to reproduce in the equivalent circuit the electrical conditions at certain regular intervals along the smooth line, we may do so by dividing this line into uniform sections and replacing each by its equivalent  $T$  or  $\Pi$ . We shall thus produce a multiple-section equivalent circuit or artificial line. Multiple-section artificial lines will be considered in the following chapter.

## CHAPTER VII

### LUMPY ARTIFICIAL LINES

Lumpy artificial lines have already been described in Chapter VI. They may be classified both in regard to the number of their main wires, and in regard to the nature of their terminal elements.

**Classification According to Number of Main Wires.**—Artificial lines are one-wire, two-wire, or three-wire, according to the

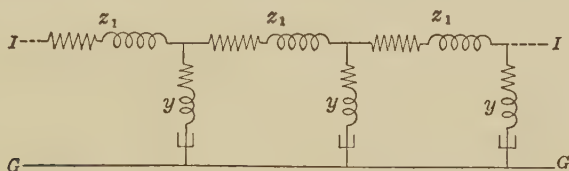


FIG. 27.—Diagram of connections between series and shunt elements in a single-wire artificial line.

number of their main-line conductors. A typical one-wire lumpy line is indicated in part of its length in Fig. 27. Here  $z_1$ ,  $z_1$ , and  $z_1$  are three equal sections or lumps of line impedance, (in c.c. cases, resistance). Three equals leak of admittance

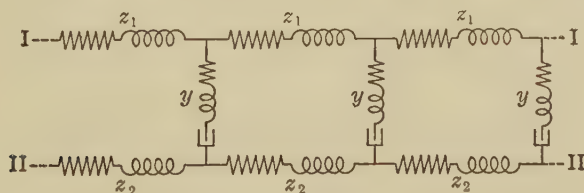


FIG. 28.—Diagram of connections between series and shunt elements in a two-wire artificial line.

(in c.c. cases conductance) are  $yyy$ , all connected to the common ground wire, or neutral connection  $GG$ . The type of impedance  $z$ , and the type of leak admittance  $y$  depend on the line to be imitated. Thus,  $z$  may be a pure resistance, or a reactance coil, or a condenser, or any combination of such elements, and simi-

larly for  $y$ . Single-wire lines, in practice, are characteristic of wire telegraphy.

A typical two-wire artificial line is shown, in part of its length, in Fig. 28. Here there are three sections, each having equal impedances  $z_1z_1z_1$  in one line, and similarly equal impedances  $z_2z_2z_2$  in the other line. Between the corresponding lumps of opposite line impedances are branched the equal leak admittances  $y_1y_1y_1$ . Two-wire lines, in practice, are characteristic of wire telephony.

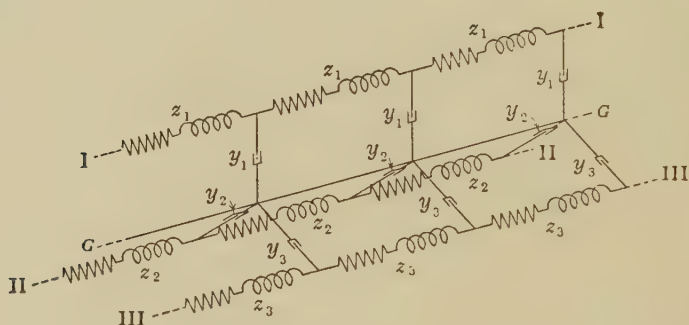


FIG. 29.—Diagram of connections between series and shunt elements in a four-wire three-phase artificial line.

A typical four-wire artificial line is similarly shown in Fig. 29, for three sections. Three equal impedances,  $z_1z_1z_1$ , in line I,  $z_2z_2z_2$  three similar equal impedances in line II,  $z_3z_3z_3$  in line III. Leak admittances  $y_1y_1y_1$ ,  $y_2y_2y_2$ ,  $y_3y_3y_3$ , are tapped off between corresponding line lumps of impedance to the ground wire or neutral connection  $GG$ . Three-wire lines, and four-wire lines, in practice, are characteristic of three-phase a.c. systems.

In theory, it is unnecessary to employ any except one-wire artificial lines, because any symmetrical two-wire or three-wire system can always be subdivided into a like number of virtually independent single-wire systems. We shall, therefore, study only the theory of single-wire artificial lines, on the understanding that the results can be readily applied to either two-wire or three-wire artificial lines.

**Classification According to Terminal Elements.**—Uniform artificial lines of the ladder type which terminate in half-lumps of line impedance, are called *T*-lines; while those which terminate in half-lumps of leak admittance are called *II*-lines.



If  $r$  be the line impedance per section (ohms  $\angle$ ) and  $g$  the leak admittance per section (mhos  $\angle$ ), then if the leak  $g$  is applied at the middle of the line section, as in Fig. 30, the section is called a  $T$ -section, as is suggested by the diagram. If, on the other hand, the leak  $g$  is divided into two half-leaks, each of  $g/2$  mhos, and one half-leak is applied at each end of the line impedance sec-

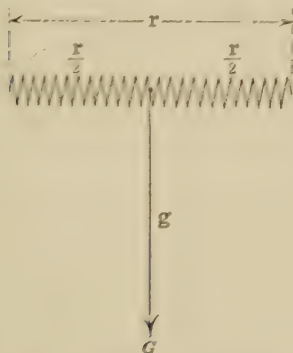


FIG. 30.— $T$ -section, comprising two equal-series elements and a leak or shunt element between them.

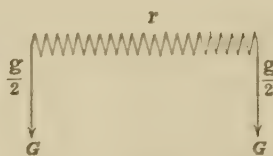


FIG. 31.— $\Pi$ -section, comprising one series element with a leak or shunt element at each end.

tion  $r$ , as shown in Fig. 31, the section is called a  $\Pi$ -section, as is also suggested by the diagram.

If a number of  $T$ -sections are connected in series, the result is a simple alternation of  $r$  and  $g$  lumps except at the terminals, where half-sections,  $r/2$ , of line impedance supervene. Thus

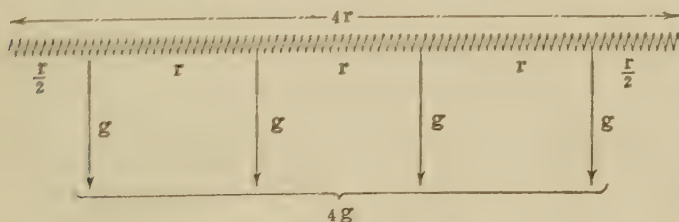


FIG. 32.—Four-section  $T$ -line.

Fig. 32 shows an artificial line of four  $T$  sections. The sum total of all the line impedances is  $4r$  ohms, and the sum total of the leak admittances is  $4g$  mhos.

If, on the other hand, a number of  $\Pi$ -sections are connected in series, the result is a simple alternation of  $r$  and  $g$  lumps, except at terminals, where half-sections of leak admittance supervene.

Thus Fig. 33 shows an artificial line of four  $\Pi$ -sections. The sum total of all the line impedance is  $4r$  ohms, and the sum total of all the leak admittances is  $4g$  mhos.

Away from the ends, there is no necessary difference between a  $T$ -line and  $\Pi$ -line. The distinction lies in the terminal elements only. Each type has, as we shall see, its own relative advantages and disadvantages.

We shall also see that each  $T$ -section, or  $\Pi$ -section, of artificial line subtends a certain hyperbolic angle  $\theta$  radians. A line of  $n$  sections then subtends a *total angle* of  $\Theta = n\theta$  hyps. A  $T$ -line or a  $\Pi$ -line also possesses a surge impedance  $r_0$  ohms, which is independent of the number of sections.

The conjugate line which a given artificial line imitates, and to which it corresponds, has the same angle  $\Theta$  and surge impedance  $r_0$  as the artificial line. The first problem which presents itself,

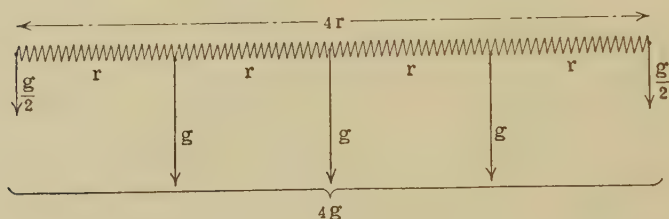


FIG. 33.—Four-section  $\Pi$  line.

therefore, in considering an artificial line of a given number of  $T$ - or  $\Pi$ -sections, each having definite lumps of line impedance and leak admittance, is the determination of its total line angle  $\Theta$  hyps. and its surge impedance  $r_0$  ohms.

**First Approximation to the Section Angle  $\theta$  and Surge Impedance  $r_0$  of a  $T$ - or  $\Pi$ -Section.**—If a single uniform smooth line has a total conductor resistance of  $R$  ohms, and a total dielectric leakance of  $G$  mhos, then we know from (35) and (43) that its line angle is

$$\theta = \sqrt{RG} \quad \text{hyps. } \angle \quad (191)$$

and its surge impedance

$$r_0 = \sqrt{\frac{R}{G}} \quad \text{ohms } \angle \quad (192)$$

In the same way, ignoring the lumpiness of the leaks in an artificial line section, having a line resistance  $r$  ohms, and a section

leak of  $g$  mhos (Figs. 30 to 34), the uncorrected section angle will be

$$\theta_a = \sqrt{rg} \text{ apparent hyps. } \angle \quad (193)$$

whether the section be a  $T$ - or a  $\Pi$ -section. Likewise, the surge impedance will be

$$r'_0 = \sqrt{\frac{r}{g}} \text{ apparent ohms } \angle \quad (194)$$

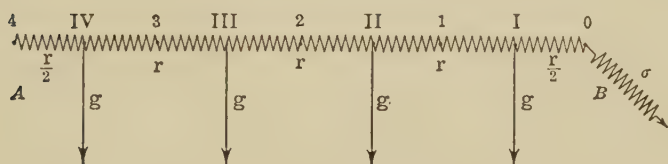


FIG. 34.—Four-section  $T$ -line grounded at motor end  $B$  through a load of  $\sigma$  ohms.

The total uncorrected angle of a line of  $n$  such sections will then be

$$\Theta_a = n\sqrt{rg} \text{ apparent hyps. } \angle \quad (195)$$

and the surge resistance of the line is the same as that of a section

$$r'_0 = r''_0 = \sqrt{\frac{r}{g}} \text{ apparent ohms } \angle \quad (194a)$$

These values require to be corrected for lumpiness. The lumpiness errors tend to increase, the larger and fewer the line sections.

The correction for lumpiness is readily obtained by considering a single section of the artificial line and reverting to its conjugate smooth line, as explained in the last chapter. In the case of a  $T$ -section belonging to a  $T$ -artificial line, we may use any of formulas (172) to (179) for finding  $\theta$  and formula (180) for finding the correct value of  $z_0$ . We may note that

$$r = 2\rho', \text{ and } g = g' \quad (196)$$

in Figs. 22 and 32, so that (193) becomes

$$\theta_a = \sqrt{2\rho'g'} \text{ apparent hyps. } \angle \quad (197)$$

or

$$\frac{\theta_a}{2} = \sqrt{\frac{\rho'g'}{2}} = \frac{\sqrt{rg}}{2} \text{ apparent hyps. } \angle \quad (198)$$

whereas the correct value of the semi-section angle is, by (176)

$$\sinh \frac{\theta}{2} = \sqrt{\frac{\rho' g'}{2}} = \frac{\sqrt{\mathbf{r} \mathbf{g}}}{2} \quad \text{hyp. } \angle \quad (199)$$

The lumpiness correction thus consists in replacing  $\frac{\theta_a}{2}$  by  $\sinh \frac{\theta}{2}$ .

An alternative equation for finding the true section angle  $\theta$  would be formula (173),

$$\theta = \cosh^{-1} (1 + \rho' g') = \cosh^{-1} \left( \frac{\rho' + R'}{R'} \right) = \cosh^{-1} \left( 1 + \frac{\mathbf{r} \mathbf{g}}{2} \right) \quad \text{hyp. } \angle \quad (200)$$

Similarly using (196), (194) and (180) become

$$z_0 = \sqrt{\frac{\mathbf{r}}{\mathbf{g}}} \cdot \cosh \left( \frac{\theta}{2} \right) = z'_0 \cosh \left( \frac{\theta}{2} \right) \quad \text{true ohms } \angle \quad (201)$$

Since  $\rho'' = \mathbf{r}$  and  $2g'' = \mathbf{g}$ , the lumpiness correction factors for a  $\Pi$ -section are obtained from (182) to (187). Thus, by (185),

$$\sinh \frac{\theta}{2} = \sqrt{\frac{\rho'' g''}{2}} = \frac{\sqrt{\mathbf{r} \mathbf{g}}}{2} \quad \text{numeric } \angle \quad (202)$$

or

$$\frac{\theta}{2} = \sinh^{-1} \left( \frac{\sqrt{\mathbf{r} \mathbf{g}}}{2} \right) \quad \text{hyp. } \angle \quad (203)$$

which coincide, with (199).

From (188) using (186)

$$z_0 = \sqrt{\frac{\mathbf{r}}{\mathbf{g}}} \cdot \operatorname{sech} \left( \frac{\theta}{2} \right) = \sqrt{\frac{\mathbf{r}}{\mathbf{g}}} \frac{1}{\cosh \left( \frac{\theta}{2} \right)} = z''_0 \operatorname{sech} \left( \frac{\theta}{2} \right) \quad \text{ohms } \angle \quad (204)$$

It is evident from (198) to (204) that the *lumpiness correction factor* of  $\theta_a$  is the same for a  $\Pi$ -section as for a  $T$ -section. The correction factor of  $z'_0$  or  $z''_0$  is not, however, the same for a  $\Pi$ -section as for a  $T$ -section. In the former case, it is  $\operatorname{sech} (\theta/2)$  and in the latter case  $\cosh (\theta/2)$ .

**Multiple-section T Artificial Line.**—As an example of a multiple-section  $T$ -artificial line and the relations to its conjugate smooth line, we may consider (see Fig. 34), the five-section line of Fig. 38, of  $\Theta = 1.75868$  and  $\mathbf{r}_0 = 1436.1$ , loaded at the motor end with  $\sigma = 750$  ohms. Here  $\mathbf{r} = 500$  ohms, and  $\mathbf{g} =$

0.00025 mho. The first-approximation section angle is, therefore,  $\sqrt{500 \times 0.00025} = \sqrt{0.125} = 0.35355$  hyp., and the first-approximation surge impedance  $r'_0 = \sqrt{500/0.00025} = \sqrt{2,000,000} = 1,414.2$  ohms. The corrected section angle is, by (199),  $\theta = 2 \sinh^{-1} \frac{0.35355}{2} = 0.35174$  hyp. The corrected surge impedance is, by (201),  $r_0 = 1,414.2 \times \cosh 0.17587 = 1,436.1$  ohms. The angle subtended by the load is, also, by (106),  $\theta' = \tanh^{-1} (750/1,436.1) = 0.57941$  hyp. If we add  $\theta'$  to  $N\theta$ , we obtain the position angles of the junctions shown in Fig. 35. At each junction, the resistance is given by (146). The resistance

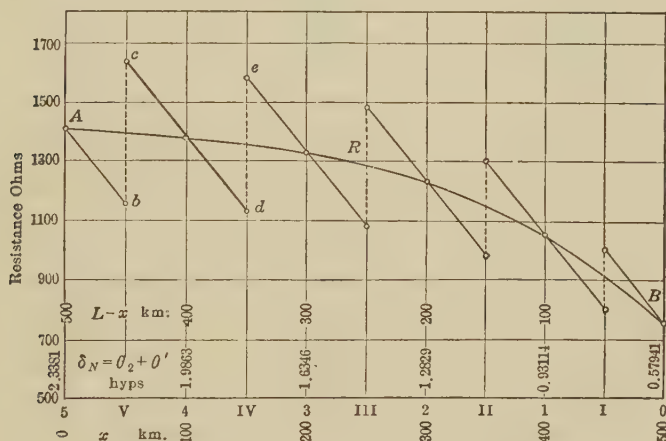


FIG. 35.—Line resistance at and beyond leaks and junctions of loaded *T*-line, and at corresponding position angles on the conjugate smooth line (see Fig. 38).

commences at 750 ohms for junction 0, rises steadily to 1,000 ohms by leak I; then falls, owing to the effect of the leak to 800 ohms; then rises to 1,050 ohms at junction 1, and so on, following the set of zigzag straight lines indicated. The conjugate smooth line of 1.7587 hyps. and surge impedance 1,436.1 ohms, loaded at *B* with 750 ohms, would offer a continuous-line resistance from point to point, following formula (146), which corresponds exactly to (143) at section junctions, as shown by the continuous curve *ARB* in Fig. 35. It is evident that each and every point of an active smooth lines possesses a corresponding position angle  $\delta_P$ ; but an artificial line can be said to have position angles only at its junctions and mid-sections.

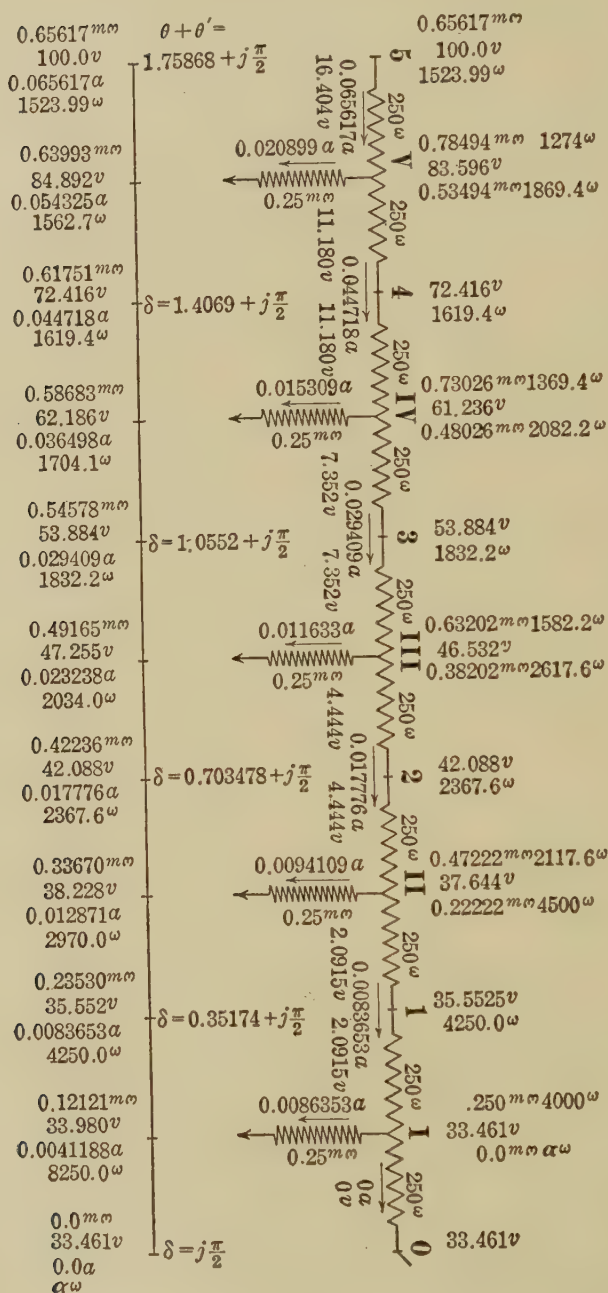


FIG. 36.—Five-section T-line freed at motor end, and its conjugate smooth line.



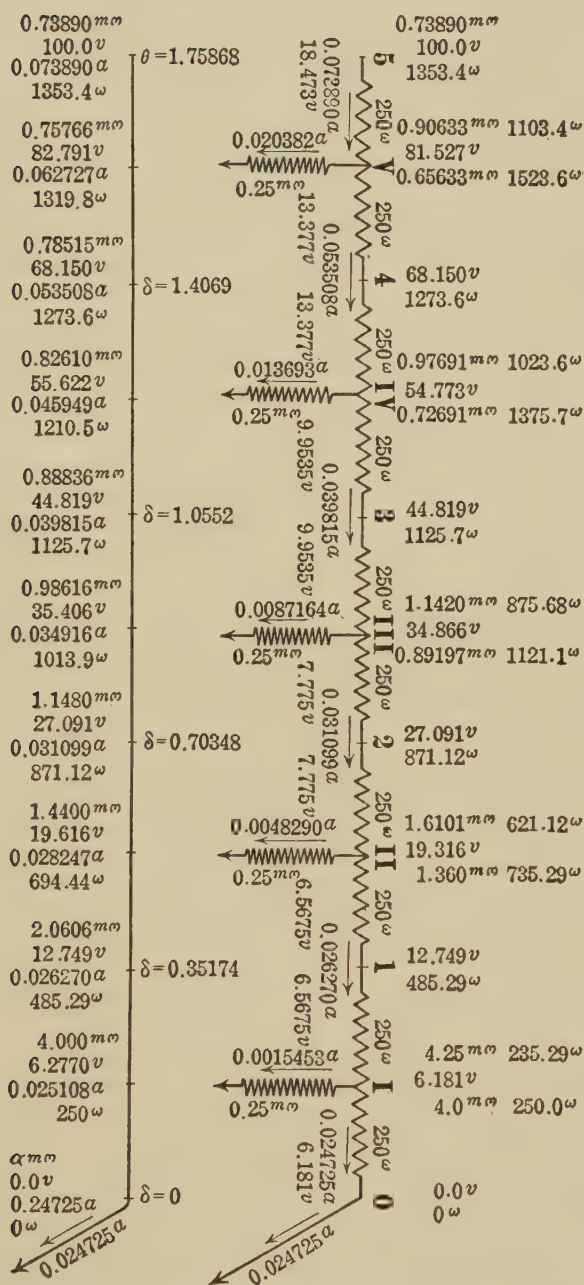


FIG. 37.—Five-section T-line grounded at motor end, and its conjugate smooth line.

**T-Section Artificial and Conjugate Lines.**—Figure 36 represents the artificial and conjugate lines freed at the far end, and energised with 100 volts at the generator end. The position angle at the free end is  $j_2^{\pi}$  hyp. and at the home end

$1.75868 + j_2^{\pi}$  hyps. The resistances, potentials, and currents are marked off at section junctions, as well as at the mid-section leaks. It will be observed that the conditions correspond at section junctions to those at corresponding points on the conjugate smooth line.

In Fig. 37, the same lines are grounded at the far end, but with the conditions otherwise unchanged. The position angle vanishes at the grounded end, while at the generator end it is 1.75868 hyps.

The same lines are grounded in Fig. 38 through a resistance  $\sigma = 750$  ohms. The position angle at the far end is here 0.57941 hyp., as is shown in Fig. 35. The position angle at the generator end is 2.3381 hyps.

**II-Section Artificial and Conjugate Lines.**—In the case of an artificial line composed of  $n$  uniform II-sections, the total angle of the line will be

$$\Theta = n\theta \quad \text{hyps. } \angle \quad (205)$$

where  $\theta$  is the angle of each section. Here again, if the architrave impedance  $\rho''$  is expressed as  $r$ , the total line resistance per section, and  $g = 2g''$  is the total leakance of the section, the apparent section angle uncorrected for lumpiness, as in (193), is:

$$\theta_a = \sqrt{rg} \quad \text{apparent hyps. } \angle \quad (206)$$

or

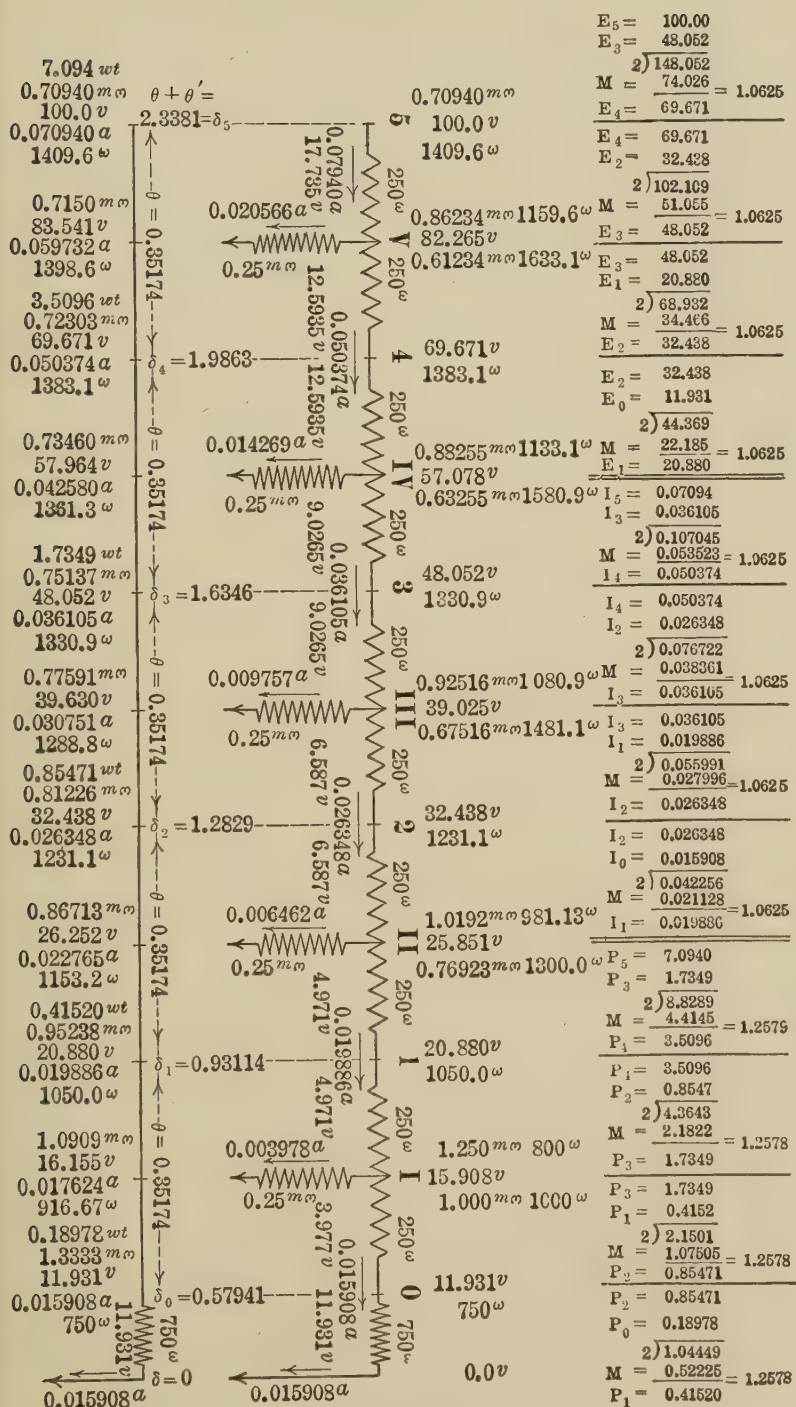
$$\frac{\theta_a}{2} = \frac{\sqrt{rg}}{2} \quad \text{apparent hyps. } \angle \quad (207)$$

But by reversion to the conjugate smooth line, using (185), the corrected section angle becomes:

$$\sinh \left( \frac{\theta}{2} \right) = \frac{\sqrt{rg}}{2} = \sqrt{\frac{\rho''g''}{2}} \quad \text{numeric } \angle \quad (208)$$

or by (183),

$$\cosh \theta = 1 + \frac{rg}{2} = 1 + \rho''g'' = \frac{\nu + g''}{\nu} \quad \text{numeric } \angle \quad (209)$$



Similarly, the apparent surge impedance of the section, neglecting lumpiness, is, by (192) and (194),

$$z_0'' = \sqrt{\frac{r}{g}} \quad \text{apparent ohms } \angle \quad (210)$$

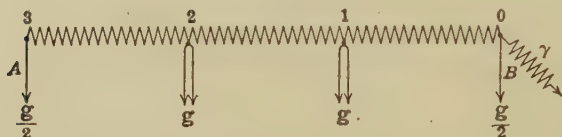


FIG. 39.—Three-section II-line grounded at motor end *B* through a load of conductance  $\gamma$  mhos.

but applying the correction factor from (204), the corrected surge impedance of the artificial line of  $n$  sections is

$$z_0 = \sqrt{\frac{r}{g}} \operatorname{sech} \frac{\theta}{2} = \sqrt{\frac{r}{g} \frac{1}{\cosh (\theta / 2)}} = \sqrt{\frac{\rho'''}{2g''}} \operatorname{sech} \frac{\theta}{2} = z_0'' \operatorname{sech} \frac{\theta}{2} \quad \text{ohms } \angle \quad (211)$$

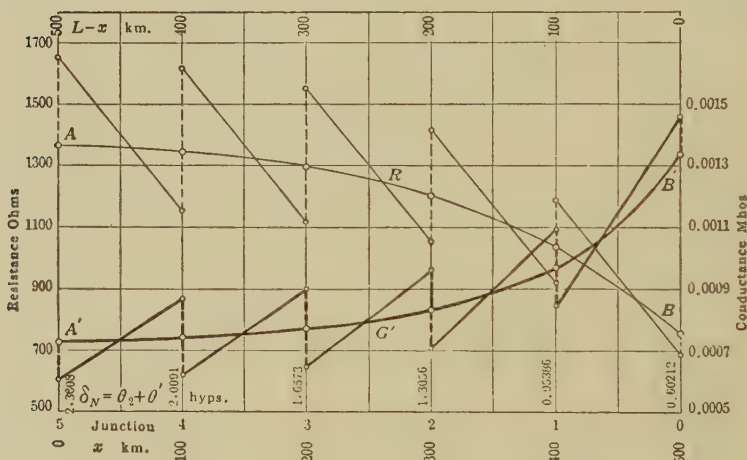


FIG. 40.—Line impedance and admittance at and beyond junctions of a loaded II-line, as well as at corresponding position angles of the conjugate smooth line.

Figure 40 gives the graphs of line impedance and admittance for the case of the five-section loaded II-line of Fig. 44. The section-line impedance is  $r = 500$  ohms, and leakance  $g = 0.00025$  mho. The uncorrected or apparent surge impedance is  $r_0'' = \sqrt{500/0.00025} = \sqrt{2,000,000} = 1,414.2$  ohms. The uncorrected or apparent section angle is  $\sqrt{500 \times 0.00025} = \sqrt{0.125}$

= 0.35355 hyp. The corrected section angle is, by (208),  $\theta = 2 \sinh^{-1}(\sqrt{0.125}/2) = 2 \sinh^{-1} 0.17678 = 2 \times 0.175868 = 0.351736$  hyp., and the angle subtended by the whole line is 1.75868 hyps. The corrected surge impedance is, by (211),  $\frac{1,414.2}{\cosh 0.175868} = 1,392.6$  ohms. The load of 750 ohms at  $B$  subtends an angle of  $\theta' = \tanh^{-1} (750/1,392.6) = 0.60212$  hyp., which, added to the successive values of  $\theta_2$  at junctions, gives the position angles  $\delta_N$  at junctions. The line resistance then varies as the tangent, and the line conductance as the cotangent of these angles. The leak distribution is seen in Fig. 39.

In Fig. 40, the curve  $ARB$  follows the line resistance of the conjugate line, having  $\Theta = 1.7587$  hyps. and  $r_0 = 1,392.6$  ohms. Such a line would possess a total conductor resistance, by (52), of

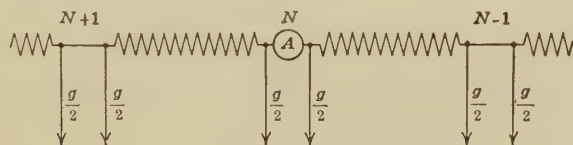
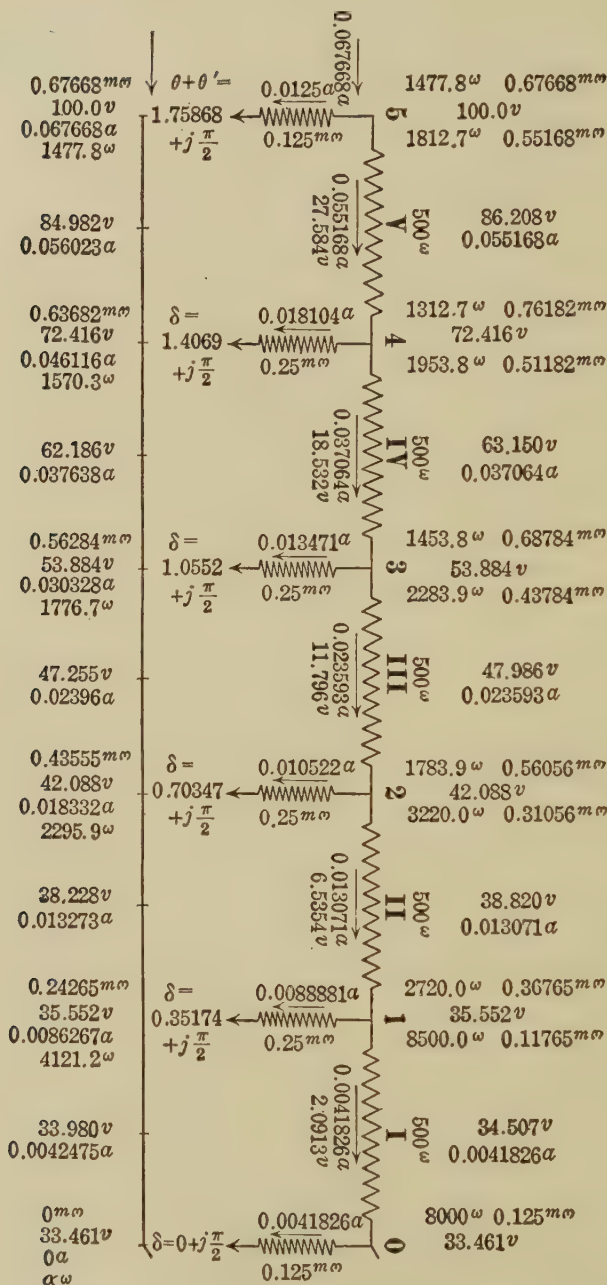


FIG. 41.—Diagrammatic representation of a  $\Pi$ -line with double leaks at each junction for the insertion of an ammeter  $A$  between successive sections.

$1.7587 \times 1,392.6 = 2,449$  ohms, and a total leakance, by (53), of  $1.7587 \div 1,392.6 = 1.263 \times 10^{-3}$  mho, whereas the artificial line has an aggregate line resistance of 2,500 ohms, and a total leakance of  $1.25 \times 10^{-3}$  mho. The zigzag line connecting  $A$  and  $B$  follows the line resistance over the  $\Pi$ -line. If measured between the leaks at each junction, the resistance coincides with the corresponding points on the curve  $ARB$ . The heavy black curve  $A'G'B'$  follows the graph of line conductance, along the conjugate line, and, at any point thereof, is the reciprocal of the corresponding value on the curve  $ARB$ . The zigzag heavy line, oscillating about  $A'G'B'$ , follows the line conductance over the  $\Pi$ -line. At section junctions, the oscillating values on the  $\Pi$ -line fall into coincidence with these smooth curves, provided that the measurements are made between the two leaks of a junction, as indicated in Fig. 41. In practice, it is customary to merge these two leaks  $g/2$  into one of  $g$  mhos, as in Fig. 33. In such a case, the agreement of line resistance and conductance at junctions is only realizable arithmetically.



FIG. 42.—Five-section  $\Pi$ -line freed at motor end, and its conjugate smooth line.



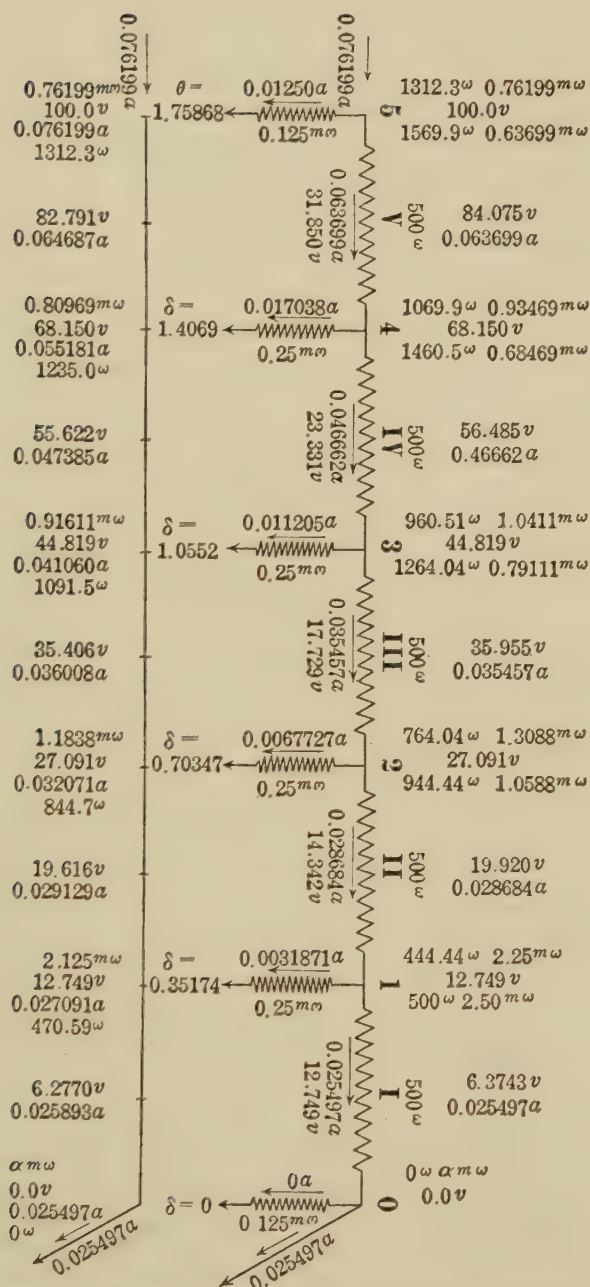


FIG. 43.—Five-section II-line grounded at motor end, and its conjugate smooth line.

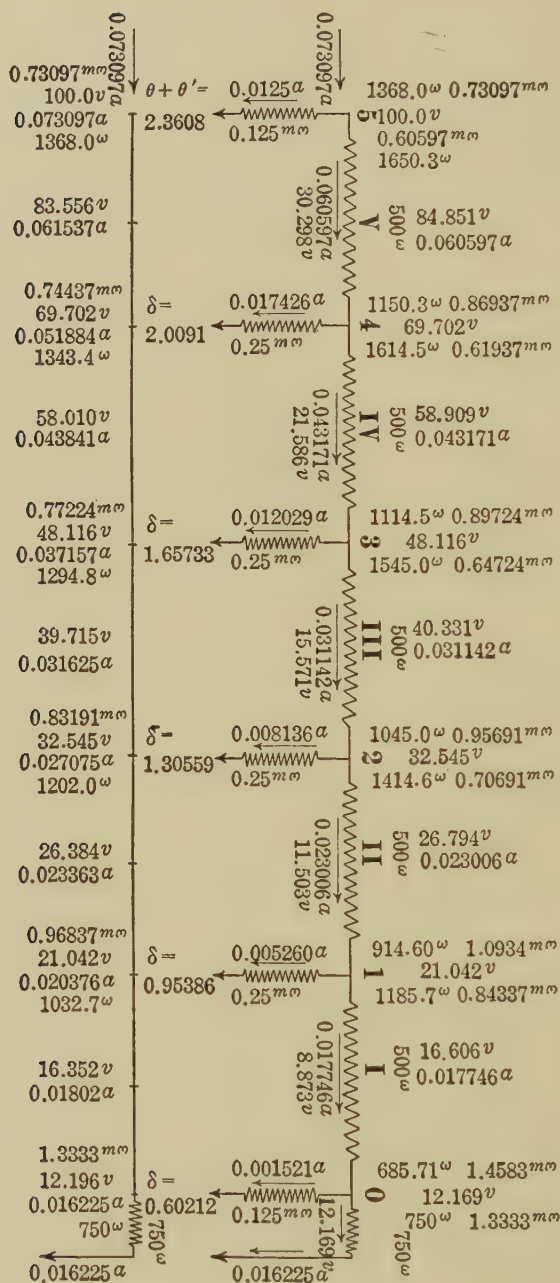


FIG. 44.—Five-section  $\Pi$ -line loaded at motor end, and its conjugate smooth line.

**General Properties of Artificial T- and  $\Pi$ -lines.**—If any uniform smooth line is terminated in any manner consistent with the steady state, such as a permanent load impedance at the motor end, and an impressed e.m.f. of single frequency at the generator end, an artificial line of  $n$  uniform  $T$ - or  $\Pi$ -sections, having the same total line angle  $\Theta$  and the same surge impedance  $z_0$  as the smooth line, will present the same terminal values of voltage, current, and power, if terminated in the same manner. These terminal identities are illustrated in Figs. 36 to 38, and 42 to 44.

Moreover, at each section junction of the artificial line, the forward impedance, voltage, current, and power will be, respectively, the same as at the corresponding point of the similarly terminated conjugate smooth line. It is to be understood, however, that in the case of a  $\Pi$ -line, the junction measurements are made between adjacent section leaks, as in Fig. 41.

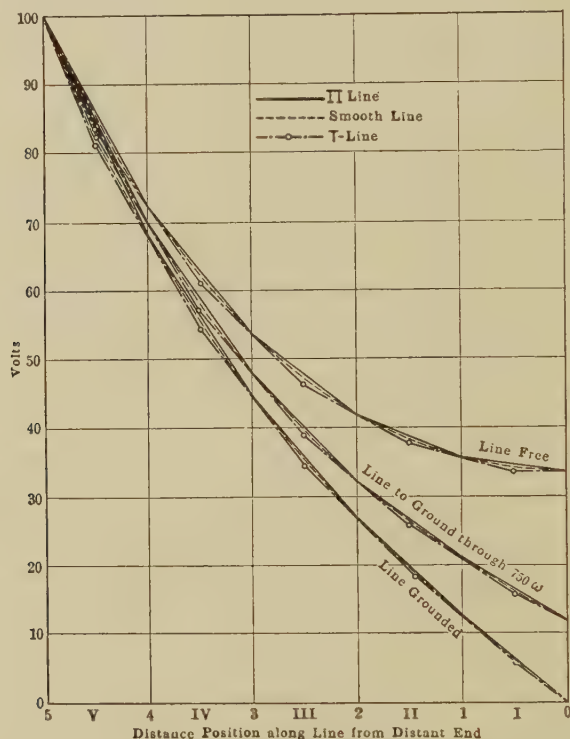
Whereas each and every point on the smooth line may be regarded as having its position angle, only the terminals and junction points of an artificial line can be said to have position angles. With this limitation, corresponding points of similarly terminated artificial and conjugate smooth lines are the same; so that the voltages, currents, and forward impedances will then be respectively proportional, in each case, to the hyperbolic sines, cosines, and tangents of these position angles.

**Fall of Potential Compared on T-,  $\Pi$ -, and Conjugate Lines Compared.**—Figures 45, 46, and 47 represent graphically the fall of potential along the  $T$ -line and  $\Pi$ -line of Figs. 36 to 38 and 42 to 44, as well as along a smooth conjugate line. Strictly speaking, it is not possible to have one and the same smooth line conjugate to both a  $T$ -line and a  $\Pi$ -line, unless the  $r$  and  $g$  in the sections of each are different, owing to differences in  $r_0$ , but the discrepancy is very small in this case.

It will be seen that taking the *line free* graphs, the dotted curve represents a true catenary for the conjugate smooth line. Contacting with this catenary at junction points, are the internal polygon representing the  $\Pi$ -line potential fall, and the external polygon representing the  $T$ -line potential fall.

These curves indicate that it is possible to arrange two loaded flexible massless strings with suitable masses in such a manner that both of them shall contact with a common catenary, one of them forming an internal string polygon, and the other an external string polygon.

**Fall of Current on T-, II-, and Conjugate Lines Compared.**—Figure 48 represents graphically the fall of current along the *T*-line of Figs. 36 to 38 and along the conjugate smooth line. The dotted smooth curves apply to the smooth line in each case. The zigzag *T*-line current graphs coincide with the smooth curves at section junctions.

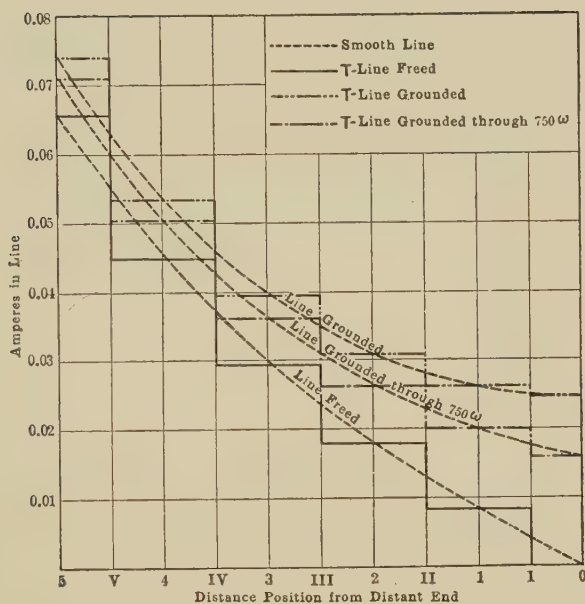
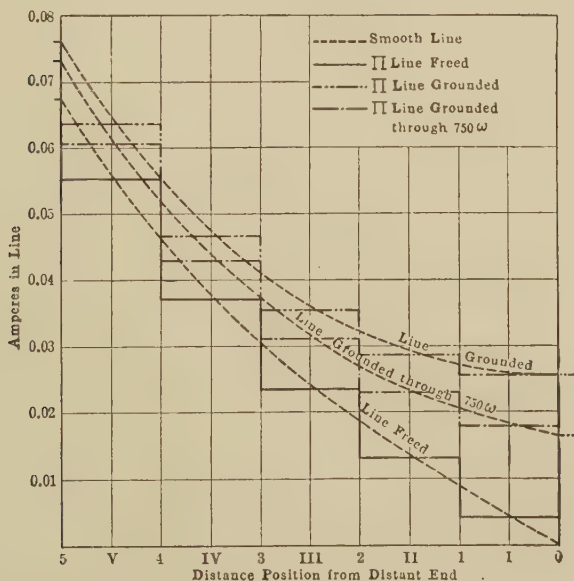


FIGS. 45, 46, and 47.—Fall of potential on artificial *T*-line, artificial *II*-line and on their conjugate smooth line.

In a similar manner, Fig. 49 shows the corresponding *II*-line current graphs. Here the mean ordinate at junction points coincides with the corresponding smooth curve.

**Artificial Line of Indefinitely Great Number of Very Small Sections.**—If a section of lumpy line is large; *i.e.*, contains a relatively large lump of resistance *r* and a large associated lump of leakance *g*, the lumpiness correction factor in angle, by (203)

$$h_v = \frac{\sinh^{-1}(\sqrt{rg}/2)}{(\sqrt{rg}/2)} = \frac{\sinh^{-1}(\theta_a/2)}{(\theta_a/2)} \quad \text{numeric } \angle \quad (211a)$$

FIG. 48.—Currents in artificial *T*-line and in conjugate smooth line.FIG. 49.—Currents in artificial *II*-line and in conjugate smooth line.

tends to be considerable, and in some a.c. cases may be enormous. The correction factor in surge impedance, either  $\cosh (\theta/2)$  or  $\operatorname{sech} (\theta/2)$  as the case may be, is also capable of assuming large proportions. As, however, the subdivision of the lumpiness is effected by placing the same total artificial-line resistance and leakance in more numerous sections, both  $r$  and  $g$  are reduced so that the value of  $k_v$  diminishes toward unity. Finally, when the successive sections are all exceedingly small and indefinitely numerous, both  $r$  and  $g$  tending toward zero, the limit of  $k_v$

$$\left( \frac{\sinh^{-1} (\theta_a/2)}{(\theta_a/2)} \right)_{\theta_a=0} = 1 \quad \text{numeric} \quad (211b)$$

or there ceases to be any correction factor, and the minute apparent angle  $\theta_a/2$  subtended by a half-section is not to be distinguished from its actual semi-angle  $\theta/2$ . At the same time the values of  $\cosh \theta/2$  and  $\operatorname{sech} \theta/2$ , as  $\theta$  approaches zero, tend to the value unity; or the apparent surge impedance by (194) becomes the true surge impedance  $r_0$ . Such a line, however, with indefinitely numerous and indefinitely small lumps of impedance and leakance is, however, a smooth line, which obviously has no lumpiness error.

#### Intermediate-point Properties of Real or Artificial Lines.—

Certain properties of voltage, current, and power pertaining to intermediate points in any uniform length of real or artificial line are often useful because they do not demand any knowledge as to the terminal conditions of the line.

If we consider a uniform line of any length, energized in any manner at its ends, such as the five-section  $T$ -artificial line of Fig. 38, or its conjugate smooth line, we may take any three uniformly spaced points. On the conjugate smooth line, the uniform spacing may have any magnitude; but in the general case of a uniform artificial line, the spacing distance must be an integral number of sections. Let the three points selected be indicated respectively by  $P_1$ ,  $P_2$ , and  $P_3$ . Thus, in Fig. 38, we may take the three-section junctions 1, 2, and 3, which are spaced one section apart. The mid-point will then be  $P_2$ . The mid-point potential will then be  $E_2$  and the mid-point current  $I_2$ . We may then define the arithmetical mean of the potentials or currents at the outer points  $P_1$  and  $P_3$  as the "mean potential" or "mean current" of the trio. Thus, the mean potential will be  $(E_1 + E_3)/2$ , and the mean current  $(I_1 + I_3)/2$ . It is then



readily shown that the ratio of the mean to the mid-potential is equal to the ratio of the mean to the mid-current, and to  $\cosh \theta$ , where  $\theta$  is the spacing angle.

In the example selected from Fig. 38,  $E_1$  is 20.880 volts, and  $E_3$  is 48.052 volts. Their mean is 34.466 volts. The mid-potential  $E_2$  is 32.438. Indicating the mean value of  $M$ , and the mid value by  $D$ , the *ratio of mean to mid* is  $M/D = 34.466/32.438 = 1.0625$ , which is  $\cosh \theta$ ,  $\theta$  being the section angle 0.35174 hyp. The same ratio holds for the mean-to-mid current. Four such ratios of potential and of current are worked out on the right-hand margin of the figure.

Since the potentials and currents are the same at a junction point of an artificial line and at the corresponding point of the conjugate smooth line, as indicated in the figure, the proposition must apply to both  $T$  and  $\Pi$  types of line, if it applies to one of them.

The proof of the proposition rests upon the fact to which attention has already been directed in Chapter IV—that every point along a smooth line, and every junction point along a uniform artificial line, possesses a position angle to the hyperbolic sine of which the potential is proportional, and the current to the hyperbolic cosine. The value of the position angle varies with the load at the motor end, but we are only interested in the differences between the position angles at the three points with a spacing angle of  $\theta$  hyps., and this spacing angle is constant under all loads.

Let  $\delta$  be the position angle of the mid-point  $P_2$ . Then the position-angle of point  $P_1$  will be  $(\delta \pm \theta)$  the upper sign being taken if the power is being transmitted in the direction 1, 2, and 3. The position angle of  $P_3$  will likewise be  $(\delta \mp \theta)$ . The potential at the midpoint  $P_2$  will then be

$$E_2 = A \sinh \delta = D \quad \text{volts } \angle \quad (212)$$

where  $A$  is a voltage constant depending on the terminal conditions.

Again the potentials at  $P_1$ , and  $P_3$ , will be respectively, by (569)

$$E_1 = A \sinh (\delta \pm \theta) = A (\sinh \delta \cosh \theta \mp \cosh \delta \sinh \theta) \quad \text{volts } \angle \quad (213)$$

and

$$E_3 = A \sinh (\delta \mp \theta) = A (\sinh \delta \cosh \theta \mp \cosh \delta \sinh \theta) \quad \text{volts } \angle \quad (213a)$$

The arithmetical mean of these two potentials (a vector mean in an a.c. case) will be

$$M = A \sinh \delta \cosh \theta \quad \text{volts } \angle \quad (214)$$

so that, dividing by (212),

$$\frac{M}{D} = \cosh \theta \quad \text{numeric } \angle \quad (215)$$

Similarly, the current in the line at the mid-point  $P_2$  is

$$I_2 = B \cosh \delta = D \quad \text{amperes } (216)$$

where  $B$  is a current constant depending on the terminal conditions.

The currents at  $P_1$ , and  $P_3$ , will be respectively, by (570),

$$I_1 = B \cosh (\delta \pm \theta) = B (\cosh \delta \cosh \theta \pm \sinh \delta \sinh \theta) \quad \text{amperes } \angle \quad (217)$$

and

$$I_3 = B \cosh (\delta \mp \theta) = B (\cosh \delta \cosh \theta \mp \sinh \delta \sinh \theta) \quad \text{amperes } \angle \quad (217a)$$

subject to the same convention as to the sign selected. The mean is:

$$M = B \cosh \delta \cosh \theta \quad \text{amperes } \angle \quad (218)$$

Dividing by (216),

$$\frac{M}{D} = \cosh \theta \quad \text{numeric } \angle \quad (219)$$

If, then, we know the potential and current at the two ends of a uniform smooth line in the steady state, we can use this proposition to find the potential and current at the mid-point of the line. Moreover, if we know the potential and current at any two points  $P_1$  and  $P_2$  on a uniform real or artificial line, the points being separated by the angle  $\theta$ , then we can use the proposition to infer the potential and current at a third point distant  $\theta$  from either  $P_1$  or  $P_2$ .

In any continuous-current line, the power at any point varies as the sine of twice the position angle. This is readily shown from the product of (212) and (216), in view of (558). Hence the mean-to-mid power ratio for any three equally spaced points of spacing distance  $\theta$ , is  $\cosh 2\theta$ . This is also shown on the right-hand margin of Fig. 38. In the a.c. case, the corresponding proposition is less simple, and is of doubtful utility.

The mean-to-mid theorem is often useful in the interpolation of sines and cosines in tables of complex functions.

## CHAPTER VIII

### THE DESIGN, CONSTRUCTION, AND TESTS OF CONTINUOUS-CURRENT ARTIFICIAL LINES

Continuous-current artificial lines may be constructed:

1. To furnish an electrical model of some particular telegraph line, with a standard or normal linear leakance in the steady state.
2. To furnish an electrical model of a low-voltage d.c. railway signal system, where a continuous signalling current is carried over the two parallel rails of a railroad track, so as to respond to the short-circuiting action of an advancing train.
3. To furnish a model for the use of students in an electrical engineering laboratory, to familiarize them with the tests and formulas pertaining to such lines, before proceeding to the less simple and much more extensive field of a.c. line testing.

We shall take up the consideration of a particular example of type (3). In this case it was desired to construct a five-section artificial line,\* which could be connected by the students either as a *T*-line or as a *II*-line, in order to aid them in forming either of these subtypes.

A rectangular box was constructed of hard wood, well soaked with molten paraffin wax. This box is 57.5 cm. (22.6 in.) long, 17.8 cm. (7 in.) wide, and 10 cm. (4 in.) high. All of the electrical parts and connections are fastened to the cover, which is removable by means of a dozen wood screws. A plan view of the box and its cover appears in Fig. 50.

Three rows of brass strips are seen fastened to the top of the cover, the upper row commencing with *1a*, *1b*, *1c*, and ending with *5a*, *5b*, *5c*. Between the members of each of these five groups are connected resistances *AA*, each of 250 ohms, of No. 32 B. & S. gage *Ia-Ia* resistance wire, double cotton-covered, anti-inductively wound and impregnated with paraffin wax. These resistances form the line sections. The second, or middle row contains resistances *B*, *B*, each of 4,000 ohms, of the same

\* "A Convenient Form of Continuous-current Artificial Line," by A. E. Kennelly, *Electrical World*, June 14, 1913.

kind of wire. These form the leaks. The third, or bottom row, is a single brass strip  $gg$ , serving as the common ground connection of the line.

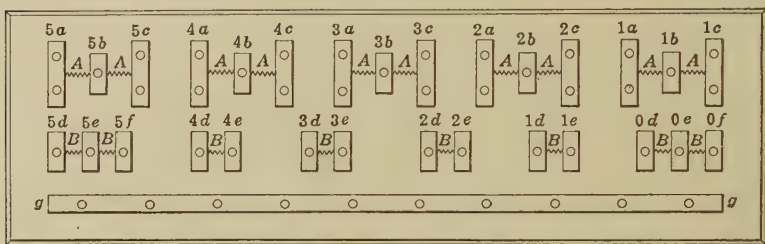


FIG. 50.—Plan view of artificial c.c. line arranged for one, two, three, four, or five sections either of  $T$ 's or  $II$ 's.

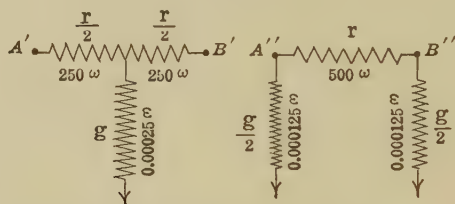


FIG. 51.—Single sections of  $T$ - and  $II$ -line.

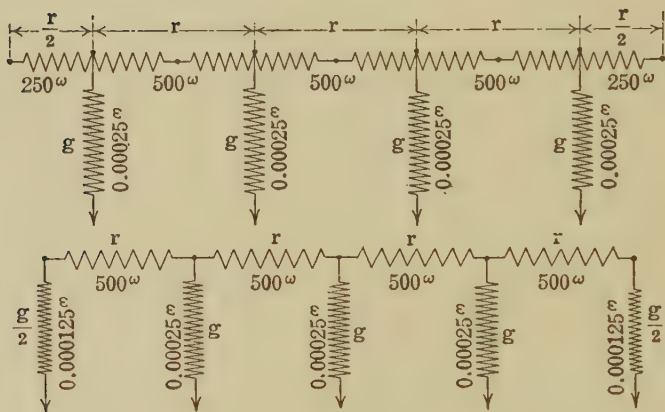


FIG. 52.—Four-section  $T$ -line and four-section  $II$ -line.

A single section of  $T$ -line connection is indicated in Fig. 51, at  $A'B'$ , and a single section of  $II$ -line connection at  $A''B''$ . A four-section  $T$  line, and also a four-section  $II$  line appear in Fig. 52. Pairs of electrically connected brass plugs serve to connect

the line into as many as five sections of the type desired. In Fig. 53, the box is shown connected as a five-section  $T$ -line.

The electrical behavior of such a five-section  $T$ - or  $\Pi$ -line is illustrated diagrammatically in Figs. 36, 37, 38, 42, 43, and 44,



FIG. 53.—Continuous-current artificial-line box connected as a five-section  $T$ -line.

for the particular cases of grounding, freeing, and loading with 750 ohms at the distant end. In either case, the section angle is 0.35174 hyp., but, for reasons already discussed in Chapter VI, the surge impedance of the  $T$ -sections is 1,436.1 ohms, while that of the  $\Pi$ -sections is 1,392.6 ohms.

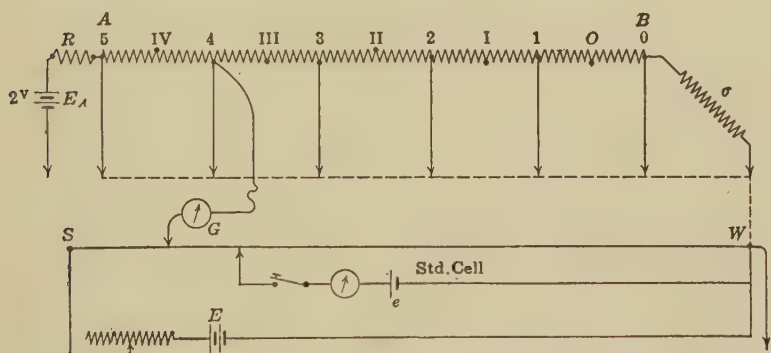


FIG. 54.—Diagram of connections for potentiometer test of c.c. artificial line of  $\Pi$ -sections.

**Potentiometer Tests of Artificial Line.**—The test for fall of potential along the junctions and mid-sections of the box, arranged as a five-section  $\Pi$ -line, loaded at  $B$  with a resistance of  $\sigma$  ohms, is indicated diagrammatically in Fig. 54. The battery  $E_A$  may be a steady storage cell, capable of maintaining, say, 2.0 volts at its terminals during the continuance of the test. The resist-



ance  $R$  at  $A$ , enables the potential impressed on the end 5 of the line, to be brought within the usual 1.6 volts capable of being read directly on an ordinary potentiometer. The slide wire of this instrument is indicated as  $SW$ , the working battery at  $E$ , the standard cell at  $e$ . As connected, the potential to ground is being measured at junction 4.

The current strengths along the artificial line may be readily measured by observing the potentiometer p.d. on each successive line element 0 1, 1 2, 2 3, 3 4, and 4 5. The entering current at  $A$  may likewise be measured by observing the drop of potential in  $R$ .

The position angles along the line are determined from the load  $\sigma$  and the line elements, in the manner described in Chapter VI. The potentials and currents at each successive junction and mid-section are then computed by reference to tables of real hyperbolic functions. The observed and computed values are finally recorded, and compared in parallel columns.

If the elements of resistance entering into the line are carefully measured in the first instance, if all of the plug contacts and connections are good, and if the potentiometer measurements are carefully made, it is customary for the student to find the observed and computed values in agreement to the third and sometimes to the fourth significant digit.

There is nothing which gives the student so complete a grasp of the principles and formulas relating to a.c. artificial lines, as preliminary tests on such d.c. artificial lines. It is important to make these d.c. lines stepping stones to a.c. lines, because the technique is easily grasped and followed, and the precision of measurement is all that can be desired. With a.c. lines, the precision attainable is ordinarily lower, disturbances due to changes in impressed frequency are very noticeable, and the computations retarded through the substitution of complex for real numbers, even though the formulas employed remain unchanged.

**Wheatstone-bridge Test of Lines.**—A useful test on c.c. lines, for  $\theta$  and  $r_0$ , is conveniently made by means of the Wheatstone bridge (see Fig. 55). This is the measurement of the line resistance at each successive junction, both with the  $B$  end freed, and with the  $B$  end grounded.

By (146) the resistance at junction  $N$ , with  $B$  grounded, is

$$R_{gN} = r_0 \tanh (N\theta) = r_0 \tanh \Theta \quad \text{ohms } \angle \quad (220)$$



With the  $B$  end freed, and with  $\delta_B = j_2^{\pi}$ , the line resistance at junction  $N$  is

$$R_{fN} = r_0 \tanh \left( N\theta + j_2^{\pi} \right) = r_0 \coth (N\theta) \quad \text{ohms } \angle \quad (221)$$

and generally

$$R_N = r_0 \tanh (N\theta + \theta') = r_0 \tanh \delta_N \quad \text{ohms } \angle \quad (222)$$

Multiplying formulas (220) and (221) together, we find

$$R_{gN} \cdot R_{fN} = r_0^2 \quad \text{ohms}^2 \angle \quad (223)$$

or, by definition, the surge impedance is

$$r_0 = \sqrt{R_{gN} \cdot R_{fN}} \quad \text{ohms } \angle \quad (224)$$

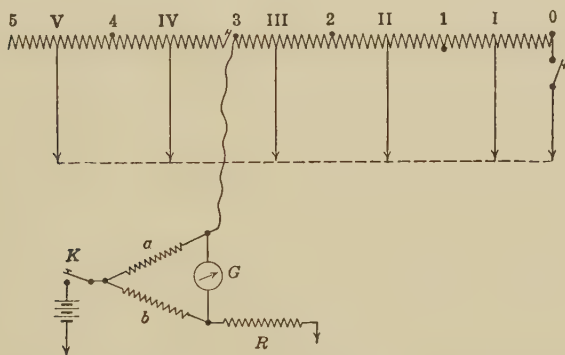


FIG. 55.—Connection diagram for line-resistance test with Wheatstone bridge.

In words, *the product of the impedance free and impedance grounded is constant at any and all section junctions, either of a T- or II-line. The square root of this product is the surge impedance of the line. In other words, the surge impedance of a line at any testing point is always the geometric mean of  $R_g$  and  $R_f$ . On a smooth line, any point may be a testing point; but on an artificial line only junctions. This may be taken as defining  $r_0$ .*

Moreover, dividing (220) by (221) we have

$$\tanh \Theta = \tanh (N\theta) = \sqrt{\frac{R_{gN}}{R_{fN}}} \quad \text{numeric } \angle \quad (225)$$

or

$$\Theta = N\theta = \tanh^{-1} \sqrt{\frac{R_{gN}}{R_{fN}}} \quad \text{hyps. } \angle \quad (226)$$

*The angle subtended by the line beyond any junction is the anti-tangent of the root of the ratio of the resistance grounded to the resistance freed. This serves to define the angle  $\Theta$ .*

*In other words, the angle subtended by a line beyond a testing point has as its tangent the geometric mean of  $R_g$ , the resistance grounded, and  $G_f$ , the conductance freed.*

When these line-resistance tests are made on a  $T$ -line, it is necessary only to break the line at the junction selected, and to connect the bridge to the end beyond the break. In the case of a  $\Pi$ -line, however, it is necessary, in addition, to change the first leak from  $g$  to  $g/2$  mhos. This may be done by substituting a transferable half-leak for the usual full leak, at the testing terminal.

As an example, consider the  $T$ -line represented in Figs. 36 and 37. If we cut in at section 3,  $R_{g3} = 1,125.7$  ohms, and  $R_{f3} = 1,832.2$  ohms. Hence  $r_0 = \sqrt{1,125.7 \times 1,832.2} = 1,436.1$  ohms, and  $N\theta = \tanh^{-1} \sqrt{1,125.7/1,832.2} = \tanh^{-1} 0.78383 = 1.0552$  hyps. Since here  $N = 3$ ,  $\theta = 0.35173$  hyp. per section.

It is instructive to make measurements of  $R_g$  and  $R_f$  at each successive junction along the line, and so to derive the values of  $\theta$  and  $r_0$ .

**Distribution of Work of Tests among Observers.**—The various tests above described can be made, if necessary, by a single observer, making all his own connections, measurements, and records. The work is done more conveniently and expeditiously by a pair of observers, one making the measurements and the other the connections and records, the two occasionally changing duties. Three observers can also advantageously divide the work between them, and even a fourth can also be occupied in computing checks, as the test advance.

**Disturbances of Potential and Current in the Artificial Line that may be produced by the Applications of a Leak Load, in making Potentiometer Measurements.**—It has been already pointed out that it is desirable, in making potentiometer measurements of voltage along the line, to keep the impressed potential at the generator end within the direct compass of the potentiometer, so as to avoid having to apply a "volt box" or "multiplier" to the line, at the testing point. Such a reducing box (see Fig. 56) virtually applies a leak load to the line at the testing point. A small leak of this kind has a surprisingly large effect in lowering the line potential at and near the leak. Figure 56 repre-

sents a four-section  $T$ -line, loaded at  $B$  with a resistance  $\sigma$ , and having the potential at mid-section II measured by potentiometer. The potential being beyond the direct compass of the instrument, a volt box  $X$ , of say 10,000 ohms, or 0.1 millimho, is applied to the line at this point, and one-tenth, say, of the voltage across the box  $X$  to ground, is measured at the potentiometer.

Since it may sometimes be necessary to employ relatively high impressed voltages on the line, and a volt-box leak of the kind described, we may consider the magnitude of the effect produced, and how to correct for it, if needful.\*

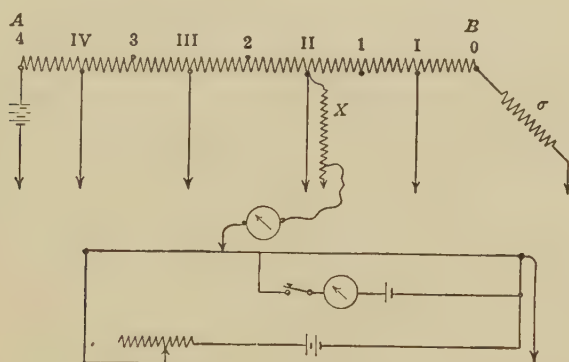


Fig. 56.—Potential test of continuous-current line by potentiometer with aid of a volt box  $X$ .

Figure 57 shows the effect of applying a leak load of 0.1 millimho (10,000 ohms), to junction 3 of the five-section line already considered in Fig. 38, voltage at  $A$  with 100 volts, and loaded at  $B$  with 750 ohms. It will be seen that the effect of the leak, such as might be used for potentiometer measurement of potential at 3, is to lower the potential from 48.052 to 45.648 volts, a reduction of 2.404, or approximately 5 per cent. At neighboring testing points, the potential is likewise lowered, although not to the same extent. Another effect of the leak is to introduce a discontinuity in the position angle at 3, from 1.6346 to 1.1503 hypos., the rationale of which will be considered under the subject of composite lines.

\* "Disturbances of Potential and Current Produced in an Active Network by the Application of a Leak Load," by A. E. Kennelly, *Electrical World*, Dec. 28, 1912.

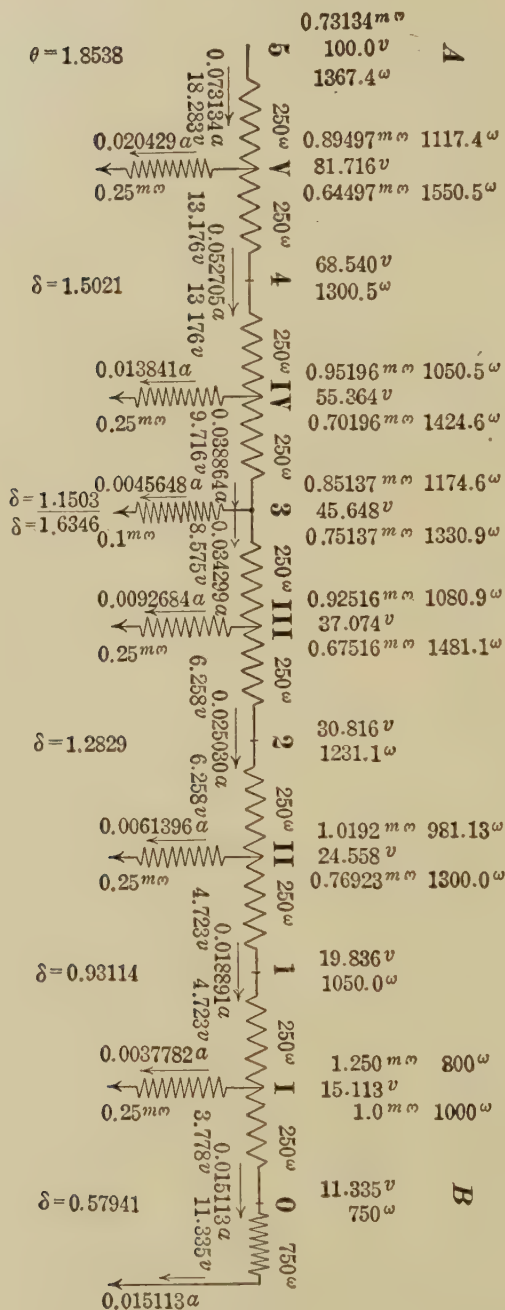


FIG. 57.—Artificial line loaded with a leak of 0.1 millimho at junction 3.

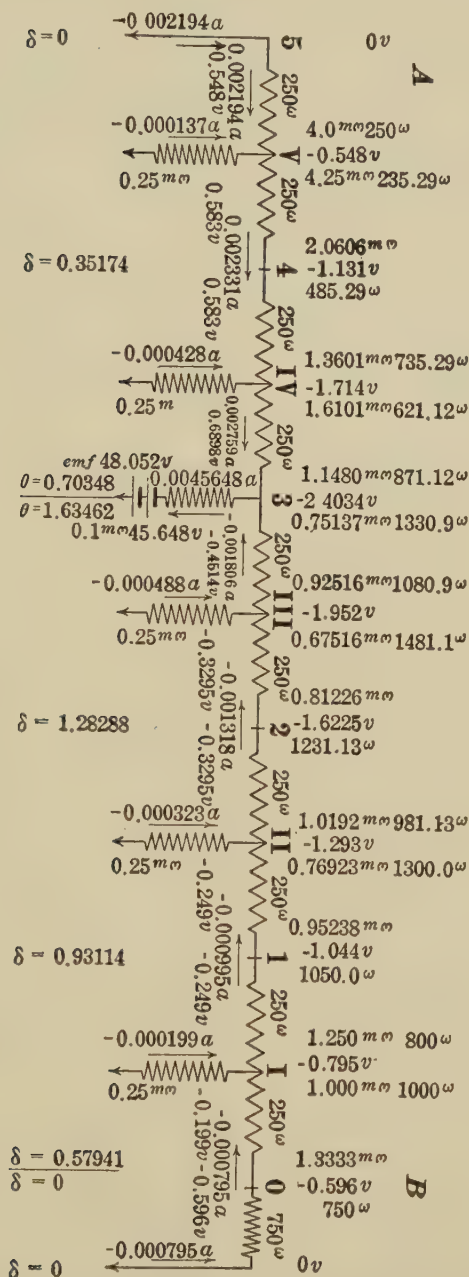


FIG. 58.—Artificial line grounded at A and with the e.m.f. of 48.052 volts inserted outwardly in the leak load at 3.





Figure 58 shows the same artificial line with the impressed e.m.f. removed at  $A$ , and with the leak applied at 3, this leak containing in it an e.m.f. of 48.052 volts, the potential existing there before applying the leak, as in Fig. 38, page 81. The effect of this e.m.f., taken negatively, is to produce a potential at 3 of  $-2.4034$  volts, and correspondingly, in diminishing extent, at more remote testing points. These are precisely the values of the disturbances produced by the leak. The currents in the line of Fig. 58, on each side of the leak, are  $+2.759$  milliamp. on the upside, and  $-1.806$  milliamp. on the downside, which correspond to the disturbances shown in Fig. 57, by reference to Fig. 38.

Fig. 59 indicates the extent of the disturbances in potential and current at the various testing points along the line, by the application of this 10,000-ohm leak.

**Correction for Potential Disturbances Due to Leak.**—Let  $V$  be the potential at the testing point before applying the leak, and  $v$  the potential at the same point after applying the leak. Then the *depression factor* of the leak is\*

$$d = \frac{v}{V} = \frac{G}{G + g} \quad \text{numeric } \angle \quad (227)$$

where  $G$  is the conductance in mhos to ground of the line from the testing point, excluding the leak, and  $g$  is the conductance of the leak itself. The factor  $k$  which should be applied to the observed potential, to correct for the action of the leak, may be called the *correcting factor of the leak at the point of application* and is:

$$k = \frac{1}{d} = \frac{V}{v} = \frac{G + g}{G} \quad \text{numeric } \angle \quad (228)$$

The conductance  $G$  will be the sum of the line conductances to ground, from the testing point, in both directions. If  $\theta_1$  is the angle subtended by the  $A$  end of the line, at the testing point, when grounded at  $A$ , and  $\theta_2$  the corresponding angle subtended by the  $B$  end of the line, then by (147)

$$G = y_0(\coth \theta_1 + \coth \theta_2) \quad \text{mhos } \angle \quad (229)$$

In the case considered,  $\theta_1 = 0.70348$  and  $\theta_2 = 1.63462$ ; also  $y_0 = 0.69633$  millimho; whence  $k = 1.05265$ . The observed potential at 3, in the presence of the leak, should be multiplied by this

\* "On the Measurement of the Insulation of Continuous-current Three-wire Systems While at Work," by E. J. Houston and A. E. Kennelly, *Electrical World*, July 25, 1896, vol. xxviii, p. 95 (7).

factor, in order to arrive at the value of the potential with the leak removed.

**Correction for Current Disturbances Due to Leak.**—Knowing either the uncorrected potential  $v$ , or the corrected potential  $V$ , at the testing point, the extent of the disturbance in current over the adjoining sections can readily be found. If  $G_1$  and  $G_2$  are the conductances to ground on each side, whose sum is  $G$ , then

$$i_1 = vg \cdot \frac{G_1}{G} \quad \text{and} \quad i_2 = vg \cdot \frac{G_2}{G} \quad \text{amp. } \angle \quad (230)$$

or

$$i_1 = Vg \cdot \frac{G_1}{G + g} \quad \text{and} \quad i_2 = Vg \cdot \frac{G_2}{G + g} \quad \text{amp. } \angle \quad (231)$$

are the changes in current due to the application of the leak load. In an artificial line subtending angles  $\theta_1$  and  $\theta_2$  on each side.

$$i_1 = vg \cdot \frac{\coth \theta_1}{\coth \theta_1 + \coth \theta_2} \quad \text{and} \quad i_2 = vg \cdot \frac{\coth \theta_2}{\coth \theta_1 + \coth \theta_2} \quad \text{amp. } \angle \quad (232)$$

or

$$i_1 = Vg \cdot \frac{y_0 \coth \theta_1}{g + y_0(\coth \theta_1 + \coth \theta_2)} \quad \text{and} \quad i_2 = Vg \cdot \frac{y_0 \coth \theta_2}{g + y_0(\coth \theta_1 + \coth \theta_2)} \quad \text{amp. } \angle \quad (233)$$

The sum of  $i_1$  and  $i_2$  in (232) is obviously

$$i_1 + i_2 = vg \quad \text{amp. } \angle \quad (234)$$

In the case considered,  $v = 45.648$ ,  $V = 48.052$ ,  $g = 0.1 \times 10^{-3}$ ,  $G_1 = 1.148 \times 10^{-3}$ ,  $G_2 = 0.7514 \times 10^{-3}$ ,  $G = 1.8994 \times 10^{-3}$ ,  $i_1 = 2.759 \times 10^{-3}$  amp., and  $i_2 = 1.806 \times 10^{-3}$  amp.

In general, a new correction factor has to be found for each successive testing point. Hence the desirability of dispensing with a reduction box when using the potentiometer.

Although an artificial line of the character shown in Fig. 50 has the advantage of serving either as a T-line or as a  $\Pi$ -line at will, yet so much care has to be taken to ensure good contacts at all the plugs, that it is doubtful whether fixed independent T-lines and  $\Pi$ -lines, with fewer switch contacts, are not preferable.

## CHAPTER IX

### COMPLEX QUANTITIES AND ALTERNATING-CURRENT QUANTITIES

It is assumed that the student is already acquainted with the elementary principles of the simple a.c. circuit; so that it will be desirable to review only those features of a.c. operation which bear immediately upon the behavior of a.c. lines.

**Complex Quantities and Plane Vectors.**—*Real quantities* are such as may be represented geometrically by the position of

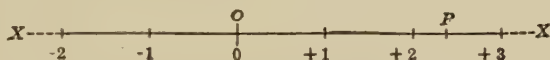


FIG. 60.—Geometrical representation of real numbers by the position of the point  $P$  on the straight line  $-XOX$ .

a movable point  $P$ , Fig. 60, with respect to a fixed point or origin  $O$ , on an indefinitely extending straight line  $-XOX$ . Real quantities include positive and negative quantities, integral as well as fractional.

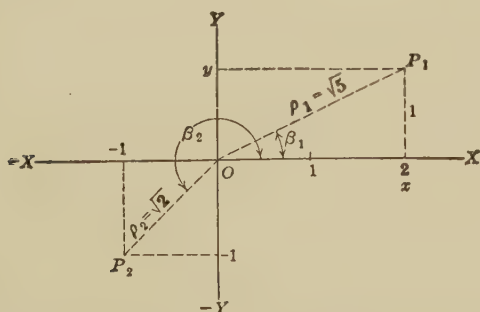


FIG. 61.—Complex numbers represented by the plane vectors  $OP_1$  and  $OP_2$ .

*Complex quantities* are such as may be represented geometrically by the position of a movable point  $P$ , in a plane, with respect to a fixed point or origin  $O$  in that plane (Fig. 61).

The position of  $P$ , with respect to  $O$ , can be defined in either of two ways, namely:

1. In rectangular coördinates, sometimes called Cartesian coördinates.

2. In polar coördinates.

In rectangular-coördinate definition, there are two fixed mutually perpendicular axes,  $-XOX$  and  $-YOY$ , in the plane of reference. The former is called the *real axis*, or *axis of reals*; since it corresponds to the axis of real quantities in Fig. 60. The latter ( $-YOY$ ), is called the *imaginary axis*, or *axis of imaginaries*. The qualifying adjective "imaginary," has historical significance only, and does not mean that there is anything indeterminate or fictitious about this axis. The *orthogonal*

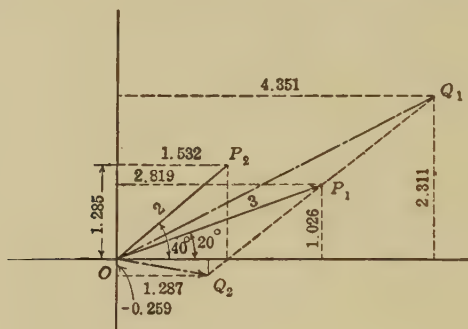


FIG. 62.—Sum and difference of two plane vectors  $OP_1$  and  $OP_2$ .

or perpendicular projections of  $OP$ , on the  $X$ - and  $Y$ -axes, are respectively the *real component*  $x$ , and the *imaginary component*  $y$ . The straight line  $OP_1$ , Fig. 62, connecting the origin  $O$  with the movable point  $P_1$  is not a *vector*, in the complete sense of that term as used in mathematics, because, although two complex quantities  $OP_1 = 3 \angle 20^\circ$  and  $OP_2 = 2 \angle 40^\circ$ , Fig. 62, have as their sum  $OP_1 + OP_2 = OQ_1$  and as their difference  $OP_1 - OP_2 = OQ_2$ , formed according to the same rules as govern true vectors, yet the product  $OP_1 \times OP_2$  of these two complex quantities is  $OQ$ , Fig. 63, and is equal to the opposite-order product  $OP_2 \times OP_1$ ; whereas two vectors, when multiplied, enjoy a scalar product, as well as a vector product, and the latter depends upon the order of multiplication.

In order to distinguish the straight lines in a plane, which geometrically represent complex quantities, from true vectors,

we may call the former *plane vectors*. In what follows, the term “vector” will mean a “plane vector.”

**Rectangular Plane Vectors.**—The magnitudes and signs of the rectangular components  $x$  and  $y$  completely determine the position of the vector  $OP$ . If  $x$  and  $y$  are both positive,  $OP$  lies in the first quadrant. If  $x$  and  $y$  are both negative,  $OP$  lies in the third quadrant. If  $x$  is  $-$  and  $y$  is  $+$ ,  $OP$  lies in the second quadrant. If  $x$  is  $+$  and  $y$  is  $-$ ,  $OP$  lies in the fourth quadrant.

To express the vector  $OP$  in polar coördinates, we take the same origin  $O$ , and axis of reference  $OX$ , as the fixed *initial line*. From this line, we measure the circular arc  $XOP$ , either in radians, degrees, quadrants, or other specified units of circular angle  $\beta$  (Fig. 61). The length of the vector  $OP$  is called the *modulus* of the polar-coördinate complex quantity; while the circular angle  $\beta$  is called the *argument* of the same. Since the mathematical terms “modulus” and “argument” are not well adapted for practical purposes, we shall follow the terminology suggested by Fleming\* and use the term *size* for the modulus, and the term *slope* for the argument of a polar complex quantity. Any plane vector is thus completely specified either by its real and imaginary components,  $x$  and  $y$ , or by its size  $\rho$  and slope  $\beta$ .† The slope may exceed the range  $+360^\circ$ , or  $+2\pi$  radians; but, in most cases, it is simpler and more convenient to keep within these limits. The positive or counter-clockwise direction of rotation in angle is understood, unless the negative sign is prefixed.

A rectangular-coördinate vector or *rectangular vector* may be written:

$$OP = x + jy \quad \text{vector} \quad (235)$$

where  $j = \sqrt{-1}$ , and indicates that  $y$  is measured along the imaginary axis. Proper signs must be given to both  $x$  and  $y$ .

**Polar Plane Vectors.**—A polar-coördinate vector, or *polar vector*, may be written:

$$OP = \rho e^{i\beta} \quad \text{vector} \quad (236)$$

where  $e$  is the base of Napierian logarithms (2.71828 . . .), and  $\beta$  is in *circular radians*. The factor  $e^{\pm i\beta}$  on being expanded, becomes:

\* See “The Wireless Telegraphist’s Pocketbook,” by Prof. J. A. Fleming, London, 1915.

† The size of a plane vector quantity  $z$  is denoted by  $|z|$ , and its slope may be denoted by  $\angle z$ . Thus if  $z = 1.5\angle 30^\circ$  say, then  $|z| = 1.5$  and  $\angle z = 30^\circ$ .



$$\epsilon^{\pm i\beta} = 1 \pm j\beta - \frac{\beta^2}{2!} \mp j\frac{\beta^3}{3!} + \frac{\beta^4}{4!} \pm j\frac{\beta^5}{5!} - \frac{\beta^6}{6!} \mp \dots \quad \text{numeric } \angle \quad (237)$$

$$= \left(1 - \frac{\beta^2}{2!} + \frac{\beta^4}{4!} - \frac{\beta^6}{6!} + \dots\right) \pm j \left(\beta - \frac{\beta^3}{3!} + \frac{\beta^5}{5!} - \dots\right) \quad (238)$$

$$= \cos \beta \pm j \sin \beta \quad \text{numeric } \angle \quad (239)$$

This is a *versor*, or operator which turns or rotates in one plane the size or modulus  $\rho$  from the original direction  $OX$ , through  $\pm\beta$  radians, as, for example, into the direction  $OP_1$  (Fig. 61).

For ordinary purposes of definition and operation, however, it is sufficient to write (236) in the simpler *slope notation*.\*

$$OP = \rho \angle \beta \quad \text{vector } \angle \quad (240)$$

which shows that  $OP$  has a size of  $\rho$  units, and is displaced in phase through a slope of  $\beta$  circ. radians in the positive direction. If  $\beta$  is expressed in degrees, we may write it

$$OP = \rho \angle \beta^\circ \quad \text{vector } \angle \quad (241)$$

If we desire to express a negative phase or angle of rotation, we may write the polar vector

$$OP = \rho \nabla \beta^\circ \text{ or } \rho \angle -\beta^\circ \quad \text{vector } \angle \quad (242)$$

The size  $\rho$  may be regarded as essentially positive; but a negative sign applied to it is equivalent to a change of  $\pi$  radians, or  $180^\circ$ , in the slope. That is

$$-\rho \angle \beta^\circ = +\rho \angle (\beta \pm 180^\circ) \quad \text{vector } \angle \quad (243)$$

### Interchangeability of Rectangular and Polar Plane Vectors.—

It is evident from the elementary trigonometry of Fig. 61, that

$$\rho \angle \beta^\circ = \sqrt{x^2 + y^2} \left| \tan^{-1} \left( \frac{y}{x} \right) \right| \quad \text{numeric } \angle \quad (244)$$

so that a vector whose rectangular coördinates  $x$  and  $y$  are given, can be converted into a polar vector, whose size is the square root of the sum of the square of the components, and the tangent of whose slope is their ratio  $y/x$ .†

\* "On the Fall of Pressure in Long-distance A. C. Conductors," by A. E. Kennelly. *Elec. W. N. Y.*, Vol. 23, p. 17, January 6, 1894. New slope notation.

† Slide rules are obtainable by which vectors can be readily transformed from polar to rectangular coördinates, or reciprocally. Curve sheets are also available graduated both in polar and rectangular coördinates, for enabling the transfer from one to the other to be effected by inspection.



We may also write (244) in a form more convenient for computation (see page 150):

$$\begin{aligned} \rho \angle \beta^\circ &= x \sqrt{1 + \left(\frac{y}{x}\right)^2} \left| \tan^{-1} \frac{y}{x} \right| = x \sec \beta^\circ \left| \tan^{-1} \frac{y}{x} \right| \\ &= x \sec \beta^\circ \angle \beta^\circ \quad \text{numeric } \angle \quad (245) \end{aligned}$$

that is, we may find  $\tan^{-1} (y/x) = \beta^\circ$ , and then  $\rho$  will be  $x \sec \beta^\circ$ ; or

$$\begin{aligned} \rho \angle \beta^\circ &= y \sqrt{1 + \left(\frac{x}{y}\right)^2} \left| \cot^{-1} \frac{x}{y} \right| = y \operatorname{cosec} \beta^\circ \left| \cot^{-1} \frac{x}{y} \right| \\ &= y \operatorname{cosec} \beta^\circ \angle \beta^\circ \quad \text{numeric } \angle \quad (246) \end{aligned}$$

Formula (245) is useful for transforming rectangular to polar coördinates, when  $y$  is smaller than  $x$ , or  $\rho$  makes an angle of less than  $45^\circ$  with the  $-XOX$ -axis; while (246) is preferable when  $\rho$  makes a large angle with that axis.

Reciprocally,

$$x + jy = \rho \cos \beta + j\rho \sin \beta \quad \text{numeric } \angle \quad (247)$$

so that the real and imaginary components of a vector are *respectively the cosine and sine components of the size*.

**Addition and Subtraction of Plane Vectors.**—To add plane vectors, express them in rectangular coördinates. *The summation vector will then have, as its real component, the algebraic sum of the reals, and, as its imaginary component, the algebraic sum of the imaginaries.*

Thus, the sum of  $(5 + j2)$  and  $(-3 - j1)$  is  $2 + j1$ . In Fig. 62, the summation  $3 \angle 20^\circ + 2 \angle 40^\circ = (2.819 + j1.026) + (1.532 + j1.285) = 4.351 + j2.311 = OQ_1$ .

Subtraction of a vector is merely its addition according to the preceding rule, after the signs of both of its components have been reversed.

Thus, to subtract  $(2 + j7)$  from  $(5 - j3)$  add  $(-2 - j7)$  to  $(5 - j3) = 3 - j10$ . In Fig. 62,  $3 \angle 20^\circ - 2 \angle 40^\circ = (2.819 + j1.026) - (1.532 + j1.285) = 1.287 - j0.259 = OQ_2$ .

**Multiplication of Plane Vectors.**—To multiply plane vectors, express them in polar coördinates, or as *polars*. *The product will then have, for its size, the product of the sizes, and for its slope, the algebraic sum of the slopes; or*

$$B \angle \beta_2 \times A \angle \beta_1 = A \angle \beta_1 \times B \angle \beta_2 = AB / \beta_1 + \beta_2 \quad \text{numeric } \angle \quad (248)$$

Thus,

$$5 \angle 30^\circ \times 2 \angle 20^\circ = 10 \angle 50^\circ$$

In Fig. 63,  $OP_1 \times OP_2 = 3 \angle 20^\circ \times 2 \angle 40^\circ = 6 \angle 60^\circ = OQ$ .

**Division of Plane Vectors.**—To divide one plane vector by a second, express both as polars, such as  $A \angle \beta_1$  and  $B \angle \beta_2$ . The quotient will then have, for its size, the quotient of the sizes, and for its slope the algebraic difference of the slopes, or

$$A \angle \beta_1 \div B \angle \beta_2 = \frac{A}{B} \angle \beta_1 - \beta_2 \quad \text{numeric } \angle \quad (249)$$

Thus

$$7 \angle 60^\circ \div 2 \angle 10^\circ = 3.5 \angle 70^\circ.$$

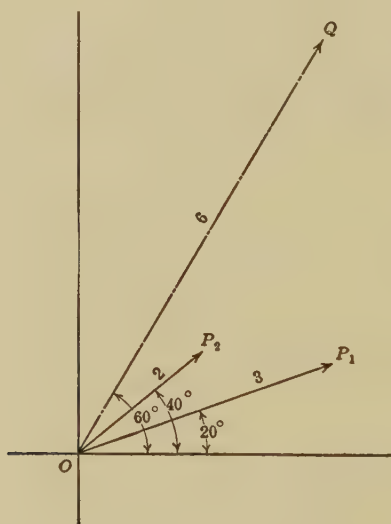


FIG. 63.—Product of two complex quantities represented as plane vectors.

Vector multiplication and division may also be effected between rectangulars, although the formulas are not so simple. Thus

$$(x_1 + jy_1)(x_2 + jy_2) = (x_1x_2 - y_1y_2) + j(x_1y_2 + x_2y_1) \quad \text{numeric } \angle \quad (250)$$

The real component of the product contains a difference, and the imaginary component a sum of products in  $x$  and  $y$ . Again

$$\frac{x_1 + jy_1}{x_2 + jy_2} = \frac{(x_1 + jy_1)(x_2 - jy_2)}{(x_2 + jy_2)(x_2 - jy_2)} = \frac{(x_1x_2 + y_1y_2) + j(x_1y_2 - x_2y_1)}{x_2^2 + y_2^2} \quad \text{numeric } \angle \quad (251)$$

These expressions (250) and (251) are so awkward, by comparison with (248) and (249), that it usually saves time to convert rectangulars to polars, in order to effect either multiplication, division, involution or evolution.

**Reciprocals of Vectors.**—If a plane vector is expressed in polar coördinates, its reciprocal has for its size the reciprocal of the vector's size, and for its slope, the negative of the vector's slope; or

$$\frac{1}{A \angle \beta} = \frac{1}{A} \nabla \beta = \frac{1}{A} \angle -\beta \quad \text{numeric } \angle \quad (252)$$

Thus

$$\frac{1}{5 \angle 60^\circ} = 0.2 \nabla 60^\circ.$$

The corresponding result in Cartesian vectors is:

$$\frac{1}{x + jy} = \frac{1}{x + jy} \times \frac{x - jy}{x - jy} = \frac{x - jy}{x^2 + y^2} \quad \text{numeric } \angle \quad (253)$$

**Involution and Evolution of Plane Vectors.**—*The  $n$ th power of a polar plane vector has for its size the  $n$ th power of the size, and for its slope  $n$  times the slope of the polar; or*

$$(A \angle \beta)^n = A^n \angle n\beta \quad \text{numeric } \angle \quad (254)$$

Thus

$$(5 \angle 20^\circ)^3 = 5^3 \angle 60^\circ = 125 \angle 60^\circ.$$

Similarly, the  $n$ th root of a polar  $A \angle \beta$ , has for its size  $A^{1/n}$ , the  $n$ th root of the size, and for its slope  $\angle \beta/n$ , the  $n$ th part of the slope.

Thus

$$(64 \angle 45^\circ)^{1/2} = 8 \angle 22^\circ.5.$$

Fractions of a degree may be expressed in minutes and seconds, but often more conveniently in decimals of a degree, when decimal tables of circular functions are available. The sexagesimal system of angles wastes, in the aggregate, a large amount of the time of engineers.

**Complex Hyperbolic Angles.**—We have already seen that a *real* hyperbolic angle is associated with a hyperbolic sector, in a manner analogous to the association of a *real* circular angle with a circular sector. We shall next see that an *imaginary hyperbolic angle* is associated with a circular sector. Similarly, an *imaginary circular angle* is associated with a hyperbolic sector. Consequently, there is a close cross-con-





**Sine of a Complex Hyperbolic Angle. Geometrical Construction.**—In the plane  $XOY$ , Fig. 65, with origin  $O$ , and unit radius  $OA$ , describe the rectangular hyperbola  $HABH'$ , whose asymptote is  $OTS$ . If the angle whose sine is required is  $1 + j2$ , draw the radius-vector  $OB$ , enclosing a hyperbolic angle  $AOB$  of 1 radian. Its sine will be  $OX = bB$ . Describe 2 circ. radians in the plane  $XOY$ , from  $OX$  to  $Od$ , enclosing the circular angle  $XOd$ . Let another plane, which we may call the reference plane, pass through  $-XOX$ , and make with the plane  $XOY$  an angle whose circular sine\* is the hyperbolic tangent  $At$ . Project the point  $d$  perpendicularly out of the plane  $XOY$ , until it meets the reference plane in the point  $P$ . Then  $OP$  in the reference plane will be the required complex sine, having components in that plane  $OM$  and  $MP$ , i.e.,  $-0.48906 + j1.4031 = 1.4859 \angle 109^\circ.12'.58''$ . It is evident that the sine of  $1 + j1.0$  hyps. would be  $OQ$ , and of  $1 + j1.5$  hyps.  $OR$ , both in the reference plane. Moreover, the locus of  $\sinh(1 + jy)$  will be the ellipse  $XQRPXb$ , whose semi-major axis is  $Ob = \cosh 1$ , and whose semi-minor axis  $OX = bB = \sinh 1$ . Thus, *the imaginary component of a hyperbolic angle, whose sine or cosine is required, may be regarded as producing rotation over a corresponding circular sector; while the real component produces rotation over a corresponding hyperbolic sector.*

**Three-dimensional Model for the Projection of Cosines and Sines of Complex Hyperbolic Angles.**—Figure 66 is a perspective view of a geometrical model† for realizing the construction of Fig. 64, and enabling cosines and sines of complex angles to be obtained by projection. A sheet of squared coördinate paper is laid on the horizontal plane  $XOY$ , the origin of coördinates being at the center  $O$ , and the distance  $OC$ —a decimeter—being taken as unity. A brass half-rod  $AOB$ , is clamped to the base-board along the  $OX$ -axis. The brass wire  $CES$ , in the vertical plane, or  $XOZ$ -plane, follows the curve of a rectangular hyperbola, having its center at  $O$  and unit radius  $OC$ . The upper end of this curved wire rests on the supporting vertical brass pillar  $BS$ . Real hyperbolic angles can be marked off along  $CES$  by a

\* Incidentally, this circular angle is called the "Gudermannian of the hyperbolic angle."

† "A New Geometrical Model for the Orthogonal Projection of the Cosines and Sines of Complex Angles," by A. E. Kennelly, *Proc. Am. Acad. Arts, Sci.*, April, 1919, vol. liv, No. 5, pp. 371-378.



thread from center  $O$  moving as radius-vector over the wire. Thus the point  $E$  on the wire  $CES$  marks a hyperbolic sector  $COE$ , corresponding to 1 hyp. radian, or 1 hyp. Following the construction described in relation to Fig. 64, we can find the cosine of the angle  $COE$ , or  $\cosh \theta$ , by dropping a perpendicular plummet and thread from the point  $E$  on to the  $OX$ -axis at  $D$ ; so that the distance  $OD$  shall measure  $\cosh \theta$ . In this case, with  $\theta = 1$ , the distance  $OD$  will be 1.543 decimeter units. If, however, the angle is complex, of the type  $(\theta_1 + j\theta_2)$  and contains the  $j$  component  $j\theta_2$ , we must execute a second stage in the process, and follow a circular path in space of  $\theta_2$  units in circular angle. At the foot of the plummet perpendicular  $ED$ , there rises from the

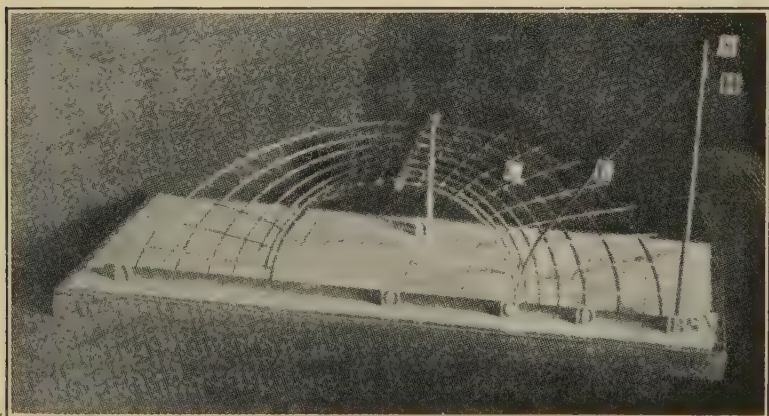


FIG. 66.—Perspective view of three-dimensional model for the projection of complex hyperbolic cosines and sines.

axis  $OX$ , an inclined brass semicircle  $DG$ . This semicircle has its center at  $O$ , and radius  $OD$ , but its plane is inclined from the vertical in such a manner that the top of the semicircle reaches an elevation of 1 decimeter unit above the base plane  $XOY$ . Eight such inclined semicircles are seen in the model, forming a skeleton frame, but, theoretically, their number should be indefinitely great, so as to provide one such semicircle for each and every plummet point along  $CX$ . The first semicircle  $OC$  has unit radius, and stands strictly vertical in the same  $XOZ$  plane as the hyperbola  $CES$ ; but all the other semicircles are inclined, with their tops on the same level, one unit above the base.

If  $\theta_2$  be taken by way of illustration as 0.6 quadrant, or  $54^\circ$ , we must follow the semicircle  $DG$  to the point  $G$ , such that the

arc  $DG$ , in the plane of the semicircle, corresponds to this angle. We now drop a plummet from this point  $G$  on to the horizontal base, so as to touch the same at some point  $g$ , not marked in the figure. The plane-vector straight line  $Og$ , in the plane  $XOY$ , will then mark the cosine of the complex angle  $(\theta_1 + j\theta_2)$  or

$$Og = \cosh (\theta_1 + j\theta_2) = x + jy = \rho \angle \beta \quad (255)$$

If  $\theta_2$  exceeds the value  $\pi/2$  or 1 quadrant, the stopping point will lie on the left-hand side of the top horizontal bar. If  $\theta_2$  should lie between  $\pi$  and  $2\pi$ , or between 2 and 4 quadrants, the stopping point will be beneath the base, and the projection to the  $XOY$ -

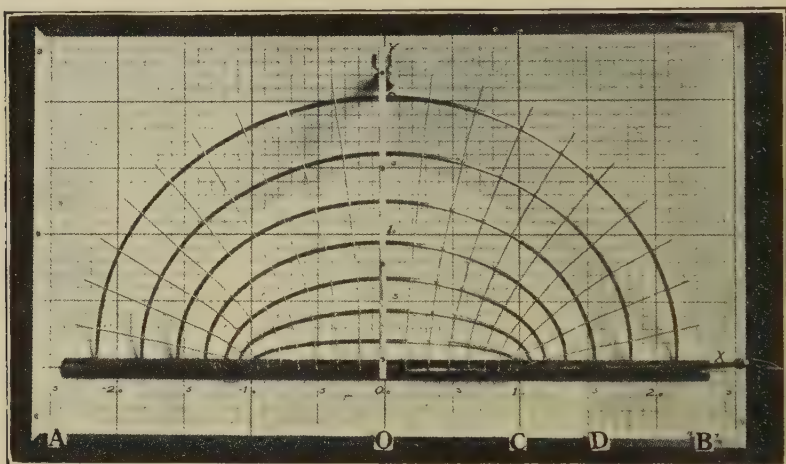


FIG. 67.—Plan view of model, taken from a point on  $OZ$  axis 15 units (decimeters) from  $O$ .

plane will be upwards, because the semicircles are supposed to be complete circles, with their lower halves invisible beneath the base. Consequently, if  $\theta_2$  contains many quadrants, each step of 4 quadrants involves one complete revolution around the circle, and may be omitted from the process. The model illustrated would serve to indicate values of  $\theta_1$  no greater than about  $\theta_1 = 1.5$ ; but values of  $\theta_2$  are included from  $+\infty$  to  $-\infty$ , noting that adding or subtracting 2 quadrants from  $\theta_2$  reverses the direction of the vector  $Og$ , without altering its magnitude.

The model is not serviceable for the numerical evaluation of  $\cosh (\theta_1 + j\theta_2)$ , for lack of geometrical precision; but it aids in giving a clear mental picture of the process indicated in Fig. 64. The brass tie wires which connect points of the same value of  $\theta_2$

in decimals of a quadrant, are horizontal. A plan view of the model as photographed from above, at a distance of 15 units, or 1.5 meters, is shown in Fig. 67. The various circles corresponding each to a different value of  $\theta_1$ , project into ellipses, and the tie wires each corresponding to a different value of  $\theta_2$ , project into hyperbolas. All the ellipses and hyperbolas are confocal, and the two common foci are situated on the  $X$ -axis, one at  $+1$  and the other at  $-1$ .

A corresponding model, conforming to the geometry of Fig. 65, could be prepared for projecting the plane-vector values of  $\sinh (\theta_1 + j\theta_2)$ ; or the model of Figs. 66 and 67, can be used to project sines as well as cosines, by using the identity

$$\sinh (\theta_1 + j\theta_2) = -j \cosh \left\{ \theta_1 + j \left( \theta_2 + \frac{\pi}{2} \right) \right\} \quad (256)$$

A region near the center of a chart used for obtaining the numerical values of  $\cosh (\theta_1 + j\theta_2)$  or of  $\sinh (\theta_1 + j\theta_2)$ , to a limited degree of precision sufficient for many engineering purposes, is presented in Fig. 219. Here the confocal ellipses and hyperbolas pertaining, respectively, to constant  $\theta_1$  and constant  $\theta_2$ , have their foci at points A and B, the center of the system being at O. This chart is readily interpreted after a comprehensive examination of the model.

**Cosine of a Complex Hyperbolic Angle. Trigonometrical Expressions.**—Referring to (588), Appendix A, the cosine of a complex angle,

$$\cosh (x \pm jy) = \cosh x \cosh jy \pm \sinh x \sinh jy \quad (257)$$

$$= \cosh x \cos y \pm j \sinh x \sin y \quad (258)$$

$$= \cosh x \cos y \pm j \cosh x \sin y \tanh x \quad (259)$$

$$= \frac{1}{2}(\epsilon^x \angle \pm y + \epsilon^{-x} \angle \pm y) \quad (260)$$

$$= \sqrt{\cosh^2 x - \sin^2 y} \angle \pm \tan^{-1} (\tanh x \tan y) \quad (261)$$

$$= \sqrt{\sinh^2 x + \cos^2 y} \angle \pm \tan^{-1} (\tanh x \tan y) \quad (262)$$

$$= \sqrt{\cosh 2x \cdot \cos 2y} \angle \pm \tan^{-1} (\tanh x \tan y) \quad (263)$$

$$\text{where } \cos 2z = \frac{\cos 2y}{\cosh 2x} \quad (264)$$

Each and all of the above formulas (257) to (264) has advantages in particular cases for purposes of computation, while (259) is the formula embodied in the construction of Figs. 64 and 66.

**Sine of a Complex Hyperbolic Angle. Trigonometrical Expressions.**—Referring to (585), Appendix A, the sine of a complex angle,

$$\sinh(x \pm jy) = \sinh x \cdot \cosh jy \pm \cosh x \cdot \sinh jy \quad (265)^*$$

$$= \sinh x \cdot \cos y \pm j \cosh x \cdot \sin y \quad (266)$$

$$= \sinh x \cdot \cos y \pm j \sinh x \cdot \sin y \cdot \coth x \quad (267)$$

$$= \frac{1}{2}(\epsilon^x \angle \pm y - \epsilon^{-x} \angle \pm y) \quad (268)$$

$$= \sqrt{\sinh^2 x + \sin^2 y} \angle \pm \tan^{-1}(\coth x \cdot \tan y) \quad (269)$$

$$= \sqrt{\cosh^2 x - \cos^2 y} \angle \pm \tan^{-1}(\coth x \cdot \tan y) \quad (270)$$

$$= \sqrt{\cosh 2x \cdot \sin z} \angle \pm \tan^{-1}(\coth x \cdot \tan y) \quad (271)^*$$

where  $z$  has the meaning given in (264)

The construction of Fig. 65 is derived from (267); but (265) to (271) are all useful.

**Tangent of a Complex Hyperbolic Angle. Trigonometrical Expression.**—A geometrical construction for  $\tanh(x + jy)$  involving orthogonally intercepting circles, has long been known,<sup>†</sup> and has been given in detail elsewhere.<sup>‡</sup> For practical purposes, however, we may obtain an expression for the tangent, by dividing the cosine into the sine, using any corresponding pairs of formulas between (257) and (271). An additional useful formula is

$$\tanh(x \pm jy) = \frac{\sinh 2x}{\cosh 2x + \cos 2y} \pm j \frac{\sin 2y}{\cosh 2x + \cos 2y} \quad (272)$$

The sines, cosines, and tangents of complex hyperbolic angles have been extensively tabulated and charted<sup>§</sup> for practical use. These will be frequently referred to in what follows. For accurate arithmetical work, the tables are the more important. For slide-rule computations, where swiftness is desired, with a correspondingly lesser degree of precision, the charts are preferable.

\* Formulas (263), (264), and (271), are due to Prof. C. L. Bouton.

† Crystal's "Algebra," Edinburgh, 1889.

‡ "Application of Hyperbolic Functions to Electrical Engineering Problems," Chapter V.

§ "Tables of Complex Hyperbolic and Circular Functions," by A. E. Kennelly, Harvard University Press, 1913.

"Chart Atlas of Complex Hyperbolic and Circular Functions," by A. E. Kennelly, Harvard University Press, 1913.



**Quadrant Measure for Circular Angles.**—It has been pointed out, in connection with Figs. 64 and 65, that the vector value of either  $\sinh (x + jy)$  or  $\cosh (x + jy)$  is cyclically repetitive, at successive intervals of  $2\pi$  circ. radians in  $y$ . This makes an awkward interval for tabulation. A much more convenient expedient is to express the imaginary component in quadrants, since 4 quadrants are equivalent to  $2\pi$ , or 6.283 . . . radians. In Figs. 64 and 65, the lower half of the  $y$  circles are indicated in quadrant measure. Thus  $\cosh (1 + j\underline{2.5}) = -1.09 - j0.83$ , and  $\sinh (1 + j\underline{2.5}) = -0.83 - j1.09$ . This division with decimal subdivisions corresponds precisely to the French system of dividing the circle in grades, or decimals of a quadrant. In order to reduce a complex angle  $(x + jy)$  to quadrant measure, the imaginary  $y$  must be *quadranted i.e.*, divided by  $\pi/2$ , or 1.57079 . . . . That is

$$x \pm jq = x \pm j \frac{y}{1.57079 \dots} = x \pm j0.63662y \text{ hyps. } \angle \quad (273)$$

Thus,  $1 + j2$  in radian measure, is  $1 + j\underline{1.2732}$  in quadrant measure. It is advisable to *underscore quadranted imaginaries*, in order clearly to distinguish them from radians circular measure.

Another advantage pertaining to the use of French quadrant measure, in dealing with the imaginary components of hyperbolic angles, is that when  $x$  exceeds 4.0, it is easily shown from (260) and (268), that for most practical purposes,\*

$$\sinh (x + jy) \cong \cosh (x + jy) \cong \frac{e^x}{2} \angle y \text{ numeric } \angle \quad (274)$$

where the result is expressed as a polar, with its argument in circular measure, which, for practical purposes, has to be reduced to degrees or *grades*, according to the tables available. But

$$\sinh (x + jq) \cong \cosh (x + jq) \cong \frac{e^x}{2} \angle q \text{ numeric } \angle \quad (275)$$

That is, *the sine or cosine of a hyperbolic angle with a large real component  $x$  has a size of half the exponential of  $x$ , and a slope equal to the imaginary  $q$ , expressed in quadrants, or in grades after shifting the decimal point.*

The tables and charts are largely based on quadrant measure in the imaginary components of the entering hyperbolic angles, and we shall often use quadrant measure in what follows.

\* The symbol  $\cong$  stands for "approximately equals."

**Simple Alternating-current Circuits.**—A simple a.c. circuit is one which has resistance and reactance (inductive, condensive, or both) and which carries a single frequency, *i.e.*, the e.m.f. and current are sinusoidal without harmonics. In Fig. 68, such a circuit is indicated as having an impressed root-mean-square (r.m.s.) e.m.f. of  $E$  volts, by voltmeter, impressed upon a non-ferrie inductive impedance  $Z$  ohms  $\angle$ , connected between the mains  $mm$ , the current supplied to this reactor being  $I$  amp.  $\angle$  r.m.s. by ammeter, and the active power  $P_a$  watts, by wattmeter. The impressed frequency  $f$  in\* cycles per second, has an angular velocity,

$$\omega = 2\pi f \quad \text{circ. radians/sec.} \quad (276)$$

In the case represented in Fig. 68, let  $f = 63.66$  cyps, for which  $\omega = 400$  radians per sec. Let the impedance of the coil, as appar-

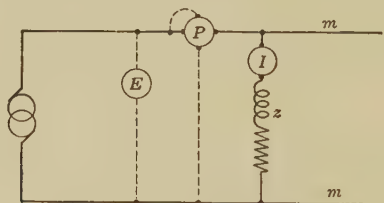


FIG. 68.—Simple alternating-current circuit with the impedance  $z$  measured both in size and in slope by volt-am-wattmeter readings.

ent from volt-am-wattmeter measurements, be 10 ohms, with a power factor of 80 per cent., *i.e.*, 8 ohms *active resistance* and 6

\* Signalling frequencies in submarine and land telegraphy range from 1 to 100 or more cyps ( $\omega = 6$  to 628). Power and lighting frequencies (low frequencies) ordinarily range from 25~ to 60~ ( $\omega = 157$  to  $\omega = 377$ ). Telephone frequencies (audio frequencies or moderate frequencies) ordinarily range from 60~ to 10,000~ ( $\omega = 377$  to  $\omega = 62,800$ ). A standard reference telephonic frequency is  $\omega = 5,000$ . Radio frequencies (high frequencies) ordinarily range from 10,000~ to 100,000,000~, or more. Alternating-current engineering, taken broadly, thus includes the range from  $f = 1$  to  $f = 10^8$ , ( $\omega = 6.28$  to  $\omega = 6.28 \times 10^8$ ).

The term "cycles" is often inaccurately employed to connote "cycles per second" in abbreviated form. But the word "cycle" cannot accurately represent both a "periodic event" and the number of such events in unit time. On the other hand, the constant repetition of the correct phrase "cycles per second" when discussing frequencies, is both burdensome and redundant. This correct phrase may however be written in the abbreviated form "cy.p.s." The periods may then, for convenience, be dropped, leaving frequencies expressed in "cyps." It is proposed to use this expression *cyps.* hereafter, as an abbreviated form of "cycles per second."



ohms *inductive reactance*. The active resistance of a coil is that which it appears to offer from such a.c. measurements. The active resistance of a coil ordinarily exceeds the d.c. resistance, and increases with the frequency. It may include elements due

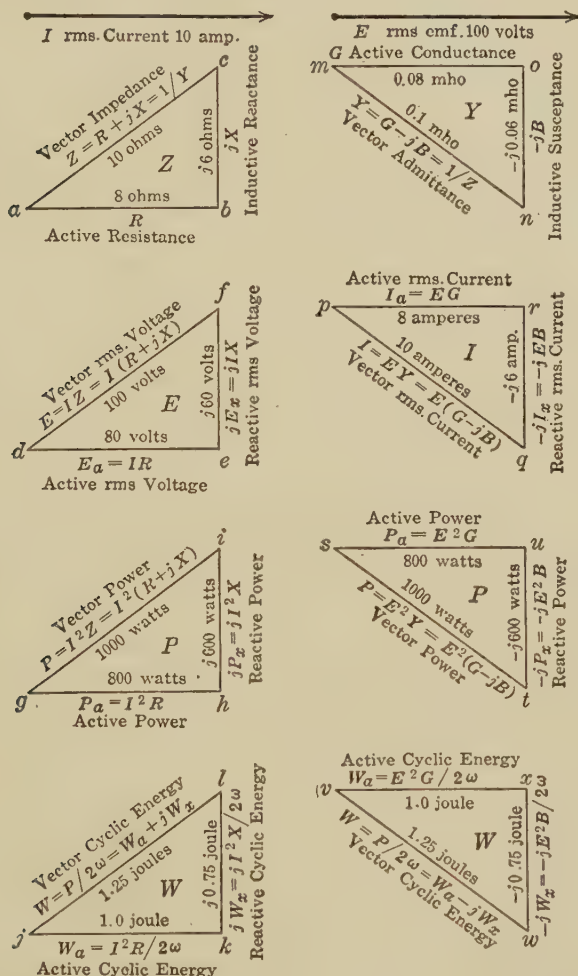


FIG. 69.—Vector diagrams for simple inductive alternating-current circuit.

to *skin effect* (imperfect current distribution over the cross-section of the conductor), eddy-current loss in the conductor, and hysteretic and eddy-current losses in neighboring iron or steel. The inductive reactance of a coil is the positive reactive resistance

which it appears to possess by reason of its e.m.f. of self-inductance, as modified by skin effect and eddy currents. It is assumed

$$jX = jL\omega \qquad j \text{ ohms} \quad (277)$$

that expresses the relation between the reactance  $jX$  of the coil at impressed angular velocity  $\omega$ , and the apparent inductance  $L$  henrys. In the case considered,  $L = 0.015$  henry.

Since the current and the impressed e.m.f. will ordinarily differ in phase, it is optional to select either of those quantities as having *reference phase*. That is, we may consider the current  $I$  as of standard phase and the impressed e.m.f.  $E$  as leading in this case with respect thereto; or, we may consider the e.m.f. as of standard phase, and the current  $I$  as lagging with respect to the same. Each assumption gives rise to a series of four simple stationary vector diagrams, as indicated in Fig. 69. The left-hand column of the *ZEPW* triangles employs the current as of standard phase; while the right-hand column of *YIPW* triangles, employs the e.m.f. as of standard phase.

**Vector Impedance.**—Commencing with the left-hand column, the impedance triangle  $abc$  has for its base, the active resistance  $R$ , in this case 8 ohms, and for its vertical side, the inductive reactance  $+jX$ ,\* in this case  $j6$  ohms. If the circuit contained condensive reactance, instead of inductive reactance, this vertical side would be in the negative† direction, or would be  $-jX$  ohms. We might also describe the inductive impedance in this case as  $10 \angle 36^\circ.52'.11''$  ohms.

**Vector Electromotive Force.**—If next we multiply this impedance by  $I = |I| \angle 0^\circ = 10 \angle 0^\circ$  amp., we obtain the  $E$  triangle  $def$ , with  $IR = 80$  active volts,  $jIX = j60$  reactive volts, and  $E = IZ = I(R + jX)$  total or vector volts. This is a stationary vector triangle, in which the horizontal or active component is the

\*  $j$  for  $\sqrt{-1}$  was first introduced into electrotechnics by Bedell and Crehore, "Alternating Currents," 1893. The application of complex arithmetic and plane vectors to impedance, and the a.c. circuit, was first introduced by the author, "Impedance," *Trans. A. I. E. E.*, vol. x, p. 175, April, 1893. The extension of complex quantities and plane vectors to potentials and currents is due to Steinmetz, "Complex Quantities and Their Use in Electrical Engineering," *Proc. Intern. Elec. Congress*, Chicago, August, 1893.

† International notation, according to the decision of the International Electrical Commission, at its Turin meeting in 1911, calls for  $R + jX$  as the impedance of an inductance coil, here followed. See Standardization Rules of the A. I. E. E.

r.m.s. voltage component consumed actively in overcoming resistance. The vertical or reactive component is the r.m.s. voltage component consumed reactively, in overcoming reactive resistance or reactance; *i.e.*, in neutralizing the c.e.m.f. of self-induction. The total or vector voltage may be described as  $100 \angle 36^\circ.52'.11''$  volts, to *current standard phase*.

**Vector Power to Current Phase.**—If we multiply the  $E$  voltage triangle by  $|I| \angle 0^\circ = 10 \angle 0^\circ$  amp., we obtain the power triangle  $ghi$ . Here  $gh$  is the active power  $P_a = I^2 R$  watts, both the average and the maximum cyclic rate of transferring energy out of the circuit, in the form either of heat, chemical, or mechanical energy. The imaginary component  $hi$  is the reactive power, or the maximum cyclic rate of transferring energy from the mains  $mm$ , Fig. 68, into the magnetic flux of the coil, and back again. When the r.m.s. current  $I$  in the coil reaches a maximum or crest value  $I_m$  amp., either plus or minus, the coil contains magnetic energy  $LI_m^2/2 = LI^2$  joules. At the current zero points, this energy disappears from the coil, returning to the mains and generator system. The maximum cyclic rate of transfer of this energy is equal to this reactive power  $jP_x$  watts. The reactive power is sometimes called “wattless power,” but the term is both erroneous and misleading. The reactive power  $jI^2 X$  is just as “wattful” as the active power  $I^2 R$ . The only difference is that  $jI^2 X$  is the activity of transferring undissipated energy from one part of the circuit to another, while  $I^2 R$  is the activity of transferring energy from the circuit to its surroundings. This  $I^2 R$  power is therefore dissipated or expended; whereas the  $I^2 X$  power is conserved and, in the steady state, requires no energy to maintain it. The energy of active power is spent outside the circuit; but the energy of reactive power is loaned to the circuit during one half of the energy cycle and returned from the circuit to the source during the other half. It is true that in ordinary industrial practice, reactive power has no effect on customers’ watt-hour meters, and therefore is not saleable, but it is illogical to deny the existence of power, merely because it is ordinarily unsaleable.

Similarly, the hypotenuse  $gi$  is the total or *vector power*  $I^2 Z$  watts. It is commonly described as volt-amperes, to distinguish it from active power. This distinction is a useful one, provided it is realized that a *vector volt-ampere* is likewise a *vector watt*. In this case, the vector power is 1 kw. or 1,000 volt-amp. with an

active component of 800 watts, and a reactive component of  $j600$  watts.

**Vector Cyclic Energy.**—If we divide the  $P$  triangle by  $2\omega$ , or twice the impressed angular velocity, we obtain the stationary vector diagram  $jkl$ . Here  $jk$  is the active maximum cyclic energy, which is added in successive + and - blocks, in each energy cycle, to the stream of outgoing active energy leaving the circuit.  $W_a$  is the cyclic active energy throb, as will be seen later. The reactive component  $jW_x$  is the maximum cyclic energy, added in successive + and - blocks to the energy of the magnetic flux linked with the coil. This *reactive energy* block  $W_x = 0.75$  joule. When at its negative maximum, it destroys the energy in the coil ( $0.75 - 0.75 = 0$  joule). When at its positive maximum, it produces the full cyclic magnetic energy in the coil ( $0.75 + 0.75 = 1.5$  joules). The r.m.s. current  $I$  being 10 amp., its maximum cyclic value is  $I\sqrt{2} = 14.14$  amp., and the maximum cyclic magnetic energy is

$$W_m = \frac{1}{2}LI_m^2 = LI^2 = 2W_x \quad \text{joules} \quad (278)$$

in this case  $\frac{1}{2} \times 0.015 \times (14.14)^2 = 1.5$  joules, as already found. The frequency of this energy cycle is  $2f$ , or twice the frequency of the impressed current; because  $LI_m^2/2$  reaches its maximum at each current wave crest, whether  $I$  is plus or minus. Its angular velocity is therefore  $2\omega$  radians per second.

**Vector Admittance.**—Turning now to the second column in Fig. 69, the vector admittance of the branch circuit in Fig. 68 is the reciprocal of the vector impedance  $Z$ . In this case  $Y = 1/10 \angle 36^\circ.52'.11'' = 0.1 \angle 36^\circ.52'.11'' = 0.08 - j0.06$  mho. This admittance is represented at *mon*. The real component  $G$ , or *mo*, is called the *active conductance*. The imaginary component *on* is  $-jB$ , the *inductive susceptance*. If the branch circuit under test in Fig. 68 were condensive, instead of being inductive; *i.e.*, if a condenser were either substituted for the reactor, or a condenser of preponderating reactance were inserted in series with the coil, then the susceptance  $jB$  would be plus, instead of minus, and would become a *condensive susceptance*. The  $Y$ -triangle, and its subordinates, may thus be either inverted or erect. Its condition in this respect must always be opposite to that of the corresponding  $Z$ -triangle.

**Vector Current.**—If taking the impressed r.m.s. e.m.f.  $E$  as of standard phase, or as inherently possessing zero slope, we mul-



tiply  $Y$  by  $E = |E| \angle 0^\circ$ , we obtain the  $I$  triangle  $prq$ . Here  $pr$  is the active current  $I_a = EG$  amp. The negative perpendicular  $rq$  is the reactive current  $-jI_x = -jEB$  amp. The active component  $I_a$  will be in phase with the impressed e.m.f.  $E$ . The reactive component will be in quadrature with  $E$ .

**Vector Power to Electromotive Force Phase.**—If we multiply the r.m.s. current  $I$ , or  $10 \angle 36^\circ.52'.11''$ , by the impressed e.m.f. at standard phase  $E = 100 \angle 0^\circ$  volts, we obtain the vector power diagram  $sut$ , or  $1,000 \angle 36^\circ.52'.11''$  watts. Here  $E^2G$ , or 800 watts, is the *active power*,  $-jE^2B$ , or  $-j600$  watts, the *reactive power*, and  $E^2Y = E^2(G - jB)$ , the *vector power*. It will be observed that the power diagram  $sut$  is the same as the power diagram  $I^2Z$ , or  $ghi$  reversed, the active 800 watts being the same in both; but the reactive components  $ut$  and  $hi$  being mutually opposite. At first sight, this looks like a contradiction; but, on further examination, the two oppositely directed triangles are consistent. Figs. 70 and 71 show that the crest value of the power always occurs midway between the maxima of voltage and of current. Consequently, *reactive power which is leading with respect to current phase, is lagging with respect to voltage.*

Similar considerations apply to the two  $W$  triangles  $kjl$  and  $vwx$ , which are likewise mutually inverted.

**Instantaneous Diagram to Current Standard Phase.**—Fig. 70 represents diagrammatically one complete cycle of current and voltage in the branch circuit of Fig. 68, under consideration. In order to simplify the diagram, all of the waves, which are actually sinusoids, are indicated by simple zigzag or saw-tooth waves. The maxima, minima, and zero points, are correctly presented by such a diagram; but the intersections of the lines do not carry the same significance.\*

The current  $I$  starts positively at  $0^\circ$ , or with standard phase, and reaches its crest value 14.14 amp. at  $90^\circ$ . The impressed e.m.f.  $E$ , reaches its crest value 141.4 volts, nearly  $37^\circ$  earlier in the cycle. It is analyzed into two components; namely, the active component  $E_a$ , 113.1 volts, in phase with  $I$ , and a leading reactive component  $E_x$ , 84.84 volts, in quadrature with  $I$ .

The successive instantaneous products of current and voltage give rise to a  $P$  sinusoid of double frequency, executing two com-

\* Corresponding diagrams with full sinusoidal curves are given in the original paper "Vector Power in Alternating-current Circuits," by A. E. Kennelly, *Trans. A. I. E. E.*, June 27, 1910.

plete cycles in one cycle of either current or voltage. This power sinusoid has its crests at +1,800 watts, just midway in time between the crests of  $I$  and  $E$ . It is therefore a leading power with respect to the current  $I$ . The power sinusoid has its axis on the line  $pp$  at +800 watts, and its lower maxima at -200 watts. It may therefore be expressed as

$$EI \{ \cos \beta + \sin (2\omega t + \beta) \} = P_a + P \sin (2\omega t + \beta) \quad \text{watts} \quad (279)$$

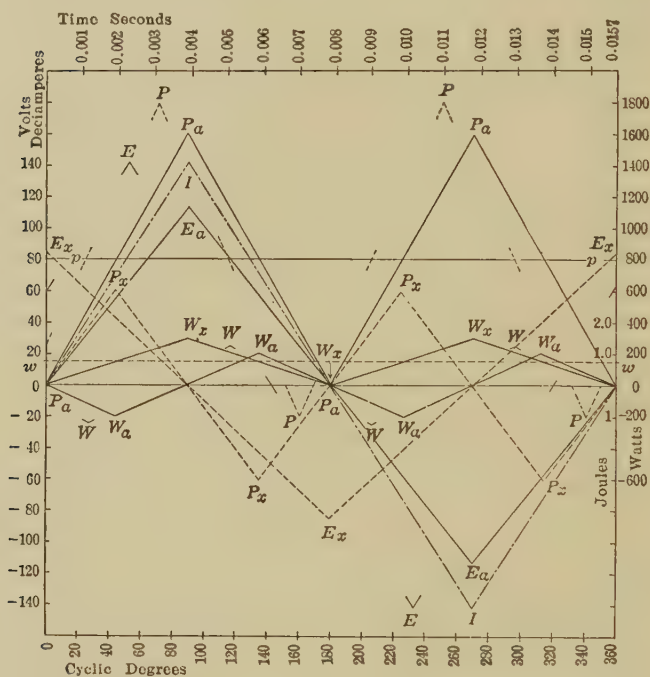


FIG. 70.—Diagram of maximum cyclic current, voltage, power and energy, to current standard phase.

or, in this case,  $800 + 1,000 \sin (2\omega t + \beta)$  watts, where  $\omega =$  radians per sec. It may be analyzed into an active power component  $P_a = 800 - 800 \cos (2\omega t)$  watts corresponding to  $gh$ , Fig. 69, and a leading reactive power component  $P_x$  in quadrature therewith,  $600 \sin (2\omega t)$ , corresponding to  $hi$ , Fig. 69.

The power  $P$  may be considered as the time rate of change of a certain cyclic energy  $W$ . This energy, being the integral of (279) will have a double-frequency sinusoid  $W$ , 1.25 joules in amplitude, and  $37^\circ$  in energy phase, ahead of its active component  $W_a$  of



1.0 joule amplitude. The leading reactive component  $W_x$  of 0.75 joule amplitude has its axis  $ww$  displaced to 0.75 joule above 00. The three powers  $P_x$ ,  $P$  and  $P_a$ , are severally  $90^\circ$  ahead of the three energies  $W_x$ ,  $W$  and  $W_a$ . The amplitude 0.75 joule of the reactive energy, in phase with  $I$ , causes the crest energy of the current  $LI_m^2/2$  to be just 1.5 joules, as has already been pointed out. At the current zeros, the total value of  $W_x$  is zero. These energy components correspond to the three vectors of the  $W$  triangle  $jkl$ , Fig. 69.

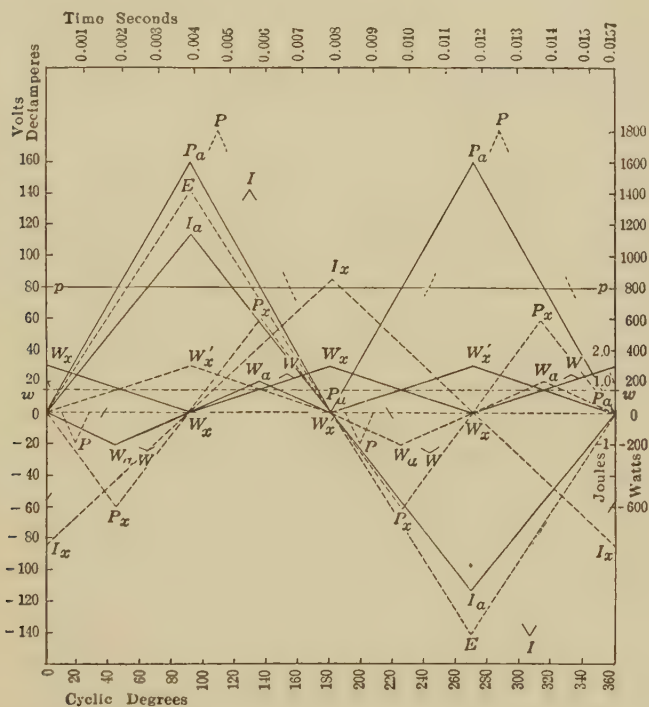


FIG. 71.—Diagram of maximum cyclic voltage, current, power and energy, to voltage standard phase.

**Instantaneous Diagram to Voltage Standard Phase.**—In Fig. 71, the corresponding series of amplitudes and phase relations is presented to voltage standard phase.  $E$  represents the voltage wave of amplitude 141.4, commencing positively at  $0^\circ$ . The current  $I$  lags  $37^\circ$  with respect thereto. The power sinusoid  $P$  has its crest midway between these, and lags  $37^\circ$  of power phase with respect to  $E$ , thus corresponding to  $st$ , in Fig. 69. This power

may be analyzed into an active component  $P_a$ , of 800 watts amplitude, and a lagging reactive component  $P_x$  of 600 watts, corresponding to *ut*, Fig. 69. To these three cyclic double-frequency powers correspond three cyclic double-frequency energies  $W_a$ ,  $W$  and  $W_x$ , of 1.0, 1.25 and 0.75 joules amplitude. The latter is the negative of an energy wave  $W'_x$ , of like amplitude, which would represent the energy in a condenser of  $+j0.06$  mho conductance, charged to a potential of 141.4 volts. The sinusoid  $W_x$  reaches its total crest value of 1.5 joules in phase with  $I_x$ . These energy relations correspond to those of the triangle *vw**x*, Fig. 69.

It will be evident from what has been pointed out in relation to Figs. 69, 70, and 71, that *inductively reactive power may properly be indicated as either  $+j$  or  $-j$  power*, according as we assume the current or the e.m.f. of the circuit as the standard reference phase. Indeed, some writers habitually indicate inductive power as  $+j$  and others as  $-j$  vector power. It is, therefore, important when presenting a vector-power diagram such as *ghi*, or *sut* in Fig. 69, to specify clearly the phase of reference, in order to avoid ambiguity.

**Rotative Properties of the E and I Vector Diagrams.**—The *Z* and *Y* triangles, Fig. 69, are essentially stationary, no benefit being derivable from their rotation. The *E* and *I* diagrams, however, *def* and *pqr*, although presented as stationary, may be made serviceable as *rotary vector diagrams*. Thus, let the *def* triangle be increased  $\sqrt{2}$  times in linear dimensions; or let the same triangle have its scale of linear interpretation increased in this ratio, and be rotated about *O*, Fig. 72, in the plane of the figure, at the angular velocity  $\omega$  radians per sec., or 63.66 revolutions per sec. Then the instantaneous projections of the points *e*, *f* and *G*, on the axis of reals  $-XOX$ , will indicate the corresponding instantaneous values of the active, total and reactive electromotive forces.

Similarly, if the *I* diagram be expanded  $\sqrt{2}$  times in linear dimensions, and be rotated about the point *O*, Fig. 73, in the plane of the paper, at the angular velocity,  $\omega = 400$  radians per sec., the instantaneous projections of *q*, *r*, and *s* on the axis of reals  $-XOX$ , starting from the proper epoch, will mark the corresponding instantaneous values of the total, active and reactive currents.

The stationary *E* and *I* diagrams are, therefore, also to be regarded as rotative, if suitably altered in scale of linear dimensions. It also follows that the *E* and *I* vectors may be mounted together, at the proper phase displacement, and rotated conjointly as a

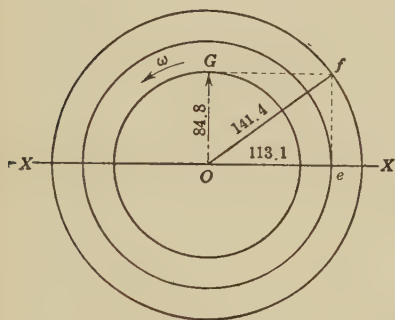


FIG. 72.—Rotation of the *E* diagram after linear expansion in ratio  $\sqrt{2}$ , for instantaneous projections.

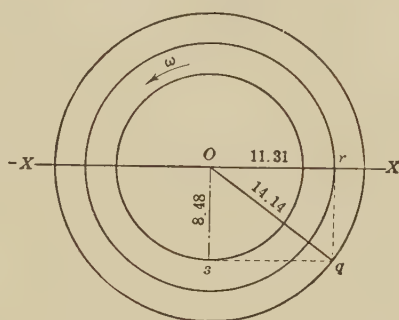


FIG. 73.—Rotation of the *I* diagram after linear expansion in ratio  $\sqrt{2}$ , for instantaneous projections.

single diagram, at the common angular velocity  $\omega$ . Such a rotative diagram, of either voltage or current, has long been used illustratively in a.c. analysis.\*

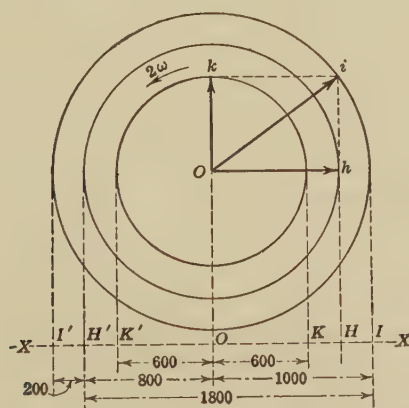


FIG. 74.—Rotative power diagram without change of scale.

**Rotative Properties of the P Vector Diagrams.**—If either of the power diagrams in Fig. 69, say *ghi*, be rotated about the point *O*, Fig. 74, without any change in scale, at the angular velocity

\* "The Alternating-current Transformer," by J. A. Fleming, vol. i, p. 110, London, 1889.

$2\omega$  or, in this case, 127.3 revolutions per sec., and instantaneous projections of  $h$ ,  $i$  and  $k$  be taken, on the axis  $-XOX$ , then these projections will mark the instantaneous values of the active, total and reactive powers. The zero of the reactive power is at  $O$ , which also corresponds to the line  $pp$  in Figs. 70 and 71; but the point  $H'$  corresponds to the power zero  $OO$  in those figures. Referring to the power triangle  $ghi$ , and  $sut$  of Fig. 69, it will be evident that *the instantaneous power in an a.c. circuit, or branch, oscillates between the sum and difference of the base and hypotenuse of the vector power triangle* ( $-200$  and  $+1800$  watts in Fig. 74).

By mounting the  $I$  and  $E$  vectors on one disk, spinning at  $\omega$  radians per sec., and the  $P$  vectors on another disk, geared with

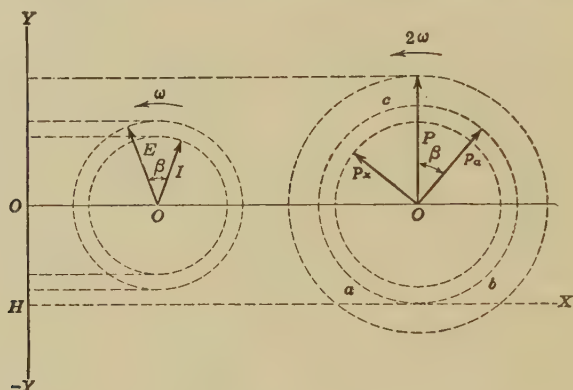


FIG. 75.—Corresponding rotations of the  $E$ ,  $I$  and  $P$  vectors.

the first in the velocity ratio of 2 to 1, so that the  $P$  disk spins at  $2\omega$  radians per sec. (Fig. 75), the instantaneous vertical projections of  $E$ ,  $I$ ,  $P_a$ ,  $P_x$  and  $P$ , on the vertical axis  $-YOY$ , will mark off the corresponding instantaneous voltage, current, active, reactive, and total power. The  $P$  vector should stand vertical, as shown, when the  $E$  and  $I$  vectors make equal and opposite angles with the vertical. Powers are read with respect to  $H$  as zero, except  $P_x$ , which is read with respect to  $O$  as zero.

**Rotative Properties of the W Vector Diagrams.**—By reference to (279), it will be seen that the time integral of the power contains a uniformly increasing term  $P_a t$ , as well as a cyclically oscillating term  $\frac{P}{2\omega} \sin(2\omega t + \beta)$ . The latter term can be developed by the projection, on a fixed axis, of the energy triangle

$jkl$ , or  $vwx$ , spinning in the plane of projection, about the points  $j$  or  $v$ , with the angular velocity  $2\omega$  radians per sec. The first term requires a constantly increasing addition to the value of  $W$  so developed. The sum of the two terms can, therefore, always be obtained by both rotating and rolling the diagram, developed as a wheel of tread radius  $W_a$  and flange radius

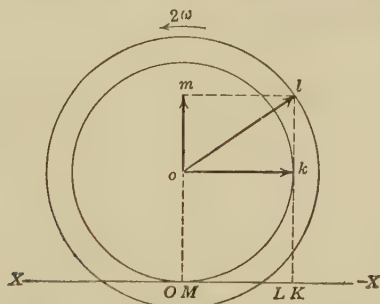


FIG. 76.—Rotation, with rolling, of the  $W$  diagram, or energy wheel.

$W$ , as indicated in Fig. 76. Here the wheel  $klm$  rolls on the rail  $+XO - X$ , at uniform angular velocity  $2\omega$ . The vertical projection of the flange point  $l$ , at  $L$  on the rail, marks the instantaneous value of the energy delivered to the circuit, for which the energy triangle  $jkl$ , Fig. 69, has been prepared.

It will be observed that, as the wheel rotates and rolls, the path of the flange point in the plane of rotation will be a prolate

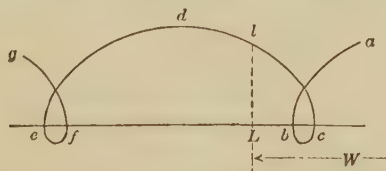


FIG. 77.—Prolate trochoid described by the moving point on the flange of the wheel representing a rotating and rolling energy diagram.

trochoid,\*  $abcdefg$ , containing a closed loop at each revolution. The instantaneous projection at  $L$  of the flange point  $l$  in this curve marks off the total energy poured into the circuit from the electric source, up to that instant.

Just as any point on the flange of a railroad-car wheel, running at say 100 km. per hr., over a railroad track, not only comes to

\* "Differential and Integral Calculus," by Greenhill, 1896, p. 39.



rest, but actually retrogresses, or reverses its direction of horizontal translatory motion, once in each wheel revolution; so, when the flange point is executing the loops *bc*, *ef*, in Fig. 77, the energy ceases to flow from the source into the circuit, and flows back from the circuit toward the source.

In the particular case of Fig. 78, when the circuit is *non-reactive*, and contains only pure resistance, the flange of the wheel dis-

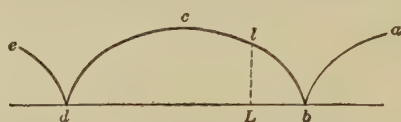


FIG. 78.—Case of reactanceless circuit corresponding to a flangeless wheel, the moving point tracing a cycloid in the plane of rotation.

appears, or the wheel becomes a simple cylinder, and the path of the rotating point *l* becomes a pure cycloid, *abcde*. In this case, the flow of energy momentarily stops at *b* and *d*, but the energy tide does not reverse.

In the opposite case, when the circuit is resistanceless or wholly reactive, the energy vector diagram *jkl* has zero base, and its hypotenuse coincides with its perpendicular. The triangle

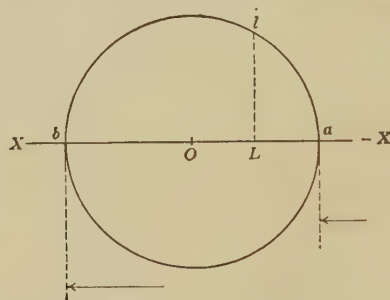


FIG. 79.—Rotation, without rolling, of *W* diagram, in limiting case of resistanceless circuit.

shrinks to a mere vertical line, and the tread radius shrinks to the axis *O*, Fig. 79, leaving the wheel all flange. This "wheel," in rotating, fails to advance by rolling, and the energy oscillates between the limits *a* and *b*.

In Fig. 75, if the power disk is allowed to roll upon the tread circle *a*, *b*, *c* over a rail *HX*, and with it the geared current-voltage disk, the moving system will project on a vertical rod, carried along with it, the instantaneous values of current, volt-



age, and power; while the vertical projection of the flange point  $P$  will trace out, to a suitable linear scale, the energy along the rail. The horizontal speed of the axle  $O$  will measure the average power, and also the *active watts* of the circuit. Such models have been constructed.\*

**Fictitious Impedance Diagrams.**—In cases where the branch circuit of Fig. 68 contains either an active c.e.m.f. such as that of a synchronous motor, or a combination of condensive and inductive reactances in series, the readings of e.m.f., current and power, will give rise to an impedance  $Z$  diagram and its series of subsidiaries, which is arithmetically correct and practically useful, but is physically incorrect as regards impedance elements. Such diagrams, although serviceable, may be described as *fictitious*.

\*“Artificial Electric Lines” pp. 137–140.

## CHAPTER X

### FUNDAMENTAL PROPERTIES OF ALTERNATING-CURRENT REAL LINES

We have already seen that all uniform real c.c. lines, in a steady state of operation, possess or subtend a *real hyperbolic angle*  $\theta$ , and have likewise a linear real hyperbolic angle  $\alpha = \theta/L = \sqrt{rg}$  hyps. per km. A c.c. artificial line also possesses a real hyperbolic angle  $\theta$  per section of its length, and, if each section represents a length of  $L$  km., a corresponding linear hyperbolic angle  $\theta/L$  is inferred.

A.c. lines differ from c.c. lines in the steady state, from the effects of inductance and of capacitance. That is, while c.c. lines call only for a consideration of linear resistance  $r$  and linear leakage  $g$ , a.c. lines call, in addition, for a consideration of linear inductance  $l$ , and linear capacitance  $c$ . Moreover, the effects of inductance and capacitance vary with the frequency.

**Linear Inductance of Real Lines.**—The *inductance* of a very long loop consisting of a pair of parallel uniform round wires, each of radius  $\rho$  cm. and set at an interaxial distance  $D$  cm., may be defined as the total magnetic flux linked with the loop per unit of current steadily passing around it. The *linear inductance* of such a loop is the total flux, per linear centimeter of the loop, and per unit of current. In c.g.s. magnetic measure, this linear inductance may be expressed in abhenrys per loop centimeter, according to the formula:\*

$$l_0 = \mu + 4 \log h \left( \frac{D}{\rho} \right) \quad \frac{\text{abhenrys}}{\text{loop cm.}} \quad (280)$$

where  $\mu$  is the magnetic permeability of the wire, assumed uniform, which for non-magnetic materials may be taken as unity, and  $\log h$  signifies hyperbolic or Napierian logarithms, to the base  $e = 2.71828 \dots$ . The first term signifies the *internal linear loop inductance*, and the second term the *external linear loop inductance*.

\* "Electricity and Magnetism," by Clerk Maxwell, vol. ii, p. 293, 1881.

"Principles of Alternating Currents," by R. R. Lawrence, Chap. XIII.

Reducing (280) to common logarithms, and to henrys per loop kilometer, we have for non-magnetic wires, in air or other non-magnetic medium, the linear loop inductance

$$l_{\text{loop}} = \left\{ 1 + 9.2103 \log \left( \frac{D}{\rho} \right) \right\} 10^{-4} \frac{\text{henrys}}{\text{loop km.}} \quad (281)$$

The linear inductance of either of the two wires to the mid-plane between them, may be called the *linear wire inductance*. It is half of the linear loop inductance (280) or

$$l = \left\{ 0.5 + 4.6052 \log \left( \frac{D}{\rho} \right) \right\} 10^{-4} \frac{\text{henrys}}{\text{wire km.}} \quad (282)$$

It is known\* that this *non-ferric linear inductance*, as above defined, by the ratio of the linear flux to the steady current supporting it, is the same for all equal values of  $D/\rho$ . In other words, the degree of proximity of the two parallel wires does not have to be considered.

In the case of three parallel and equally spaced wires† forming a three-phase, a.c. line system, the linear wire inductance is advantageously obtained from (282). In such a case,  $D$  is the interaxial distance between any pair of the three wires.

As an example, the linear wire inductance of a pair of No. 10 A.W.G. copper wires of diameter 0.2589 cm. interaxially separated by 30.48 cm. (1 ft.) is

$$\begin{aligned} \left( 0.5 + 4.6052 \log \frac{30.48}{0.12945} \right) 10^{-4} &= (0.5 + 4.6052 \times 2.3719) 10^{-4} \\ &= (0.5 + 10.923) 10^{-4} = 11.423 \times 10^{-4} = 1.1423 \text{ millihenrys} \\ &\text{per wire km. (1.839 mh. per wire mile.)} \end{aligned}$$

Tables of linear wire inductances for different sizes of wire at various spacings have been worked out by‡ various writers.

**Linear Capacitance of Real Lines.**—It follows from the theorem of the propagation of electric disturbances over a pair of uniform parallel conductors in free space at the speed of light, that for

\* A. Russell, "A Treatise on the Theory of Alternating Currents," Cambridge University Press, 1904, vol. i, Chapter II, pp. 57–60.

† If the wires are unequally spaced, the linear inductances differ, and the linear resistances, also virtually differ. The corrections for dissymmetrical spacing, are considered in the footnote on page 138.

‡ "The Inductance and Capacity of Suspended Wires," by E. J. Houston and A. E. Kennelly, *Electrical World*, July 7, 1894, vol. xxiv, pp. 6–7, also various handbooks, such as "The Standard" or "The American" handbook.

any such pair of conductors, of any cross-sectional shape,\* their linear loop capacitance expressed in statfarads per loop centimeter is the reciprocal of their external linear loop inductance expressed in abhenrys per loop centimeter. Consequently, the linear loop capacitance of a pair of round wires in air is by (280)

$$c_0 = \frac{1}{4 \log h (D/\rho)} \quad \frac{\text{statfarads}}{\text{loop cm.}} \quad (283)$$

Reducing to common logarithms, kilometer lengths, and remembering that 1 statfarad =  $10^9 \mu\mu\text{f.}$  (micromicrofarads) this becomes:

$$c_{,,} = \frac{0.0120635}{\log (D/\rho)} \times 10^{-6} \quad \frac{\text{farads}}{\text{loop km.}} \quad (284)$$

If, however, the wires are not separated by a distance of many radii, *i.e.*, if  $D/\rho$  is less than 10, say, these formulas (283) and (284) are unreliable and a formula may be substituted, which is correct for all distances, in air,  $d$  being the diameter of the wire in cm.† The short-separation linear loop capacitance is

$$c_0 = \frac{1}{4 \cosh^{-1} (D/d)} \quad \frac{\text{statfarads}}{\text{loop cm.}} \quad (285)$$

reduced to farads per loop kilometer this is,

$$c_{,,} = \frac{0.027778}{\cosh^{-1} (D/d)} \times 10^{-6} \quad \frac{\text{farads}}{\text{loop km.}} \quad (286)$$

Thus the linear loop capacitance of a pair of wires at an interaxial distance of 50 diameters, or 100 radii, is by (284)  $0.0120635/2 = 0.006032 \mu\text{f./loop km.}$ , and by the strict formula (286),  $0.027778/4.6051 = 0.006032$ , to four significant digits the same result. At an interaxial distance, however, of 2 diameters or 4 radii, the linear loop capacitance by (284) is  $0.0120635/0.60206 = 0.02004 \mu\text{f./loop km.}$ ; while by the strict formula (286) it is  $0.027778/1.3170 = 0.02109$ .‡

\* *Trans. A. I. E. E.*, June 29, 1909, vol. xxviii, part I, p. 702.

† "Principles of Alternating Currents," by R. R. Lawrence, Chap. XIV.

‡ Seeing that (285) is the correct formula for the linear loop capacitance of a pair of parallel cylinders in air at any distance, the proposition cited connecting linear inductance and capacitance would indicate that (280) should be:

$$l_0 = 4 \cosh^{-1} \left( \frac{D}{d} \right) \quad \frac{\text{abhenrys}}{\text{loop cm.}} \quad (289)$$

This question has been investigated experimentally. See Dr. F. B. Silsbee on "Inductance of Conductors at Close Spacings," *Elec. World*, July

The *linear wire capacitance* is just double the linear loop capacitance, and in the c.g.s. system, is the capacitance per linear cm. of either wire in a uniform insulated loop to the zero-potential mid-plane between them. Hence,

$$c = \frac{0.05556}{\cosh^{-1}(D/d)} \times 10^{-6} \quad \frac{\text{farads}}{\text{wire km.}} \quad (287)$$

or, for ordinary interaxial distances,  
very nearly

$$c = \frac{0.024127}{\log(D/\rho)} \times 10^{-6} \quad \frac{\text{farads}}{\text{wire km.}} \quad (288)$$

The curves of Fig. 80 show the linear wire capacitance of straight round parallel wires in air (uncorrected for insulators, towers or neighboring wires) up to interaxial distances of 25 diameters, in accordance with (287). Fig. 81 shows the corresponding linear wire capacitances up to interaxial distances of 10,000 diameters, in accordance with either (287) or (288).

Thus, in a three-phase aerial line, with the wires separated interaxially by 100 diameters, each wire would have a linear capacitance of  $\frac{0.0556}{\cosh^{-1} 100} = 0.0556/5.298 = 0.01049$  microfarad per wire km., *i.e.*, between each wire and the neutral or zero-potential surface.

In the case of three parallel and equally spaced wires forming a three-phase a.c. line system, the linear wire capacitance is

15, 1916, vol. lxxviii, pp. 125-126. The results indicate that at very high frequencies, formula (289) appears to be correct; but that at low frequencies (280) is correct. The reason seems to be that at low frequencies, the resistivity of the conductor tends to equalize the current density over the cross-section; whereas at high frequencies, the current density is non-uniform and superficial, such as would give effect to (289).

The following references bear upon the linear capacitance formula.

"The Linear Resistance between Parallel Conducting Cylinders in a Medium of Uniform Conductivity," by A. E. Kennelly, *Proc. Am. Phil. Soc.*, April, 1909, vol. xlviii, pp. 142-165.

"The Electrostatic Capacity between Equal Parallel Wires," by H. Pender and H. S. Osborne, *Electrical World*, vol. lvi, No. 12, pp. 667-670.

"Graphic Representations of the Linear Electrostatic Capacity between Parallel Equal Wires," by A. E. Kennelly, *Electrical World*, October 27, 1910.

A. Russell, "Alternating Currents," Cambridge University Press, 1904, vol. i, Chapter 2, p. 59.



advantageously found from (288). In such a case,  $D$  is the inter-axial distance between any pair of the three wires.\*

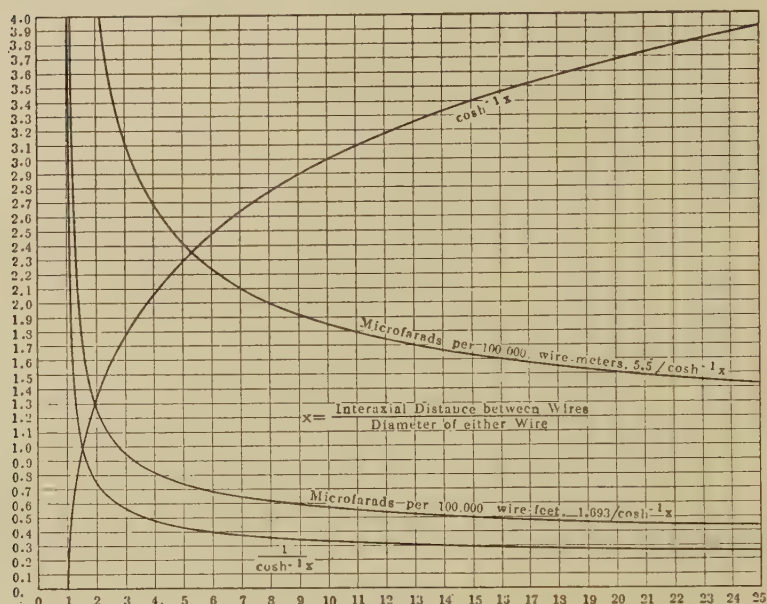


FIG. 80.—Linear capacitance per 100,000 wire-feet and wire-meters. Graphs of  $\cosh^{-1} x$ ,  $1/\cosh^{-1} x$  and linear capacitances of bare, equal, parallel, round wires in air for interaxial distances up to 25 diameters.

**Linear Constants.**—The *linear wire reactance*  $x = l\omega$  of the conductor in ohms per wire kilometer, is the product of  $l$  the linear wire inductance, and the impressed angular velocity  $\omega$ . The linear wire reactance manifestly increases directly with the frequency  $f$ . It is just half the *linear loop reactance*  $l, \omega$  ohms per loop km.

The *linear wire susceptance*  $b = c\omega$  of the dielectric, in mhos per wire kilometer, is the product of  $c$  the linear wire capacitance, and the impressed angular velocity  $\omega$ . It also manifestly

\* If the three wires of a three-phase transmission line are unequally spaced, as for instance, when all three are mounted on the same cross-arm of each pole, the linear inductances and capacitances of the three loops will be different. Unless the differences are eliminated by symmetrical transposition, they tend to produce differences in the drops of potential on the three-wires, and dissymmetry in the three-phase system. If, however, the wires are regularly transposed, it is shown in text-books on line Power Transmission that the effective or geometric distance between wires is  $\sqrt[3]{D_1 D_2 D_3}$ , where  $D_1$  and  $D_2$ , and  $D_3$  are the distances between the respective pairs.



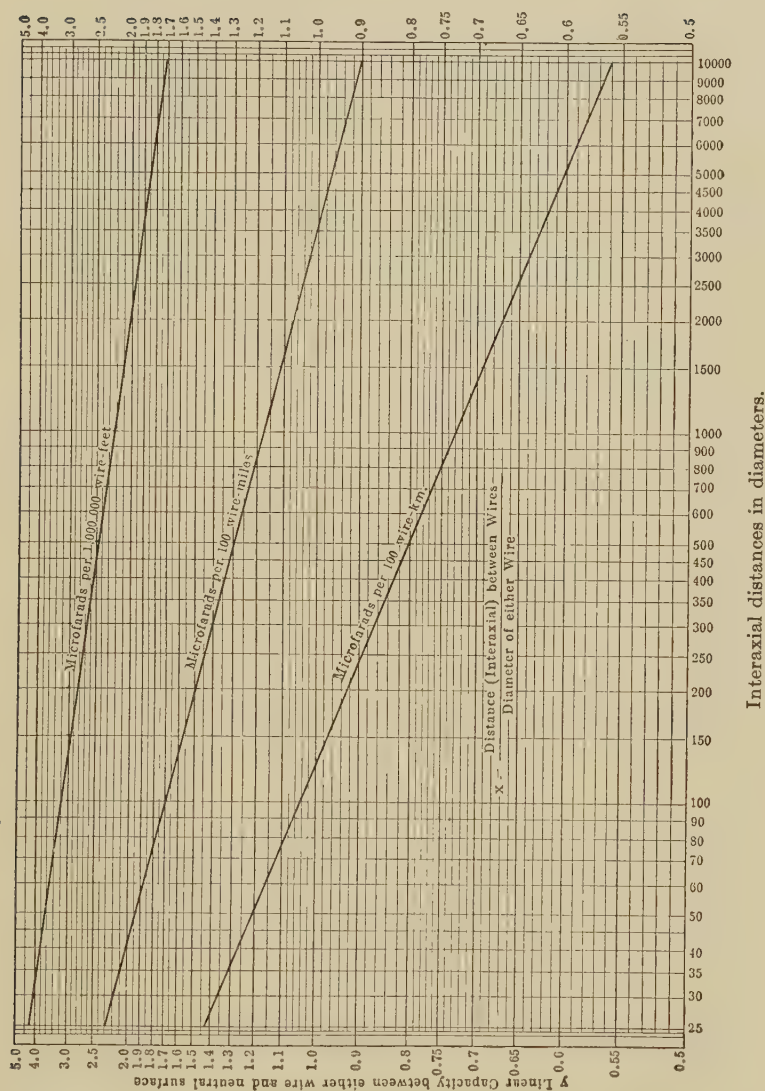


FIG. 81.—Graphs of linear wire capacitances of bare, equal, parallel, round wires in air for interaxial distances from 25 to 10,000 diameters, in microfarads per 1,000,000 wire-feet, per 100 wire-miles and per 100 wire-kilometers;

$$y = \frac{16.93}{\cosh^{-1} x} \mu\text{f. per 1,000,000 wire-feet}; \quad y = \frac{8.941}{\cosh^{-1} x} \mu\text{f. per 100 wire-miles};$$

$$y = \frac{5.556}{\cosh^{-1} x} \mu\text{f. per 100 wire-kilometers.}$$

increases directly with the frequency of operation, and is just double the *linear loop susceptance*  $b_{,,}$  mhos per loop km.

The *linear wire impedance* of a real a.c. line is

$$z = r + j\omega = r + jx \quad \frac{\text{ohms}}{\text{wire km.}} \quad \angle \quad (290)$$

Here  $r$ , the real component of the plane vector  $z$ , is the linear wire resistance, and, at low frequencies, is the same as though the wire were operated by continuous currents, at the same temperature. At high frequencies, "skin effect," or non-uniform a.c. density, tends to increase  $r$ .

**Skin-effect Formulas for Round Wires.**—In the ordinary case of round wires of radius  $X$  cm. and electric conductivity  $\gamma$  abmhos per cm. (the reciprocal of the resistivity  $\rho$  in abohm-centimeters), operated at  $\omega$  radians per sec., a fundamental formula for the internal linear impedance  $z'$  of the wire due to "skin effect," i.e., to auto-disturbance of a.c. density over the cross-section, when not too close to neighboring active conductors, is\*

$$z' = r \cdot \frac{\alpha_0 X}{2} \cdot \frac{J_0(\alpha_0 X)}{J_1(\alpha_0 X)} \quad \frac{\text{ohms}}{\text{wire km.}} \quad \angle \quad (291)$$

where

$$\alpha_0 = \sqrt{-j4\pi\gamma\mu\omega} = \sqrt{4\pi\gamma\mu\omega} \angle 45^\circ = \sqrt{2\pi\gamma\mu\omega} - j\sqrt{2\pi\gamma\mu\omega} = \alpha_2 - j\alpha_2 \quad \text{cm}^{-1} \quad \angle \quad (292)$$

$r$  is the ordinary linear resistance of the wire to continuous currents, in ohms per wire kilometer.

$\gamma = 1/\rho$  is the conductivity of the wire, abmhos per cm.

$\mu$  is the permeability of the substance of the wire assumed as uniform and as unity for non-magnetic substances.

$\alpha_2$  stands for the size of either component of a semi-imaginary  $\alpha_0$ .

$J_0(\alpha_0 X)$  is a plane-vector Bessel function of  $\alpha_0 X$ , of zero order† (numeric  $\angle$ ).

\* "Funktionentafeln mit Formeln und Kurven," by Jahnke and Emde, Teubner's, Berlin, 1909, pp. 142-144.

† These vector Bessel functions have been tabulated and charted over a convenient range. See "Experimental Researches on Skin Effect in Conductors," by Kennelly, Laws and Pierce, *Proc. A. I. E. E.*, September, 1915, and also for more elaborate Tables "Calculation of Mathematical Tables," Part III, "Bessel Functions of Negative Semi-imaginary Argument, Section A, Report, *British Assoc.*, Liverpool, 1923, pp. 7-12.

$J_1(\alpha_0 X)$  is a plane-vector Bessel function of  $\alpha_0 X$ , of first order (numeric  $\angle$ ).

The real component of  $z'$  is the apparent linear a.c. resistance of the wire, including skin effect, in ohms per wire kilometer. The imaginary component of  $z'$  is the apparent linear internal reactance of the wire in  $j$  ohms per wire kilometer. The external reactance, due to magnetic flux encircling the whole wire, in the air or other external insulating material, is the same as though no skin effect existed, and does not appear in the formula.

At very low frequencies when  $\omega$  approaches zero, the expression  $\alpha_0 X/2 \cdot J_0(\alpha_0 X)/J_1(\alpha_0 X)$  approaches  $1.0 \angle 0^\circ$ . At very high frequencies, when  $\alpha_0$  becomes a large inverted semi-imaginary quantity, the limit of  $\alpha_0 X/2 \cdot J_0(\alpha_0 X)/J_1(\alpha_0 X)$  becomes:

$$\left| \frac{\alpha_0 X}{2} \right| \angle 45^\circ = \frac{\alpha_2 X}{2} + \frac{j\alpha_2 X}{2} = \frac{\alpha_2 X}{\sqrt{2}} \angle 45^\circ \quad \text{numeric } \angle \quad (293)$$

or the internal linear impedance of the wire at very high frequencies is large and semi-imaginary, especially when the radius  $X$  of the wire is large.

As an example, a No. 8 A.W.G. copper wire has a radius  $X = 0.1632$  cm., a resistivity at  $20^\circ\text{C.}$  of  $1,724$  absohm-cm. ( $\gamma = 0.5801 \times 10^{-3}$ ), and a linear resistance at  $20^\circ\text{C.}$  of  $2.061$  ohms per wire km., required its *internal linear impedance* at  $820\sim = 5,152$  radians per sec.

Here  $\alpha_0 X = \sqrt{12.566 \times 0.5801 \times 10^{-3} \times 5.152 \times 10^3} \angle 45^\circ \times 0.1632 = 1.0 \angle 45^\circ = 0.707 - j0.707$ . Hence by Bessel Tables

$$\begin{aligned} z' &= 2.061 \times \frac{1.0 \angle 45^\circ}{2} \times \frac{1.0155 \angle 14^\circ.217}{0.5014 \angle 37^\circ.837} \\ &= 2.061 (1.01266 \angle 7^\circ.054) = 2.061 (1.0050 + j0.12436) = 2.0713 \\ &+ j0.2563 \frac{\text{ohms}}{\text{wire km.}} \end{aligned}$$

The *virtual linear resistance* has thus increased 0.5 per cent. by skin effect. The linear inductance is  $0.2563/5,152 = 0.4976 \times 10^{-4}$  henry per wire km. =  $0.4976$  abhenry per wire cm., which is 0.48 per cent. below the normal value of 0.5 (see (282 and 289)).

When the value of  $\alpha_2 X$  does not exceed unity, as in the above example, the change in internal reactance is so small that it may ordinarily be ignored, and an approximate formula for change of

linear resistance, due in its original form to Lord Rayleigh,\* may be used, ordinarily only as far as two terms:

$$r' = r \left\{ 1 + \frac{(\alpha_2 X)^4}{48} - \frac{(\alpha_2 X)^8}{2,880} + \dots \right\} \frac{\text{ohms}}{\text{wire km.}} \quad (294)$$

Thus in the case above considered with  $\alpha_2 X = 0.707$ , this becomes

$$\begin{aligned} r' &= 2.061 \left( 1 + \frac{0.25}{48} - \dots \right) \\ &= 2.061(1 + 0.0052 - \dots) \text{ ohms per wire km.} \end{aligned}$$

When  $\alpha_2 X$  exceeds 2, the last formula (294) becomes unsuitable, and Russell's formula† may be employed, ordinarily only as far as two terms:

$$r' = r \left( \frac{\alpha_2 X}{2} + \frac{1}{4} + \frac{3}{32 \alpha_2 X} - \dots \right) \frac{\text{ohms}}{\text{wire km.}} \quad (295)$$

**Potentials Electrostatically Induced on Neighboring Parallel Wires.**—A high-tension active conductor, suspended in the air, creates an electrostatic field in its vicinity, and an insulated passive parallel wire in that vicinity assumes a potential which may be a considerable fraction of that of the active wire. The theory of this inductive action is important in the study of anti-inductive protection.

The uniform conducting wire is assumed to be horizontally supported on insulators, in the air, at an axial height of  $h$  meters above the flat conducting surface of the ground. The radius of the wire is  $\rho$  meters. When a steady potential of  $+V$  volts is impressed on the wire, its cylindrical surface retains this potential, and the ground retains zero potential. The potential will decrease from the wire, through the air, to ground, in a well-known regular manner. The equipotential surfaces surrounding the wire will be a system of eccentric cylinders, their horizontal axes lying in the vertical plane passing through the axis of the wire. This cylindrical distribution of potential is such as would be produced, if the ground were removed and replaced by air, with an "image wire" supported at a depth of  $h$  meters beneath the original ground plane. If the image wire were steadily maintained at a potential  $-V$  volts, the conjoint action of the real wire and its image would create, by symmetry, a

\*Lord Rayleigh, *Phil. Mag.*, May December, 1886.

†Russell, A.; *Phil. Mag.*, 1909, vol. xvii, p. 524.

neutral surface, or surface of zero potential, at the horizontal plane originally coinciding with the ground surface. Moreover, it is shown in textbooks on electrostatics, that the potential induced at any point  $P$  distant  $r$  and  $r'$  from the polar axes of the image and real wires, respectively, is proportional to the logarithm of their ratio, or to  $\log (r/r')$ . The ratio  $(r/r')$  for the point, is called its *polar ratio*. The polar axes of the wires do not coincide with their geometrical axes; but, in any ordinary case of parallel wires suspended in air, the difference is negligible, and we may consider  $r$  and  $r'$  as measured from the point  $P$ , perpendicularly to the axes of the two wires. In the same way, the potential of any point on the surface of the real wire is proportional to its *log polar ratio*, or to  $\log (2h/\rho)$ ; because\* for any point on the real wire's surface, the distance  $r$  will be very nearly  $2h$ , and the distance  $r'$  will be the wire radius  $\rho$ . In this way, we arrive at the well-known approximate equation

$$\frac{v}{V} = \frac{\log r/r'}{\log 2h/\rho} \quad \text{--- numeric} \quad (296)$$

where  $v$  is the potential at the point  $P$ . If a passive insulated wire is supported parallel to the real and image wires at the distance ratio  $r/r'$ , it will acquire this potential inductively, and an electrostatic voltmeter connected from ground to the passive wire might indicate this potential. It is evident from (296), that at any point with unity polar ratio, or equidistant from the real and image wires, the logarithm of its polar ratio must vanish, or the potential must be zero.

In Fig. 82, which represents a vertical plane across a set of three mutually equidistant three-phase transmission wires  $a$ ,  $b$ , and  $c$ , the point  $O$  on the ground surface  $GG$ , is taken as the zero of coördinates. The top wire  $a$  is 10 m. vertically above the point  $O$  and its coördinates are therefore  $x = 0$  and  $y = 10$ . The wires  $b$  and  $c$ , being axially separated 1.5 m., have coördinates of  $-0.75, 8.7$ , and  $+0.75, 8.7$  respectively. On a cross-arm, beneath the three-phase wires, are two telephone wires on insulators marked 1 and 2 on the diagram, with coördinates  $-0.6, 7.0$ , and  $-0.3, 7.0$ , respectively. The three image wires  $a'$ ,  $b'$  and  $c'$ , are indicated in the figure. Each has the same  $x$ -coördinate, and the opposite  $y$ -coördinate, as its real wire. The

\* See "The Transmission of Electrical Energy," by E. J. Berg, and "Principles of Alternating Currents," by R. R. Lawrence, Chap. XIV.







radius  $\rho$  of each real and image wire is 0.0059 m. (0.01936 ft. or 0.2323 in.). The radius of the telephone wires is practically unimportant. From these data, we have to find the polar ratios of the telephone-wire axes, either geometrically from the drawing board, or arithmetically from the relative coördinates, or preferably by both methods as mutual checks. The polar distances, in meters, are marked on the diagram. Thus the polar distances of the axis of telephone wire No. 1 from the axes of real wire  $a$  and image wire  $a'$  are respectively  $r_a = 3.059$  m. (10.037 ft.) and  $r'_a = 17.01$  m. (55.81 ft.). The polar ratio for wire 1 with respect to real and image wires  $a$  is thus  $r'_a/r_a = 17.01/3.059 = 55.81/10.037 = 5.560$ , the logarithm of which, to five places, is 0.74507. The polar ratio for the surface of wire  $a$  is  $20.0/0.0059$  in meter measure, or  $65.62/0.01936$  in foot measure, or 3,390 (to four figures), the logarithm of which is 3.5302. Dividing the log polar ratios according to (296), we have  $v/V = 0.7451/3.530 = 0.2110$ ; so that the potential of the insulated telephone wire 1 will be 21.1 per cent. of the potential of the inducing wire  $a$ . If we assume that the three-phase system of potentials impressed on the three wires  $a$ ,  $b$ , and  $c$  is symmetrical, with 63,000 volts effective or r.m.s. between any pair, the star-voltage of any one wire to neutral or ground potential will be  $63,000/\sqrt{3}$  or 36,370 r.m.s. volts. The potential induced on insulated telephone wire No. 1 will, therefore, be 7,676 volts, of the same frequency as the potential of  $a$ , and in phase with the same.

If we compute the log polar ratios,  $\log (r'_b/r_b)$  and  $\log (r'_c/r_c)$  of wire 1, with respect to wires  $b$  and  $c$ , we find them to be 0.2777 and 0.2482, respectively, which represent 10,102 and 9,028 volts, each in phase with the potential of its working wire. There are thus three independent a.c. potentials induced on wire 1, differing in phase by  $120^\circ$ , and the resultant potential of wire 1 will be the plane-vector sum of the three. This is indicated in Fig. 83, the phase of potential  $v_a$  being taken as standard, and the direction of positive rotation being assumed as shown. If the direction of rotation should actually be the opposite, the phase but not the magnitude of the resultant would be changed. Ordinarily, the phase of the resultant induced potential is unimportant. The three induced potentials being  $v_{01a} = 7,676 \angle 0$ ;  $v_{01b} = 10,102 \angle 120^\circ$ , and  $v_{01c} = 9,028 \angle 240^\circ$ , the resultant is

$v_{01} = -1,889 + j932 = 2,106 \angle 153.7^\circ$  r.m.s. volts, as obtained either graphically or arithmetically.

Computing the log polar ratios of wire 2 with respect to the axes of wires  $a$ ,  $b$ , and  $c$ , we obtain the three correspondingly induced potentials  $v_{02a} = 7,740 \angle 0^\circ$ ,  $v_{02b} = 9,966 \angle 120^\circ$ , and  $v_{02c} = 9,392 \angle 240^\circ$ , the resultant of which is  $v_{02}$ , Fig. 83, or  $-1,939 + j497 = 2,002 \angle 165.6^\circ$ , the difference of potential  $V_{21}$  between the two passive wires will be  $438.0 \angle 83^\circ.5 = 50 + j435$  r.m.s. volts, as shown in the figure. While, therefore, the potential induced in each wire separately is roughly 2,000 volts, the potential difference between them is over 400 volts, mainly due to the phase difference of the two individual potentials.

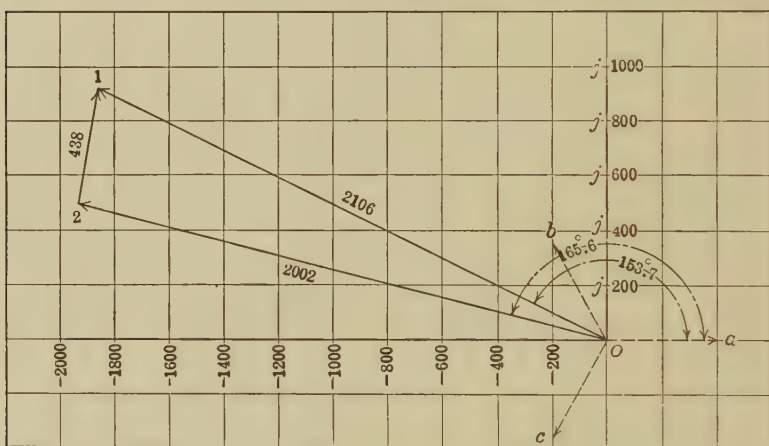


FIG. 83.—Vector diagram of statically induced potentials.

These statically induced potentials are independent of the inducing frequency, and of the length of the parallel system of wires, except that when the parallel exposure is long, the potentials are more likely to be retained in spite of leakage in the telephone wire system than when the exposure is short.

It is theoretically possible to place a single passive insulated wire at a neutral position with respect to the inducing conductors, but practically it is much better to place the telephone wire or wires as far as practicable from the high-tension wires. By *transposing* the two telephone wires with respect to the inducing wires, *i.e.*, exchanging relative positions in a regular manner, such as by twisting the telephone pair, the difference of potential at their terminals may be made to disappear: but transposition

of this kind will not annul the relatively high induced potentials of both the passive wires with respect to ground. Those may be removed, however, by connecting a *drainage coil*, i.e., a reactor, between them, with a ground connection at the center. The coil will develop its full reactance to the potential difference  $v_{12}$ , Fig. 83, but will develop little reactance to the potentials  $v_{01}$ ,  $v_{02}$ , which tend to cancel each other's magnetizing force.

The preceding theory applies with precision, only if there are no grounded wires on the poles or towers supporting the wires, and if the ground surface is at zero potential. It is found experimentally that the level upper surface of ordinary soil may be taken as a zero-potential surface, when wet after rain. When dry, however, the equivalent surface of zero potential descends below the ground surface towards the level at which water is found on digging. On the other hand, a flat layer of wet snow covering the ground only a few decimeters thick, has been found to raise the zero-potential surface substantially to the top of the snow. Over dry rock, the zero level may lie at considerable depth for low-frequency voltages. When the telephone wires are connected through apparatus to ground, the conditions are still more complex.

**Voltages Magnetically Induced in Parallel Wire Loops.**—If alternating currents are flowing in the three-phase system of Fig. 82, there will be alternating magnetic fields in the vicinity, and magnetically induced voltages will develop in the conducting loop formed by neighboring wires, such as the loop 1, 2, in Fig. 82. It is shown in textbooks dealing with mutual inductance, that if a horizontal wire, such as the wire  $a$ , Fig. 83, is at inter-axial distances of  $r_{a1}$  and  $r_{a2}$  from the sides 1 and 2, of a parallel conducting loop, the linear mutual inductance of the wire, with respect to the loop, will be

$$M_a = 2 \log h \frac{r_{a1}}{r_{a2}} = 4.605 \log \frac{r_{a1}}{r_{a2}} \quad \frac{\text{abhenries}}{\text{linear cm.}} \quad (297)$$

where  $\log h$  denotes the hyperbolic or Napierian logarithm, and  $\log$  the common logarithm of the distance ratio.  $M_a$  will be positive or negative, according as  $r_{a1}$  is greater or less than  $r_{a2}$ . If the two distances happen to be equal, the linear mutual inductance will vanish. If the wire  $a$  carries an alternating current of the single frequency  $f$  cyps., and of effective or r.m.s. value  $I$  abamp. ( $10 \times I$  amp.), the magnetic flux linked with the loop

per linear centimeter of the system, will be  $IM_a$  maxwells r.m.s. per linear cm., and the rate of change of this flux in the loop will develop therein a linear e.m.f. of

$$e_a = j\omega IM_a = j\omega I2 \log \frac{r_{a1}}{r_{a2}} \frac{\text{abvolts}}{\text{linear cm.}} \quad (298)$$

where  $\omega = 2\pi f$  is the angular velocity of the alternating current in radians per second. The induced e.m.f. per linear kilometer will be  $e_a$  r.m.s. millivolts, and the induced e.m.f. per linear mile 1.609  $e_a$  r.m.s. millivolts.

If we take as an example the three-phase system of Fig. 83, and assume that a simple alternating current of 100 amp. or 10 abamp. r.m.s. flows in each wire, we have first to find the linear mutual inductances from the axial distances indicated. These are  $M_a = +0.02899$ ,  $M_b = -0.05969$ ,  $M_c = +0.1659$  abhenries/cm. Each of the three magnetic fluxes, linked with the loop, will have the same phase as the current generating it. If we take the phase of  $I_a$  as standard, and the frequency as 60 cyps., the corresponding angular velocity will be  $\omega = 377$ ; so that the linear e.m.f. due to the flux from  $I_a$  will be  $e_a = 0.02899 \angle 0^\circ \times 10 \times j377 = 108.9 \angle 90^\circ$  abvolts per linear cm. Similarly,  $e_b$  will be  $225.0 \angle 30^\circ$  and  $e_c = 625.5 \angle 30^\circ$ . The resultant of these three linear e.m.fs. is  $742.3 \angle 7^\circ$ , abvolts per cm. or 742.3 millivolts per km., the phase being ordinarily of no importance. This corresponds to 1.195 volts per mile of system length.

Contrary to the conditions already noted for statically induced voltages, magnetically induced voltages increase with the frequency and with the current strength. Moreover, if harmonics are present in the current waves, they will develop e.m.fs. in relative proportion to their frequencies. The telephonic disturbance due to relatively feeble harmonics may be much greater than that due to the fundamental working current. It is possible theoretically to reduce the resultant induced e.m.f. in the loop to zero by twisting the telephone wires, *i.e.*, by thorough transposition, as well as by thorough transposition of the power wires.

**Vector Linear Wire Constants.**—In all a.c. problems, the *vector linear wire impedance*  $z$  replaces the real linear wire resistance  $r$  of corresponding d.c. problems. Nevertheless,  $r$  may be retained in a.c. problems, if it is borne in mind that it has been changed from a real to a complex quantity. The linear wire impedance  $z$  of an a.c. loop circuit, is manifestly just half the linear loop impedance  $z_{\text{loop}}$ , of the same.



The *linear wire admittance* of a real a.c. line is

$$y = g + j\omega = g + jb \quad \frac{\text{mhos}}{\text{wire km.}} \angle \quad (299)$$

Here  $g$ , the real component of the plane vector  $y$ , is the linear wire conductance, and is ordinarily greater than the corresponding leakage conductance of the same line when operated by continuous currents. It is, therefore, necessary to measure  $g$  in a.c. cases. The linear wire admittance  $y$  of a loop circuit, formed of two uniform parallel wires, is just double the *linear loop admittance*  $y_{\text{L}}$ , of the same circuit, in mhos per loop kilometer.

In all a.c. problems, the vector linear wire admittance  $y$  replaces the real linear wire conductance  $g$  of corresponding d.c. problems. Nevertheless,  $g$  may be retained in a.c. problems, if it is remembered that  $g$  has been changed from a real to a complex quantity.

The *linear hyperbolic angle* of a real a.c. line is the vector,

$$\alpha = \sqrt{zy} = \sqrt{(r + jx)(g + jb)} = \alpha_1 + j\alpha_2 \quad \frac{\text{hyps.}}{\text{wire km.}} \angle \quad (300)$$

The real and imaginary components  $\alpha_1$  and  $\alpha_2$  of this vector are:

$$\begin{aligned} \alpha_1 &= \sqrt[1]{2} \left\{ \sqrt{(r^2 + x^2)(g^2 + b^2)} + (gr - bx) \right\} \\ &= \sqrt[1]{2} \left\{ |\alpha^2| + (gr - bx) \right\} \quad \frac{\text{hyps.}}{\text{wire km.}} \end{aligned} \quad (301)$$

$$\begin{aligned} \alpha_2 &= \sqrt[1]{2} \left\{ \sqrt{(r^2 + x^2)(g^2 + b^2)} - (gr - bx) \right\} \\ &= \sqrt[1]{2} \left\{ |\alpha^2| - (gr - bx) \right\} \quad \frac{\text{cir. radians}}{\text{wire km.}} \end{aligned} \quad (302)$$

where  $|\alpha^2|$  means the size of the plane vector  $\alpha^2$  defined by:

$$|\alpha^2| = \sqrt{(r^2 + x^2)(g^2 + b^2)} = |z| \cdot |y| \quad \text{numeric} \quad (303)$$

It is, however, ordinarily more convenient and expeditious to express  $z$  and  $y$  as polars, and then to find  $\alpha$  as a polar; thus:

$$\begin{aligned} \alpha &= \sqrt{|z| \angle \beta_1^\circ |y| \angle \beta_2^\circ} = \sqrt{|zy|} \angle \frac{\beta_1^\circ + \beta_2^\circ}{2} = \sqrt{|zy|} \angle \beta^\circ \\ &\quad \frac{\text{hyps.}}{\text{wire km.}} \angle \end{aligned} \quad (304)$$

We may take, as an example to be worked out in each way, the case of a loop of standard telephone twisted-pair circuit, consisting of two No. 19 A.W.G. copper wires, 0.0912 cm. in diam-

eter, paper-insulated and lead-sheathed. The loop-mile constants of this circuit are taken as  $r_{,,} = 88$  ohms/l.m.,  $l_{,,} = 10^{-3}$  h/l.m.,  $g_{,,} = 5 \times 10^{-6}$  mho/l.m.,  $c_{,,} = 0.054 \times 10^{-6}$  f/l.m. The corresponding wire kilometer values are  $r = 27.34$ ,  $l = 0.3107 \times 10^{-3}$ ,  $g = 6.214 \times 10^{-6}$ ,  $c = 0.6711 \times 10^{-7}$ . At the standard telephonic angular velocity,  $\omega = 5,000$ , ( $f = 796\sim$ ),  $x = 1.5535$  ohms per wire km., and  $b = 335.5 \times 10^{-6}$  mho per wire km. Then by (301):

$$\begin{aligned}\alpha_1 &= \sqrt{\frac{1}{2} \left\{ \sqrt{(27.34^2 + 1.554^2) (6.214^2 + 335.5^2) 10^{-12} + (6.214 \times 27.34 \times 10^{-6} - 1.5535 \times 335.5 \times 10^{-6})} \right.} \\ &= \sqrt{\frac{1}{2} \left\{ \sqrt{(747.476 + 2.413) (38.61 + 112,560.25) 10^{-12} + (169.891 - 521.288) 10^{-6}} \right.} \\ &= \sqrt{\frac{1}{2} \left\{ \sqrt{(749.889)(112,598.9 \times 10^{-12}) - 351.397 \times 10^{-6}} \right.} \\ &= \sqrt{\frac{1}{2} \left\{ \sqrt{0.749889 \times 1.125989 \times 10^{-4} - 3.51397 \times 10^{-4}} \right.} \\ &= \sqrt{\frac{1}{2} \left\{ \sqrt{0.844365 \times 10^{-4} - 0.0351397 \times 10^{-2}} \right.} \\ &= \sqrt{\frac{1}{2} \left\{ 0.918893 \times 10^{-2} - 0.035140 \times 10^{-2} \right.} \\ &= \sqrt{\frac{1}{2} \left\{ 0.883753 \times 10^{-2} \right\}} = \sqrt{0.441876 \times 10^{-2}} \\ &= 0.66474 \times 10^{-1} = 0.066474 \\ \alpha_2 &= \sqrt{\frac{1}{2} \left\{ (0.918893 \times 10^{-2} + 0.035140 \times 10^{-2}) \right.} \\ &= \sqrt{\frac{1}{2} \left\{ 0.954033 \times 10^{-2} \right.} \\ &= \sqrt{0.477017 \times 10^{-2}} = 0.69066 \times 10^{-1} = 0.069066\end{aligned}$$

so that

$$\begin{aligned}\alpha &= 0.066474 + j0.069066 \quad \text{hyps. per wire km.} \\ &= 0.066474 + j0.043969 \quad \text{hyps. per wire km.}\end{aligned}$$

Using the polar method by (300) and (304), with (245) and (246)

$$\begin{aligned}\alpha &= \sqrt{(27.34 + j1.5535) (6.214 + j335.5) 10^{-6}} \\ &= \sqrt{\left\{ 27.34 \sec \beta_1 \angle \tan^{-1} \frac{1.5535}{27.34} \right.} \\ &\quad \left. \left\{ 335.5 \operatorname{cosec} \beta_2 \angle \cot^{-1} \frac{6.214}{335.5} \right\} 10^{-6} \right.} \\ &= \sqrt{\left\{ (27.34 \sec 3^\circ.15'.08'') \angle 3^\circ.15'.08'' \right.} \\ &\quad \left. \left\{ (335.5 \times 10^{-6} \operatorname{cosec} 88^\circ.56'.20'') \angle 88^\circ.56'.20'' \right\} \right.} \\ &= \sqrt{27.384 \angle 3^\circ.15'.08'' \times 335.56 \times 10^{-6} \angle 88^\circ.56'.20''} \\ &= \sqrt{9,188.91 \times 10^{-6} \angle 92^\circ.11'.28''} = 95.859 \times 10^{-3} \angle 46^\circ.5'.44'' \\ &= 0.095859 \angle 46^\circ.5'.44''\end{aligned}$$



$$\begin{aligned}
 &= 0.066474 + j0.069066 && \text{hyps. per wire km.} \\
 &= 0.066474 + j0.043969 && \text{hyps. per wire km.}
 \end{aligned}$$

The steps of the computation in the latter case are indicated geometrically in Fig. 84.

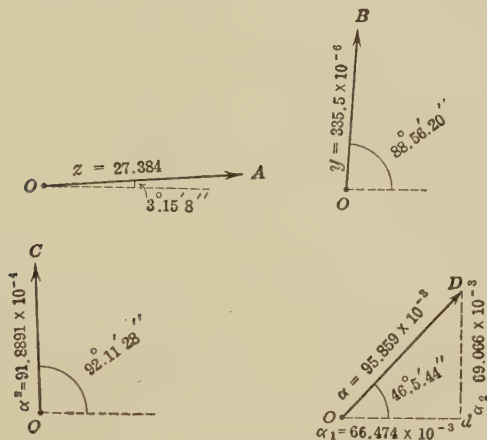


Fig. 84.—Polar development of linear hyperbolic angle.

**Alternating-current Attenuation Constant.**—We have already seen in Chapter III that the linear hyperbolic angle  $\alpha$  of a c.c. line measures the attenuation of either potential or current along a line of great length. In the a.c. case, the linear hyperbolic angle has a *real component*  $\alpha_1$  and an *imaginary component*  $\alpha_2$ . On an a.c. line of very great length; or of short length, but grounded at the motor end through an impedance equal to the surge impedance  $z_0$ , the steady-state potential being taken as  $V$  volts  $\angle$  at any point on the line, the potential  $V_1$  at a point 1 km. further along will be, by (37):

$$V_1 = V\epsilon^{-\alpha} = V\epsilon^{-(\alpha_1 + j\alpha_2)} = V\epsilon^{-\alpha_1} \cdot \epsilon^{-j\alpha_2} = V\epsilon^{-\alpha_1} \angle \alpha_2 \quad \text{volts } \angle \quad (305)$$

That is, the *real part* of  $\alpha$  determines the attenuation in size, and the *imaginary part* the attenuation in slope, or phase, per unit length of the line. From (38) and (39) the same proposition applies to the normal attenuation of both potential and current.

The *linear phase attenuation*  $\alpha_2$  may here be considered as the decay of phase in  $V$ , expressed in circular radians per kilometer.

If we consider an a.c. generator applied to the home end of a line, the waves of potential and current flow down the line, each retaining its original phase, *i.e.*, a crest persisting as a crest, and a

zero as a zero. But the generator is steadily impressing a new and advancing phase on the line; so that, with respect to the generator, the phases of the waves, as they advance, steadily fall behind that at the generator end. The greater the velocity of wave propagation, the less will be the loss of phase, or phase attenuation  $\alpha_2$  in any single kilometer of line; while on the contrary, the less rapidly the waves advance, the greater will be the phase attenuation.

**Wave Length.**—The distance in which the phase attenuation amounts to  $360^\circ$ , or  $2\pi$  circ. radians, will be 1 wave length,  $\lambda$  km. For this reason  $\alpha_2$  is sometimes called the *wave-length constant*. Consequently,

$$\lambda \alpha_2 = 2\pi \quad \text{radians} \quad (306)$$

$$\lambda = \frac{2\pi}{\alpha_2} = \frac{4}{\alpha_2} \quad \text{km.} \quad (307)$$

where  $\alpha_2$  is the wave-length constant in quadrant measure.

**Apparent Velocity or Group Velocity of Propagation.**—Moreover, the number of waves per sec. emitted by the generator, or passing any point on the line, must be equal to the impressed frequency  $f$  in cycles per second; so that the distance through which any wave will advance in 1 second must be  $f\lambda$  km., or the *apparent velocity of propagation*  $v$  will be

$$v = f\lambda = \frac{2\pi f}{\alpha_2} = \frac{\omega}{\alpha_2} = \frac{4f}{\alpha_2} \quad \frac{\text{km.}}{\text{sec.}} \quad (308)$$

In the case already considered, the normal attenuation will be approximately 0.06647 per unit, per km., or 6.647 per cent. per km.\* The phase attenuation is 0.069066 circ. radian per km., or  $3^\circ.57'.26''$  per km. The wave length  $\lambda$  is  $6.2832/0.069066 = 90.974$  km., and  $v$ , the apparent velocity of propagation,  $5,000/0.069066 = 72,395$  km. per sec.

The *actual velocity of propagation* of electric waves over circuit wires in air is accepted as equal to the velocity of light in air, or very closely 300,000 km. per sec. In a dielectric of permittivity  $\kappa$ , and permeability  $\mu$ , the actual velocity is theoretically reduced in the ratio  $1/\sqrt{\kappa\mu}$ . The apparent velocity is less than the actual velocity, owing to the effects of attenuation; whereby the advanc-

\*  $e^{-0.06647}$  is actually 0.93569, or 0.06431 per unit loss, and not 0.06647. This discrepancy is due to the fact that  $\alpha_1$  is here so large that the square and higher powers of  $\alpha_1$  are not negligible; see (37).

ing waves disappear before reaching their final goal, thus diminishing their apparent speed. In the case of an overhead aerial line, with no losses, *i.e.*, with negligible linear conductor resistance  $r$  and dielectric conductance  $g$ , the linear hyperbolic angle would be

$$\alpha = \sqrt{j\bar{l}\omega \cdot j\bar{c}\omega} = j\omega\sqrt{\bar{c}l} = j\alpha_2 \quad \frac{\text{hyp.}}{\text{km.}} \angle \quad (309)$$

or  $\alpha$  would be all imaginary. The apparent velocity of propagation would then, by (308), be  $v = 1/\sqrt{\bar{c}l}$ . If the wires had negligible internal inductance, and the insulators supporting the wires had negligible capacitance, the value of  $1/\sqrt{\bar{c}l}$  for such an aerial line would be 300,000 km. per sec. Internal inductance, and extra external capacitance tend to lower this slightly. Linear resistance and leakance lower it still more, especially at low frequencies. Solid dielectrics reduce it still further, and loading the line with coils in series, or leaks in shunt, may yet further lower it.

**Special Cases of Linear Hyperbolic Angle.**—We have already seen that in the particular case of a line with negligibly small  $r$  and  $g$ , the linear hyperbolic angle  $\alpha$  becomes a pure imaginary, with zero attenuation, or for an ideal *lossless line*  $\alpha_1 = 0$ .

In the case of negligible leakance  $g$ , and negligible inductance  $l$ , we have  $x = 0$  and

$$\alpha = \sqrt{jrc\omega} = \sqrt{jrb} = \sqrt{rb} \angle 45^\circ \quad \frac{\text{hyp.}}{\text{km.}} \angle \quad (310)$$

and

$$\alpha_1 = \alpha_2 = \frac{|\alpha|}{\sqrt{2}} \quad \frac{\text{radians}}{\text{km.}} \quad (311)$$

Here  $\alpha$  is a *semi-imaginary quantity*, *i.e.*, a complex quantity having equal real and imaginary components, or having an argument of  $45^\circ$ . This case corresponds very nearly to cabled lines operated at low frequencies.

Thus, if in the example of a standard twisted pair of #19 A.W.G. paper covered wires, worked out on page 150, if we make  $l = 0$  and also  $g = 0$ , we obtain

$$\begin{aligned} \alpha &= \sqrt{27.34 \times j335.54 \times 10^{-6}} = \sqrt{9174 \times 10^{-6}} \angle 45^\circ \\ &= 95.781 \times 10^{-3} \angle 45^\circ = 0.095781 \angle 45^\circ \text{ hyp./km. } \angle \\ &= 0.06773 + j0.06773 \quad \text{hyp./km. } \angle \\ &= 0.06773 + j0.04312 \quad \text{hyp./km. } \angle \\ &= 0.1090 + j0.1090 \quad \text{hyp./mile } \angle \\ &= 0.1090 + j0.06939 \quad \text{hyp./mile } \angle \end{aligned}$$

These values of  $\alpha$  correspond to the linear hyperbolic angle of one statute loop mile of standard artificial telephone cable ( $r_{\infty} = 88$ ,  $c = 0.054 \times 10^{-6}$ ,  $\omega = 5,000$ ).

In the case when  $r$ ,  $x$ , and  $b$  are definite, but  $g$  is negligibly small,  $\beta_2^\circ \cong 90^\circ$  and  $\beta^\circ \cong \frac{\beta_1^\circ}{2} + 45^\circ$ . This case corresponds very closely to well-insulated overhead aerial lines.

In the case when  $r$ ,  $x$ , and  $g$  are definite, but  $b$  is negligibly small,  $\beta_2^\circ \cong 0^\circ$  and  $\beta^\circ \cong \frac{\beta_1^\circ}{2}$ . This case corresponds very closely to an a.c. signal circuit comprising the two rails of a railroad track.

In the case where  $l/r = c/g$ ,  $\beta_1^\circ = \beta_2^\circ = \beta^\circ$ , and we have Heaviside's distortionless circuit.\*

When the linear inductance is very appreciable, as in ordinary aerial lines, the real attenuation constant  $\alpha_1$  may be approximately expressed as follows, especially at high frequencies,

$$\alpha_1 \cong \frac{r/2}{\sqrt{l/c}} \left( 1 + \frac{gl}{cr} \right) = \frac{1}{2} \frac{r}{z_{00}} \left( 1 + \frac{gl}{cr} \right) = \frac{1}{2} \left( \frac{r}{z_{00}} + gz_{00} \right) = \frac{1}{2} \left( \frac{r}{z_{00}} + \frac{g}{y_{00}} \right) \frac{\text{hyp.}}{\text{km.}} \quad (312)$$

When the linear leakance  $g$  is negligible, this reduces to

$$\alpha_1 \cong \frac{r/2}{\sqrt{l/c}} = \frac{1}{2} \frac{r}{z_{00}} \frac{\text{hyp.}}{\text{km.}} \quad (313)$$

Prof. G. W. Pierce has shown† that in the case of negligible leakance, the value of the linear hyperbolic angle becomes

$$\alpha = \omega \sqrt{l/c} (\sinh u + j \cosh u) \quad \text{hyp. per km. } \angle \quad (314)$$

and the surge impedance

$$z_0 = z_{00} (\cosh u - j \sinh u) \quad \text{ohms } \angle \quad (315)$$

where

$$u = \frac{1}{2} \sinh^{-1} \left( \frac{r}{x} \right) = \frac{1}{2} \sinh^{-1} \left( \frac{r}{lw} \right) \quad \text{hyp.} \quad (316)$$

and

$$z_{00} = \sqrt{\frac{l}{c}} \quad \text{ohms} \quad (317)$$

\* O. Heaviside, "Reprinted Papers," 1892, vol. ii, p. 307 (*The Electrician*, 1887, 1888).

† *Proc. Am. Acad. of Arts Sci.*, April, 1922, vol. 57, No. 7, pp. 175-191.

He has computed, and published in the same paper, a table (to four decimal places) of  $\cosh u$  and  $\sinh u$  for values of  $(r/x)$  from 0 to 250.

Thus for an overhead aerial telephone pair of No. 10 A.W.G. wires 0.2589 cm. (0.1019 in.) in diameter, inter-axially separated by 1 ft. (30.48 cm.) we may take  $l = 1.142 \times 10^{-3}$  henry,  $r = 3.293$  ohms,  $c = 0.9964 \times 10^{-8}$  farad,  $g = 0$ , all per wire kilometer. At  $\omega = 10,000$ ,  $x = 11.42$  ohms per wire km. The value of  $r/x$  is then 0.28835. The value of  $\sinh^{-1}$  (0.28835) is 0.2845 hyp. The tabular value of  $\cosh 0.14225$  is 1.010 and of  $\sinh 0.14225$  is 0.1427, as obtainable for 0.28835 from the Pierce table. We also find for  $\omega\sqrt{lc}$ , 0.03373 and for  $z_0$ , 338.55 ohms. We then have by (314),  $\alpha = 0.03373$  ( $0.1427 + j1.010$ ) =  $0.00481 + j0.0341$  hyp. per km., and  $z_0 = 338.55$  ( $1.010 - j0.1427$ ) =  $342 - j48.3$  ohms.

Formulas (314) and (315) have also been extended, in the original paper, to cases of uniformly leaky lines; but they become somewhat less simple.

**Linear Hyperbolic Angle as Affected by Unit of Length.**—As already pointed out in relation to (36), the value of the linear hyperbolic angle is directly proportional to the unit of length selected. Thus, since 1 naut., or nautical mile, is 1.853 km., the value of  $\alpha$  referred to  $r$ ,  $l$ ,  $g$  and  $c$ , in linear nautical measure, would be 85.3 per cent greater than in linear kilometer measure. Thus, in the case considered (page 150),

$$\alpha_{km} = 0.095859 \angle 46^\circ.05'.44'' = 0.066474 + j0.069066 \text{ hyp. per km.}$$

This becomes, proportionately,

$$\alpha_{nt} = 0.1776 \angle 46^\circ.05'.44'' = 0.1232 + j0.1280 \text{ hyp. per naut.}$$

**Linear Hyperbolic Angle as Affected by Single-wire or Two-wire Lines.**—We have already seen that the value of  $\alpha$  is the same whether we form it from loop-kilometer or wire-kilometer linear constants. With respect to wire-linear values, the loop-linear values of conductor impedance ( $r + jx$ ) will be doubled; while those of dielectric admittance ( $g + jb$ ) will be halved. It is, therefore, entirely optional whether we enter (300) or (304) with *loop* or *wire-linear constants*, provided we keep entirely to one or the other plan. The values of  $\alpha$  and of  $\theta$  will in either case be the same. Telephone engineers ordinarily use loop-linear values. Telegraph and power-transmission engineers ordinarily use wire-



linear values. For simplicity and uniformity, we shall use wire-linear values throughout.

**Hyperbolic Angle Subtended by an Alternating-current Line.** Since, by (35),  $L\alpha = \theta$ , it follows that the hyperbolic angle  $\theta$  subtended by an a.c. line is:

$$\theta = L\alpha = L(\alpha_1 + j\alpha_2) = L\alpha_1 + jL\alpha_2 = \theta_1 + j\theta_2 \quad \text{hyp. } \angle \quad (318)$$

*This angle consists of a real or hyperbolic component  $\theta_1$ , and an imaginary or circular component  $\theta_2$ . The former measures the normal attenuation of potential or of current over the line, and the latter the attenuation of phase.*

Another expression for  $\theta$  following (35), is

$$\theta = L\sqrt{z.y} = \sqrt{Z.Y} = \sqrt{(R + jX)(G + jB)} \quad \text{hyp. } \angle \quad (319)$$

In the case of a "reactanceless track circuit," i.e., a railway-track signal circuit, with negligible rail reactance by comparison with the rail resistance, and with negligible track susceptance by comparison with the track leakance ( $X = 0$ ,  $B = 0$ ),  $\theta$  is a pure real, or a real hyperbolic angle. This corresponds also to the d.c. case.

In the ideal case of a "lossless line" ( $R = 0$ ,  $G = 0$ ),  $\theta$  is a pure imaginary, or corresponds to a circular angle. High-frequency, large, well-insulated aerial lines approximate to this case.

In the case of a "pure cable" ( $X = 0$ ,  $G = 0$ ),  $\theta$  is a semi-imaginary quantity at all frequencies.

As an example, we may consider 50 km. of the paper and air insulated twin-wire standard telephone cabled conductor, the linear hyperbolic angle of which we have already seen to be, at  $\omega = 5,000$ ,  $\alpha = 0.095859 \angle 46^\circ.05'.44'' = 0.066474 + j0.069066$  hyp. per km. Here  $\theta = 50\alpha = 4.79295 \angle 46^\circ.05'.44'' = 3.3237 + j3.4533$  hyps. This means that with normal attenuation, both the potential and the current would attenuate in 50 km. to  $e^{-3.3237} \times e^{-j3.4533} = 0.0362 \angle 3.4533$  radians  $= 0.0362 \angle 197^\circ.51'.34''$ . *Normal attenuation is the exponential attenuation which occurs on either an indefinitely long line, or on a line of moderate length, rendered equivalent in behavior to part of an infinite line, by being grounded at the far end through an impedance equal to its surge impedance  $z_0$ .*

**Normal Attenuation Factor.**—As already explained in connection with (40) and (41), a line of  $\theta$  hyps. developing normal



attenuation, has an attenuation factor, for both potential and current, of

$$\begin{aligned}\epsilon^{-\theta} &= \epsilon^{-\theta_1 \searrow \theta_2} \text{ cir. radians} = \epsilon^{-\theta_1 \searrow \theta_2} \cdot \frac{180}{\pi} \text{ degrees} \\ &= \epsilon^{-\theta_1 \searrow \theta_2} \cdot \frac{2}{\pi} \text{ quadrants} \quad \text{numeric } \angle \quad (320)\end{aligned}$$

In cases of *non-normal attenuation*, such as ordinarily present themselves in practice, the attenuation factor is the ratio of a pair of hyperbolic functions.

**Distance in Which the Normal Attenuation Factor Attains Specified Values.**—If we desire to know the distance  $L_{1/n}$  in which the magnitude or vector size either of potential or current will fall to  $1/n$ th of its initial value, we have

$$\epsilon^{-\theta_1} = n^{-1} \quad \text{numeric} \quad (321)$$

or

$$\theta_1 = \text{logh } n \quad \text{hyp.} \quad (322)$$

Thus to fall to  $1/2$ ,  $\theta_1$  must be  $\text{logh } 2 = 0.69315$ ; so that  $L_{1/2} \alpha_1 = 0.69315$ , or  $L_{1/2} = \frac{0.69315}{\alpha_1}$ . Again, to fall to  $1/\epsilon$ , or to  $0.3679$ ,

$\theta_1 = 1$  and

$$L_{1/\epsilon} = \frac{1}{\alpha_1} \quad \text{km.} \quad (323)$$

In the case already considered, where  $\alpha_1 = 0.066474$ , the potential and current will normally fall to one-epsilonth in a distance of  $L_{1/\epsilon} = 1/0.066474 = 15.04$  km., and will fall to one-half in a distance of  $L_{1/2} = 0.69315/0.066474 = 10.4$  km.

Similarly, if we desire to know the distance in which the phase of either potential or current will normally fall or lag 1 radian with respect to the phase at the line point considered,

$$L_\beta = \frac{1}{\alpha_2} \quad \text{km.} \quad (324)$$

Thus in the case considered, where  $\alpha_2 = 0.069066$ , the distance of normally attenuating 1 circ. radian in phase would be  $1/0.069066 = 14.48$  km. The distance for  $1^\circ$  would be  $57.296$  times shorter or  $14.48/57.296 = 0.2527$  km. The distance for losing  $30^\circ$  would be  $7.581$  km.

**Polar Graph of Normal Attenuation on an Alternating-current Line.**—*The polar graph of normal attenuation on any a.c. line*

is an inward equiangular spiral, in which the circular angle between the tangent and the radius-vector is  $\beta^\circ$ , the slope of  $\alpha$ .

An equiangular spiral may be expressed by the formula\*

$$\rho = a^\gamma = ce^{\gamma \cot \beta^\circ} \text{ vector size} \quad (325)$$

where  $\rho$  is the size and  $\gamma$  the slope of the radius-vector in circular radians. Here  $a$  and  $c$  are constants, and  $\beta^\circ$  is the circular angle of the spiral.

When the real attenuation component  $\alpha_1$  is small by comparison with the imaginary component  $\alpha_2$ , the circular angle approaches  $90^\circ$  or  $\pi/2$  radians. In such a case, the tangent of the *normal attenuation spiral* is nearly perpendicular to the radius-vector, and the spiral departs but little from a pure circle, making many revolutions before collapsing. On the contrary, when  $\alpha_1$  is large with respect to  $\alpha_2$ , as in the case of heavy attenuation, the tangent is nearly coincident with the radius-vector, and the spiral approaches a straight line directed toward the origin.

The normal attenuation spiral for the standard telephone cable, at  $\omega = 5,000$ , above considered, is shown in Fig. 85, at *ABC-DEFG*. The initial radius-vector  $OA = 1$ , represents the value of voltage measurable at a given point on the line, say the generator end. The tangent  $AT$  makes with this radius-vector the circular angle  $OAT = \beta^\circ = 46^\circ.05'.44''$ , and this property holds for any and all points on the curve. The successive points† *B, C, D, E, F, G*, have been chosen as marking off successive, equal circular angles at *O*, in this case  $30^\circ$ .

*Such equal angles subtend, in all normal attenuation cases, equal lengths of the line.* In this case,  $30^\circ$  corresponds to 7.581 km. Each of these successive radii-vectores *OB, OC, OD*, etc., is 60.41 per cent of the length of its predecessor, or has attenuated in size 39.59 per cent in the preceding  $30^\circ$ . The polar equation (325) of this particular spiral is  $\rho = 1.0e^{-\gamma \cot 46^\circ.5'.44''} = 1.0e^{-0.96247\gamma}$ .

It will be observed that at *OG*, 45.487 km. from *A*, the potential is oppositely directed to, or  $180^\circ$  in phase from, the initial value *OA*. In this half-revolution, the remnant is reduced to 0.0486 of the original, and in one complete revolution, or 90.973 km., the remnant would be  $(0.0486)^2 = 0.002364$  of the original,

\* Greenhill's "Differential and Integral Calculus," The Macmillan Company, 1896, p. 55.

† C. V. Drysdale, "The Theory of Alternate-current Transmission in Cables," *The Electrician*, December, 1907 and January, 1908.

an insignificantly small amount. In the case, however, of a well-insulated power-transmission line,  $\beta$  might readily attain  $88^\circ$ , and the normal attenuation of potential or current may be less than 20 per cent in one complete revolution. In such a case, the direction of the current may be reversed many times, over a long line, without falling to insensible magnitudes. *The higher the frequency, the more numerous and closer these reversals are*

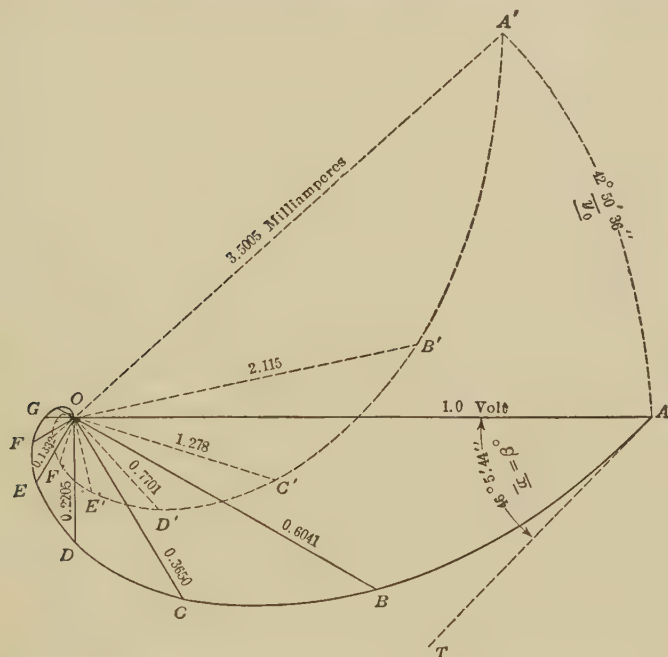


FIG. 85.—Normal attenuation spirals of potential and current.

likely to be along the line, and the more numerous the spiral convolutions in the normal attenuation graph.

#### Graphical Relation between Potential and Current Spirals.—

If we express the normal attenuation of potential along any actual line by the formula:

$$V_x = V_A e^{-\alpha x} \quad \text{volts } \angle \quad (326)$$

where  $x$  is the distance in kilometers from the point where the potential is  $V_A$  volts, it follows that

$$\frac{dV_x}{dx} = -\alpha V_A e^{-\alpha x} = -\alpha V_x \quad \frac{\text{volts}}{\text{km.}} \angle \quad (327)$$

or the rate of change of potential is  $-\alpha$  times the potential itself. But the normal attenuation graph is an inward equiangular spiral; so that the rate of change of potential along the line is also an equiangular spiral, multiplied by the vector  $\alpha$ ; *that is the negative differential of the potential spiral is the same spiral altered in scale by the size of  $\alpha$ , and changed in phase by the slope  $\beta^\circ$  of  $\alpha$* , in this case  $46^\circ.5'.44''$ . This differential spiral would start from a line near  $OF$ , drawn parallel to  $AT$ , and its radii-vectores would lag  $133^\circ.54'.16''$  behind those of the potential  $A, B, C, D, E$ .

We know from the fundamental theory discussed in Chapter IV, in relation to (54), that:

$$\frac{dV_x}{dx} = -\alpha V_x = -Iz = -I(r + j\omega) \quad \frac{\text{volts}}{\text{km.}} \angle \quad (328)$$

or

$$I = -\frac{1}{z} \cdot \frac{dV_x}{dx} \quad \text{amp.} \angle \quad (329)$$

This means that if we operate upon the differential spiral by  $-1/z$ , we shall obtain the graph of the current. Consequently, *the graph of a normally attenuating current is also an equiangular spiral, to an altered scale, and advanced  $\beta^\circ - \beta_1^\circ = \overline{y_0}$  beyond the potential spiral*. In this case  $A'B'C'D'$ , Fig. 85, is the current spiral to a scale of milliamperes, advanced  $46^\circ.5'.44'' - 3^\circ.15'.08'' = 42^\circ.50'.36''$  beyond  $ABCD$ . The initial current at  $OA'$  is numerically equal to  $y_0$ , and the current spiral may be regarded as the potential spiral after being operated upon by the plane vector  $y_0$ .

Again, following (60), if we differentiate the potential spiral twice, we obtain the same spiral operated upon by the plane vector  $\alpha^2$ ; *i.e.*, altered in scale by  $|\alpha^2|$  and advanced in phase by  $\overline{\alpha^2} = 2\beta^\circ$ .

In the case of a distortionless circuit, in which  $z_0$  and  $y_0$  are real quantities, or  $\beta^\circ = 0$ , the normal attenuation spirals of  $V$  and  $I$  have the same direction in the plane of reference, so that one and the same spiral will serve for both with a suitable change in dimensional scale.

**Similarity of Sectors in a Normal Attenuation Spiral.**—If a normal attenuation spiral of potential or current is subdivided into sectors subtending equal circular angles at the origin, like  $AOB, BOC, COD$ , etc., Fig. 85, it is evident from the laws of the equiangular spiral, that these sectors are similar; that is

$OA:OB::OB:OC$ , and if we draw chords  $AB$ ,  $BC$ ,  $CD$ , etc., we shall also have  $OA:OB::AB:BC$ . These successive chords, being equally dephased by the sectorial angle, may be also represented in a similar equiangular spiral.

**Alternating-current Surge Impedance.**—In accordance with (224) and (43), which must be now interpreted vectorially, the surge impedance  $z_0$  for a.c. lines is

$$\begin{aligned} z_0 &= \sqrt{\frac{R_f}{G_g}} = \sqrt{\frac{\bar{Z}}{\bar{Y}}} = \sqrt{\frac{R + jX}{G + jB}} = \sqrt{\frac{z}{y}} = \sqrt{\frac{r + jx}{g + jb}} \\ &= \sqrt{\frac{|z| \angle \beta_1^\circ}{|y| \angle \beta_2^\circ}} = \sqrt{\frac{|z|}{|y|} \frac{\beta_1^\circ - \beta_2^\circ}{2}} = \sqrt{\frac{|z|}{|y|}} \angle \beta_0^\circ \text{ ohms } \angle \quad (330) \end{aligned}$$

In the standard telephone cable case already considered, we have

$$\begin{aligned} z_0 &= \sqrt{\frac{27.34 + j1.5535}{(6.214 + j335.5)10^{-6}}} = 10^3 \sqrt{\frac{27.384 \angle 3^\circ.15'.08''}{335.56 \angle 88^\circ.56'.20''}} \\ &= 285.67 \angle 42^\circ.50'.36'' \text{ ohms.} \end{aligned}$$

An indefinitely long line of this type would therefore offer this impedance, for  $\omega = 5,000$ , at and beyond any point. In this case, because  $\beta_2^\circ$  is so much larger than  $\beta_1^\circ$ , the surge impedance is nearly a semi-imaginary quantity. It behaves like a condenser in series with a resistance. If, on the contrary,  $\beta_1^\circ > \beta_2^\circ$ , the slope of  $z_0$  would be positive, and the surge impedance would be an inductive instead of a condensive impedance.

*A long line whose surge impedance is inductive calls for expenditure of  $+j$  reactive power, as well as of active power from a traversing electric wave; while a line whose surge impedance is condensive, calls for the expenditure of  $-j$  reactive power, as well as of active power, from such waves.* A line whose surge impedance is reactanceless, absorbs only active power in transit, without reactive, *i.e.*, stored or transformed, power. Reactively absorbed power involves subsequent release, with corresponding after-effects, or disturbance. Actively absorbed power, *i.e.*, dissipated power, involves no subsequent reaction or disturbance.

It is for this reason that the Heaviside distortionless circuit has at all frequencies a reactanceless  $z_0$ . That is since  $x/r = b/g$ ,  $\beta_1^\circ = \beta_2^\circ$  at all frequencies, and  $\beta_0^\circ = 0$ .

**Loop Surge Impedances.**—We have already seen (49), that the surge impedance of a loop line is just double the surge impedance of a wire line. Thus, in the telephone case considered, if we take the linear constants  $r_{..}$ ,  $l_{..}$ ,  $g_{..}$ , and  $c_{..}$ , on the loop-kilometer basis



instead of on the wire-kilometer basis, the use of (330) would yield  $z_{0,,} = 571.34 \angle 42^\circ.50'.36''$  ohms instead of  $285.67 \angle 42^\circ.50'.36''$ .

At high frequencies, since  $x$  and  $b$  tend to become large with respect to  $r$  and  $g$ , the surge impedance tends to the reactanceless value:

$$z_{00} = \sqrt{\frac{\bar{l}}{c}} = \sqrt{\frac{\bar{L}}{C}} \quad \text{ohms} \quad (331)$$

**Initial Current at Sending End.**—When an indefinitely long idle line is suddenly switched upon a single-frequency a.c. generator, there will immediately be an outgoing a.c. wave projected over the line. In general, this consists of two parts, namely: (1) the “*normal wave*,” such as will be delivered to the line in the final steady state; and (2) a “*transient wave*,” which rapidly decays exponentially with time, and, in the course of a few cycles, practically disappears. This transient wave may be called, for convenience, a “*splash*.” The splash will be greatest if the line switch is closed at or near a voltage crest of the generator. It will be least, if closed at or near a zero point of current and voltage. We may assume that by choosing the proper instant for closing the line switch, the splash may be ignored. In that case, if  $V_A$  be the vector r.m.s. potential of the generator at standard phase, the initial outgoing current will be a sinusoidal function of time, whose r.m.s. value will be

$$I_A = \frac{V_A}{z_0} = V_A y_0 \quad \text{amp. } \angle \quad (332)$$

Similarly, at any point along the line, the r.m.s. current will be at the outset, and at all subsequent times, equal to the r.m.s. local potential divided by the surge impedance. This means that the potential and current waves advance steadily along the line with their amplitudes in fixed ratio, and their phases displaced by the angle  $\bar{y}_0$  (see Chapter XI).

In the case of a finite line grounded at the far end through  $z_0$  ohms  $\angle$ , or shorted in the double-wire case through  $z_{0,,} = 2z_0$  ohms  $\angle$ , the condition is the same. Ignoring splash, the initial values of outgoing r.m.s. potential and current remain the final values, because the condition is one of normal attenuation, with no reflected waves returning from the distant end. In the case, however, of a finite line grounded at the far end through an impedance other than  $z_0$ , there will be waves reflected from that end, which, running to and fro over the line, will superpose themselves upon the outgoing normal waves. In the final steady



state, the outgoing current will settle down to the value (see (149))

$$I_A = \frac{V_A}{z_0 \tanh \delta_A} = V_A \cdot y_0 \coth \delta_A \quad \text{amp. } \angle \quad (333)$$

and at any point  $P$  along the line

$$I_P = \frac{V_P}{z_0 \tanh \delta_P} = V_P \cdot y_0 \coth \delta_P \quad \text{amp. } \angle \quad (334)$$

Here the vector factor  $\tanh \delta_P$  takes into account all of the superposed reflected waves which enter into the final steady stream, after theoretically infinite time; but, ordinarily, for practical purposes in the course of a few cycles. *This factor  $\tanh \delta_P$  therefore converts the initial line impedance into the final line impedance at  $P$ .*

**Alternating-current Surge Admittance.**—The surge admittance  $y_0$  of a wire line is the reciprocal of the surge impedance. The size of  $y_0$  is therefore the reciprocal of the size of  $z_0$ , and the slope of  $y_0$  is the negative of the slope of  $z_0$ . Thus, in the case considered,  $y_0 = 1/(285.67 \angle 42^\circ.50'.36'') = 3.5005 \times 10^{-3} \angle 42^\circ.50'.36''$  mho.

The surge admittance of a loop line is manifestly one-half that of either of its component wire lines.

The surge admittance at high frequencies evidently tends to the limiting and reactanceless value

$$y_{00} = \sqrt{\frac{C}{L}} = \sqrt{\frac{C}{L}} \quad \text{mhos} \quad (335)$$

**General Relations of Potential, Current, Impedance and Admittance with the Position Angle in Alternating-current Circuits.**—The fundamental formulas for single-frequency a.c. circuits in the steady state are (119), (131), (143), (144) and (161), already considered in connection with c.c. lines. They are here collected for convenience of comparison.

$$\frac{V_P}{V_C} = \frac{\sinh \delta_P}{\sinh \delta_C} \quad \text{numeric } \angle \quad (336)$$

$$\frac{I_P}{I_C} = \frac{\cosh \delta_P}{\cosh \delta_C} \quad \text{numeric } \angle \quad (337)$$

$$\frac{Z_P}{Z_C} = \frac{\tanh \delta_P}{\tanh \delta_C} \quad \text{numeric } \angle \quad (338)$$

$$\frac{Y_P}{Y_C} = \frac{\coth \delta_P}{\coth \delta_C} \quad \text{numeric } \angle \quad (339)$$

$$\left| \frac{P_P}{P_C} \right| = \left| \frac{\sinh 2\delta_P}{\sinh 2\delta_C} \right| \quad \text{numeric } \angle \quad (340)$$

*That is, the potential, current, impedance, admittance and volt-amperes at any point  $P$ , bear to the corresponding known quantities at some given point  $C$ , a simple ratio of sines, cosines, tangents and cotangents of the position angles of  $P$  and  $C$ .*

## CHAPTER XI

### OUTLINE THEORY OF THE INITIAL TRANSIENT STATE IN SIMPLE ALTERNATING-CURRENT LINES

A transient in any dynamical system is any phenomenon incident to the transition from one steady state of the system to another. Transients present themselves in many branches of engineering. The transients of actual alternating-current lines are here under consideration, and particularly the electromagnetic-wave transients that occur when a single uniform line  $A, B$ , Fig. 86, loaded at  $B$  with a fixed impedance  $\sigma$  ohms  $\angle$  is suddenly switched at  $A$  to a simple a.c. generator. These

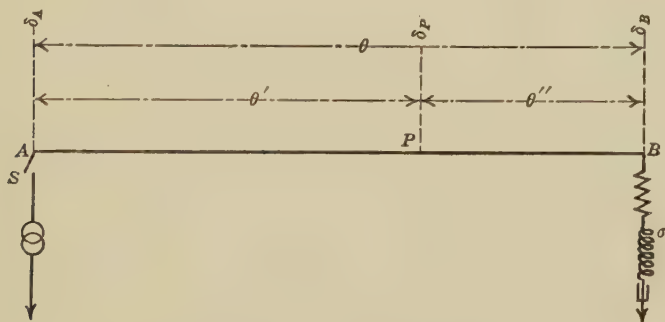


FIG. 86.—Uniform line  $AB$ , energised at  $A$  through switch  $S$ , from an alternating-current source of negligible impedance.

transients are referred to in Chapter XVII, especially in relation to Table XXVII. It is proposed to consider the elementary theory of such initial transients in somewhat more detail in this chapter.

**Assumptions.**—It is assumed that the line  $AB$  of Fig. 86 is uniform, smooth, and inactive before closing the switch  $S$ . The load  $\sigma$  ohms  $\angle$  is fixed and known. The circuit is indicated as having a ground return; but this may be regarded as equivalent to one side of a balanced two-wire metallic circuit, of doubled e.m.f.  $E$ , and doubled load  $\sigma$ . The e.m.f. is sinusoidal, so as to have one and only one frequency. If the switch  $S$  is closed at

an instant when the e.m.f. is, say, near the maximum cyclic value, the first waves of e.m.f., and current sent out over the line will not be sinusoidal, or there will be an initial disturbance that may be described as an electric splash. If, however, the switch is closed at a *zero instant*, *i.e.*, at an instant when the e.m.f. of the generator is passing through zero in the positive direction, and so that there is no splash,\* the initial and all subsequent waves of voltage and current sent out to the line are assumed to be sinusoidal.† Finally, the internal impedance of the generator is taken as negligibly small.

A voltage wave may be regarded as a wave of electric flux, and a current wave as one of the magnetic flux. Both waves have the same apparent velocity, as expressed in (308) and their combination is an electromagnetic wave.

**Normal Attenuation of Voltage and Current Waves.**—When a sinusoidal voltage or current wave is delivered to a line, without splash, from the generator to A, Fig. 86, it is subject to normal attenuation as defined by (40), (41) and (138). The wave attenuates in magnitude and lags in phase. This lagging in phase is due to the fact that the wave leaves the generator with the phase it possesses at that instant, while the generator continues to produce new waves, or advance its phase, at the rate of  $360f$  electrical degrees per sec. Any sinusoidal wave advancing over an angular distance of  $\theta = \theta_1 + j\theta_2$  hyps., undergoes an attenuation of

$$\epsilon^{-\theta} = \epsilon^{-(\theta_1 + j\theta_2)} = \epsilon^{-\theta_1} \cdot \epsilon^{-j\theta_2} = \epsilon^{-\theta_1} \angle \theta_2 \quad (341)$$

These attenuations are exemplified in Figs. 185 and 186.

**Terminal Reflections at A and B.**—An advancing voltage wave, *i.e.*, an electric-flux wave arriving at the end of the line and striking either a terminal impedance  $\sigma = z_2$  ohms  $\angle$ , or a different line of surge impedance  $z_2$  ohms  $\angle$ , will be disrupted at the transition, in the manner originally analyzed, but without vector signification, by Heaviside.‡ The transmission coeffi-

\* The assumption that, in the general case, there will be no splash if the switch is closed at a zero instant of e.m.f. is not quite correct; but the error may be neglected as a first approximation.

† For actual tests of the theory on a long artificial line, see "The Transient Process of Establishing a Steadily Alternating Current on a Long Line from Laboratory Measurements on an Artificial Line," A. E. Kennelly and U. Nabeshima. *Proc. Am. Phil. Soc.* Vol. 44, April 1920, pp. 325-370.

‡ "Reprinted Electrical Papers," by O. Heaviside, London, 1892, vol. 1.

cient,  $m_v$  or coefficient of voltage transmission is (see Appendix D),

$$m_v = \frac{z_2}{\left(\frac{z_1 + z_2}{2}\right)} = \frac{2z_2}{z_1 + z_2} \quad \text{numeric } \angle \quad (342)$$

and the reflection coefficient  $-(1 - m_v)$  is\*

$$m_v - 1 = \frac{z_2 - z_1}{z_1 + z_2} \quad \text{numeric } \angle \quad (343)$$

On the other hand, a current wave, *i.e.*, a magnetic-flux wave, advancing from  $z_1$  to  $z_2$ , will be disrupted, with a transmission coefficient  $m_c$

$$m_c = \frac{z_1}{\left(\frac{z_1 + z_2}{2}\right)} = \frac{2z_1}{z_1 + z_2} \quad \text{numeric } \angle \quad (344)$$

and a reflection coefficient  $-(1 - m_c)$ \*

$$m_c - 1 = \frac{z_1 - z_2}{z_1 + z_2} \quad \text{numeric } \angle \quad (345)$$

Thus, a wave of voltage  $100 \angle 0^\circ$  volts passing from a section of surge impedance  $z_1 = 100 \angle 0^\circ$  ohms to another of surge impedance  $z_2 = 300 \angle 0^\circ$  ohms, develops a transmission coefficient, by (342), of  $m_v = 1.5 \angle 0^\circ$ , or rises to  $150 \angle 0^\circ$  volts, after passing the junction. The reflected wave has a coefficient  $0.5 \angle 0^\circ$ , or a value of  $+50 \angle 0^\circ$  volts. This reflected wave retreats along  $z_1$ , and raises the voltage on that side of the junction to  $150 \angle 0^\circ$  volts. There is thus no discontinuity of voltage at the junction, after the incoming wave has split. The incoming current on  $z_1$  was  $100 \angle 0^\circ / 100 \angle 0^\circ = 1.0 \angle 0^\circ$  amp. On reaching the junction, it splits, the transmitted current, by (344), being  $0.5 \angle 0$  amp., and the reflected current, by (345),  $-0.5 \angle 0^\circ$  amp. Before the transition, there was  $100 \angle 0^\circ$  volts and  $1.0 \angle 0^\circ$  amp. on  $z_1$ . After the transfer there is  $150 \angle 0^\circ$  volts and  $0.5 \angle 0^\circ$  amp. on both. The *effect of the transition* is, therefore, to raise the voltage and to lower the current in the system, so far as this particular set of waves is concerned.

It may be noticed that

$$m_v + m_c = 2 \quad (346)$$

or

$$1 - m_v = m_c - 1 \quad (347)$$

\* The negative sign applies to the reflection coefficients because the direction in which these waves advance after reflection is opposite to that of the original or transmitted waves.



**Voltage Waves Arriving Successively at an Intermediate Point P.**—If any point  $P$  is selected along the line, distant  $\theta'$  hyps. from  $A$ , as shown in Fig. 86, the first wave to arrive at  $P$ , after closing the switch  $S$ , comes from  $A$  directed towards  $B$ . The second arrives from  $B$ , directed towards  $A$ . It is evident that all the odd-numbered waves come from  $A$ , and may be called  $A$  waves; while all the even-numbered waves may be called  $B$  waves. The time required for a wave to travel in one direction over the whole line, is given in (439).

Table VIII gives a schedule of the successive  $A$  and  $B$  voltage waves arriving at  $P$ , and also at each end of the line. The coefficient  $m$  here stands for  $m_v$ . Under  $C$  is given the vector values of the voltage waves transmitted to ground through the load  $\sigma$ .

It will be observed that the successive  $A$  waves of voltage arriving at  $P$  are given in Table VIII in column  $P$  by alternate arrivals:

$$\epsilon^{-\theta'}, (1 - m_v)\epsilon^{-(2\theta+\theta')}, (1 - m_v)^2\epsilon^{-(4\theta+\theta')}, \dots \text{volts } \angle \quad (348)$$

The ratio of each wave in this series to its predecessor is

$$(1 - m_v)\epsilon^{-2\theta} = \epsilon^{-2(\theta+\delta_B)} = \epsilon^{-2\delta_A} \quad (349)$$

where, by (343) and (551),

$$(1 - m_v) = \frac{z_0 - \sigma}{z_0 + \sigma} = \frac{1 - \tanh \delta_B}{1 + \tanh \delta_B} = \epsilon^{-2\delta_B} \quad (350)$$

$\delta_B$  and  $\delta_A$  are the position angles of the terminals  $B$  and  $A$  in the steady state, as defined in (106) and (107).

Similarly, the successive  $B$  waves arriving at  $P$  in Table VIII under column  $P$  are:

$$(m_v - 1)\epsilon^{-(2\theta-\theta')}, -(m_v - 1)^2\epsilon^{-(4\theta-\theta')}, (m_v - 1)^3\epsilon^{-(6\theta-\theta')}, \dots \quad (351)$$

The ratio of each term to its predecessor is again

$$-(m_v - 1)\epsilon^{-2\theta} = (1 - m_v)\epsilon^{-2\theta} = \epsilon^{-2\delta_A} \quad (352)$$

Successive pairs of  $A$  and  $B$  waves are periodic, and may be described as  $AB$  waves. The ratio of each  $AB$  wave to its predecessor is  $\epsilon^{-2\delta_A}$ , the same as that of its two components.

If we sum up vectorially the  $AB$  waves arriving either at  $P$ , or at  $B$ , up to the  $k$ th inclusive, it is indicated in Table VIII, that the total amounts to

$$E_\alpha (1 - \epsilon^{-2k\delta_A}) \quad \text{volts } \angle \quad (353)$$

where  $E_\alpha$  is the r.m.s. voltage established in the final steady state at  $P$ , and the quantity  $(1 - \epsilon^{-2k\delta_A})$  is the growth factor of the

TABLE VIII

Schedule of voltage-wave arrivals and reflections at a point  $P$  on a uniform line  $AB$ , on which unit maximum cy. e.m.f. is impressed at  $A$ , and a load  $\sigma$  vector ohms is connected at  $B$

Number of wave	Time at $A$ , $t$ sec.	$A$	$P$	$B$	$C$	Time at $C$ , $t$ sec.
1A	0	1.0	$\epsilon^{-\theta'}$	$\epsilon^{-\theta}$	$m\epsilon^{-\theta}$	$T$
2A	2T	$(m-1)\epsilon^{-\theta}$	$(m-1)\epsilon^{-(\theta+\theta')}$	$(m-1)\epsilon^{-\theta}$	.....	$T$
2A	2T	$(1-m)\epsilon^{-\theta}$	$(1-m)\epsilon^{-(\theta+\theta')}$	$(1-m)\epsilon^{-\theta}$	$m(1-m)\epsilon^{-\theta}$	3T
3A	4T	$-(m-1)^2\epsilon^{-\theta}$	$-(m-1)^2\epsilon^{-(\theta+\theta')}$	$-(m-1)^2\epsilon^{-\theta}$	.....	3T
3A	4T	$(1-m)^2\epsilon^{-\theta}$	$(1-m)^2\epsilon^{-(\theta+\theta')}$	$(1-m)^2\epsilon^{-\theta}$	$m(1-m)^2\epsilon^{-\theta}$	5T
3A	6T	$(m-1)^3\epsilon^{-\theta}$	$(m-1)^3\epsilon^{-(\theta+\theta')}$	$(m-1)^3\epsilon^{-\theta}$	.....	5T
4A	.....	$(1-m)^{k-1}\epsilon^{-\theta(k-1)}$	$(1-m)^{k-1}\epsilon^{-(\theta+\theta')}$	$(1-m)^{k-1}\epsilon^{-\theta}$	$m(1-m)^{k-1}\epsilon^{-(\theta+\theta')}$	$(2k-1)T$
4A	2(k-1)T	$= \epsilon^{-2(k-1)\delta_A}$	$= \epsilon^{-(2k-1)\delta_A+\theta'}$	$= \epsilon^{(2k-1)\delta_A+\theta}$	$= 2 \sinh \delta_B \epsilon^{-(2k-1)\delta_A}$	$(2k-1)T$
kB	2kT	$-(1-m)^k\epsilon^{-\theta}$	$-(1-m)^k\epsilon^{-(\theta+\theta')}$	$-(1-m)^k\epsilon^{-(\theta+\theta')}$	.....	$(2k-1)T$
		$= -\epsilon^{-2k\delta_A}$	$= -\epsilon^{-(2k\delta_A+\theta')}$	$= -\epsilon^{-(2k-1)\delta_A-\delta_B}$		
Sum to	2kT	1.0	$\frac{\sinh \delta_P}{\sinh \delta_A} (1 - \epsilon^{-2k\delta_A})$	$\frac{\sinh \delta_B}{\sinh \delta_A} (1 - \epsilon^{-2k\delta_A})$		Sum to $2(k-1)T$
Sum to	2kT	1.0	$\frac{\sinh \delta_P}{\sinh \delta_A} \cdot 2\epsilon^{-k\delta_A} \sinh k\delta_A$	$\frac{\sinh \delta_B}{\sinh \delta_A} \cdot 2\epsilon^{-k\delta_A} \sinh k\delta_A$		Sum to $2(k-1)T$
Sum to	2kT	1.0	$E_{P\sigma} \cdot 2\epsilon^{-k\delta_A} \sinh k\delta_A$	$E_{B\sigma} \cdot 2\epsilon^{-k\delta_A} \sinh k\delta_A$		Sum to $2(k-1)T$

waves up to the completion of the  $k$ th  $AB$  wave. If  $k = 0$ , no waves have arrived at  $P$ , and the growth factor is zero. If  $k = \infty$ , the growth factor is 1.

**Current Waves Arriving Successively at an Intermediate Point P.**—Table IX gives the schedule of the successive  $A$  and  $B$  current waves arriving at  $P$ , and also at each end of the line. The coefficient  $n$  here stands for  $m_c$ . Under  $C$  is given the vector values of the current waves successively transmitted to ground through the load  $\sigma$ .

It will be observed that the successive  $A$  waves of current arriving at  $P$  are, counting the initial outgoing wave as  $1.0 \angle 0^\circ$ ;  $\epsilon^{-\theta'}$ ,  $(m_c - 1)\epsilon^{-(2\theta+\theta')}$ ,  $(m_c - 1)^2\epsilon^{-(4\theta+\theta')}$  . . . amp.  $\angle$  (354) and the corresponding  $B$  waves are:

$$(m_c - 1)\epsilon^{-(2\theta-\theta')}, \quad (m_c - 1)^2\epsilon^{-(4\theta-\theta')}, \quad (m_c - 1)^3\epsilon^{-(6\theta-\theta')} \dots \text{amp. } \angle \quad (355)$$

In each of these series, the vector ratio of any wave to its predecessor is  $(m_c - 1)\epsilon^{-2\theta}$ . By (347) this is the same vector ratio as in the series of voltage waves, and is equal to  $\epsilon^{-2\delta_A}$ .

Table IX also shows that the sum of the first  $k$   $AB$  waves at either  $P$  or  $B$  is  $I_\infty (1 - \epsilon^{-2k\delta_A})$ ; where  $I_\infty$  is the final r.m.s. alternating-current strength, and  $(1 - \epsilon^{-2k\delta_A})$  is the growth factor. We may, therefore, conclude that in any simple line circuit, like that of Fig. 86, energized splashlessly at  $A$ , the growth factor for  $A$ ,  $B$ , or  $AB$  waves of either voltage or current is the same, at all points along the line.

**Geometrical Representation of Vector Growth. Equiangular Spiral Polygons.**—If we consider any regular plane polygon, such as a square or hexagon, it is evident that the internal angles of such a polygon are equal, and that the sides are also equal, or that the ratio of successive side lengths is unity. If, however, we attempt to draw a plane polygon with constant internal angles, but with the ratio of successive side lengths some constant differing from unity, we are led to a construction of the type indicated in Fig. 87, and which may be called an *equiangular spiral polygon*; because the spiral curve enveloping the vertices  $ABCD$  of the polygon is an equiangular spiral, or a spiral in which the radius vector from the pole  $P$ , to the curve at any point has a constant inclination to the local tangent. In the particular equiangular spiral polygon of Fig. 87, each side is two-thirds of the length of its predecessor, and the interior angles  $OAB$ ,

TABLE IX

Schedule of current wave arrivals and reflections at a point  $P$  on a uniform line  $AB$ , on which a current of maximum cv. strength  $I_0 = E/z_0$  vector amperes is launched at  $A$ , and to which a load of  $\sigma$  vector ohms is connected at  $B$

Number of wave	Time at $A$ , $t$ sec.	$A$	$P$	$B$	$C$	Time at $C$ , $t$ sec.
1A	0	1.0	$\epsilon^{-\theta'}$	$\epsilon^{-\theta}$	$n\epsilon^{-\theta}$	$T$
1B	$2T$	$(n-1)\epsilon^{-\theta\theta}$	$(n-1)\epsilon^{-(\theta\theta-\theta')}$	$(n-1)\epsilon^{-\theta}$	.....	$T$
2A	$2T$	$(n-1)\epsilon^{-\theta\theta}$	$(n-1)\epsilon^{-(\theta\theta+\theta')}$	$(n-1)\epsilon^{-\theta\theta}$	$n(n-1)\epsilon^{-3\theta}$	$3T$
2B	$4T$	$(n-1)^2\epsilon^{-4\theta}$	$(n-1)^2\epsilon^{-(4\theta-\theta')}$	$(n-1)^2\epsilon^{-4\theta}$	.....	$3T$
3A	$4T$	$(n-1)^2\epsilon^{-4\theta}$	$(n-1)^2\epsilon^{-(4\theta+\theta')}$	$(n-1)^2\epsilon^{-4\theta}$	$n(n-1)^2\epsilon^{-6\theta}$	$5T$
3B	$6T$	$(n-1)^3\epsilon^{-6\theta}$	$(n-1)^3\epsilon^{-(6\theta-\theta')}$	$(n-1)^3\epsilon^{-6\theta}$	.....	$5T$
...	...	...	...	...	.....	...
kA	$2(k-1)T$	$(n-1)^{k-1}\epsilon^{-2(k-1)\theta}$ $= \epsilon^{-2(k-1)\delta_A}$	$(n-1)^{k-1}\epsilon^{-\{2(k-1)\theta+\theta'\}}$ $= \epsilon^{-2(k-1)\delta_A+\theta'}$	$(n-1)^{k-1}\epsilon^{-(2k-1)\theta}$ $(n-1)^{k-1}\epsilon^{-(2k-1)\theta}$	$n(n-1)^{k-1}\epsilon^{-(2k-1)\theta}$ $= 2 \cosh \delta_B \epsilon^{-(2k-1)\delta_A}$	$(2k-1)T$
kB	$2kT$	$(n-1)^k\epsilon^{-2k\theta} = \epsilon^{-2k\delta_A}$	$(n-1)^k\epsilon^{-(2k\theta-\theta')} = \epsilon^{-(2k\delta_A-\theta')}$	$(n-1)^k\epsilon^{-(2k-1)\theta}$ $= \epsilon^{-(2k\delta_A-\theta')}$	.....	$(2k-1)T$
Sum to	$2kT$	$I_0 \cosh \delta_P (1 - \epsilon^{-2k\delta_A})$ $I_A \cosh \delta_A$	$I_0 \cosh \delta_P (1 - \epsilon^{-2k\delta_A})$ $I_A \cosh \delta_P (1 - \epsilon^{-2k\delta_A})$	$I_0 \cosh \delta_B (1 - \epsilon^{-2k\delta_A})$ $I_A \cosh \delta_A$	.....	Sum to $2(k-1)T$
Sum to	$2kT$	$I_A \cosh \delta_P (1 - \epsilon^{-2k\delta_A})$ $I_{A\alpha} (1 - \epsilon^{-2k\delta_A})$	$I_A \cosh \delta_P (1 - \epsilon^{-2k\delta_A})$ $I_{P\alpha} (1 - \epsilon^{-2k\delta_A})$	$I_A \cosh \delta_B (1 - \epsilon^{-2k\delta_A})$ $I_{B\alpha} (1 - \epsilon^{-2k\delta_A})$	.....	Sum to $2(k-1)T$
Sum to	$2kT$	$I_{A\alpha} (1 - \epsilon^{-2k\delta_A})$ $I_{A\alpha} \cdot 2\epsilon^{-k\delta_A} \sinh k\delta_A$	$I_{P\alpha} (1 - \epsilon^{-2k\delta_A})$ $I_{P\alpha} \cdot 2\epsilon^{-k\delta_A} \sinh k\delta_A$	$I_{B\alpha} (1 - \epsilon^{-2k\delta_A})$ $I_{B\alpha} \cdot 2\epsilon^{-k\delta_A} \sinh k\delta_A$	.....	Sum to $2(k-1)T$
Sum to	$2kT$	$I_{A\alpha} (1 - \epsilon^{-2k\delta_A})$ $I_{A\alpha} \cdot 2\epsilon^{-k\delta_A} \sinh k\delta_A$	$I_{P\alpha} (1 - \epsilon^{-2k\delta_A})$ $I_{P\alpha} \cdot 2\epsilon^{-k\delta_A} \sinh k\delta_A$	$I_{B\alpha} (1 - \epsilon^{-2k\delta_A})$ $I_{B\alpha} \cdot 2\epsilon^{-k\delta_A} \sinh k\delta_A$	.....	Sum to $2(k-1)T$
including ( $k+1$ )A	$2kT$	$I_{A\alpha} (1 - \epsilon^{-2k\delta_A})$ $+ I_0 \epsilon^{-2k\delta_A}$				

$ABC$ , etc. are all  $120^\circ$ . Such a polygon commencing at the origin  $O$ , will terminate at the pole  $P$ , after an infinite number of steps taken in uniformly decreasing geometrical ratio. In any such polygon, the angles  $OPA$ ,  $APB$ ,  $BPC$ , etc., subtended at the pole by successive sides, are equal, the successive triangles  $OAP$ ,  $ABP$ ,  $BCP$ , etc. are all similar, and the radii from the pole to the successive vertices,  $PO$ ,  $PA$ ,  $PB$ , etc., diminish in the same ratio as the sides.

If we take the plane vector  $OP$  as unity, and draw the polygon\* so that the ratio of successive sides  $AB/OA$  and of successive

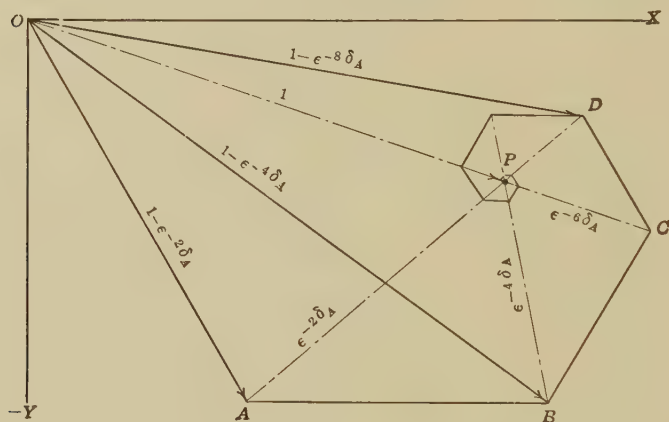


FIG. 87.—Example of equiangular spiral polygon.

radii  $BP/AP$  is equal to  $e^{-2\delta_A}$ ; then the radii  $AP$ ,  $BP$ ,  $CP$ , etc. will have the respective vector lengths  $e^{-2\delta_A}$ ,  $e^{-4\delta_A}$ ,  $e^{-6\delta_A}$ , etc.; while the vectors  $PA$ ,  $PB$ ,  $PC$ , etc. will be  $-e^{-2\delta_A}$ ,  $-e^{-4\delta_A}$ ,  $-e^{-6\delta_A}$ , etc. It is then evident that the vectors  $OA$ ,  $OB$ ,  $OC$ , etc. are respectively  $(1 - e^{-2\delta_A})$ ,  $(1 - e^{-4\delta_A})$ ,  $(1 - e^{-6\delta_A})$ , etc. This will be the vector growth of a voltage or current whose final value is  $OP$ , and whose transient value after  $k$   $AB$  wave arrivals is, by (353),  $(1 - e^{-2k\delta_A})$ . To each particular length of line in Fig. 86, impressed frequency  $f$ , and terminal load  $\sigma$ , there will correspond one and only one spiral polygon, having the vector ratio  $e^{-2\delta_A}$ , and growth factor  $(1 - e^{-2k\delta_A})$ .

\*"Equiangular Spiral Polygons as Presenting Themselves in Electrical Engineering" A. E. Kennelly, *Proc. Am. Phil. Soc.*, Apr., 1926, Vol. 65, No. 1, pp. 326-348.



**Determination of the Pole of a Spiral Polygon from Any Known Pair of Successive Wave Vectors.**—In Fig. 88, let  $AB$  and  $BC$  be two successive known vectors,  $A$  being the origin, and  $AX$  the initial line, or phase reference. It is required to find the vector  $AP$  of the pole. Let  $AB$  be taken as unity; then  $BC$  will be vectorially

$$\epsilon^{-n} = \epsilon^{-(\alpha-j\beta)} = \epsilon^{-\alpha} \cdot \epsilon^{j\beta} = \epsilon^{-\alpha} \angle \beta \quad (356)$$

where  $\epsilon^{-\alpha}$  is the size ratio of each side to its predecessor, in this case  $0.754 = \epsilon^{-0.2825}$  and  $\beta$  is the angle in circular radians that each side makes with its predecessor, in this case  $\pi/3$  or  $1.0472$ ,

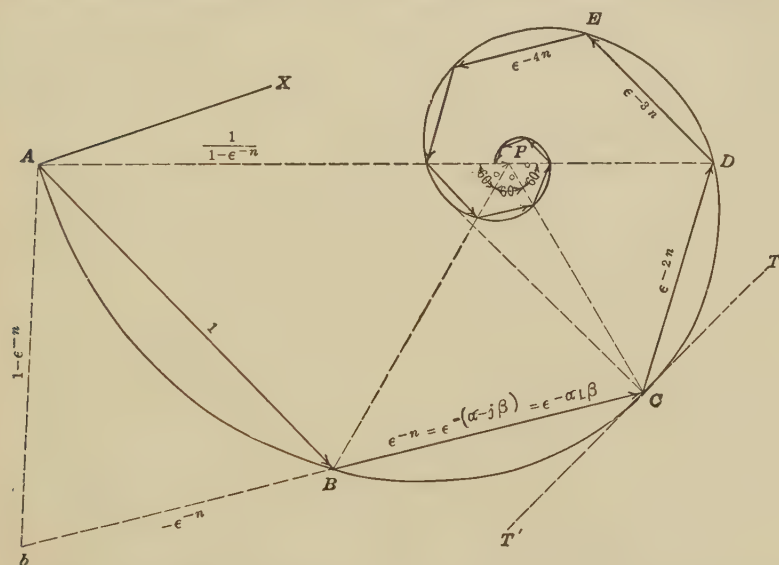


FIG. 88.—Construction for finding the pole  $P$  of an equiangular spiral polygon, when two successive sides are given, such as  $AB$  and  $BC$ . Here  $n = 2\delta_A$ .

corresponding to  $60^\circ$ . That is,  $BC$  makes an angle of  $60^\circ$  with  $AB$  produced. Continuing the construction,  $CD$  will be vectorially  $\epsilon^{-2n}$ ,  $DE$  will be  $\epsilon^{-3n}$ , and so on. The vector  $AP$  will therefore be the sum of the infinite series;

$$1 + \epsilon^{-n} + \epsilon^{-2n} + \epsilon^{-3n} + \dots = \frac{1}{1 - \epsilon^{-n}} \quad (357)$$

If  $CB$  is produced to  $b$ , so that  $bB = BC$ , we have  $Bb = -\epsilon^{-n}$  and  $Ab = 1 - \epsilon^{-n}$ . The vector reciprocal of  $Ab$  will then be  $AP$ , the required vector to the pole. We make the angle  $BAP$  equal to the angle  $bAB$ , and make  $AP$  a third proportional to  $Ab$  and  $AB$ .

The angle of the *enveloping spiral* is *PCT* and is constant. We have this angle defined by the relation

$$\tan \phi = \frac{\beta}{\alpha} \quad (358)$$

If we consider the exponent  $n$  as a plane vector with a real component  $\alpha$  and an imaginary component  $\beta$ , the slope of  $n$  is the angle  $\phi$ . In the case of Fig. 88,  $\beta = 1.0472$  and  $\alpha = 0.2825$ ; so that  $\tan \phi = 1.0472/0.2825 = 3.7069$  and  $\phi = 75^\circ$ , nearly.

**Particular Case of a Sixteenth-wave Line Freed at B.**—Figure 89, illustrates the case of a sixteenth-wave line of  $\theta = 0.34658 + \frac{2\pi}{16} = 0.34658 + j0.25$ , freed at  $B$ , and energized at  $A$  with an e.m.f. of  $100 \angle 0^\circ$  r.m.s. volts. The wave arrivals are reckoned at a point  $P$ , half way along the line. The position angle of  $A$ , due to the freeing of  $B$  is,

$$\delta_A = 0.34658 + j1.25 \quad \text{hyps. } \angle \quad (359)$$

and

$$2\delta_A = 0.69315 + j2.5 \quad \text{hyps. } \angle \quad (360)$$

Each  $A$  wave will bear to its predecessor the ratio

$$e^{-0.69315 \angle 225^\circ} = 0.5 \angle 225^\circ = 0.5 \angle 135^\circ$$

The first  $A$  voltage wave to arrive at the mid-point  $P$  is  $100e^{-0.17329 \angle 0.125} = 84.1 \angle 11^\circ.25$ . This is represented by the vector  $OA$ , Fig. 89. The next  $A$  wave is half  $OA$  in size, and makes an angle of  $225^\circ$  with  $OA$ , or  $AB = 42.05 \angle 236^\circ.25 = 42.05 \angle 123^\circ.75$ . Each succeeding  $A$  wave is half the last in size, and makes an internal angle with it of  $45^\circ$ . The pole of this spiral polygon is found at  $R$  with a vector  $OR$ .

Similarly, the first  $B$  voltage wave arriving at  $P$  is, by the series (351),  $Oa = 59.5 \angle 0.375 = 59.5 \angle 33^\circ.75$ . Its successors are  $ab$ ,  $bc$ ,  $cd$ , etc., each half its predecessor, and enclosing the same angle of  $45^\circ$ . The pole of the  $B$  series is at  $r$ . The resultant of both  $A$  and  $B$  voltage waves is  $OE'$ , the vector sum of  $OR'$  and  $Or$ , amounting to  $100.7 \angle 5.8^\circ$  volts. We may, however, consider the successive  $AB$  waves, each formed by one  $A$  and the next  $B$  wave. This is shown by the vectors  $OA + Aa'$ ,  $a'B' + B'b'$ ,  $b'C' + C'c'$ , etc. If we draw the lines  $Oa'$ ,  $a'b'$ ,  $b'c'$ , etc., these will denote the successive  $AB$  waves. Each is half its predecessor, and encloses with it an angle of  $45^\circ$ . The pole of the  $AB$  polygon is at  $E'$ , and the vector  $OE'$  measures  $100.7 \angle 5.8^\circ$ .

The  $A$ ,  $B$  and  $AB$  polygons thus have each the same ratio  $e^{-2\delta_A}$ , and the same growth factor. The final voltage at  $P$  in the steady state is, by (118).

$$E_P = E_A \frac{\sinh \delta_P}{\sinh \delta_A} = E_A \frac{\cosh (0.1733 + j0.125)}{\cosh (0.3466 + j0.25)} = 100.7 \angle 5.8^\circ \text{ volts } \angle \quad (361)$$

If, as in the case just considered, the point  $P$  is midway between  $A$  and  $B$ , the successive  $A$  and  $B$  waves arrive at  $P$  at

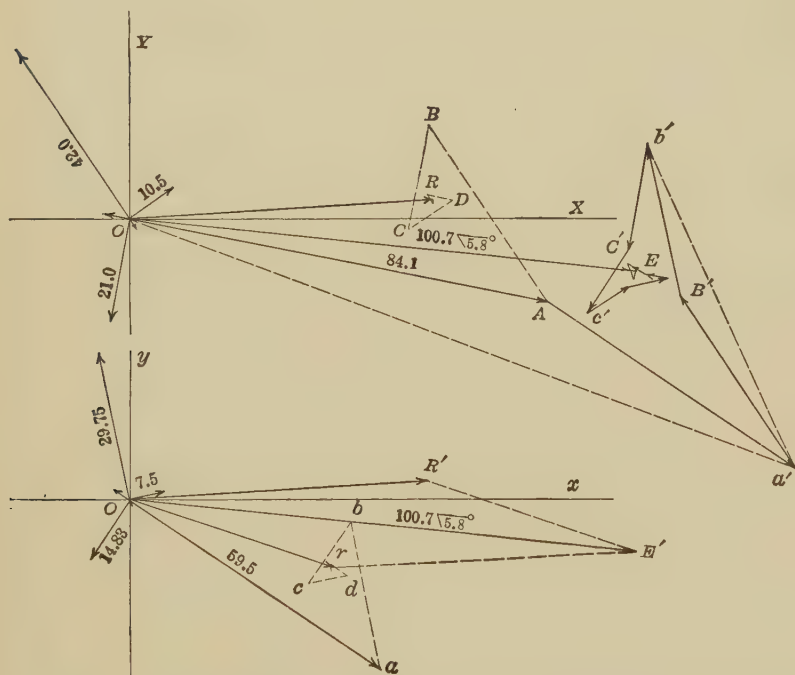


FIG. 89.— $A$ ,  $B$ , and  $AB$  spiral polygons of voltage-wave arrivals at a point  $P$  on a sixteenth-wave line freed at  $B$ , and for which  $\theta = 0.34658 + j\frac{\pi}{8}$ .

successive equal intervals of time. If, however,  $P$  is moved towards the end  $B$ , the time interval between an  $A$  wave and its successor  $B$ , is less than the interval between a  $B$  wave and its successor  $A$ . Finally, if  $P$  is moved to the far end, so as to coincide with  $B$ , the  $A$  and  $B$  waves will coalesce, and produce their effects at the same instants.

**Case of an Eighth-wave Line.**—Figure 90 presents the polygon of vector voltage wave, arriving at the free end  $B$  of a line having an angle

$$\theta = 0.3466 + j\frac{2\pi}{8} = 0.3466 + j0.7854 = 0.3466 + j\underline{0.5}$$

and therefore having one-eighth of a wave length. The position angle at the  $A$  end of the line is  $\delta_A = 0.3466 + j\underline{1.5}$  and  $\epsilon^{-2\delta_A} = \epsilon^{-(0.69315+j3)} = 0.5\angle 270^\circ = 0.5\angle 90^\circ$ . Each wave has half the size of its predecessor, and leads the latter by  $90^\circ$ .

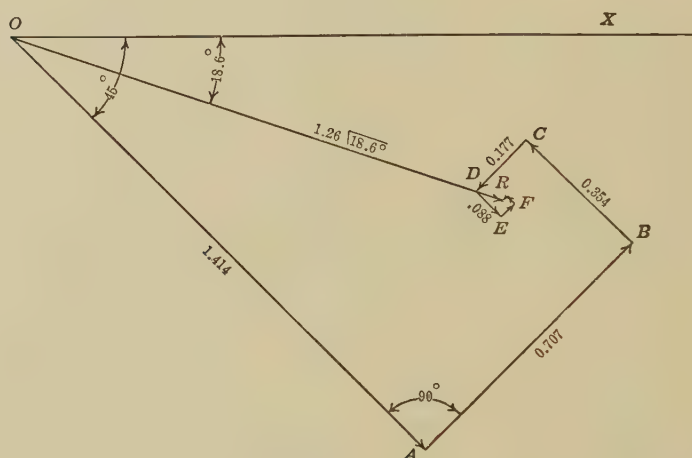


Fig. 90.—Spiral polygon of voltage waves building up at the free end  $B$  of an eighth-wave line having an angle  $\theta = 0.34658 + j\frac{\pi}{4} = 0.34658 + j\underline{0.5}$ .

The first  $A$  wave to arrive at  $B$ , from a generator at  $A$  of  $1.0\angle 0^\circ$  r.m.s. volt, is  $\epsilon^{-0.3466}\angle 0.5 = 0.707\angle 45^\circ$ . The  $B$  wave reflected from the same open end immediately merges with this, and doubles it to form the first  $AB$  wave  $OA$ , Fig. 90, of  $1.414\angle 45^\circ$  volts. If no other reflections arrived later, the voltage at  $B$  would remain 1.414 volts, lagging  $45^\circ$ , or one-eighth of a cycle, behind the generator at  $A$ . The next  $AB$  wave is, however,  $AB = 0.707\angle 45^\circ$ , and so on, until after what is theoretically an infinite time, but, from an engineering standpoint, is apparently only a few milliseconds, the final steady voltage becomes

$$OR = 1.26\angle 18^\circ.6 = 1.0 \times \text{sech } (0.3466 + j\underline{0.5}) \text{ volts } \angle \quad (362)$$

The successive vector stages of growth of this terminal e.m.f. at  $B$  are  $OA$ ,  $OB$ ,  $OC$ ,  $OD$ , etc., represented by the expression

$$1.26\angle 18^\circ.6(1 - \epsilon^{-2k\delta_A}) = 1.26\angle 18^\circ.6 \{1 - 0.5^k \angle (k \times 90^\circ)\}$$

**Case of Quarter-wave Lines.**—When a line has quarter-wave length, its angle is  $\theta = \theta_1 + j\frac{2\pi}{4} = \theta_1 + j1$ . When freed at the distant end, its position angle at  $A$  is

$$\delta_A = \theta_1 + j2 \quad \text{hyps. } \angle \quad (363)$$

so that

$$2\delta_A = 2\theta_1 + j4 \quad \text{hyps. } \angle \quad (364)$$

Consequently

$$\epsilon^{-2\delta_A} = \epsilon^{-2\theta_1} \angle 360^\circ = \epsilon^{-2\theta_1} \angle 0^\circ \quad (365)$$

or each successive wave of either voltage or current has the same phase as its predecessor. Vectorially, all the waves fall upon one and the same straight line.

An example of the behavior is given in Fig. 91. Here a line having an angle  $\theta = 0.6 + j1$ , is freed at  $B$ , and is energized splashlessly at  $A$ , with  $1.0 \angle 0^\circ$  r.m.s. volt. The voltage waves are reckoned at the free end  $B$ . The first  $A$  wave to arrive there is in the condition  $1.0 \times \epsilon^{-\theta} = \epsilon^{-0.6} \angle 90^\circ = 0.5488 \angle 90^\circ$  volt. There is an immediate  $B$  reflection of equal amount from the open end and the first  $AB$  wave is  $2 \times 0.5488 \angle 90^\circ = 1.0976 \angle 90^\circ$ , as is shown by the vector  $OA$ . The vector ratio being  $\epsilon^{-1.2} \angle 0^\circ$  or  $0.3012 \angle 0^\circ$ , the next  $AB$  wave is  $0.3306 \angle 90^\circ$ , or  $AB$ . Proceeding in this way, the final voltage is  $OR = 1.5707 \angle 90^\circ$  r.m.s. volts, at  $B$ . This value is also given by the well-known formula:

$$\begin{aligned} E_B &= \frac{E_A}{\cosh \theta} = \frac{1.0 \angle 0^\circ}{\cosh (0.6 + j1)} \\ &= 1.5707 \angle 90^\circ \quad \text{volts } \angle \quad (366) \end{aligned}$$

As is pointed out in Chapter XII, this straight-line vector summation may amount to large values when  $\theta_2$  is small. The phenomenon is known as the "Ferranti effect."

Figures 92 and 93 represent the corresponding voltage polygons for a point  $P$ , two-thirds of the line length away from  $A$ , and one-third from  $B$ , the same line being assumed, and freed at  $B$ , as in the preceding illustration. The vector ratio  $\epsilon^{-2\delta_A}$ , therefore, remains unchanged at  $0.3012 \angle 0^\circ$ . The first  $A$  wave to arrive at  $P$  is  $\epsilon^{-0.4} \angle 0.667 = 0.6703 \angle 60^\circ$  or  $OA$ , in Fig. 92. The first



FIG. 91.—Vector voltage building up at the free end of a quarter-wave line, having an angle  $\theta = 0.6 + j\frac{\pi}{2} = 0.6 + j1$ .



$B$  wave, is  $\epsilon^{-0.8} \sphericalangle 1.33 = 0.4493 \sphericalangle 120^\circ$ , or  $oa$  in the figure. All the  $A$  waves add up along the line  $OABC$ , and all the  $B$  waves along the line  $Oabc$ . The final value of the  $A$  summation is  $0.9571 \sphericalangle 60^\circ$ , and that for the  $B$  summation is  $0.6411 \sphericalangle 120^\circ$ . The total final voltage at  $P$  is the vector sum of these quantities, or  $OR = 1.394 \sphericalangle 83.^\circ 7$ . We may, however, study the  $AB$

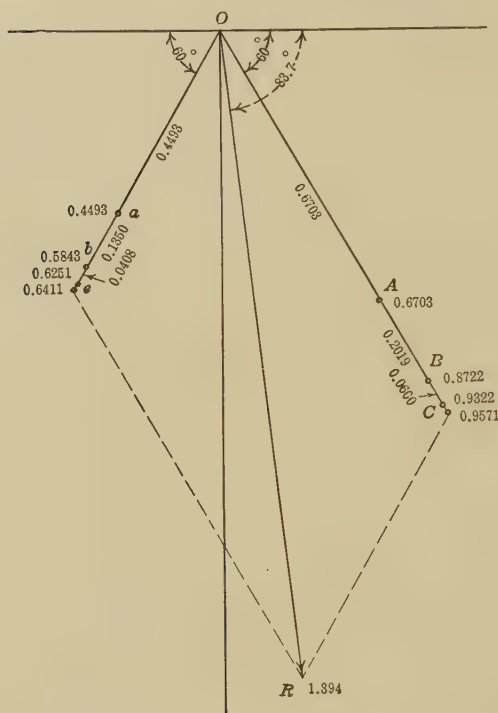


FIG. 92.— $A$  and  $B$  voltage polygons, and their resultant  $OR$ , at an intermediate point  $P$ , on a quarter-wave line freed at  $B$ .

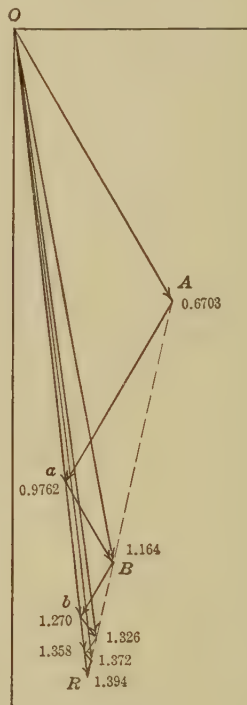


FIG. 93.—The  $AB$  polygon for the same case and intermediate point. Line angle  $\theta = 0.6 + j\frac{\pi}{2} = 0.6 + j1$ .

waves, as in Fig. 93. Here the first  $AB$  wave is  $Oa = 0.9762 \sphericalangle 83.^\circ 7$ , the sum of  $OA$  and  $Oa$  of Fig. 92. The next  $AB$  wave is  $ab$ , the third  $bc$ , and so on, the final value being  $OR = 1.394 \sphericalangle 83.^\circ 7$  as in the previous case.

Finally, the  $A$ ,  $B$ , and  $AB$  current waves polygons for the same point  $P$ , are indicated in Figs. 94 and 95. Counting the outgoing current wave

$$I_A = \frac{E_A}{Z_0} \quad \text{amp. } \angle \quad (367)$$

as unity, at standard phase, the first  $A$  wave to arrive is  $OA$ , Fig. 94, or  $0.6703 \angle 60^\circ$ , the same as  $OA$  in the  $A$  voltage case of Fig. 92; but the first  $B$  wave is  $Oa = 0.4493 \angle 60^\circ$ , Fig. 94, in the opposite direction to  $Oa$  in Fig. 92. The final resultant current wave is  $OR = 0.8446 \angle 18.83^\circ$ , which is quite different from the resultant voltage wave  $OR \dots 1.394 \angle 83^\circ.7$  of Fig.

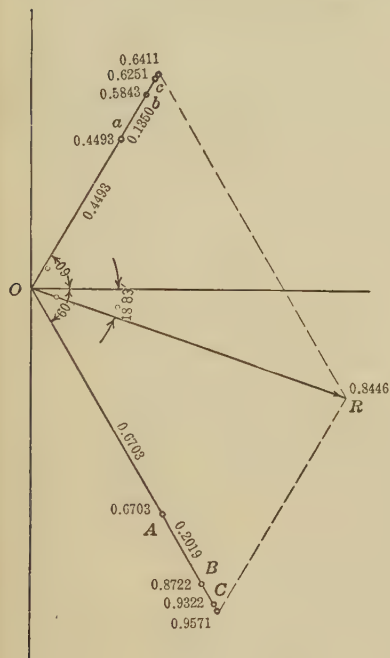


FIG. 94.—Vector current waves building up at an intermediate point  $P$  on a quarter-wave line freed at  $B$ .

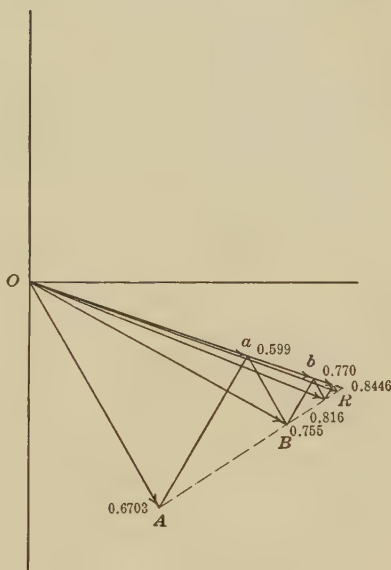


FIG. 95.—Vector  $AB$  polygon of current waves for same case and intermediate point.

92. The corresponding  $AB$  wave development is given in Fig. 95. In each of the cases presented in Figs. 92 to 95, the vector polygon is a straight line, and the vector ratio  $\epsilon^{-2\delta_A} = 0.3012 \angle 0^\circ$ . Each point  $P$  along this line, develops its own *straight line polygon* of voltage and current; but no two points have the same polygon; because the first  $AB$  wave has its own size and slope, and all the subsequent  $AB$  waves follow in the same straight line.

Lines of odd-quarter wave length ( $\frac{1}{4}$ ,  $\frac{3}{4}$ ,  $\frac{5}{4}$ , etc.), develop straight-line polygons, in which the successive vectors are cophasal, or in simple straight-line summation. Lines of even-quarter wave length ( $\frac{2}{4}$ ,  $\frac{4}{4}$ ,  $\frac{6}{4}$ , etc.), develop straight-line

polygons in which the successive vectors have opposite phases, or a phase difference of  $180^\circ$ .

Summing up the preceding discussions, we may conclude that in the case of a simple smooth line  $AB$ , connected to ground or neutral potential at  $B$  through a simple impedance  $\sigma$ , and voltaged splashlessly at  $A$  by a single-frequency generator of negligible impedance, the voltage and the current at any point  $P$  along the line, build up to their final steady a.c. states by successive vector steps, following respective spiral polygons. No two points will, in general, have the same polygon, but all will have the same growth factor, which depends only upon the position angle of the  $A$  end of the line, as developed in the final steady state.

## CHAPTER XII

### QUARTER-WAVE AND HALF-WAVE REAL LINES IN THE STEADY STATE

If an a.c. line has quarter-wave length to a given frequency, it follows that its hyperbolic angle is then expressible in the form

$$\theta_{1/4} = \theta_1 + j\frac{\pi}{2} = \theta_1 + j1 \quad \text{hyps. } \angle \quad (368)$$

When such a line is freed at the motor end, we know that the ratio of the generator-end to motor-end voltage, at the same frequency, is, by (121) or (133),

$$\frac{V_A}{V_B} = \cosh \theta_{1/4} = \cosh \left( \theta_1 + j\frac{\pi}{2} \right) = j \sinh \theta_1 \quad \text{numeric } \angle \quad (369)$$

On a line of small transmission losses and low attenuation, the real quantity  $\theta_1$  may be much less than unity, in which case  $\sinh \theta_1 \cong \theta_1$ , and the  $A/B$  voltage ratio on the quarter-wave line is very nearly

$$\frac{V_A}{V_B} \cong j\theta_1 \quad \text{numeric } \angle \quad (370)$$

or the voltage at  $A$  is to that at  $B$  in the quadrature ratio of  $\theta_1$ . Such a line develops what is commonly called a large Ferranti effect at no load, in the manner discussed in the preceding chapter.

Similarly, if this quarter-wave line is shorted or grounded at the far end, we have, by (131),

$$\frac{I_A}{I_B} = \frac{\cosh \theta_{1/4}}{\cosh 0} = \frac{\cosh \left( \theta_1 + j\frac{\pi}{2} \right)}{1} = j \sinh \theta_1 \quad \text{numeric } \angle \quad (371)$$

which is the same ratio as in (369), or the ratio of currents at generator and motor ends (grounded) are approximately in the quadrature ratio of  $\theta_1$ .

An approximate particular case is presented in Fig. 163, where a line of  $1.405 \angle 69^\circ.7 = 0.487 + j1.318 = 0.487 + j0.839$  hyp. This line had only 83.9 per cent of a quadrant or quarter-wave length, but its observed free-end voltage ratio was about 1.75; or  $V_A/V_B = 0.57$ , and  $\sinh 0.487 = 0.506$ .

Similarly a quarter-wave line whose angle was  $0.1 + j1$  would have an  $A/B$  voltage ratio of approximately 0.1 or  $B/A$  voltage ratio of 10. In power transmission, at fundamental frequencies of 60~ or less, lines are hardly ever sufficiently long to reach quarter-wave length; so that this large resonant quarter-wave rise of potential on open circuit was computed\* before it was even observed on artificial lines in the laboratory.

An experimental test of this resonant rise was made† on the laboratory artificial line of Table XVIII page 221, with the connections shown in Fig. 96. The line had a length of 240 miles (386 km.) corresponding to 500,000 circ. mils or 250 sq. mm. cross-section, in eight sections of 30 miles (48.3 km.) each. In order to make

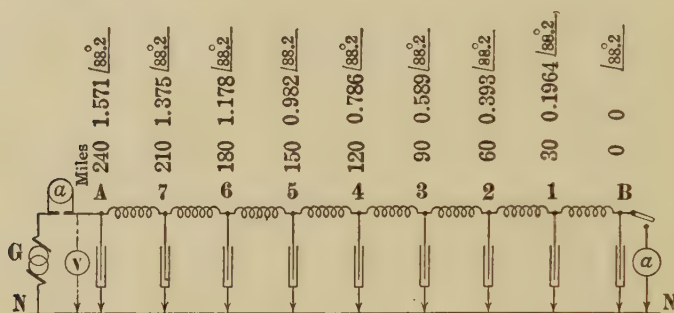


FIG. 96.—Connections for quarter-wave line tests.

this a quarter-wave line, the impressed frequency was raised to 189~. The data concerning the line at this frequency are given in Table X. The angle subtended by the line was then found to be  $1.5712 \angle 88.2 = 0.0493 + j1.5706 = 0.0493 + j1$  hyp. According to (369), the ratio of home to far free-end potential should be 0.0493, with a resonant-rise ratio of  $1/0.0493 = 20.28$ . This was, in fact, observed within the limits of experimental error. The dots in Fig. 97 indicate observations and the curve

\* "Resonance in Alternating-current Lines," by E. J. Houston and A. E. Kennelly, *Trans. A. I. E. E.*, April, 1895.

† "The Influence of Frequency on the Equivalent Circuits of Alternating-current Transmission Lines," by A. E. Kennelly, *Electrical World*, Jan. 21, 1909.

"The Application of Hyperbolic Functions to Electrical Engineering Problems," Chapter VII.

† "Resonance Tests of a Long Transmission Line," by A. E. Kennelly and Harold Pender, *Electrical World*, Aug. 8, 1914.



connects the computed corresponding values. Table X gives the observations at junctions and their position angles. In this case, therefore, 1,000 volts applied at the generator end between any pair of the three conjugate smooth-line conductors, at  $189^\circ$ , would produce more than 20,000 volts at the free ends 240 miles (386 km.) distant. A corresponding current ratio was also measured with the line grounded at the distant end, in accordance with (371).

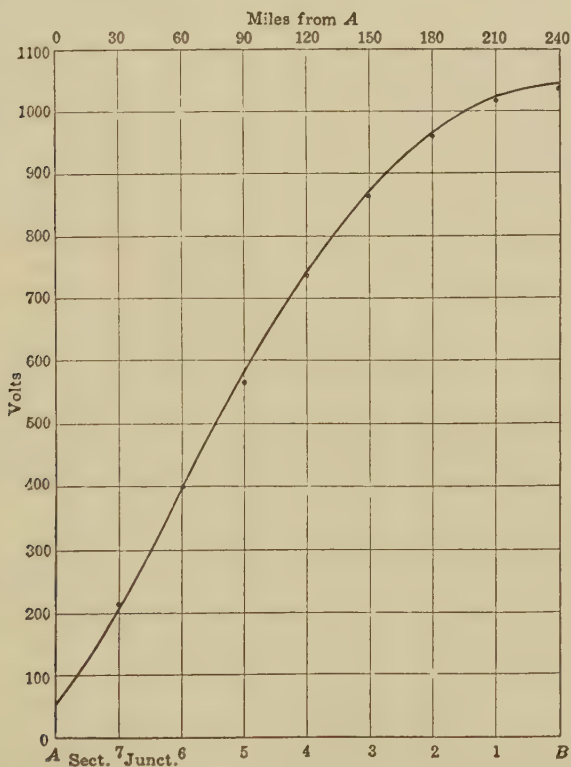


Fig. 97.—Theoretical curve of voltage along conjugate smooth line and observed values at artificial-line junctions.

In power-transmission practice, there is probably no reason for fearing the results of any such large resonant rise of potential, partly because of the great length of line necessary, at  $25^\circ$  or even at  $60^\circ$ , to approximate quarter-wave conditions, and partly because expedients are available for keeping down the motor-end voltage at light load, should it rise seriously. This

TABLE X.—VOLTAGES AT SECTION JUNCTIONS OF QUARTER-WAVE ARTIFICIAL LINE FREED AT FAR END

Position	Position angle $\delta_P$ hyps. with $B$ grounded	Cosh $\delta_P$ by chart	Potential $V_P$	
			Computed, volts	Observed, volts
$B$	0	1.000 $\angle 0^\circ.0$	1,044 $\angle 90^\circ.0$	1,033
1	0.1964 $\angle 88^\circ.2$	0.98 $\angle 0^\circ.10$	1,023 $\angle 89^\circ.9$	1,015
2	0.393 $\angle 88^\circ.2$	0.924 $\angle 0^\circ.25$	965 $\angle 89^\circ.75$	960
3	0.589 $\angle 88^\circ.2$	0.832 $\angle 0^\circ.75$	869 $\angle 89^\circ.25$	860
4	0.786 $\angle 88^\circ.2$	0.708 $\angle 1^\circ.3$	739 $\angle 88^\circ.7$	735
5	0.982 $\angle 88^\circ.2$	0.555 $\angle 2^\circ.7$	579 $\angle 87^\circ.3$	559
6	1.178 $\angle 88^\circ.2$	0.383 $\angle 5^\circ.3$	400 $\angle 84^\circ.5$	397
7	1.375 $\angle 88^\circ.2$	0.200 $\angle 11^\circ.5$	209 $\angle 78^\circ.5$	211
$A$	1.571 $\angle 88^\circ.2$	0.0493 $\angle 90^\circ.0$	51.5 $\angle 0^\circ.0$	51.5 $\angle 0^\circ$

may be done by means of a synchronous-motor reactance at the far end, or of inductive reactances applied at points along the line. It may be expected, however, that harmonic frequencies in the impressed voltage wave, on a relatively short line, may happen to excite quarter-wave resonance, and so produce, by perpendicular summation, a relatively large rise at the distant free end. Thus, a 5 per cent. harmonic, multiplied twenty-fold by accidental quarter-wave resonance, would produce a 100 per cent. harmonic component at the distant open end, which, by (421), would give rise to 41.4 per cent. increase in local r.m.s. voltage, neglecting any normal rise in voltage due to the fundamental frequency alone.

Three-quarter, five-quarter and odd-quarter wave lines, in general, give rise to resonant free-end voltages of the same general character as those on quarter-wave lines, but ordinarily much less marked in size.

**Half-wave Lines.**—On the other hand, half-wave, whole-wave, and even-quarter wave lines generally, are characterized by comparative uniformity between the potentials at their terminals.\* A half-wave line has an angle  $\theta_{\frac{1}{2}}$

$$\theta_{\frac{1}{2}} = \theta_1 + j\pi = \theta_1 + j2 \quad \text{hyps. } \angle \quad (372)$$

\* "An Artificial Transmission Line with Adjustable Line Constants," by C. E. Magnusson and S. R. Burbank, *Proc. A. I. E. E.*, Sept. 5, 1916.

and when freed at  $B$ , the  $A/B$  potential ratio is, by (117),

$$\frac{V_A}{V_B} = \frac{\sinh\left(\theta_{1/2} + j\frac{\pi}{2}\right)}{\sinh j\frac{\pi}{2}} = \cosh \theta_{1/2} = -\cosh \theta_1 \quad \text{numeric} \quad (373)$$

When  $\theta_1$  is less than 0.2,

$$\cosh \theta_1 \cong 1 + \theta_1 \quad \text{numeric} \quad (374)$$

so that for half-wave lines of very small attenuation,

$$\frac{V_A}{V_B} \cong -(1 + \theta_1) = (1 + \theta_1) \angle 180^\circ \quad \text{numeric} \angle \quad (375)$$

or  $V_A$  is greater in size than  $V_B$ ,

Similarly, if a half-wave line is grounded or shorted at the motor end  $B$ , the currents at  $A$  and  $B$  have, by (129), the ratio

$$\frac{I_A}{I_B} = \frac{\cosh \theta_{1/2}}{\cosh 0} = \frac{\cosh (\theta_1 + j\pi)}{1} = -\cosh \theta_1 = \cosh \theta_1 \angle 180^\circ \quad \text{numeric} \quad (376)$$

or in the case of small real attenuation with  $\cosh \theta_1 \cong 1 + \theta_1$ , the currents at the two ends of the line will have opposite phases but nearly the same strength.\*

**General Remarks Concerning Voltage and Current Ratios on Single Lines.**—It follows from (117) and (129) that if a single uniform line of any length or number of waves, is freed at the motor end, and the  $A/B$  voltage ratio under a given impressed frequency is denoted by the complex number  $N$ , then when the same line is shorted or grounded directly at the motor end, the  $A/B$  current ratio under the same frequency must also be  $N$ ; because, while the  $A/B$  voltage ratio is a sine ratio, yet because the open end virtually adds an imaginary quadrant to the position angles throughout, this ratio becomes virtually a cosine ratio, similar to the  $A/B$  current ratio.

As an example to illustrate the above relations, we may consider the case of the smooth line referred to on page 241, having a linear hyperbolic angle of  $\alpha = 0.0025 + j0.01$  hyp.  $\angle$  per km., and a surge impedance of  $z_0 = 400 \angle 8^\circ$  ohms. This 800-km. line, when grounded at the motor end  $B$  and voltaged at the generator end with  $1.0 \angle 0^\circ$  volt, develops the distribution of position angles, potentials and currents shown in Table XI (p. 190) and indicated

\* "The Propagation of Electric Energy by Standing and Traveling Waves, Experimental Test of an Artificial Transmission Line," by John F. H. Douglas, *Electrical World*, Aug. 10, 1912.

to polar coördinates in Fig. 98. Referring to the table, the first column indicates positions along the line, with their corresponding distances from  $A$  in the second column. The third column gives the position angles of those positions. Column IV gives the sines of the position angles, from pages 90 to 105 of the "Tables of Complex Hyperbolic Functions." The potentials

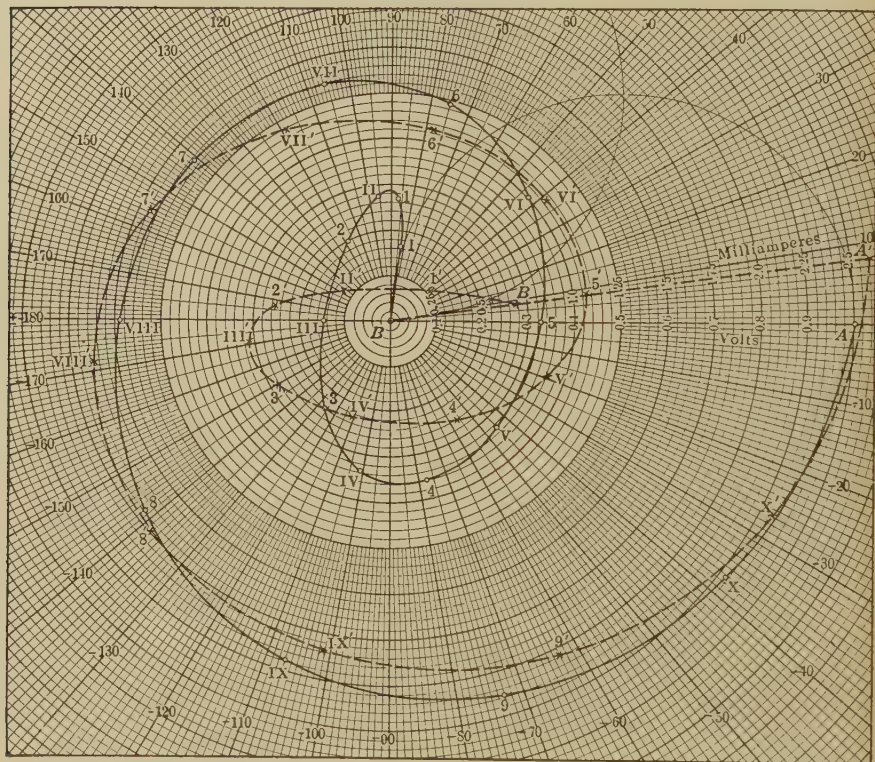


FIG. 98.—Graphs of potential and current along line of  $\theta = 2 + j8$  and  $z_0 = 400 \angle 8^\circ$  grounded at  $B$ .

in column V are in direct proportion to the sines of column IV, starting with  $V_A = 1.0 \angle 0^\circ$ . Column VI gives the cosines of the position angles from pages 106 to 121 of the book of tables. The currents in column VII are directly proportional to the cosines in column VI, starting with  $I_A = V_A / (z_0 \tanh \delta_A)$  amp. Because all the position angles have round numbers, their sines and cosines can be taken directly from the tables, to five decimal places, by direct inspection. In more general cases, either



numerical interpolation would be required for any high degree of precision; or the chart atlas could be used for swift graphical interpolation of lesser precision.\*

In Fig. 98, the heavy line is the potential graph; while the broken line is the current graph. The current leads the potential over considerable portions of the line. Both the potential and

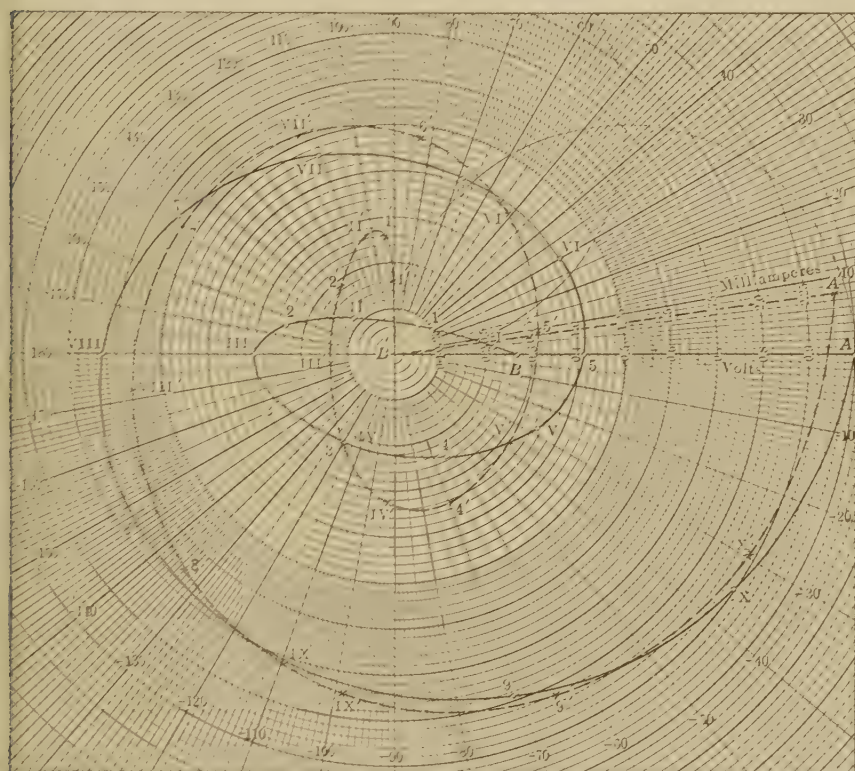


FIG. 99.—Graphs of potential and current along line of  $\theta = 2 + j8$  and  $z_0 = 400 \angle 8^\circ$  when freed at B.

current curves describe two complete revolutions in phase; but the difference of phase between them is not constant.

\* It may be noted that when, as in the case considered, the potential or current distribution extends over a considerable range of circular angle or phase displacement, the points along the line at which the position angles are quadrantal, or have an integral number of quadrants in the imaginary, can always be found, and at these points the sines or cosines are always obtainable, from tables of real hyperbolic functions, to at least five places of decimals.

In Table XII and Fig. 99, the same line is considered as freed at the *B* end, and voltaged at *A* with  $1.0\angle 0^\circ$  volts. The table is prepared in the same manner as its predecessor No. XI. The position angles of Table XII exceed the corresponding position angles of Table XI by one imaginary quadrant, since the free end adds  $j\frac{\pi}{2}$ , or  $j1$ , to all the position angles. It will be seen on comparing the two tables, that the sizes of the sines in one are the same as those of the corresponding cosines in the

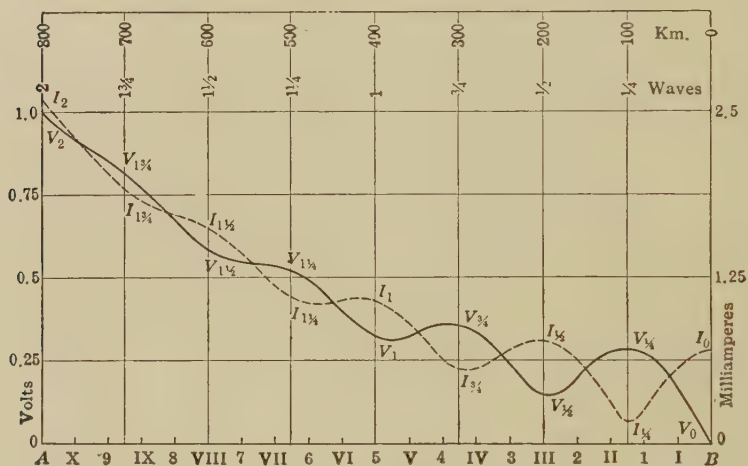


FIG. 100.—Sizes of potentials and currents along smooth line of  $\theta = 2 + j8$  and  $z_0 = 400\angle 8^\circ$  when grounded at *B* and subjected at *A* to  $1.0\angle 0^\circ$  volt.

other; or, from (133) and (134),

$$\left| \sinh \left( \alpha + j\frac{\pi}{2} \right) \right| = \left| \cosh \alpha \right| \quad \text{numeric} \quad (377)$$

and

$$\left| \cosh \left( \alpha + j\frac{\pi}{2} \right) \right| = \left| \sinh \alpha \right| \quad \text{numeric} \quad (378)$$

Consequently, the relative sizes of the currents along the line to ground are identical with the relative sizes of the potentials along the line freed, and reciprocally. The same relation can be observed in Fig. 98, which gives the graphs of potential and current along the line, and which may be compared with Fig. 99 for this purpose.

Figures 100 and 101 are corresponding “size-distance” diagrams of voltage and current for the same line, grounded and



freed at  $B$ , respectively. Referring to Fig. 100, the continuous line  $V_2 \dots V_0$  follows the size of potential along the line from 1 to 0; while the broken line  $I_2 \dots I_0$  follows the size of the current from 2.59 to 0.689 milliamp. The abscissas are marked off in positions, in kilometer distances, and in wave lengths from  $B$ . It will be observed that the  $V$  curve passes through either an actual maximum, or a tendency to a maximum size, at each odd quarter-wave distance from  $B$ . The maximum at the first quarter is the most marked, and the successive subsequent maxima dwindle and gradually disappear. The  $I$  curve shows on

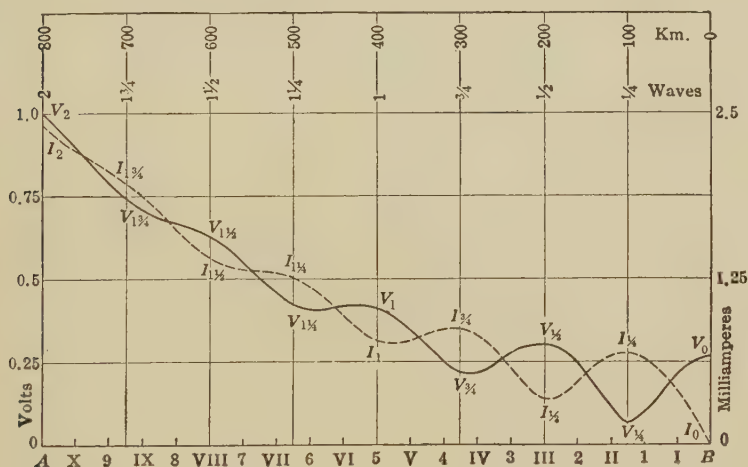


Fig. 101.—Sizes of potentials and currents along smooth line of  $\theta = 2 + j8$  and  $z_0 = 400\angle 8^\circ$ , when freed at  $B$  and subjected at  $A$  to  $1.0\angle 0^\circ$  volt.

the other hand, minima at the quarter-wave points and maxima at the zero and half-wave points, the oscillation in size being greatest near the  $B$  end, and gradually disappearing.

Turning now to Fig. 101, where the conditions are represented for an open end at  $B$ , the  $V$  line has its minima at odd-quarter wave points and the  $I$  line its maxima at these points. If the scale of potential and current sizes were suitably selected, the two sets of curves in Figs. 100 and 101 would completely coincide, the  $V$  curve in one with the  $I$  curve in the other. With the particular scales shown, the agreement is fairly close.

In the case of a large slope  $\beta^\circ$  in the linear hyperbolic angle  $\alpha$ , that is, in lines having small linear losses and large linear reactances, as for example a large-conductor aerial line operated at a high frequency, the successive oscillations in the sizes of poten-

TABLE XI

Distribution of potential and current over a uniform smooth line of  $\theta = 2.0 + j\bar{8}$  and  $z_0 = 400 \angle 8^\circ$ , when grounded at  $B$  and voltage at  $A$

I Position	II $x$ km.	III $\delta_P$ hyps.	IV $\sinh \delta_P$ by tables	V $V_P$ volts	VI $\cosh \delta_P$ by tables	VII $I_P$ milliamp.
A	0	$2.0 + j\bar{8}.0$	$3.62686 \angle 0^\circ$	$1.00 \angle 0^\circ$	$3.76220 \angle 0^\circ$	$2.59328 \angle 8^\circ$
X	40	$1.9 + j\bar{7}.6$	$3.32060 \angle 37^\circ.227$	$0.91556 \angle 37^\circ.227$	$3.36681 \angle 34^\circ.789$	$2.32074 \angle 26^\circ.789$
9	80	$1.8 + j\bar{7}.2$	$3.09206 \angle 72^\circ.900$	$0.85255 \angle 72^\circ.900$	$2.95835 \angle 71^\circ.059$	$2.03919 \angle 63^\circ.059$
IX	120	$1.7 + j\bar{6}.8$	$2.81138 \angle 106^\circ.906$	$0.77516 \angle 106^\circ.906$	$2.66361 \angle 109^\circ.155$	$1.83602 \angle 101^\circ.155$
8	160	$1.6 + j\bar{6}.4$	$2.44721 \angle 141^\circ.752$	$0.67475 \angle 141^\circ.752$	$2.50955 \angle 146^\circ.192$	$1.72983 \angle 138^\circ.192$
VIII	200	$1.5 + j\bar{6}.0$	$2.12928 \angle 180^\circ$	$0.58709 \angle 180^\circ$	$2.35241 \angle 180^\circ$	$1.62151 \angle 172^\circ$
7	240	$1.4 + j\bar{5}.6$	$1.99295 \angle 140^\circ.627$	$0.54950 \angle 140^\circ.627$	$2.06903 \angle 147^\circ.249$	$1.42618 \angle 155^\circ.249$
VII	280	$1.3 + j\bar{5}.2$	$1.94654 \angle 105^\circ.642$	$0.53670 \angle 105^\circ.642$	$1.72627 \angle 110^\circ.659$	$1.18992 \angle 118^\circ.659$
6	320	$1.2 + j\bar{4}.8$	$1.78409 \angle 74^\circ.844$	$0.49191 \angle 74^\circ.844$	$1.54077 \angle 68^\circ.706$	$1.06205 \angle 76^\circ.706$
VI	360	$1.1 + j\bar{4}.4$	$1.45926 \angle 42^\circ.227$	$0.40235 \angle 42^\circ.227$	$1.56156 \angle 30^\circ.182$	$1.07638 \angle 38^\circ.182$
5	400	$1.0 + j\bar{4}.0$	$1.17520 \angle 0^\circ$	$0.32403 \angle 0^\circ$	$1.54308 \angle 0^\circ$	$1.06364 \angle 8^\circ$
V	440	$0.9 + j\bar{3}.6$	$1.18289 \angle 45^\circ.407$	$0.32615 \angle 45^\circ.407$	$1.30700 \angle 27^\circ.493$	$0.90091 \angle 19^\circ.493$
4	480	$0.8 + j\bar{3}.2$	$1.30124 \angle 77^\circ.825$	$0.35878 \angle 77^\circ.825$	$0.94033 \angle 63^\circ.927$	$0.64817 \angle 55^\circ.927$
IV	520	$0.7 + j\bar{2}.8$	$1.21653 \angle 101^\circ.110$	$0.33542 \angle 101^\circ.110$	$0.81911 \angle 118^\circ.263$	$0.56461 \angle 110^\circ.263$
3	560	$0.6 + j\bar{2}.4$	$0.86650 \angle 126^\circ.471$	$0.23892 \angle 126^\circ.471$	$1.02948 \angle 158^\circ.685$	$0.70962 \angle 150^\circ.685$
III	600	$0.5 + j\bar{2}.0$	$0.52110 \angle 180^\circ$	$0.14368 \angle 180^\circ$	$1.12763 \angle 180^\circ$	$0.77727 \angle 172^\circ$
2	640	$0.4 + j\bar{1}.6$	$0.71708 \angle 117^\circ.607$	$0.19771 \angle 117^\circ.607$	$0.90732 \angle 164^\circ.568$	$0.62542 \angle 172^\circ.568$
II	680	$0.3 + j\bar{1}.2$	$0.99862 \angle 95^\circ.407$	$0.27534 \angle 95^\circ.407$	$0.43385 \angle 138^\circ.122$	$0.29905 \angle 146^\circ.122$
1	720	$0.2 + j\bar{0}.8$	$0.97213 \angle 86^\circ.331$	$0.26804 \angle 86^\circ.331$	$0.36882 \angle 31^\circ.277$	$0.25423 \angle 39^\circ.277$
I	760	$0.1 + j\bar{0}.4$	$0.59626 \angle 82^\circ.189$	$0.16440 \angle 82^\circ.189$	$0.81520 \angle 4^\circ.142$	$0.56192 \angle 12^\circ.142$
B	800	$0.0 + j\bar{0}.0$	$0 \angle 0^\circ$	$0 \angle 0^\circ$	$1.00 \angle 0^\circ$	$0.68930 \angle 8^\circ$

TABLE XII

Distribution of potential and current over a uniform smooth line of  $\theta = 2.0 + j8$  and  $z_0 = 400 \angle 8^\circ$  when freed at  $B$  and voltaged at  $A$

I Position	II $x$ km.	III $\delta_P$ hyps.	IV $\sinh \delta_P$ by tables	V $V_P$ volts	VI $\cosh \delta_P$ by tables	VII $I_P$ milliamp.
A	0	<u>2.0 + j9.0</u>	3.76220 $\angle 90^\circ$	1.00 $\angle 0^\circ$	3.62686 $\angle 90^\circ$	2.4101 $\angle 8^\circ$
X	40	<u>1.9 + j8.6</u>	3.36681 $\angle 55^\circ.211$	0.89490 $\angle 34^\circ.879$	3.32060 $\angle 52^\circ.773$	2.2066 $\angle 29^\circ.227$
9	80	<u>1.8 + j8.2</u>	2.95835 $\angle 18^\circ.941$	0.78634 $\angle 71^\circ.059$	3.09206 $\angle 17^\circ.100$	2.0547 $\angle 64^\circ.900$
IX	120	<u>1.7 + j7.8</u>	2.66361 $\angle 19^\circ.155$	0.70799 $\angle 109^\circ.155$	2.81138 $\angle 16^\circ.906$	1.8682 $\angle 98^\circ.906$
8	160	<u>1.6 + j7.4</u>	2.50955 $\angle 56^\circ.192$	0.66704 $\angle 146^\circ.192$	2.44721 $\angle 51^\circ.752$	1.6262 $\angle 133^\circ.752$
VIII	200	<u>1.5 + j7.0</u>	2.35241 $\angle 90^\circ$	0.62528 $\angle 180^\circ$	2.12928 $\angle 90^\circ$	1.4149 $\angle 172^\circ.0$
7	240	<u>1.4 + j6.6</u>	2.06903 $\angle 122^\circ.751$	0.54995 $\angle 147^\circ.249$	1.99295 $\angle 129^\circ.373$	1.3243 $\angle 148^\circ.627$
VII	280	<u>1.3 + j6.2</u>	1.72627 $\angle 159^\circ.341$	0.45885 $\angle 110^\circ.659$	1.94654 $\angle 164^\circ.358$	1.2935 $\angle 133^\circ.642$
6	320	<u>1.2 + j5.8</u>	1.54077 $\angle 158^\circ.706$	0.40954 $\angle 68^\circ.706$	1.78409 $\angle 164^\circ.844$	1.1855 $\angle 82^\circ.844$
VI	360	<u>1.1 + j5.4</u>	1.56156 $\angle 120^\circ.182$	0.41507 $\angle 30^\circ.182$	1.45926 $\angle 132^\circ.227$	0.96969 $\angle 50^\circ.227$
5	400	<u>1.0 + j5.0</u>	1.54308 $\angle 90^\circ$	0.41015 $\angle 0^\circ$	1.17520 $\angle 90^\circ$	0.78093 $\angle 8^\circ$
V	440	<u>0.9 + j4.6</u>	1.30700 $\angle 62^\circ.507$	0.34740 $\angle 27^\circ.493$	1.18289 $\angle 44^\circ.593$	0.78604 $\angle 37^\circ.407$
4	480	<u>0.8 + j4.2</u>	0.94033 $\angle 26^\circ.073$	0.24994 $\angle 63^\circ.927$	1.30124 $\angle 12^\circ.175$	0.86469 $\angle 69^\circ.825$
IV	520	<u>0.7 + j3.8</u>	0.81911 $\angle 28^\circ.263$	0.21772 $\angle 118^\circ.263$	1.21653 $\angle 11^\circ.110$	0.80840 $\angle 93^\circ.110$
3	560	<u>0.6 + j3.4</u>	1.02948 $\angle 68^\circ.685$	0.27364 $\angle 158^\circ.685$	0.86650 $\angle 36^\circ.471$	0.57580 $\angle 118^\circ.471$
III	600	<u>0.5 + j3.0</u>	1.12763 $\angle 90^\circ$	0.29973 $\angle 180^\circ$	0.52110 $\angle 90^\circ$	0.34628 $\angle 172^\circ$
2	640	<u>0.4 + j2.6</u>	0.90732 $\angle 105^\circ.432$	0.24117 $\angle 164^\circ.568$	0.71708 $\angle 152^\circ.393$	0.47651 $\angle 125^\circ.607$
II	680	<u>0.3 + j2.2</u>	0.43385 $\angle 131^\circ.878$	0.11532 $\angle 138^\circ.122$	0.99862 $\angle 174^\circ.593$	0.66359 $\angle 103^\circ.407$
1	720	<u>0.2 + j1.8</u>	0.36882 $\angle 121^\circ.277$	0.09803 $\angle 31^\circ.277$	0.97213 $\angle 176^\circ.331$	0.64599 $\angle 94^\circ.331$
I	760	<u>0.1 + j1.4</u>	0.81520 $\angle 94^\circ.142$	0.21668 $\angle 4^\circ.142$	0.59626 $\angle 172^\circ.189$	0.39622 $\angle 90^\circ.189$
B	800	<u>0.0 + j1.0</u>	1.00 $\angle 90^\circ$	0.26580 $\angle 0^\circ$	0 $\angle 90^\circ$	0 $\angle 8^\circ$

tial and current continue for a number of waves, with but little damping or diminution. In the case of the line represented in Figs. 100 and 101, the oscillations in size rapidly diminish after the first wave length. In lines of large losses and low linear reactance, even the first oscillation may be imperceptible.

Figures 100 and 101, show in connection with Tables XI and XII, that if the line therein considered is open at *B*, a potential of 0.06716 volt at the quarter-wave point 100 km. from *B*, would develop 0.2658 volt at *B*, a resonant *B/A* voltage ratio of nearly 4. At the half-wave point III, 200 km. from *B*, an impressed potential of 0.2997 volt would produce 0.2658 volt at *B*, a drop of 0.1276 per unit, or 12.76 per cent. By proceeding in this way, the ratio of generator to motor end potential or current can be found from these figures for any length of this type of line, at the selected angular frequency of  $\omega = 5,000$ , ( $f = 796\sim$ ), with the line either open or shorted at the motor end.

If the smooth line considered in Figs. 100 and 101 were replaced by its equivalent *T* or  $\Pi$  line, the graph of potential and current sizes would manifestly be a succession of straight lines. For example, if the artificial line was a  $\Pi$  line of eight sections, each representing a quarter wave at the selected frequency, the potential sizes at terminals and junctions would coincide with those indicated at the points  $V_2, V_{1\frac{3}{4}}, V_{1\frac{1}{2}} \dots V_0$ , and would fall from one such point to the next in a simple straight line. The current size on the other hand would be constant in successive horizontal sections with sudden drops at leaks.

**Quarter-wave Artificial Lines.**—A quarter-wave artificial line, which needs only to be constructed of a single section, has the property of producing a relatively large rise of voltage at the motor free end, when voltaged at the generator end with the correct frequency. Such a device becomes, in effect, a frequency-change detector, since if the frequency varies, in either direction, from the normal for which the line section is designed, the motor-end voltage falls off rapidly. Such a quarter-wave artificial line is, however, only a particular set of connections for producing resonance between inductive and condensive reactances at a critical frequency.

## CHAPTER XIII

### REGULARLY LOADED LINES AND ATTENUATION MEASURE

Regular loads on a line are similar loads which recur at regular intervals. They may be either regular series loads (impedance loads) or regular leak loads. Regular series loads are well known and much used in long-distance telephony.

In dealing with series loads, their easiest elucidation is perhaps through the use of the equivalent  $T$ , while in dealing with leak loads, the equivalent  $\Pi$  may be used.

**Regular Series Loads.**—Let a uniform line, of surge impedance  $r_0$  ohms  $\angle$ , be divided into uniform sections of angle  $\theta$  hyps.  $\angle$ . Let an impedance load of

$$\Sigma = 2\sigma \quad \text{ohms } \angle \quad (379)$$

be inserted between adjacent sections  $ab$ ,  $cd$ ,  $ef$ , as shown in Fig. 102. The end sections will, by symmetry, terminate in a terminal impedance load of  $\sigma$  ohms  $\angle$ . It is required to find the angle and surge impedance which each loaded section  $AB$ ,  $CD$ ,  $EF$ , appears to possess.

First form the equivalent  $T$  of any unloaded section by formulas (163) to (166). These are indicated in Fig. 102 at  $a'b'$ ,  $c'd'$ , and  $e'f'$ . These are the artificial-line  $T$  sections conjugate to those of the original smooth line. Each has arms of  $\rho'$  ohms, and a leak of  $g'$  mhos.

Next add to each arm of a  $T$  its adjacent semi-load  $\sigma$  ohms  $\angle$ , as indicated at  $A'B'$ ,  $C'D'$ , and  $E'F'$ . The leaks  $g'$  remain unchanged. These  $T$ 's, as amended, are clearly equivalent to the reverted sections  $A_1B_1$ ,  $C_1D_1$ ,  $E_1F_1$ .

Finally revert from the amended  $T$ 's to their equivalent smooth lines, using (173) to (180), or (199) and (201), finding  $\theta_1$  and  $z_0$ . This completes the required solution.

In the particular case of Fig. 102, each unloaded section subtends an angle of  $\theta = 0.35174$  hyp. with a surge impedance of  $z_0 = 1,436.1$  ohms. The nominal  $T$  of such a section has, therefore, a total line impedance of  $0.35174 \times 1,436.1 = 505.14$



ohms, and a total line admittance of  $0.35174/1,436.1 = 0.24492 \times 10^{-3}$  mho. The correcting factor for the  $T$  arms is  $\tanh \frac{0.17587}{0.17587} = 0.98982$ , and that for the  $T$  staff,  $\frac{\sinh 0.35174}{0.35174} = 1.0208$ . Applying these factors, the equivalent  $T$  has a resist-

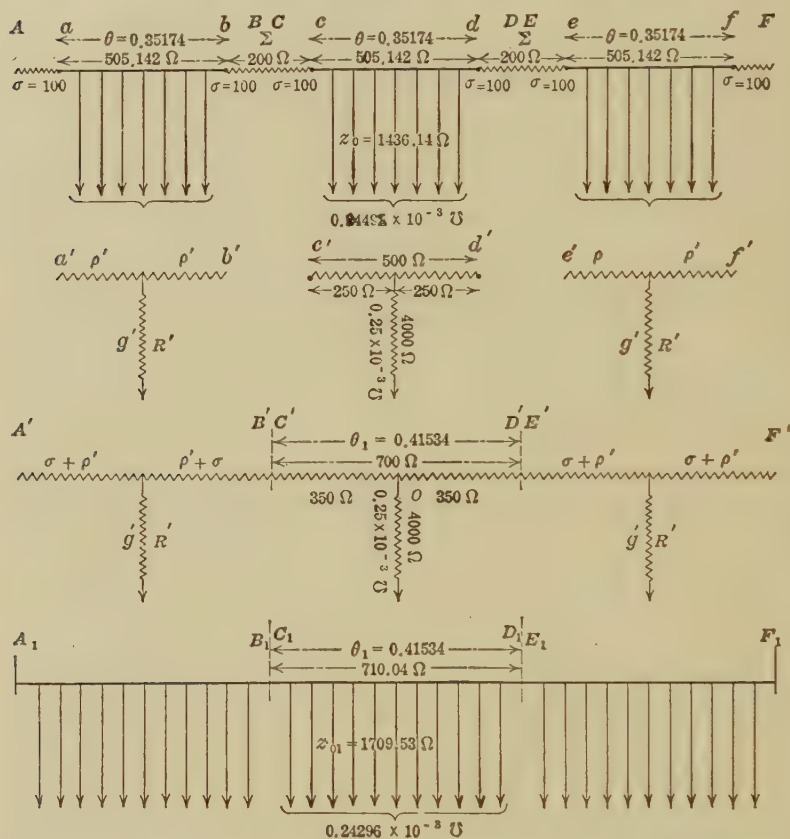


FIG. 102.—Smooth line sections and their equivalents before and after series loading.

ance in each arm of  $\rho' = 250.0$  ohms, and a staff admittance of  $0.250 \times 10^{-3}$  mho. Adding in the impedance semiloads  $\sigma$  to each arm, the amended  $T$  has arms of  $C'O$ ,  $OD' = 350.0$  ohms. In the amended  $T$  line, therefore,  $r = 700$ , and  $g = 0.25 \times 10^{-3}$ . The apparent angle of a half-section is  $\theta/2 = \sqrt{0.175}/2 = 0.41833/2 = 0.20917$  hyp. The corrected semi-section angle is  $\sinh^{-1} (0.20917) = 0.20767$  hyp. and  $\theta_c =$



0.41534 hyp. The apparent surge impedance of the amended  $T$  sections is  $z_0 = \sqrt{700/0.25 \times 10^{-3}} = \sqrt{2.8 \times 10^6} = 1,673.3$  ohms, and the corrected value  $z_0 = 1,673.3 \cosh 0.20767 = 1,673.3 \times 1.0216 = 1,709.5$  ohms. The loading of the line has, therefore, changed the section angles from 0.35174 to 0.41534 hyp. and the surge impedance from 1,436.1 to 1,709.5 ohms. The new sections behave as though they contained 710.04 ohms smoothly distributed resistance and  $0.24296 \times 10^{-3}$  mho smoothly distributed leakance.

It should be observed that whereas before the loading, any section length of the smooth line had the same values of  $\theta$  and  $z_0$ , after the loading the new values  $\theta$ , and  $z_0$ , apply only at section junctions, or mid-load points. If we cut into the loaded line at random, we cannot expect to find these values in a section length on either side of the cut.

If we analyze algebraically the steps of the process above indicated, we are led to the following formulas:

If  $\theta$  be the angle of a smooth line section before loading,  
 $\theta$ , be the angle of the same line section after loading,  
 $z_0$  be the surge impedance of the section before loading,  
 $z_0$ , be the surge impedance of the section after loading,

then

$$\tanh \left( \frac{\theta}{2} \right) = \sqrt{\tanh \left( \frac{\theta}{2} \right) \cdot \tanh \left( \frac{\theta}{2} + \delta \right)} \quad \text{numeric } \angle \quad * (380)$$

where

$$\tanh \delta = \frac{\sigma}{z_0} \quad \text{numeric } \angle \quad (381)$$

or

$$\delta = \tanh^{-1} \left( \frac{\sigma}{z_0} \right) \quad \text{hyps. } \angle \quad (382)$$

Also

$$\cosh \theta = \cosh \theta + \frac{\sigma}{z_0} \sinh \theta \quad \text{numeric } \angle \quad \dagger (383)$$

$$\frac{z_0}{z_0} = \frac{\sinh \theta}{\sinh \theta} \quad \text{numeric } \angle \quad (384)$$

\* "Artificial Lines for Continuous Currents in the Steady State," by A. E. Kennelly, *Proc. Am. Acad. Arts & Sciences*, Nov., 1908., Vol. 44, No. 4, pp. 97-130.

† "On Loaded Lines in Telephonic Transmissions," by G. A. Campbell, *Phil. Mag.*, March, 1903, series vi, vol. v, p. 313.

As an a.c. example, consider the case represented in Fig. 103 of a twisted-pair telephone cable having the linear constants presented in Table XIII and loaded in sections of 2.607 km. (1.62 miles) with  $4.535 + j441.5$  ohms per wire. The angle subtended by a section at  $\omega = 5,000$  radians per sec., before loading, is  $0.20065 + j0.20720$  hyp., as shown at  $AB$ , Fig. 103, the surge impedance being  $247.284 \angle 43.48'.16''$  ohms. The nominal  $T$  of such a section is indicated at  $aOb$ . The equivalent and the amended  $T$ , after the addition of a semi-load on one side, are marked at  $A'OB'$ . The conjugate smooth-line section of

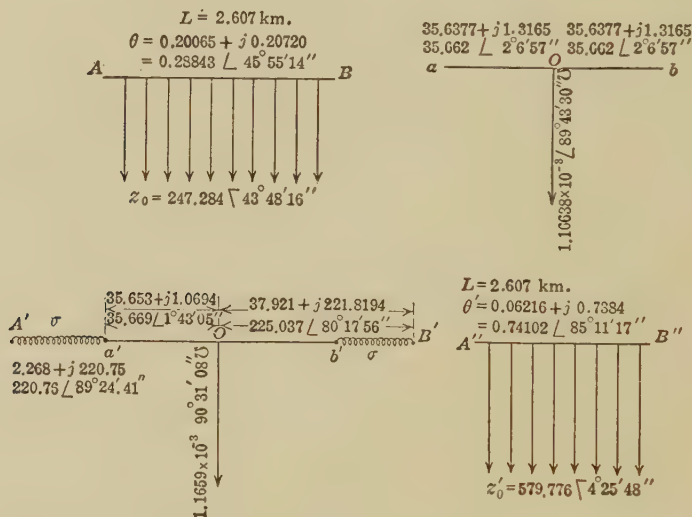


FIG. 103.—Series loaded section of standard telephone cable treated through the substitution of its equivalent  $T$ .

the amended  $T$  appears at  $A''B''$ . It will be seen that the loading has changed the section angle from  $0.20065 + j0.20720$  to  $0.06216 + j0.7384$ ; while it has changed the surge impedance from  $247.284 \angle 43.48'.16''$  to  $579.776 \angle 4.25'.48''$ .

Without going through the process indicated in Fig. 103, we may use (380) as follows:

$$\tanh\left(\frac{\theta}{2}\right) = 0.144243 \angle 45.31'.21''$$

$$\tanh \delta = \frac{\sigma}{z_0} = \frac{220.76 \angle 89.24'.41''}{247.284 \angle 43.48'.16''} = 0.89274 \angle 133.12'.57''$$

TABLE XIII

Linear constants of twisted-pair cabled conductor referred to in Figs. 103 and 107, before being loaded

Linear quantity	Per loop mile	Per wire mile	Per loop km.	Per wire km.
Conductor resistance, ohms....	$r'' = 88$	$r, = 44$	$r'' = 54.68$	$r = 27.34$
Conductor inductance, henrys...	$l'' = 0.65 \times 10^{-3}$	$l, = 0.325 \times 10^{-3}$	$l'' = 0.404 \times 10^{-3}$	$l = 0.202 \times 10^{-3}$
Dielectric conductance, mhos...	$g'' = 1.73 \times 10^{-6}$	$g, = 3.46 \times 10^{-6}$	$g'' = 1.075 \times 10^{-6}$	$g = 2.15 \times 10^{-6}$
Dielectric capacitance, farads...	$c'' = 0.072 \times 10^{-6}$	$c, = 0.144 \times 10^{-6}$	$c'' = 0.04474 \times 10^{-6}$	$c = 0.08948 \times 10^{-6}$

whence

$$\frac{\theta,}{2} = 0.37051 \angle 85^{\circ}.11'.17''$$

and

$$\theta, = 0.74102 \angle 85^{\circ}.11'.17'' \text{ hyp.}$$

Also by (384)

$$z_0, = 247.284 \angle 43^{\circ}.48'.16''$$

$$\times \frac{0.675966 \angle 86^{\circ}.5'.20''}{0.288311 \angle 46^{\circ}.42'.52''}$$

$$= 579.776 \angle 4^{\circ}.25'.48'' \text{ ohms.}$$

**Regular Leak Loads.**—If the smooth line  $A'E$ , Fig. 104, is divided into equal sections, and a leak of  $\Gamma$  mhos is applied at each junction, with half-leaks of  $\gamma$ ; or

$$\Gamma = 2\gamma \text{ mhos } \angle \quad (385)$$

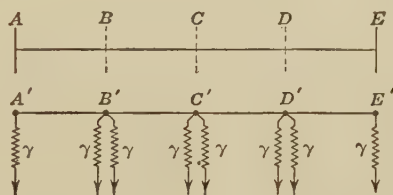


FIG. 104.—Four-section line with leaks at junctions.

at terminals  $(A'B'C'D'E')$ . Then each smooth section may be replaced by its equivalent  $\Pi$ . To each pillar leak of a  $\Pi$  is added the leak  $\gamma$ , thereby producing an amended  $\Pi$ . This amended  $\Pi$  is then reverted to its conjugate smooth line of angle  $\theta,$ , and surge impedance,  $z_0,$ .

As an example consider the case represented in Figs. 105 and 106. Here a uniform smooth-line section of surge impedance  $z_0 = 2,000$  ohms, or surge admittance  $y_0 = 0.5 \times 10^{-3}$

mho, and linear hyperbolic angle 0.005 hyp. per km., is loaded at each end  $A'$ ,  $B'$ , with a leak of 0.5 millimho. The unloaded section  $AB$  subtends an angle of 0.25 hyp. It contains a total conductor impedance of  $0.25 \times 2,000 = 500$  ohms and a total dielectric admittance of  $0.25 \times 0.5 \times 10^{-3} = 0.125 \times 10^{-3}$  mho. These are the values to be inserted in the nominal  $\Pi$ , which has an architrave impedance of 500 ohms, and two leaks each of  $0.0625 \times 10^{-3}$  mho. The correcting factors are  $\sinh 0.25/0.25 = 0.25261/0.25 = 1.01044$ , and  $\tanh 0.125/0.125 = 0.12435/0.125$

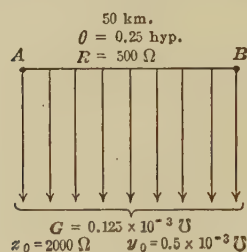


FIG. 105.—Uniform unloaded line and its equivalent  $\Pi$ .

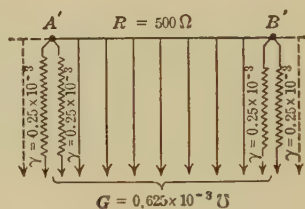


FIG. 106.—Leak loaded-line section and its equivalent  $\Pi$ .

$= 0.99480$ . Applying these to the elements of the nominal  $\Pi$ , we obtain the equivalent  $\Pi$ ,  $ab$ , Fig. 105, with an architrave of 505.22 ohms, and two leaks, each of  $0.062175 \times 10^{-3}$  mho. We now increase each pillar leak to  $0.312175 \times 10^{-3}$  mho, leaving the architrave unaltered as at  $a'b'$ , Fig. 106. The total line impedance  $r$  of a section is thus 505.22 ohms and the total leak admittance  $g$ ,  $0.62435 \times 10^{-3}$  mho. The apparent angle subtended by half the amended  $\Pi$  is thus

$$\frac{\sqrt{505.22 \times 0.62435 \times 10^{-3}}}{2}$$

$= 0.280818$  hyp. The corrected value is  $\sinh^{-1} (0.280818)$   
 $= 0.27725$  hyp. The apparent surge impedance is  $z_0' =$

$\sqrt{505.22/624.35 \times 10^{-6}} = 899.552$  ohms. The corrected value is  $z_0 = \frac{899.552}{\cosh 0.27725} = 899.552/1.03868 = 866.05$  ohms, and  $y_0 = 1.1546 \times 10^{-3}$  mho.

The loaded sections, therefore, behave as though they had a total conductor impedance of  $0.5545 \times 866.05 = 505.22$  ohms uniformly distributed, and a total dielectric leakance of  $0.5545 \times 1.1546 \times 10^{-3} = 0.62435 \times 10^{-3}$  mho, uniformly distributed.

Instead of going through the steps indicated in Figs. 105 and 106, we may derive the following formulas directly,  $\theta$  being the unloaded section angle,  $\theta$ , the loaded section angle,  $y_0$  the surge admittance before loading,  $y_0$ , the surge admittance after loading.

$$\tanh\left(\frac{\theta'}{2}\right) = \sqrt{\tanh\left(\frac{\theta}{2}\right) \cdot \tanh\left(\frac{\theta}{2} + \delta\right)} \quad \text{numeric } \angle \quad * (386)$$

where

$$\tanh \delta = \frac{\gamma}{y_0} \quad \text{numeric } \angle \quad (387)$$

or

$$\delta = \tanh^{-1}\left(\frac{\gamma}{y_0}\right) \quad \text{hyps. } \angle \quad (388)$$

Also

$$\cosh \theta' = \cosh \theta + \frac{\gamma}{y_0} \sinh \theta \quad \text{numeric } \angle \quad (389)$$

$$\frac{y_0'}{y_0} = \frac{\sinh \theta'}{\sinh \theta} \quad \text{numeric } \angle \quad (390)$$

A remarkable analogy is presented between the groups of formulas (380 to 384) and (386 to 390).

In the case above considered  $\delta = \tanh^{-1}(0.25 \times 10^{-3}/0.5 \times 10^{-3}) = \tanh^{-1} 0.5 = 0.549307$  hyp. so that

$$\tanh\left(\frac{\theta'}{2}\right) = \sqrt{\tanh 0.125 \times \tanh 0.674307}$$

$= \sqrt{0.12435 \times 0.58780} = 0.270357$ ; whence  $\theta'/2 = 0.27725$  and  $\theta' = 0.5545$  hyp., as already found. Again

$$\frac{y_0'}{0.5 \times 10^{-3}} = \frac{\sinh 0.5545}{\sinh 0.2500} = \frac{0.58336}{0.25261} = 2.30931.$$

whence  $y_0' = 1.15466 \times 10^{-3}$  mho, and  $z_0' = 866.05$  ohms, as above.

\* *Loc. cit.* See (380).

The effect of leak leading in this example has been to increase the section angle from 0.25 to 0.5545 hyp. and to diminish the surge impedance from 2,000 to 866.05 ohms.

As an a.c. example, we may consider 2.607-km. sections of smooth standard twisted-pair cable, referred to in Table XIII and\* Fig. 103. This line is loaded with leaks of  $\Gamma = (0.013332 - j1.3332)10^{-3} = 1.33327 \times 10^{-3} \angle 89^\circ.25'.37''$  mho per wire at

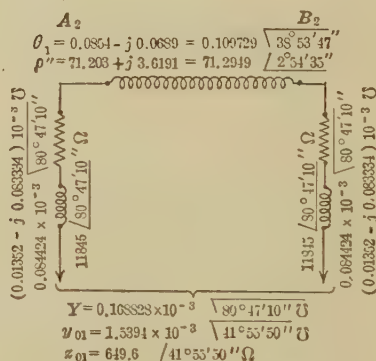
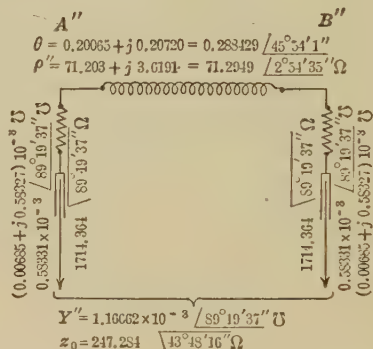
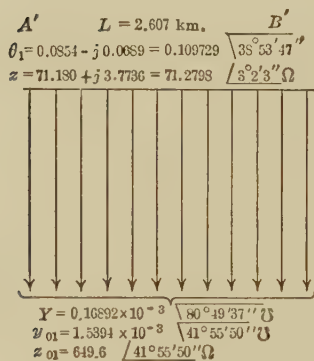
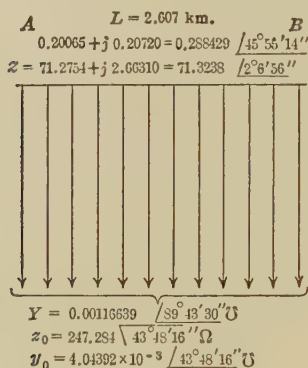


FIG. 107.—Smooth line and its equivalent II before and after regular leak loading.

junctions, such as would be produced by a reactor of 7.5 ohms and 0.15 millihenry, to ground at each junction. Thus  $\gamma = (0.006666 - j0.6666)10^{-3} = 0.666635 \times 10^{-3} \angle 89^\circ.25'.37''$  mho.

The unloaded section is indicated at AB, Fig. 107 and its equivalent II at A''B''. After adding in the leaks, we obtain

\* Further particulars concerning the effects of series loading are given in Chapter VIII of "The Application of Hyperbolic Functions to Electrical Engineering Problems."



the amended  $\Pi$ ,  $A_2B_2$ , and finally, by reversion, the conjugate smooth section  $A'B'$ . It will be observed that the loading has changed the section angle from  $0.20065 + j0.20720$  to  $0.0854 - j0.0689$  hyp., and the surge impedance from  $247.284 \angle 43^\circ.48'.16''$  to  $649.6 \angle 41^\circ.55'.50''$ .

Although these leak loads have reduced the real component of the section angle nearly as much as the series loads of Fig. 103, yet, in general, the benefit of reduced attenuation is much more localized toward a critical frequency in leak loading than in series loading. In other words, the benefits of series loading extend in this case over a larger range of frequencies than those of leak loading.

#### Impedance-frequency Method of Locating a Fault in a Line.\*

It often happens that, either in a loaded or unloaded line, some fault or discontinuity occurs, such as an omitted loading coil, a broken insulator or a defective loading coil. The impedance  $Z_A$  of such a line  $AB$ , assumed as normally uniform, and terminated at  $B$  in its surge impedance  $z_0$ , is measured at  $A$ , under varied impressed frequency, with an impedance bridge. Sensibly smooth curves of resistance and reactance components *versus* frequency are then normally obtained, such as curve 1 in Fig. 108, where the resistance component of  $Z_A$  falls fairly steadily from 1,450 ohms at 300~ to about 300 ohms at 2,300~.

If a marked discontinuity, such as an omitted or shorted loading coil, occurs on the line at some point  $x$  km. from the testing station  $A$ , reflections of voltage and current will be set up from the fault, and these will cause the resistance or reactance component of the observed sending-end impedance to fluctuate with impressed frequency.

If  $I_A$  is the current strength entering the line at  $A$ , the fault will, by reflection, superpose vector additions in this current, the phase of which will vary from one frequency to another, thus causing  $I_A$  to fluctuate between successive maxima and minima. The amplitude of the fluctuations will depend, among other things, upon the magnitude of the irregularity. As a result of this variation in current  $I_A$  with impressed frequency  $f$ , the resistance and reactance components of  $Z_A$  will fluctuate in the manner shown by curve 2 in Fig. 108.

\* W. H. Harden, "Practices in Telephone Transmission Maintenance Work," *Bell System Technical Journal*, January, 1925, vol. iv, No. 1, p. 49.

Let  $f_1, f_2, f_3$ , etc., be the frequencies of successive maxima in the component quantity, and let us first assume that the apparent velocity  $v$  of propagation remains sensibly constant over the range of frequencies employed. As we increase the frequency from  $f_1$  to  $f_2$ , we add one complete wave length to the distance that the reflected current wave must travel.

Let  $\lambda_1$  be the wave length corresponding to  $f_1$ , and  $\lambda_2$  the corresponding wave length for frequency  $f_2$ , and so on,  $n$  being the number of complete wave lengths included in  $2x$  km., the distance traveled by the reflected current wave.

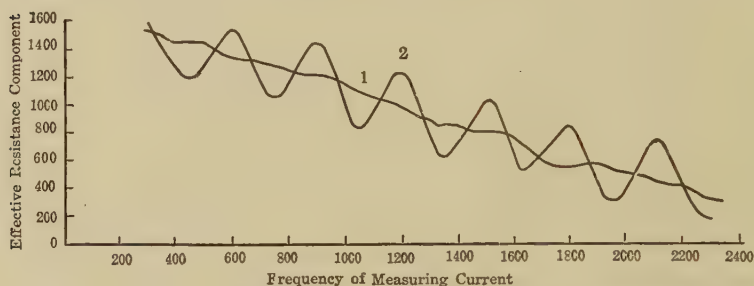


FIG. 108.—Curves of resistance component of sending-end impedance versus impressed frequency for (1) a particular line in substantially normal condition, and (2) the same line containing a fault or reflecting discontinuity.

At frequency  $f_1$

$$n = \frac{2x}{\lambda_1} \quad \text{numeric} \quad (391)$$

Again, at frequency  $f_2$ , there will be  $n + 1$  waves included in the distance  $2x$ , since the wave length is now shorter, so that

$$n + 1 = \frac{2x}{\lambda_2} \quad \text{numeric} \quad (392)$$

But

$$\lambda_1 = \frac{v}{f_1} \quad \text{km.} \quad (393)$$

and

$$\lambda_2 = \frac{v}{f_2} \quad \text{km.} \quad (394)$$

Substituting (393) in (391) and (394) in (392), we obtain

$$= \frac{2xf_1}{v} \quad \text{numeric} \quad (395)$$

and

$$n + 1 = \frac{2xf_2}{v} \quad \text{numeric} \quad (396)$$

Subtracting (395) from (396)

$$1 = \frac{2x}{v} (f_2 - f_1) \quad \text{numeric} \quad (397)$$

or

$$x = \frac{v}{2(f_2 - f_1)} \quad \text{km.} \quad (398)$$

Similarly

$$x = \frac{v}{2(f_3 - f_2)} \quad \text{etc.} \quad \text{km.} \quad (399)$$

The successive maxima in the curve of Fig. 108 enable an average value of the distance  $x$  to be obtained, according to the series of (398) and (399). Both resistance and reactance curves may be used. If the line is loaded, the frequency range should not be carried too near the cutoff value at one end, or too low at the other.

A correction may be made for known variations of velocity  $v$  with frequency by first preparing a table of  $v$  versus  $f$ , and using the velocity corresponding to the mean  $\frac{f_{n+1} + f_n}{2}$  between each pair of successive maxima.

In some cases, the line construction near the testing station may differ from that more remote, so that the first line section  $AB$ , with velocity  $v_1$ , may be connected at junction  $B$ , to a second section  $BC$ , with velocity  $v_2$ . The distance to the fault is then computed as before, using the velocity  $v_1$  of the first section. If the fault then appears to be beyond the junction  $B$ , the apparent distance must be corrected for the change of velocity beyond the junction. In that case,

let  $x_c$  be the fault's distance using velocity  $v$  (km.)

$X$  be the length of the first section  $AB$  (km.)

$x_2$  be the distance from junction  $B$  to the fault (km.)

$v_1$  be the propagation velocity in section  $AB$  (km./sec.)

$v_2$  be the propagation velocity in section  $BC$  (km./sec.)

$x$  be the corrected distance from  $A$  to the fault (km.)

Since  $x_c$  is greater than  $X$ ,  $x_c - X$  is the length of first section having the same delay as  $x_2$ . Now the length for a given delay is directly proportional to the velocity; so that

$$x_2 = (x_c - X) \frac{v_2}{v_1} \quad \text{kilometers} \quad (400)$$

or

$$x = X + x_2 = X + (x_c - X) \frac{v_2}{v_1} \quad \text{kilometers} \quad (401)$$

The same method may be employed to locate an irregularity in an artificial line.

**Attenuation Expressed in Transmission Units.**—Attenuation of voltage or of current has been referred to in Chapters III and X, in relation to the reductions in these quantities which occur over a specified length of a given type of telephone line, at a standard frequency, such as that for  $\omega = 5,000$ , ( $f = 796.4\sim$ ). More recently, however, a new "telephone transmission unit" has been adopted in this country, which has the advantage of being independent of any particular frequency, and of being applied to any uses of power besides wire telephony. Moreover, it is equally as applicable to a communication line interrupted by relays or repeaters as to a continuous single- or composite-section circuit.

**Transmission Unit.**—When power to the extent of  $P_A$  active watts is steadily supplied to a transmission system  $AB$ , in such a manner that the output delivered at  $B$  is  $P_B$  active watts, the ratio  $P_A/P_B$  is the *power-transmission ratio*. Under ordinary circumstances, owing to loss of power in transmission, this ratio is greater than unity. Then the number of "transmission units" lost in the system is, by definition,

$$\text{T.U.} = 10 \log \left( \frac{P_A}{P_B} \right) = 10 (\log P_A - \log P_B)$$

transmission units (402)

If, for instance,  $P_A = 10 P_B$ , so that the power loss is 90 per cent. of the input,  $\text{T.U.} = 10 \log (10) = 10$  units. In other words, there are 10 transmission units lost in a 10 to 1 input-output power system.

Again, since  $\log (1.259) = 0.1$ , it follows that when  $P_A/P_B = 1.259$ , there is 1 transmission unit of loss.

Again, if in a direct-current system of power supply to constant-potential mains, at 100 volts, from central-station busbars at 112.2 volts, for every watt delivered to the mains, 1.122 watts would be taken from the busbars. The ratio  $P_A/P_B = 1.122$ , and  $\log (P_A/P_B) = 0.05$ , so that the transmission units would be 0.5, or half a unit. This would be a moderate loss in power distribution. In general, the ratio  $P_A/P_B$ , when the transmission loss is small, contains about 25 per cent. per unit of transmission loss, as the following table shows.

$$\text{That is, } P_A/P_B = 1 + \frac{25}{100} \times \text{T.U., approximately.}$$

TABLE XIV

Input-output rates for transmission unit measure up to T.U. = 1

T.U.	$\log \left( \frac{P_A}{P_B} \right)$	$\frac{P_A}{P_B}$	T.U.	$\log \left( \frac{P_A}{P_B} \right)$	$\frac{P_A}{P_B}$
0.1	0.01	1.024	0.6	0.06	1.153
0.2	0.02	1.047	0.7	0.07	1.177
0.3	0.03	1.071	0.8	0.08	1.202
0.4	0.04	1.099	0.9	0.09	1.233
0.5	0.05	1.127	1.0	0.10	1.259

The number of transmission units of power loss that can be tolerated in telephonic communication depends upon a number of circumstances, and does not admit of a brief categorical statement. In commercial telephony, however, over ordinary cabled pairs of wires, and in the absence of repeaters, it may be taken as about 30 T.U. This means that  $\log (P_A/P_B) = 3.0$ , or  $P_A = 1,000 P_B$ . The power delivered at  $B$  would be the one-thousandth part of the input power at  $A$ .

**Comparison of Transmission Units with Other Modes of Expressing Attenuation.**—We have seen that in normal attenuation of voltage or current, over a very long a.c. line, or over any finite line with a surge impedance load, is by (320),  $\epsilon^{-\theta_1}$ , where  $\theta_1$  is the real part of the line angle  $\theta$ , neglecting questions of phase. Over such a circuit, the normal power loss would be  $\epsilon^{-2\theta_1}$ .

Any two quantities  $A$  and  $B$ , expressible in the same physical unit, will have a ratio  $A/B = \epsilon^n$ . The exponent  $n$  is then the Napierian logarithm of this ratio, and the ratio is said to be  $n$  *napiers*, the name being taken in recognition of the inventor and first tabulator of logarithms to the base  $\epsilon$ . One napier is therefore a ratio of 2.718 . . . or  $\epsilon^1$ , and  $n$  napiers, therefore, define a ratio of  $\epsilon^n$  between the two quantities considered. Consequently, a line of angle  $\theta$ , whose real part is  $\theta_1$ , will in normal attenuation have  $2\theta_1$  napiers of power attenuation and since

$$\epsilon^{2\theta_1} = 10^{0.4343 \times 2\theta_1} = 10^{0.8686\theta_1} \quad (403)$$

this will correspond to 8.686  $\theta_1$  T.U. That is, in normal attenuation,

$$1 \text{ napier in voltage or current} = 8.686 \text{ T.U. of power loss} \quad (404)$$



One mile of standard cable as used in America, with the constants

$r = 88$  ohms per loop mile,

$c = 0.054 \times 10^{-6}$  farad per loop mile,

with  $g = l = 0$ , and under an impressed angular velocity of  $\omega = 5,000$ , develops a linear hyp. angle, by (310), of

$$\alpha = \sqrt{88 \times j2.7 \times 10^{-4}} = \sqrt{j2.376 \times 10^{-2}}$$

$$= 1.541 \times 10^{-1} / 45^\circ$$

$$= 0.109 + j0.109 \text{ hyps. per mile (see page 153).}$$

The normal attenuation of current or voltage, over such a standard cable mile, will thus be

$$0.109 \text{ napier} = 0.947 \text{ T.U.} \quad (405)$$

1 mile of standard cable thus involves, at  $\omega = 5,000$ , a power loss of nearly 1 T.U. Since the mile of standard cable was formerly the generally used standard of attenuation in telephone engineering, this approximate relation was a strong argument for the adoption of the T.U. as a general attenuation unit in American telephony.

The following table\* gives the relations between the attenuation units:

TABLE XV

	Miles of standard cable at $\omega = 5,000$	Napiers in $\theta_1$	T.U. in power
1 Mile standard cable.....	1	0.109	0.947
1 Napier in $\theta_1$ (normal attenuation)....	9.175	1	8.686
1 T.U. in power.....	1.056	0.115	1

\* See also "Transmission Circuits for Telephonic Communication," by K. S. Johnson, Chapter II; "The Transmission Unit and Telephone Transmission Reference Systems," by W. H. Martin, *The Bell System Technical Journal*, 1924, vol. iii, pp. 400-408.



## CHAPTER XIV

### DESCRIPTIVE OUTLINE OF ALTERNATING-CURRENT ARTIFICIAL LINES, THEIR HISTORY, AND USES

An artificial electric line is a model line constructed of such materials, dimensions, and parts, so connected, that it shall, at certain assigned terminals, be the electrical counterpart of a corresponding imitated real electric line. When the artificial line is connected to suitable terminal apparatus, such as a generator at one end, and a motor at the other, the voltage, current, and power, at its assigned terminals, will be respectively the same as the corresponding quantities on the imitated real line, similarly connected to the same terminal apparatus. An artificial line corresponding to high-tension a.c. real lines, is ordinarily arranged for operation at some convenient low tension a sub-multiple of the real-line tension.

The principal purpose of an artificial line is thus to furnish an electric model of a corresponding real line, so that the electrical behavior of the real line can be imitated by the model in a manner suitable for either demonstration or observation in the laboratory. Not only may the electrical behavior of a projected real line be predetermined from observations on its model in the laboratory, but the behavior of an existing long real line may also be measured much more conveniently on a laboratory model than is possible for simultaneous measurements at distant points on the real line.

The behavior investigated may relate either to the steady state of electric flow over the line or to the transient states of electric flow, during disturbances. Since, however, the steady state is much the easier to examine, and is much more thoroughly understood in the present state of engineering knowledge, we shall confine ourselves, in the main, to the study of the steady states of artificial and real a.c. lines. Artificial lines for continuous currents have already been discussed in Chapters VII and VIII.

Alternating-current artificial lines may be divided into two general types, namely:

1. Smooth lines, or lines in which the linear constants are distributed smoothly and uniformly throughout. Thus a smooth a.c. artificial line would have its resistance, inductance, capacitance, and leakance all intimately associated and continuously distributed.

2. Lumpy lines, or lines in which the linear constants are connected in successive lumps or localized units. Thus a lumpy a.c. artificial line would have alternate lumps of conductor impedance and dielectric admittance, *i.e.*, alternate reactors in series and condensers in shunt.

Smooth artificial lines have the advantage of being capable of imitating the electric conditions of real lines for all frequencies and transient conditions. Lumpy artificial lines have the advantages of being much simpler, more compact, more durable, cheaper, and easier to construct. They react differently, however, to different frequencies, so that either some correction, or some examination for assurance, is necessary to make certain that the electrical behavior of a lumpy line is applicable to the real line imitated.

The theory of both real and artificial lines in the steady state naturally finds expression in hyperbolic functions. With the aid of these functions all the essential formulas are brief, easy, and difficult to forget. Without them, the expressions to a like degree of precision are lengthy, ponderous, and hard to remember.

**Historical Outline of Smooth Artificial Lines.**—The artificial line of series resistance and shunt capacitance first came into use as an adjunct of duplex submarine-cable telegraphy. In its first form it was a lumpy line with alternate lumps of resistance and capacitance, as represented in Fig.\* 109. A similar artificial line for duplex telegraphy was also employed by J. B. Stearns.

These telegraph artificial lines were designed and used for dot-and-dash signaling impulses, which do not have the regularity of simple alternating currents.

In a later form, introduced by H. A. Taylor and Alex. Muirhead, the artificial line for duplex submarine-cable telegraphy was a smooth line† in which resistance and capacitance were distributed uniformly together, as shown in Fig. 110. The construction employed for effecting the distribution of resistance and capacitance is indicated in Fig. 111. The first or upper electrode sheet of each paraffined paper layer is cut out into the

\* C. F. Varley, British Patent No. 3453 of 1862.

† H. A. Taylor and Alex. Muirhead, British Patent No. 684 of 1875.

form of a grid of such dimensions that the resistance of the strip between its ends *A* and *B* is such as should be associated with the capacitance of the condenser. The second or opposing sheet electrode remains uncut. All the upper sheets in each box are then connected in series, and all the lower sheets in parallel.

In the ordinary duplex system of land-line telegraphy, only a very crude model of the real line needs to be embodied in the artificial line, because the duplex balance is so crude, and the

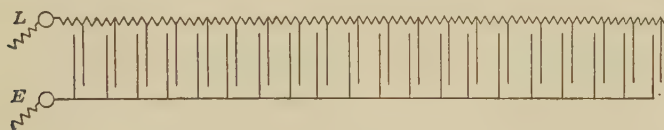


FIG. 109.—Varley artificial submarine cable of 1862.

receiving instrument so relatively insensitive to imperfections of balance. In the duplex system as applied to long submarine cables, however, the siphon recorder, or other receiver used, is relatively very sensitive to feeble current changes; so that a high degree of electrical symmetry is required between the artificial and real cables at and near the sending ends. That is, the artificial cable must imitate the real cable closely, not only in steady states, but also throughout a large class of unsteady or

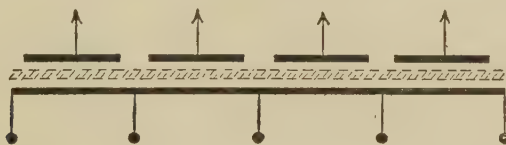


FIG. 110.—Muirhead smooth artificial cable of 1875.

transient states. A lumpy artificial line is, therefore, likely to be serviceable for submarine long-cable duplex balances only at a certain electrical distance from the sending end. Close to the sending end, it is important to have the artificial cable smooth and in close imitation of the real cable. Beyond the design of the artificial cable so as to attain the required degree of electrical imitation, the operation of duplex-cable telegraphy did not demand a knowledge of the quantitative relations of artificial lines in the steady state.

An artificial line with distributed resistance, inductance, and capacitance was constructed by Prof. M. I. Pupin in 1898, and

measurements on it were published by him in 1899.\* The sections of this line consisted of coils of insulated wire having tinfoil sheets between the layers. These tinfoil sheets, connected together, formed one plate of a condenser, the other plate of which

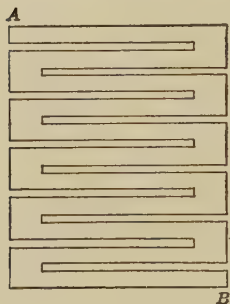


FIG. 111.

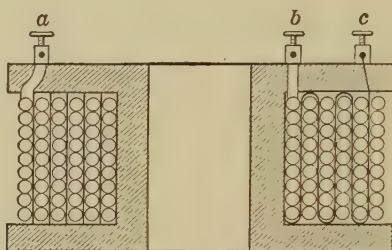


FIG. 112.—Longitudinal section of one coil of Pupin line containing resistance inductance and capacitance in association.

was formed by the insulated wire. A longitudinal section of one coil is shown in Fig. 112. One assemblance of coils into an artificial line is shown in Fig. 113.

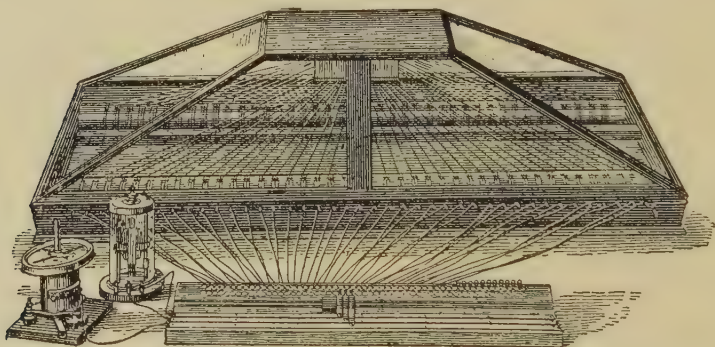


FIG. 113.—Section of an artificial line at Columbia University containing alternate lumps of inductive resistance and capacitance.

A smooth artificial power-transmission line with distributed resistance, inductance, and capacitance is described in the *A. I. E. E. Transactions* for 1911,† as having been installed at

\* "Propagation of Long Electrical Waves," by M. I. Pupin, *Trans. A. I. E. E.*, March, 1899, vol. xvi, pp. 93-142.

† "Design, Construction, and Test of an Artificial Transmission Line," by J. H. Cunningham, *Trans. A. I. E. E.*, February, 1911, vol. xxx, part 1, pp. 245-256.



Union College, Schenectady. Its electrical length is stated as being 130 miles (209 km.) of a one-wire line of No. 1 A.W.G. copper wire, with resistance 93.6 ohms, inductance 0.3944 henry

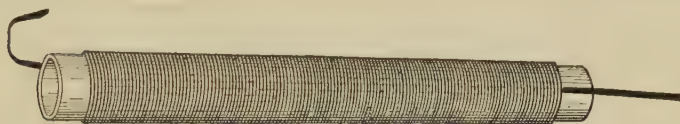


FIG. 114.—Unit tube of smooth artificial power line.

and capacitance  $1.135 \mu f$ . The wire, No. 8 A.W.G. copper, was wound on glass cylinders, in 240 turns per cylinder. On the inside of each such tube was a tinfoil layer forming the grounded

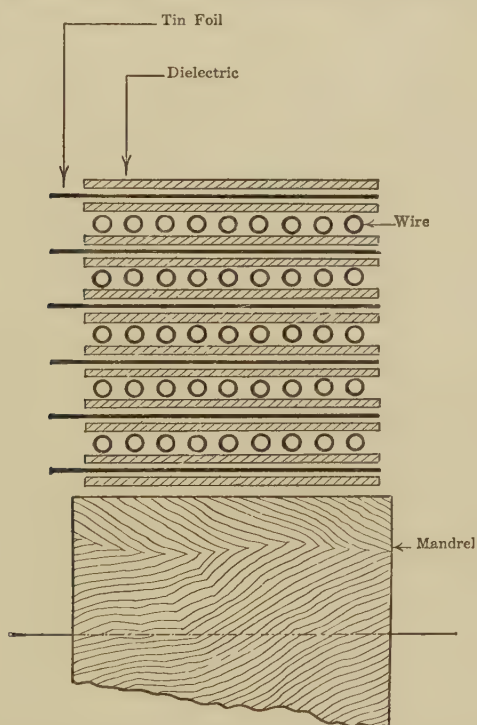


FIG. 115.—Part of a smooth-line coil in axial section, showing 5 layers of enamel-insulated wire, with tinfoil between and outside the layers. The tinfoil is covered by insulator on each side.

side of the condenser. There were about 400 of these wound glass tubes. Each tube was about  $4\frac{1}{2}$  ft. (1.37 m.) long, and 6 in. (15 cm.) in diameter, weighed complete some 40 lb. (18 kg.), and represented about 0.5 km. (0.3 mile) of the imitated line.



The tubes were mounted on wooden racks, each about 9 ft. (2.74 m.) long, by  $4\frac{1}{2}$  ft. (1.37 m.) wide, and 8 ft. (2.44 m.) high, occupying about 324 cu. ft. (9.15 cu. m.) and holding 100 tubes. The total space occupied was thus about 1,300 cu. ft. (36.8 cu. m.) with over 7,000 lb. (3,180 kg.) of copper wire. A unit tube is illustrated in Fig. 114. Such a line is particularly well adapted for the study of very rapid transient phenomena.

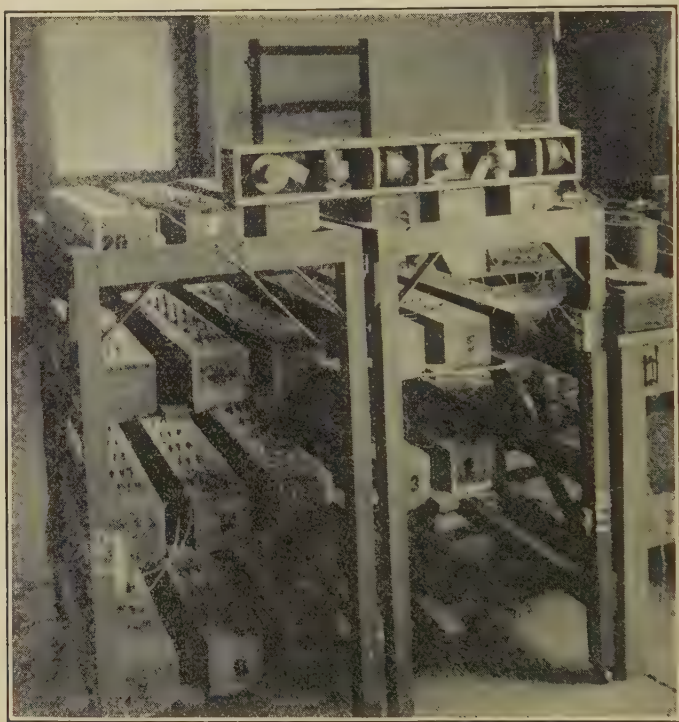


Fig. 116.—Smooth alternating-current artificial line of 1,600 km. assembled in boxes and supporting frames. The coils are supported so as to have minimum mutual inductance.

The construction of smooth artificial a.c. lines makes the maintenance of their insulation more difficult than that of lumpy a.c. lines. Glass tubes are also brittle and liable to fracture.

Dellenbaugh has described\* a type of smooth a.c. artificial line, using coils of a type similar to that of Fig. 112, which have given satisfactory results. Figure 115 shows part of an axial section

\* "Artificial Transmission Lines with Distributed Constants" by F. S. Dellenbaugh, Jr., *Trans. A. I. E. E.*, 1923, vol. xlii, pp. 803-823.

of one coil of this type, having 45 turns. Alternate layers of enamel-insulated wire and tinfoil coated inside and out with dielectric, are wound on the coil. A smooth line of 1,600 km. (1,000 miles) of this type, mounted in wooden boxes, is shown in Fig. 116.

**Lumpy Line Reactors.**—The line reactors should be as simple to construct as possible. They should be capable of being adjusted into close mutual agreement. They should be so mounted that the mutual inductance between adjacent reactors should be negligible. They should be easily insulated from ground, and should be impregnated with a waterproof insulating compound so as to maintain good internal insulation. Finally, they should be solidly constructed so that their electrical constants may remain unaltered with time.

A question which naturally arises early in the design is whether the reactors should be *ferric* or *non-ferric*, *i.e.*, whether they should have, or should not have, subdivided iron cores. The advantage of iron cores is that they enable the needed amount of reactance to be obtained with cheaper, smaller, more compact, and less mutually reactive toroids than if wooden or air cores are used, so that the whole artificial line can be compressed into a relatively small compass. On the other hand, the disadvantage of iron cores is that the electrical constants of their coils vary appreciably, not only with the frequency, but also with the strength of exciting alternating current, at one and the same frequency.

If, therefore, an artificial line with reactors is needed for first approximation purposes only, and especially if it is required to be semi-portable, cores of either laminated or pulverized steel should be used, preferably in toroid coils. If, however, the line is needed for quantitative purposes, and especially for careful study in the laboratory, non-ferric reactors should be selected. Up to the present time, artificial lines used industrially, for practical checks, commonly use ferric reactors, and artificial lines in the testing laboratories of technical colleges ordinarily employ non-ferric reactors.

Non-ferric reactors for artificial lines have been constructed in three forms, namely: (1) toroids with wooden ring cores; (2) square wooden frames intended roughly to simulate closed circular solenoids; and (3) toroidal coils of wire wound on forms and assembled in air, so as to approximate closed circular solenoids.

The first type was described by G. M. B. Shepherd.\* "They are wooden-core toroids of nearly the same dimensions as the loading coils commonly used for underground cables." There are two windings on opposite halves of the ring, the middle point of each being brought out and connected to the capacity as shown in Fig. 117. This figure shows a two-wire artificial line in  $I$  sections, each representing 8 miles (12.9 km.) of overhead telephone copper pair conductor, except one section of 4 miles (6.45 km.). The loop resistance is 72 ohms per section, the loop inductance is 0.0296 henry per section, the loop capacitance 0.08  $\mu$ f. per section, and the loop leakance adjustable in three steps between 8 and 80 micromhos per section. There are altogether 26 sections (two of 4 miles each), representing in all 200 miles

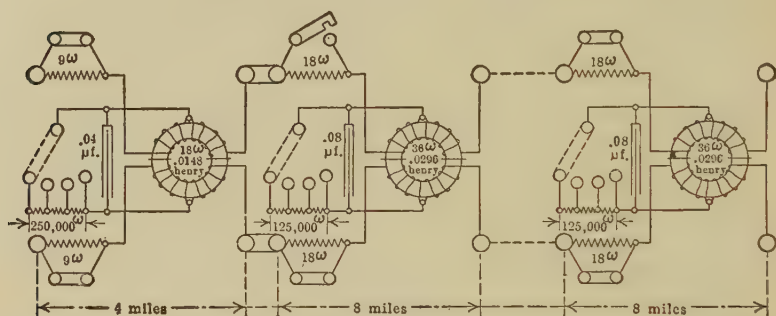


FIG. 117.—Artificial telephone line in  $I$  sections, with adjustable section resistances and leakances.

(322 km.) of aerial loop pair. This line is made up in two wooden-frame cases, each about 37 in. by 7 in. by 10 in. high (94 cm. by 17.8 cm. by 25.4 cm. high).

The second type was described† in the *Electrical World* of Feb. 17, 1912. It consists of a four-section square wooden frame, such as is indicated in Fig. 118. Each coil is separately wound in the lathe, with double cotton-covered copper wire, and then thoroughly impregnated with paraffin wax. The ends of

\* "An Artificial Equivalent of an Open-wire Line for Telephonic Experiments," by G. M. B. Shepherd, *The Post Office Electrical Engineers' Journal* October, 1914, vol. vii, part 3.

† "An Artificial Power-transmission Line," by A. E. Kennelly and H. Tabossi, *Electrical World*, Feb. 17, 1912. See also "Measurements of Voltage and Current over a Long Artificial Power-transmission Line at 25 and 60 Cycles per Second," by A. E. Kennelly and F. W. Lieberknecht, *Trans. A. I. E. E.*, June, 1912.

each coil are soldered to small brass terminal plates, and the direction of winding is such as to imitate that of a closed circular solenoid. The wooden cores are assembled into square frame reactors by a single brass screw bolt *S*, at each corner. Such a frame reactor possesses an appreciable amount of external magnetic leakage; so that it is desirable to screw them down to

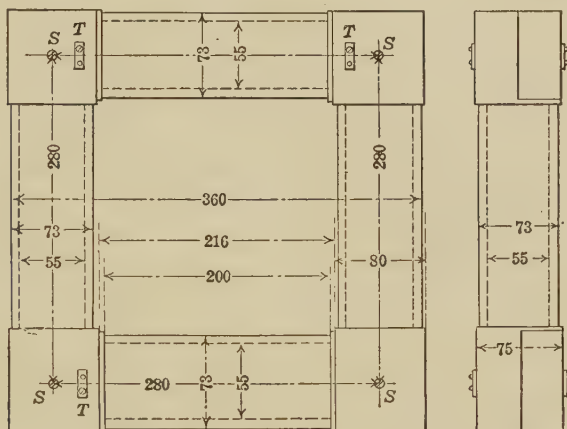


FIG. 118.—Outline sketch of one coil. Dimensions in millimeters.

the supporting shelf alternately in perpendicular planes as is indicated in Figs. 119 and 120. The particular frame reactor of Fig. 118 weighs, unwound, 2.8 kg. (6.2 lb.). The insulated wire on the frame weighs 5.6 kg. (12.4 lb.). Each of the four component coils is wound with 1,190 turns of double cotton-covered No. 19 A.W.G. wire, of bare diameter 0.915 mm. (0.036

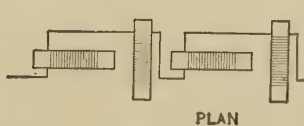


FIG. 119.



FIG. 120.

FIGS. 119 and 120.—Plan and side elevation of the grouping of reactors on shelf.

in.), and of mean covered diameter 1.14 mm. (0.045 in.), occupying approximately seven layers of 170 turns each. The total inductance of each frame reactor averages 90 millihenrys. The total resistance of each frame reactor at 20°C. averages 24.1 ohms. The constants of the line appear in Table XVI, p. 217.

In the particular  $\Pi$ -line into which these frame reactors enter, there are 30 reactors in all. Each section approximately repre-

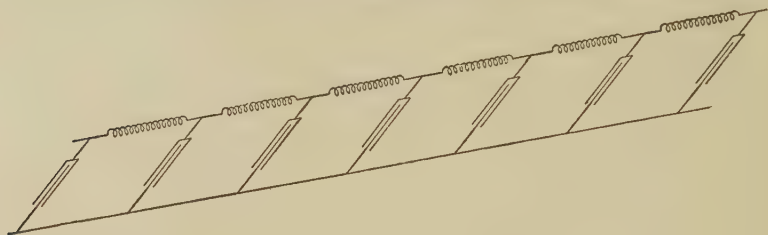


FIG. 121.—Connection of sections when operated as a single-phase line.

sents 80 km. (49.7 miles) of No. 000 A.W.G. aluminum-stranded three-phase conductor of overstrand diameter 1.195 cm. (0.47 in.), suspended parallel in air, at equal interaxial distances of

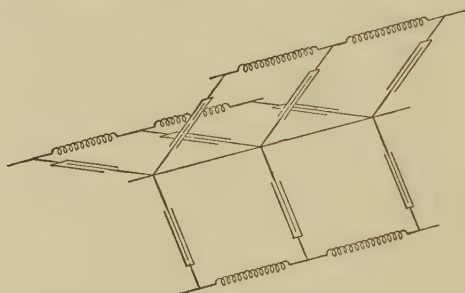


FIG. 122.—Connection of sections when operated as a three-phase line.

230 cm. (90.5 in.). The total length of the artificial line is, therefore, 2,400 km. (nearly 1,500 miles) if connected single-phase, as in Fig. 121, or 800 km. (nearly 500 miles) if connected three-

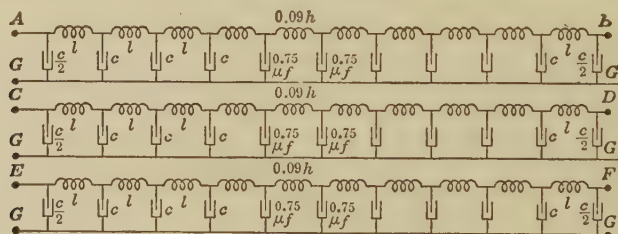


FIG. 123.—Diagram of connections of artificial  $\Pi$ -line.

phase, as in Figs. 122 and 123. The line is mounted on three shelves, in a wooden cabinet with sliding glass doors. For many purposes, a much shorter artificial line would suffice.



The condensers are of leadfoil and impregnated paper, of the type employed in telephony. Each section condenser averages  $0.75 \mu\text{f}$ . The six terminal condensers of Fig. 123 are each of  $0.375 \mu\text{f}$ . Each condenser is placed in a separate tin box, 20 cm. by 5.6 cm. by 14.2 cm. high (7.9 by 2.2 by 5.6 in.), which is then filled up with paraffin wax. They are tested initially to withstand 500 volts a.c. They have a small dielectric leakance at a low frequency, which, if fairly uniform, measured, and taken into account, is no practical disadvantage.

The total weight of insulated copper wire in the entire 30-frame line is 168 kg. (370 lb.), and the total capacitance  $22.5 \mu\text{f}$ .

The constants of the conjugate smooth line at low frequencies not exceeding  $60\sim$  are given in the accompanying table.\*

TABLE XVI

Nominal linear constants of artificial 85 sq. mm. (168,000 circ. mils) aluminum power-transmission line, taking each section as representing 80 km. (49.7 miles) of conductor

	Per wire km.	Per wire mile
Linear resistance $r$ ohms at $0^\circ\text{C}$ .....	0.278	0.445
Linear resistance $r$ ohms at $20^\circ\text{C}$ .....	0.301	0.485
Linear inductance $l$ henrys.....	$1.13 \times 10^{-3}$	$1.82 \times 10^{-3}$
Linear capacitance $c$ farads.....	$9.38 \times 10^{-9}$	$15.1 \times 10^{-9}$
Linear leakance $g$ mhos.....	$0.12 \times 10^{-6}$	$0.19 \times 10^{-6}$
Linear hyperbolic angle hyps. at $60\sim$ ...	$0.00135 \angle 71^\circ.5$	$0.00218 \angle 71^\circ.5$

The angle  $\theta$  subtended by each section at  $60\sim$  is  $0.108 \angle 71^\circ.5$  hyp. The angle subtended by each half-section at  $60\sim$  is  $0.054 \angle 71^\circ.5$  hyp. The lumpiness correction factor, at  $60\sim$ , is  $1.0007 \angle 0^\circ.03$ ; so that there is practically no correction for lumpiness at this frequency. The total angle subtended by the whole single-phase line of 30 sections, at  $60\sim$ , is  $3.24 \angle 71^\circ.5 = 1.028 + j3.072 = 1.028 + j1.956$  hyps.

This type of artificial power-transmission line has been found convenient for experimental investigations at low frequencies. It has been found practicable to insert a small manganin wire resistor in circuit with each reactor when it is desired to have the

\* Tests of one of the reactors removed from the line at different impressed frequencies, have shown that its effective resistance at  $28^\circ\text{C}$ . was 25.3 ohms at zero frequency, 26.8 ohms at  $1,000\sim$ , 31.5 ohms at  $2,000\sim$ , and 35.5 ohms at  $2,500\sim$ .

line approximately imitate a telephone overhead copper line, say 3.65 mm. (0.144 in.) in diameter. The line is then, however, not well adapted for use with telephonic frequencies, because of the large lumpiness correction factor, and for telephonic measurements, a similar line has been constructed with smaller and more numerous frame reactors and sections.

The dimensions of the frame in this higher-frequency line are indicated in Fig. 124. The winding consists of No. 24 A.W.G., double cotton-covered copper wire, diameter bare 0.51 mm. (0.020 in.), covered 0.76 mm. (0.03 in.). Each of the four limbs composing the frame carries 975 turns in approximately  $7\frac{3}{4}$  layers of 125 turns per layer. The mean diameter of the winding

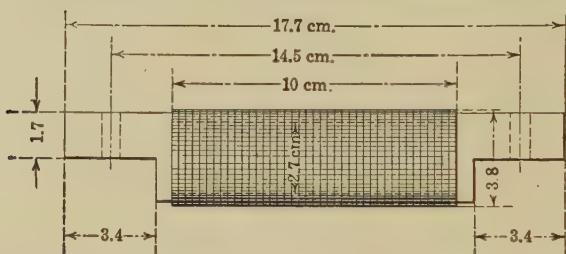


FIG. 124.—Single coil and wooden core of square-frame reactor.

is 32.5 mm. (1.27 in.), and the length of wire on each limb is 100 m. (328 ft.). The total length per frame is thus 400 m. (1,310 ft.), with a total frame resistance of 33.0 ohms at 20°C., and a total frame inductance of 0.031 henry. The weight of wire on each frame is approximately 0.735 kg. (1.62 lb.).

There are 80 frame reactors and sections in the line, making the total weight of wire 58.8 kg. (130 lb.). The total line resistance of the 80 reactors is 2,640 ohms at 20°C., and their total inductance 2.48 henrys. They are connected as a  $\Pi$ -line. The reactors are arranged alternately in mutually perpendicular upright planes, as in Figs. 119 and 120. The line occupies two shelves of a pair of cabinets which, in combination, are 6.75 m. (22 ft. 2 in.) long, 45.7 cm. wide (18 in.) and 88 cm. (34.5 in.) high. These cabinets are provided in front with sliding glazed doors.

The condensers are selected telephone condensers of leadfoil and paper, tested up to 500 volts, a.c., r.m.s. The average capacitance of each condenser is 0.325  $\mu$ f., making the aggregate capacitance of the 80 sections, 26  $\mu$ f. Each section is intended

to represent 30 km. (18.7 miles) of heavy long-distance aerial telephone wire, according to the data in Table XVII.

TABLE XVII

Nominal linear constants of artificial telephone line for 15.67 sq. mm. (30,000 circ. mils) copper aerial conductor at interaxial distance of 30 cm. from its parallel return conductor, each section being taken as representing 30 km. (18.7 miles) of wire

	Per wire km.	Per wire mile
Linear resistance $r$ ohms at 0°C.....	1.013	1.63
Linear resistance $r$ ohms at 20°C.....	1.1	1.77
Linear inductance $l$ henrys.....	$1.03 \times 10^{-3}$	$1.66 \times 10^{-3}$
Linear capacitance $c$ farads.....	$10.8 \times 10^{-9}$	$17.4 \times 10^{-9}$
Linear leakance $g$ mhos.....	$1.2 \times 10^{-8}$	$1.93 \times 10^{-8}$
$\alpha$ at 20°C. and $\omega = 5,000$ .....	$0.00178 + j0.0107$	hyp./km.
$\theta$ per section $\omega = 5,000$ .....	$0.0533 + j0.32$	hyp.

The conjugate smooth line is 2,400 km. (1,490 miles) of aerial copper conductor, one of a pair of parallel copper wires 0.447 cm. in diameter (0.176 in.) at an interaxial distance of 30 cm. (11.8 in.). The cross-section of such a wire would be 15.67 sq. mm. (0.0243 sq. in. or 30,900 circ. mils) between the sizes of Nos. 5 and 6 A.W.G.

The third type of non-ferrie reactor was described by R. D. Huxley,\* and by Prof. C. E. Magnusson.† In each case, there are wooden-cored or air-cored coils of insulated wire mounted on a base, in such a manner as to approximate the structure and behavior of a closed circular solenoid, or toroid.

In the Pender and Huxley design, there are eight coils in an octagonal reactor group, as shown in plan by Fig. 125. Each coil is wound in the lathe on a wooden form. The axial length is 2.5 cm., the internal winding diameter 5.75 cm., the external winding diameter about 16.0 cm. or the winding depth 5.13 cm. in 23 layers of about 10 turns each, or 230 turns in all, per coil of No. 12 A.W.G. double cotton-covered copper wire 0.0808 in. (2.05 mm.) bare, 0.092 in. (2.35 mm.) covered diameter. The weight of wire in each reactor group of eight coils is approxi-

\* R. D. Huxley, "Design for Artificial Transmission Line," *Electrical World*, May 2, 1914, p. 980.

† C. E. Magnusson, J. Gooderham, and R. Rader, "A 200-mile Artificial Transmission Line," *Electrical World*, June 22, 1915. See also "An Artificial Transmission Line with Adjustable Line Constants," by C. E. Magnusson, and S. R. Burbank, *Trans. A. I. E. E.*, September, 1916.

mately 43 lb. (19.5 kg.). The d.c. resistance of each reactor group at 20°C. averages 3.39 ohms. Its average inductance at low frequencies is 0.056 henry.

As each coil was completed, it was transferred from the lathe to an oven, where it was dried for several hours. It was then thoroughly impregnated in a bath of molten beeswax and rosin.

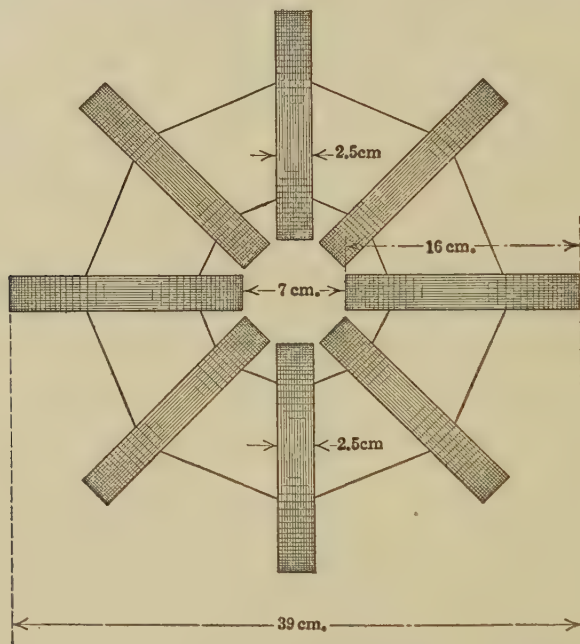


FIG. 125.—Non-ferrie reactor for artificial power-transmission line. Plan view. Wooden wedge-shaped spacing pieces between coils.

The coils, painted with paraffin wax, are mounted by setting them in channel holes cut out in a wooden base, and the connections between coils are soldered together.

The capacitance per section is 0.485  $\mu\text{f.}$  in paper condensers of the telephone type, sealed in tinned iron cases and individually designed to withstand 2,000 volts. At 60~, the condenser phase-angle defect was less than 15' of arc. These condensers were specially selected for uniformity.

Each section of the artificial line represents approximately 30 miles (48.25 km.) of aerial power-transmission copper conductor of 500,000 circ. mils (253 sq. mm.) cross-section, spaced at equal interaxial distances of 9 ft. (275 cm.). The entire line of 26 H-

sections thus represents 780 miles (1,250 km.) of single-phase conductor. The total weight of insulated wire is about 1,100 lb. (500 kg.). The sections are mounted in racks five shelves deep in two cabinets, each capable of holding 15 sections. Each cabinet measures approximately 185 cm. by 61 cm. by 167.5 cm. high, with a floor space of 1.1 sq. m.

The linear constants of the conjugate smooth line at low frequencies are given in Table XVIII.

TABLE XVIII

Nominal linear constants of 250 sq. mm. (500,000 circ. mils) copper artificial power-transmission line taking each section as representing 30 miles (48.3 km.)

	Per wire km.	Per wire mile
Linear resistance $r$ ohms at 20°C.....	0.0702	0.113
Linear inductance $l$ henrys.....	$1.16 \times 10^{-3}$	$1.87 \times 10^{-3}$
Linear capacitance $c$ farads.....	$1.004 \times 10^{-8}$	$1.617 \times 10^{-8}$
Linear leakance $g$ mhos.....	$0.013 \times 10^{-6}$	$0.021 \times 10^{-6}$
Linear hyperbolic angle $\alpha$ hyps. at 189.4~.....	$0.00407 \angle 88^\circ.2$	$0.00655 \angle 88^\circ.2$

No lumpiness correction factor has to be applied on this line, in practice, below 200~. The section angle at 189.4~ is  $0.1964 \angle 88^\circ.2$  hyp. At 189.4~, the lumpiness correcting factor is  $1.002 \angle 0^\circ.01$ .

This line is relatively heavy to construct, but is very well adapted to manifest a.c. and transient phenomena, owing to its relatively very low linear resistance, and its small section angle.

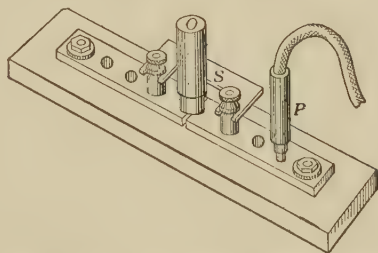


FIG. 125A.—Convenient form of plug contact piece.

**General Remarks Concerning Artificial-line Connections.**—In establishing the connections of an artificial line, it is important to have as few and firm electric contacts as possible, and to provide convenient means for testing the continuity and uniformity of the sections. A particular form of plug contact piece having some advantages for connecting consecutive II-sections is shown in Fig. 125A. The condenser is connected to the brass split or tapered plug,  $P$ , capable of being tightly inserted in the piece and of



being speedily removed. By throwing off all the condenser plugs, a Wheatstone-bridge test of the line circuit, or of any part thereof, can be speedily made. The open-circuiting plug *O*, permanently short-circuited by the removable brass strip *S*, enables the line to be opened conveniently at that point, or permits the insertion of a small resistance in the line, for measuring line current by potentiometer.

One of the most important requirements of any artificial line is obviously uniformity among the sections. It is usually more important that they should be all alike, even if they are somewhat off standard, than that some should approach the standard electric conditions very closely while others depart appreciably therefrom. It is very disconcerting to observers and computers to find certain sections too far off the average. If electrical discrepancies exist, it is usually better to place them near the motor end of the line, and to have the highest available degree of uniformity in the generator-end sections, where the fall of potential and current is greatest.

It is found advantageous to insulate elaborately all parts of the line circuit, and to ground carefully the ground side. For some purposes it is insufficient to employ the ground side as a mere return conductor, and actual grounding to water pipes is to be preferred as a general practice.

**Relative Merits of *T*- and  $\Pi$ -Sections.**—As to the choice between *T*- and  $\Pi$ -sections, assuming that they are both readily realizable, *T*-sections have the advantage that the ammeters, or equivalent current-measuring devices, can be inserted at section junctions, without disturbing adjacent leaks. Moreover, series-loading coils at junctions can much more easily be inserted experimentally in *T*-lines than in  $\Pi$ -lines. On the other hand, the terminal sections of a *T*-line call for half reactors. It is often inconvenient to supply terminal reactors of half the usual section reactance, or to find the correct mid-points of the section reactances. It is ordinarily preferable to make all the line reactors similar and equal without mid-point taps. Two section reactors may be used in parallel to form each terminal semi-reactance, but this is wasteful of material. It is easier in such cases to employ  $\Pi$ -sections, with full reactors throughout, and semi-leaks at the terminals. Each of these two types of artificial line has, therefore, its particular advantages and disadvantages, and the selection between them will depend on the merits of each case.

**Alternating-current Track-signaling Circuits.**—Many steam railroads employ automatic block-signal systems, in which the bonded track rails form the operating conductors. A very simple set of connections in such a system is indicated in Fig. 126. An a.c. transformer  $T$ , at position  $A$ , supplies, say, 8 volts, at 25~, to the rails of the track  $AB$ , through the current-limiting resistance,  $r$ . The rails are electrically disconnected at the insulating points  $I, I; I, I$ . A track relay  $R$ , at the distant end  $B$  of the section, is arranged to be operated by the alternating current from  $A$ , unless a train  $N$ , at any position between  $A$  and  $B$ , establishes a short-circuit between the rails. As soon as the train clears the section, the relay  $R$  will become reënergized.

The two rails of the track, if properly and uniformly bonded at joints, form the two conductors of a two-wire circuit, with an impressed e.m.f. at  $A$ , and a permanent load at  $B$ . The leakage

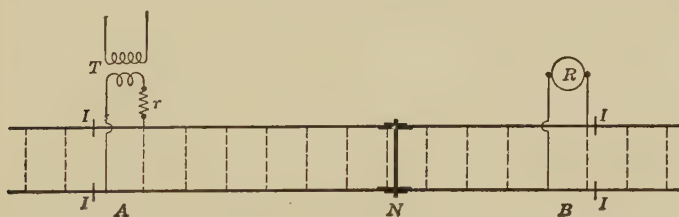


FIG. 126.—Elementary-connection diagram of a railway-track signal system.

across the track due to moisture in the ties and ballast, will tend to develop a uniformly distributed leakance, the linear value of which will depend upon the chemical and mechanical conditions of the track, and also on the weather. It is reported, as the result of many electrical observations on a variety of lengths and locations of track, that this linear leakance, at any one locality and time, is substantially uniform and uniformly distributed; so that this distributed leakance obeys Ohm's law sufficiently nearly to admit of being treated as uniform, in the engineering application of the hyperbolic theory.

The linear impedance of the track rails will depend upon their size and shape, the conductivity and permeability\* of the steel at the working temperature, on the impressed frequency, the current strength, and on the nature of the bonding. Tables of linear

\* "Experimental Researches on the Skin Effect in Steel Rails," by A. E. Kennelly, F. H. Achard, and A. S. Dana, *Journal of the Franklin Institute*, August, 1916, pp. 135-189.

impedance\* for different sizes of rails and different kinds of bonding have been prepared by Railway Signal Engineers. Its size is estimated to vary between 0.3 and 1.5 ohms per track km. (0.1 and 0.5 ohm per track 1,000 ft.), and its slope between  $12^\circ$  and  $66^\circ$ . The linear leakance may also vary between 0.15 and 1.2 mhos per track km. (0.05 and 0.4 mho per track 1,000 ft.), according to the nature of the ballast, and the wetness of the same. This linear leakance is relatively so large that the capacity susceptance is ordinarily negligible.

In preparing an artificial line to represent a signal circuit of given length and track conditions, the linear resistance would be taken from tables, for the rail size and character of bonding, as well as for the impressed frequency of the signaling current. The linear leakance would naturally be selected at a reasonable maximum value† likely to be met with under the worst prevailing weather conditions. If the signaling apparatus worked with an ample margin of safety in the laboratory on such an artificial line, it might be expected to work satisfactorily over the corresponding actual track circuit under all normal operating conditions, all defective rail bonds having been removed.

A particular 1-km. section of track is indicated at  $AB$  in Fig. 127. Here the linear impedance is taken as  $z_{,,} = 1.18 \angle 22^\circ.2$  ohms per track km. ( $0.36 \angle 22^\circ.2$  ohm per track 1,000 ft.) and  $y_{,,} = 0.563 \angle 0^\circ$  mho per track km. ( $0.172 \angle 0^\circ$  mho per track 1,000 ft.). These conditions lead to  $\theta = 0.815 \angle 11^\circ.1$  hyp. per km, and  $z_{0,,} = 1.45 \angle 11^\circ.1$  ohm ( $y_{0,,} = 0.690 \angle 11^\circ.1$  mho) or  $z_0 = 0.725 \angle 11^\circ.1$  ohm, ( $y_0 = 1.380 \angle 11^\circ.1$  mhos).

The correcting factors for the equivalent circuits of this length of track are indicated in Fig. 127. The larger is  $1.106 \angle 2^\circ.3$ . For shorter lengths of track, these correcting factors would be nearer to unity. For lengths of 0.25 km. or less, the nominal  $T$ 's and  $\Pi$ 's would be substantially equivalent  $T$ 's and  $\Pi$ 's.

The equivalent  $I$ -section for 1 km. is indicated at  $A'B'$ . Each line wire has  $0.562 \angle 21^\circ.1$  ohms, and the central leak has  $1.608 \angle 2^\circ.3$  ohms. The equivalent  $T$  is found on either side of the neutral line  $NN'$ .

\* "Alternating-current Signaling," by Harold McCready, Union Switch and Signal Co., Swissvale, Pa., 1915, p. 440.

† "Electric Interlocking," by the Engineering Staff of the General Railway Signal Co., Rochester, N. Y., 1915.

† "Data on Electric Railway Track Leakage," by G. H. Ahlborn, *Technological Papers of the Bureau of Standards*, No. 75, August, 1916.

The equivalent  $O$  section is shown at  $A''B''$ . It has  $0.653 \angle 24^\circ.5$  ohm on each side, and  $3.81 \angle 1^\circ.1$  ohms in each leak. On each side of the neutral line  $N''N''$  is an equivalent  $\Pi$ .

At  $a'b'$  is the equivalent  $T$  with double surge resistance, and at  $a''b''$  is the corresponding equivalent  $\Pi$  with double surge resistance.

By making up a set of such similar equivalent sections for various lengths of track, say three of 1 km., two of 0.5 km., two

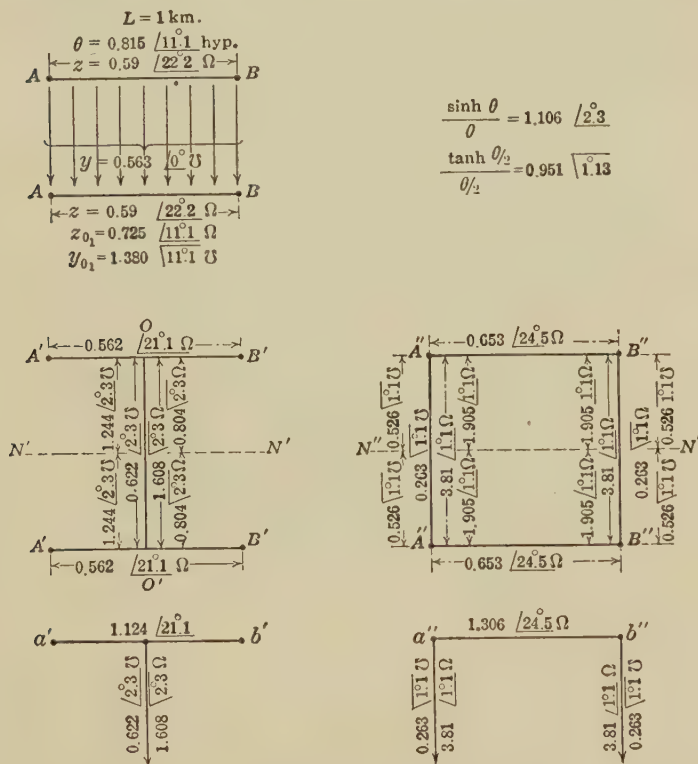


FIG. 127.—Diagrams of a particular 1-km. track section and its equivalent circuits.

of 0.25 km., and two of 0.125 km., it would be readily possible to connect up an artificial track line of any desired length from 0.125 km. up to 4.75 km. On this artificial line, any specific piece of apparatus such as a track relay might be tested under conditions resembling those occurring in actual operation.\*

\* L. V. Lewis, *The Signal Engineer*, July, 1911. "Analytic Method of Solving Track Circuit Problems," by C. F. Estwick, *Journal of the Railway Signal Association*, May, 1916, 21st year, No. 2, pp. 348-362.



**Artificial Telephone Lines.**—Figure 128A shows a convenient and portable form of artificial twisted-pair standard telephone

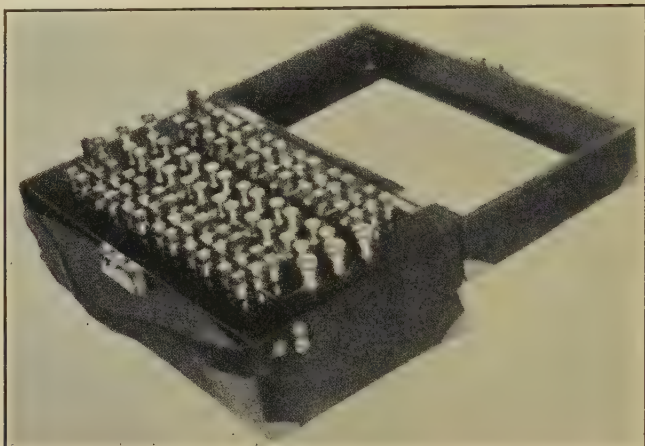


FIG. 128A.—32 mile artificial twisted-pair standard telephone cable.

cable as constructed by the Western Electric Co. for comparative tests, either electrical or auditory, on actual operating telephone

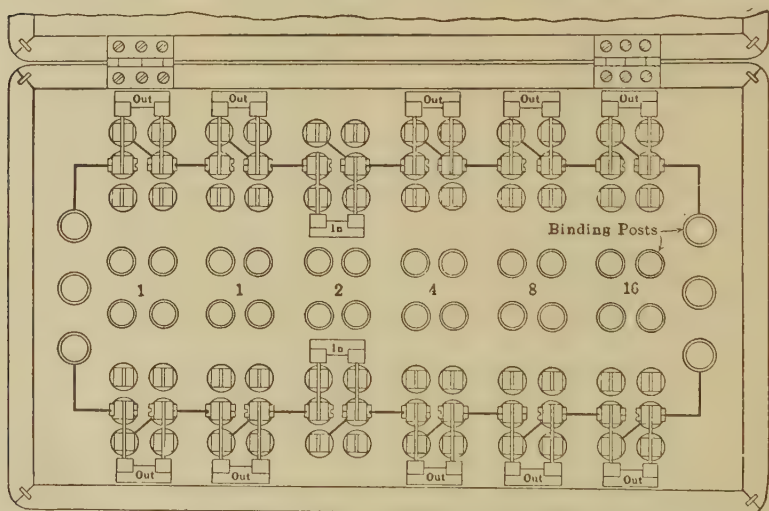


FIG. 128B.—Connection-diagram of Western Electric artificial telephone line.

circuits. The approximate inside dimensions of the box are 35.5 cm. by 19 cm. by 14 cm. deep (14 in. by 7.5 in. by 5.5. in. deep). The electrical connections are indicated in Fig. 128B. The box



contains 32 miles (51.5 km.) of artificial cable in *I*-sections of 16, 8, 4, 2, 1, and 1 miles. Each 1-mile section has 88 ohms conductor resistance and 0.054  $\mu\text{f.}$  intercapacitance, as at *AB*, Fig. 152 page 273. These sections are connected each to a quadruple group of binding posts along the central line. A pair of throw-over double-blade switches are also connected to each section, in such a manner that when *AA* and *BB* are made the main terminals of the line, each pair of switches brings in a section when thrown inward, and cuts it out of circuit when thrown outward. As con-



FIG. 128C.—Western Electric Company's aerial telephone line.

nected in Fig. 128*B*, there is one section of 2 miles (3.2 km.) left inserted in the line. By selecting the proper combination of switches, any integral number of miles of standard cable between 1 and 32, inclusive, can be connected in circuit.

A larger Western Electric Company's artificial telephone line box is illustrated in Fig. 128*C*. It contains *I*-sections of artificial No. 12 N.B.S. gage, diameter 0.104 in. (2.64 mm.) aerial open two-wire line of the following constants,  $r_{,,} = 10.4$  ohms/loop mile (6.46 ohms/loop km.),  $l_{,,} = 3.67$  millihenrys/loop mile (2.28 millihenrys/loop km.), and  $c_{,,} = 8.35$  m $\mu\text{f.}$ /loop mile (5.19 m $\mu\text{f.}$ /loop km.).\* The plan of connection by switches is the same as in the box of Fig. 128*B*. By means of these switches,

\* m $\mu\text{f.}$  is a symbol for millimicrofarad or  $10^{-9}$  farad.

any length between 10 miles (16 km.) and 600 miles (966 km.) of two-wire line may be inserted by 10-miles steps.

**Artificial Submarine Cables.**—A box of smooth artificial line containing resistance and associated distributed capacitance for a particular type of submarine cable is represented in Fig. 129. The box contains the equivalent of about 60 nauts. of ordinary cable (112 km.). The distributive association of resistance and capacitance in such a box has already been described earlier in this chapter (see page 210).

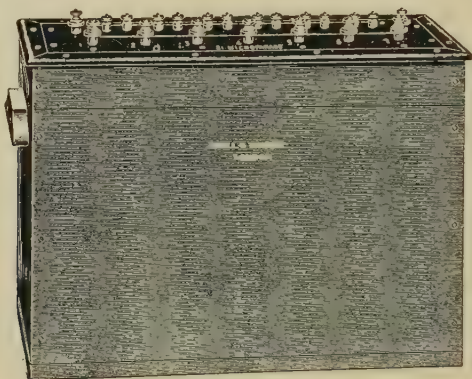


FIG. 129.—Box of artificial line for submarine telegraph cable, containing distributed resistance and capacitance.

**Distortionless Attenuators.**—Since artificial lines of series inductive reactance and shunt condensance, like those shown in Fig. 123C, involve distortion when applied as attenuators on multi-frequency circuits, it has been found desirable to employ artificial lines of pure resistance in both shunt and series elements, when distortion is to be avoided. Such reactanceless artificial lines introduce real values, for both  $\theta$  and  $z_0$ . Their attenuation is independent of the impressed frequency. They are adjusted into sections graded in transmission units (see Chapter XIII) so as to insert attenuation in suitable steps up to 100 T. U. or over.

## CHAPTER XV

### FUNDAMENTAL PROPERTIES OF ALTERNATING-CURRENT ARTIFICIAL LINES

Artificial lines may be classified conveniently in accordance with the arrangement of their elements and terminals, and in view of the real lines or systems that they are designed to represent. We may consider, for this purpose, the group of real and artificial lines or systems indicated in Fig. 130.

**Single-wire Lines.**—In section 2 of Fig. 130, a single uniform section of real line is indicated at  $AB$ . As shown, it is a single-wire c.c. line with ground return, having a total conductor resistance of  $R$  ohms, and total leakance of  $G$  mhos, so as to subtend a total angle of  $\theta$  hyps, and to have a surge resistance of  $z_0$  ohms. It might, however, also serve to designate an a.c. line with conductor impedance  $Z$  ohms  $\angle$ , and dielectric admittance  $Y$  mhos  $\angle$ . It might, likewise, be taken to represent one wire of a pair of parallel conductors employing a complete metallic circuit, such as one-half of the two-wire line of section 5.

Conjugate with the line  $AB$  of Fig. 130-2 are the  $\Pi$  artificial line of section 1, and the  $T$  artificial line of section 3. Each of these two artificial lines has three elements of resistance in the c.c. case, and of impedance in the general a.c. case. We have already seen in Chapter VI that, by properly proportioning the impedance elements, each of these two artificial lines subtends the same angle  $\theta$ , and offers the same surge impedance  $z_0$ , as the real line, at the terminals  $A$  and  $B$ , with ground or neutral return.

**Two-wire Lines.**—In Fig. 130-5, a uniform two-wire line is indicated with input terminals at  $AG$ , and output terminals at  $BH$ . If the line system is symmetrical, the neutral or zero-potential plane will divide the system into two equal and opposite halves or single-wire systems, as is indicated by the dotted lines  $NN$ . The artificial lines conjugate to the double-wire system of section 5 are the  $O$ -line of section 4 and the  $I$ -line of section 6. The former comprises four impedance elements and the latter five.

If the single-wire line of section 2 is regarded as being one of the conductors in the two-wire line of section 5, and is operated to neutral potential, then we have found, in Chapter III, in relation to Figs. 10 and 11, that the angle  $\theta$  subtended by both

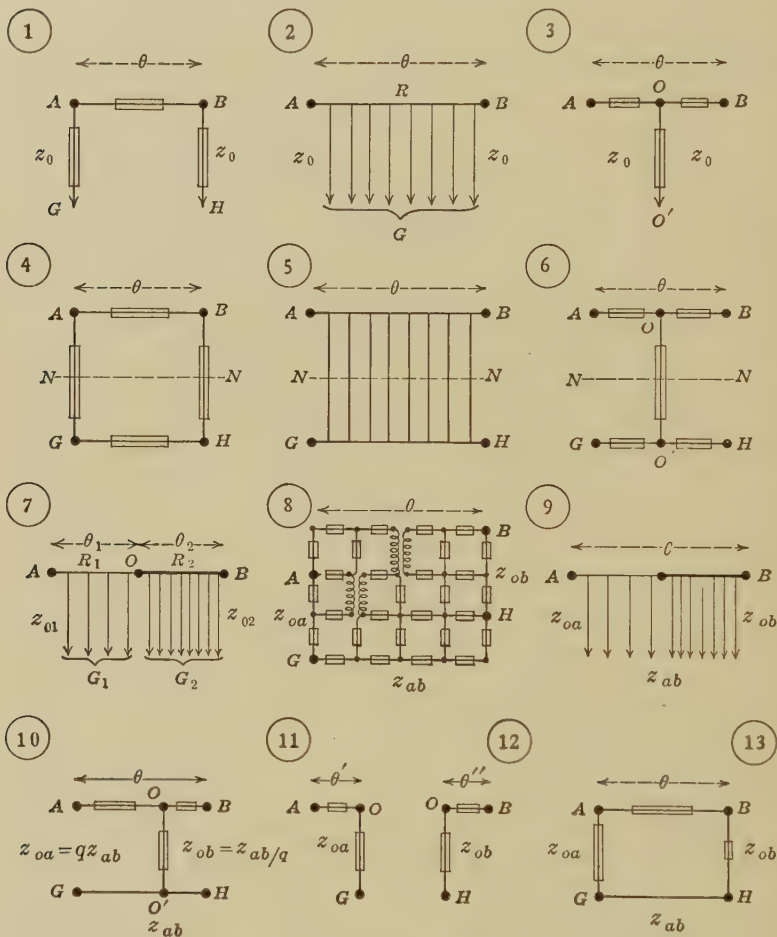


FIG. 130.—Group of real lines and systems together with various types of artificial lines conjugate to the same.

systems will be the same, but that the surge impedance  $z_{0,}$  of the two-wire line of section 5 will be double the surge resistance  $z_0$ , of the single-wire line in section 2. The same relations hold for the conjugate artificial lines; that is, the surge impedance of the

$O$ -line will be twice that of the  $\Pi$ -line, and that of the  $I$ -line twice that of the  $T$ -line.

If we describe the lower half  $NNGH$  of section 4 as a  $U$ -line, and the lower half  $NNGH$  of section 6 as an *anchor line*, then we may say that an  $O$ -line of double surge impedance may be formed by the cross connection of a  $\Pi$ -line and a  $U$ -line, the  $\Pi$ ,  $U$ , and  $O$ -lines all having the same angle  $\theta$ . Similar conditions apply to the  $I$ -line of section 6, and its equal components of  $T$ - and anchor lines.

If, in sections 4 and 6, we move the dividing lines  $NN$  upwards or downwards, it is evident that the  $O$  and  $I$ -lines may be split up into unequal  $\Pi$ - $U$  pairs, and likewise the  $I$ -line into unequal pairs of  $T$ - and anchor components. In either case, the two components will have different values of  $\theta$  and  $z_0$ . In other words, a uniform two-wire real line of section 5 may be resolved into an infinite number of conjugate  $\Pi$ - $U$  pairs, to form its  $O$ -conjugate, and also into an infinite number of  $T$ -anchor pairs, to form its  $I$ -conjugate.

**Composite Lines.**—Section 7 represents a composite real line of two lengths  $A-O$  and  $O-B$  in series. Each length has its own angle and surge impedance. A conjugate artificial-line system for this composite line would be a series combination of conjugates for the different lengths. There might be any one of four such series combinations; namely, a  $\Pi$ - $T$ , a  $T$ - $\Pi$ , a  $\Pi$ - $\Pi$  and a  $T$ - $T$ . In each case, the artificial network or *net* would be *dissymmetrical* because the surge impedances of the component lines, real or artificial, would, in general, be different.

A two-wire composite line corresponding to the system of section 7 would have as conjugates any one of the four following series pairs of artificial lines;  $O-I$ ,  $I-O$ ,  $O-O$ , and  $I-I$ . In any such conjugate series pair, the potential, current, and power at the junction point  $O$  would be the same as at the junction  $O$  of the corresponding real-line pair in section 7.

If the same pair of real lines  $AO$ ,  $OB$  are connected to form the composite line of section 9, we may consider the system as forming a single-element dissymmetrical line system of total angle  $\theta$ , and with two terminal surge impedances, namely  $z_{0a}$  from the  $A$  end and  $z_{0b}$  from the  $B$  end. In this case, the total angle  $\theta$  will, in general, differ from the sum  $\theta_1 + \theta_2$  of the component line angles of section 7. We are thus led to the consideration of *dissymmetrical electrical nets*.



**Dissymmetrical Nets.**—A net or network is any aggregation of electrical conductors connected together in any definite manner, each element of the system being assumed to obey a.c. Ohm's law. Conducting lines, resistances, inductances, condensers, or transformers may enter, in any order or number, into any element of the net. A simple particular form of net is represented in section 8. Two terminals  $A$  and  $G$ , selected arbitrarily, may constitute the input terminals; while two others, such as  $B$  and  $H$ , constitute the output terminals. The symbol  $\equiv$  represents any combination of definite impedance at any single impressed frequency. Such a net may be described as a *four-terminal net*. When two opposite-end terminals  $G$  and  $H$  are united, the system becomes a *three-terminal net*. Any composite line such as that of section 9 may be regarded as a particular case of a dissymmetrical net.

The discussion of dissymmetrical nets will be taken up in Chapter XVIII. We are here mainly concerned with the classification of lines, systems, and parts. It will be shown that any dissymmetrical net can be completely represented, at input and output terminals, for any single impressed frequency, by a certain dissymmetrical  $T$  as in section 10, or by a certain dissymmetrical  $\Pi$  as in section 13. Similarly, the net may be represented, at input and output terminals, by any one of an infinite series of dissymmetrical  $I$ -lines or any one of an infinite series of  $O$ -lines. All these different conjugates will have, at the assigned frequency, the same total angle  $\theta$  and the same pair of terminal surge impedances  $z_{0a}$  and  $z_{0b}$ , as the net.

**Resolution of a  $T$  or  $\Pi$  into a Pair of Cantilevers.**—A *cantilever* may be described as either a  $T$ -line with one of its arms suppressed by being reduced to zero, or as a  $\Pi$  with one of its pillars suppressed by being made infinite in impedance. A cantilever may be either a *7-line* as in section 11 at  $AOG$ , or a *gamma-line* ( $\Gamma$ ) as in section 12, at  $OBH$ . It can be shown that any  $T$ -line, such as that of section 10, may be resolved\* into a  $7$ -line  $AOG$ , series connected to a  $\Gamma$ -line  $OBH$ , such that the sum of the cantilever angles  $\theta' + \theta''$  is equal to the angle  $\theta$  of the  $T$ , and the surge impedances  $z_{0a}$  and  $z_{0b}$  of the cantilevers are, respectively, equal to those of the  $T$ .

\* Two such  $7$ - $\Gamma$  or  $\Gamma$ - $7$  pairs of cantilevers can, in general, be found, whose series connection will result in the required  $T$ - or  $\Pi$ -line (see Chapter XIX).

Similarly, any  $\Pi$ -line, such as that of section 13, may be resolved into a  $\Gamma$ -line  $OBH$ , series connected to a  $\gamma$ -line  $AOG$ , such that the sum of the cantilever angles  $\theta' + \theta''$  is equal to the angle  $\theta$  of the  $\Pi$ , and the surge impedances at the ends correspond completely.

In the same way, any  $I$ -line may be resolved into a pair of series-connected bracket lines ( $[|]$ ), an *end-bracket*  $] at AG and a fore bracket [ at BH, such that the sum of the two component bracket angles is equal to the angle  $\theta$  of the  $I$ , and the surge impedances on the concave sides of the brackets are respectively equal to the  $z_{0a}$  and  $z_{0b}$  of the  $I$ .$

Again, any  $O$ -line may be resolved into a pair of series-connected bracket lines ( $[|]$ ), a fore bracket  $[ at AG, and an end bracket ] at BH, such that the sum of the component bracket angles is equal to the angle  $\theta$  of the  $O$ , and the surge impedances on the convex sides of the brackets are respectively equal to the  $z_{0a}$  and  $z_{0b}$  of the  $O$ . In general, this substitution of bracket lines can be effected in an infinite variety of ways.$

To summarize, any three-terminal net may be replaced by one  $T$  or one  $\Pi$ . Any four-terminal net may be replaced by any one of an infinite series of  $I$ 's or any one of an infinite series of  $O$ 's. Any  $T$  may be replaced by two series-connected cantilevers, a  $\gamma$  and a  $\Gamma$ . Any  $\Pi$  can be replaced by two series-connected cantilevers, a  $\Gamma$  and a  $\gamma$ . Any  $I$  can be replaced by any one of an infinite series of brackets, a  $] and a [ . Any  $O$  can be replaced by any one of an infinite series of brackets, a  $[ and a ]$ .$

Symmetrical  $\Pi$ 's and  $T$ 's, or  $O$ 's and  $I$ 's, pertain more particularly to the representation of real uniform lines in the laboratory. Dissymmetrical  $T$ 's and  $\Pi$ 's, or  $I$ 's and  $O$ 's, with their cantilever or bracket components, pertain more particularly to general nets, and their applications.

**Alternating-current Artificial Lines.**—Alternating-current artificial lines are ordinarily composed of uniform sections, either  $T$ 's or  $\Pi$ 's. The series elements of these sections ordinarily contain resistance and reactance, and the shunt elements, or leaks, conductance and susceptance.

There are two fundamental problems which frequently present themselves in discussing the relations between real and artificial a.c. lines. The first is to find the elements of a  $T$ - or  $\Pi$ -section which shall make the section correspond to an assigned length of real line at an assigned frequency. The second is,

knowing the impedance and admittance elements of an artificial line section, at a given frequency, to find the line angle and surge impedance of the section at that frequency. We shall consider these two problems in the above order.

**To Find the Elements of a T or  $\Pi$  Which Shall Form a Section Equivalent to a Given Length of Real Line at a Given Frequency.**

The procedure is the same as in the d.c. case already considered in Chapters VI and VII, but with the formulas interpreted vectorially. That is, we find the angle  $\theta$  subtended by the given length of real line, at the assigned frequency, and also its surge impedance  $z_0$ . The conductor impedance of the real section is, therefore,  $Z = \theta z_0$  ohms, and the dielectric admittance is  $Y = \theta/z_0 = \theta y_0$ . We then map out the nominal  $T$  and  $\Pi$  containing

these quantities. We next find\* the correcting factors  $\frac{\sinh \theta}{\theta}$  and  $\frac{\tanh (\theta/2)}{\theta/2}$ , which, applied to the elements of the nominal sections, gives the corrected elements of the equivalent sections.

As an example, we may consider a length of 7.581 km. (4.71 miles) of the telephone line already employed, at the angular frequency of  $\omega = 5,000$ . We have already seen (p. 158) that, at this frequency, 7.581 km. subtend a circular angle of  $30^\circ$ , and have a total angle  $\theta = 0.726726 \angle 46^\circ.05'.44''$  hyp.  $= 0.50394 + j0.52360 = 0.50394 + j0.33333$ . The surge impedance  $z_0$  is  $285.67 \angle 42^\circ.50'.36''$  ohms. The conductor impedance of this length is, therefore,  $0.726726 \angle 46^\circ.05'.44'' \times 285.67 \angle 42^\circ.50'.36'' = 207.602 \angle 3^\circ.15'.8''$  ohms. The dielectric admittance is  $0.726726 \angle 46^\circ.5'.44''/285.67 \angle 42^\circ.50'.36'' = 2.5439 \times 10^{-3} \angle 88^\circ.56'.20''$  mho. We draw the nominal  $T$  and  $\Pi$  containing these values, as shown at  $AOB$ , and  $A''B''$ , Fig. 131. We now find the correcting factors

$$\frac{\sinh (0.726726 \angle 46^\circ.5'.44'')}{0.726726 \angle 46^\circ.5'.44''} \text{ and } \frac{\tanh (0.363363 \angle 46^\circ.5'.44'')}{0.363363 \angle 46^\circ.5'.44''}$$

\* Tables of these correcting factors have already been published within certain limits of  $\theta$ , in the author's "Tables of Complex Hyperbolic and Circular Functions," and graphical interpolation charts in his "Chart Atlas of Complex Hyperbolic and Circular Functions;" but in cases where it is desired to work out these correcting factors, a good plan is to find  $\sinh (\theta/2)$  and also  $\cosh (\theta/2)$  as polars. Twice their product is then  $\sinh \theta$ , and their ratio is  $\tanh (\theta/2)$ . These expressed as polars are then divided by  $\theta$  and  $\theta/2$ , respectively.

to the required degree of precision, from charts, tables, or calculation. They are as shown in Fig. 131,  $0.998189 \angle 5^{\circ}.2'.36''$ , and  $1.00033 \angle 2^{\circ}.31'.22''$ , respectively. These are the lumpiness corrections. For many practical purposes, these correcting factors are so near to  $1.0 \angle 0^{\circ}$  as to be negligible. In other words, up to the frequency  $\omega = 5,000$ , the nominal sections of artificial-line  $T$ 's or  $\Pi$ 's may be regarded as substantially the same as the equivalent sections up to line lengths of 7.58 km. (4.7 statute

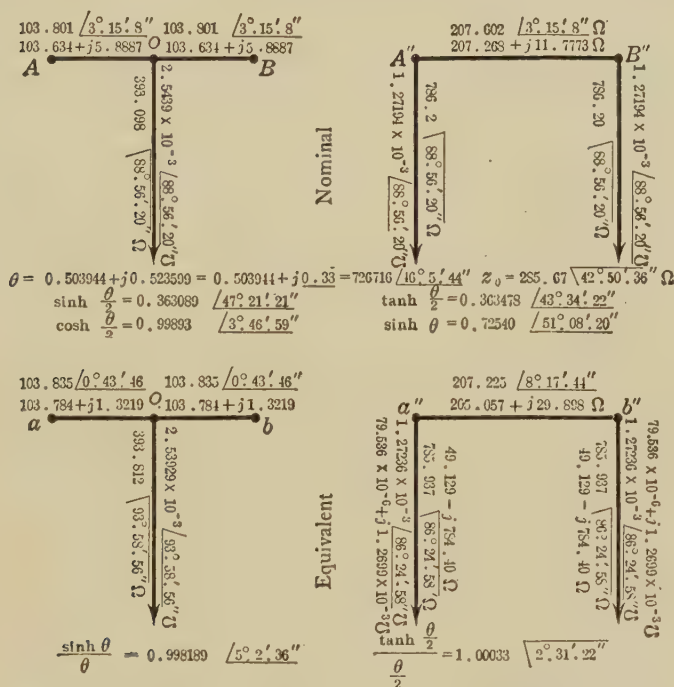


FIG. 131.—Nominal and equivalent  $T$  and  $\Pi$  artificial-line sections.

miles). The equivalent sections are indicated at  $aob$  and  $a''b''$ , Fig. 131.

**I- and O-Sections of Double-wire Artificial Line.**—If we desired two-wire artificial-line sections, we should connect a pair of equivalent  $T$ 's, or a pair of equivalent  $\Pi$ 's by their feet, to form what may be called an equivalent  $I$  and an equivalent  $O$  section, respectively, as in Fig. 132. The angle subtended by an equivalent  $I$  or  $O$  is identical with that subtended by the corresponding equivalent  $T$  or  $\Pi$ . The surge impedance of the  $I$  or  $O$  is, as we

have already seen, just double the surge impedance of the  $T$  or  $\Pi$ , respectively.

If we connect in series a number of such equivalent  $T$ 's or  $\Pi$ 's, we obtain a corresponding length of artificial  $T$  or  $\Pi$  line, as in Fig. 133, which shows the distribution of current and voltage over the first four sections of such a pair of lines. Each line is supposed to have been rendered virtually infinite by grounding, after any desired number of sections, through an impedance of  $285.67 \angle 42^\circ.50'.36''$  ohms. An impressed a.c. potential of 1.0

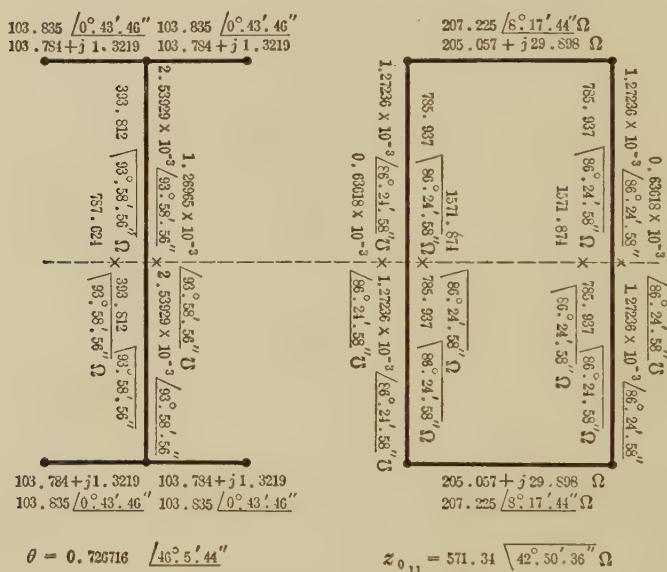


FIG. 132.—Double-wire  $I$  and  $O$  artificial-line sections.

r.m.s. volt is applied at  $A$ , the generating end, at a frequency of  $f = 796\sim$ , or  $\omega = 5,000$ .

**Unrealizable Artificial-line Sections.**—It will be noticed in Figs. 131 and 132, that there should be no difficulty in constructing and adjusting the elements of the equivalent  $\Pi$  or  $O$ . The architrave should have an inductance of  $29.898/5,000 = 5.9796 \times 10^{-3}$  henry, with resistance added up to 205.06 ohms, preferably of insulated manganin wire. The  $\Pi$  leaks should have  $1,269.9/5,000 = 0.254 \mu\text{f.}$  capacitance, at the impressed frequency, with an associated leakance of 79.5 micromhos. By taking sufficient pains, these values could be adjusted to within



desirable limits of precision. In the case, however, of the equivalent  $T$  and  $I$ , there would be no way of obtaining, without the aid either of inductive devices or of parallel branches, the required staff elements, by simple series connection of resistance and capacitance, because the slopes of the  $T$ -leaks exceed  $90^\circ$ . In the case of this length of real line section, and for this assigned frequency, the equivalent  $T$ -sections would have arithmetical significance only, and would not be physically realizable, in the laboratory, by ordinary simple means. At other frequencies, or with other lengths of real-line section, we might find both  $T$  and  $\Pi$  realizable. It sometimes happens that neither the  $T$  nor the  $\Pi$  is realizable. In such cases, another length of real-line section should be selected for imitation.

**Graphs of Normal Attenuation on Alternating-current Real and Artificial Lines.**—If we plot the values of potential and current over the virtually infinite artificial lines of Fig. 133, by comparison with the corresponding values over the conjugate smooth line, as in Fig. 85, we are led to the constructions of Fig. 134, where  $ABCD$  is the potential spiral,  $A'B'C'D'$  the current spiral, and the constant phase difference between these two spirals is left out of consideration, in order to facilitate inspection. Turning to the potential spiral, Fig. 134,  $OA$  being the impressed unit r.m.s. potential at  $A$ , to standard phase, then the curve  $ABCD$ - $EFG$  represents the fall of potential along the conjugate smooth line, as in Fig. 85. The potential drops in the line elements of the  $\Pi$  line are indicated, both in magnitude and phase, by the interior straight lines, or chords,  $AB$ ,  $BC$ ,  $CD$ , etc. Similarly, the potential drops in the line elements of the  $T$  line are indicated, both in magnitude and phase, by the exterior straight lines  $Ak$ ,  $kBl$ ,  $lCm$ , etc. At the junctions the potentials are the same, on both the artificial lines, as well as on the real conjugate line. *The  $T$ -line normal-attenuation potential thus falls on an external contacting equiangular-spiral polygon, and the  $\Pi$ -line potential falls on an internal contacting polygon, the points of contact representing the terminals and junction points of the sections.* To construct these polygons, first draw the equiangular spiral  $ABCD$  for the conjugate smooth line or real line. Mark off a mid-section point such as  $i$ , where the radius-vector  $Oi$  bisects the circular section angle  $AOB$ . Operate on the vector  $Oi$  by  $\cosh (\theta/2)$ , and  $\operatorname{sech} (\theta/2)$ , so as to produce the vectors  $Oj$  and  $Ok$ , respectively. In the case of Fig. 134,  $\cosh (\theta/2) = 0.99893 \angle 3^\circ.46'.59''$ , and  $\operatorname{sech}$

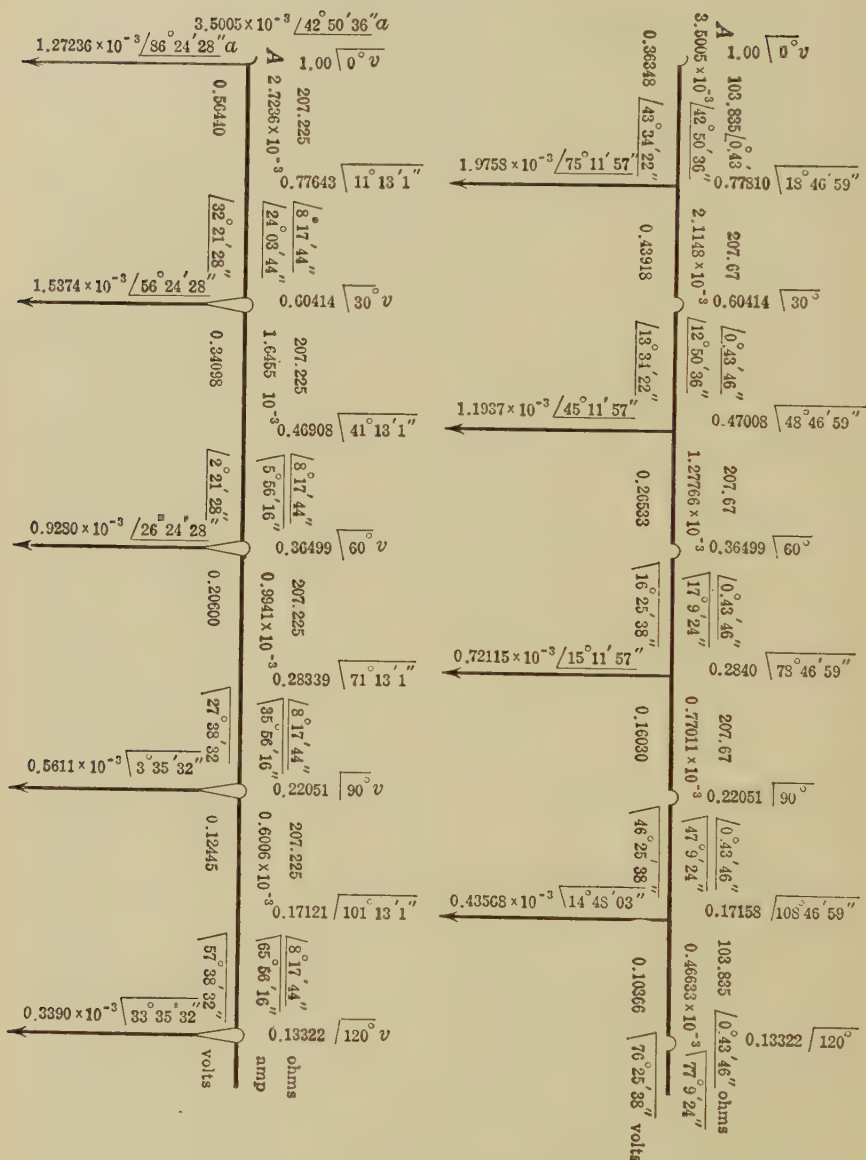


FIG. 133.—Normal attenuation over artificial T- and II-lines.

$(\theta/2) = 1.00107 \angle 3^\circ.46'.59''$ . The point  $j$  will bisect  $AB$ . Join  $Ak$  and  $Bk$ , which will be the vector drops in the arms of the  $T$ -section, to scale and phase. Moreover,  $kB$  will be equal to and in line with  $lB$ .

The graph of normal power attenuation on any real line is also an equiangular spiral. The power delivered at  $B$  if  $P_A$  is the active power input at  $A$ , becomes

$$P_B = P_A e^{-2\theta_1} \quad \text{watts} \quad (405a)$$

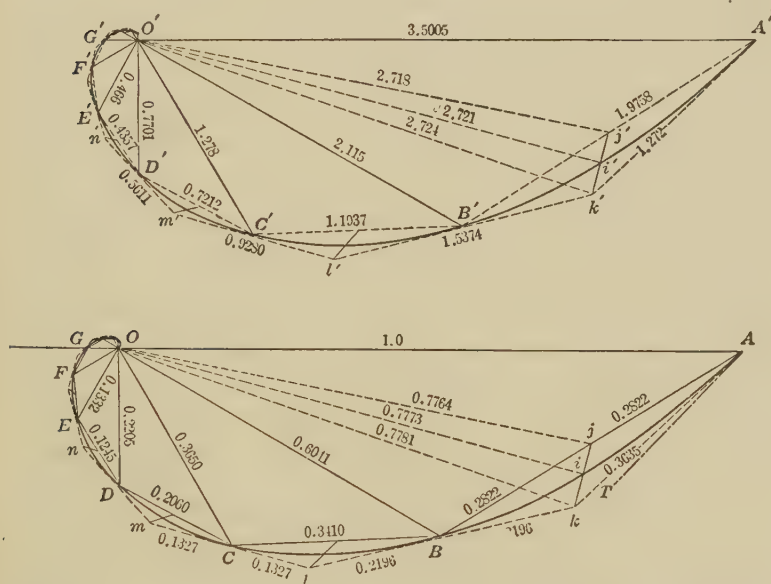


FIG. 134.—Normal attenuation graphs on a real line and on its conjugate artificial  $T$  and  $\Pi$  lines.

where  $\theta_1$  is the real part of the angle  $\theta$  subtended by the line. The efficiency of the line is, therefore,

$$\eta = e^{-2\theta_1} \quad \text{numeric} \quad (405b)$$

The same efficiency pertains to the conjugate artificial lines, at the same impressed frequency.

Turning now to the current graph  $A'B'C'D'$ , Fig. 134, the curve is the normal attenuation spiral of the conjugate smooth line to initial current standard phase. At junction points  $B'C'D'$ , the line currents are in coincidence with each other, and with the contacting equiangular spiral. If we operate on the mid-section vector such as  $Oi'$  by  $\cosh (\theta/2)$  and  $\operatorname{sech} (\theta/2)$ , as before, we

obtain the vectors  $Oj'$  and  $Ok'$ , the former bisects  $A'B'$ , and represents the vector arithmetical means of the line currents  $3.5005 \angle 0^\circ$  and  $2.1148 \angle 30^\circ$ , in the two branches of the first  $T$ -section. The latter,  $Ok'$  represents the current at the middle of the first  $\Pi$ -section, *i.e.*, the current in the architrave of that section. *Thus the  $\Pi$ -line normal-attenuation current falls on an external contacting equiangular spiral polygon, and the  $T$ -line current falls on an internal contacting polygon, the points of contact representing the terminals and junction points of the lines.* The successive sides of these current polygons represent the magnitudes and phases of the leak currents. Each polygonal side may be regarded as equivalent to the vector sum of all the infinitesimal leaks in the subtended smooth section. It will be understood that at any  $\Pi$ -line junction, the true line current requires replacing the single leak at that junction by a pair of parallel half-leaks, and placing the ammeter in the line between them, as in Fig. 41. Otherwise the true line current will be only arithmetically realizable, as the vector arithmetical mean of the two line currents on each side of the junction. Thus, at the end of the first  $\Pi$ -line section, the true line current would be to voltage standard phase

$$\frac{2.7236 \times 10^{-3} \angle 24^\circ.03'.44'' + 1.6455 \times 10^{-3} \angle 5^\circ.56'.15^\circ}{2} = 2.1148 \angle 12^\circ.50'.36'' \text{ milliamp.}$$

In regard to potential and current, therefore, the  $T$ - and  $\Pi$ -lines are mutually reciprocal. The  $\Pi$  line always follows, for potentials, the inside polygon, and, for currents, the outside polygon. This is true not only in the equiangular spiral graphs, controlling normal attenuations; but also in the hyperbolic-function graphs, which, as we shall see, control in the general case, and of which the equiangular spiral is but a limiting instance.

**Deduction of Section Elements from Their Measured Values of  $\theta$  and  $z_0$ .**—Another form in which the preceding problem may present itself, is where measurements of an artificial line, at a given frequency, in the manner described in the next chapter, and based on formulas (224) and (226), lead to correspondingly deduced values of the section angle  $\theta$  and surge impedance  $z_0$ . The problem then is to find the elements of the section in line impedance and leak admittance at that frequency. The procedure is the same as that above outlined. The nominal line impedance of the section is  $\theta z_0$  ohms, and the nominal leak admit-

tance  $\theta y_0$  mhos, in either one or two leaks, according as the section is a  $T$ - or a  $\Pi$ -section. The nominal  $T$  or  $\Pi$  is thus formed, and correcting factors  $\frac{\sinh \theta}{\theta}$  and  $\frac{\tanh (\theta/2)}{\theta/2}$  applied to their elements, to form the equivalent elements. These equivalent values are the respective line impedances and leak admittances, which the section elements possess at the frequency of the measurements.

**To Find the Line Angle  $\theta$  and Surge Impedance  $z_0$  of a  $T$ - or  $\Pi$ -section of Given Elements.**—In this problem, we start with either  $T$ - or  $\Pi$ -sections, all similar and symmetrical, the line impedance and leak admittance elements of which, at a given frequency, are known. We then have to find the section line angle  $\theta$  and the surge impedance  $z_0$ .

The procedure corresponds, under a.c. conditions, to that already found, under d.c. conditions, for a  $T$ -section by (174) and (180), or for a  $\Pi$ -section by (183) and (188). These formulas are now applied vectorially. We may take the following illustrative example.

A  $\Pi$ -line  $AB$ , of ten sections, is grounded at  $B$  through an impedance of  $\sigma = 1,216.936 \angle 72^\circ.329 = 369.4 + j1159.5$  ohms, the impressed angular frequency being  $\omega = 5,000$

radians per sec. Such a terminal load would be produced by a resistance of 369.4 ohms, containing an inductance of 231.9 millihenrys at this frequency. Each line section has a line impedance of  $r = 388.853 \angle 78^\circ.331 = 78.651 + j380.816$  ohms, and a pair of leaks each of admittance  $1.82858 \times 10^{-3} \angle 86^\circ.047 = (126.05 + j1824.2)10^{-6}$  mho, as shown in Fig. 134A, the measurements being made at  $\omega = 5,000$ . Required the line angle and surge impedance of each section. These particular element values are selected, partly because they approximately correspond to an artificial line\* on which similar tests have been already made and reported, partly because such an artificial line corresponds fairly well to a particu-

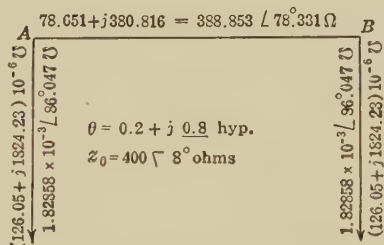


FIG. 134A.— $\Pi$  section of elements from which the section angle  $\theta$  and surge impedance  $z_0$  are deduced.

\* "Test of an Artificial Aerial Telephone Line at a Frequency of 750 Cycles per Second," by A. E. Kennelly and F. W. Lieberknecht, *Proc. A. I. E. E.*, June, 1913.



lar actual aerial telephone line, and partly because the position angles come out in simple round numbers, which may be found in the published tables without interpolation.

Following formula (202) we have

$$\sinh \frac{\theta}{2} = \sqrt{\frac{388.853}{2} \angle 78^\circ.331 \times 1.82858 \times 10^{-3} \angle 86^\circ.047}$$

$$= \sqrt{0.355524 \angle 164^\circ.378} = 0.59626 \angle 82^\circ.189.$$

In the published tables and charts (Table X), it is found that this corresponds precisely to  $\theta/2 = 0.1 + j0.4 = 0.1 + j0.62832 = 0.63623 \angle 80^\circ.957$  hyp. In general, it would be necessary to employ interpolation in the charts or tables, with some sacrifice of numerical precision, or else to use formula (591), Appendix A.

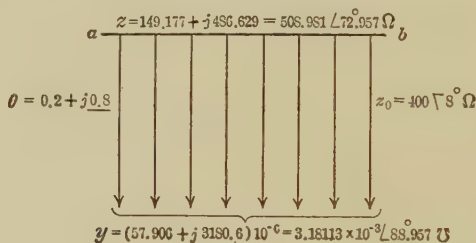


FIG. 135.—Smooth-line section conjugate to assigned II.

In this case, the section angle  $\theta = 0.2 + j0.8 = 0.2 + j1.2566 = 1.27246 \angle 80^\circ.957$  hyps. The angle subtended by the whole line of ten sections would therefore be  $2.0 + j8.0$  hyps. The normal attenuation factor of potential or current on such a line would be  $e^{-2} = 0.13533$ . The *normal phase attenuation* would be eight quadrants, or two complete waves of potential or current developed over the line, or the line would include two wave lengths. At this frequency it would be a *two-wave line*, and the artificial line would have five sections to a wave.

The apparent or uncorrected surge impedance of the line would be, by (194),

$$z_0'' = \sqrt{\frac{388.853 \angle 78^\circ.331}{3.65718 \times 10^{-3} \angle 86^\circ.047}} = \sqrt{10.6327 \times 10^4 \angle 7^\circ.716}$$

$$= 326.078 \angle 3^\circ.858 \quad \text{ohms}$$

and the true or corrected surge impedance by (204) is

$$z_0 = z_0'' / \cosh (0.1 + j0.4) = \frac{326.078 \angle 3^\circ.858}{0.81520 \angle 4^\circ.142} = 400 \angle 8^\circ \text{ ohms.}$$

The conjugate smooth line would, therefore, have a total angle of  $2 + j8 = 2 + j12.566 = 12.7245 \angle 80^\circ.957$  hyps., and a surge impedance of  $400 \angle 8^\circ$  ohms. If this line had a length of say 800 km., then a length of 80 km. would correspond to one section of the artificial line, and would subtend  $0.2 + j0.8 = 0.2 + j1.2566 = 1.27245 \angle 80^\circ.957$  hyps. The conductor impedance of the 80 km. smooth-line section, would be  $1.27245 \angle 80^\circ.957 \times 400 \angle 8^\circ = 508.981 \angle 72^\circ.957 = 149.177 + j486.629$  ohms. The linear impedance of the smooth line would be  $6.36225 \angle 72^\circ.957 = 1.8647 + j6.08286$  ohms per wire km., corresponding to a linear inductance of 1.2166 millihenrys per wire km. The dielectric admittance of the 80-km. smooth-line section would be  $1.27245 \angle 80^\circ.957 / (400 \angle 8^\circ) = 3.18113 \times 10^{-3} \angle 88^\circ.957 = (57.906 + j3180.6)10^{-6}$  mho. The linear dielectric admittance would thus be  $(0.72383 + j39.757)10^{-6}$  mho per wire km., corresponding to a linear capacitance of 0.0079515  $\mu$ f. per wire km. The smooth section is indicated at  $ab$ , Fig. 135.

The equivalent  $T$  of the section is shown in Fig. 136 at  $A'OB'$ . It will be seen that it happens to be unrealizable, because the slope of the leak admittance is  $94^\circ.331$ , and no simple admittance can have a slope exceeding  $90^\circ$ . We may assume, however, for the purpose of comparison between equivalent  $\Pi$ - and  $T$ -lines, that this  $T$ -section is not only arithmetically realizable, but is also physically realizable, by some special means, employing, say the aid of mutual inductance.

### Fall of Potential Along Artificial and Conjugate Smooth Lines.

To illustrate the comparative behavior of  $T$ -,  $\Pi$ -, and conjugate smooth lines,

we may consider 10-section lines of the three types shown in Figs. 136, 134, and 135, respectively, operated at the  $A$  end with an impressed potential of 1.0 volt r.m.s., at  $\omega = 5,000$  and with a terminal load at  $B$ , in each case, of  $\sigma = 1,216.94 \angle 72^\circ.329$  ohms. The angle subtended by the  $B$  terminal load is by (106)

$$\theta' = \tanh^{-1} \left( \frac{1,216.94 \angle 72^\circ.329}{400 \angle 8^\circ} \right) = \tanh^{-1} (3.04234 \angle 80^\circ.329) \\ = 0.05 + j0.8 \text{ hyp.}$$

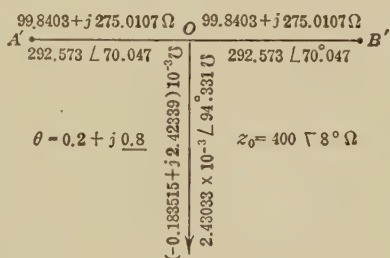


FIG. 136.— $T$  section equivalent to assigned  $\Pi$ .

The three types of  $\Pi$ -,  $T$ -, and smooth lines are indicated in Figs. 137, 138, and 139 respectively. The position angles of the junctions are also indicated, as pertaining to each of the three lines.

Remembering that the potentials along any such line are as the sines of the position angles, we obtain the results presented in Table XIX. The first column marks the position along the line, and the second column the distance  $x$  in kilometers from the generator end. Column III gives the corresponding position angles, from  $0.05 + j0.8$  hyp. at the  $B$  end, to  $2.05 + j8.8$  hyps. at the  $A$  end. The sines of these position angles, as given in the published tables of "Complex Hyperbolic Functions," appear in



Artificial  $\Pi$ - and  $T$ -lines with their conjugate smooth line.

the fourth column. In the fifth column of potential  $V_P$ , starting with the impressed potential of  $1.0 \angle 0^\circ$  volt r.m.s., at  $A$ , the remaining values are simply proportional to the sines of the position angles. The last two columns contain the particulars for the  $\Pi$ - and  $T$ -lines respectively. At junction points, denoted by the arabic numerals, the potentials on all three lines are identical. At mid-sections, the  $\Pi$ -line potentials are, by (215),  $\cosh v$  times the corresponding mid-section potentials on the smooth line; while the  $T$ -line potentials are  $\frac{1}{\cosh v} = \operatorname{sech} v$  times the same. We have already seen that  $\cosh v$  is, by tables,  $0.81520 \angle 4^\circ.142$ , and  $\operatorname{sech} v = 1.2267 \angle 4^\circ.142$  where  $v = \theta/2$ . These are the multipliers for the last two columns in Table XIX.

The numerical values of  $V_P$  recorded in Table XIX, are plotted in Fig. 140. Here  $OA$  is the vector  $1.0 \angle 0^\circ$  corresponding to the assumed impressed potential. The inwardly directed spiral curve  $A, 9, 8, 7, 6$ , etc., represents the fall of potential from the

TABLE XIX  
Distribution of potential over T-line, II-line and the conjugate smooth line

1 Position	2 $x$ km.	3 $\delta_P$ hyps.	4 $\sinh \delta_P$	5 $V_P$ r.m.s. volts	6 II-line r.m.s. volts	7 $T$ -line r.m.s. volts
A	0	2.05 + <u><math>j8.8</math></u>	3.93620 $\angle 72^\circ.551$	1.000 $\angle 0^\circ$		
X	40	1.95 + <u><math>j8.4</math></u>	3.49302 $\angle 37^\circ.110$	0.88741 $\angle 35^\circ.441$	0.72341 $\angle 31^\circ.299$	1.08858 $\angle 39^\circ.583$
9	80	1.85 + <u><math>j8.0</math></u>	3.10129 $\angle 0^\circ$	0.78789 $\angle 72^\circ.551$		
IX	120	1.75 + <u><math>j7.6</math></u>	2.85165 $\angle 322^\circ.339$	0.72448 $\angle 110^\circ.212$	0.59060 $\angle 106^\circ.070$	0.88873 $\angle 114^\circ.354$
8	160	1.65 + <u><math>j7.2</math></u>	2.68178 $\angle 286^\circ.794$	0.68131 $\angle 145^\circ.757$		
VIII	200	1.55 + <u><math>j6.8</math></u>	2.44238 $\angle 253^\circ.464$	0.62049 $\angle 179^\circ.087$	0.50582 $\angle 174.945$	0.76116 $\angle 183^\circ.229$
7	240	1.45 + <u><math>j6.4</math></u>	2.09821 $\angle 219^\circ.047$	0.53307 $\angle 213^\circ.504$		
VII	280	1.35 + <u><math>j6.0</math></u>	1.79909 $\angle 180^\circ$	0.45706 $\angle 252^\circ.551$	0.37260 $\angle 248^\circ.409$	0.56068 $\angle 256^\circ.693$
6	320	1.25 + <u><math>j5.6</math></u>	1.70635 $\angle 139^\circ.420$	0.43350 $\angle 293^\circ.131$		
VI	360	1.15 + <u><math>j5.2</math></u>	1.70971 $\angle 104^\circ.880$	0.43436 $\angle 327^\circ.671$	0.35408 $\angle 323^\circ.529$	0.53282 $\angle 331^\circ.813$
5	400	1.05 + <u><math>j4.8</math></u>	1.57374 $\angle 75^\circ.747$	0.39981 $\angle 356^\circ.804$		
V	440	0.95 + <u><math>j4.4</math></u>	1.24674 $\angle 44^\circ.483$	0.31674 $\angle 28^\circ.068$	0.25820 $\angle 23^\circ.926$	0.38854 $\angle 32^\circ.210$
4	480	0.85 + <u><math>j4.0</math></u>	0.95612 $\angle 0^\circ$	0.24290 $\angle 72^\circ.551$		
IV	520	0.75 + <u><math>j3.6</math></u>	1.01079 $\angle 311^\circ.160$	0.25670 $\angle 121^\circ.391$	0.20934 $\angle 117^\circ.249$	0.31501 $\angle 125^\circ.533$
3	560	0.65 + <u><math>j3.2</math></u>	1.17892 $\angle 280^\circ.523$	0.29951 $\angle 152^\circ.028$		
III	600	0.55 + <u><math>j2.8</math></u>	1.11300 $\angle 260^\circ.763$	0.28276 $\angle 171^\circ.788$	0.23050 $\angle 167^\circ.646$	0.34686 $\angle 175^\circ.930$
2	640	0.45 + <u><math>j2.4</math></u>	0.74969 $\angle 239^\circ.856$	0.19047 $\angle 192^\circ.695$		
II	680	0.35 + <u><math>j2.0</math></u>	0.35719 $\angle 180^\circ$	0.09075 $\angle 252^\circ.551$	0.07398 $\angle 248^\circ.409$	0.11132 $\angle 256^\circ.693$
1	720	0.25 + <u><math>j1.6</math></u>	0.63977 $\angle 108^\circ.629$	0.16254 $\angle 323^\circ.922$		
I	760	0.15 + <u><math>j1.2</math></u>	0.96290 $\angle 92^\circ.769$	0.24463 $\angle 339^\circ.782$	0.19942 $\angle 335^\circ.640$	0.30008 $\angle 343^\circ.924$
B	800	0.05 + <u><math>j0.8</math></u>	0.95237 $\angle 89^\circ.070$	0.24195 $\angle 343^\circ.481$		



generator end at *A*, to the motor end *B*, using the values in column 4 of the table, and also intermediate values. The smooth-line potential graph is seen to be a smooth spiral, *i.e.*, a complex hyperbolic sinusoid, making not quite two turns. The voltage attenuation factor of the whole line is shown in Table XIX to be 0.24195, as against 0.13533 in the normal case, and the lag in

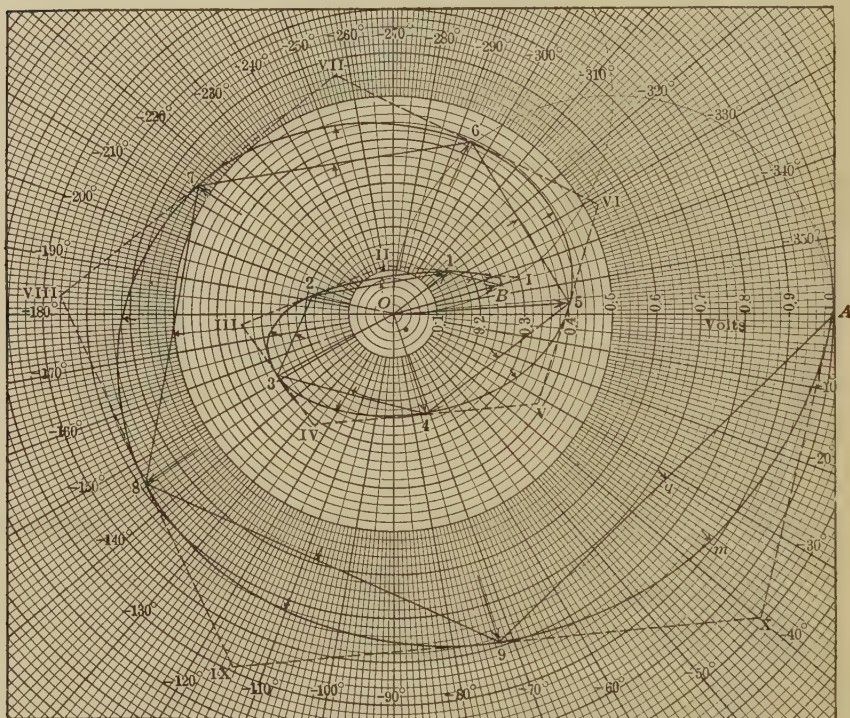


FIG. 140.—Potential distribution over real and artificial lines.

phase amounts to  $703^{\circ}.481$ , as against  $720^{\circ}$  in the normal case. The same is true for the conjugate artificial lines. On these, however, the fall of potential takes place in successive straight lines. For the  $\Pi$ -line, these straight lines are internal chords to the spiral; while, for the  $T$ -line, they are external chords, marked in broken lines. Thus, in the first  $\Pi$ -section, the potential drop is  $A9 = 1.0716 \angle 44^{\circ}.542 = 2.7557 \times 10^{-3} \angle 33^{\circ}.789 \times 388.853 \angle 78^{\circ}.331$  volts, a value greater than the initial impressed e.m.f. The drop in the first half of the first  $T$ -section, is



similarly  $AX = 2.43385 \times 10^{-3} \angle 6^{\circ}.883 \times 292.573 \angle 70^{\circ}.047 = 0.71208 \angle 76^{\circ}.930$ . The mid-section point of the smooth line has its potential indicated at  $Om = 0.88741 \angle 35^{\circ}.441$ . If this is multiplied by  $\cosh \left( \frac{\theta}{2} \right)$ , or  $0.81520 \angle 4^{\circ}.142$ , we obtain the mid-point potential  $Oq = 0.72341 \angle 31^{\circ}.299$ , in the middle of the chord A9. Again, if we divide  $Om$  by  $0.81520 \angle 4^{\circ}.142$ , we obtain  $OX = 1.08858 \angle 39^{\circ}.583$  volts, the potential at the first  $T$ -leak.

Proceeding in this way, the lines joining the mid  $T$ -section points X, IX, VIII, etc., contact with the spiral at their respective centers. At the junction points 9, 8, 7, etc., the internal and external spiral polygons contact with the smooth-line spiral.

**General Considerations of Alternating-current Potential Fall.** Although the numerical values tabulated and charted in Table XIX and Fig. 140, pertain to this particular line, operated at the selected frequency, and under the particular assigned motor load, yet the results indicated are typical of fairly long aerial lines operated at any moderate or audio frequency (between  $100\sim$  and  $10,000\sim$ ), under any ordinary load. The procedure is the same in all cases, except when the terminal load happens to have an impedance very nearly equal to the line's surge impedance, in which case the voltage spiral approaches, as we have seen, the equiangular spiral of normal attenuation, instead of a sinusoidal spiral of *stationary-wave attenuation*, corresponding to the general case of superposed waves reflected from the motor end of the line. When the impedance of the motor load differs from the line's surge impedance, the position angle at  $B$  may always be found by (106), from tables, charts or computation, whether the size of the motor load impedance is large or small, *i.e.*, whether the line at  $B$  is freed, grounded, or in any intermediate state differing from  $z_0$ . The potential at any position angle then follows the sinh of that angle, and there is no exchange from sinh to cosh, as we have seen may occur in the c.c. case with large motor-load impedances. In this respect, the a.c. interpretation of the algebraic theory is simpler than the c.c. interpretation.

**Current Distribution over Artificial and Conjugate Smooth Lines.**—The distribution of current over the lines, at the selected frequency and motor load, is shown in Table XX, which is drawn up like Table XIX. Column 4 gives the tabular values of the cosines of the position angles at junctions and mid-sections. The r.m.s. current entering the line at  $A$  is  $2.43385 \times 10^{-3} \angle 6^{\circ}.883$

TABLE XX  
Distribution of current over T-line, II-line, and conjugate smooth line

1	2	3	4	5	6	7
Position	$x$ km.	$\delta_P$ hyps.	$\cosh \delta_P$	$I_P$ milliamp. r.m.s.	T-line milliamp. r.m.s.	II-line milliamp. r.m.s.
A	0	2.05 + $\overline{j8.8}$	3.83206 $\angle 71^\circ.434$	2.43385 $\angle 6^\circ.883$		
X	40	1.95 + $\overline{j8.4}$	3.53698 $\angle 34^\circ.904$	2.24643 $\angle 29^\circ.647$	1.83128 $\angle 25^\circ.505$	2.7557 $\angle 33^\circ.789$
9	80	1.85 + $\overline{j8.0}$	3.25853 $\angle 0^\circ$	2.06958 $\angle 64^\circ.551$		
IX	120	1.75 + $\overline{j7.6}$	2.90532 $\angle 325^\circ.630$	1.84525 $\angle 98^\circ.921$	1.50424 $\angle 94^\circ.779$	2.26357 $\angle 103^\circ.063$
8	160	1.65 + $\overline{j7.2}$	2.52644 $\angle 289^\circ.280$	1.60461 $\angle 135^\circ.271$		
VIII	200	1.55 + $\overline{j6.8}$	2.27074 $\angle 250^\circ.426$	1.44221 $\angle 174^\circ.125$	1.17568 $\angle 169^\circ.983$	1.76916 $\angle 178^\circ.267$
7	240	1.45 + $\overline{j6.4}$	2.17067 $\angle 213^\circ.055$	1.37865 $\angle 211^\circ.496$		
VII	280	1.35 + $\overline{j6.0}$	2.05833 $\angle 180^\circ$	1.30730 $\angle 244^\circ.551$	1.0657 $\angle 240^\circ.409$	1.60367 $\angle 248^\circ.693$
6	320	1.25 + $\overline{j5.6}$	1.79462 $\angle 148^\circ.354$	1.13981 $\angle 276^\circ.197$		
VI	360	1.15 + $\overline{j5.2}$	1.45399 $\angle 111^\circ.670$	0.92347 $\angle 312^\circ.881$	0.75281 $\angle 308^\circ.739$	1.13282 $\angle 317^\circ.023$
5	400	1.05 + $\overline{j4.8}$	1.29137 $\angle 67^\circ.432$	0.82019 $\angle 357^\circ.119$		
V	440	0.95 + $\overline{j4.4}$	1.36505 $\angle 28^\circ.257$	0.86698 $\angle 36^\circ.294$	0.70676 $\angle 32^\circ.152$	1.06353 $\angle 40^\circ.436$
4	480	0.85 + $\overline{j4.0}$	1.38353 $\angle 0^\circ$	0.87872 $\angle 64^\circ.551$		
IV	520	0.75 + $\overline{j3.6}$	1.15356 $\angle 335^\circ.228$	0.73276 $\angle 89^\circ.323$	0.59726 $\angle 85^\circ.181$	0.89875 $\angle 93^\circ.465$
3	560	0.65 + $\overline{j3.2}$	0.76220 $\angle 299^\circ.613$	0.48409 $\angle 124^\circ.938$		
III	600	0.55 + $\overline{j2.8}$	0.65555 $\angle 237^\circ.010$	0.41636 $\angle 187^\circ.541$	0.33941 $\angle 183^\circ.399$	0.51075 $\angle 191^\circ.683$
2	640	0.45 + $\overline{j2.4}$	0.93330 $\angle 197^\circ.042$	0.59277 $\angle 227^\circ.509$		
II	680	0.35 + $\overline{j2.0}$	1.06188 $\angle 180^\circ$	0.67443 $\angle 244^\circ.551$	0.54979 $\angle 240^\circ.409$	0.82732 $\angle 248^\circ.693$
1	720	0.25 + $\overline{j1.6}$	0.84754 $\angle 169^\circ.910$	0.53830 $\angle 254^\circ.641$		
1	760	0.15 + $\overline{j1.2}$	0.34375 $\angle 155^\circ.382$	0.21833 $\angle 269^\circ.169$	0.17798 $\angle 265^\circ.027$	0.21833 $\angle 273^\circ.311$
B	800	0.05 + $\overline{j0.8}$	0.31304 $\angle 8^\circ.741$	0.19882 $\angle 55^\circ.810$		

amp. from (148). The line currents at the other positions are then simply proportional to the cosines of the position angles. At junctions, the currents in the artificial lines are identical with the currents in the smooth line; except that in the case of the  $\Pi$ -line, in order to measure the line current at a junction, it is necessary to substitute a pair of semi-leaks, each of  $g/2$  mhos, for the single leak  $g$  mhos, and to insert the ammeter in the line between

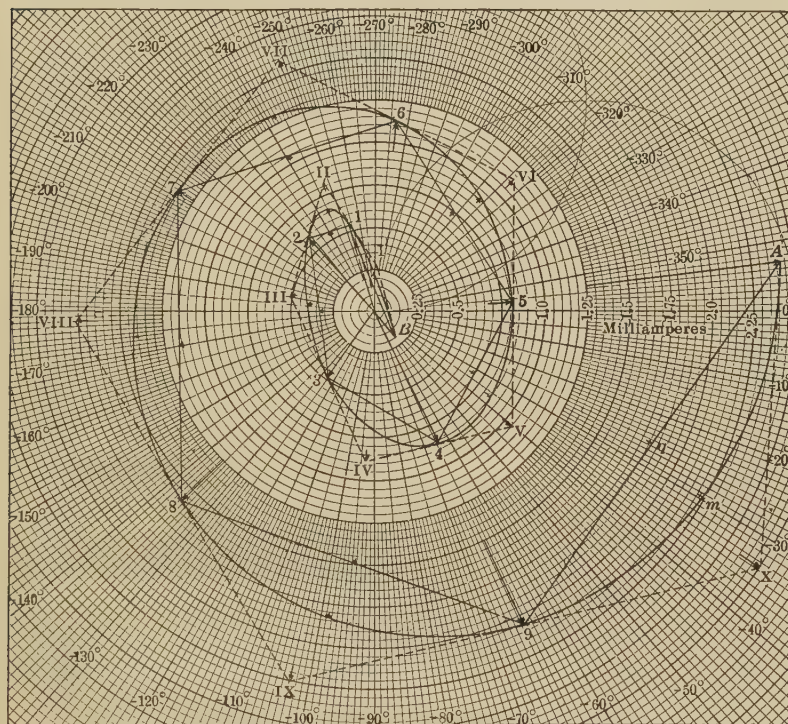


FIG. 141.—Current distribution over real and artificial lines.

the two semi-leaks (Fig. 41). Otherwise only the  $\Pi$  mid-section currents can be measured.

Column 6 gives the  $T$  mid-section currents, while column 7 gives the  $\Pi$  mid-section currents.

The polar graph of the current distribution over the three lines is given in Fig. 141, to voltage standard phase. The entering current is  $OA = 2.43385 \angle 6^\circ.883$  milliamp., as in Table XX, or a current leading the impressed voltage at  $A$  by  $6^\circ.883$ . Along the smooth line, the current changes its phase from point to

point, along the complex cosh curve, or inwardly directed *hyperbolic cosine spiral*  $A, 9, 8, 7 \dots B$ , making in all,  $782^\circ.693$  of rotation or more than two complete revolutions.

The internal spiral polygon  $A, 9, 8 \dots B$ , belongs to the  $T$ -line, and the external polygon to the  $\Pi$ -line. The vector  $Om$  indicates the smooth-line current at the first mid-section  $X$ .  $Oq = Om \cosh v$ , and  $OX = Om \operatorname{sech} v$ . Consequently, when an ammeter is inserted in this architrave of the  $\Pi$ -line, the current observed is  $Oq$ .

The chords of the artificial-line spiral polygons necessarily measure the currents in the leaks. Thus  $OA - O9 = 9A$ , the vector current in the  $T$ -line leak  $X$ , namely,  $1.08858 \angle 39^\circ.583 \times 2.43033 \times 10^{-3} \angle 94^\circ.331 = 2.6456 \times 10^{-3} \angle 54^\circ.748$  amp. Similarly,  $XA$  is the vector current in the semi-leak at the entering end of the  $\Pi$ -line,  $9X$  and  $IX$  9, the currents in the semi-leaks at  $\Pi$  junction 9. If there is only one full leak  $g$  at this junction, the current in it will be  $IX - X$  milliamperes.

**General Considerations Affecting Alternating-current Graphs of Potential and Current.**—It will be observed that the spiral relations of potential and current graphs on  $T$ - and  $\Pi$ -lines are mutually inverted. *The  $T$ -line graphs are the internal spiral polygons on the current diagram, but they are the external polygons on the voltage diagram.*

It will also be noticed that the circular angle subtended on these graphs by a section, although identical for any one section on all three types of line, are very different for different sections. Thus in Fig. 141, or Table XX, the last section  $B-1$  subtends an arc of nearly  $160^\circ$ ; while the next section, 1-2, subtends only about  $27^\circ$ . The same remark applies to the potential graph. Consequently, *although in the equiangular spirals of normal attenuation, equal line sections subtend equal circular arcs, yet in the ordinary case of a hyperbolic sine or cosine spiral of standing-wave attenuation, equal line sections do not, in general, subtend equal circular arcs, especially near the motor end of the line.* For this reason, these two-dimensional graphs of potential or current are inadequate to present a correct idea of distances along the line,\*

\* "Telephonic Transmission Measurements" by B. S. Cohen and G. M. Shepherd, *Journal of Proceedings Institute Electrical Engineers*, London, 1907, vol. xxxix, p. 503.

See also "The Theory of Alternate-current Transmission in Cables," by C. V. Drysdale, *The Electrician*, December, 1907, and January, 1908.



and some other device such as a three-dimensional model must be resorted to, if a correct distance representation is called for. Nevertheless, the relatively simple two-dimensional diagrams of Figs. 140 and 141 suffice for many purposes.

**Distribution of Impedance over Alternating-current Artificial and Conjugate Smooth Lines.**—It is evident from (146) that the line impedance of any real uniform line, in a steady a.c. state, must be a continuous quantity, without sudden changes or discontinuities, in the absence of localized leaks or inserted loads. In the case of lumpy artificial lines, however, the line impedance undergoes a discontinuity, or takes a sudden jump, at each leak.

Table XXI shows the distribution of line impedance for the particular case already discussed. Column 4 gives the tangents of the position angles, and column 5 the line impedance, respectively proportional to them. In column 6 and 7 are the corresponding values for the  $\Pi$ - and  $T$ -lines.

It will be observed that the line impedance commences, for all three lines, at  $A$  with  $410.872 \angle 6^\circ.883$  ohms. An indefinitely long line of this type would offer  $z_0 = 400 \angle 8^\circ$  ohms. The line impedance ends at  $B$ , with  $1,216.936 \angle 72^\circ.329$ , for all three types, this being the assigned impedance of the motor load.

In the case of the  $\Pi$ -line, of column 6, the impedance falls at the entrance leak from  $410.872 \angle 6^\circ.883$  to  $362.885 \angle 33^\circ.789$  ohms, see p. 82. At the mid-section  $X$ , it is  $262.512 \angle 2^\circ.490$ . At the upside of leak 9, it is  $285.913 \angle 38^\circ.762$  ohms, and in the middle of that leak, *i.e.*, at junction 9, it is  $380.700 \angle 8^\circ$ . Similarly, for the  $T$ -line in column 7, the entering impedance at  $A$  is  $410.872 \angle 6^\circ.883$  ohms. At the upside of the leak  $X$ , it is  $447.265 \angle 46^\circ.466$  ohms, and at the downside it is  $525.987 \angle 24^\circ.968$  ohms. Twice the impedance in parallel of these last two values is  $594.437 \angle 14^\circ.078$  ohms, which is obtained from  $Z_p$  in column 5 at  $X$ , by multiplying with  $\text{sech}^2 \frac{\theta}{2}$  or  $1.50477 \angle 8^\circ.284$ , in accordance with (215) and (219).

The graph of line impedance over the conjugate smooth line is indicated in Fig. 142. Starting with  $OB = 1,216.936 \angle 72^\circ.329$  ohms at the motor end, the line impedance in the first half section exceeds 4,000 ohms, in a widely extending spiral. There are, in all, about four turns in this inwardly directed *hyperbolic tangent spiral*, or about twice as many convolutions as in either of the potential or current graphs.



TABLE XXI  
Distribution of impedance over T-line,  $\Pi$ -line, and the conjugate smooth line

1 Position	2 $x$ km.	3 $\delta_P$ hyps.	4 $\tanh \delta_P$	5 $Z_P$ ohms	6 $\Pi$ -line ohms	7 $T$ -line ohms
A	0	$2.05 + j8.8$	$1.02718 \angle 1^\circ.117$	$410.872 \angle 6^\circ.883$		
X	40	$1.95 + j8.4$	$0.98757 \angle 2^\circ.206$	$395.028 \angle 5^\circ.794$	$362.885 \angle 33^\circ.789$ $262.512 \angle 2^\circ.490$ $285.913 \angle 38^\circ.762$	$447.265 \angle 46^\circ.466$ $594.437 \angle 14^\circ.078$ $525.987 \angle 24^\circ.968$
9	80	$1.85 + j8.0$	$0.95175 \angle 0^\circ$	$380.700 \angle 8^\circ$		
IX	120	$1.75 + j7.6$	$0.98153 \angle 3^\circ.291$	$392.612 \angle 11^\circ.291$	$348.074 \angle 30^\circ.512$ $260.907 \angle 3^\circ.007$ $300.991 \angle 42^\circ.694$	$429.408 \angle 49^\circ.803$ $590.801 \angle 19^\circ.575$ $553.838 \angle 20^\circ.917$
8	160	$1.65 + j7.2$	$1.06149 \angle 2^\circ.486$	$424.596 \angle 10^\circ.486$		
VIII	200	$1.55 + j6.8$	$1.07559 \angle 3^\circ.038$	$430.236 \angle 4^\circ.962$	$385.105 \angle 32^\circ.510$ $285.910 \angle 3^\circ.322$ $301.305 \angle 35^\circ.237$	$474.351 \angle 47^\circ.958$ $647.418 \angle 13^\circ.246$ $552.097 \angle 28^\circ.267$
7	240	$1.45 + j6.4$	$0.96665 \angle 5^\circ.993$	$386.660 \angle 2^\circ.007$		
VII	280	$1.35 + j6.0$	$0.87405 \angle 0^\circ$	$349.620 \angle 8^\circ$	$332.398 \angle 35^\circ.189$ $232.337 \angle 0^\circ.284$ $270.325 \angle 44^\circ.438$	$406.682 \angle 45^\circ.197$ $526.107 \angle 16^\circ.284$ $491.899 \angle 19^\circ.504$
6	320	$1.25 + j5.6$	$0.95082 \angle 8^\circ.933$	$380.328 \angle 16^\circ.933$		
VI	360	$1.15 + j5.2$	$1.17587 \angle 6^\circ.790$	$470.348 \angle 14^\circ.790$	$382.676 \angle 23^\circ.892$ $312.565 \angle 6^\circ.506$	$447.461 \angle 55^\circ.616$ $707.778 \angle 23^\circ.074$

5	400	$1.05 + j4.8$	$1.21866 \angle 8^\circ.315$	$487.464 \angle 0^\circ.315$	$352.936 \angle 39^\circ.781$	$649.632 \angle 25^\circ.306$
V	440	$0.95 + j4.4$	$0.91333 \angle 16^\circ.226$	$365.332 \angle 8^\circ.226$	$375.931 \angle 43^\circ.632$	$473.719 \angle 35^\circ.091$
4	480	$0.85 + j4.0$	$0.69107 \angle 0^\circ$	$276.428 \angle 8^\circ$	$242.778 \angle 16^\circ.510$	$549.750 \angle 0^\circ.058$
IV	520	$0.75 + j3.6$	$0.87623 \angle 24^\circ.068$	$350.492 \angle 32^\circ.068$	$228.395 \angle 32^\circ.115$	$442.164 \angle 32^\circ.341$
3	560	$0.65 + j3.2$	$1.54680 \angle 19^\circ.090$	$618.720 \angle 27^\circ.090$	$270.269 \angle 20^\circ.914$	$358.483 \angle 60^\circ.982$
III	600	$0.55 + j2.8$	$1.69780 \angle 23^\circ.753$	$679.120 \angle 15^\circ.753$	$232.917 \angle 23^\circ.784$	$527.419 \angle 40^\circ.352$
2	640	$0.45 + j2.4$	$0.80327 \angle 42^\circ.815$	$321.308 \angle 34^\circ.815$	$333.248 \angle 58^\circ.563$	$650.710 \angle 0^\circ.595$
II	680	$0.35 + j2.0$	$0.33638 \angle 0^\circ$	$134.552 \angle 8^\circ$	$586.412 \angle 39^\circ.655$	$716.510 \angle 50^\circ.992$
1	720	$0.25 + j1.6$	$0.75486 \angle 61^\circ.281$	$301.944 \angle 69^\circ.281$	$451.304 \angle 24^\circ.037$	$1,021.94 \angle 7^\circ.469$
I	760	$0.15 + j1.2$	$2.80120 \angle 62^\circ.612$	$1,120.480 \angle 70^\circ.612$	$372.907 \angle 1^\circ.012$	$585.153 \angle 51^\circ.579$
B	800	$0.05 + j0.8$	$3.04234 \angle 80^\circ.329$	$1,216.936 \angle 72^\circ.329$	$230.216 \angle 55^\circ.998$	$187.791 \angle 29^\circ.184$
					$809.415 \angle 0^\circ.284$	$202.473 \angle 16^\circ.284$
					$196.460 \angle 75^\circ.229$	$206.792 \angle 2^\circ.052$
					$606.884 \angle 50^\circ.611$	$557.464 \angle 89^\circ.283$
					$744.605 \angle 62^\circ.318$	$1,686.61 \angle 78^\circ.896$
					$903.415 \angle 70^\circ.170$	$1,509.31 \angle 71^\circ.886$

The parts nearer to the origin of Fig. 142 are repeated, in Fig. 143, on an enlarged scale. The  $T$ -line impedances are also indi-

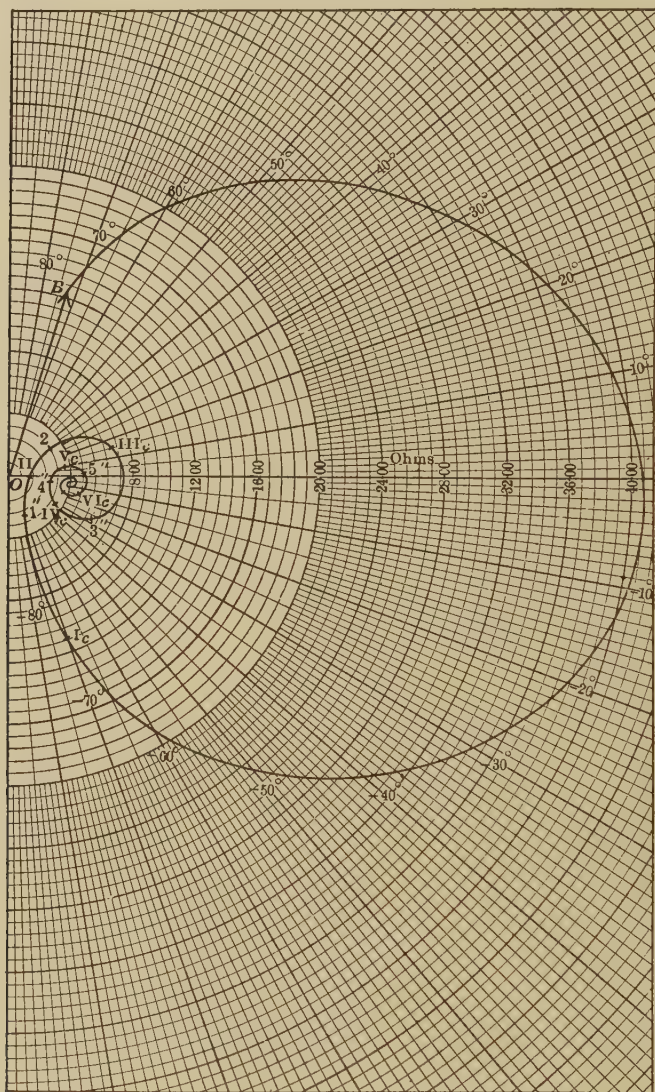


FIG. 142.—Impedance of conjugate smooth line.

cated therein. Each junction point 1, 2, 3, etc., on the spiral, is intersected by a straight line extending  $292.573 \angle 70^\circ.047$  in each

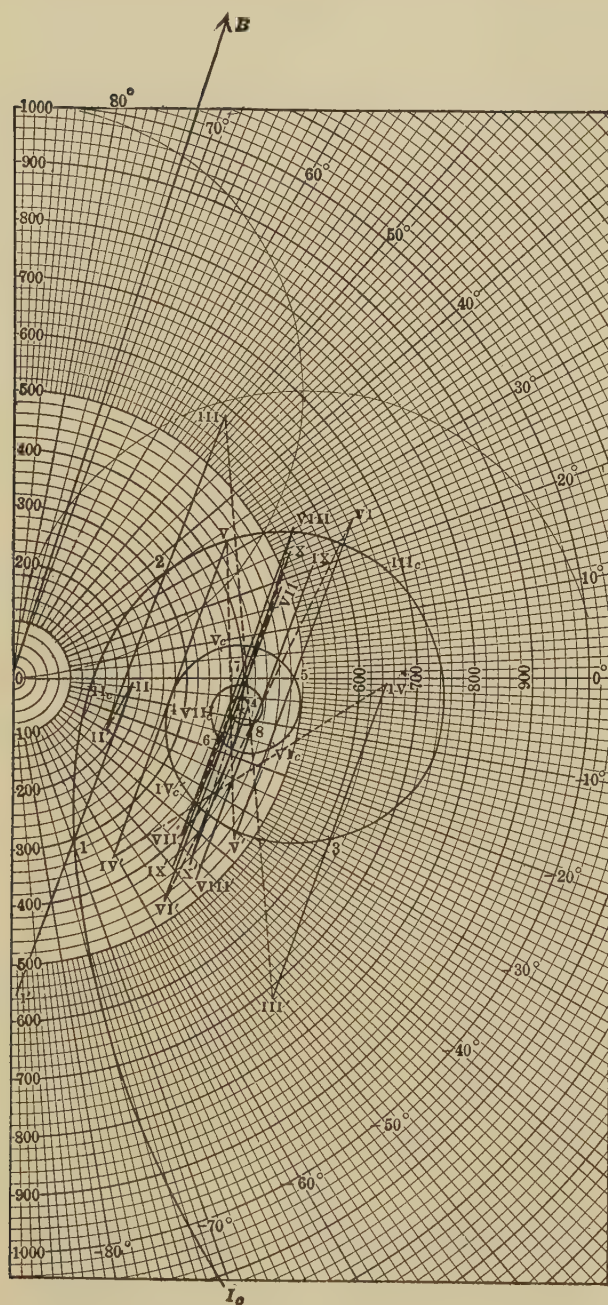


FIG. 143.—Line impedance on *T*-line and on conjugate smooth line.



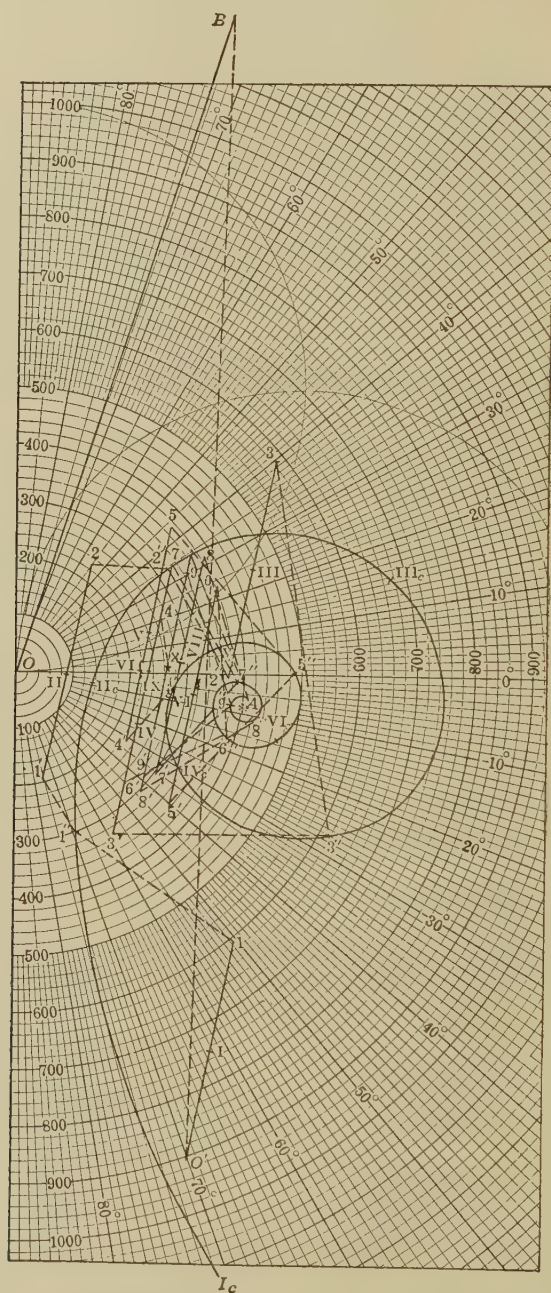


FIG. 144.—Line impedance on II-line and on conjugate smooth line.



direction, or having a length of 585.146 ohms in all. These straight lines are the continuous portions of the  $T$ -line impedance graph. Between their ends, there are jumps or discontinuities, due to the sudden effects of the leaks, and indicated by broken connecting lines. Thus the graph jumps from II to II', from III to III', and so on. *The continuous portions of the  $T$ -line impedance graphs are thus a bundle of equal and parallel straight lines, whose middle points coincide with corresponding junction points on the smooth-line spiral.*

The corresponding graph for the  $\Pi$ -line is presented in Fig. 144. Here the continuous portions are a bundle of equal and parallel straight lines, or vectors of 388.853  $\angle 78^\circ.331$  ohms, the mid-points of which are related to the corresponding smooth-line mid-points by the operator,  $\cosh^2 (\theta/2)$ .

**General Considerations Concerning Line Impedance.**—The foregoing discussion indicates that the line-impedance graph of a smooth line, in the general case, is a *tanh spiral* of two convolutions per wave of voltage or current, and confined to the right-hand half of the complex plane, the phase angles being ordinarily limited to  $\pm 90^\circ$ . The line-impedance graphs of artificial lines are discontinuous, and more complicated. At junction points, however, coincidence is complete, assuming that  $\Pi$ -line leaks are provided in contiguous pairs.

Since the phase-angle variation of line impedance is approximately twice as rapid as that of potential or current ( $1.7^\circ$  per km. in the case considered), the measurements of line impedance at the successive section junctions are particularly liable to be vitiated by accidental changes in impressed frequency.

**Distribution of Power over Alternating-current Lines.**—The distribution of power over a smooth a.c. line may be computed in two ways. First, the local potential and current may be found, as in Tables XIX and XX. The complex power has then, as its size, the volt-amperes, *i.e.*, the product of the sizes of the volts and the amperes, and, for its slope, the difference of the slopes of the volts and amperes. Thus, if at position  $P$ , the potential is  $V_P = |V_P| \angle \beta_V^\circ$  volts, and to the same reference phase, the current is  $I_P = |I_P| \angle \beta_I^\circ$  amp., the power at  $P$  is either:

$$P_P = |V_P| \cdot |I_P| \angle (\beta_V^\circ - \beta_I^\circ) \quad \text{watts} \quad \angle \quad (406)$$

or

$$P_P = |V_P| \cdot |I_P| \angle (\beta_I^\circ - \beta_V^\circ) \quad \text{watts} \quad \angle \quad (407)$$

according as the power is reckoned to current or potential phase as reference standard (Fig. 69). In the case of the c.c. circuit, the power  $P_P = V_P I_P$  watts, where all of the three quantities  $P$ ,  $V$  and  $I$  are real. In the case of the a.c. circuit, this equation will hold only if one of the two complex quantities has  $\angle 0^\circ$  slope, or is taken as of local standard phase, and the phase of the other is reduced to this local standard. Thus if to the same reference phase,  $V = 100 \angle 60^\circ$  r.m.s. volts, and  $I = 2 \angle 30^\circ$  r.m.s. amp., the local complex power will be  $200 \angle 30^\circ$  watts to local current standard phase, or  $200 \angle 30^\circ$  watts to local voltage standard phase. (Page 125.)

The second method of computing the distribution of power over the a.c. line is to write down the sinh of twice the position angle opposite each position. The size of the power will then be directly proportional to the size of  $\sinh 2\delta_P$ , and the slope of the power, to current standard phase, will be the slope of the line impedance at that point.

That is, if  $V_C$  and  $I_C$  are the vector potential and current at some point  $C$ , whose position angle is  $\delta_C$ .

$$\frac{V_P \cdot I_P}{V_C \cdot I_C} = \frac{\sinh \delta_P \cdot \cosh \delta_P}{\sinh \delta_C \cdot \cosh \delta_C} = \frac{\sinh (2\delta_P)}{\sinh (2\delta_C)} \quad \text{numeric } \angle \quad (408)$$

or

$$\frac{|P_P|}{|P_C|} = \frac{|\sinh (2\delta_P)|}{|\sinh (2\delta_C)|}$$

or the size of the vector power is as the sinh of twice the position angle. Moreover,

$$\frac{\overline{P_P}}{\underline{I_P}} = \frac{E_P}{I_P} = \overline{z_0 \tanh \delta_P} = \overline{Z_P} \quad \text{cir. degrees} \quad (409)$$

or the slope of the power at any point is the slope of the line impedance at that point, to current phase as standard.

Therefore, to local current standard phase,

$$P_P = \frac{|P_C|}{|\sinh 2\delta_C|} \cdot |\sinh 2\delta_P| \cdot \overline{Z_P} \quad \text{watts } \angle \quad (410)$$

The real component of the local vector power  $P_P$  is active power, or the rate of energy flow past the point, outward bound from the circuit; while the imaginary component of  $P_P$  is reactive power, or the rate of energy flow past the point into storage, or for retention in the circuit.

TABLE XXII  
Distribution of power over conjugate smooth line

1 Position	2 $x$ km.	3 $\delta_P$ hyps.	4 $2\delta_P$ hyps.	5 $\left  \frac{1}{\sinh 2\delta_P} \right $	6 $\frac{1}{Z_P}$	7 $P_P$ milliwatts	8 $P_{P_a}$ milliwatts	9 $P_{P_r}$ milliwatts
A	0	2.05 + <u><math>j8.8</math></u>	4.1 + <u><math>j17.6</math></u>	30.170	$\angle 6^\circ.883$	2.43385 $\angle 6^\circ.883$	2.41631	- $j0.29158$
X	40	1.95 + <u><math>j8.4</math></u>	3.9 + <u><math>j16.8</math></u>	24.709	$\angle 5^\circ.794$	1.99350 $\angle 5^\circ.794$	1.98332	- $j0.20115$
9	80	1.85 + <u><math>j8.0</math></u>	3.7 + <u><math>j16.0</math></u>	20.211	$\angle 8^\circ$	1.63060 $\angle 8^\circ$	1.61473	- $j0.22694$
IX	120	1.75 + <u><math>j7.6</math></u>	3.5 + <u><math>j15.2</math></u>	16.570	$\angle 11^\circ.291$	1.33685 $\angle 11^\circ.291$	1.31097	- $j0.26175$
8	160	1.65 + <u><math>j7.2</math></u>	3.3 + <u><math>j14.4</math></u>	13.551	$\angle 10^\circ.486$	1.09324 $\angle 10^\circ.486$	1.07498	- $j0.19897$
VIII	200	1.55 + <u><math>j6.8</math></u>	3.1 + <u><math>j13.6</math></u>	11.092	$\angle 4^\circ.962$	0.89501 $\angle 4^\circ.962$	0.89165	- $j0.07741$
7	240	1.45 + <u><math>j6.4</math></u>	2.9 + <u><math>j12.8</math></u>	9.1093	$\angle 2^\circ.007$	0.73492 $\angle 2^\circ.008$	0.73447	- $j0.02575$
VII	280	1.35 + <u><math>j6.0</math></u>	2.7 + <u><math>j12.0</math></u>	7.4063	$\angle 8^\circ$	0.59751 $\angle 8^\circ$	0.59170	- $j0.08316$
6	320	1.25 + <u><math>j5.6</math></u>	2.5 + <u><math>j11.2</math></u>	6.1245	$\angle 16^\circ.933$	0.49411 $\angle 16^\circ.934$	0.47268	- $j0.14392$
VI	360	1.15 + <u><math>j5.2</math></u>	2.3 + <u><math>j10.4</math></u>	4.9718	$\angle 14^\circ.790$	0.40112 $\angle 14^\circ.790$	0.38783	- $j0.10240$
5	400	1.05 + <u><math>j4.8</math></u>	2.1 + <u><math>j9.6</math></u>	4.0646	$\angle 0^\circ.315$	0.32792 $\angle 0^\circ.315$	0.32792	+ $j0.00180$
V	440	0.95 + <u><math>j4.4</math></u>	1.9 + <u><math>j8.8</math></u>	3.4037	$\angle 8^\circ.226$	0.27461 $\angle 8^\circ.226$	0.27178	+ $j0.03929$
4	480	0.85 + <u><math>j4.0</math></u>	1.7 + <u><math>j8.0</math></u>	2.6456	$\angle 8^\circ$	0.21344 $\angle 8^\circ$	0.21136	- $j0.02971$
IV	520	0.75 + <u><math>j3.6</math></u>	1.5 + <u><math>j7.2</math></u>	2.3320	$\angle 32^\circ.068$	0.18810 $\angle 32^\circ.068$	0.15940	- $j0.09987$
3	560	0.65 + <u><math>j3.2</math></u>	1.3 + <u><math>j6.4</math></u>	1.7972	$\angle 27^\circ.090$	0.14499 $\angle 27^\circ.090$	0.12908	- $j0.06603$
III	600	0.55 + <u><math>j2.8</math></u>	1.1 + <u><math>j5.6</math></u>	1.4593	$\angle 15^\circ.753$	0.11773 $\angle 15^\circ.753$	0.11331	+ $j0.03196$
2	640	0.45 + <u><math>j2.4</math></u>	0.9 + <u><math>j4.8</math></u>	1.3994	$\angle 34^\circ.815$	0.11291 $\angle 34^\circ.814$	0.09270	+ $j0.06446$
II	680	0.35 + <u><math>j2.0</math></u>	0.7 + <u><math>j4.0</math></u>	0.75858	$\angle 8^\circ$	0.06121 $\angle 8^\circ$	0.06061	- $j0.00852$
1	720	0.25 + <u><math>j1.6</math></u>	0.5 + <u><math>j3.2</math></u>	1.08446	$\angle 69^\circ.281$	0.08750 $\angle 69^\circ.281$	0.03096	- $j0.08184$
I	760	0.15 + <u><math>j1.2</math></u>	0.3 + <u><math>j2.4</math></u>	0.66200	$\angle 70^\circ.612$	0.05341 $\angle 70^\circ.613$	0.01773	- $j0.05038$
B	800	0.05 + <u><math>j0.8</math></u>	0.1 + <u><math>j1.6</math></u>	0.59626	$\angle 72^\circ.329$	0.04811 $\angle 72^\circ.329$	0.01460	+ $j0.04584$

If we seek for the vector power to potential local standard phase, we must reverse the slope of (410) or

$$P_P = \frac{|P_c|}{|\sinh 2\delta_c|} \cdot |\sinh 2\delta_P| \cdot \overline{Y_P} \quad \text{watts } \angle \quad (411)$$

where  $Y_P$  is the line admittance at and beyond  $P$ .

Table XXII gives the distribution of vector power over the conjugate smooth line under consideration. Column 4 shows the doubled position angles, and column 5 the sizes of the corresponding tabular sines. The slope of  $Z_P$ , taken from Table XXI, appears in column 6, as the slope of the power. Column 7 gives

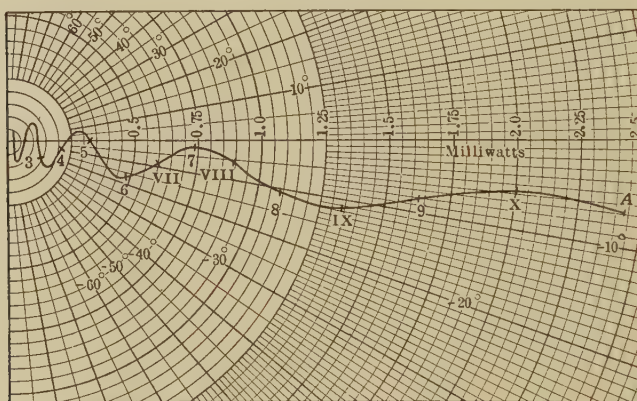


FIG. 145.—Graph of vector power along conjugate smooth line.

the vector power, proportional to the value in column 5, and also equal to the local product of  $V_P$  and  $I_P$  (Tables XIX and XX), with  $I_P$  at local standard phase. The real components, or local active powers, appear in column 8, and the reactive components in column 9. The active power is always positive, and steadily diminishes from the generator toward the motor end. The successive differences are due to the local values of  $I_P^2 r$  and  $V_P^2 g$ , along the line. The reactive power changes sign several times.

Figure 145 gives the graph, in polar coordinates, of the vector power along the line. Near the generator end, the power increases rapidly in size, but approaches the limiting value of  $-8^\circ$  in slope. The power graph for an indefinitely long uniform a.c. conductor would be a radial straight line. Near the motor end, the fluctuations of power are rapid both in size and slope.

The active and reactive power components of the power are plotted separately in Fig. 146. The active power falls off with distance along an approximately exponential curve. The reactive power fluctuates through about four waves.

The powers at junctions along the artificial line are vectorially identical with those at corresponding junction points on the conjugate smooth line. At mid-sections, the volt-amperes or power sizes agree with those at smooth-line mid-sections, but the slopes are different; so that the active and reactive components do not tally, unless corrected.

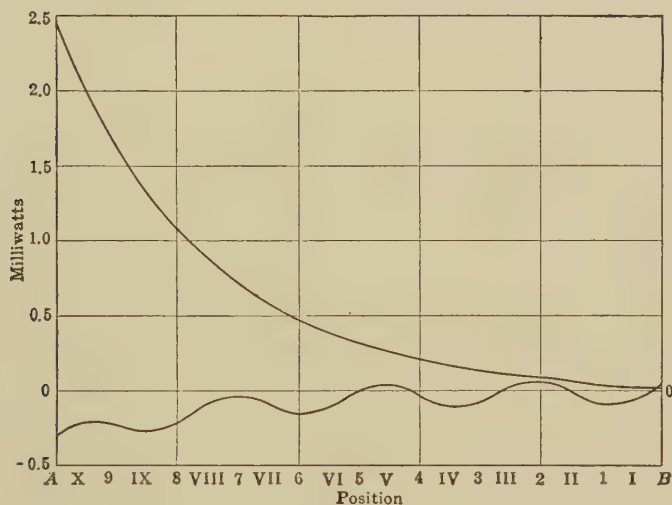


FIG. 146.—Active and reactive components of power along conjugate smooth line.

Thus, if we consider the first II section at the generator end, we find from Tables XIX and XX that

$V_x = 0.72341 \angle 31^\circ.299$  volts, and  $I_x = 2.7557 \angle 33^\circ.789$  milliamp. To local current standard phase, these become

$V'_x = 0.72341 \angle 2^\circ.490$  volts, and  $I'_x = 2.7557 \angle 0^\circ$  milliamp. The power at this mid-section point of the II line is then

$P_x = 0.72341 \times 2.7557 \angle 2^\circ.490 = 1.9935 \angle 2^\circ.490$  milliwatts. But the power at the corresponding point on the smooth line (Table XXII) is  $P_{cx} = 1.9935 \angle 5^\circ.794$  milliwatts; so that  $P_x = P_{cx} \angle 8^\circ.284$ ; or the power at the II-line mid-section has a slope  $8^\circ.284$  greater than that at the corresponding smooth-line mid-



section. This condition will be found to apply throughout. The slope of  $\cosh^2 (\theta/2)$  is  $8^\circ.284$ , and at any midsection,

$$P_{cx} = |P_x| \angle \{ \overline{P_x} - \overline{\cosh^2 (\theta/2)} \} \quad \text{watts } \angle \quad (412)$$

or

$$P_x = |P_{cx}| \angle \{ \overline{P_{cx}} + \overline{\cosh^2 (\theta/2)} \} \quad \text{watts } \angle \quad (413)$$

**Surge-impedance Load.**—If to the conjugate lines of Figs. 137, 138, and 139, we apply a surge-impedance load ( $\sigma = 400 \angle 8^\circ$  ohms), we produce the condition of normal attenuation already discussed in Chapter X, in connection with Fig. 85. The polar graphs of voltage and current distribution over the line become equiangular spirals, and those for the artificial lines equiangular spiral polygons. This condition is shown in Fig. 147. Here the curve  $A, 9, 8, \dots B$  is the equiangular spiral of either voltage or current over the line, commencing with  $OA = 1.0 \angle 0^\circ$  volt at  $A$ , or  $2.5 \angle 8^\circ$  milliamperes, under the constant impressed angular velocity of  $\omega = 5,000$ . We have seen that at this angular velocity the line subtends a hyperbolic angle of  $\theta = 12.725 \angle 80^\circ.957 = 2 + j8$  hyps. The constant angle of the equiangular spiral is, by (356),  $80^\circ.957$ , or the tangent to the spiral at any point makes this circular angle with the radius vector.

It may be observed that in Figs. 140 and 141, the graphs of voltage and current over the same line subtend a total circular angle of  $703^\circ.481$  and  $782^\circ.693$ , respectively; whereas the circular component of the line angle  $\theta$  is 8 quadrants, or just  $720^\circ$ . In the case of Fig. 147 for normal attenuation, the polar graph subtends exactly 8 quadrants. This is manifestly a characteristic property of any uniform line under surge-impedance load. Its polar graph of voltage or current subtends a circular angle equal to the imaginary component  $j\theta_2$  of its total hyperbolic angle, while the ratio of  $A$  to  $B$  terminal sizes is the exponential of  $\theta_1$ .

The internal polygon  $A, 9, 8, \dots B$  represents the distribution of voltage over the 10 sections of  $\Pi$  artificial line of Fig. 137; while the external polygon  $A, X, 9, IX, 8, \dots B$  represents the corresponding distribution of voltage over the 10-section  $T$ -line of Fig. 138. The voltages at the three mid-points of the conjugate first sections are, respectively,  $Oq$ ,  $Om$ , and  $OX$ . The ratio of any adjacent pair is the cosine of half the section angle; *i.e.*,  $\cosh (0.1 + j0.4)$ .

The entering current  $I_A$  at  $A$ , will be numerically equal to  $y_0$  and in this case is 2.5 milliamp., leading the impressed voltage

by  $8^\circ$ . If, however, we present the current distribution graph to current standard phase at  $A$ , the same spiral  $A, 9, 8, \dots B$  will serve, where the initial vector  $OA$  represents  $0.0025 \angle 0^\circ$  amp. In this case, the internal polygon represents the current distribution over the  $T$ -line and the external polygon that over the  $\Pi$ -line. The salient angle of each polygon is  $72^\circ$  or that of one sector or the equiangular spiral.

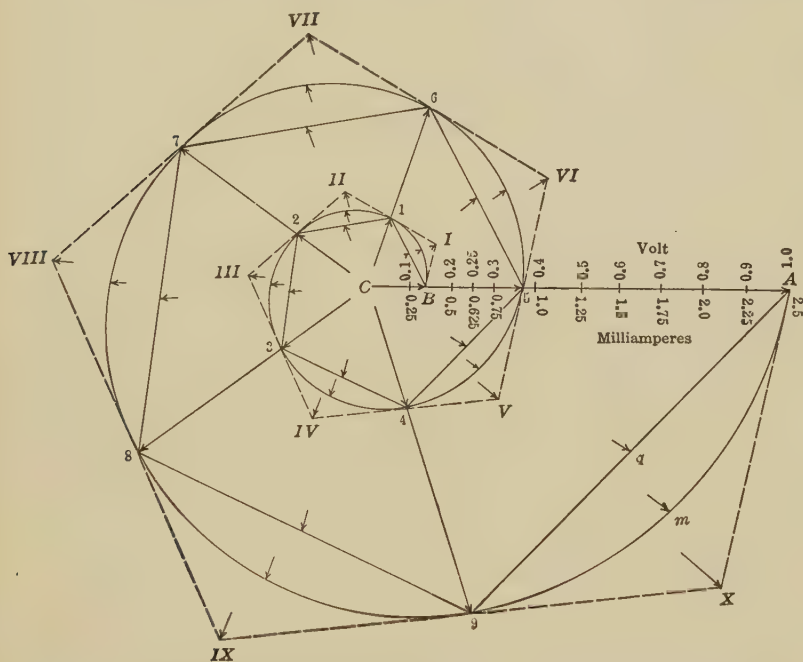


FIG. 147.—Potential and current distribution over real and artificial lines with normal attenuation.

Comparing Figs. 85 and 147, it will be evident that as the real part  $\alpha_1$  of the linear hyperbolic angle  $\alpha$  diminishes, the equiangular spiral of normal attenuation approaches nearer to the circular form. In fact a lossless line with  $\theta = 0 + j\theta_2$  would develop a circular graph of  $\theta_2$  radians for both voltage and current distribution, in the normal attenuation case. On the other hand, a line of very large losses and with  $\alpha_1$  large with respect to  $\alpha_2$ , would develop a very flat equiangular spiral under surge-impedance load, and in the limiting case, the spiral would become a straight line.

**Power Distribution under Surge-impedance Load.**—If we prepare the graph of vector power distribution for the case of the normal attenuation case of Fig. 147, corresponding to Fig. 145 for the non-normal case, we obtain a single radius vector of size 0.250 milliwatt, and of slope  $-8^\circ$  to voltage standard phase, or of  $+8^\circ$  to current standard phase. At the inner end  $B$ , the vector will terminate at  $0.04534 \angle \pm 8^\circ$  milliwatt. In other words, the graph will resemble that of Fig. 145, without undulations. Again, if we prepare the scalar diagram of active and reactive power distribution along the line to correspond with Fig. 146, we find two smooth descending exponential curves, which, drawn on arith-log paper, form straight lines. These are drawn in Fig. 148. The active power falls from 2.47567 milliwatts at  $A$ , to 0.04534 milliwatt at  $B$ , following the right-hand scale; while the reactive power (condensive) falls from 0.347934 milliwatt at  $A$  to 0.0063726 milliwatt at  $B$ , following the left-hand scale. In each case the ratio of  $A$  to  $B$  power is  $54.5983 = e^4 = 10^{1.737179} = (1.259)^{17.37179}$ . If we call the exponent of this ratio, to Napierian base, the *napiers*, the common logarithm or logarithm to base 10, the *orders*, and the logarithm to base 1.259 the T.U. or *transmission units*, it will be seen that the power ratio expended in the line, either active or reactive, is 4.0 napiers, 1.737 orders, or 17.37 T.U. Moreover, the napiers are always just twice the hyps. in  $\theta_1$ . A uniform scale of T.U. is marked off on each side of Fig. 148. It will be seen that the power-consumption ratio in any single section of the line is 1.737 T.U., either for active or reactive power, and for any one of the three conjugate lines considered. This uniformity of power-consumption ratio only presents itself when the line is indefinitely long, or is made virtually infinite by reason of a surge-impedance load, as may be seen by examining the non-normal attenuation case of Fig. 146. The consumption-of-power ratio is also non-uniform within the limits of any single section of artificial line, even in the normal attenuation case. It only appears to be uniform for the artificial lines in Fig. 148. by taking successive section junctions into account.

The numerical data for the normal-attenuation case considered are presented in Table XXIII. Column 2 shows the angular distance from the generator end of the line, Column 3 the local voltage, Column 4 the local current, and Column 5 the local vector power to voltage standard phase. Columns 6 and 7 give, respec-

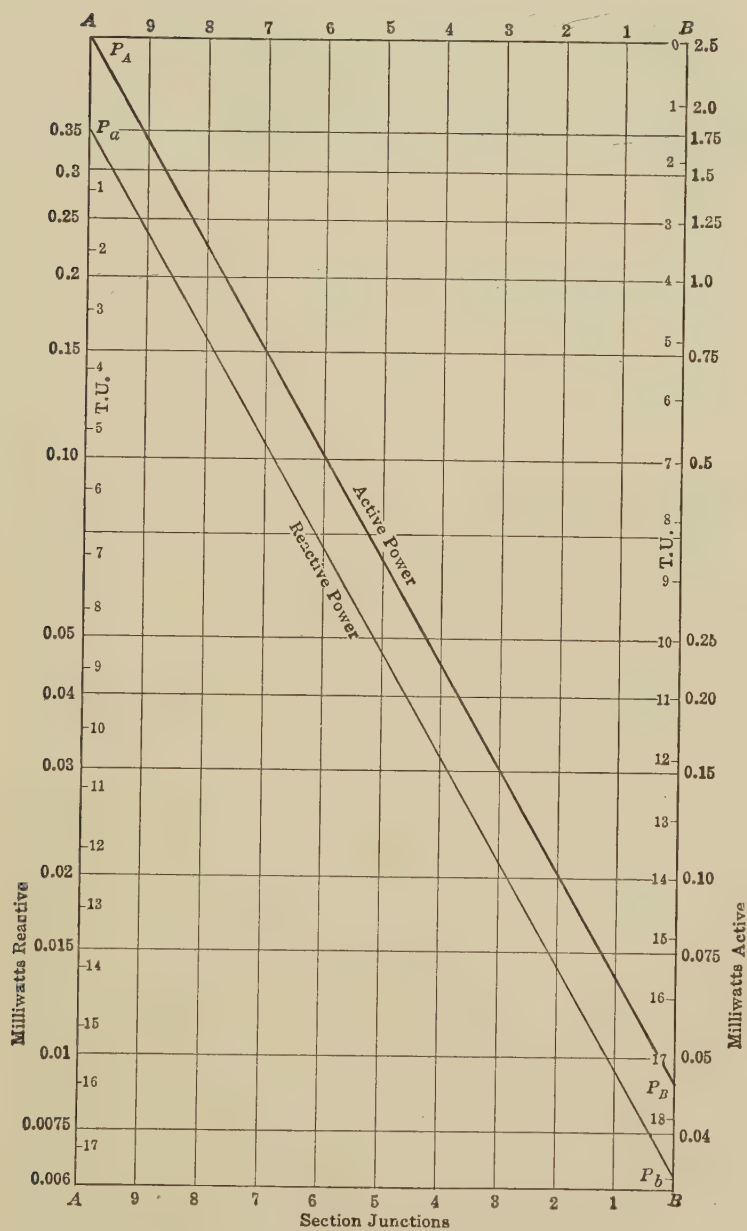


FIG. 148.—Active and reactive power along the line.

tively, the local active and reactive power, the latter being  $+j$  power to voltage standard phase, *i.e.*, condensive power.

**Lossless Line on a Purely Reactive Load.**—If we consider the line of  $\theta = 2 + j8$ , with  $z_0 = 400\angle 8^\circ$ , already discussed, and suppose the line losses reduced to the ideal limit of  $\theta = 0 + j8$ , with  $z_0 = 400\angle 0^\circ$ , we reach the unrealizable condition of a

TABLE XXIII

Distribution of voltage, current, and power over conjugate real and artificial lines of Figs. 137, 138, and 139 with normal attenuation

1	2 $\theta_1$ hyps.	3 $E_P = E_A e^{-\theta_1}$ volts	4 $I_P = E_P / Z_0$ milliamp.	5 Vector power $P_P$ milliwatts $\angle$	6 Active power $P_{Pa}$ milliwatts	7 Reactive power $P_{Pr}$ milliwatts
A	0 + $j0$	1.000 $\angle 0^\circ$	2.50 $\angle 8^\circ$	2.50 $\angle 8^\circ$	2.475670	$j0.347934$
X	0.1 + $j0.4$	0.904837 $\angle 36^\circ$	0.904837 $\angle 36^\circ$	0.904837 $\angle 36^\circ$	0.904837	$j0.233226$
9	0.2 + $j0.8$	0.818731 $\angle 72^\circ$	0.818731 $\angle 72^\circ$	0.818731 $\angle 72^\circ$	0.818731	$j0.233226$
1X	0.3 + $j1.2$	0.740818 $\angle 108^\circ$	0.740818 $\angle 108^\circ$	0.740818 $\angle 108^\circ$	0.740818	$j0.233226$
8	0.4 + $j1.6$	0.670320 $\angle 144^\circ$	0.670320 $\angle 144^\circ$	0.670320 $\angle 144^\circ$	0.670320	$j0.233226$
VIII	0.5 + $j2.0$	0.606531 $\angle 180^\circ$	0.606531 $\angle 180^\circ$	0.606531 $\angle 180^\circ$	0.606531	$j0.233226$
7	0.6 + $j2.4$	0.548812 $\angle 216^\circ$	0.548812 $\angle 216^\circ$	0.548812 $\angle 216^\circ$	0.548812	$j0.233226$
VII	0.7 + $j2.8$	0.496585 $\angle 252^\circ$	0.496585 $\angle 252^\circ$	0.496585 $\angle 252^\circ$	0.496585	$j0.233226$
6	0.8 + $j3.2$	0.449329 $\angle 288^\circ$	0.449329 $\angle 288^\circ$	0.449329 $\angle 288^\circ$	0.449329	$j0.233226$
VI	0.9 + $j3.6$	0.406570 $\angle 324^\circ$	0.406570 $\angle 324^\circ$	0.406570 $\angle 324^\circ$	0.406570	$j0.233226$
5	1.0 + $j4.0$	0.376879 $\angle 360^\circ$	0.376879 $\angle 360^\circ$	0.376879 $\angle 360^\circ$	0.376879	$j0.233226$
V	1.1 + $j4.4$	0.332871 $\angle 396^\circ$	0.332871 $\angle 396^\circ$	0.332871 $\angle 396^\circ$	0.332871	$j0.233226$
4	1.2 + $j4.8$	0.301194 $\angle 432^\circ$	0.301194 $\angle 432^\circ$	0.301194 $\angle 432^\circ$	0.301194	$j0.233226$
IV	1.3 + $j5.2$	0.272532 $\angle 468^\circ$	0.272532 $\angle 468^\circ$	0.272532 $\angle 468^\circ$	0.272532	$j0.233226$
3	1.4 + $j5.6$	0.246597 $\angle 504^\circ$	0.246597 $\angle 504^\circ$	0.246597 $\angle 504^\circ$	0.246597	$j0.233226$
III	1.5 + $j6.0$	0.223130 $\angle 540^\circ$	0.223130 $\angle 540^\circ$	0.223130 $\angle 540^\circ$	0.223130	$j0.233226$
2	1.6 + $j6.4$	0.201897 $\angle 576^\circ$	0.201897 $\angle 576^\circ$	0.201897 $\angle 576^\circ$	0.201897	$j0.233226$
II	1.7 + $j6.8$	0.182684 $\angle 612^\circ$	0.182684 $\angle 612^\circ$	0.182684 $\angle 612^\circ$	0.182684	$j0.233226$
I	1.8 + $j7.2$	0.165299 $\angle 648^\circ$	0.165299 $\angle 648^\circ$	0.165299 $\angle 648^\circ$	0.165299	$j0.233226$
I	1.9 + $j7.6$	0.149569 $\angle 684^\circ$	0.149569 $\angle 684^\circ$	0.149569 $\angle 684^\circ$	0.149569	$j0.233226$
B	2.0 + $j8.0$	0.135335 $\angle 720^\circ$	0.135335 $\angle 720^\circ$	0.135335 $\angle 720^\circ$	0.135335	$j0.233226$

lossless line with vanishing conductor resistance as well as vanishing dielectric leakance. If, furthermore, the load at the B end of the line is assumed to be purely reactive, we reach the limiting ideal case of a lossless system, carrying reactive power, but with no active power in the steady state. Thus, if a line of  $\theta = j8$  and  $z_0 = 400\angle 0^\circ$ , is connected at B to a load of  $\sigma = j1231.07$  ohms, the position angle  $\delta_B = 0 + j0.8$  and  $\delta_A$  will be  $0 + j8.8$ . Table XXIV shows the distribution of voltage, current, and power over such a purely reactive system. In column 2, the position angles are all imaginary, or represent circular angles only. In view of the relations given in Appendix



TABLE XXIV

Distribution of voltage, current, and power over conjugate real and artificial lines of Figs. 137, 138, and 139, assumed lossless, and with pure inductively reactive load

1 <i>P</i>	2 $\delta_P$ hyps.	3 $\sinh \delta_P$	4 $\cosh \delta_P$	5 $E_P$ volts	6 $I_P$ millamp.	7 $P_P$ milliwatts
A	$j8.8$	0.951057 $\angle$ 90°	0.309017 $\angle$ 0°	0.951057 $\angle$ 0°	0.772543 $\angle$ 90°	0.734732 $\angle$ 90°
X	$j8.4$	0.587785 $\angle$ 90°	0.809017 $\angle$ 0°	0.587785 $\angle$ 0°	2.022543 $\angle$ 90°	1.188794 $\angle$ 90°
9	$j8$	0	1.0 $\angle$ 0°	0	2.50 $\angle$ 90°	0
IX	$j7.6$	0.587785 $\angle$ 90°	0.809017 $\angle$ 0°	0.587785 $\angle$ 180°	2.022543 $\angle$ 90°	1.188794 $\angle$ 90°
8	$j7.2$	0.951057 $\angle$ 90°	0.309017 $\angle$ 0°	0.951057 $\angle$ 180°	0.772543 $\angle$ 90°	0.734732 $\angle$ 90°
VIII	$j6.8$	0.951057 $\angle$ 90°	0.309017 $\angle$ 180°	0.951057 $\angle$ 180°	0.772543 $\angle$ 270°	0.734732 $\angle$ 90°
7	$j6.4$	0.587785 $\angle$ 90°	0.809017 $\angle$ 180°	0.587785 $\angle$ 180°	2.022543 $\angle$ 270°	1.188794 $\angle$ 90°
VII	$j6.0$	0	1.0 $\angle$ 180°	0	2.5 $\angle$ 270°	0
6	$j5.6$	0.587785 $\angle$ 270°	0.809017 $\angle$ 180°	0.587785 $\angle$ 360°	2.022543 $\angle$ 270°	1.188794 $\angle$ 90°
VI	$j5.2$	0.951057 $\angle$ 270°	0.309017 $\angle$ 180°	0.951057 $\angle$ 236°	0.772543 $\angle$ 270°	0.734732 $\angle$ 90°
5	$j4.8$	0.951057 $\angle$ 270°	0.309017 $\angle$ 360°	0.951057 $\angle$ 360°	0.772543 $\angle$ 450°	0.734732 $\angle$ 90°
V	$j4.4$	0.587785 $\angle$ 270°	0.809017 $\angle$ 360°	0.587785 $\angle$ 360°	2.022543 $\angle$ 450°	1.188794 $\angle$ 90°
4	$j4$	0	1.0 $\angle$ 360°	0	2.5 $\angle$ 450°	0
IV	$j3.6$	0.587785 $\angle$ 450°	0.809017 $\angle$ 360°	0.587785 $\angle$ 540°	2.022543 $\angle$ 450°	1.188794 $\angle$ 90°
3	$j3.2$	0.951057 $\angle$ 450°	0.309017 $\angle$ 360°	0.951057 $\angle$ 540°	0.772543 $\angle$ 450°	0.734732 $\angle$ 90°
III	$j2.8$	0.951057 $\angle$ 450°	0.309017 $\angle$ 540°	0.951057 $\angle$ 540°	0.772543 $\angle$ 630°	0.734732 $\angle$ 90°
2	$j2.4$	0.587785 $\angle$ 450°	0.809017 $\angle$ 540°	0.587785 $\angle$ 540°	2.022543 $\angle$ 630°	1.188794 $\angle$ 90°
II	$j2$	0	1.0 $\angle$ 540°	0	2.5 $\angle$ 630°	0
I	$j1.6$	0.587785 $\angle$ 630°	0.809017 $\angle$ 540°	0.587785 $\angle$ 720°	2.022543 $\angle$ 630°	1.188794 $\angle$ 90°
I	$j1.2$	0.951057 $\angle$ 630°	0.309017 $\angle$ 540°	0.951057 $\angle$ 720°	0.772543 $\angle$ 630°	0.734732 $\angle$ 90°
B	$j0.8$	0.951057 $\angle$ 630°	0.309017 $\angle$ 720°	0.951057 $\angle$ 720°	0.772543 $\angle$ 810°	0.734732 $\angle$ 90°

A, viz.,  $\sinh j\theta = j \sin \theta$ , and  $\cosh j\theta = \cos \theta$ , the hyperbolic functions in columns 3 and 4 reduce to simple circular functions. The voltages in column 5 are then all real; either positive, negative, or zero, and the currents in column 6 are all purely reactive, or quadrature currents. The powers in column 7 are thus purely reactive, here given to voltage standard phase. Some of

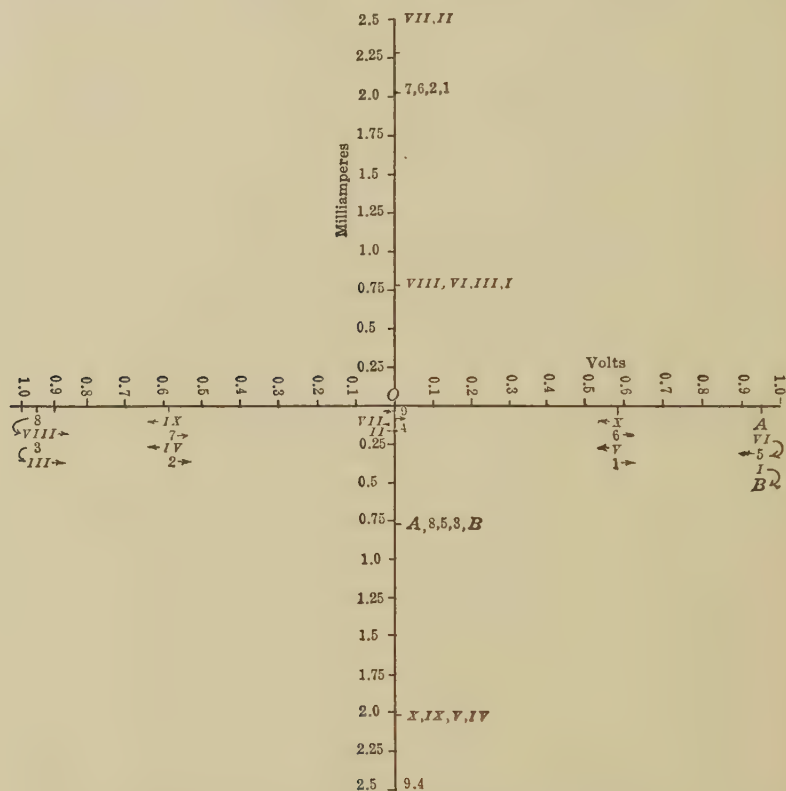


FIG. 149.—Straight-line graphs of voltage and current for ideal case of a lossless line under terminal load of pure inductive reactance.

$$\theta = j8, z_0 = 400 \angle 0^\circ, \sigma = j1231.07.$$

them are inductive, and others condensive, in regular sequence.

The conditions last named are presented graphically in Fig. 149. The e.m.f.  $E_A$  impressed at A is  $0.951 \angle 0^\circ$  volt, effective or root-mean-square. As we advance, from position to position, along the line, the voltage changes sign, between the limits  $+1$  and  $-1$ , but does not rotate in phase. Its vector graph is the horizontal straight line. The current graph is, likewise, the

perpendicular straight line, so that at each and every point on the line, the voltage and current remain in quadrature. The conjugate artificial lines of Figs. 137 and 138 now contain reactances only, and their graphs of voltage and current also follow the perpendicular straight lines of Fig. 149.

The scalar power graph in the same lossless system appears in Fig. 150. It is a regular sinusoid of four complete waves or cycles. The reactive power input at *A* is equal, in this case, to the reactive power output at *B*.

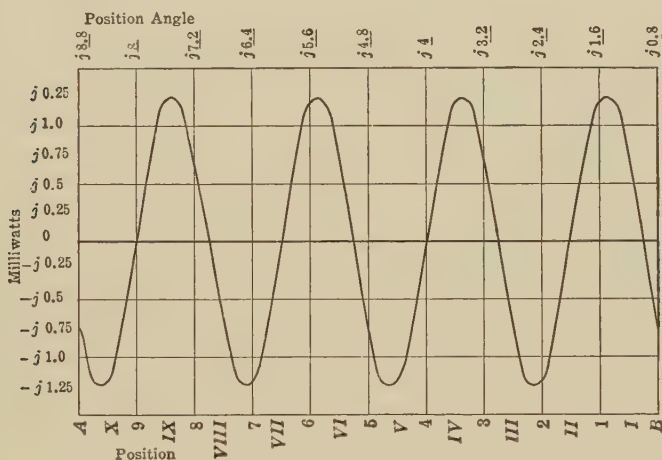


Fig. 150.—Scalar graph of power distribution over lossless line.

**Normal Attenuation over Lossless Line.**—If the lossless line of  $\theta = j8$  and  $z_0 = 400 \angle 0^\circ$  is connected at *B* to a surge-impedance load  $\sigma = 400 \angle 0^\circ$  ohms, the line will deliver active power to the load, and will receive a like amount of active power from the generator at *A*. The vector conditions are indicated for this case in Fig. 151, which may be compared with Fig. 147 for the corresponding case of normal attenuation, when moderate losses are distributed along the line. The equiangular spiral of Fig. 147, with its constant angle of  $80^\circ.957$ , is replaced in the lossless case of Fig. 151, by the pure circle of constant angle  $90^\circ$ . This circular graph represents the distribution of both voltage and current over the line. Both quantities remain constant in magnitude along the line, and only change uniformly in phase, the total phase shift being  $720^\circ$ , or 2 cycles. The phases at input *A*, and at output *B*, are the same, and the active power

delivered is the same at both, *i.e.*, 2.5 milliwatts. The conjugate artificial line *T*- and *II*-sections, like those of Figs. 137 and 138, each subtend a hyperbolic angle of  $j0.8$ , or a circular angle of 0.8 quadrant, *i.e.*,  $72^\circ$ . Their series elements are composed of pure inductive reactances, and their shunt elements of pure condensive reactances. At section junctions, the voltages and, likewise, the currents, on the three conjugate lines are in agreement. The interior pentagon follows the potential distribution

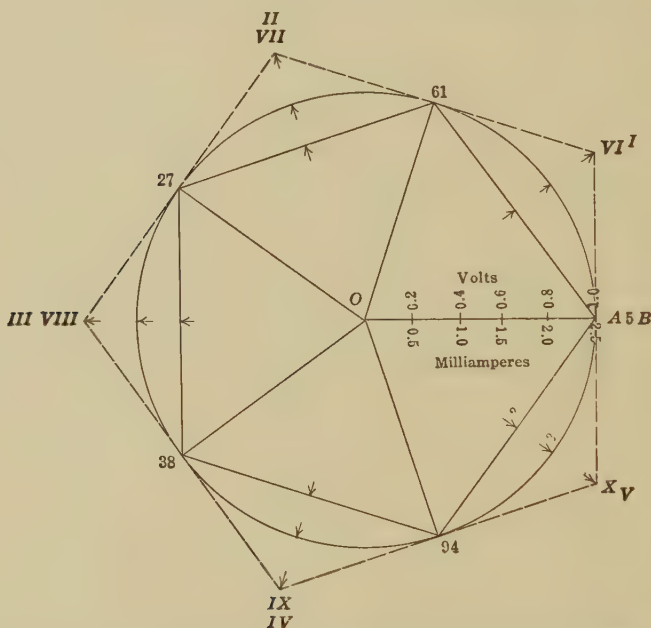


FIG. 151.—Normal attenuation of voltage and current over the lossless line.  $\theta = j8$ ,  $z_0 = 400\angle 0^\circ$ , with surge-impedance load  $\sigma = 400\angle 0^\circ$ .

of voltage over the *II*-line, and the external pentagon the corresponding potential distribution over the *T*-line. In the current distributions, these relations are mutually reversed. At each mid-section, such as *X*, the conjugate vector voltages *Oq*, *Om*, and *OX*, existing on the three lines, are in the successive ratio of  $\cosh j0.4$ , *i.e.*,  $\cos 0.4$  or  $\cos 36^\circ$  or 0.809017, as will be evident from an inspection of the figure.

**Range of Normal Attenuation Graphs.**—On comparing the normal attenuation graphs of Figs. 134, 147, and 151, it will be seen that the normal-attenuation vector diagram of voltage and

current distribution over a line is a circle, for the limiting and hypothetical case of zero loss. As the line losses increase, the circle becomes an equiangular spiral of smaller constant angle; until when the line losses become very great, the spiral becomes, in the limiting case, a straight line.

**Range of Non-normal Attenuation Graphs.**—Comparing Figs. 98, 99, 140, 141, and 151, it appears that in the limiting hypothetical case of a uniform lossless line, grounded or freed at the *B* end, so as to deliver no power, the vector diagrams of voltage and current distribution over the line become two mutually perpendicular straight lines. The same holds true if there is a load at *B* which is purely reactive. As active load is applied, however, to the line, the voltage and current graphs become hyperbolic sine and cosine spirals, respectively, and widen out from the straight-line form. If the line has more than 1 wave length at the impressed frequency ( $\theta_2$  more than  $\underline{4}$ ), the successive spiral loops recur, one above the other, or coincide. If, however, losses occur in the line, as is the rule at the present time in all actual lines, the successive sine and cosine spirals do not coincide, but lie one within the other.

**Impedance Distribution between Elements of I- and O-sections.**—If we consider section 4 of Fig. 130, it is evident that this *O*-section comprises four elements of impedance, namely, *AB* and *GH* in series, with *AG* and *BH* in shunt. It is important to ascertain how far variations may be admitted into these pairs, without altering either the angle  $\theta$  or the surge impedance  $z_0$  of the section.

We may assume that a certain voltage, say 1 volt, is maintained across the shunt element *AG*. If the remaining three elements are simple resistances, we may suppose that the series pair *AB* and *GH* are each 1,000 ohms; while the resistance of the shunt element *BH*, allowing for the influence of such *O*-sections as may lie beyond, is 500 ohms. Then the total resistance in the branch circuit *ABHG* will be 2,500 ohms and the current in each of the two series elements will be 0.4 milliamp. The potential difference established across the shunt element *BH* will also be 0.2 volt.

It will be evident that if we change the distribution of resistance between the two series elements *AB* and *GH* while retaining their sum at 2,000 ohms, we shall neither alter the current strength in them, nor affect the value of the p.d. maintained at



the shunt terminals  $BH$ . Thus, we may place the entire 2,000 ohms of series resistance in  $AB$ , and leave  $GH$  devoid of resistance, or put all in  $GH$ , and leave none in  $AB$ . We may assign any share of the total 2,000 ohms to  $AB$  and insert the balance in  $GH$ . The resulting current in the series elements will be left constant at 0.4 milliamp., and the resulting p.d. across  $BH$  at 0.2 volt. The same proposition must apply in an  $O$ -section carrying an alternating current. The total series impedance in the elements  $AB$  and  $GH$  together, may be distributed in any manner between the upper and lower sides, either as to resistance or as to reactance, without affecting the current strength in these elements, or the p.d. across  $BH$  in magnitude or in phase.

If all of the series impedance in an  $O$ -section is transferred to one side, the section becomes either a  $\Pi$ -section or a  $U$ -section, without altering either the angle  $\theta$  or the surge impedance  $z_0$  of the section.

On the other hand, no transfer of impedance from one shunt element to the other of an  $O$ -section can be made without affecting the characteristic constants of the section, and its behavior in an artificial line.

Similar deductions apply to an  $I$ -section of the type indicated in Fig. 130 part 6. We may alter in any manner the series impedance distribution on one side of the shunt element  $OO'$ , provided that the vector sum of the two impedances on that side of the leak remains unchanged.

**Balanced Artificial Lines.**—Although, as we have seen, the distribution of impedance between series elements of an artificial-line section comprised between two successive leaks is a matter of indifference, so far as concerns the  $\theta$  and  $z_0$  of that section, yet the distribution of potentials with respect to ground can be profoundly affected by such changes of series impedance. In order to secure a *balanced two-wire artificial line*, it is ordinarily necessary to secure the balance of potentials on each side of the line, by maintaining strict equality between the series impedances in each section. Thus, in Fig. 130-4, in order to have the line of zero or neutral potential  $NN$  pass through the center of the shunt elements  $AG$  and  $BH$  of an artificial line, it is necessary that the series impedances  $AB$  and  $GH$  shall be equal in each section. Under these conditions, if a balanced alternating source of e.m.f. is applied to the input terminals, with zero potential midway between them, the e.m.f. at each successive leak will be

balanced, and the capacitance currents or charging currents in the two sides of the artificial line will remain balanced and equal. The higher the voltage and frequency impressed upon the line, the more important this condition of balance is likely to be in making reliable measurements upon the artificial line. For this reason, *O*- and *I*-lines are sometimes more desirable to work with in the laboratory than lines made up of their constituent half-sections  $\Pi$ 's and  $T$ 's, or *U*'s and anchors. Aside from this consideration of balance in absolute potentials, and of charging currents, the  $\Pi$ - and  $T$ -sections are somewhat easier to deal with than *O*- and *I*-sections both in construction and in computation.

**$T$  and  $\Pi$  Artificial Lines of Double Surge Impedance.**—We have seen that  $T$  and  $\Pi$  artificial lines are single-wire lines with ground or zero-potential return. Consequently, when an actual

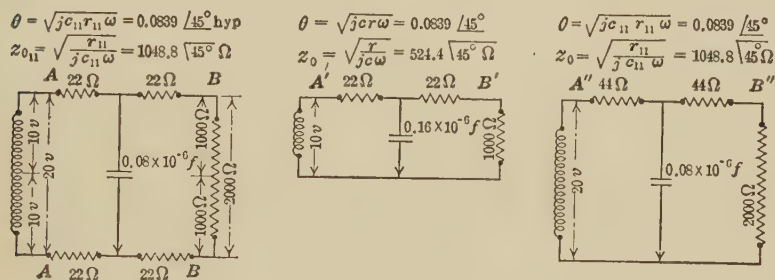


FIG. 152.—*I* section and *T* section, with a *T* of double surge impedance.

two-wire line circuit is imitated by a  $T$  or  $\Pi$  artificial line, the latter should be operated with half the e.m.f. applicable to the two-wire line at the generator end, and with half the impedance load at the motor end, as is indicated in Figs. 10 and 11. In some practical cases, there may be difficulty in testing the artificial line with half the voltage and half the load that should be applied to a double-wire model, *i.e.*, an artificial line of *I*- or *O*-sections. This objection may be overcome in a  $T$ - or  $\Pi$ -line by employing sections of *double surge impedance*.

In Fig. 152, a single-section *I* artificial line is indicated at *AB* *AB*, with 20 volts applied across the two sides at *A*, and a 2,000-ohm load across the two sides at *B*. This line nominally represents a single mile (1.6 km.) of standard telephone twisted-pair cable, having a capacitance of 0.08  $\mu$ f. and a total conductor resistance of 88 ohms, half in each conductor. At  $\omega = 5,000$ , the angle subtended by this *I* line is  $0.0839 \angle 45^\circ \text{ hyp.}$ , uncorrected

for lumpiness, and the uncorrected surge impedance is  $z_{0,,} = 1,048.8 \angle 45^\circ$  ohms at this frequency.

The nominal  $T$ -section corresponding to this line is shown at  $A'B'$ . It has 44 ohms conductor resistance and  $0.16 \mu\text{f.}$  capacitance to ground return. It should be operated with 10 volts at  $A'$  and with 1,000 ohms at  $B'$ , in order to develop the same distribution of position angles, potential and current as the  $I$  line at  $AB$ . The nominal angle subtended by the  $T$ -section  $A'B'$  is the same as that of the  $I$ -section ( $0.0839 \angle 45^\circ$  hyps.); but its surge impedance is only half that of the  $I$  section.

If, however, the  $T$ -section be given the same total conductor resistance as the  $I$ -section (88 ohms) as at  $A''B''$ , Fig. 152, with the same capacitance as the  $I$ -section, we obtain a  $T$  of the same section angle as before; but with *double surge impedance*. This  $T$ -section may now be operated with full voltage at  $A''$  and full impedance at  $B''$ , in order to develop the same distribution of position angles, potentials and currents as the  $I$ -section, neglecting balance. The correcting factors for lumpiness will also be the same for all three types of equivalent circuit. Moreover, the equivalent  $\Pi$  can be similarly produced for double surge impedance by keeping the same leaks as in the  $O$  section, but putting all of the conductor impedance into one line, and using the other as a ground return.

**Plural Frequencies or Complex Harmonic Potentials and Currents.**—We have hitherto assumed that the impressed a.c. voltages employed possessed one and only one frequency, or were purely sinusoidal; so that, in the absence of iron-cored coils in the circuit, the currents over the line were also of single frequency. We may now consider the effects of plural impressed frequencies, *i.e.*, of the ordinary complex harmonic impressed e.m.f., containing a fundamental frequency associated with multiple frequency harmonics. The  $n$ th multiple of the frequency is called the  $n$ th harmonic. The fundamental may thus be included as the first harmonic.

In order to deal with the plural-frequency case quantitatively, it is necessary to analyze the impressed potential wave into its harmonic components. As is well known, the complete Fourier analysis of a complex wave may be written

$$V_0 + V'_1 \sin \omega t + V'_2 \sin 2\omega t + V'_3 \sin 3\omega t + V'_4 \sin 4\omega t + \dots \\ + V''_1 \cos \omega t + V''_2 \cos 2\omega t + V''_3 \cos 3\omega t + V''_4 \cos 4\omega t + \dots$$

volts (414)

where  $V_0$  is a continuous potential, such as might be developed by a storage battery, ordinarily absent in an a.c. generator wave,  $V'_1, V''_1, V'_2, V''_2$ , etc., maximum cyclic amplitudes of the various sine and cosine components. The even harmonics are ordinarily negligible in an a.c. generator wave; so that  $V'_2, V''_2, V'_4, V''_4$ , etc., are ordinarily all zeros. If we count time from some moment when the fundamental component passes through zero in the positive direction,  $V''_1 = 0$  and the series becomes

$$\begin{aligned} V'_1 \sin \omega t + V'_3 \sin 3\omega t + V'_5 \sin 5\omega t + \dots \\ V''_3 \cos 3\omega t + V''_5 \cos 5\omega t + \dots \end{aligned} \quad \text{volts} \quad (415)$$

Compounding sine and cosine harmonic components into resultant harmonics of displaced phase, this may be expressed as

$$V_{r1} \sin \omega t + V_{r3} \sin (3\omega t + \beta^\circ) + V_{r5} (5\omega t + \beta^\circ) + \dots \quad \text{volts} \quad (416)$$

where

$$V_{rn} = \sqrt{V'^2_n + V''^2_n} \quad \text{volts} \quad (417)$$

and

$$\tan \beta_n^\circ = \frac{V''_n}{V'_n} \quad \text{numeric} \quad (418)$$

Formulas (414) and (415) give the wave analysis in *sine and cosine harmonics*, while (416) gives it in *resultant sine harmonics*.

When considering a plural-frequency a.c. line, we require to know the harmonic analysis of the impressed potential, either in sine and cosine harmonics, or in resultant harmonics. The latter analysis is preferable, as being shorter and containing fewer terms. A decision must be made as to the number of frequencies or upper harmonics which must be taken into account.

Ordinarily, the sizes of the harmonics diminish as their order increases; but there are numerous exceptions to this rule, as when some particular tooth frequency in the a.c. generator establishes a prominent size for that harmonic. Care must therefore be exercised not to exclude any important harmonics. On the other hand, the fewer the harmonics to be dealt with, the better, because the labor involved, in correctly solving the problem, increases in nearly the same ratio as the number of harmonics retained.

The rule is to work out the position angle, r.m.s. potential, and r.m.s. current distributions, over the artificial or conjugate smooth line, for each harmonic component in turn, as though it existed alone, and then to combine them, at each position, in the well-known way for root mean squares.



**Combination of Components of Different Frequencies into a R. m. s. Resultant.**—Let the r.m.s. value of each a.c. harmonic component be obtained from dividing its amplitude by  $\sqrt{2}$  in the usual way, and let

$$V_n = \frac{V_{rn}}{\sqrt{2}} = \sqrt{\frac{V'^2_n + V''^2_n}{2}} \text{ r.m.s. volts} \quad (419)$$

be the r.m.s. value of the  $n$ th harmonic. Then the r.m.s. value of all the harmonics together, over any considerable number of cycles, will be

$$V = \sqrt{V_1^2 + V_2^2 + V_3^2 + \dots} \text{ r.m.s. volts} \quad (420)$$

or, as is well known, the joint r.m.s. value of a plurality of r.m.s. values of different frequency, is the square root of the sum of their squares. If a continuous potential  $V_0$  be present, this may be regarded as a r.m.s. harmonic of zero frequency, and be included thus:

$$V = \sqrt{V_0^2 + V_1^2 + V_2^2 + V_3^2 + \dots} \text{ r.m.s. volts} \quad (421)$$

Moreover, from (417), it is evident that the squares of the r.m.s. values of the sine and cosine terms of any harmonic may be substituted for the square of their resultant; or that, in this respect, the sine and cosine terms may be treated as though they were components of different frequencies.

The same procedure applies to plural-frequency currents. Find the individual r.m.s. resultant harmonics. The r.m.s. value of all together will be the square root of the sum of their squares. A continuous current, if present, may be included, as the r.m.s. value of an alternating current of zero frequency.

**Graphical Representation of R.m.s. Plural-frequency Combination.**—The process represented algebraically in (420) or (421) may be represented graphically by the process of successive perpendicular summation, or *crab addition*. An example will suffice to make this clear. A fundamental alternating current of 100 amp. r.m.s., is associated with a continuous current of 50 amp., and with two other alternating currents of other frequencies of 20 and 10 amp. r.m.s., respectively. What will be the joint r.m.s. current? Here by (421),

$$\begin{aligned} I &= \sqrt{100^2 + 50^2 + 20^2 + 10^2} = \sqrt{10,000 + 2,500 + 400 + 100} \\ &= \sqrt{13,000} = 114.0175 \text{ amp. r.m.s.} \end{aligned}$$



In Fig. 153,  $OA$  represents the fundamental r.m.s. current.  $AB$ , added perpendicularly to  $OA$ , represents the continuous current, or current of 50 r.m.s. amp. at zero frequency. The perpendicular sum of  $OA$  and  $AB$  is  $OB = 111.8034$  amp. Adding similarly the other frequency components  $BC$  and  $CD$ , the total perpendicular sum is  $OD = 114.0175$  amp. The order in which the components are added manifestly does not affect the final result, and it is a matter of insignificance whether the various

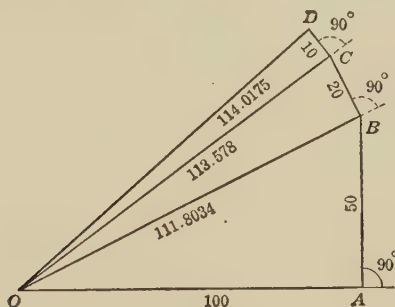


FIG. 153.—Geometrical representation of a joint r.m.s. value of plural-frequency components by perpendicular summation or "crab addition."

frequencies coacting are "harmonic," *i.e.*, are integral multiples of a fundamental, or not, so long as they are different.

The complete solution of an a.c. line with complex harmonic potentials and currents thus requires an independent solution of potential and current for each single frequency in turn, as though the others were non-existent, and then the r.m.s. value at any point on the line is the perpendicular sum of the separate frequency values. The powers and energies of the different frequencies are independent of each other, and the total transmitted energy is the scalar sum of the energies transmitted at the separate component frequencies.

## CHAPTER XVI

### TESTS OF ALTERNATING-CURRENT ARTIFICIAL LINES

Steady-state tests of artificial lines are ordinarily of three kinds, namely: (1) tests of plane-vector impedance or admittance; (2) tests of plane-vector potential; (3) tests of plane-vector current. These tests may need to be made at any point along the line, and especially at any section junction.

**Impedance Tests.**—Impedance or admittance tests are ordinarily one of two types: (1) bridge tests by some null method; and (2) equality of potential-difference tests, by electrostatic voltmeter.

**Bridge Balances.**—In order to measure the vector impedance or admittance of an a.c. line, it is necessary to obtain a bridge

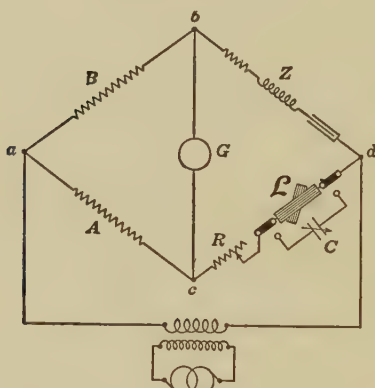


FIG. 154.—Rayleigh bridge.

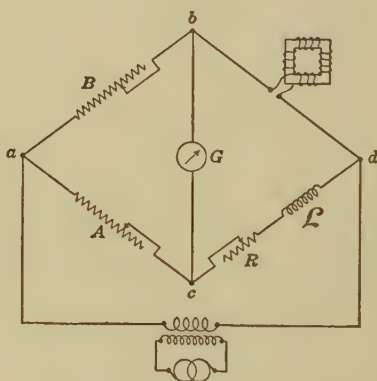


FIG. 155.—Modified Rayleigh bridge for measurement of one of a series of nearly uniform impedances in terms of a fixed inductance standard.

balance with both resistance and reactance. One method of such measurement employs the Rayleigh bridge, which has an adjustably variable inductance  $L$  in that arm of the quadrilateral (Fig. 154) which balances the line to be measured. When the line is condensively reactive, an adjustable capacitance  $C$  may be used instead of an adjustable inductance or the balancing inductance

transferred to the unknown arm. The balance is noted either on a vibration galvanometer, tuned to the measured frequency of the testing alternating e.m.f., or on a pair of head telephones substituted for the galvanometer. In case a variable inductance standard is not available, a fixed standard inductance may be employed of the same order of magnitude as that to be measured. In that case (Fig. 155), the ratio arms  $A$  and  $B$  must be so adjusted for balance with the aid of a rheostat  $R$ , that their ratio corresponds both to the resistances and inductances of the arms  $bd$  and  $cd$ . This dual ratio is sometimes tedious to attain.

**Tests of Equality of Potential Difference.**—Figure 156 indicates a method of measuring line impedance when a bridge balance or

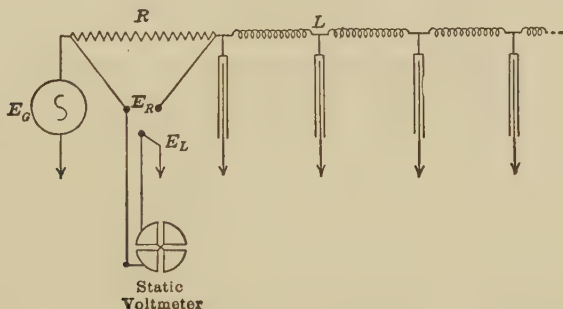


FIG. 156.—Connections for sending-end impedance measurement.

equivalent null method is unavailable, and when a suitable electrostatic voltmeter or electron-tube voltmeter is at hand.

The a.c. testing source  $E_G$  of carefully measured and controlled frequency, is impressed upon the artificial line to be tested, through the non-inductive adjustable resistance  $R$ . The electrostatic voltmeter is connected alternately to read the voltage drop in the resistance  $R$ , and that from the line to ground. The resistance  $R$  must then be adjusted, by successive trials, until these two readings are equal. This means that the size of the line impedance is equal to the numerical value of the resistance  $R$ , in ohms. By repeating the observations many times, this adjustment can be made with considerable precision. After equality has been obtained, the two voltmeter readings are recorded, and the reading from the generator to ground is noted. This reading, the voltmeter connections for which are indicated in Fig. 156, corresponds to the total drop in line  $L$  and resistance  $R$  together.

From the calibration curve of the voltmeter, the three voltage drops or potential differences  $E_G$ ,  $E_L$ , and  $E_R$ , are found. The former represents the size of the total p.d. The other two have been made equal by adjustment, and represent the sizes of the line p.d. and resistance p.d. In Fig. 157, let  $OG$  be drawn to scale to represent  $E_G$ , and likewise  $OA$  and  $GA$ , to represent  $E_R$

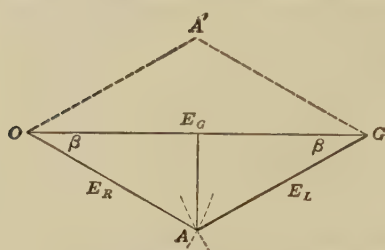


FIG. 157.—Graphic method of determining the line impedance.

and  $E_L$ . Then, since the same a.c. produces all three p.d.s., the diagram may be regarded as an impedance diagram to a suitable scale, as well as a voltage diagram. The impedance scale must be such that if the length of  $OA$  be taken numerically equal to the adjusted resistance  $R$  at

equality,  $E_L$  will represent the impedance offered by the line, both in size and slope.

The line impedance, whose size is  $R$ , will now have a slope of  $2\beta^\circ$ , where  $\beta^\circ$  is the angle  $AOG$ .

In practice, it is not necessary to draw the diagram, because evidently

$$\cos \beta^\circ = \frac{E_G}{2E_R} \quad \text{numeric} \quad (422)$$

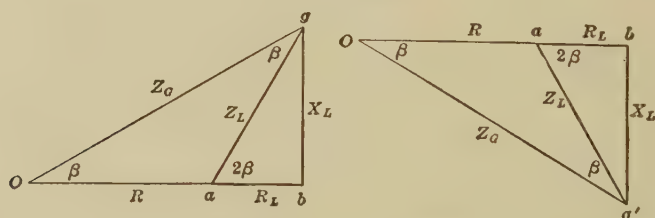


FIG. 158.—Indeterminate alternative vector diagrams obtainable from line-impedance measurements conducted as in Fig. 156.

Knowing  $E_G$  and  $E_R$ ,  $\beta^\circ$  may be immediately obtained from tables of circular functions.

Strictly speaking, the method is open to ambiguity in interpretation because the line impedance may be either  $R \angle 2\beta^\circ$ , or  $R \angle 2\beta^\circ$ , as is shown by Fig. 158. The uncertainty may be overcome, either by preliminary rough computation, as to whether the line is inductive or condensive; or else a definite increment of reactance, such as a suitable reactor or condenser, should be added

to the testing end of the line, and the test repeated. Knowing the sign and approximate magnitude of the reactance increment, the interpretation of the sign of the slope  $\beta^\circ$  should thus be reduced to certainty.

The precision of the test in regard to the slope  $\beta^\circ$  is usually distinctly less than in regard to the size  $R$ , because of the effect a small error in voltmeter reading or in the voltmeter calibration may have in (422).

**Potential Tests.**—There are two types of tests for measuring the potential along the line, namely; (1) a.c. potentiometer tests; and (2) electron-tube voltmeter or electrostatic voltmeter tests.

Alternating-current potentiometer tests may be made with either a *polar potentiometer*\* or with a *rectangular potentiometer*. The former gives readings in polar form, *i.e.*, in size and slope, or volts and reference phase. The latter instrument gives readings in rectangular form, *i.e.*, in two quadrature components. From these, the size of the observed voltage can be read as the vector sum of the two components, while the slope of the same can be found with respect to some particular voltage as phase reference. Descriptions of these instruments, and of their use, may be found in textbooks on a.c. measuring instruments.

With either form of potentiometer, it is advantageous to use a vibration galvanometer, tuned to the test frequency, as a null instrument, or indicator of zero current.

Electron-tube voltmeters and electrostatic voltmeters, as ordinarily used, give readings of sizes and not of slopes for the voltages they serve to measure. Consequently, when they are used, additional measurements are necessary, in order to evaluate the slopes or phase angles of the voltages observed.

**Line Potentials by Electron-tube Voltmeter or Electrostatic Voltmeter.**—If an a.c. voltmeter is used to determine the potentials at line junctions or mid-sections, it is very desirable to use an electron-tube-voltmeter or electrostatic voltmeter, in order to avoid the reduction of potential brought about by the admittance of the instrument. In practice, a good arrangement is to employ one voltmeter over the range between, say, 0.01 and 1 volt, another over the range between 1 and 10 volts, and a third for

\* See also "Artificial Lines" by the author, McGraw-Hill Book Company, Inc., 1917, p. 222, for a description of the Drysdale-Tinsley polar potentiometer.



higher voltages. Electron-tube voltmeters will give good readings for voltages below those at which electrostatic voltmeters are ordinarily used. The calibrations should be carefully checked, from time to time.

Since a voltmeter, used in the ordinary way, measures the size but not the slope of the a.c. voltage to which it is applied, additional measurements are needed in order to evaluate the slope.

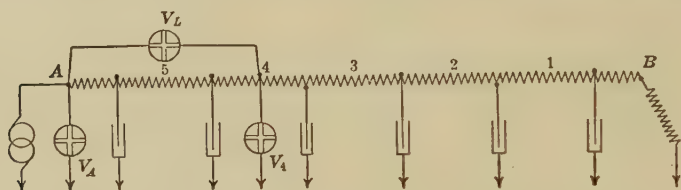


FIG. 159.—Connection diagram for plane-vector potential test along a.c. artificial line.

Figure 159 shows a method for carrying out this plan. If the potential  $V_4$  has to be measured between junction 4 and ground, the potential  $V_A$ , at the generator end is also measured, as well as  $V_L$  the voltage drop between A and 4. In practice,  $V_A$  is measured once for all, and held constant by means of an auxiliary a.c. voltmeter, which need not be electrostatic. A single testing electrostatic voltmeter is used to measure  $V_L$  and  $V_4$ , alternately

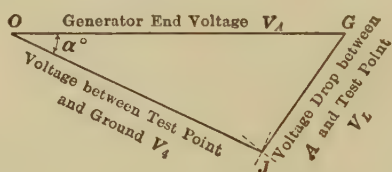


FIG. 160.—Triangle of three observed voltages for determining their phase relations.

in succession. The three values  $V_A$ ,  $V_L$  and  $V_4$  determine a voltage triangle, from which the phase or slope of  $V_4$  can be determined, in the manner indicated in Fig. 160, where  $OG$  is the generator voltage  $V_A$  at A,  $GJ$  the voltage drop on the line, and  $OJ$  the voltage  $V_4$  at the test point. The size of this voltage in Fig. 160 would be  $OJ$ , and its slope  $\sphericalangle \alpha^\circ$ , taking  $OG$  as at standard phase. The triangle is easily produced graphically, using the points  $O$  and  $G$  as successive centers, with intersecting arcs at  $J$ . The circular angle  $\alpha^\circ$  is then measured with a protractor.

There is a possible ambiguity as to the side of  $OG$  on which the triangle should lie, which means that the slope  $\alpha^\circ$  might be either  $\angle\alpha^\circ$  or  $\angle\alpha^\circ$ ; but ordinarily there is no difficulty in deciding this either by the aid of a rough calculation, or by means of a special test with an added known reactance.

The triangulation is repeated at each junction on the same sheet of polar coordinate paper, keeping the generator end

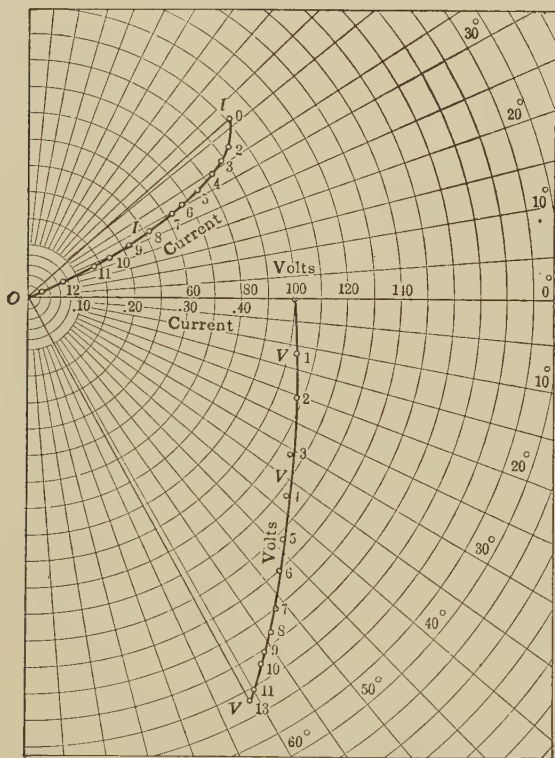


FIG. 161.—Curves showing phase relations of voltage and current for points on the open line.

voltage  $V_A$  constant, say at  $100\angle 0^\circ$  volts. Figure 161 gives an example of this procedure in the particular case of a 13-section line of the type defined in Table XVI and representing 1,040 km. of aerial power-transmission conductor operated at  $60.7\sim$ , with the distant end free, and with 100 volts r.m.s. impressed at the generator end. The successive vertices of the triangles obtained

TABLE XXV  
Distribution of voltage and current over the line at 60.7 cycles per second, distant end free

Junction	Distance from receiving end		Angular distance from receiving end, hyps.	Potential at each junction, volts						Current in each mid-section, amperes			
	Km.	Miles		Observed by potentiometer		Observed by static voltmeter		Computed		Observed by potentiometer	Computed		
				Magni- tude	Phase	Magni- tude	Phase	Magni- tude	Phase		Magni- tude	Phase	
0	1,040	646.1	1.405/89° 7	100.0	∞0°	.....	.....	100.0	∞0°	0.506	/41° 9	0.506	/41° 9
1	960	596.0	1.297 "	102.8	∞11° 8	101.8	.....	102.4	∞11° 2	0.475	/38° 0	0.472	/38° 2
2	880	547.0	1.243 "	108.5	∞21° 9	108.1	.....	107.0	∞21° 7	.....	.....	.....	.....
			1.189 "	.....	.....	.....	.....	.....	.....	.....	.....	.....	.....
3	800	497.0	1.135 "	115.3	∞30° 6	115.5	∞30° 5	114.6	∞30° 5	0.446	/36° 2	0.446	/36° 3
4	720	447.0	1.081 "	123.7	∞37° 5	124.0	∞37° 9	121.1	∞36° 1	0.414	/34° 2	0.416	/34° 7
5	640	398.0	1.027 "	132.5	∞43° 2	132.8	∞43° 0	132.2	∞43° 1	0.377	/33° 0	0.383	/33° 3
			0.973 "	.....	.....	.....	.....	.....	.....	.....	.....	.....	.....
6	560	348.0	0.865 "	.....	.....	.....	.....	.....	.....	.....	.....	.....	.....
			0.811 "	140.7	∞47° 7	141.2	∞48° 0	141.5	∞47° 7	0.344	/31° 1	0.345	/32° 0
7	480	298.0	0.757 "	149.2	∞51° 2	148.3	∞52° 2	149.8	∞51° 4	0.305	/30° 0	0.305	/31° 0
			0.703 "	155.7	∞53° 9	155.7	∞54° 5	157.7	∞54° 3	0.262	/28° 5	0.266	/30° 1
8	400	249.0	0.649 "	.....	.....	.....	.....	.....	.....	.....	.....	.....	.....
			0.594 "	.....	.....	.....	.....	.....	.....	.....	.....	.....	.....
9	320	199.0	0.540 "	.....	.....	.....	.....	.....	.....	.....	.....	.....	.....
			0.486 "	161.5	∞57° 0	161.8	∞56° 8	164.1	∞56° 5	0.214	/28° 1	0.210	/29° 2
10	240	149.0	0.432 "	166.0	∞58° 7	167.0	∞58° 7	169.4	∞58° 2	0.170	/25° 4	0.166	/28° 7
			0.375 "	169.7	∞60° 0	170.7	∞59° 4	173.4	∞59° 3	0.124	/25° 0	0.124	/28° 3
11	160	99.4	0.324 "	.....	.....	.....	.....	.....	.....	.....	.....	.....	.....
			0.270 "	.....	.....	.....	.....	.....	.....	.....	.....	.....	.....
12	80	49.7	0.216 "	.....	.....	.....	.....	.....	.....	.....	.....	.....	.....
			0.162 "	172.6	∞60° 9	172.0	∞60° 8	175.8	∞60° 0	0.077	/21° 7	0.074	/28° 0
3	0	0	0.108 "	173.8	∞61° 0	173.3	∞60° 8	176.6	∞60° 2	0.023	/20° 5	0.023	/27° 9
			0.054 "	.....	.....	.....	.....	.....	.....	.....	.....	.....	.....
I	II	III	IV	V	VI	VII	VIII	IX					

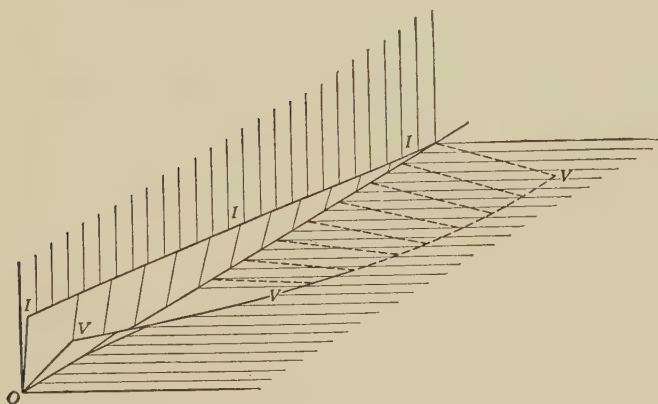


FIG. 162.—Line free at distant end—60 cycles per second.

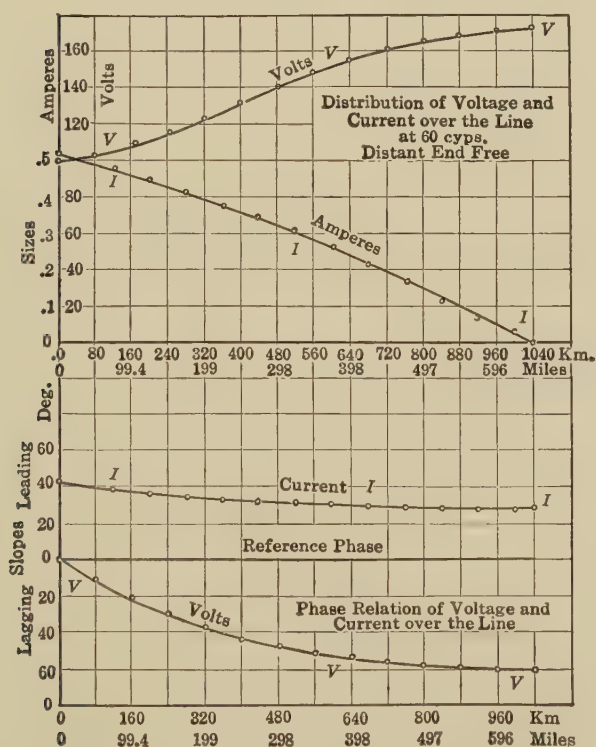


FIG. 163.—Voltage, current, and phase relations along line at 60 cycles per second and no-load. Rectangular coordinates.

from electrostatic voltmeter measurements fall on the points 1, 2, 3, . . . 13, which, connected by the line  $VVV$ , show the graph of potential along the artificial line, and also, by inference, on the conjugate smooth line at this frequency. The open-end voltage is  $173.8\angle 61^\circ$ . The observations are recorded both by voltmeter and potentiometer for this case in Table XXV.\* Two other methods of presenting the results of these observations to the eye are given in Figs. 162 and 163.

**Relative Advantages of Potentiometer and Voltmeter Methods.** The electrostatic voltmeter method of measuring line potentials has the advantage that its technique is simple and requires but little preparation. Impressed potentials of 100 volts r.m.s. are ordinarily applicable with it. Disadvantages are that its precision is seldom very high, because it is a deflection method, and moreover, if there are harmonics in the wave of impressed voltage, these enter into the measurements by perpendicular summation, as already described, and vitiate the results for the fundamental frequency as obtained by computation. The potentiometer method, on the other hand, is capable of much greater precision, and the tuned vibration galvanometer responds almost entirely to the fundamental sinusoid, but it involves a more elaborate technique. For class-laboratory work, therefore, the easier voltmeter method is to be preferred, unless the generated voltage wave available is very impure. For research purposes, the potentiometer is superior. In potentiometer measurements, it may be advisable to limit the impressed voltage at the generator end to 1.8 volts, so as to dispense with multipliers and their attendant errors. (Page 98.)

**Relations between the Impressed Voltage, the Current and Power.**—In Fig. 164, we have an artificial line whose line impedances and leak admittances may be assumed properly to correspond with those of a certain imitated conjugate smooth line. The motor-end load  $Z_r$ , also has the same apparent impedance as the load which the actual line has to carry, as determined by the vector ratio of receiving-end volts to amperes. We have to consider how the current and power in the artificial-line impedance model compare with those on the actual line as the impressed voltage is varied.

\* "Measurements of Voltage and Current over a Long Artificial Power-transmission Line at 25 and 60 Cycles per Second," by A. E. Kennelly and F. W. Lieberknecht, *Proc. A. I. E. E.*, June 25, 1912.



It will be evident, on examination, that if the voltage impressed on the artificial line in the laboratory is  $1/n$ th of that impressed on the actual line at the same frequency, the artificial-line currents will be  $1/n$ th those at corresponding points on the actual conjugate smooth line, and the artificial line powers will be  $1/n^2$  those on the actual line. Thus if the star voltage on a three-phase transmission line is say 10,000 volts r.m.s. to neutral, and its conjugate artificial-line impedance model is operated at 10 volts r.m.s. to ground, or  $1/1,000$ th of the actual working pressure, then each milliampere of observed current at junctions will correspond to an ampere on the actual line, and each micro-watt of power on the artificial line will represent 1 watt on the actual line. The results obtained in the laboratory are, therefore, readily interpretable in ordinary magnitudes, if we maintain the correct motor-end load impedance.

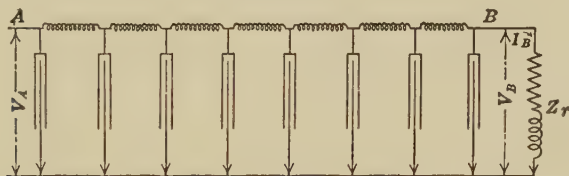


FIG. 164.—Impedance model of a single-phase, single-wire line and its receiving-end load.

The effects of synchronous-motor or “rotary-condenser” compensation at any point on the line, say at the receiving end, on the voltage regulation, can be investigated experimentally by connecting the proper equivalent reactance to the line at that point, and studying the corresponding distributions of potential and current.

**Current Tests.**—There are three types of tests for alternating current along an artificial line, *viz.*, potentiometer tests, fall of potential tests, and ammeter tests.

**Potentiometer Tests for Vector Current.**—In this method, a small non-inductive resistance of manganin strip, say 0.1 ohm, is inserted in the line at the test junction, and the vector voltage drop in this measured at its terminals by a.c. potentiometer. This method succeeds well at low frequencies, and the error introduced by the insertion of 0.1 ohm at any junction is ordinarily unimportant. This is a useful “research method.” An appropriate set of contact plug connections is indicated in Fig. 165.

**Sectional Fall of Potential Tests.**—When an electrostatic voltmeter capable of measuring from 2 to 20 volts is used, the voltage drop upon a reactor in the line, adjacent to the test point, can be observed. Knowing the vector impedance of the reactor, and the slope of the vector drop from triangulation, as above described, the vector current strength in the reactor can be immediately deduced by Ohm's law. This is a useful "laboratory-class method."

**Ammeter Tests.**—Occasionally, the line currents may be observed directly by the insertion of a suitable a.c. ammeter at the test junction. Ordinarily, however, the impedance of the ammeter is sufficiently great to introduce an appreciable error into the line distributions.

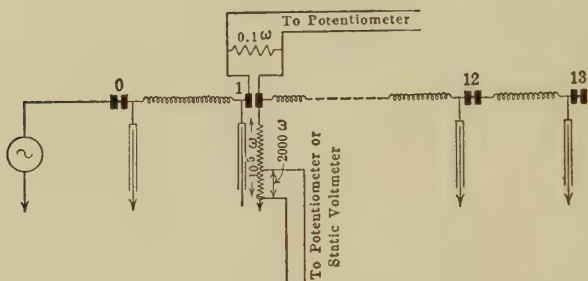


FIG. 165.—Connections used in a series of measurements of potential and current along the line.

**Distribution of Test Operations among Observers.**—It is possible for a single observer, if he has ample time at his disposal, to make, unaided, all the observations of potential and current along an artificial line, if all the apparatus and controlling devices are conveniently arranged. It is much easier, however, for two observers to carry on the work between them. As many as six observers may coöperately take part in the observations, with mutual advantage, especially if the electrostatic voltmeter methods are used.

There are a number of tests which can be effectively carried out by students of electric transmission on an artificial line with different line lengths, impressed frequencies, loads, load power factors and positions of load. As a rule, such tests on a.c. artificial lines should be preceded by preliminary tests on c.c. artificial lines. Such a.c. experiments properly checked, and

supported by computation, give the student an unassailable comprehension of essential steady-state a.c. line phenomena.

**Frequency Measurements.**—Artificial-line tests conducted at power-distribution frequencies call for no recommendations as to the measurement of impressed frequency beyond watchfulness and care. The ordinary laboratory frequency meters, properly checked and calibrated, are satisfactory. A good means of checking the frequency of a vibrating-reed frequency meter is to examine it, in a good light, through the vibrating slits of a *stroboscopic tuning fork*.\*

At telephonic frequencies, however, special methods are needed for measuring frequency with the necessary degree of precision. One means is an improved stop-watch electromagnetic revolution counter.†

A second means is a stroboscopic tuning fork applied to a target mounted on the shaft of the alternator supplying the testing current. In practice it is found convenient to place the testing apparatus within view of, but at a suitable distance from, the alternator. The observer at the apparatus can then control the speed and delivered frequency of the alternator by a hand rheostat, while he watches the stroboscopic image of the illuminated rotating target on the alternator, at a distance of say 15 m., through a small telescope which has a stroboscopic fork mounted in front of its eyepiece.

A third means is the *acoustic tonometer*, or series of small tuning forks, such as are found in acoustic laboratories. The testing alternating current is supplied through a suitable impedance to an ordinary telephone receiver, and the observer finds by trial the tuning fork giving the pitch nearest to that of the telephonically

\* "The Measurement of Rotary Speeds of Dynamo Machines by the Stroboscopic Fork," by A. E. Kennelly and S. E. Whiting, *Trans. A. I. E. E.*, July, 1908, vol. xxvii, pp. 727-742.

"Stroboscopic Measurements of Alternating-current Frequency with Electric Lamps," by A. E. Kennelly, *Electrical World*, Dec. 26, 1908. "Separation of the No-load Stray Losses in a Continuous-current Machine by Stroboscopic Running-down Methods," by D. Robertson, *Journ. Inst. Elect. Engrs.*, February, 1915, vol. liii, pp. 308-322.

"The Stroboscope in Speed Measurements and Other Engineering Tests," by D. Robertson, *Trans. Institute Engineering and Ship Builders*, 1912-1913, vol. vi, pp. 37-82; *Mech. Eng.*, 1913, vol. xxxi, pp. 512-515, 539-543.

† "Experimental Researches on Skin Effect in Conductors," A. E. Kennelly, F. A. Laws, and P. H. Pierce, *Trans. A. I. E. E.*, September, 1915, p. 1757.

emitted tone. When the a.c. frequency is steady, as, for example, when it is delivered from a carefully operated Vreeland oscillator, the difference in pitch between the a.c. telephonic tone and the tuning-fork tone can be found by counting acoustic beats during a measured time interval, such as half a minute.

A fourth means is a calibrated vacuum-tube oscillator.

**Frequency Limitations of Artificial Lines.**—It will be evident from an inspection of Figs. 140, 141, 147, and 151 with their polygonal section voltages and currents, that as the frequency impressed upon an artificial line is increased, the number of sections per wave is diminished, and the lumpiness correction factors tend to increase. There is ordinarily no difficulty in

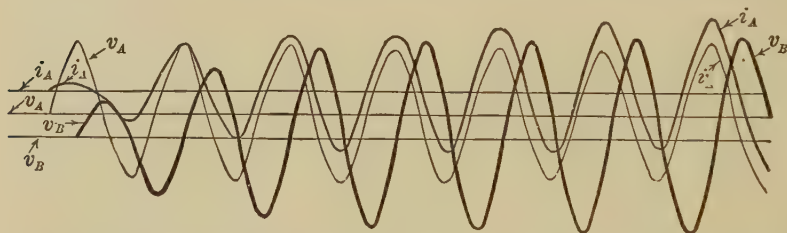


FIG. 166.—Oscillogram showing the time and phase intervals between the impressed voltage  $V_A$  and the delivered voltage  $V_B$  on an artificial power-transmission line at frequency of 60.6 cyps.

operating an artificial line up to the frequency which provides on the average three sections per wave, although the correction factor is then sensitive to small frequency changes. Operation ordinarily becomes impracticable at or below two sections per wave.\*

**Measurement of Apparent Velocity of Propagation on an Artificial Line.**—If we impress a single-frequency source of electromotive force on the  $A$  end of an artificial line and record  $V_A$  and  $V_B$  on an oscillograph film we have a means of measuring the angle  $\theta_2$  between  $V_A$  and  $V_B$ . Knowing the length of line,  $x$  km. we may solve for apparent velocity,  $v$ .

$$\frac{\theta_2}{x} = \alpha_2 \quad \text{and since } v = \frac{\omega}{\alpha_2} \quad \text{by (308),}$$

$$v = \frac{\omega x}{\theta_2} \quad \frac{\text{km.}}{\text{sec.}} \quad (423)$$

The application of this is illustrated by Figs. 166 and 167.

\* "Behavior of a Lumpy Artificial Line as the Frequency Is Indefinitely Increased," by Edith Clarke, Thesis, Mass. Inst. Technology, 1919, 42 pp.

In Fig. 166 we have an oscillogram taken on 1,255 km. of artificial power line freed at the distant end.  $f = 60.6$  cyps.  $V_B$  starts approximately one-quarter cycle behind  $V_A$ . Therefore,  $\theta_2 = \pi/2$

$$v = \frac{2\pi \times 60.6 \times 1,255}{\pi/2} = 242.4 \times 1,255 = 304,000 \frac{\text{km.}}{\text{sec.}}$$

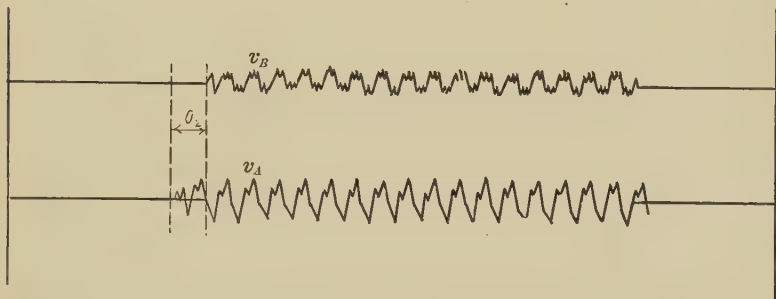


FIG. 167.—Oscillogram showing time and phase intervals between  $V_A$  and  $V_B$  at an audio frequency of 1,000 cyps.

This is a little high, the result depending upon the accuracy with which  $\theta_2$  and  $f$  are measured.

Figure 167 shows the same method on a 1,000-cyps. e.m.f. impressed on an artificial line representing 189 miles (305 km.) of No. 12 N.B.S. open-wire telephone line. Assuming a complete cycle delay between  $V_A$  and  $V_B$ , we get 189,000 miles for  $v$  (305,000 km./sec).



## CHAPTER XVII

### COMPOSITE LINES

A composite line is a line composed of a plurality of single lines in series, each possessing its own linear electric constants. In practice, composite lines are more frequently met than single lines, especially when long circuits are used. Thus, a telephone circuit may include an underground-cable twisted pair, from the subscribers' set to his local exchange, then a different size of underground-cable pair to the outskirts of the city, then one or more different sizes of overhead copper-pair lines, and finally underground lines to the called subscriber's set. No steady-state working theory of a.c. lines can therefore be satisfactory, which fails to deal with composite lines in a reasonably simple way.

We may first consider the d.c. theory of composite lines employing real hyperbolic functions, and then apply it to a.c. cases, by vector interpretation of the formulas, *i.e.*, by extending them from one dimension to two dimensions.

**Case of Two Sections Having Different Linear Constants but the Same Surge Impedance.**—If two single lines  $AB$ ,  $CD$ , Fig. 168, are joined at  $BC$ , and these lines happen to possess the same value of surge impedance  $z_0$ , then the composite line  $AD$  has very simple properties.

Suppose the composite line  $AD$  to be grounded at  $D$  and voltage at  $A$ . Let  $\theta_1$  be the angle subtended (35) by  $AB$ , and  $\theta_2$  that subtended by  $CD$ . Then, if we assign position angles to the system, commencing at  $D$  where  $\delta_D = 0$ , we find the position angle at  $C$  is  $\delta_C = \theta_2$ . The line impedance at  $C$  is also

$$Z_C = z_0 \tanh \delta_C = z_0 \tanh \theta_2 \quad \text{ohms } \angle \quad (424)$$

The section  $CD$  may now be regarded in its entirety as a single motor-end load applied to the section  $AB$ . Then by (106),  $\sigma = Z_C$  and

$$\tanh \theta' = \frac{\sigma}{z_0} = \frac{z_0 \tanh \theta_2}{z_0} = \tanh \theta_2 \quad \text{numeric } \angle \quad (425)$$

whence  $\theta' = \theta_2$ . Consequently, at a junction between single lines possessing identical vector surge impedances, the position angles

on each side of the junction are equal. The reason for this is that each and every individual electric wave which passes a junction, either way, undergoes no disruption, unless the surge impedances of the sections differ. The wave passes over from one section to the other as though the junction did not exist.

The position angle at  $A$ , Fig. 168, will now be  $\delta_A = \theta_1 + \theta_2$  in this case 3.0 hyps., and the distributions of potential, current

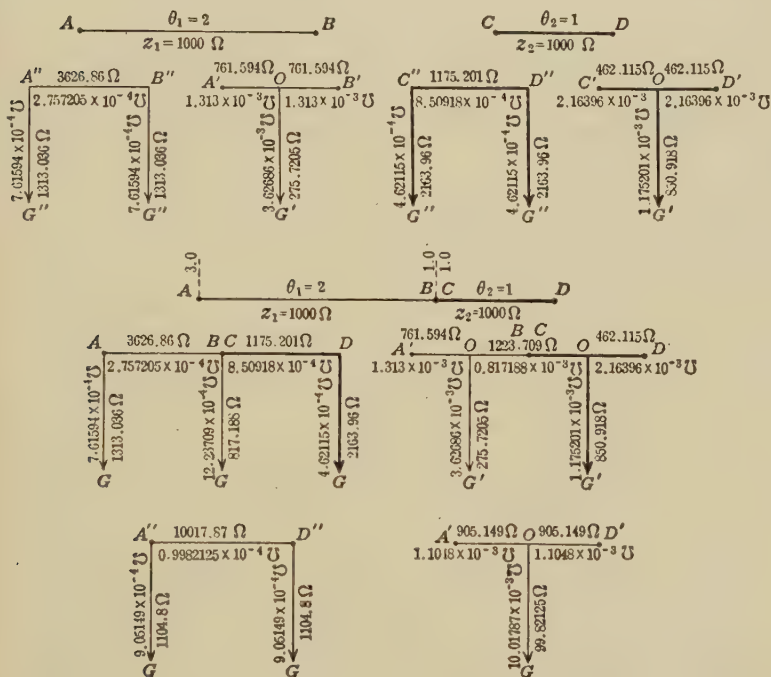


FIG. 168.—Two-section composite-line merger and hyperbolic equivalent circuits.

and impedance will be continuously proportional, respectively, to the sinh, cosh and tanh of the position angle, as on an ordinary single line.

Similar conditions will present themselves if we ground the composite line  $AD$  of Fig. 168, at  $A$ , and voltage it at  $D$ . The position angles will distribute themselves over the system without any discontinuity at the junction  $BC$ . Again, if one terminal of the composite line, having unchanged surge impedance, is grounded through a terminal load, subtending a terminal angle

$\theta'$ , the position angles will increase continuously to  $\delta_A = \delta_D = \theta_1 + \theta_2 + \theta'$  hyps.  $\angle$  at the other end.

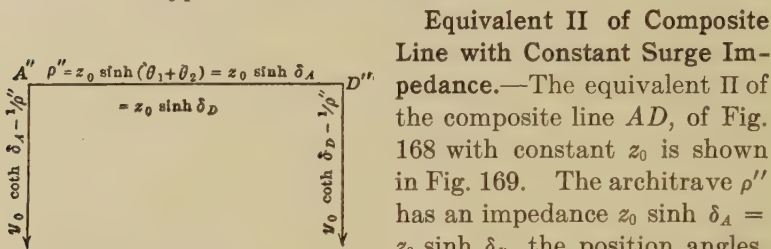


FIG. 169.—Equivalent II of two-section composite line with constant surge impedance.

**Equivalent II of Composite Line with Constant Surge Impedance.**—The equivalent II of the composite line  $AD$ , of Fig. 168 with constant  $z_0$  is shown in Fig. 169. The architrave  $\rho''$  has an impedance  $z_0 \sinh \delta_A = z_0 \sinh \delta_D$ , the position angles,  $\delta_A$  and  $\delta_D$  being each reckoned from the opposite grounded end.

The admittance of the  $A$  leak is

$$g_A'' = Y_A - \frac{1}{\rho''} = y_0 \coth \delta_A - \frac{1}{\rho''} = y_0 \coth \delta_A - \nu \text{ mhos } \angle \quad (426)$$

Similarly, the  $D$  leak admittance is

$$g_D'' = Y_D - \frac{1}{\rho''} = y_0 \coth \delta_D - \frac{1}{\rho''} = y_0 \coth \delta_D - \nu \text{ mhos } \angle \quad (427)$$

where the architrave admittance is

$$\nu = \frac{1}{\rho''} \text{ mhos } \angle \quad (428)$$

These two leaks are equal. The rule is: Ground the composite line at the distant end. *The home-end leak will then be equal to the line admittance at the home end, minus the architrave admittance  $\nu$ .*

In Fig. 168, we have a particular case of a composite line with elements of equal surge impedance. The line  $AB$  has an angle  $\theta_1 = 2.0$  hyps., and  $z_1 = 1,000$  ohms. The line  $CD$  has  $\theta_2 = 1.0$ , and  $z_2 = 1,000$  ohms. Beneath each line is placed its equivalent II and equivalent  $T$ . The two lines are connected at the junction  $BC$ . The merger II and  $T$  are indicated underneath the composite line  $AD$ . The merger II,  $A''D''$ , is such as can be obtained by direct computation from (425) to (428) and Fig. 169. The merger  $T$ ,  $A'D'$ , can also be computed by hyperbolic formulas,\* but we shall, for simplicity, here confine ourselves to a consideration of merger equivalent II's, and hyperbolic equivalent II's.

**Merger, Hyperbolic, and Net II or T of a Composite Line or System.**—In all cases of composite lines, it is possible to replace

\* "The Equivalent Circuits of Composite Lines in the Steady State" by A. E. Kennelly, *Proc. Am. Acad. of Arts. and Sciences*, September, 1909, vol. 45, No. 3, pp. 31-75.

each single-line section by its equivalent  $\Pi$  or  $T$ , in the manner indicated in Fig. 168, to connect these end to end, and to resolve them by successive arithmetical steps, into a single resultant or *merger*  $\Pi$  or  $T$ . Thus, in Fig. 168, the central star or  $T$ ,  $ABCDG$ , of the double  $\Pi$  immediately under and to the left of the composite line  $AD$ , can be replaced through known formulas, by its equivalent delta and so lead to the merger equivalent  $\Pi$ ,  $A''D''$ . This process is very laborious and liable to error. The process of obtaining the final or *net equivalent*  $\Pi$  or  $T$  of a composite line, system, or network, by the use of hyperbolic or complex angles is much simpler and speedier. This process leads to what may be called the *hyperbolic*  $\Pi$  or  $T$ , *i.e.*, a net  $\Pi$  or  $T$ , arrived at with the aid of hyperbolic functions. In the examples furnished throughout this chapter, the net  $\Pi$  has been obtained by both the merger and hyperbolic methods, as mutual checks, but only the hyperbolic method is, as a general rule, to be recommended. There is ordinarily nothing about a net  $\Pi$  to show whether it is a merger  $\Pi$  or a hyperbolic  $\Pi$ , or how it was arrived at.

It may be observed that the net  $\Pi$  of a composite line, in which the surge impedance  $z_0$  of the various sections is the same, is always symmetrical in the absence of terminal or intermediate loads. Thus, in Fig. 168, the net  $\Pi$   $A''D''$  of the two section composite line, each section having  $z_0 = 1,000$  ohms, has equal pillar leaks. The corresponding net  $T$ ,  $A'D'$  is likewise symmetrical, having equal arms.

**Composite Lines Having Different Sectional Surge Impedances.**—If the component sections of a composite line differ in their surge impedances, either as to size or slope, the waves of voltage and current traveling over the line will be subject to disruption into transmitted and reflected components in the manner discussed in Chapter XI, so that the angle of the net  $\Pi$  for the line will not be the sum of the constituent section angles. If, however, we know the values of  $\theta$  and  $z_0$  for each section at a given frequency, we can find the distributions of voltage, current, and power over the entire line at that frequency; or, without computing these distributions, we can find the net  $\Pi$  of the system. In either case, we commence by finding the distribution of position angles over the entire line from the motor to the generator end.

**General Case of Composite Lines with Differing Surge Impedances.**—In Fig. 170, three-line sections are presented with the following constants:

For  $AB$ ,  $\theta_1 = 2.0$ ,  $z_1 = 1,000$ .

For  $CD$ ,  $\theta_2 = 1.5$ ,  $z_2 = 2,000$ .

For  $EF$ ,  $\theta_3 = 0.5$ ,  $z_3 = 2,500$ .

We proceed to determine the distribution of position angles, potential and current over the composite line  $AF$ , when grounded at  $A$  and voltage at  $F$ .

**Position-angle Distribution.**—Starting from the grounded motor end at  $A$ , the position angle  $\delta_A = 0$ . At  $B$ , the position angle is evidently  $\delta_B = \theta_1$ . The line impedance of  $BA$  at  $B$  is  $z_1 \tanh \theta_1 = 1,000 \tanh 2.0 = 1,000 \times 0.96403 = 964.03$  ohms, and this may be regarded as a terminal load  $\sigma$  at  $C$ , applied to the section  $DC$ . The position angle at  $C$  just across the junction from  $B$  is therefore, by (106),

$$\tanh \delta_C = \frac{Z_{gB}}{z_2} = \frac{z_1}{z_2} \tanh \theta_1 = \frac{964.03}{2,000} = 0.482015,$$

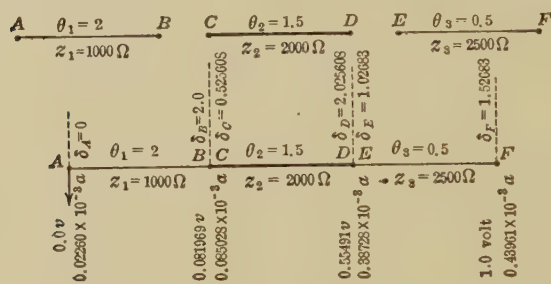


FIG. 170.—Three-section composite line grounded at  $A$ .

from which  $\delta_C = 0.525608$  hyp. The junction  $BC$  thus introduces a discontinuity into the position angle. On the  $B$  side of the junction, this angle is 2.0. On the  $C$  side, it is 0.525608.

From  $C$  to  $D$ , the position angle increases in the regular way, and at  $D$  it has reached the value 2.025608 hyps. The line impedance at  $D$  is thus  $Z_{gD} = z_2 \tanh \delta_D = 2,000 \tanh 2.025608 = 2,000 \times 0.96579 = 1,931.58$  ohms. This may again be regarded as a terminal load to the section  $FE$ . The angle subtended by this load will be

$$\tanh \delta_E = \frac{Z_{gD}}{z_3} = \frac{z_2}{z_3} \tanh \delta_D = \frac{1,931.58}{2,500} = 0.772632,$$

from which  $\delta_E = 1.02683$  hyps. This position angle is marked off on the upside of the  $DE$  junction.

From  $E$  to  $F$ , the position angle increases regularly to 1.52683 hyps. at  $F$ .



**Potential Distribution.**—Considering now a potential steadily applied at  $F$ , Fig. 170, the potential at any point along any section of the composite line will be simply proportional to the sine of the position angle. At the junctions there is discontinuity of position angle, but no discontinuity of potential. If, therefore, the potential at any point of the composite line is given, the potentials at the ends of that section are readily found, and these give known potentials at the terminals of the next adjacent sections, which likewise can be worked up for potential distribution, and so on, throughout all the sections.

Thus, having given that the impressed potential at  $F$  is 1.0 volt, the potential  $V_E$  is

$$1.0 \times \frac{\sinh 1.02683}{\sinh 1.52683} = 0.55491 \text{ volt}$$

This must also be the potential  $V_D$  at the beginning of the  $DC$  section. Consequently, the potential  $V_C$  is

$$0.55491 \times \frac{\sinh 0.525608}{\sinh 2.025608} = 0.081969 \text{ volt}$$

This must also be the potential  $V_B$  at the beginning of the  $BA$  section, while  $V_A = 0$ , since the line is assumed to be grounded at  $A$ .

**Line-admittance Distribution.**—The line admittance in each section will be, by (147), proportionate to the cotangent of the position angle; so that, in Fig. 170.

$$Y_{gB} = y_1 \coth \delta_B = 10^{-3} \times \coth 2.0 = 1.0373 \times 10^{-3} \text{ mho;}$$

$$Y_{gD} = y_2 \coth \delta_D = 0.5 \times 10^{-3} \times \coth 2.025608 = 0.51771 \times 10^{-3} \text{ mho;}$$

$$Y_{gF} = y_3 \coth \delta_F = 0.4 \times 10^{-3} \times \coth 1.52683 = 0.43961 \times 10^{-3} \text{ mho.}$$

The entering current  $I_F$  at  $F$  is therefore  $0.43961 \times 10^{-3}$  amp.

**Line-current Distribution.**—The line current in each section may either be determined by the formula (148), or by taking the cosines of position angles and using formula (131). Thus

$$I_E = 0.43961 \times 10^{-3} \times \frac{\cosh 1.02683}{\cosh 1.52683} = 0.38728 \times 10^{-3} \text{ amp.}$$

This must also be the current  $I_D$ , just beyond the  $DE$  junction. Again,

$$I_C = 0.38728 \times 10^{-3} \times \frac{\cosh 0.525608}{\cosh 2.025608} = 0.085028 \times 10^{-3} \text{ amp.}$$

This must also be the current  $I_B$  just beyond the  $BC$  junction. Finally,

$$I_A = 0.085028 \times 10^{-3} \times \frac{\cosh 0}{\cosh 2.0} = 0.022600 \times 10^{-3} \text{ amp.}$$

**Power Distribution.**—The power distribution over the composite line may be obtained either from the product of the local volts and amperes, or, in each section successively, by taking its size proportional to the sine of twice the position angle, and its slope from the line impedance, as previously described.

**General Case of Composite Line with Terminal Load.**—If the line, instead of being grounded directly at  $A$ , had been grounded

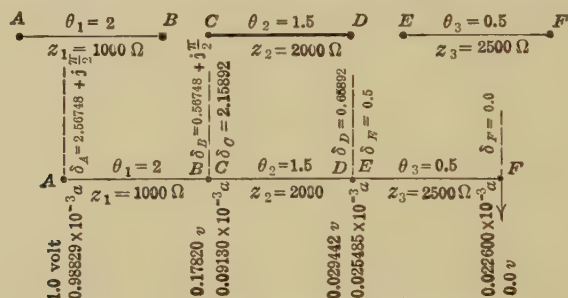


FIG. 171.—Three-section composite line grounded at  $F$ .

through a motor-end load of assigned actual or virtual impedance, the procedure would be the same, except that instead of starting with a position angle of zero at  $A$ , there would be a definite starting position angle  $\delta_A = \tanh^{-1} (\sigma/z_1)$  hyps.

**Reversed Distribution of Position Angles.**—If instead of grounding the composite line at  $A$ , Fig. 170, and voltageing it at  $F$ , we ground it at  $F$ , and voltage it at  $A$ , the distribution of position angles will be different from that already found, but will be determinable by the same process. The distribution is shown in Fig. 171, for the three-section composite line above considered. Starting from  $F$  grounded, where  $\delta_F = 0$ ,  $\delta_E = 0.5$  hyp. At the other side of the junction  $DE$ , however, the line angle is

$$\begin{aligned} \delta_D &= \tanh^{-1} \left( \frac{z_3}{z_2} \tanh \delta_E \right) = \tanh^{-1} (1.25 \tanh 0.5) \\ &= \tanh^{-1} 0.57765 = 0.65892. \end{aligned}$$

The position angle then regularly increases to 2.15892 hyps. at  $C$ . Again,

$$\begin{aligned}\delta_B &= \tanh^{-1} \left( \frac{z_2}{z_1} \tanh \delta_c \right) = \tanh^{-1} (2.0 \tanh 2.15892) \\ &= \tanh^{-1} (2 \times 0.97369) = \tanh^{-1} (1.94738)\end{aligned}$$

The antitangent of a quantity greater than unity must contain an imaginary quadrant or  $j_2^\pi$  (see Fig. 17); so that

$$\delta_B = \coth^{-1}(1.94738) + j_2^\pi = 0.56748 + j_2^\pi = 0.56748 + j\underline{1.0} \text{ hyp.}$$

The position angle now increases regularly to  $2.56748 + j_2^\pi$  at  $A$ .

The effect of the imaginary quadrant in the position angles on the  $AB$  section will be virtually to transmute sines into cosines, cosines into sines, and tangents into cotangents in using the standard formulas. This complication presents itself only in c.c. cases. It does not intrude in a.c. cases.

Repeating the development of potential and current distributions, we find that the current  $I_F$  to ground at  $F$  is  $0.022600 \times 10^{-3}$  amp., which is the same as  $I_A$  in Fig. 170. This is a general law which may be expressed as follows.\*

Any composite line of any number of sections, with or without loads of any kind, operated in the steady state either by a direct current or by a single-frequency alternating current, has the same receiving-end impedance from each end; so that if say 1 volt is applied to each end in turn, the current strength received to ground at the other end will be the same. This is equivalent to stating that such a composite line may be represented by a net II, the architrave of which is the receiving-end impedance to ground from either end of the whole line.

It is assumed in the above proposition that all the elements of the composite-line system are subject to Ohm's law in complex arithmetic, *i.e.*, that there are no faults, or bad contacts, subject to erratic variation.

**Formation of the Hyperbolic Equivalent II of Composite Line.**—In order to form the hyperbolic II of the composite line represented in Figs. 170 and 171, we first find the value of the architrave impedance and then, in turn, the value of each terminal leak admittance.

\* *Am. Acad. Arts and Sciences, loc. cit.*, 1909.

The steps in the process are indicated in Fig. 172. The architrave impedance by (169), if there were only a single section  $AB$  in Fig. 171, grounded at  $B$ , and voltaged from  $A$ , would be

$$\rho'' = z_1 \sinh \delta_A \quad \text{ohms } \angle \quad (429)$$

At each transition down line from the voltaged end, take the ratio of the cosine of the downside terminal position angle to the cosine of the upside terminal position angle. As there are two transitions in Fig. 171, namely at  $B - C$  and  $D - E$ , the composite architrave impedance working from the voltage end  $A^*$  is

$$\rho'' = z_1 \sinh \delta_A \cdot \frac{\cosh \delta_C}{\cosh \delta_B} \cdot \frac{\cosh \delta_E}{\cosh \delta_D} \quad \text{ohms } \angle \quad (430)$$

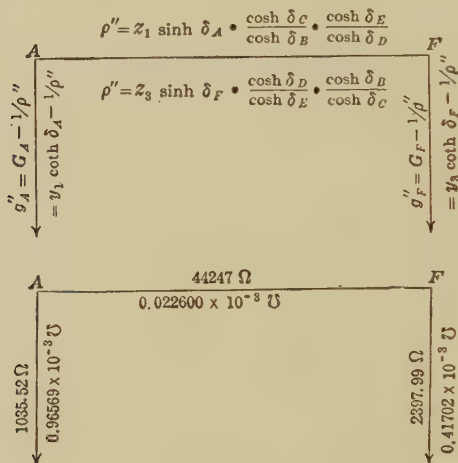


Fig. 172.—Equivalent II of three-section composite line.

If we worked from the  $F$  voltaged end, with  $A$  grounded, we should have for the first section  $EF$  (Fig. 170).

$$\rho'' = z_3 \sinh \delta_F \quad \text{ohms } \angle \quad (432)$$

Applying cosine ratios at transitions in position angles we obtain

$$\rho'' = z_3 \sinh \delta_F \cdot \frac{\cosh \delta_D}{\cosh \delta_E} \cdot \frac{\cosh \delta_B}{\cosh \delta_C} \quad \text{ohms } \angle \quad (433)$$

\* It may be noted that this formula (430) for evaluating the architrave impedance from the position angles is not the only one available. An alternative formula is

$$\rho'' = z_1 \sinh \theta_1 \cdot \frac{\sinh \delta_D}{\sinh \delta_C} \cdot \frac{\sinh \delta_F}{\sinh \delta_E} \quad \text{ohms } \angle \quad (431)$$

This is called the "second method" in the original paper, *Proc. Am. Acad. Arts and Sciences*, November, 1909. The first method only will be developed here. See also Appendix E.

The same process would be continued for any number of transitions, one cosine ratio being applied for each in turn. The value of  $\rho''$  working from either end will be the same; i.e.,  $\rho''$  is identical in (430) and (433).

Hence to find the architrave impedance of a composite line: Ground one end, and determine the distribution of position angles at transitions. The architrave  $\rho''$  has then the value which would present itself if the last single line were the only line, but multiplied by the ratio of the cosines of the down to the up terminal position angles, at each transition in turn.

The process is well adapted to either slide-rule or logarithmic computation, when a number of transitions occur. A composite line containing  $n$  single lines will embody  $n - 1$  transitions and  $n - 1$  cosine ratios.

Thus, in the case above represented in Fig. 170, using (433),

$$\begin{aligned}\rho'' &= 2,500 \times \sinh 1.52683 \times \frac{\cosh 2.025608}{\cosh 1.02683} \times \frac{\cosh 2.0}{\cosh 0.525608} \\ &= 2,500 \times 2.1932 \times \frac{3.8563}{1.5752} \times \frac{3.7622}{1.1414} = 44,247 \text{ ohms.}\end{aligned}$$

Again, in the case of Fig. 171, using (430),

$$\begin{aligned}\rho'' &= 1,000 \times \sinh \left( 2.56748 + j_2^{\pi} \right) \times \frac{\cosh 2.15892}{\cosh \left( 0.57648 + j_2^{\pi} \right)} \\ &\quad \times \frac{\cosh 0.5}{\cosh 0.65892} \\ &= 1,000 \times j \cosh 2.56748 \times \frac{\cosh 2.15892}{j \sinh 0.57648} \times \frac{\cosh 0.5}{\cosh 0.65892} \\ &= 1,000 \times 6.5549 \times \frac{4.3886}{0.59843} \times \frac{1.1276}{1.2251} = 44,247 \text{ ohms}\end{aligned}$$

**Leak Admittances of Equivalent II.**—The admittance of the leak  $g_A'$  of the hyperbolic II is equal to the line admittance at  $A$ , minus the architrave admittance. By (147) the line admittance at  $A$  to ground at  $F$  is  $G_{gA}$  in the c.c. case or  $Y_{gA}$  in an a.c. case. Using the latter for generality,

$$\begin{aligned}Y_{gA} &= y_3 \coth \delta_A \\ &= 10^{-3} \times \coth \left( 2.56748 + j_2^{\pi} \right) = 10^{-3} \times \tanh 2.56748 \\ &= 0.98829 \times 10^{-3} \text{ mho.}\end{aligned}$$



The architrave admittance will be  $\nu = 1/\rho'' = 1/44,247 = 0.02260 \times 10^{-3}$ ; so that

$$\begin{aligned} g_A &= Y_{gA} - \nu = y_1 \coth \delta_A - \nu && \text{mhos } \angle \quad (434) \\ &= (0.98829 - 0.02260)10^{-3} = 0.96569 \times 10^{-3} \text{ mho} \end{aligned}$$

Similarly, the admittance of the leak  $g''_F$  is equal to the line admittance at  $F$  minus the architrave admittance. The line admittance at  $F$  to ground at  $A$  (Fig. 170), is  $G_{gF}$  (or  $Y_{gF}$  in the general case)

$$\begin{aligned} Y_{gF} &= y_3 \coth \delta_F && \text{mhos } \angle \quad (435) \\ &= 0.4 \times 10^{-3} \coth 1.52683 = 0.4 \times 10^{-3} \times 1.09905 \\ &= 0.43962 \times 10^{-3} \text{ mho} \end{aligned}$$

so that

$$\begin{aligned} g''_F &= y_3 \coth \delta_F - \nu && \text{mhos } \angle \quad (436) \\ &= (0.43962 - 0.02260)10^{-3} = 0.41702 \times 10^{-3} \text{ mho} \end{aligned}$$

*The leak admittance at either terminal of the equivalent  $\Pi$  of a composite line is therefore the line admittance of that terminal, reduced by the architrave admittance.*

**General Considerations Concerning the Equivalent  $\Pi$  of a Composite Line.**—Since the line admittance will, in general, have different values at the two terminals of a composite line, *it follows that the terminal leaks of the equivalent  $\Pi$  of a composite line have, in general, different values, or a composite line has a dissymmetrical net  $\Pi$ .* Similarly, a composite line has, in general, a dissymmetrical equivalent  $T$ .

If, therefore, a motor-end load, of impedance  $\sigma$  ohms  $\angle$ , be applied successively to each terminal of a composite line, and the other terminal is at the same time voltaged to the same potential  $V$ , the current received through the load will, in general, be different in the two cases, unless  $\sigma = 0$ . This is for the reason that the value of the shunt applied to  $\sigma$  by the leak at that terminal will be different in the two cases.

In order to find the architrave and the leak at one terminal of a composite line, it is only necessary to work out the distribution of position angles over the system in the direction toward the required leak. If, however, both leaks are required, so as to complete the equivalent  $\Pi$ , then it becomes necessary to work out the position-angle distributions in both directions over the system.

**Terminal Cantilevers.**—Cantilever is the name proposed for the architrave and one leak\* of an equivalent  $\Pi$ . The architrave and the leak at the voltaged end, such as can be computed from one series of position angles toward that end, as in Fig. 173, may

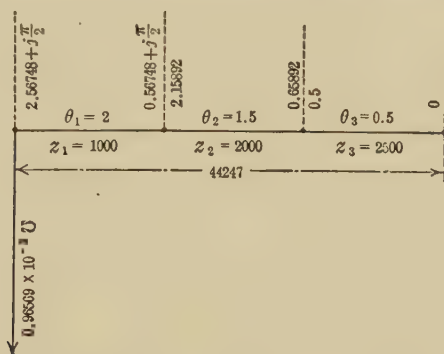


FIG. 173.—A-cantilever of three-section composite line.

be called the “A cantilever” or  $\Gamma$  of the composite line. The corresponding oppositely developed architrave and leak as in Fig. 174 may be called the “F cantilever” or 7 of the same line. Although both cantilevers have to be worked out, in order to

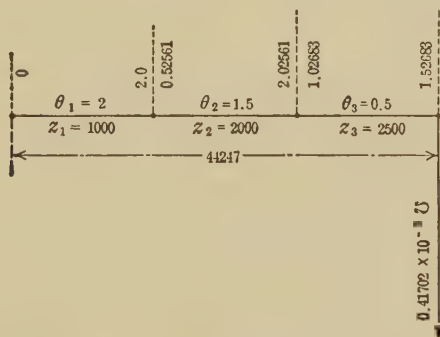


FIG. 174.—F-cantilever of three-section composite line.

complete the net  $\Pi$  of a composite line, yet, in particular cases, it may only be necessary to work out one of them. For example, if the composite line is to be voltaged at  $A$  and grounded at  $F$ , it is

\* The term “gamma” ( $\Gamma$ ) has been suggested to denote the generator-end leak and the architrave of an equivalent  $\Pi$ ; while the term *seven* has been suggested for the motor-end leak and the architrave (7). The term “cantilever” may be considered as applying to either case ( $\Gamma$  or 7) (in Fig. 130, 11 and 12).

of no immediate practical interest to determine the  $F$  leak of the equivalent  $\Pi$ , because, by assumption, that leak is to remain short-circuited. It is, therefore, only necessary in that case, to work out the  $A$  cantilever, and to ground the distant end of the architrave. When, however, the complete equivalent  $\Pi$ , and both cantilevers, are computed, there is the advantage of the check that the architrave impedance  $\rho''$  should be the same in both.

**Alternating-current Example of Composite Line.**—The following example may illustrate the application of the foregoing principles to an a.c. case. In Fig. 175, we have a diagrammatic representation of a three-section composite telephone line. At  $A$  is the generator, of *angular frequency* 5,000 radians per sec. ( $f = 796\sim$ ), impressed on a 5-km. section of a standard twisted-



FIG. 175.—Composite telephone circuit of central overhead section and terminal cable sections.

pair telephone cable from  $A$  to  $B$ . Then from  $C$  to  $D$  there is a 250-km. overhead section of open-wire telephone line, and finally from  $E$  to  $F$  another 5 km. of underground wire like that between  $A$  and  $B$ . At  $F$  is a terminal load, such as a receiving set between the wires of the circuit. The impedance of this load, at impressed frequency, is taken as  $1,500\angle 70^\circ$  ohms per loop, *i.e.*,  $750\angle 70^\circ$  ohms per wire. It is required to find the distributions of position angle, potential and current over the composite line, assuming  $2.0\angle 0^\circ$  volts applied across the lines at  $A$ , *i.e.*,  $1.0\angle 0^\circ$  volt per wire.

The linear constants of the three single lines are recorded in Table XXVI. The angle subtended by each underground line is  $0.3324 + j0.2199 = 0.4793\angle 46^\circ.096$  hyp., and that subtended by the overhead line  $1.171 + j2.785$  hyp.  $= 1.171 + j4.375 = 4.53\angle 75^\circ.017$  hyp.

In Fig. 176, we have at the top, the three sections. Their respective single equivalent  $\Pi$ 's are given below these. The underground-section  $\Pi$ 's are clearly realizable in the laboratory. The overhead-section  $\Pi$  is not, however, realizable by ordinary simple impedances. At  $A'' B'' E'' F''$ , the three  $\Pi$ 's are joined

TABLE XXVI  
Linear constants of the sections of composite line in Fig. 175

	Section A-B	Section C-D	Section E-F
Section length, km.....	5.0	250.0	5.0
Linear resistance, $r$ , ohms per loop km.....	54.68	6.586	54.68
Linear inductance, $l$ , henrys per loop km.....	$0.6213 \times 10^{-3}$	$2.284 \times 10^{-3}$	$0.6213 \times 10^{-3}$
Linear capacitance, $c$ , farads per loop km.....	$0.3355 \times 10^{-7}$	$0.4982 \times 10^{-8}$	$0.3355 \times 10^{-7}$
Linear leakance, $g$ , mhos per loop km.....	$3.107 \times 10^{-6}$	0	$3.107 \times 10^{-6}$
Hyperbolic angle $\theta$ , at $\omega = 5,000$ , hyps.....	$0.3324 + j0.2199$	$1.171 + j2.785$	$0.3324 + j0.2199$
Linear hyperbolic angle $\alpha$ , at $\omega = 5,000$ , $\frac{\text{hyps.}}{\text{km.}}$ .....	$0.06647 + j0.04398$	$0.004684 + j0.01114$	$0.06647 + j0.04398$
Surge impedance per wire, at $\omega = 5,000$ , ohms.....	$285.7 \angle 42^\circ.843$	$363.7 \angle 14^\circ.983$	$285.7 \angle 42^\circ.843$

end to end, and adjoining leaks are merged by vector addition. The central II, at  $B'' E''$ , is then replaced by its equivalent  $T$  at  $B''' E'''$ . As the next step, the  $T$  at  $A''' F'''$ , which happens to

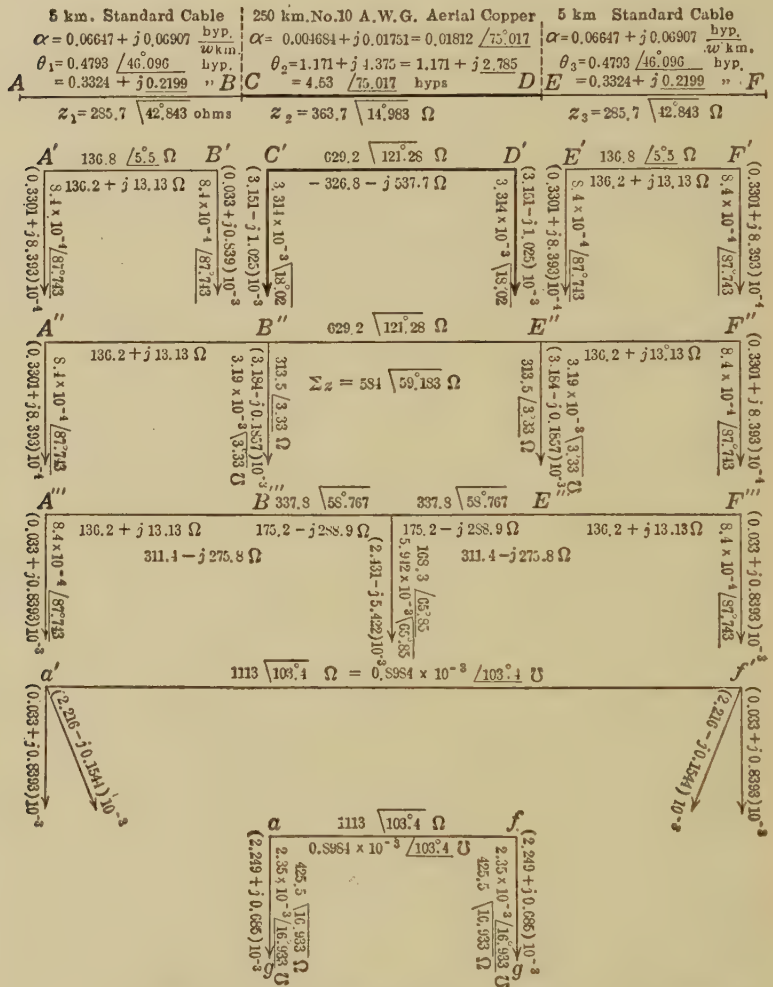


FIG. 176.—Successive steps in determining the merger II of the three-section composite line.

be symmetrical in this case, is replaced by its equivalent II,  $a'f'$ , with sloping pillars. Finally, the terminal leaks are merged by vector addition, and we obtain the merger II of the system, at  $afgg$ . The architrave has an impedance of  $1,113 \sqrt{103.4}$  ohms,



an unrealizable value with ordinary simple impedance elements in series. Each leak has  $2.35 \angle 16^\circ.933$  millimho. The merger  $\Pi$  of a three-section line calls for two  $\Pi - T$  or  $T - \Pi$  transformations, and a merger  $\Pi$  of an  $n$ -section line calls, in general,

$\left[ \begin{array}{l} 5 \text{ km. Standard Cable} \\ \alpha = 0.06647 + j0.06907 \\ \theta_1 = 0.4793 \angle 46^\circ.096 \\ = 0.3324 + j0.2199 \text{ hyp.} \end{array} \right]$	$\left[ \begin{array}{l} 250 \text{ km. No. 10 A.W.G. Aerial Copper} \\ \alpha = 0.004664 + j0.01751 = 0.01812 \angle 75^\circ.017 \\ \theta_2 = 1.171 + j4.375 = 1.171 + j2.785 \\ = 4.53 \angle 75^\circ.017 \text{ hyps.} \end{array} \right]$	$\left[ \begin{array}{l} 5 \text{ km. Standard Cable} \\ \alpha = 0.06647 + j0.06907 \\ \theta_3 = 0.4793 \angle 46^\circ.096 \\ = 0.3324 + j0.2199 \text{ hyps.} \end{array} \right]$
$A \quad z_1 = 285.7 \angle 42^\circ.843 \Omega$	$B \quad C \quad z_2 = 363.7 \angle 14^\circ.983 \Omega$	$D \quad E \quad z_3 = 285.7 \angle 42^\circ.843 \Omega \quad F$

$$\delta_D = \tanh^{-1} \left( \frac{z_3}{z_2} \tanh \delta_E \right) = \tanh^{-1} \left( \frac{285.7 \angle 42^\circ.843}{363.7 \angle 14^\circ.983} \times 0.4713 \angle 41^\circ.5 \right) = \tanh^{-1} (0.3703 \angle 13^\circ.64)$$

$$\delta_D = 0.36 + j0.065$$

$$\theta_2 = 1.171 + j2.785$$

$$\delta_C = 1.531 + j2.850$$

$$\delta_D = \tanh^{-1} \left( \frac{z_2}{z_1} \tanh \delta_C \right) = \tanh^{-1} \left( \frac{363.7 \angle 14^\circ.983}{285.7 \angle 42^\circ.843} \times 1.094 \angle 2^\circ.43 \right) = \tanh^{-1} (1.393 \angle 30^\circ.29)$$

$$\delta_D = 0.575 + j0.685$$

$$\theta_1 = 0.332 + j0.220$$

$$\delta_A = 0.907 + j0.906$$

$$\rho_{11} = z_1 \sinh \delta_A \cdot \frac{\cosh \delta_C}{\cosh \delta_D} \cdot \frac{\cosh \delta_E}{\cosh \delta_D}$$

$$= z_1 \sinh (0.907 + j0.906) \cdot \frac{\cosh (1.531 + j2.850)}{\cosh (0.575 + j0.685)} \cdot \frac{\cosh (0.3324 + j0.220)}{\cosh (0.36 + j0.065)}$$

$$= 285.7 \angle 42^\circ.843 \times 1.434 \angle 89^\circ.9 \times \frac{2.263 \angle 25^\circ.3}{0.780 \angle 43^\circ.9} \times \frac{1.00 \angle 6^\circ.5}{1.062 \angle 2^\circ.1} = 1119 \angle 103^\circ.1 \Omega$$

$$Y_{AG} = y_1 / \tanh \delta_A = 3.500 \times 10^{-3} \angle 42^\circ.843 / 1.368 \angle 5^\circ.6 = 2.559 \times 10^{-3} \angle 37^\circ.243 = (2.037 + j1.549) 10^{-3} \Omega$$

$$1/\rho_{11} = 0.8937 \times 10^{-3} \angle 103^\circ.1 = (-0.203 + j0.870) 10^{-3} \Omega$$

$$Y_{ag} = (2.240 + j0.679) 10^{-3} \Omega$$

$$= 2.341 \times 10^{-3} \angle 16^\circ.87 \Omega$$

$$\begin{array}{c} a \\ \left( \begin{array}{l} 2.240 + j0.679 \end{array} \right) 10^{-3} \Omega \\ \downarrow \\ g \\ \left( \begin{array}{l} 2.341 \times 10^{-3} \angle 16^\circ.87 \end{array} \right) \Omega \end{array} \quad \begin{array}{c} 1119 \angle 103^\circ.1 \Omega \\ \downarrow \\ 0.8937 \times 10^{-3} \angle 103^\circ.1 \Omega \end{array} \quad \begin{array}{c} f \\ \left( \begin{array}{l} 2.240 + j0.679 \end{array} \right) 10^{-3} \Omega \\ \downarrow \\ 2.341 \times 10^{-3} \angle 16^\circ.87 \Omega \end{array}$$

FIG. 177.—Full computation of hyperbolic  $\Pi$  for the three-section composite line, for  $n - 1$  such transformations, besides incidental auxiliary computations. It is a tedious, and error-provoking process.

It is evident from this merger  $\Pi$ , that if the composite line were directly grounded at  $F$ , and voltaged with  $1.0 \angle 0^\circ$  at  $A$ , the received current at  $F$  would be  $0.8984 \angle 103^\circ.4$  milliamp. Although apparently leading the impressed e.m.f. by  $103^\circ.4$ , the

received current would actually lag  $360^\circ - 103^\circ.4 = 256^\circ.6$  behind it.

The hyperbolic II is worked out in full in Fig. 177, with the aid of the "Chart Atlas of Complex Hyperbolic Functions." The first step is to lay off the position angles, each of which takes one line on the page, and two references to the chart. Thus, in finding  $\delta_D$ , we require to find  $\tanh \delta_E = \tanh (0.3324 + j0.2199)$ . The charts do not, as a rule, admit of being used to this degree of precision, but we can readily find from Chart IX<sub>A</sub>,  $\tanh (0.33 + j0.22) = 0.471 \angle 41^\circ.5$ , the last digit of the size being doubtful. We then have to find from the same chart  $\tanh^{-1} (0.3703 \angle 13^\circ.64)$ , by entering on the rectilinear background for  $0.370 \angle 13^\circ.6$ , and interpolating on the curvilinear system,  $0.36 + j0.065$  hyp.

After establishing the position angles, we know that in any one section, the potentials are as their sines, and the currents as their cosines, there being no discontinuity at junctions. We start at *A*, where the potential is given, and where the current is, by (148),  $I_A = y_1 \coth \delta_A = 2.559 \angle 37^\circ.243$  milliamp.

The architrave  $\rho''$  of the hyperbolic II, by (430), appears beneath  $\delta_A$  in Fig. 177. In the formula, there are five successive references to chart X-XI. The result is  $1,119 \angle 103^\circ.1$ , as against  $1,113 \angle 103^\circ.4$  by the merger method. The discrepancy is attributable to the limits of graphic interpolation precision in the charts. By numerical interpolation in the corresponding tables, a closer approximation would be obtainable, at a greater expenditure of time.

At the bottom of the arithmetic is the computation for the *a* leak; namely  $2.341 \times 10^{-3} \angle 16^\circ.87$  mho. Ordinarily, the *f* leak could not be found without a new distribution of position angles from *A* to *F*; but, in this case, by symmetry, the *f* and *a* leaks are identical.

In Fig. 178, we have the merger II extended to include the receiving instrument between *f* and *G*. The new II, which is dissymmetrical, has an architrave impedance  $a'g$  of  $2,100 \angle 26^\circ.4$  ohms. One volt applied at *a'* would, therefore, deliver a current through the receiving instrument of  $0.4763 \angle 26^\circ.4$  milliamp. Fig. 179 gives the corresponding *A* cantilever by the hyperbolic-function method. The position angles have been recast from *G* to *A*. The final result gives an architrave impedance  $a'g'$  of  $2,108 \angle 26^\circ.5$  ohms, and an *a'* leak admittance of  $2.406 \angle 37^\circ$

millimhos. One volt at  $A$  would, therefore, send  $0.4744 \angle 26^\circ.5$  milliamp. through the receiving instrument, which means that 2.0 volts across the circuit in Fig. 175 would send this same current through the  $1,500 \angle 70^\circ$ -ohm instrument at  $F$ . The potentials and currents at transitions are also indicated in the upper part of Fig. 179. The discrepancy of 0.4 per cent. between the hyperbolic and merger architraves is again attributable to the limits of graphic interpolation in the use of charts.

**Alternating-current Case of Impedance Loads at Each Terminal.**—As an instance of terminal loads at each end of a line, the case of Fig. 180 may be taken. Here the single line subtends

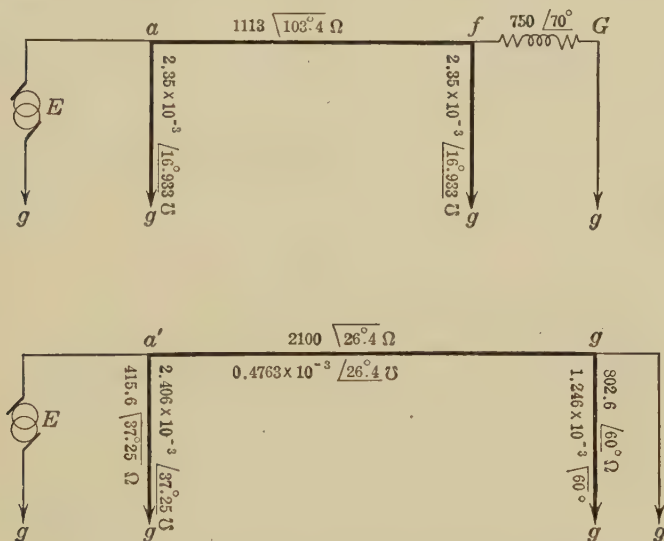
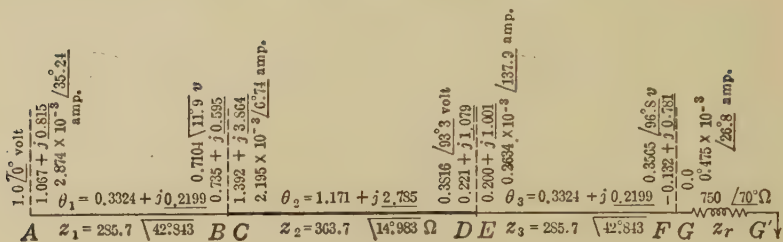


FIG. 178.—Merger II of composite line including terminal load at  $G$ .

an angle of  $\theta = 1.871 + j1.835 = 1.871 + j1.168$  hyps., and has a surge impedance of  $285.5 \angle 45^\circ$  ohms. The motor-end load  $DE$  has an impedance  $Z_r = 776.4 \angle 86^\circ.55$ ; so that it subtends a virtual angle of  $\theta' = \tanh^{-1} (776.4 \angle 86^\circ.55) / 285.5 \angle 45^\circ = \tanh^{-1} (2.719 \angle 131^\circ.55) = -0.23 + j0.820$  hyp. by Chart XII. Similarly, the virtual angle of the generator-end impedance is  $\tanh^{-1} (71.8 \angle 82^\circ.8 / 285.5 \angle 45^\circ) = \tanh^{-1} (0.2515 \angle 127^\circ.8) = -0.149 + j0.128$  hyp. also by chart. The sum of the line angle and the two terminal angles is  $1.492 + j2.116$ . The  $A$  cantilever of this system has therefore an architrave impedance of\*

\*See "Artificial Electric Lines" page 260, formula (434).



$$\delta_P = \tanh^{-1} \left( \frac{Z_P}{Z_3} \right) = \tanh^{-1} \left( \frac{750 \angle 70^\circ}{285.7 \angle 42.843} \right) = \tanh^{-1} (2.625 \angle 112.843) = \tanh^{-1} (-1.019 + j2.420)$$

$$\delta_P = -0.132 + j0.791$$

$$\theta_3 = 0.332 + j0.220$$

$$\delta_E = 0.200 + j1.001$$

$$\delta_D = \tanh^{-1} \left( \frac{Z_D}{Z_2} \tanh \delta_E \right) = \tanh^{-1} \left\{ \frac{285.7 \angle 42.843}{363.7 \angle 14.983} \tanh (0.200 + j1.001) \right\} = \tanh^{-1} (3.98 \angle 28.31)$$

$$\delta_D = 0.221 + j1.079$$

$$\theta_2 = 1.171 + j2.785$$

$$\delta_C = 1.392 + j3.864$$

$$\delta_B = \tanh^{-1} \left( \frac{Z_B}{Z_1} \tanh \delta_C \right) = \tanh^{-1} \left\{ \frac{363.7 \angle 14.983}{285.7 \angle 42.843} \tanh (1.392 + j3.864) \right\} = \tanh^{-1} (1.137 \angle 24.86)$$

$$\delta_B = 0.735 + j0.595$$

$$\theta_1 = 0.332 + j0.220$$

$$\delta_A = 1.067 + j0.815$$

$$\begin{aligned} \rho_{11} &= Z_1 \sinh \delta_A \frac{\cosh \delta_C}{\cosh \delta_B} \cdot \frac{\cosh \delta_E}{\cosh \delta_D} \cdot \frac{\cosh \delta_G}{\cosh \delta_F} \\ &= 235.7 \angle 42.843 \cdot \sinh (1.067 + j0.815) \frac{\cosh (1.392 + j3.864)}{\cosh (0.735 + j0.595)} \frac{\cosh (0.200 + j1.001)}{\cosh (0.221 + j1.079)} \cdot \frac{\cosh 0}{\cosh (-0.132 + j0.791)} \\ &= 236.7 \angle 42.843 \cdot 1.602 \angle 76.9 \cdot \frac{2.125 \angle 11^\circ}{1.002 \angle 40.3} \cdot \frac{0.201 \angle 90.6}{0.255 \angle 120.16} \cdot \frac{1.0 \angle 0^\circ}{0.363 \angle 26.5} = 2108 \angle 26.5^\circ \Omega \end{aligned}$$

$$\begin{aligned} Y_{AG} &= y_1 / \tanh \delta_A = 3.500 \times 10^{-3} \angle 42.843 / 1.218 \angle 7.6 = 2.874 \times 10^{-3} \angle 35.243 = (2.347 + j1.655) \times 10^{-3} \text{ } \Omega^{-1} \\ 1/\rho_{11} &= 0.4744 \times 10^{-3} \angle 26.5 = (0.425 + j0.212) \times 10^{-3} \text{ } \Omega^{-1} \\ Y_{AG} &= (1.922 + j1.446) \times 10^{-3} \text{ } \Omega^{-1} \\ &= 2.406 \times 10^{-3} \angle 37.0 \end{aligned}$$

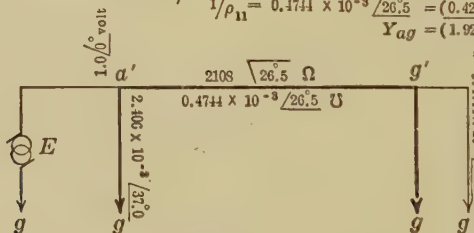


FIG. 179.—Complete computation of the A cantilever of the three-section composite line including the terminal load at G.

$$\begin{aligned} \rho'' &= 285.5 \angle 45^\circ \times \frac{\sinh (1.492 + j2.116)}{\cosh (-0.149 + j0.128)} \times \frac{\cosh 0}{\cosh (-0.23 + j0.820)} \\ &= 285.5 \angle 45^\circ \times \frac{2.118 \angle 168.5}{0.363 \angle 37.8} \times \frac{1.0 \angle 0^\circ}{0.9912 \angle 1.75} = \\ &= 1,680 \angle 173.95 \text{ ohms.} \end{aligned}$$

A potential of  $1.0 \angle 0^\circ$  volt impressed at *A*, Fig. 180, would thus send a current of  $0.0595 \angle 173^\circ.95$  milliamp. through the terminal impedance at *DE*.

**Intermediate Loads.**—Formulas have been developed\* for computing the architrave impedance of the net  $\Pi$  of a composite line taking into account intermediate series and leak loads applied at the junctions. Such formulas are lengthy, when there are several sections and intermediate loads. Such cases are often

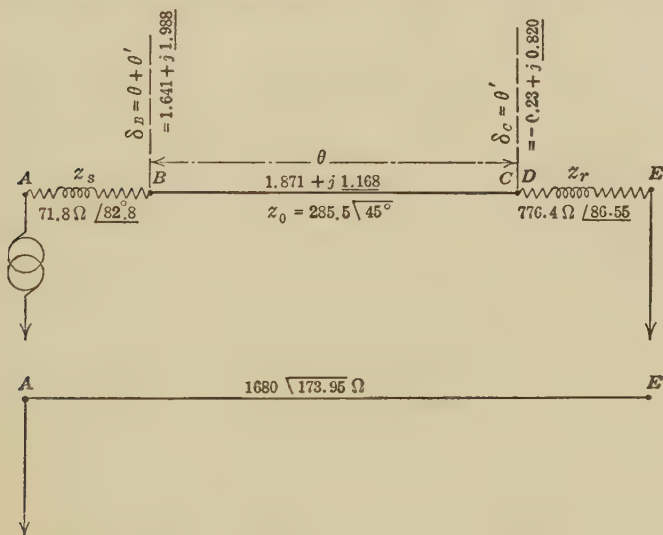


FIG. 180.—Line loaded at each end and the *A* cantilever.

more easily dealt with by the theory of general nets, to be considered in the next chapter. It may suffice here to point out that the effect of a given intermediate load, say a given series impedance, on the architrave impedance of the net  $\Pi$  may be very different at different junctions. Thus, to take a simple c.c. case, the effect of inserting 100 ohms, either as a terminal load, or as an intermediate load, at various points in the composite line in Fig. 170, is illustrated in Fig. 181. It will be seen that the architrave resistance of the line being 44,247 ohms without the load, is variously increased from 45,680 to 48,620 ohms, according to the position of the load. In a.c. cases, such differences may be surprisingly large.

\* See "Artificial Electric Lines," by same author and publisher, Chapter XIV.



**Case of an Alternating-current Transformer Inserted in Composite Line.**—In Fig. 182, we have a composite line  $AB, CD$  connected inductively through a transformer with another composite

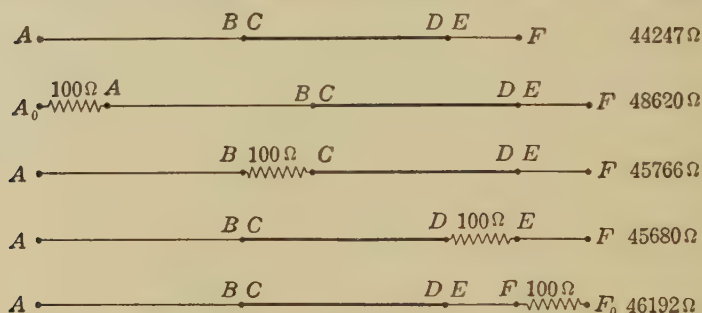


FIG. 181.—Effect of position of a series load in a composite line upon the arch-trove resistance.

line  $EF, GH$  grounded at  $H$ , through a terminal load  $\sigma$  ohms. The four single lines have the respective angles and surge impedances  $\theta_1, \theta_2, \theta_3, \theta_4$  and  $z_1, z_2, z_3, z_4$ . The transformer may be assumed to have a voltage ratio of  $n$ , in the sense that after

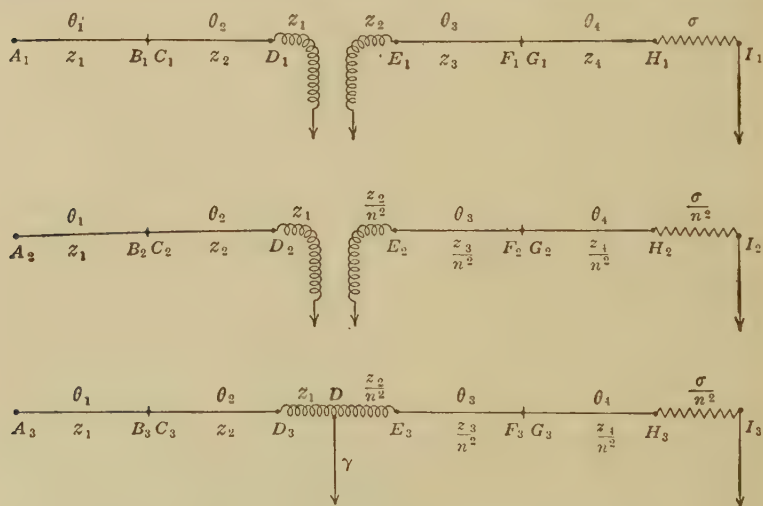


FIG. 182.—Treatment of inductively connected composite lines.

deducting the primary  $IZ$  drop, 1 volt of internally induced primary c.e.m.f. will be associated with  $n$  volts in the secondary winding. Both the primary and secondary windings have impedances comprising the effective resistance  $r$ , and the effective

self-reactance  $jx$  ohms. The leakage-reactance is that reactance which is due to magnetic flux not linked with the other winding. From this standpoint, a transformer contains a pure resistance-less mutual reactance and a pair of external impedances, one in each circuit.

We may next assume that the transformer is changed to a level transformer, with ratio 1, and with equal numbers of mutual turns in primary and secondary winding. The levelling may be imagined as effected to either primary or secondary voltage. We may assume, as in Fig. 182, that the primary winding remains unchanged, but the secondary winding is levelled to it. All impedances in the secondary system must now be divided by  $n^2$ , and all admittances multiplied by  $n^2$ . This condition is indicated at  $E_2, F_2, G_2, H_2$ . The two level-voltage composite systems may now be joined conductively at  $D$ , at a leak  $\gamma$ , which has such admittance as will carry the observed exciting current of the transformer when a corresponding exciting voltage is applied at  $D$ . The composite system  $A_3 - I_3$  is now a four-section composite line, with a terminal impedance of  $\sigma/n^2$  ohms  $\angle$  at  $HI$ , an intermediate impedance  $D_3E_3$ , and a leak  $\gamma$  in the same. The section angles  $\theta_3, \theta_4$ , have not been altered by the ideal process described.

After the position angles have been assigned to the modified through composite line  $A_3I_3$ , the potentials and currents may be worked out in the usual way. The resulting potentials are then multiplied by  $n$ , between  $D_1$ , and  $I_1$ , to derive the actual potentials with the actual unlevel transformer, and the resulting currents are likewise divided by  $n$ , between  $D_1$  and  $I_1$ . The vector powers on the imaginary level system will agree with the vector powers at corresponding points of the actual system.\*

If more than one transformer link occurs in the system, the procedure is the same. There will then be three or more voltage levels, any one of which may be selected as reference level, and the others reduced thereto, by the proper transformation ratios. Thus, if there is a step-up transformer at one end of a section, and

\* The Application of Hyperbolic Functions to Electrical Engineering Problems," p. 157.

"Theory and Calculation of Alternating-current Phenomena," by C. P. Steinmetz, New York, 1897.

"On the Predetermination of the Regulation of Alternating-current Transformers," by A. E. Kennelly, *Electrical World*, New York, Sept. 2, 1899, vol. xxxiv, p. 343.

a similar step-down transformer at the other, then either the high-voltage or low-voltage level may be accepted as the reference level, in constructing the conductive system. Ordinarily, the low-voltage level is the more convenient. The levelling process introduces no change into the angles which the various sections subtend. It changes only the surge impedance along with all the impedances and admittances of the same circuit. If there were negligible impedance and negligible losses in the transformers, their effect would be confined arithmetically to changing the surge impedances of the sections affected.

**Composite-line Tests in the Laboratory.**—The following case is taken from experimental tests, at 60~, of a two-section composite line consisting of a telephonic resistance-condensance line, joined to part of the line specified\* in Table XVII. The connections are indicated in Fig. 183. At the impressed frequency of 60.5~, the artificial telephone line *AB* subtended  $0.654 + j0.4068$  hyp., with a surge impedance of  $1,365\angle 44^\circ.02$  ohms: while the artificial power line *CD* subtended  $0.127 + j1.008$  hyp., with a surge impedance of  $347.6\angle 3^\circ.92$  ohms. The equivalent  $\Pi$  of each section and the equivalent  $\Pi$  of the composite line *AD* are also shown in Fig. 183. The composite line equivalent  $\Pi$  has an architrave of  $535\angle 107^\circ.5$  ohms, and two dissymmetrical leaks, one of them having a size more than three times that of the other, the slopes also being very different. The composite line was loaded at *D* with  $1,000\angle 0^\circ$  ohms.

The results of the Drysdale potentiometer tests, reduced to  $100\angle 0^\circ$  volts at *A*, appear in Fig. 184. The curves show the computed values of potential and current over the conjugate smooth line, while the circles represent the observations at selected junctions along the composite artificial line. It will be seen that the voltage falls along a nearly straight line over the artificial telephone line, from  $100\angle 0^\circ$  at *A*, to  $11.07\angle 14^\circ.76$  at *B*. It then rises to  $23.21\angle 103^\circ.44$  at *D*.

Figure 185, is a schematic representation of reflected voltage waves over the composite line, assuming that an outgoing wave of  $100\angle 0^\circ$  volts is suddenly launched from *A* without any accompanying splash or oscillatory disturbance. The coefficients used are given in Table XXVII, based on (320), (342), (343), (344), and (345).

\* These tests are recorded in theses at the Mass. Inst. Tech. by C. W. Whitall and F. W. McKown, June, 1916.

Thus, the first outgoing wave from  $A$ , in Fig. 185, arrives at  $B$  in the condition  $52.00 \angle 36^\circ.61$  (line 5, column 1, Table XXVII), or  $41.74 - j31.01$  volts. At junction  $BC$  this wave splits, the transmitted portion is  $21.96 \angle 4^\circ.33$ , and the reflected portion

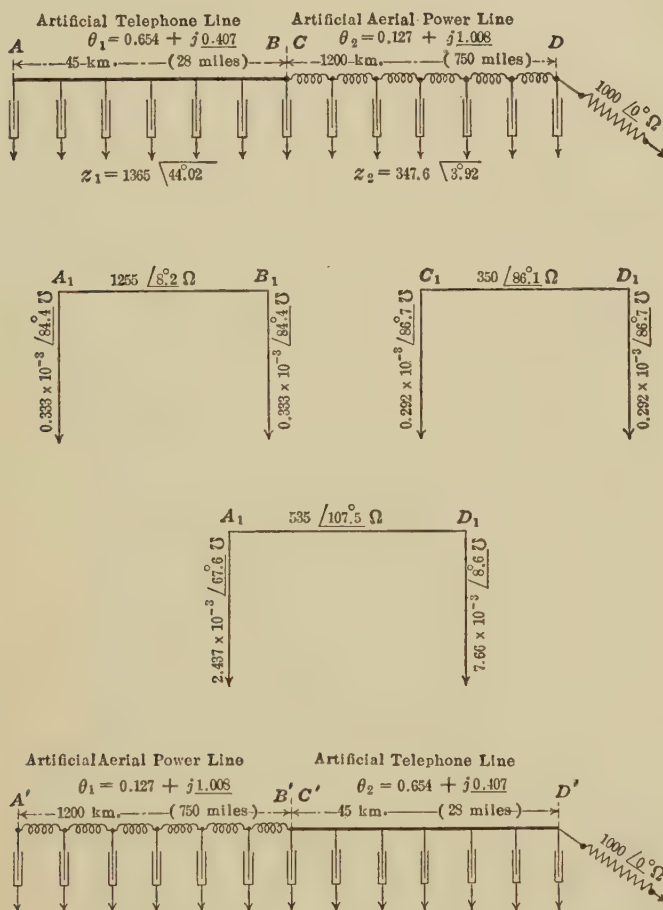


FIG. 183.—Connections of composite artificial line in laboratory test.

$35.43 \angle 124^\circ.06$ . This reflected portion returns to  $A$  under attenuation, then to  $B$ , again is partially reflected back to  $A$ , and so on, for four  $ABBA$  return trips, before it is exhausted to below 0.1 volt in size, after which it is ignored in the schedule.

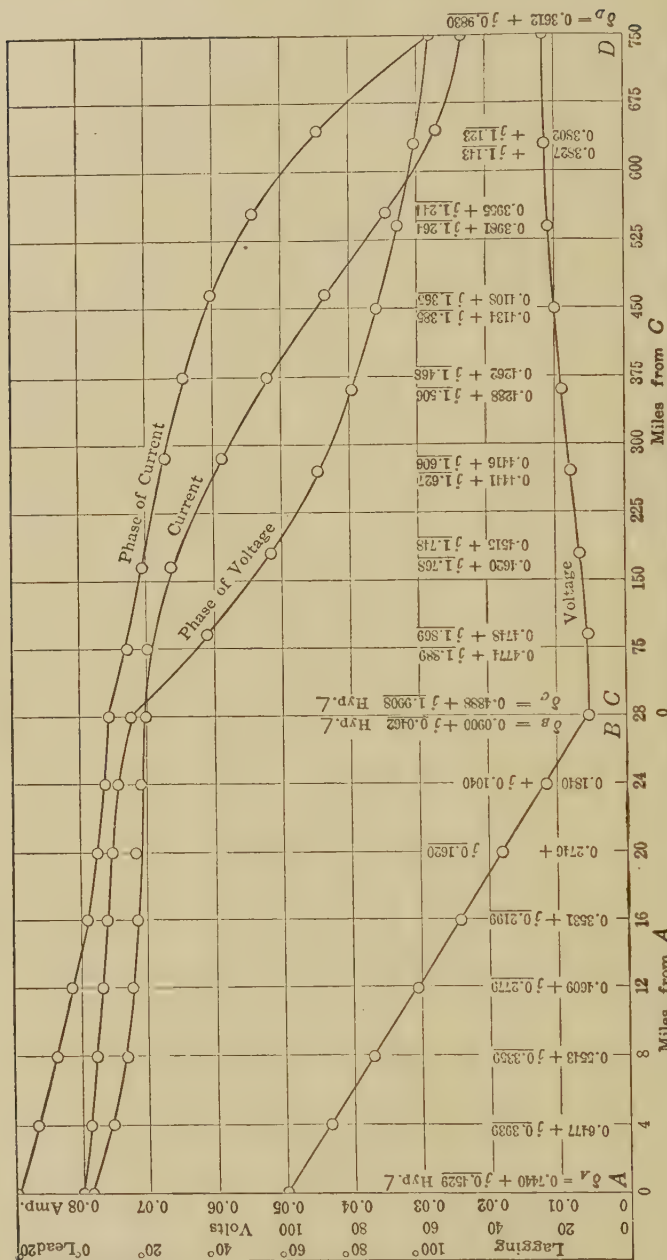


Fig. 184.—Observed distributions of voltage and current over composite artificial line and computed curves for conjugate smooth line. Centers of small circles represent observed values.



TABLE XXVII  
Constants and coefficients for the composite line of Fig. 183

		I		II	
		Art. telephone line		Art. power line	
1	Angle subtended at $f = 60.5\sim$ , hyps.....				
2		0.654 + $j0.6390$		0.1273 + $j1.5831$	
3	Surge impedance at $f = 60.5\sim$ , ohms.....	1.365 $\angle 44^\circ .02$		0.1273 + $j1.008$ 347.6 $\angle 3^\circ .92$	
4	Normal attenuation coefficient.....				
5		A to B or B to A $\epsilon = 0.484 - j0.6390$ 0.520 $\angle 36^\circ .612$		C to D or D to C $\epsilon = 0.172 - j1.4841$ 0.8805 $\angle 90^\circ .705$	
6	Reflection coefficient, voltage.....	B toward A 0.6814 $\angle 160^\circ .666$		D toward C 0.4853 $\angle 3^\circ .094$	
7		A toward B 1.00 $\angle 180^\circ$		C toward D 0.6814 $\angle 19^\circ .334$	
8	Reflection coefficient, current.....	B toward A 0.6814 $\angle 19^\circ .334$		D toward C 0.4853 $\angle 176^\circ .906$	
9		A toward B 1.00 $\angle 0^\circ$		C toward D 0.6814 $\angle 160^\circ .666$	
10	Transmission coefficient, voltage.....	$\frac{2z_2}{z_1 + z_2}$		B to C 0.4224 $\angle 32^\circ .282$	
11		$\frac{2z_1}{z_1 + z_2}$		C to B 1.6583 $\angle 7^\circ .818$	
12		$\frac{2\sigma}{z_2 + \sigma}$		D to $\sigma$ 1.4848 $\angle 1^\circ .011$	
13	Transmission coefficient, current.....	$\frac{2z_1}{z_1 + z_2}$		B to C 1.6583 $\angle 7^\circ .818$	
14		$\frac{2z_2}{z_1 + z_2}$		C to B 0.4224 $\angle 32^\circ .282$	
15		$\frac{2z_2}{z_2 + \sigma}$		D to $\sigma$ 0.5161 $\angle 2^\circ .909$	
16	Time occupied in one transit—Time interval at $\omega = 350$ , (seconds).....			C to D or D to C	
17	Number of single transits per second.....	A to B or B to A 0.00168 595		0.00416 240	
18	Apparent velocity of transmission, km.....	26,810		288,000	
19	Apparent velocity of transmission, $\frac{\text{stat. miles}}{\text{sec.}}$ .....	16,660		179,000	

Figure 185 recognizes 40 successive vector increments at *B*, 32 such increments at *C*, and 29 at *D*. The vector sums of these various series appear at the foot of each column. The vector sum at *B* is  $11.33\angle 13^{\circ}.73$  volts, and at *C*  $11.17\angle 16^{\circ}.37$ . These sums differ because of the neglect of wave tailings below 0.1 volt in size. If the summations were extended, without mistakes, to a sufficiently great number of terms and wave increments, they would agree with each other, and with the steady-state hyperbolic function value  $11.07\angle 14^{\circ}.76$  volts, as shown below on the lowest line.

Figure 186 is a similar schedule of current waves, and of their descendants by rupture at junctions. Here 29 increments are included at *A*, 38 at *B*, 50 at *C* and 49 at *D*, before extinction to below 0.1 milliamp. The vector sums are compared with the steady-state hyperbolic values on the two lowest lines of the schedule.

It is clear from Figs. 185 and 186 that if we had to depend on vector summation of reflected and transmitted waves for arriving at final steady states, as in these schedules, the work would frequently be prohibitively laborious. The hyperbolic-function method, on the other hand, by virtually summing up to infinity all these series of vector increments, is a most effective labor-saving device.

**Time Interval of a Line.**—The apparent velocity of transmission over an artificial line of hyperbolic angle  $\theta_1 + j\theta_2$  and representing *L* km. (or miles) of actual conjugate-line length varies somewhat with the frequency, and is by (308),

$$v = \frac{\omega}{\alpha_2} = \frac{L\omega}{\theta_2} \quad \frac{\text{km.}}{\text{sec.}} \quad (437)$$

and the number of transits per second made by a wave at this velocity, in either direction over the line is

$$n = \frac{\omega}{\theta_2} \quad \text{numeric} \quad (438)$$

while the time consumed in any transit in either direction is

$$T = \frac{1}{n} = \frac{\theta_2}{\omega} \quad \text{sec.} \quad (439)$$

This may be called the *time interval* of an a.c. real or artificial line, for the impressed angular frequency  $\omega$ .

In the last three formulas,  $\omega$  is expressed in radians per second, and  $\theta_2$  in circular radians; but if  $\theta_2$  is expressed in circular quad-

A

D

B

C

A

D

B

C

100 + 7.0

-100.0°

41.74

-731.01

52.00

32.00

38.01

21.96

47.33

31.00

+ 739.35-19.84

-6.05-7.43

5.58

+11.17-1.31

0.58

0.22

-0.20

-70.10

0.82

145.11

+ 739.35-19.84

-6.05-7.43

5.58

+11.17-1.31

0.58

0.22

-0.20

-70.10

0.82

145.11

+ 739.35-19.84

-6.05-7.43

5.58

+11.17-1.31

0.58

0.22

-0.20

-70.10

0.82

145.11

+ 739.35-19.84

-6.05-7.43

5.58

+11.17-1.31

0.58

0.22

-0.20

-70.10

0.82

145.11

+ 739.35-19.84

-6.05-7.43

5.58

+11.17-1.31

0.58

0.22

-0.20

-70.10

0.82

145.11

+ 739.35-19.84

-6.05-7.43

5.58

+11.17-1.31

0.58

0.22

-0.20

-70.10

0.82

145.11

+ 739.35-19.84

-6.05-7.43

5.58

+11.17-1.31

0.58

0.22

-0.20

-70.10

0.82

145.11

+ 739.35-19.84

-6.05-7.43

5.58

+11.17-1.31

0.58

0.22

-0.20

-70.10

0.82

145.11

+ 739.35-19.84

-6.05-7.43

5.58

+11.17-1.31

0.58

0.22

-0.20

-70.10

0.82

145.11

+ 739.35-19.84

-6.05-7.43

5.58

+11.17-1.31

0.58

0.22

-0.20

-70.10

0.82

145.11

+ 739.35-19.84

-6.05-7.43

5.58

+11.17-1.31

0.58

0.22

-0.20

-70.10

0.82

145.11

+ 739.35-19.84

-6.05-7.43

5.58

+11.17-1.31

0.58

0.22

-0.20

-70.10

0.82

145.11

+ 739.35-19.84

-6.05-7.43

5.58

+11.17-1.31

0.58

0.22

-0.20

-70.10

0.82

145.11

+ 739.35-19.84

-6.05-7.43

5.58

+11.17-1.31

0.58

0.22

-0.20

-70.10

0.82

145.11

+ 739.35-19.84

-6.05-7.43

5.58

+11.17-1.31

0.58

0.22

-0.20

-70.10

0.82

145.11

+ 739.35-19.84

-6.05-7.43

5.58

+11.17-1.31

0.58

0.22

-0.20

-70.10

0.82

145.11

+ 739.35-19.84

-6.05-7.43

5.58

+11.17-1.31

0.58

0.22

-0.20

-70.10

0.82

145.11

+ 739.35-19.84

-6.05-7.43

5.58

+11.17-1.31

0.58

0.22

-0.20

-70.10

0.82

145.11

+ 739.35-19.84

-6.05-7.43

5.58

+11.17-1.31

0.58

0.22

-0.20

-70.10

0.82

145.11

+ 739.35-19.84

-6.05-7.43

5.58

+11.17-1.31

0.58

0.22

-0.20

-70.10

0.82

145.11

+ 739.35-19.84

-6.05-7.43

5.58

+11.17-1.31

0.58

0.22

-0.20

-70.10

0.82

145.11

+ 739.35-19.84

-6.05-7.43

5.58

+11.17-1.31

0.58

0.22

-0.20

-70.10

0.82

145.11

+ 739.35-19.84

-6.05-7.43

5.58

+11.17-1.31

0.58

0.22

-0.20

-70.10

0.82

145.11

+ 739.35-19.84

-6.05-7.43

5.58

+11.17-1.31

0.58

0.22

-0.20

-70.10

0.82

145.11

+ 739.35-19.84

-6.05-7.43

5.58

+11.17-1.31

0.58

0.22

-0.20

-70.10

0.82

145.11

+ 739.35-19.84

-6.05-7.43

5.58

+11.17-1.31

0.58

0.22

-0.20

-70.10

0.82

145.11

+ 739.35-19.84

-6.05-7.43

5.58

+11.17-1.31

0.58

0.22

-0.20

-70.10

0.82

145.11

+ 739.35-19.84

-6.05-7.43

5.58

+11.17-1.31

0.58

0.22

-0.20

-70.10

0.82

145.11

+ 739.35-19.84

-6.05-7.43

5.58

+11.17-1.31

0.58

0.22

-0.20

-70.10

0.82

145.11

+ 739.35-19.84

-6.05-7.43

5.58

+11.17-1.31

0.58

0.22

-0.20

-70.10

0.82

145.11

+ 739.35-19.84

-6.05-7.43

5.58

+11.17-1.31

0.58

0.22

-0.20

-70.10

0.82

145.11

+ 739.35-19.84

-6.05-7.43

5.58

+11.17-1.31

0.58

0.22

-0.20

-70.10

0.82

145.11

+ 739.35-19.84

-6.05-7.43

5.58

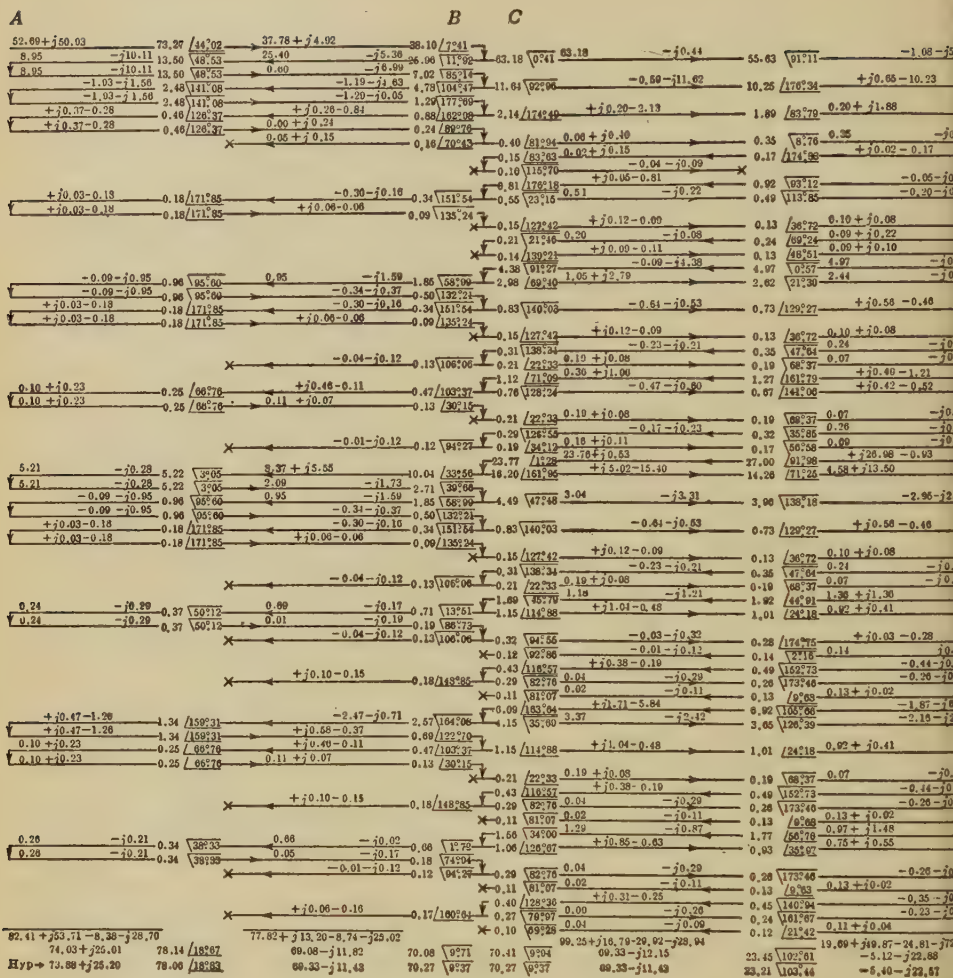


Fig. 186.—Summation of currents in milliamperes neglecting residues below 0.1 milliamperes.

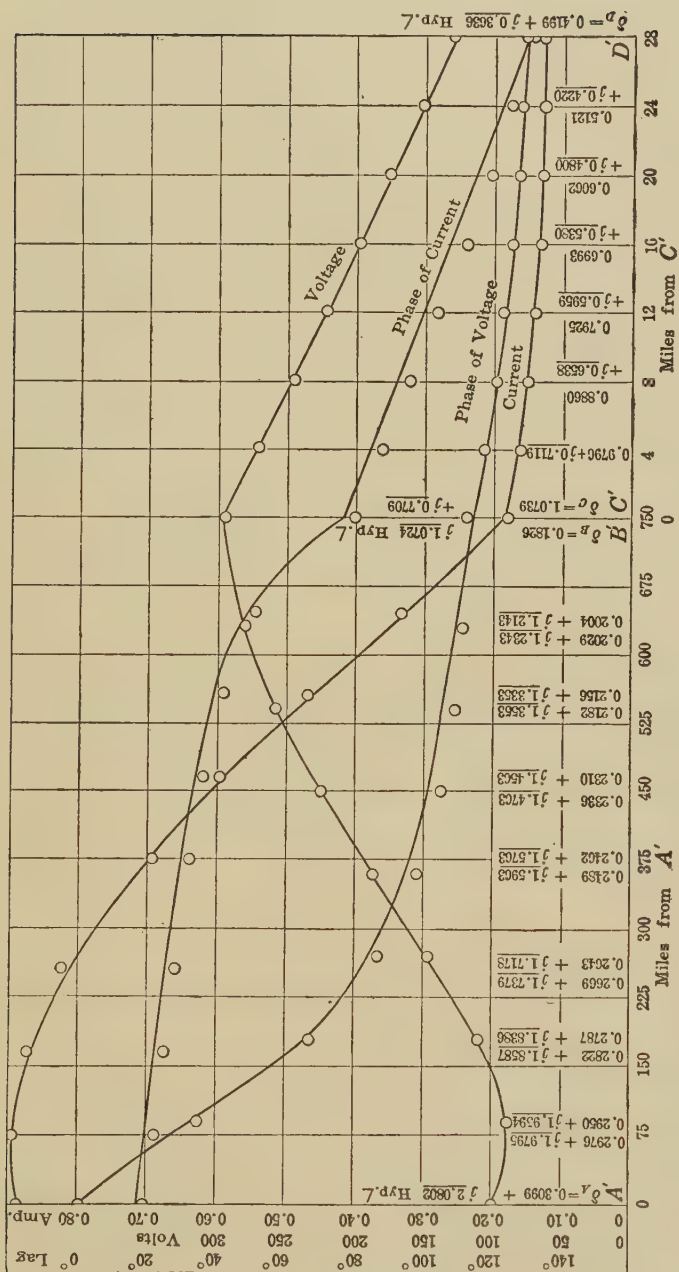


FIG. 186A.—Observed distributions of voltage and current over composite line reversed and computed curves for conjugate smooth line centers of small circles represent observed values.



rants,  $\omega$  may be correspondingly expressed in quadrants per second, where

$$\omega_q = 4f \frac{\text{quadrants}}{\text{sec.}} \quad (440)$$

Thus, the artificial power line  $CD$ , 1,200 km. long, subtending an angle of  $0.1273 + j1.008$  hyps., and the impressed frequency being 60.5~, the quadrantal angular velocity would be  $\omega_q = 242$ . Hence  $n = 242/1.008 = 240$  single transits per second,  $T = 1.008/242 = 0.00416$  second, and  $v = 1200 \times 240 = 288,000$  km./sec.

It is, therefore, evident that all of the vector increments scheduled in Figs. 185 and 186 are delivered in less than  $\frac{1}{4}$  sec. after closing the switch at the generator end  $A$  of this composite line. The smaller the losses in the sections, and the higher the attenuation coefficient size  $\epsilon^{-\theta_1}$ , the more numerous these successive increments must be, in order to reach exhaustion below assigned limits of voltage and current. On the other hand, either on an infinite line, or on a finite line with very great attenuation, the first wave will be the only one to consider in determining the steady state.

Figure 186A shows the results of the tests on the composite line when the power line was connected to the generator and the telephone line loaded with 1,000  $\angle 0^\circ$ , ohms as at  $A'D'$ , in Fig. 183. Here the voltage rises from 100  $\angle 0^\circ$  volts at  $A'$ , to 294  $\angle 112^\circ.9$  volts at  $B'$ , and then falls nearly on a straight line to 129.9  $\angle 128^\circ.6$  volts at  $D$ . The curves follow the computed values over the conjugate smooth line and the circles mark the observed values on the artificial line.

## CHAPTER XVIII

### ELECTRIC NETWORKS IN THE STEADY STATE

A network of conductors may be defined as an assemblage of conducting elements, each of which obeys Ohm's law as extended to alternating currents.\* These elements may be connected together at their terminals in any manner. A relatively simple network of some twenty elements, including also a transformer  $T$ , is represented in Fig. 187. Two pairs of terminals are selected on this network, as the input and output pairs, such as  $ag$  and

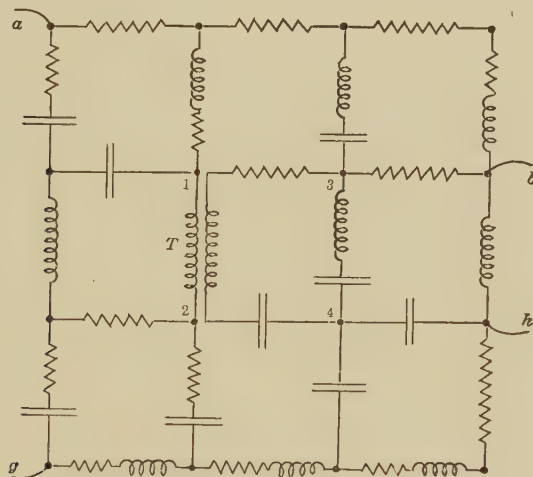


FIG. 187.—Simple rectilinear four-terminal net.

$bh$ . It is assumed that the network or *net* is inert, or devoid of e.m.f. when the terminals  $ag$  and  $bh$  are disconnected as shown. The net of Fig. 187 may be described as a *rectangular net*. Disregarding the separation between primary and secondary transformer terminals, a rectangular net of  $m$  rows of squares by  $n$  columns of squares, will have  $mn$  squares in all, and  $(m + 1)(n + 1)$  terminals.

\* "Impedance," by A. E. Kennelly, *Proc. A. I. E. E.*, April, 1893, vol. x, p. 175.

Any net may be resolved,\* so far as relates to the two pairs of terminals  $ag$  and  $bh$ , into a simple equivalent  $T$ , Fig. 188, or a simple† equivalent  $\Pi$ , Fig. 189. These equivalent triple-

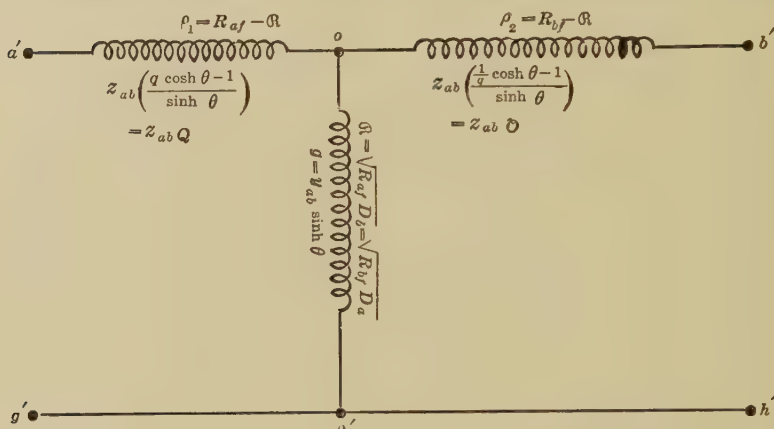


FIG. 188.—Dissymmetrical  $T$  equivalent to the four-terminal net of Fig. 187.

element nets will, in general, be dissymmetrical. All three nets, namely, the full net of Fig. 187, the  $T$  of Fig. 188, and the  $\Pi$  of Fig. 189, will have the same hyperbolic angle  $\theta$  hyps.  $\angle$ .

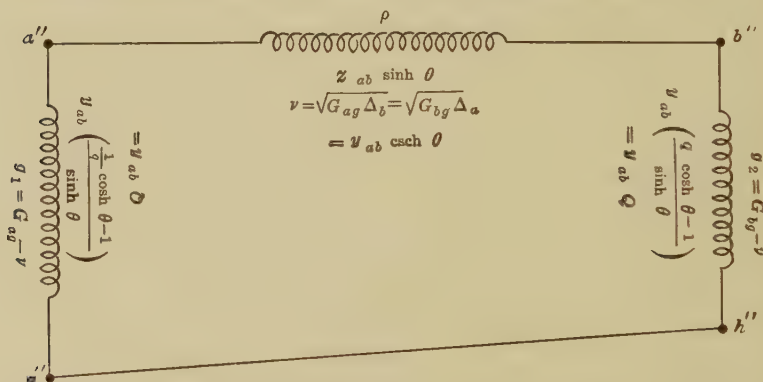


FIG. 189.—Dissymmetrical  $\Pi$  equivalent to the four-terminal net of Fig. 187.

**Surge Impedances of a Net.**—We have seen in (42) and (330), that a smooth uniform line offers to any advancing wave of single

\* "Leerlauf und Kurzschluss," J. L. La Cour, 1904.

† "Alternating Current Plane-vector Potentiometer Measurements at Telephonic Frequencies" by A. E. Kennelly and Edy Velander, *Proc. Amer. Phil. Soc.*, April, 1919, vol. lviii, p. 122.

a.c. frequency, a certain natural or characteristic impedance  $z_0 = \sqrt{\frac{z}{y}}$  which has been called the surge impedance of the line for that frequency, and which, at high frequencies, tends to the reactanceless limit  $z_{00} = \sqrt{\frac{l}{c}}$ . Consequently, the terms "natural impedance," "characteristic impedance," "iterative impedance," and "surge impedance" are all applicable to this impedance  $z_0$  of a smooth line. The term "surge impedance" has the advantage of being the briefest, as well as of having been in early use. Moreover, the value of the surge impedance of any smooth line is most easily measured by (45) and (46), taking the geometrical mean of the impedance offered by the line at one end, when the other is first grounded or shorted and then freed, or opened. That is, for any uniform line,

$$z_{0a} = z_{0b} = z_0 = \sqrt{R_{ag}R_{af}} = \sqrt{R_{bg}R_{bf}} \quad \text{ohms } \angle \quad (441)$$

Here  $z_{0a}$  and  $z_{0b}$  denote the surge impedances measured at the *A* and *B* ends of the line. By symmetry, these values are identical and equal to  $z_0$ .

A net of impedance elements like that of Fig. 187, cannot offer a constant surge impedance to a traveling wave, so that in this sense the term does not conform to such a net. Nevertheless, we may define the two impedances by:

$$z_{0a} = \sqrt{R_{ag}R_{af}} \quad \text{ohms } \angle \quad (442)$$

and

$$z_{0b} = \sqrt{R_{bg}R_{bf}} \quad \text{ohms } \angle \quad (443)$$

which measured at opposite ends of the net, by shorting and opening the distant terminals, are characteristic of the net, as is also their geometrical vector mean

$$z_{ab} = \sqrt{z_{0a}z_{0b}} = \sqrt[4]{R_{ag}R_{af}R_{bg}R_{bf}} \quad \text{ohms } \angle \quad (444)$$

Formulas (442) and (443) might properly be called the *A*- and *B*-characteristic impedances of the net and (444) the "geometrical mean characteristic impedance." As these terms are lengthy, it may be permissible to call  $z_{0a}$  and  $z_{0b}$  the *A* and *B* "surge impedances" and  $z_{ab}$  the "geomean surge impedance" of the net. Any term adopted for  $z_{0a}$  and  $z_{0b}$  for a net would preferably

be likewise applicable to  $z_0$  for a smooth line, in the interest of simplicity and consistency.\*

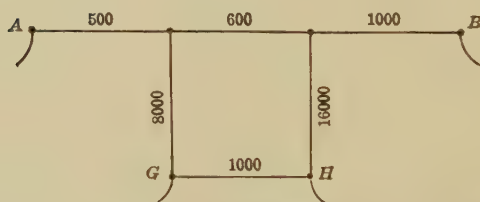
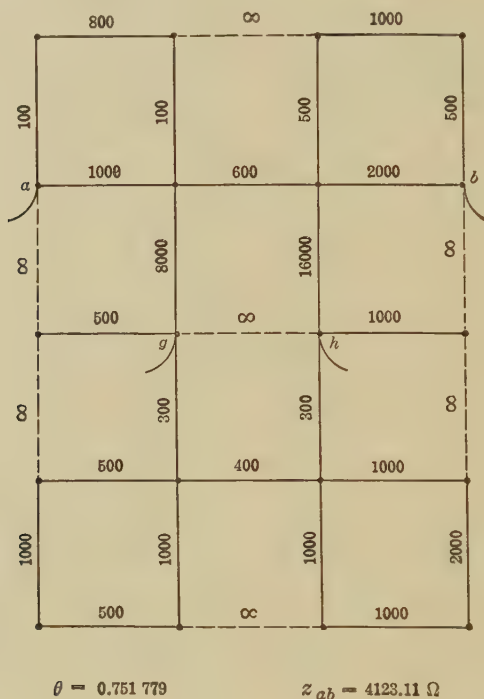
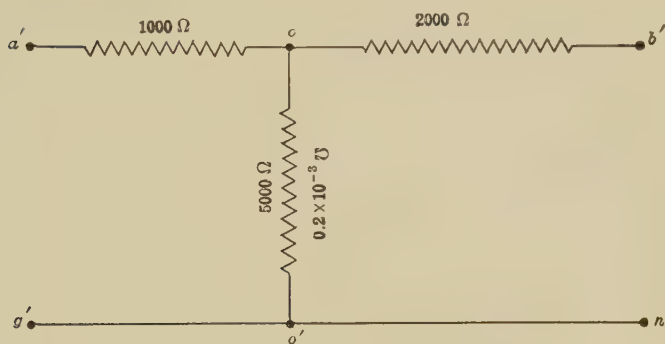


FIG. 190.—Simple c.c. net of 24 resistance elements, and the six-element net to which it is equivalent.

**Angle  $\theta$  of a Net.**—A relatively simple d.c. or zero-frequency rectangular net is indicated in Fig. 190. It is further simplified

\* The end impedances  $z_{0a}$  and  $z_{0b}$  have also been called “image impedances” by K. S. Johnson, for the reason that, as will be presently shown, if the  $B$  terminals are closed upon the load  $z_{0b}$  and the  $A$  terminals upon the load  $z_{0a}$ , each load is equal to, or is the image of, the impedance of the net at that end. See “Transmission Circuits for Telephonic Communication,” Chapter XI.





$$R_{ag} = 2428.57 \, \Omega$$

$$R_{bg} = 2883.33 \, \Omega$$

$$R_{af} = 6000 \, \Omega$$

$$R_{bf} = 7000 \, \Omega$$

$$\tanh^2 \theta = 0.404762$$

$$\tanh \theta = 0.636209$$

$$\theta = 0.751779$$

$$Z_{oa} = 3817.26 \, \Omega$$

$$Z_{ab} = 4123.11 \, \Omega$$

$$Z_{ob} = 4453.46 \, \Omega$$

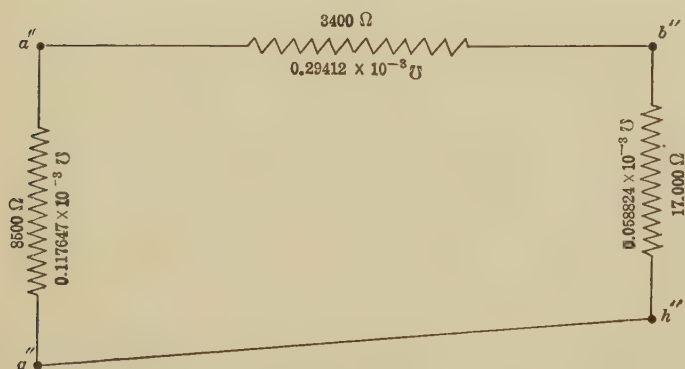
$$q = 0.92582$$

$$1/q = 1.08012$$

$$v_{oa} = 0.261967 \times 10^{-3} \, \text{V}$$

$$v_{ab} = 0.242585 \times 10^{-3} \, \text{V}$$

$$v_{ob} = 0.224545 \times 10^{-3} \, \text{V}$$



FIGS. 191 and 192.—Equivalent  $T$  and  $\Pi$  of the net in Fig. 190, together with their constants.

to six elements in the lower part of the same figure. Its equivalent  $T$  and  $\Pi$  appear in Figs. 191 and 192.

If the resistances  $R_{ag}$  and  $R_{af}$  of the net are measured at the  $ag$  terminals, with the  $bh$  terminals grounded (shorted) and freed (opened), respectively, we secure two observations at the  $A$  end. Similarly, if the resistances  $R_{bg}$  and  $R_{bf}$  of the net are measured at the  $bh$  terminals, with the  $ag$  terminals respectively grounded and freed, we secure two corresponding observations at the  $B$  end. We then have:\*

$$\tanh \theta = \sqrt{\frac{R_{ag}}{R_{af}}} = \sqrt{\frac{R_{bg}}{R_{bf}}} \quad \text{numeric } \angle \quad (445)$$

That is, the ratio of resistance shorted to resistance open is the same at each end of the net, and its square root is the hyp. tangent of the angle  $\theta$  of the net between the two end pairs of terminals. The real part  $\theta_1$  of this angle, or the hyperbolic part, measures the *electrical separation* between the two ends, in terms of attenuation, while the imaginary part  $\theta_2$  or circular part, measures, in normal attenuation, the *phase separation* between them.

The complex angle  $\theta$  of any net, symmetrical or dissymmetrical, including smooth lines, composite line systems, or air-core transformers, may be defined as

$$\theta = \tanh^{-1} \sqrt{\frac{R_{ag}}{R_{af}}} = \tanh^{-1} \sqrt{\frac{R_{bg}}{R_{bf}}} \quad \text{hyps. } \angle \quad (445a)$$

If the  $a$  and  $b$  terminals (Fig. 190) are brought into contact and likewise the  $g$  and  $h$  terminals, so that the electrical separation vanishes,  $\theta_1 = 0$ . If, on the other hand, the two ends are electrically indefinitely remote,  $\theta_1 = \infty$ .

**Characteristic Constants of a Net.**—A symmetrical net, such, for instance as a smooth real line, has two, and only two, characteristic constants, namely,  $\theta$  and  $z_0$ , the angle and the surge impedance. These two constants may be determined by two measurements of impedance,† as defined in (150) and (151). Both these measurements may be made at either end of the line, or one may be made at one end and the other at the other end.

\* "Dissymmetrical Electric Conducting Networks" by A. E. Kennelly, *Proc. A. I. E. E.*, February, 1923.

† "On Electric Conducting Lines of Uniform Conductor and Insulation Resistance" by A. E. Kennelly, *Harvard Engineering Journal*, May, 1903.

A dissymmetrical net, such, for instance as that of Fig. 190, is defined by three constants, and only three; but some latitude exists in their selection. One set of three constants capable of completely defining a dissymmetrical net, is  $\theta$ ,  $z_{0a}$  and  $z_{0b}$ , *i.e.* the angle of the net between the selected pairs of *A* and *B* terminals, at the selected frequency, and the *two surge impedances, as measured at the two ends*. Three independent measurements are necessary to determine these constants. Two measurements may be made from one end, say  $R_{ag}$  and  $R_{af}$  at *A*. The third measurement may be made from the other end, say either  $R_{bg}$  or  $R_{bf}$ . Formula (445) shows that from any three of the four measurements  $R_{ag}$ ,  $R_{af}$ ,  $R_{bg}$ , and  $R_{bf}$ , the fourth can be immediately deduced. In practice, however, there is an advantage in securing all four, since the two pairs from opposite ends furnish the mutual check afforded by (445).

Another triple group of constants completely defining a dissymmetrical net, and offering special advantages in so doing, is  $\theta$ ,  $z_{ab}$  and  $q$ , that is, the angle of the net, the *geomean surge impedance* and the *inequality factor*. This latter is defined by the relation:

$$q = \sqrt{\frac{z_{0a}}{z_{0b}}} = \sqrt[4]{\frac{R_{ag} \cdot R_{af}}{R_{bg} \cdot R_{bf}}} = \frac{z_{0a}}{z_{ab}} = \frac{z_{ab}}{z_{0b}} \quad \text{numeric } \angle \quad (446)$$

The inequality factor is a vector numeric, and may be regarded as measuring the ratio of transformation of the net, as though a transformer were inserted in the net between the *A* and *B* ends. The inequality factor being  $q$  at the *A* end of the net, that at the *B* end is  $1/q$ . In a symmetrical net,  $q = 1 \angle 0^\circ$ .

**Equivalent T of Net.**—After having obtained  $\theta$ ,  $z_{ab}$  and  $q$ , with the aid of formulas (445), (444), and (446), using any three observed vector values of the four measurable quantities  $R_{ag}$ ,  $R_{af}$ ,  $R_{bg}$ , and  $R_{bf}$ , the equivalent *T* of the net is readily found by noting that the staff admittance  $g'$ , Fig. 188, is

$$g' = y_{ab} \sinh \theta = \frac{\sinh \theta}{z_{ab}} = \frac{1}{\mathfrak{R}} \quad \text{mhos } \angle \quad (447)$$

which corresponds to (166) for a symmetrical *T*, since  $y_{ab}$  degrades to  $y_0$ , when  $q = 1 \angle 0^\circ$ . The staff impedance  $\mathfrak{R}$  is, therefore,

$$\mathfrak{R} = \frac{1}{g'} = \frac{z_{ab}}{\sinh \theta} \quad \text{ohms } \angle \quad (448)$$

This is sometimes called the “mutual impedance” of the net, because from Fig. 188, it can be seen that a given entering cur-

rent  $I$ , applied at one end, will produce in  $\mathcal{R}$  a drop of pressure  $I\mathcal{R}$  equal to the vector voltage at the other end (free).

The impedance of the  $A$  arm of the  $T$  in Fig. 188 is then

$$\rho_1 = R_{af} - \mathcal{R} \quad \text{ohms } \angle \quad (449)$$

and that of the  $B$  arm,

$$\rho_2 = R_{bf} - \mathcal{R} \quad \text{ohms } \angle \quad (450)$$

Alternative but less simple forms for these arm impedances are

$$\rho_1 = z_{ab} \left( \frac{q \cosh \theta - 1}{\sinh \theta} \right) = z_{ab} Q \quad \text{ohms } \angle \quad (451)$$

$$\rho_2 = z_{ab} \left( \frac{\frac{1}{q} \cosh \theta - 1}{\sinh \theta} \right) = z_{ab} \mathcal{Q} \quad \text{ohms } \angle \quad (452)$$

$Q$  and  $\mathcal{Q}$  being the *branch factors* of the net.

In a symmetrical net, when  $q = 1 \angle 0^\circ$ , both  $Q$  and its complement  $\mathcal{Q}$  degrade into

$$Q = \mathcal{Q} = \frac{\cosh \theta - 1}{\sinh \theta} = \tanh \frac{\theta}{2} \quad \text{numeric } \angle \quad (453)$$

which agrees with (165) and Fig. 22.

Another expression for the staff impedance is, as shown in Fig. 188,

$$\mathcal{R} = \sqrt{R_{af}(R_{bf} - R_{bg})} = \sqrt{R_{af}D_b} = \sqrt{R_{bf}(R_{af} - R_{ag})} = \sqrt{R_{bf}D_a} \quad \text{ohms } \angle \quad (454)$$

Figures 191 and 193 illustrate the preceding relations for a c.c. and an a.c. net respectively. The staff impedance in the a.c. case happens to be only arithmetically and not physically realizable, its slope being in excess of  $90^\circ$ .

**Equivalent II of Net.**—The architrave impedance of the equivalent II of a net is shown in Fig. 189 to be

$$\rho'' = z_{ab} \sinh \theta = \frac{1}{\nu} \quad \text{ohms } \angle \quad (455)$$

which corresponds to (169) for the symmetrical net. The architrave admittance is, therefore,

$$\nu = \frac{y_{ab}}{\sinh \theta} = \frac{1}{\rho''} \quad \text{mhos } \angle \quad (456)$$

This is sometimes called the “mutual admittance” of the net, because from Fig. 189 it can be seen that a given applied voltage

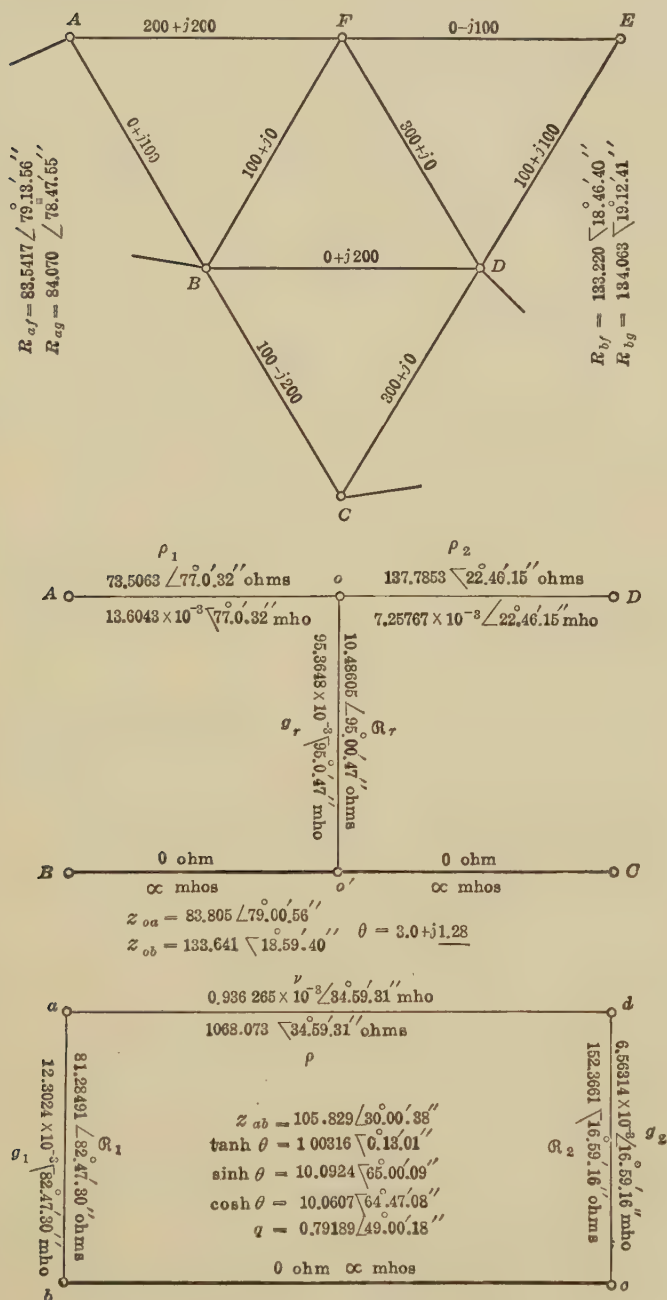


Fig. 193.—Nine-element a.c. net, with its equivalent T and II.



$E$ , at one end will produce in  $\nu$  a current  $E\nu$  equal to the vector current received at the other end (shorted).<sup>-</sup>

The admittance of the  $A$  leak will be

$$g_1 = G_{ag} - \nu \quad \text{mhos } \angle \quad (457)$$

where  $G_{ag} = 1/R_{ag}$  is the admittance measurable at the  $A$  end when the  $B$  end is grounded.

Similarly, the admittance of the  $B$  leak in Fig. 189 is

$$g_2 = G_{bg} - \nu \quad \text{mhos } \angle \quad (458)$$

Alternative but less simple forms for these leaks are

$$g_1 = y_{ab} \left( \frac{\frac{1}{q} \cosh \theta - 1}{\sinh \theta} \right) = y_{ab} Q \quad \text{mhos } \angle \quad (459)$$

and

$$g_2 = y_{ab} \left( q \frac{\cosh \theta - 1}{\sinh \theta} \right) = y_{ab} Q \quad \text{mhos } \angle \quad (460)$$

In a symmetrical net, with  $q = 1 \angle 0^\circ$ , these last two expressions coincide with each other and with  $y_0 \tanh (\theta/2)$ . This conforms with (170) and Fig. 22. Another expression for the architrave impedance, as shown in Fig. 189,

$$\nu = \sqrt{G_{ag}(G_{bg} - G_{bf})} = \sqrt{G_{ag}\Delta_b} = \sqrt{G_{bg}(G_{ag} - G_{af})} = \sqrt{G_{bg}\Delta_a} \quad \text{mhos } \angle \quad (461)$$

The last six equations are readily checked upon the numerical values appearing on the equivalent  $\Pi$ 's of Figs. 192 and 193.

**Sending-end Impedances of a Net.**—If the  $B$ -end terminals\* are left open or free, the impedance of the net as measurable from the  $A$ -end terminals is

$$R_{af} = z_{0a} \coth \theta = qz_{ab} \coth \theta \quad \text{ohms } \angle \quad (462)$$

If the  $B$ -end terminals are shorted or grounded, the  $A$ -end impedance is

$$R_{ag} = z_{0a} \tanh \theta = qz_{ab} \tanh \theta \quad \text{ohms } \angle \quad (463)$$

The product of the last two equations reduces to (442), while their ratio reduces to (445).

Similarly, if the tests are made from the  $BH$  terminals at the  $B$  end of the net, with the  $AG$  terminals first opened or freed and

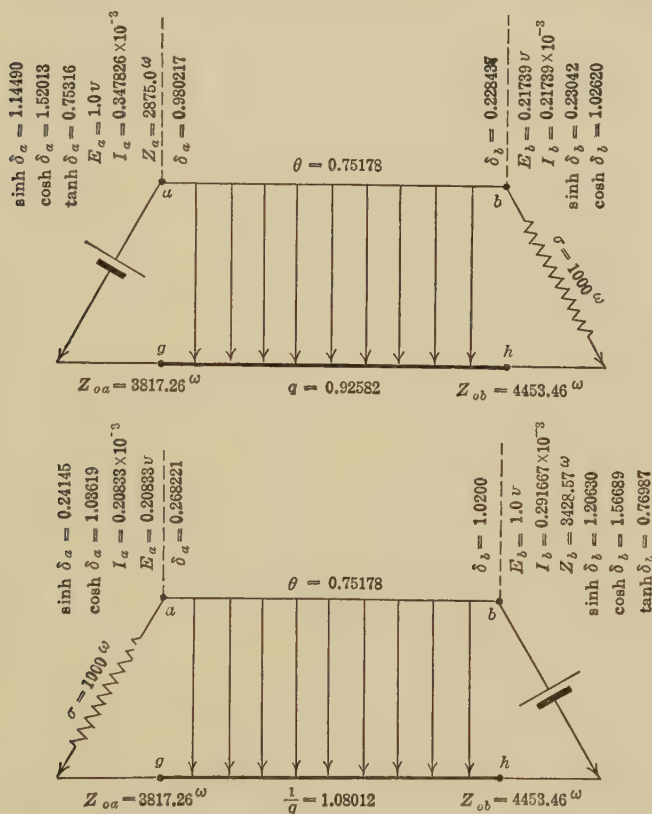
\* A fairly complete set of formulas relating to symmetrical and dissymmetrical nets, as well as to their  $T$  and  $\Pi$  equivalent is found in Appendix O of "The Appl. of Hyp. Fun. to El. Eng'g. Probs." 3rd Edition, 1925.

then shorted or grounded, we have the measurable impedances  $R_{bf}$  and  $R_{bg}$

$$R_{bf} = z_{0b} \coth \theta \quad \text{ohms } \angle \quad (464)$$

$$R_{bg} = z_{0b} \tanh \theta \quad \text{ohms } \angle \quad (465)$$

These are consistent, not only with (462) and (463), but also with (150) and (151), and (220) and (221), by noting that in any dissymmetrical net or line system, the measured sending-end



FIGS. 194 and 195.—Net of Fig. 190 indicated as a dissymmetrical line and with a load of 1,000 ohms applied at each end in turn.

impedances  $R_g$  and  $R_f$  are the products of the surge impedance at that end with  $\tanh \theta$ , and  $\coth \theta$ , respectively.

**Position Angles on a Net.**—We have seen, in connection with formulas (106) to (134) and (336) to (340), that on either a simple or a composite line, there exists a position angle  $\delta_p$  at each point, such that the potential, current, and impedance are respectively

proportional to the hyperbolic sine, cosine and tangent of the same. This proposition likewise applies to a net; except that only at the  $A$  and  $B$  terminals, can the position angles, in general, be assigned.

If the output terminals  $BH$  are closed on a load impedance  $\sigma$ , then, following (106), the position angle  $\delta_B$  is defined by the relation

$$\tanh \delta_B = \frac{\sigma}{z_{ob}} \quad \text{numeric } \angle \quad (466)$$

using the  $B$ -end surge impedance in the denominator. Then, following (107),

$$\delta_A = \theta + \delta_B \quad \text{hyps. } \angle \quad (467)$$

The impedance at the input terminals  $AG$  is then, following (149),

$$Z_A = z_{oa} \tanh \delta_A \quad \text{ohms } \angle \quad (468)$$

Reciprocally, it follows that if we invert the net, making  $BH$  the input, and  $AG$  the output terminals, the output-end position angle  $\delta$  becomes

$$\delta_A = \tanh^{-1} \left( \frac{\sigma}{z_{oa}} \right) \quad \text{hyps. } \angle \quad (469)$$

and the input-end position angle  $\delta_B = \theta + \delta_A$ , so that the input-end impedance

$$Z_B = z_{ob} \tanh \delta_B \quad \text{ohms } \angle \quad (470)$$

Thus the sending-end impedance always employs the sending-end surge impedance, and the receiving-end position angle the receiving-end surge impedance. These conditions are illustrated in Figs. 194 and 195, where the net of Fig. 190, characterized by  $\theta = 0.75178$ ,  $z_{ab} = 4,123.11$  and  $q = 0.92582$ , is loaded, at each end in turn, with  $\sigma = 1,000$  ohms, and energized at the other with 1.0 volt.

**Receiving-end Impedance.**—It follows from (475) below, that the current  $I_b$  received at  $B$ , through a load  $\sigma$  is

$$I_b = \frac{E_a}{z_{ob} \sinh \theta + \sigma q \cosh \theta} = \frac{E_a}{Z_l} \quad \text{amperes } \angle \quad (471)$$

where  $Z_l$  is defined as the receiving-end impedance in the presence of  $\sigma$ . Hence

$$Z_l = q(z_{ob} \sinh \theta + \sigma \cosh \theta) = z_{ab} \sinh \theta + \sigma q \cosh \theta \quad \text{ohms } \angle \quad (472)$$

which agrees with (155) when the net is symmetrical, or  $q = 1$ . Moreover, if  $\sigma = 0$ , the receiving-end impedance reduces to  $z_{ab}$

$\sinh \theta$ , which is the architrave of the equivalent  $\Pi$  of the net, as shown in (455). The effect, therefore, of the load  $\sigma$  is to increase the receiving-end impedance by  $q \cosh \theta$  times its own vector value.

**Voltage and Current Distribution at Ends of Net.**—We assume that the position angles at the ends of the net have been assigned in accordance with (466) and (467), and also that the voltage and current are known at one end. Then the voltage, current, and power can be found at the other end, in terms of the position angles, as well as in terms of the given values of voltage and current directly. We assume that  $A$  is the input end, and  $B$  the output end.

If the input values  $E_a$  and  $I_a$  are given we have:

$$E_b = \frac{1}{q}(E_a \cosh \theta - I_a z_{oa} \sinh \theta) = \frac{E_a}{q} \left( \frac{\sinh \delta_b}{\sinh \delta_a} \right) \text{ volts } \angle \quad (473)$$

and

$$I_b = q(I_a \cosh \theta - E_a y_{oa} \sinh \theta) = I_a q \left( \frac{\cosh \delta_b}{\cosh \delta_a} \right) \text{ amperes } \angle \quad (474)$$

If, on the other hand, the output values  $E_b$  and  $I_b$  are given, then

$$E_a = q(E_b \cosh \theta + I_b z_{ob} \sinh \theta) = E_b q \left( \frac{\sinh \delta_a}{\sinh \delta_b} \right) \text{ volts } \angle \quad (475)$$

and

$$I_a = \frac{1}{q}(I_b \cosh \theta + E_b y_{ob} \sinh \theta) = \frac{I_b}{q} \left( \frac{\cosh \delta_a}{\cosh \delta_b} \right) \text{ amp. } \angle \quad (476)$$

These equations may be checked by an inspection of Figs. 194 and 195.

It will be seen that in the case of  $q = 1$ , for a symmetrical net, or uniform line, the last equations agree with (77), (87), (117), and (129).

In particular, (475) shows that when the output terminals  $BH$  are free or open, the charging voltage of any net is

$$E_a = E_b q \cosh \theta \quad \text{volts } \angle \quad (476a)$$

This is the vector component of input voltage necessary at  $AG$ , in order to charge the net and maintain the free output voltage  $E_{bf}$  under no load ( $\sigma = \infty$ ). The additional vector component of input voltage due to maintaining the load current  $I_b$ , is  $I_b z_{ab} \sinh \theta$ , or the drop of that current in the architrave impedance  $z_{ab} \sinh \theta$  of the net's equivalent  $\Pi$ .

Moreover, if the input e.m.f.  $E_a$  is regarded as primarily assigned, it follows that the free output voltage  $E_{bf}$  of any net is:

$$E_{bf} = \frac{E_a}{q \cosh \theta} \quad \text{volts } \angle \quad (476b)$$

which agrees with (95b) when the net is symmetrical.

Again, from (476)

$$I_a = E_{bf} y_{ab} \sinh \theta = E_b g' \quad \text{amperes } \angle \quad (476c)$$

That is the charging current of any net at no load ( $\sigma = \infty$ ), is the current which the free output e.m.f.  $E_b$  would deliver to the staff admittance  $g'$ , of the net's equivalent  $T$  (Fig. 188). The additional input vector component of current due to the load  $I_b$  is then  $I_b (\cosh \theta)/q$ .

If the output terminals  $BH$  of a net are initially shorted, or grounded so that  $E_b = 0$ , the output short-circuit current  $I_{bg}$  is, by (474), (473) and (455),

$$I_{bg} = \frac{I_a q}{\cosh \theta} = \frac{E_a y_{ab}}{\sinh \theta} = E_a \nu \quad \text{amperes } \angle \quad (476d)$$

This is the current which the input e.m.f., will deliver through the architrave admittance  $\nu$  of the net.

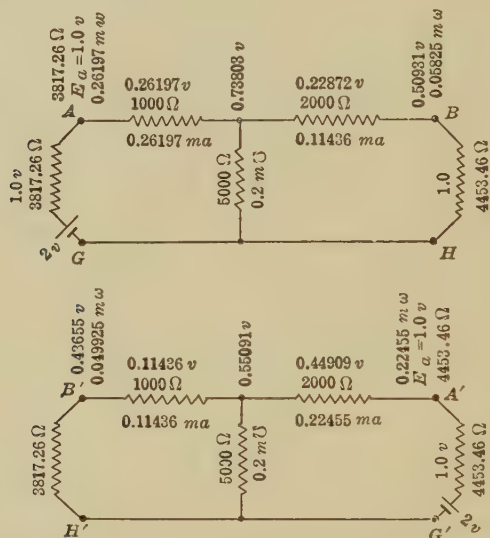
With the voltage and current ascertained at either end of the net, the power at that end follows at once, by taking their plane-vector product, one of them being first reduced to local standard phase. Thus, taking  $I$  as of standard phase or  $I = |I| \angle 0^\circ$  amperes,  $E$  will, if leading, be  $|E| \angle \beta^\circ$  volts. Their product  $P = |EI| \angle \beta^\circ$ , will be the local vector power. The real component will be active power, and the imaginary component reactive power, with  $+j$  reactive power representing inductively reactive power, or power supplied to actuate magnetic fields. Taking, on the contrary,  $E$  as of standard local reference phase, or  $E = |E| \angle 0^\circ$  volts,  $I$ , now lagging, will be  $|I| \angle \beta^\circ$  amperes. Their product  $P = |EI| \angle \beta^\circ$  will be the local vector power. The real component will be active power, as before, and the imaginary component, now of reversed sign, will be reactive power with  $+j$  reactive power representing condensively reactive power, or power supplied to actuate electrostatic fields.

**Normal Attenuation over Nets.**—If the load  $\sigma$  at the output terminals  $BH$  of a net be made equal to  $z_{ob}$  the surge impedance at that end, the position angle  $\delta_b$  of that end becomes infinite





its image impedances at the two ends, as in Figs. 198 and 199, it will be seen that a given value of impressed e.m.f. inserted at each end in turn, in this case 2 volts, will deliver the same strength of current at the other end of the net, in this case 0.11436 milliamp., the entering currents being inversely in the ratio of the two image impedances, or  $q^2$ . In this manner, any net may be equalized for equal current delivery at the two ends, under constant inserted terminal e.m.f.



FIGS. 198 and 199.—Net equalized for current delivery under constant e.m.f. impressed at either end, by application of image-impedance loads.

The receiving-end impedance with normal-attenuation net conditions takes a very simple form. If, in (472), we assign to  $\sigma$  the value  $z_{ob} = z_{ab}/q$ , we obtain

$$Z_l = z_{ab} (\sinh \theta + \cosh \theta) = z_{ab} e^{\theta} \text{ ohms } \angle \quad (478)$$

That is, the receiving-end impedance of a net under surge-impedance load is equal to the geometric mean surge impedance, multiplied by the exponent of the line angle. This corresponds to (156a) for a symmetrical net, or simple line.

Following (139) and (141), the delivered voltage and current at output terminals connected through  $z_{ob}$  become, from (473) and (474), when  $\delta_b = \alpha$ , since  $E_a = I_a z_{oa}$ ,

$$E_b = \frac{E_a e^{-\theta}}{q} \text{ volts } \angle \quad (479)$$

and

$$I_b = I_a \epsilon^{-\theta} \cdot q \quad \text{amperes } \angle \quad (480)$$

When  $q = 1$ , these expressions correspond to normal attenuation over a simple smooth line, as expressed in (140a) and (142a).

If we consider the power in a net under exponential conditions, then in the case of a c.c. net, with the slopes of current and voltage everywhere zero, the output power  $P_b$  will be the product  $E_b I_b$ , as obtained from the last two equations, and will be entirely active power.

$$P_b = E_b I_b = E_a I_a \epsilon^{-2\theta} = P_a \epsilon^{-2\theta} \quad \text{watts} \quad (481)$$

and the efficiency of power delivery over the net will be

$$\eta = \epsilon^{-2\theta} = \frac{1}{\epsilon^{2\theta}} \quad \text{numeric} \quad (482)$$

In an a.c. net, however, the size  $|P_a|$  of the input vector power, or the volt-amperes at  $A$ , will be the size of the  $E_a I_a$  product, or

$$|P_a| = |E_a I_a| \quad \text{volt-amperes} \quad (483)$$

The slope  $\overline{P_a}$  of this vector input power, to local current standard phase, must be the same as the slope of the sending-end impedance  $Z_a$ , or

$$\overline{P_a} = \overline{Z_a} = \overline{z_{oa}} \quad \text{degrees} \quad (484)$$

so that the complete vector input power will be

$$P_a = |E_a I_a| \angle \overline{Z_a} = |E_a I_a| \angle \overline{z_{oa}} \quad \text{watts } \angle \quad (485)$$

Again, the size  $|P_b|$  of the vector output power, or the volt-amperes at  $B$ , is the size of the  $E_b I_b$  product, or

$$|P_b| = |E_b I_b| = |E_a I_a \epsilon^{-2\theta}| = |P_a \epsilon^{-2\theta}| \quad \text{volt-amperes} \quad (486)$$

and the slope of this vector output power, to local current reference phase (inductively reactive power  $+j$ ) will be the same as that of  $\sigma$  or  $z_{ob}$ .

$$\overline{P_b} = \overline{\sigma} = \overline{z_{ob}} \quad \text{degrees} \quad (487)$$

and the complete vector output power is:

$$P_b = |P_a \epsilon^{-2\theta}| \angle \overline{z_{ob}} \quad \text{watts } \angle \quad (488)$$

The apparent efficiency or volt-ampere efficiency of the net is:

$$\left| \frac{P_b}{P_a} \right| = |\epsilon^{-2\theta}| = \epsilon^{-2\theta_1} \quad \text{numeric} \quad (489)$$

But the active power efficiency is:

$$\eta = \frac{|P_b| \cos \overline{z_{ob}}}{|P_a| \cos \overline{z_{oa}}} \quad \text{numeric} \quad (490)$$

If  $z_{ob} = z_{oa}$ , so that  $q = 1\angle 0^\circ$ ; or if the sizes of  $z_{ob}$  and  $z_{oa}$  differ, but their slopes are the same, the active power efficiency coincides with (489) in conformity with (142c) and (405b).

Figure 200 represents the equivalent  $T$  of a certain a.c. net with surge-impedance load and normal attenuation. The volt-ampere efficiency is 0.24377, which agrees with (489), but the active power efficiency is 0.23782.

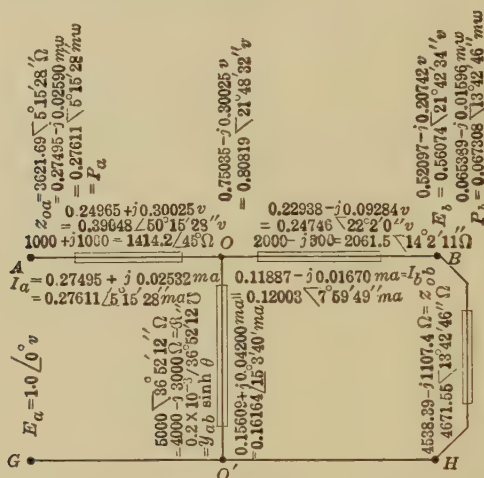


FIG. 200.—A. C. net with normal attenuation.  $\theta = 0.70577 + j0.19425$ ;  $z_{ob} = 4671.6 \angle 13^\circ.42'.46''$ ;  $q = 0.88049 \angle 4^\circ.13'.39''$ .

**Conditions for Maximum Power Output from a Net.**—If we assign to the load at the  $B$  end of any net, the particular value  $\sigma = R_{bg} = z_{ob} \tanh \theta$ , it will be evident from (466), that the position angle  $\delta_b$  at the output terminals is equal to  $\theta$ , and that at the input terminals becomes  $\delta_a = 2\theta$ . It follows from (468) that the sending-end impedance, or the impedance of the net at terminals  $AG$ , when this particular load is applied at  $BH$ , is

$$Z_a = z_{oa} \tanh (2\theta) \quad \text{ohms } \angle \quad (491)$$

and the input current, under impressed e.m.f.  $E_a$

$$I_a = \frac{E_a}{Z_a} = E_a Y_a = E_a y_{oa} \coth (2\theta) \quad \text{amperes } \angle \quad (492)$$

The input power is then:

$$P_a = |E_a^2 y_{oa} \coth (2\theta)| \angle \overline{Z_a} \quad \text{watts} \quad (493)$$

In a c.c. net, the slope is zero.

The voltage delivered at the loaded terminals is, by (473),

$$E_o = \frac{E_a \left( \frac{\sinh \theta}{\sinh 2\theta} \right)}{q} = \frac{E_a}{2q \cosh \theta} = \frac{E_{bf}}{2} \text{ volts } \angle \quad (494)$$

It is seen from (476*b*) that the voltage  $E_{bf}$  maintained at the freed or open output terminals of any net, under an impressed voltage  $E_a$  at  $AG$ , is

$$E_{bf} = \frac{E_a}{q \cosh \theta} \text{ volts } \angle \quad (495)$$

so that the voltage delivered under  $R_{bg}$  load has half the size and just the same slope as  $E_{bf}$ . In other words, if we steadily apply an e.m.f. of  $E_a$  volts, at standard phase, to the input terminals of a net, and note the voltage  $E_{bf}$  thereby produced, on open circuit, at output terminals  $BH$ ; then the load at  $BH$ , which will just reduce this to half size at the same slope, is  $\sigma = R_{bg}$ .

Again, the current delivered to the load  $\sigma$  under  $E_a$  at  $A$ , is:

$$I_b = \frac{E_b}{\sigma} = \frac{E_b}{z_{ob} \tanh \theta} = \frac{E_a}{2z_{ab} \sinh \theta} = \frac{E_a}{2\rho} = \frac{E_a \nu}{2} = \frac{I_{bg}}{2} \text{ amperes } \angle \quad (496)$$

An inspection of Fig. 189 shows that if we ground the  $B$  end, or short the  $BH$  terminals, of a net, the output current  $I_{bg}$  will be equal to the input e.m.f.  $E_a$  divided by the architrave impedance  $\rho$ , or multiplied by the architrave admittance  $\nu$ . That is

$$I_{bg} = \frac{E_a}{z_{ab} \sinh \theta} = \frac{E_a}{\rho} = E_a \nu \text{ amperes } \angle \quad (497)$$

Consequently, the current delivered to the particular load  $\sigma = R_{bg}$  in (496), has half the size and the same slope as the short-circuit current  $I_{bg}$ . In other words, if we maintain constant impressed e.m.f.  $E_a$  at input terminals, and note the strength and phase of the output current through a short at  $BH$ , the load  $\sigma$  inserted between those terminals which will halve the size of this current without altering its slope is  $\sigma = R_{bg} = z_{ob} \tanh \theta$ .

The power delivered to this load at  $B$  will be

$$P_b = \left| \frac{E_a^2}{2z_{oa} \sinh (2\theta)} \right| \angle \bar{\sigma} \text{ watts } \angle \quad (498)$$

The volt-ampere efficiency, or apparent efficiency, in an a.c. case, which corresponds to the real efficiency in a c.c. case is

$$\left| \frac{P_b}{P_a} \right| = \frac{\left| \frac{P_a (\operatorname{sech} 2\theta)}{2} \right| \cos \bar{\sigma}}{|P_a| \cos \underline{Z}_a} \text{ numeric } \quad (499)$$



In a c.c. case, however, the cosine factors both become unity and disappear, so that the efficiency of the net becomes:

$$\eta = \frac{\operatorname{sech} 2\theta}{2} = \frac{1}{2 \cosh 2\theta} = \frac{1}{\epsilon^{2\theta} + \epsilon^{-2\theta}} \quad \text{numeric} \quad (500)$$

It can be shown that for a given value of input e.m.f.  $E_a$  maintained at the  $AG$  terminals, the output of active power at  $BH$  is a maximum when the resistance of the load is  $R_{bg}$  for a c.c. net, and in an a.c. net, when the impedance of the load has the same size as the impedance  $R_{bg}$ . The maximum active output requires that the slope of  $\sigma$  should be the reverse of the slope of  $R_{bg}$ . That is, the impedance of  $\sigma$  should be the conjugate\* of the

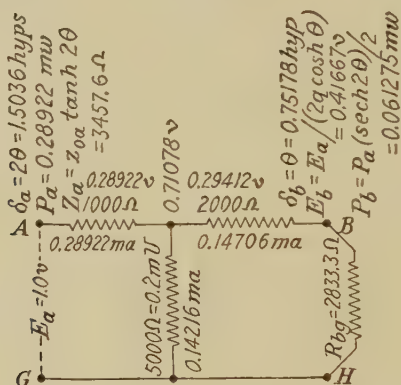


FIG. 201.—Net of Fig. 190 loaded at  $B$  with  $\sigma = R_{bg}$  for maximum output under constant e.m.f. input.

impedance  $R_{bg}$ , their resistances being equal and their reactances equal but opposite. If the nature of the load which can be applied at  $BH$  is such that its reactance cannot conveniently be made equal and opposite to that of  $R_{bg}$ , then the size of  $\sigma$  should be adjusted equal to the size of  $R_{bg}$  and its slope made as much greater than zero as is possible, in the direction opposite to that of  $R_{bg}$ .

It may be noted that, according to (500), the efficiency of a short net, as  $\theta$  approaches the limit 0, tends to become one-half or 50 per cent, for maximum output. This means that a practical power-transmission net, confining itself to an efficiency of say 90 per cent, is thereby compelled to deliver considerably less than its maximum possible output, under constant-voltage input.

\* "Transmission Circuits for Telephonic Communication" by Johnson, Chapter VIII.

In other words, efficiency of transmission, good regulation of pressure, and other considerations, are ordinarily more important than the maximum possible output.

Figure 201 illustrates the case of the c.c. net of Fig. 190, loaded at  $BH$  with  $\sigma = R_{bg} = 2,833.3$  ohms. The output voltage is 0.41667 volt or half that obtained with  $BH$  open. The output current is 0.14706 milliamp., which is half that which would be delivered in Fig. 192, through shorted  $BH$  terminals, and the output power is 0.061275 milliwatt, which is the maximum that can be furnished with 1 volt maintained at  $AG$ .

**Maximum Output at Constant Current.**—If we assign to the load at the  $B$  end of a net, the value  $\sigma = R_{bf} = z_{ob} \coth \theta$ , it will be evident from (466), that the output-end position angle is  $\delta_b = \theta + j1$ , and that at the input end becomes  $\delta_a = 2\theta + j1$ , and the sending-end impedance, by (468)

$$Z_a = z_{oa} \tanh \delta_a = z_{oa} \coth 2\theta \quad \text{ohms } \angle \quad (501)$$

If we assume that  $I_a$ , the current entering the net, is kept constant and taken as of standard phase, the input voltage will be

$$E_a = I_a Z_a = I_a z_{oa} \coth 2\theta \quad \text{volts } \angle \quad (502)$$

and the input power

$$P_a = |I_a^2 z_{oa} \coth 2\theta| \angle \overline{Z_a} \quad \text{watts } \angle \quad (503)$$

The voltage at output terminals is then by (473) (502) and (446),

$$E_b = \frac{I_a z_{ab}}{2 \sinh \theta} = \frac{I_a \Re}{2} \quad \text{volts } \angle \quad (504)$$

which has the same slope, and half the size, of the output voltage on open  $BH$  terminals, with  $I_a$  constant.

The output current through the load will also be

$$I_b = \frac{I_a q}{2 \cosh \theta} \quad \text{amperes } \angle \quad (505)$$

The output power is

$$P_b = \left| \frac{I_a^2 z_{oa}}{2 \sinh 2\theta} \right| \angle \overline{\sigma} \quad \text{watts } \angle \quad (506)$$

and the volt-ampere, or apparent efficiency, is:

$$\left| \frac{P_b}{P_a} \right| = \frac{\operatorname{sech} 2\theta}{2} = \frac{1}{2 \cosh 2\theta} = \frac{1}{\epsilon^{2\theta} + \epsilon^{-2\theta}} \quad \text{numeric} \quad (507)$$

while the real efficiency is

$$\eta = \frac{|P_b| \cos \overline{\sigma}}{|P_a| \cos \overline{Z_a}} \quad \text{numeric} \quad (508)$$

In a c.c. net, the real efficiency is, by (507)

$$\eta = \frac{\operatorname{sech} 2\theta}{2} \quad \text{numeric} \quad (509)$$

which agrees with (500), the efficiency for maximum output at constant  $E_a$ .

It may be noted that the output current through this load is of the same phase and half the size as the current produced through shorted  $BH$  terminals, with  $I_a$  constant (see (476d)).

It can be readily shown that in any c.c. net, the maximum power output is obtained, with constant-current input, when the load  $\sigma$  is equal in resistance to  $R_{bf} = z_{ob} \coth \theta$ , with an efficiency given by (509). In the case of an a.c. net, however, the corresponding rule is that the impedance of the load  $\sigma$  should be the conjugate of the impedance  $R_{bf}$ . If the reactance of the load cannot conveniently be adjusted into opposition equality with the reactance of  $R_{of}$ , then the size of  $\sigma$  should be made equal to the size of  $R_{bf}$ , and the slope of  $\sigma$  given the opposite sign to that of  $R_{bf}$ , and with a value as nearly as practicable equal to that of  $R_{bf}$ .

It can also be shown that in the case of a c.c. net, operated with constant power  $P_a$  at the input terminals, the output power will be a maximum when the load  $\sigma$  has a resistance equal to the surge resistance at that end. We have already seen that the efficiency of power delivery by the net is then, by (482),  $1/\epsilon^{2\theta}$ . This is greater than the efficiency under constant impressed e.m.f. or constant impressed current, although the difference may be very small when  $\theta$  is considerable.

In Fig. 202, the output power  $P_b$  is plotted against load resistance  $\sigma$  for the c.c. net of Figs. 190 and 192. The three curves refer to the three conditions of constant e.m.f.  $E_a$ , constant current  $I_a$  and constant power  $P_a$  at the input terminals, respectively. It will be seen that the output power is a maximum for the values  $R_{bg}$ ,  $R_{bf}$ , and  $z_{ob} = \sqrt{R_{bg} \cdot R_{bf}}$ , respectively.

With an electrically short net ( $\theta_1$  less than say 0.5), the three values of  $\sigma$ , i.e.,  $R_{bg}$ ,  $R_{bf}$ , and  $z_{ob}$ , differ considerably, and as  $\theta_1$  approaches zero, the differences become enormous. On the other hand, with an electrically long net ( $\theta_1$  greater than 3, say), these three values tend to coincide. In the case of a long telegraph line, it has long been known that the best resistance of the receiving instrument should be  $z_0$  for continuous currents,

and the conjugate of  $z_0$  for alternating\* currents. By "resistance" is here meant not joulean resistance, which would convert the output power into heat, but electrodynamic resistance or *motional resistance*, which would convert the output power into mechanical power. It is desirable that the motional resistance of the receiver should form as large a part as is practicable of the total apparent resistance of the receiver.

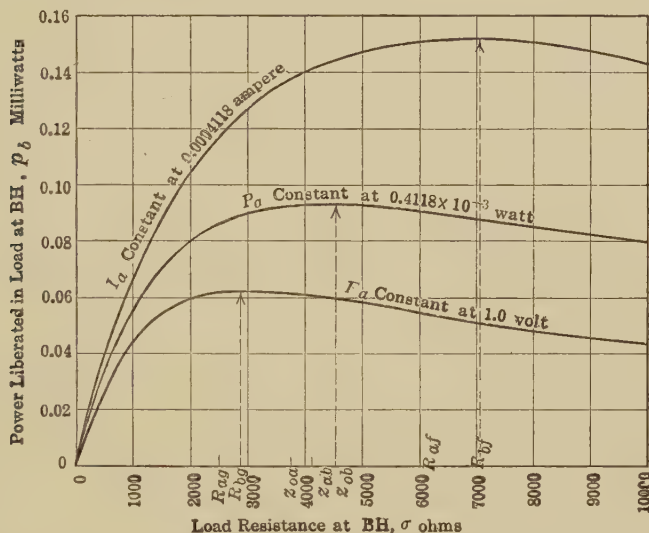


FIG. 202.—Curves of maximum power output from network of Fig. 190, under constant impressed voltage, current and power. Load resistance  $\sigma$  varied.

**The Equivalent Circuits of a Transformer.**—If we take, to begin with, an *ideal level transformer*, i.e., a transformer of unity ratio, devoid of hysteresis, resistance, and losses, it will have, by symmetry, equal inductances, and the same number of turns in both primary and secondary windings. Let such a transformer be represented by  $AG$  and  $BH$  in Fig. 203. Let the inductances in the primary and secondary windings be respectively  $\mathcal{L}_1$  and  $\mathcal{L}_2$  henrys. The mutual inductance of these will be

$$\mu = \pm k\sqrt{\mathcal{L}_1\mathcal{L}_2} \quad \text{henrys} \quad (510)$$

\* "The Best Resistance for the Receiving Instrument on a Leaky Telegraph Line" by W. E. Ayrton and C. S. Whitehead, *Jour. Inst. Elec. Engrs.*, London, 1894. "The Alternating-current Theory of Transmission Speed over Submarine Telegraph Cables" by A. E. Kennelly, *Proc. Int. Elec. Congress*, St. Louis, 1904.

where  $k$  is the coupling coefficient, a numeric which may vary between 0 and 1. The mutual reactance will then be

$$M = \pm j\mu\omega = \pm jk\omega\sqrt{\mathcal{L}_1\mathcal{L}_2} \quad j \text{ ohms } \angle \quad (511)$$

$\omega$  being the impressed angular velocity of the alternating current.

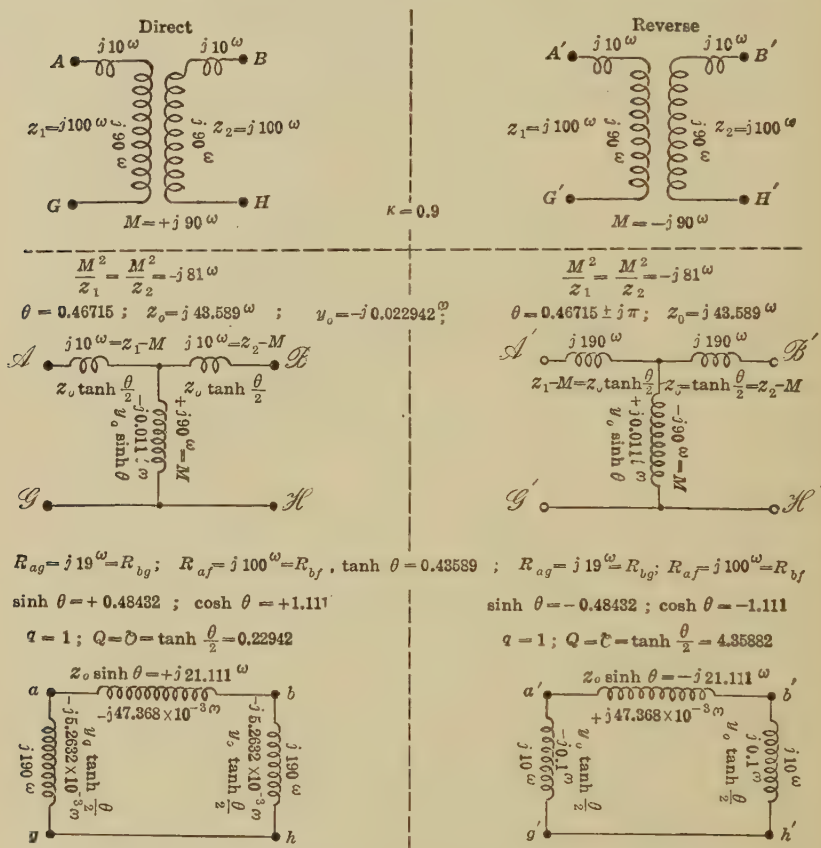


FIG. 203.—A level and lossless transformer with its two alternative  $T$ 's and  $\Pi$ 's, according to the connections of its primary and secondary windings.

This means that there are two values of the mutual reactance  $M$ , which are imaginary, and differ in sign. The primary and secondary impedances  $z_1$  and  $z_2$  will be  $j\mathcal{L}_1\omega$  and  $j\mathcal{L}_2\omega$ , respectively.

If we regard this transformer as a particular kind of net, we may measure the impedance of the primary winding at terminals  $AG$  with the  $BH$  secondary terminals open and closed, and likewise at the  $BH$  terminals with  $AG$  open and closed. We then



have according to the procedure of (445), with  $M = \pm j90$  ohms,

$$R_{af} = z_1, \quad R_{ag} = z_1 + \frac{M^2}{z_2} \quad \text{ohms } \angle^* \quad (512)$$

$$R_{bf} = z_2, \quad R_{bg} = z_2 + \frac{M^2}{z_1} \quad \text{ohms } \angle \quad (513)$$

In the case of Fig. 203,

$$z_1 = z_2 = j100, \quad k = 0.9$$

and

$$\frac{M^2}{z_1} = \frac{M^2}{z_2} = \frac{(\pm j90)^2}{j100} = -j81;$$

so that

$$R_{af} = R_{bf} = j100; \quad R_{ag} = R_{bg} = j19. \quad (514)$$

$$\tanh \theta = \sqrt{\frac{R_{ag}}{R_{af}}} = \sqrt{\frac{R_{bg}}{R_{bf}}} = \sqrt{\frac{j19}{j100}} = \sqrt{0.19} = 0.43589 \quad (515)$$

The ordinary solution of this equation, either by tables or charts, is  $\theta = 0.46715$ . There exists, however, another solution which, in the case of a transformer, is significant, namely,  $\theta = 0.46715 + j\pi = 0.46715 + j\bar{2}$ . It is always permissible to add  $\pi$  radians or 2 quadrants to the imaginary component of a hyperbolic angle, without altering the value of its tangent. In other words,  $\tanh(\theta_1 + j\theta_2)$  is a periodic function of  $\theta_2$  with  $\pi$  radians as the period.

This dual solution of (515) has, up to the present time, only become significant in dealing with nets containing transformers.

If we construct the  $T$  and  $\Pi$  of the transformer net following (447) to (461), with  $q = 1$ , and  $z_{ab} = z_o$ , we find that there are two possible  $T$ 's and two possible  $\Pi$ 's, according to whether we take one or the other of the two values of  $\theta$ , because  $\sinh(0.46715) = 0.48432$ ; but  $\sinh(0.46715 + j\bar{2}) = -0.48432$ , and  $\cosh(0.46715) = 1.111$ ; but  $\cosh(0.46715 + j\bar{2}) = -1.111$ . The two  $T$ 's are shown in the Figure at  $\mathcal{Q}\mathcal{B}\mathcal{E}\mathcal{C}$  and  $\mathcal{Q}'\mathcal{B}'\mathcal{E}'\mathcal{C}'$ . In each case the staff impedance is  $M$  ohms, but as there are two values of  $M$ , one of these is  $+j90$  ohms, and the other is  $-j90$  ohms. The branches of each  $T$  have such impedances as will make the total impedance  $\mathcal{Q}\mathcal{E}$  and  $\mathcal{B}\mathcal{C}$ , equal, respectively, to the measured impedances  $z_1$  and  $z_2$  of the primary and secondary windings, respectively.

\*"Impedance of Mutually Inductive Circuit" by A. E. Kennelly, *The Electrician*, London, Vol. 31, pp. 699-700 Oct. 27th, 1893.

One of the  $T$ 's is indicated in Fig. 203 as being "direct," and the other as being "reverse." It does not seem to be possible to distinguish between the existence of these two  $T$ 's, by any electrical tests at any one pair of terminals, with any load attached to the other. For instance, if we apply a load of 100 ohms to the secondary terminals  $\mathcal{B}\mathcal{C}$  or  $\mathcal{B}'\mathcal{C}'$  of the transformer, and apply an e.m.f. of 100 volts at the primary terminals  $\mathcal{A}\mathcal{C}$ ; the currents, voltages, and powers at these respective terminals will be the same, as if the corresponding conditions existed at the terminals of either  $T$  or of either  $\Pi$ . Any one of the four equivalent circuits will meet the external conditions equally well. So long as the primary and secondary windings are insulated from each other, this ambiguity will persist. If, however, we connect the two circuits conductively, the ambiguity can be cleared up, and only one  $T$  and its corresponding  $\Pi$  can meet the conditions. Thus, if the primary terminal  $\mathcal{C}$  is joined to the secondary terminal  $\mathcal{C}$ , and the remaining terminals  $\mathcal{A}\mathcal{B}$  of the transformer are connected to an e.m.f. of 100 volts, the current in the transformer would be  $-j5$  amp. in the direct connection, but only  $-j0.265$  amp. in the reverse connection, as is shown by considering what would happen if the corresponding  $T$ 's and  $\Pi$ 's were so treated. In the direct case, there would be a nearly direct short circuit, in the reverse case, there would be the feeble excitation current due to the effect of quadrupled self-inductance. In the direct case, the magnetic fields in the main windings would oppose. In the reverse case they would assist.

In Fig. 204, a less simple transformer is indicated with a coupling coefficient of  $k = 0.9035$  and with resistances both internal and external to the windings. The terminals of the windings or parts internal to the transformer are  $aG$  for the primary and  $bH$  for the secondary. The external fixed impedances are  $Aa$  and  $Bb$ . Here the angle  $\theta$  is again ambiguous, being either  $1.50156 + j2.3066$  or  $1.50156 + j5.4482$ , the two values differing by  $j3.1416$  or  $j2$ . The ambiguity may be cleared by suitably connecting the primary and secondary terminals.

The conclusion is, therefore, that when a transformer is included in a net, like that say of Fig. 190, the system can be reduced to an equivalent  $T$  or  $\Pi$ , without enquiring concerning the way in which the primary and secondary windings are brought out and connected. If, however, the transformer is considered, alone, as in Figs. 203 and 204, there are two possible

$T$ 's and  $\Pi$ 's,\* each of which will represent the transformer under any assigned loads, so long as the primary and secondary circuits are kept electrically separated. If, however, they are

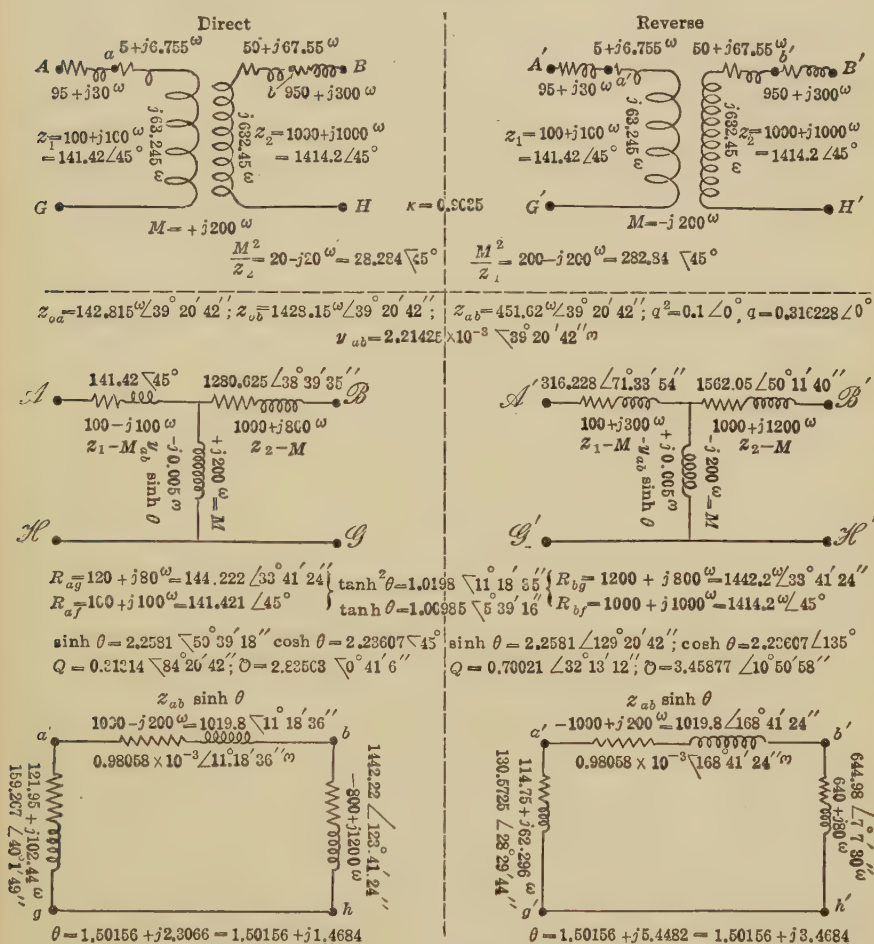


FIG. 204.—Alternative  $T$ 's and  $\Pi$ 's of an air-core transformer.

connected together at some link or links, or pairs of such transformers are connected in parallel, one or the other of these alternatives will disappear, according to the way in which the two

\* "Telephone Transformers" by W. L. Casper, *Jour. A. I. E. E.*, March, 1924, pp. 197-209; "Some Properties of Simple Electric Conducting Networks," by A. E. Kennelly, *Proc. Am. Phil. Soc.*, April, 1924, vol. lxiii, No. 2, pp. 171-189.

windings become excited, in mutual magnetic opposition, or in mutual magnetic aid.

In all cases, the ratio of transformation of the transformer is  $q$ .

**Three-terminal Nets.**—If the input and output pairs of terminals on a net have one terminal in common as in Fig. 205, the net becomes a *three-terminal net*. With respect to these three terminals, the net becomes an equivalent delta, or an equivalent  $\Pi$ , at the particular frequency considered. The three test leads may be described as the  $a$ ,  $b$  and  $g$ - $h$  test leads respec-

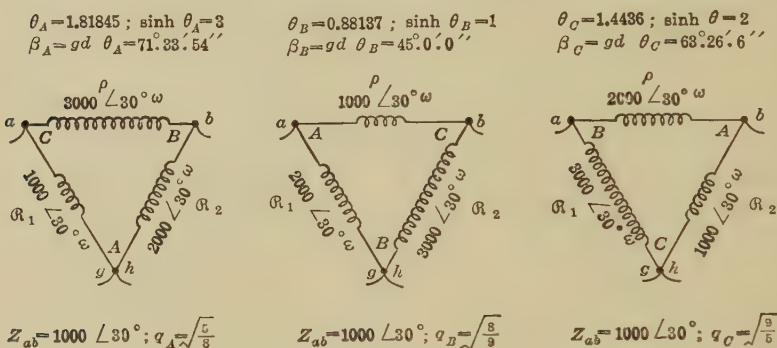


FIG. 205.—A three-terminal net in three successive aspects with respect to input and output terminals.

tively. The leads  $a$  and  $g$  belong to the input or generator test set, while  $b$  and  $h$  belong to the output or motor test set. Leads  $g$  and  $h$  are joined.

The three leads may be applied to the three terminals of the net in three different aspects, as indicated in Fig. 205. Certain properties pertain to these three different applications.\* Among them are the following:

1. The three vector values of the inequality factor, when multiplied together, give  $1 \angle 0^\circ$  as their product.
2. The geomean surge impedance  $z_{ab}$  of the net in the three aspects is the same.
3. The three angles  $\theta$  of the net in the three aspects are such that

$$\sinh \theta_A + \sinh \theta_B + \sinh \theta_C = \sinh \theta_A \cdot \sinh \theta_B \cdot \sinh \theta_C$$

numeric  $\angle$  (516)

\* "Some Properties of Three-terminal Electrical Conducting Networks," by A. E. Kennelly, *Proc. Am. Acad. Arts and Sciences*, July, 1924, vol. lix, No. 13, pp. 297-311.

If all three hyperbolic angles are real, there will correspond to each a real circular angle, known as the *gudermannian angle*  $\beta$ , see (552) to (554), such that  $\sinh \theta = \tan \beta$ . In any such case, (516) becomes

$$\tan \beta_A + \tan \beta_B + \tan \beta_C = \tan \beta_A \cdot \tan \beta_B \cdot \tan \beta_C \quad \text{numeric } \angle \quad (517)$$

which is the well-known relation connecting the three angles  $A$ ,  $B$ , and  $C$  of any plane triangle. Consequently, the three gudermannian angles, corresponding to the three aspects of the net, define the three interior angles of a certain family of similar triangles, and their sum is exactly  $\pi$  radians, or  $180^\circ$ .

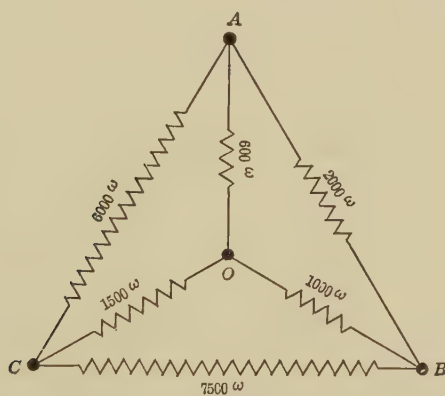


FIG. 206.—Net of six resistances, offering four sets of three-terminal subordinate nets.

As a simple example of the above relations, we may consider the six-element net of pure resistances shown in Fig. 206. The four terminals offered by the net are  $A$ ,  $B$ ,  $C$ , and  $O$ . These permit of selecting four triangles,  $ABC$ ,  $OBA$ ,  $OAC$ , and  $OBC$ . Each of these triangles offers a three-terminal arrangement, with three successive aspects. Thus the  $ABC$  triangle offers  $AC$  and  $BC$  as the input and output pairs of leads, also  $BA$  and  $CA$  and finally  $CB - AB$ . The values of  $\theta$ ,  $z_{ab}$ ,  $q$ , and other quantities, are presented in the accompanying table for all twelve of these sets. It will be seen that in each triangle, the product of the three  $q$ 's is unity, the value of  $z_{ab}$  is constant, the product of the  $\sinh \theta$ 's is equal to their sum, and the sum of the  $qd \theta$ 's is  $180^\circ$ .

**Circular Variation in Nets.**—A circular variation of any plane-vector quantity, such as voltage, current, or power, is a variation



TABLE

Data relating to the six-element

	Triangle ABC			Triangle OBA			
Terminal pairs	AC-BC	BA-CA	CB-AB	OA-BA	BO-AO	AB-OB	
$R_{ag}$	666.66	750.0	1,200	348.0	619.217	433.915	
$R_{af}$	1,333.3	833.33	1,500	468.33	668.33	833.33	
$R_{bg}$	750.0	1,200	666.66	619.217	433.915	348.0	
$R_{bf}$	1,500	1,333.3	833.33	833.33	468.333	668.333	
$\tanh^2 \theta = \frac{R_{ag}}{R_{af}} = \frac{R_{bg}}{R_{bf}}$	0.5	0.9	0.8	0.74306	0.92651	0.52070	
$\tanh \theta$	0.70711	0.94868	0.89443	0.86201	0.96255	0.72159	
$\theta$	0.88137	1.81845	1.4436	1.30112	1.97955	0.91097	
$z_{oa} = \sqrt{R_{ag} \cdot R_{af}}$	942.809	790.569	1,341.64	403.708	643.307	601.328	
$z_{ob} = \sqrt{R_{bg} \cdot R_{bf}}$	1,060.66	1,264.91	745.356	718.341	450.796	482.265	
$z_{ab} = \sqrt{z_{oa} \cdot z_{ob}}$	1,000	1,000	1,000	538.517	538.517	538.517	
$y_{ob} = \sqrt{y_{oa} \cdot y_{ob}} \times 10^3$	1.0	1.0	1.0	1.85695	1.85695	1.85695	
$q = \sqrt{\frac{z_{oa}}{z_{ob}}}$	0.94281	0.79057	1.34164	0.74967	1.19459	1.11664	
$\frac{1}{q} = \sqrt{\frac{z_{ob}}{z_{oa}}}$	$\Pi = 1$ 1.06066   1.26493   0.74536			$\Pi = 1$ 1.33393   0.83711   0.89555			
$Q = \frac{q \cosh \theta - 1}{\sinh \theta}$	0.33333	$\Pi = 1$ 0.50	1.0	0.28164	$\Pi = 1$ 0.95943	0.58804	
$Q = \frac{\frac{1}{q} \cosh \theta - 1}{\sinh \theta}$	0.50	1.0	0.3333	0.95943	0.58804	0.28164	
$\sinh \theta$	1.0	3.0	2.0	1.70058	3.55066	1.04229	
$\cosh \theta$	$\Sigma = \Pi = 6.0$ 1.414   3.1623   2.2361			$\Sigma = \Pi = 6.29353$ 1.97281   3.68874   1.4444			
$gd \theta$	45° .0' .0''   71° .33' .54''   63° .26' .6''			59° .32' .35''   74° .16' .15''   46° .11' .10''			
	180°			180°			
Elements of equivalent $\Pi$	$\rho$	1,000	3,000	2,000	915.789	1,912.09	561.29
	$\nu \times 10^9$	1.0	0.333	0.5	1.09195	0.52299	1.78161
	$R_1$	2,000	1,000	3,000	561.29	915.789	1,912.09
	$R_2$	3,000	2,000	1,000	1,912.09	561.290	915.789
Elements of equivalent $T$	$\rho_1$	333.33	500	1,000	151.66	516.66	316.66
	$\rho_2$	500	1,000	333.3	516.66	316.66	151.66
	$R$	1,000	333.3	500	316.66	151.66	516.66
	$g \times 10^3$	1.0	3.0	2.0	3.15789	6.59341	1.93548

## XXVIII

resistance network of Fig. 296

Triangle <i>OAC</i>			Triangle <i>OBC</i>		
<i>OC-AC</i>	<i>AO-CO</i>	<i>CA-OA</i>	<i>OC-BC</i>	<i>BO-CO</i>	<i>CB-OB</i>
367.50	458.658	1,046.26	466.66	655.223	1,047.38
1,068.33	468.33	1,333.33	1,068.33	668.33	1,500
458.658	1,046.27	367.50	665.226	1,047.38	466.66
1,333.33	1,068.33	468.33	1,500	1,068.33	668.33
0.34399	0.97934	0.78470	0.43682	0.98039	0.69826
0.58651	0.98962	0.88583	0.66092	0.99014	0.83562
0.67233	2.62776	1.4022	0.79445	2.65402	1.20646
626.59	463.47	1,181.11	706.085	661.746	1,253.42
782.01	1,057.24	414.864	991.382	1,057.81	558.470
700.0	700.0	700.0	836.66	836.66	836.66
1.42857	1.42857	1.42857	1.19523	1.19523	1.19523
0.89513	0.162093	1.68730	0.84393	0.79094	1.49813
$\Pi = 1$			$\Pi = 1$		
1.11716	1.51036	0.59266	1.18493	1.26432	0.66750
$\Pi = 1$			$\Pi = 1$		
0.14524	0.52381	1.38095	0.14143	0.65738	1.13546
0.52381	1.38095	0.14524	0.65738	1.13546	0.14143
0.72414	6.88525	1.90909	0.88070	7.07036	1.52120
$\Sigma = \Pi = 9.51848$			$\Sigma = \Pi = 9.47226$		
1.23466	6.9575	2.15514	1.33253	7.14073	1.82045
35° 54' 35"	81° 44' 10"	62° 21' 15"	41° 22' 13"	81° 56' 59"	56° 40' 48"
180°			180°		
506.896	4,819.67	1,336.37	736.842	5,915.49	1,272.73
1.97279	0.20748	0.74830	1.35714	0.169048	0.78571
1,336.37	506.896	4,819.67	1,272.73	736.842	5,915.49
4,819.67	1,336.37	506.896	5,915.49	1,272.73	736.842
101.66	366.66	966.66	118.33	550.0	950.00
366.66	966.66	101.66	550.0	950.0	118.33
966.66	101.66	366.66	950.0	118.33	550.0
1.03448	9.83607	2.72727	1.05263	8.45070	1.81818

of the vector over some circular arc. In other words, the locus of variation of the quantity is a circle. There are two kinds of circular variation of voltage, current, and power at a pair of output terminals of a net, namely, (1) that produced by a change of frequency impressed at the input pair of terminals, either the input voltage or the input current strength being left unchanged, and (2) that produced by circularly varying either the impressed voltage or the impressed current at the input terminals, keeping the frequency constant. Circular variation is imparted to an impressed voltage or current, if the vector change of that quantity is over some circular arc. Since a straight line is a limiting geometrical case of a circle having infinite radius, probably the simplest example of impressed circular variation is when the input impedance is made to vary along a straight-line vector locus. Thus, if from a pair of constant-potential mains, current is led to the input terminals of a net, through a variable rheostat, the impedance of the net plus rheostat will vary along a straight line as the resistance in the rheostat is changed, the frequency being kept constant. This is a circular variation of impedance at the constant potential mains, and involves circular variation both of voltage and current at the  $A$  input terminals. If the net be replaced by its equivalent  $T$  or with respect to input and output terminals, it can be readily shown\* that circular variation will also be imported into the vector voltage, current, and power at the output terminals under any constant-load impedance  $\sigma$ . Moreover, by successive repetitions of the demonstration with respect to different elements of the net, it will follow that circular variation of voltage, current, and power will be imposed in each and every element or link of the net, although the kind of circular variation is, in general, very different in different elements. It may thus be inferred that if circular variation is imparted to any element of the net, including input or output terminals, corresponding circular variations will be repeated all over the net and in each element of the same.

**Identical Nets Connected in Series.**—When two identical nets with corresponding pairs of terminals are connected in series, the connection can be made in three ways; namely

\* "Alternating-Current Plane-vector Potentiometer Measurements at Telephonic Frequencies," A. E. Kennelly and Edy Velandar, *Proc. Am. Phil. Soc.*, vol. lviii, April, 1919, pp. 97-132; and "Cisoidal Oscillations" by G. A. Campbell *Trans. A. I. E. E.*, April, 1911, vol. xxx, part 2, p. 873.

1. In back-to-back *A*-connection with *AG* connected to *A'G'*.
2. In back-to-back *B*-connection with *BH* connected to *B'H'*.
3. In forward connection, with *BH* connected to *A'G'*, or *B'H'* to *AG*.

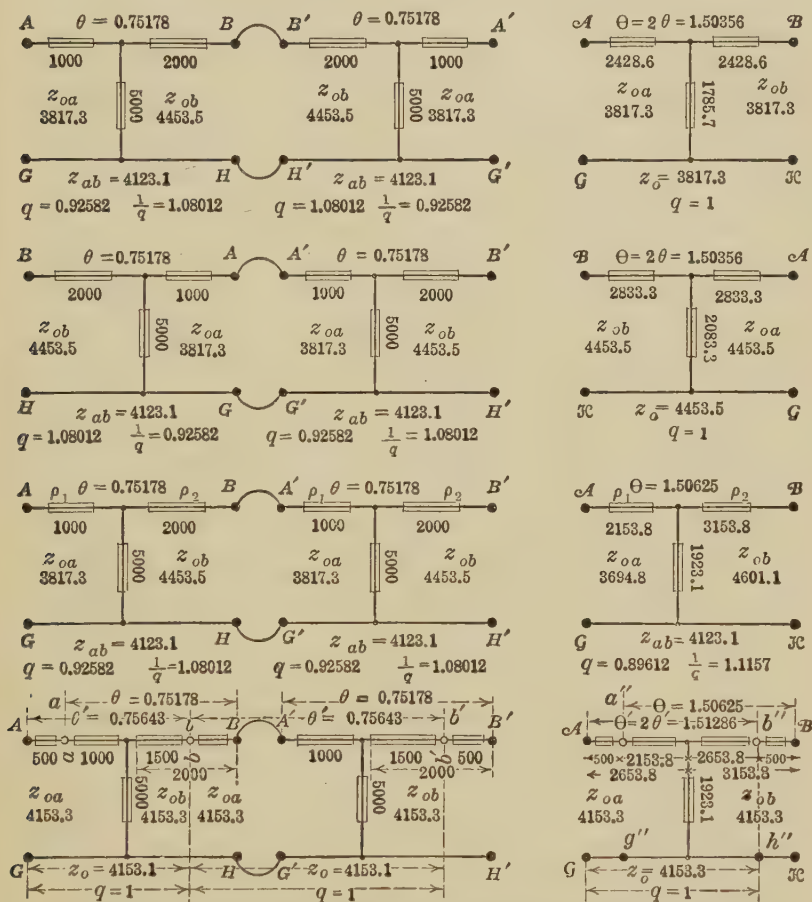


Fig. 207.—Methods of dealing with pairs of identical networks in series.

These different cases are illustrated in Fig. 207. On the first line, we have two identical *T*'s connected back-to-back *B*. Each of these *T*'s represents the c.c. net of Fig. 190. Each has the net constants  $\theta = 0.75178$ ,  $z_{ab} = 4,123.1$ , and  $q = 0.92582$ . When connected in series at their *B* ends, the equivalent *T* of the combination is shown at  $\mathcal{A}\mathcal{B}\mathcal{C}$ . Here the angle  $\Theta$  of the final net is the sum of the two component angles  $\theta$ . The final net is

symmetrical, or  $q = 1$ . The surge impedances are the same at both ends, and equal to  $z_{oa}$  of the component nets.

On the second line of Fig. 207, we have the same two nets connected back-to-back *A*. The resultant net has for its angle  $\Theta$ , the sum of the two component angles, and is symmetrical, its surge impedance  $z_0$  being equal to that of  $z_{ob}$  in the component nets.

On the third line of the figure, the same two nets are joined in simple forward connection, the *A* end of the second net being case connected to the *B* end of the first. The resultant net in this has an angle  $\Theta$  which is not the sum of the two component angles, and the surge impedances at the two ends are not the same as those of the components. The  $q$  of the resultant net is not that of the components, although the geomean surge impedance  $z_{ab}$  remains the same as that of the components.

We may now state the following propositions based upon these and similar series connections:

1. When two nets are connected in series, the angle of the combination net will be the sum of the two component angles only when the surge impedances of the two connected ends are the same, both in size and slope.

2. The back-to-back connection of two identical dissymmetrical nets produces a symmetrical resultant net of doubled angle, and of surge impedance equal to the external surge impedances of the components.

3. Any symmetrical net may be split up into a pair of component half-angle nets connected back-to-back, the external surge impedances of the components being equal to each other and to the surge impedance of the original. Moreover, since this splitting of the original net into two identical semi-angle components may be made for each and every value of  $q$ , the splitting can be effected in an infinite number of ways.

When we join two identical nets in simple forward connection, as on line 3 of Fig. 207, the following relations hold for the  $\theta$  and  $q$  of the combination net:

$$\sinh \Theta = \left( q + \frac{1}{q} \right) \sinh \theta \cosh \theta \quad \text{numeric } \angle \quad (518)$$

and

$$q' = \sqrt{\frac{(q^2 + 1) \cosh^2 \theta - 1}{(1/q^2 + 1) \cosh^2 \theta - 1}} \quad \text{numeric } \angle \quad (519)$$



It is evident that when  $q = 1$ , or the component nets are symmetrical,  $\Theta = 2\theta$ , and  $q' = 1$ , or the angles are summative and the combination net\* is symmetrical.

If the impedances of the  $A$  and  $B$  branches of a component net are denoted by  $\rho_1$  and  $\rho_2$  vector ohms, respectively, it may be noted that the difference  $\rho_2 - \rho_1$  for the combination net is the same as that for each of its identical components. The same is true for a resultant net of any number of identical component nets in simple forward connection. This suggests the following method of treating the forward connection of any number of identical dissymmetrical nets, illustrated at line 4 of Fig. 207. Reduce the artificial line of  $n$  identical nets to the equivalent of  $n$  symmetrical sections, by removing the half-branch difference  $(\rho_2 - \rho_1)/2$  from one end to the other. In Fig. 207, the branch difference of each component  $T$  is 1,000 ohms, so that if 500 ohms is taken off the  $B$  end at  $bB$ , and added to the  $A$  end at  $Aa$ , we virtually produce a two-section artificial line of uniform sections, each section having 1,500 ohms in each  $T$  branch. The angle of each symmetrical section is changed to  $\theta' = 0.75643$ , with  $z'_0 = 4,153.3$ . The combination net of  $n$  such sections will have an angle  $n\theta$ , and the same surge impedance throughout. We now form the equivalent  $T$  of this combination at  $@@b''h''$ , which will be symmetrical. Finally, we remove the half-difference  $(\rho_2 - \rho_1)/2$ , in this case 500 ohms, from the  $A$  to the  $B$  end, forming the  $T$ ,  $a''g''@3C$ , which agrees with the dissymmetrical  $T$ ,  $@@3C$  immediately above it.

\*"Identical Electrical Networks in Series." A. E. Kennelly. *Proc. Am. Phil. Soc.*, Vol. 64, April, 1925.

## CHAPTER XIX

### USE OF AN ARTIFICIAL LINE AS A FILTER FOR ALTERNATING-CURRENT FREQUENCIES

Artificial-line filters may be classified, with reference to their selective action, into the following groups:

1. Low-pass filters
2. High-pass filters
3. Band-pass filters
4. Band-suppression filters

In a mixed-frequency alternating-current stream, class 1 is intended to suppress all frequencies above a certain critical value, called the cutoff frequency. Class 2 is intended to suppress all frequencies below an assigned cutoff frequency. Class 3 should give passage only to a certain band of frequencies above an assigned lower cutoff and below an assigned upper cutoff, while class 4 is intended to suppress such a band only.

Filters may also be classified, with reference to their electric structure, into the following groups:

- a.* Single-section filters (either  $T$  or  $\Pi$ ).
- b.* Multiple-section filters. This class may again be subdivided as follows:
  - (1) Uniform-section filters, in which all the sections are identical; so that all have the same section angle  $\theta$ , and the same surge impedance  $z_0$ .
  - (2) Composite-section filters in which all the surge impedances are matched or made equal at section junctions, although not necessarily uniform as to either  $z_0$  or  $\theta$ , per section.
  - (3) Non-uniform-section filters, in which the sections differ both as to  $\theta$ , as to  $z_0$ , and as to  $z_0$  connections.

Classes *a*, *b*(1) and *b*(2) may be investigated according to the principles of artificial lines, as discussed in preceding chapters. We shall first assume that a filter belongs to class *b*(1) by being composed of uniform sections, with the understanding that the discussion can be extended to filters of class *b*(2), ordinarily with

but little additional difficulty. We may select for consideration the five-section low-pass filter shown in Figs. 208 and 209, which is arranged as an artificial line of  $T$ -sections. Each  $T$ -section has a total series inductance of 0.04 henry, and a shunt capacitance of  $10^{-6}$  farad, or 1  $\mu$ f. From what has been discussed in Chapter XV, concerning  $I$ - and  $O$ -sections, it will be evident that the  $T$ -sections of Fig. 208 might be converted into balanced  $I$ -sections of the same electrical behavior, by taking 0.01 henry

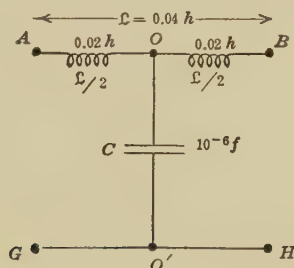


FIG. 208.—Single low-pass  $T$  filter section.

from the branch  $AO$ , and inserting it in the branch  $G'O$ , and likewise taking 0.01 henry from  $OB$ , and inserting it in  $O'H$ .

It is also assumed, at the outset, that the inductances and capacitances used in the filter are pure, or that the resistances they contain may be neglected. This restriction may be removed later, with but little extra difficulty.

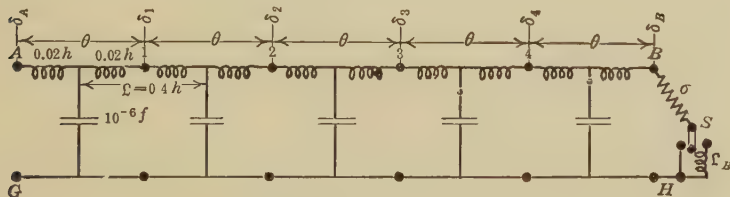


FIG. 209.—Five-section filter of the type of Fig. 208.

**Section-angle  $\theta$ .**—The cutoff properties of any uniform filter, such as that of Fig. 209, depend upon the section-angle  $\theta$ , and upon the surge impedance  $z_0$ . These may be found from (176) and (180), if, as is usually the case, the filter sections are symmetrical  $T$ -sections. If they are  $\Pi$ -sections, they may be found from (185) and (188). The ordinary artificial line is considered from the standpoint of substantially constant impressed frequency, and with relation to different lengths or

different terminal conditions. A filter is primarily considered, however, from the standpoint of substantially constant terminal conditions, but of variable impressed frequency. We have, therefore, to prepare a table or diagram indicating how  $\theta$  and  $z_0$  change under impressed changes in frequency  $f$ , or angular velocity  $\omega$ .

Following (193) and (199), for the case, say, of a low-pass filter section, like that of Fig. 208, we have:

$$\mathbf{r} = j\mathcal{L}\omega \quad \text{ohms } \angle \quad (520)$$

$$\mathbf{g} = jC\omega \quad \text{mhos } \angle \quad (521)$$

so that the first-approximation section-angle  $\theta_a$ , uncorrected for lumpiness, is

$$\theta_a = \sqrt{\mathbf{r}\mathbf{g}} = j\omega\sqrt{\mathcal{L}C} \quad \text{hyps. } \angle \quad (522)$$

and the approximate half-section angle is, therefore,

$$\frac{\theta_a}{2} = \frac{\sqrt{\mathbf{r}\mathbf{g}}}{2} = j\frac{\omega\sqrt{\mathcal{L}C}}{2} \quad \text{hyps. } \angle \quad (523)$$

The true section-angle  $\theta$ , corrected for lumpiness, is then, by (199),

$$\sinh \frac{\theta}{2} = \frac{\sqrt{\mathbf{r}\mathbf{g}}}{2} = j\frac{\omega\sqrt{\mathcal{L}C}}{2} \quad \text{numeric } \angle \quad (524)$$

From this formula,  $\theta/2$  and  $\theta$  may be found as a function of the impressed angular velocity  $\omega$ . A somewhat more convenient formula, however, is obtained if we find the cut-off angular velocity  $\omega_0$ , which will be shown to be, in this case,

$$\omega_0 = \frac{2}{\sqrt{\mathcal{L}C}} \quad \text{radians/sec.} \quad (525)$$

In the case of Fig. 208,

$$\omega_0 = \frac{2}{\sqrt{0.04 \times 10^{-6}}} = \frac{2}{\sqrt{4 \times 10^{-8}}} = 10^4 \frac{\text{rad.}}{\text{sec.}}$$

We may then define the ratio of the impressed frequency to the cutoff frequency as the *frequency ratio*  $u$ , or

$$u = \frac{\omega}{\omega_0} = \frac{f}{f_0} \quad \text{numeric} \quad (526)$$

From this standpoint, (524) becomes

$$\sinh \frac{\theta}{2} = ju \quad \text{numeric } \angle \quad (527)$$

or

$$\frac{\theta}{2} = \sinh^{-1}(ju) \quad \text{hyps. } \angle \quad (528)$$

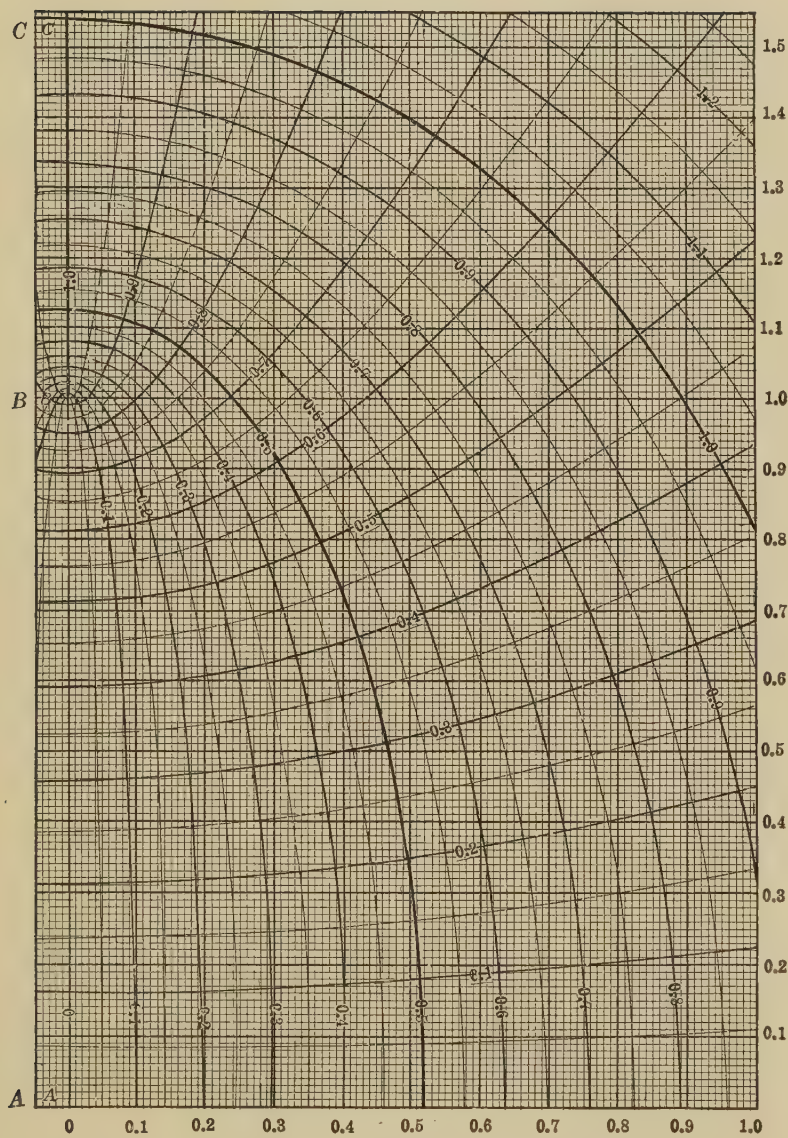


FIG. 210.—Chart for evaluating  $\sinh^{-1} ju$ .



The problem is, therefore, that of finding the inverse sinh function or antisinh of a quantity  $ju$ , which, in the case of this filter section, assumed to have no losses, is a pure imaginary or simple  $j$  number.

Figure 210 shows a portion of a chart\* from which  $\theta/2$  can be found in (528). Consider this diagram as mounted on a wall facing the observer, so that the line  $AB$  or  $j$  axis is vertical. Enter the chart at the point  $A$ , and follow the vertical line  $AB$ , until the position by the rectilinear background coördinates is equal to  $ju$ . The figure extends as far as  $ju = j1.55$ . Having found a point on  $AB$  corresponding to the given value of  $ju$ , read off this point with reference to the curvilinear coördinates, which are read along the ellipses in  $\theta_1$ , and along the hyperbolas in  $\theta_2$ , as quadrants.

Thus, at the point on the line  $AB$  corresponding to  $j0.71$ , nearly halfway up the diagram, we find that  $\theta_1 = 0$  and  $\theta_2 = 0.5$ , or half a quadrant.  $\theta_1$  is zero for all points along the line  $AB$ , up to and including  $ju = j1.0$ . We are thus able to prepare Table XXIX. Here the first column contains the impressed angular velocity  $\omega$ , and the next the corresponding pure imaginary frequency ratio  $ju$ . The third column gives the value of  $\theta/2$ , as found in Fig. 210, with  $\theta_2/2$  expressed in quadrant measure. The fourth column substitutes for the latter circular-radian measure, in the ratio of  $\pi/2$  radians per quadrant. The two last columns give the doubled corresponding values for the section-angle  $\theta$ .

Following Fig. 210 and Table XXIX, up to  $ju = j1.0$ , it will be seen that  $\theta/2$  increases regularly up to  $0 + j1.0$ . As soon as we go beyond this value of  $ju$ , we reach a region in the diagram of Fig. 210 where the points on the line  $AB$  are no longer accessible by the central flat ellipse of  $\theta_1 = 0$ . They can only be reached by taking some other  $\theta_1$  ellipse, although  $\theta_2$  continues at  $1.0$  or 1 quadrant ( $\pi/2$  radians or  $90^\circ$ ). Thus at  $ju = j1.15$ , the point on  $AB$  is found at the intersection of ellipse  $\theta_1 = 0.5$  and of hyperbola  $\theta_2 = 1.0$ ; so that  $\theta/2 = 0.5 + j1.0$ . When using the chart inversely for the first time, all the points in Table XXIX should be identified upon it.

If we plot the section angle  $\theta$  for the filter section of Fig. 208, against  $u$ , the frequency ratio, using the entries in the last

\* Part of Chart VII-VIIIA of the "Chart Atlas of Complex Hyperbolic and Circular Functions."

TABLE XXIX

Section angle  $\theta$  for a  $T$ -filter of the type shown in Fig. 208 as a function of the frequency ratio  $u$

$\omega$	$j\omega = \frac{j\omega}{\omega_0}$	$\frac{\theta}{2} = \sinh^{-1}(ju)$		$\theta = \theta_1 + j\theta_2$	
		$q$ Quadrants	$\theta_2$ Circ. radians	$q$ Quadrant	$\theta_2$ Circ. radians
1	2	3	4	5	6
		$\frac{\theta_1}{2} + j\frac{q}{2}$	$\frac{\theta_1}{2} + j\frac{\theta_2}{2}$	$\theta_1 + jq$	$\theta_1 + j\theta_2$
0	0	$0 + j0$	$0 + j0$	$0 + j0$	$0 + j0$
1,000	$j0.1$	$0 + j0.0638$	$0 + j0.1062$	$0 + j0.1276$	$0 + j0.2004$
2,000	$j0.2$	$0 + j0.1283$	$0 + j0.2014$	$0 + j0.2566$	$0 + j0.4028$
3,000	$j0.3$	$0 + j0.191$	$0 + j0.3047$	$0 + j0.388$	$0 + j0.6094$
4,000	$j0.4$	$0 + j0.262$	$0 + j0.4115$	$0 + j0.524$	$0 + j0.8230$
5,000	$j0.5$	$0 + j0.333$	$0 + j0.5236$	$0 + j0.666$	$0 + j1.0472$
6,000	$j0.6$	$0 + j0.4095$	$0 + j0.6435$	$0 + j0.819$	$0 + j1.2870$
7,000	$j0.7$	$0 + j0.493$	$0 + j0.7753$	$0 + j0.986$	$0 + j1.5506$
8,000	$j0.8$	$0 + j0.590$	$0 + j0.9273$	$0 + j1.180$	$0 + j1.8546$
9,000	$j0.9$	$0 + j0.712$	$0 + j1.1197$	$0 + j1.424$	$0 + j2.2394$
10,000	$j1.0$	$0 + j1.0$	$0 + j1.5708$	$0 + j2.0$	$0 + j3.1416$
11,000	$j1.1$	$0.4436 + j1.0$	$0.4436 + j1.5708$	$0.8872 + j2.0$	$0.8872 + j3.1416$
12,000	$j1.2$	$0.6223 + j1.0$	$0.6223 + j1.5708$	$1.2446 + j2.0$	$1.2446 + j3.1416$
13,000	$j1.3$	$0.7565 + j1.0$	$0.7565 + j1.5708$	$1.513 + j2.0$	$1.513 + j3.1416$
14,000	$j1.4$	$0.8670 + j1.0$	$0.8670 + j1.5708$	$1.734 + j2.0$	$1.734 + j3.1416$
15,000	$j1.5$	$0.9624 + j1.0$	$0.9624 + j1.5708$	$1.9248 + j2.0$	$1.9248 + j3.1416$

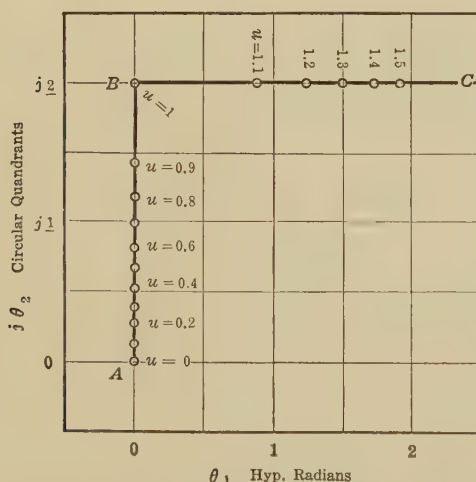


FIG. 211.—Vector graph of  $\theta$  as a function of frequency ratio  $u$  for the  $T$  filter section of Fig. 208.

column but one of Table XXIX, we produce the vector diagram of Fig. 211, where the origin of coordinates is at  $A$ ; and  $AB$  is the  $j$ -axis. It is seen that as  $u$  increases from 0 to 1.0, *i.e.*, as the impressed frequency increases from zero to the cutoff frequency,  $\theta$ , is a purely imaginary quantity  $0 + j\theta_2$ . Immediately we pass  $u = 1$ , or exceed the cutoff frequency, the locus changes

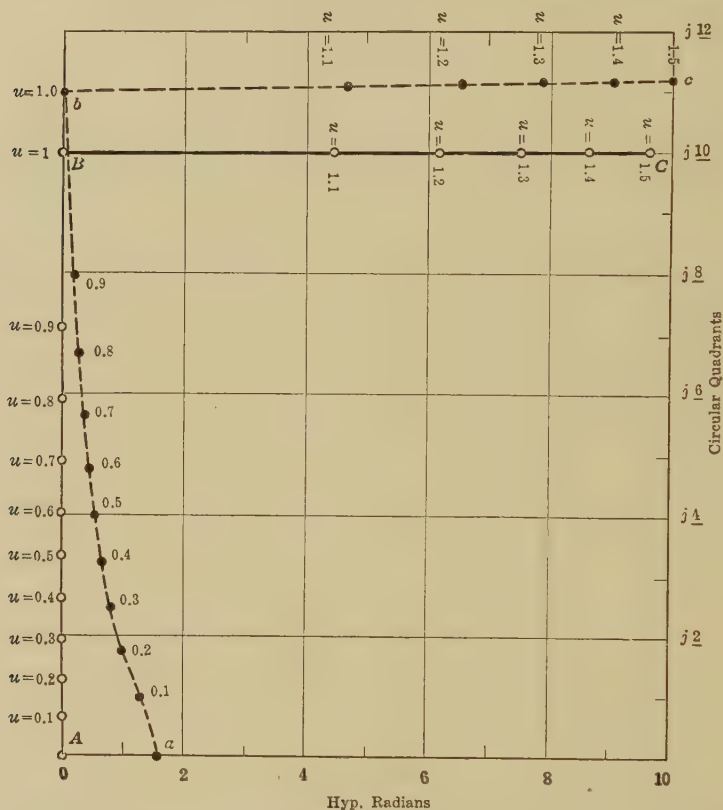


FIG. 212.—Graph of  $\theta$  or total angle of the low-pass  $T$ -filter of Fig. 208, as a function of the frequency ratio  $u$ . Also the graph of  $\delta_A$  for the 5-section filter of Fig. 209, when the load  $\sigma$  is 183.3 ohms with 0.0265 henry.

abruptly to the horizontal line  $BC$ . At  $u = 1.1$ , for instance,  $\theta = 0.89 + j2.0$ . As  $u$  is further increased, the real part  $\theta_1$  increases rapidly.

If we consider what happens when such an artificial line section is used on a surge-impedance load  $\sigma = z_0$ , we find, from (320), that the potential and current at  $B$  are attenuated rela-

tively to the impressed potential and current at  $A$ , in the ratio  $\epsilon^{-\theta} = \epsilon^{-(\theta_1 + j\theta_2)} = \epsilon^{-\theta_1} \angle \theta_2$ . When, therefore,  $\theta_1$  vanishes, the attenuation ratio is simply  $1.0 \angle \theta_2$ . That is, there is phase attenuation or slope attenuation but there is no size attenuation. The potential and current at the output terminals  $BH$ , Fig. 209, differ only in phase from those at the input terminals  $AG$ . There is no loss of potential or current in this artificial-line section. Consequently, when  $\omega$  is less than the cut-off value  $\omega_0$ , or  $u$  is less than 1.0, the filter section, assumed as having reactance but no resistance in its construction, will produce no loss of a.c. voltage, current, or power, but only change of phase. As soon, however, as we pass  $\omega = \omega_0$ , or  $u = 1$ ,  $\theta_1$ , the real part of  $\theta$ , springs into existence, and attenuation on a surge-impedance load will occur in both voltage and current, to the amount of  $\epsilon^{-\theta_1}$ , together with a change in phase of 2 quadrants, or  $180^\circ$  per section.

The *total angle* subtended by a filter artificial line of  $n$  sections is

$$\Theta = n\theta = n(\theta_1 + j\theta_2) \quad \text{hyps. } \angle \quad (529)$$

Consequently, the rapidity of cutoff with a filter of  $n$  sections is  $n$  times swifter than with a filter of one section. This is indicated in the vector diagram of Fig. 212; where the angle  $\Theta$  of a five-section filter is comparable with that of the one-section filter in Fig. 211.

Although the vector value of  $\Theta$  is indicative of the cutoff properties of any filter, when plotted as a function of  $u$ , yet it is necessary to determine the value of the surge impedance  $z_0$  as a function of  $\omega$  or of  $u$ , in order to compute the behavior of a filter under given terminal conditions.

**Surge Impedance  $z_0$ .**—Following (201), the surge impedance of any  $T$ -section or series of similar  $T$ -sections is

$$z_0 = \sqrt{\frac{\mathbf{r}}{\mathbf{g}}} \cdot \cosh \frac{\theta}{2} \quad \text{ohms } \angle \quad (530)$$

For the case of a section like that of Fig. 208, this becomes

$$z_0 = \sqrt{\frac{j\mathfrak{L}\omega}{jC\omega}} \cdot \cosh \frac{\theta}{2} = \sqrt{\frac{\mathfrak{L}}{C}} \cdot \cosh \frac{\theta}{2} = z_{00} \cosh \frac{\theta}{2} \quad \text{ohms } \angle \quad (531)$$

With the values of  $\mathfrak{L}$  and  $C$  taken in our example, and

$$z_0 = 200 \cosh \frac{\theta}{2} \quad \text{ohms } \angle \quad (532)$$

That is, the surge impedance varies over a wide range with the impressed frequency. A vector graph of  $z_0$ , with respect to  $u$ , is given in Fig. 213. It will be seen that the graph is discontinuous, diminishing from a real resistance  $200\ \Omega$  at  $u = 0$  down to zero at the cutoff ( $u = 1$ ). At the cutoff frequency, therefore, the impedance of a long artificial-line filter of this type would constitute a direct short-circuit, if it were not for the

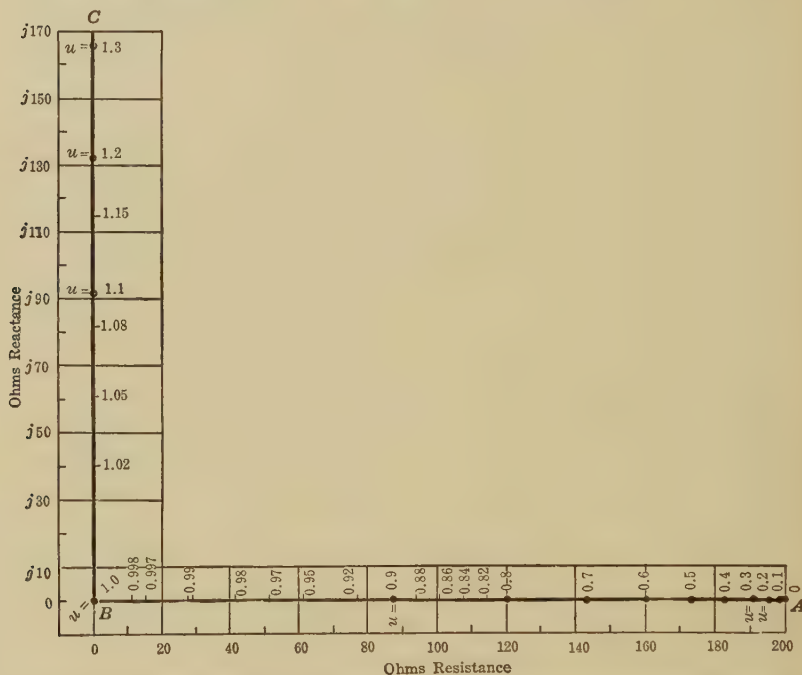


FIG. 213.—Vector graph of  $z_0$  for the particular low-pass  $T$ -filter of Figs. 208 and 209.

small internal resistances in the elements, here neglected. Beyond  $u = 1$ ,  $z_0$  increases in value indefinitely, as a pure inductive reactance.

**Behavior of Filter under Load.**—In order to determine the behavior of a filter artificial line under assigned terminal conditions as the impressed frequency changes, we follow the procedure indicated in (106), (107) and (108), illustrated in Figs. 36 to 38, and find the position angle at  $B$ , from the formula

$$\tanh \delta_B = \frac{\sigma}{z_0} \quad \text{numeric } \angle \quad (533)$$



Unless  $\sigma$  is a pure resistance, it will change with change in impressed frequency, and we have seen that  $z_0$  also changes materially with  $\omega$ , so that  $\delta_B$  varies with  $\omega$ . A vector diagram of  $\delta_B$  is given in Fig. 214, for several different loads, in the arrangement of the five-section low-pass filter of Fig. 209. For a pure resistance of  $\sigma = 183.3\Omega$ , the vector graph is  $Ab'd'Df$ , as far as  $u = 1.5$ . This graph consists of four straight lines, parallel to either the real or imaginary axis. If an inductance 0.0225 henry is added to the resistance of 156 ohms in  $\sigma$ , the

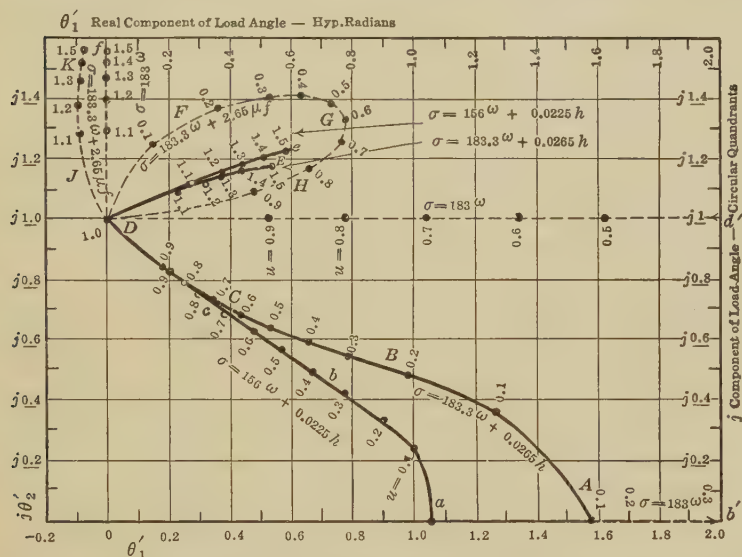


FIG. 214.—Vector graphs of  $\delta_B$  for the filter of Fig. 209 under different terminal loads, as a function of frequency ratio.

graph becomes  $abcDe$ . Increasing the inductance to 0.0265 henry, and the resistance to 183.3 ohms, changes this graph to  $ABCDE$ . If a condenser of  $2.65\ \mu\text{f.}$  replaces the inductance in the load  $\sigma$ , the graph is changed to  $DFGHDJK$ .

The position angle at  $A$  is obtained by adding  $\theta$  to  $\delta_B$ , according to (107). This varies with  $\omega$ , since both  $\delta_B$  and  $\theta$  depend upon  $\omega$ . In order to study the properties of a given filter, it is advantageous to prepare a graph of  $\delta_A$ , as a function of  $\omega$  or of  $u$ . Thus the broken line in Fig. 212 traces the vector  $\delta_A$ , from  $u = 0$  to  $u = 1.5$ , over the path  $abc$  when  $\sigma$  contains 183.3 ohms and 0.0265 henry.



will be seen that at  $u = 0$ , the received current is  $PA = 0.005$  amp. with  $1.0\angle 0^\circ$  volt, of zero frequency or continuous current, at  $A$ . At  $u = 0.3$ , the current  $I_B$  is  $PB$  nearly  $180^\circ$  in phase behind  $PA$ . At  $u = 0.6$ ,  $I_B = PC$ , about  $0.06\angle 360^\circ$ . At or near  $u = 0.8$ , it is  $PD = 0.087\angle 530^\circ$ , and at  $u = 0.95$ , it is  $PE = 0.016\angle 720^\circ$ . Beyond  $u = 0.972$ , the received current goes up very rapidly, and out of bounds for the figure, but a

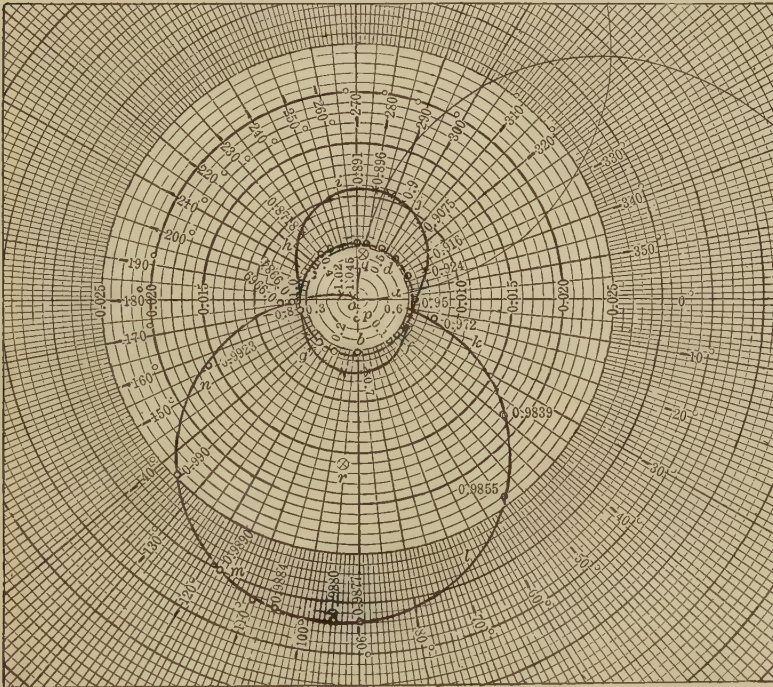


FIG. 216.—Vector graph of  $I_B$  for the 5-section  $T$ -filter of Fig. 209, delivered through a terminal load of 183 ohms, as a function of frequency ratio  $u$ .

little beyond cutoff, at  $u = 1.02$ , it has come back along the line  $GP$  to  $0.003\angle 990^\circ$ , and at  $u = 1.046$ , it is  $0.001\angle 990^\circ$ . It soon becomes vanishingly small as  $u$  further increases. The algebraical expression for  $I_B$  under constant  $E_A$  voltage at  $A$  is

$$I_B = E_A \cdot y_{00} \sec\left(\frac{\beta}{2n}\right) \angle \beta = E_A \cdot y_{00} \sec \beta' \angle (2n\beta') \text{ amp. } \angle \quad (533a)$$

where  $y_{00} = 1/z_{00}$ , or in this case 0.005 mho, and  $u = \sin \beta'$ . Also  $\beta = 2n\beta'$ ,  $n$  being the number of sections in the filter. Such a spiral may be described as a "secant spiral." Analogous



spirals, with successively varying integral values of  $n$ , will present themselves in the values of the current at successive junctions along the filter.

In order to apply a surge-impedance load for the case just considered, it would be necessary to vary  $\sigma$ , step by step, as the frequency was varied, and to make  $\sigma = 0$  at  $u = 1.0$ . With any fixed load  $\sigma$  of resistance, or mixed resistance and reactance, the conditions would be likely to be very different. Thus, if in Fig. 209, the load  $\sigma$  be made a pure resistance of 183.3 ohms, with  $1.0 \angle 0^\circ$  volt at  $A$ , and varied frequency, the same formulas (118) to (131) give for  $I_B$ , the vector graph of Fig. 216, assuming no resistance in the five-section filter. At  $u = 0$ ,  $Oa = 0.005 \angle 0^\circ$ .

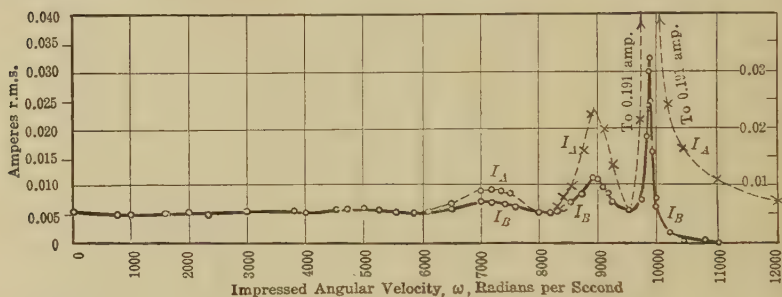


FIG. 217.—Scalar diagram of sending- and receiving-end currents for the 5-section filter of Fig. 209 with a B-terminal load of 183 ohms and variable impressed angular velocity.

At or near  $u = 0.6$ ,  $I_B = 0.055 \angle 370^\circ$ . At  $u = 0.95$ ,  $I_B = 0.0055 \angle 720^\circ$ . At  $u = 0.9877$ ,  $I_B = 0.032 \angle 810^\circ$ , and at  $u = 1.0$ ,  $I_B = 0.006 \angle 900^\circ$ ; but rapidly dwindling. The loops of this graph are nearly circular, with centers near the straight line  $qopr$ .

The scalar graphs of  $I_B$  and  $I_A$  are given for this case in Fig. 217, with ordinates, amperes, and abscissas impressed frequency. It will be seen that both  $I_B$  and  $I_A$  graphs practically coincide as far as  $\omega = 6,000$ . Above that angular velocity,  $I_B$  falls below  $I_A$ . There are five current rises at or near  $\omega = 3,000$ , 5,000, 7,200, 9,000, and 9,900, with the last one the principal peak. In general, there is one such rise for each section in the filter. At 9,900, the input current  $I_A$  rises to 0.191 amp., and  $I_B$  to 0.032. Above  $\omega = 10,000$ ,  $I_B$  falls off\* rapidly.

\* "Computation of the Behavior of Electric Filters under Load," by A. E. Kennelly and A. Slepian, *Proc. Am. Ac. Arts & Sciences*, October, 1925, vol. lx, No. 10, pp. 461-483.

Figure 218 gives the vector graph of  $I_B$  for the same filter, when an inductance of 0.0265 henry is added in the load  $\sigma$  to the resistance of 183.3 ohms. The e.m.f. at  $A$  is  $1.0\angle 0^\circ$  volt, as before. The effect of the added inductance at  $B$  is seen, by comparison with Fig. 216, to enlarge the loops, diminish their approach to circularity, and rotate in a clockwise direction the line of approximate centers.

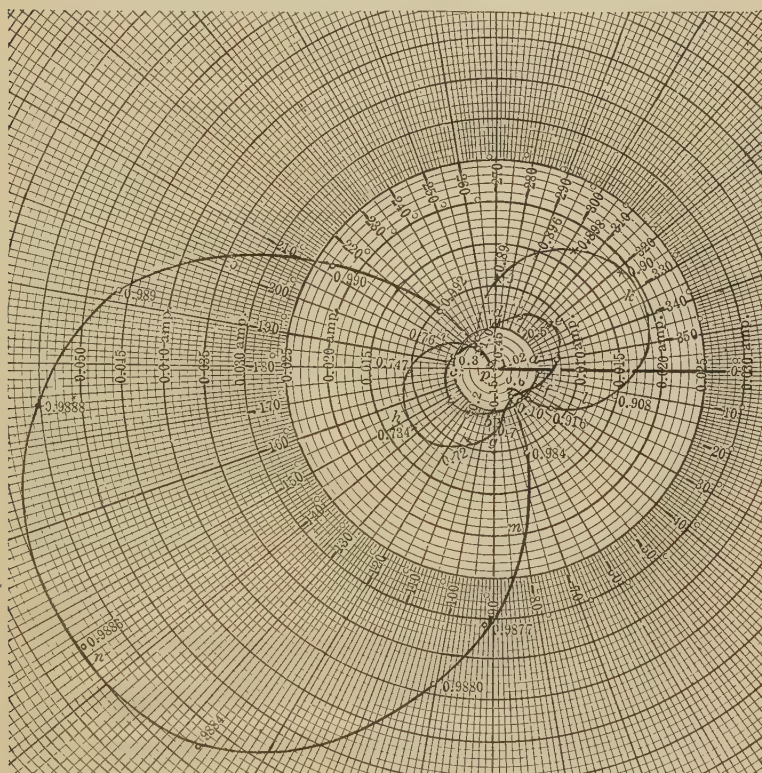


FIG. 218.—Vector diagram of received current  $I_B$  under conditions similar to those for Fig. 215, except that the load at  $B$  has an inductance of 0.0265 henry, in addition to a resistance of 183 ohms.

Table XXX gives a set of five computations for  $I_A$ ,  $E_B$ , and  $I_B$ , for the particular frequency ratios  $u = 0.2, 0.4, 0.6, 0.8$ , and  $0.99$  for the case of  $\sigma = 183.3$  ohms, the pure resistance load to which Figs. 216 and 217 refer.

**High-pass Filter.**—If we take an artificial line of the condensance-inductance type with condensers in series and induc-



TABLE XXX

Examples of tabular computation of five-section filter in Fig. 209, under different successive frequencies, with 1.0  $\angle 0^\circ$  volt impressed at  $A$ , and a load of 183.3 ohms at  $B$

$u$	$\frac{\theta}{2}$ hypos.	Section angle $\theta$ hypos.	Total angle $\Theta_q$ hypos.	$\cos \frac{\theta}{2}$	$z_0$ ohms	$\sigma_{z_0}$	$\delta_B$ hypos.	$\delta_A$ hypos.	$\tanh \delta_A$	$Z_A =$ $z_0 \tanh \delta_A$ ohms
0.2	$j0.2014$	$j0.4028$	$j1.282$	0.9797	195.9	0.935	1.70	$1.700 + j1.282$	$1.043 \angle 3^\circ.0$	$204.4 \angle 3^\circ.0$
0.4	$j0.4115$	$j0.8230$	$j2.620$	0.9165	183.3	1.00	$\alpha$	$1.347 + j1$	1.0	$183.3 \angle 0^\circ$
0.6	$j0.6435$	$j1.287$	$j4.093$	0.800	160	1.145	$1.347 + j1$	$1.347 + j5.093$	$1.138 \angle 2^\circ.35$	$182.2 \angle 2^\circ.35$
0.8	$j0.9273$	$j1.8546$	$j5.905$	0.600	120	1.528	$0.783 + j1$	$0.783 + j6.905$	$1.490 \angle 7^\circ.5$	$178.8 \angle 7^\circ.5$
0.99	$j1.429$	$j2.858$	$j9.10$	0.141	28.2	6.50	$0.155 + j1$	$0.155 + j10.1$	$0.220 \angle 44^\circ$	$6.20 \angle 44^\circ$

$u$	$I_A = Y_A = \frac{1}{\text{amp.} \times 10^{-3}}$	$\cosh \delta_A$	$\cosh \delta_B$	$I_B$ amp. $\times 10^{-3}$	$\sinh \delta_A$	$\sinh \delta_B$	$E_B$ volts	$\sigma = \frac{E_B}{I_B}$ ohms
0.2	$4.892 \angle 3^\circ.0$	$2.675 \angle 117^\circ$	$2.828 \angle 0^\circ$	$5.172 \angle 114^\circ$	$2.800 \angle 113^\circ.8$	$2.646 \angle 0^\circ$	$0.945 \angle 113^\circ.8$	$182.7 \angle 0^\circ.2$
0.4	$5.455 \angle 0^\circ$	$\alpha$	$\alpha$	$5.455 \angle 235^\circ.8$	$\alpha$	$\alpha$	$1.0 \angle 235^\circ.8$	$183.3 \angle 0^\circ$
0.6	$5.488 \angle 2^\circ.35$	$1.80 \angle 99^\circ.3$	$1.793 \angle 90^\circ$	$5.467 \angle 6^\circ.9$	$2.055 \angle 97^\circ$	$2.053 \angle 90^\circ$	$0.999 \angle 7^\circ$	$182.7 \angle 0^\circ.1$
0.8	$5.593 \angle 7^\circ.5$	$0.88 \angle 257^\circ$	$0.8655 \angle 90^\circ$	$5.501 \angle 174^\circ.5$	$1.315 \angle 264^\circ.2$	$1.323 \angle 90^\circ$	$1.006 \angle 174^\circ.2$	$182.8 \angle 0^\circ.3$
0.99	$161.2 \angle 44^\circ$	$1.020 \angle 182^\circ$	$1.0120 \angle 90^\circ$	$24.6 \angle 136^\circ$	$0.225 \angle 226^\circ$	$0.1556 \angle 90^\circ$	$4.498 \angle 136^\circ$	$182.8 \angle 0^\circ$

tances in shunt with a total capacitance of  $C$  farads in series, per section, *i.e.*, two condensers of  $2C$  each, and an inductance of  $\mathcal{L}$  henrys in shunt, the value of  $\mathbf{r}$  is  $-j\frac{1}{C\omega}$  and that of  $\mathbf{g} = -j\frac{1}{\mathcal{L}\omega}$ .

The section angle, by (203), is defined by

$$\sinh \frac{\theta}{2} = j\frac{1}{2\omega} \cdot \frac{1}{\sqrt{\mathcal{L}C}} \quad \text{numeric } \angle \quad (533b)$$

If we write for the cut-off angular velocity

$$\omega_0 = \frac{1}{2\sqrt{\mathcal{L}C}} \quad \text{radians/sec.} \quad (534)$$

Then

$$\sinh \frac{\theta}{2} = j\frac{\omega_0}{\omega} \quad \text{numeric } \angle \quad (535)$$

So long as  $\omega$  is greater than  $\omega_0$ ,  $\theta/2$  and  $\theta$  are pure imaginary hyperbolic angles; *i.e.*, real circular angles, and for a surge-impedance load, there is attenuation in slope only. When, however,  $\omega$  falls below  $\omega_0$ ,  $\theta/2$  and  $\theta$  develop real components, and attenuation of size sets in. Thus, if  $\mathcal{L} = 0.04$  henry, and  $C = 10^{-6}$  farad, as before,  $\omega = 2,500$  rad./sec., or  $f_0 = 398$  cyps. This is the cutoff frequency for such a filter. Above this frequency, the section angle  $\theta$  is a  $j$  quantity. Below 398 cyps., it is a complex quantity, and the real component increases as the frequency is diminished. The chart of Fig. 210 is applicable for the solution of (535).

**Alternative Method for Finding  $\theta$ .**—Another formula for computing  $\theta$  from the branch impedance  $\rho = \mathbf{r}/2$  and staff impedance  $\mathcal{R} = 1/\mathbf{g}$  of a symmetrical low-pass  $T$ -section is\*

$$\cosh \theta = \frac{\mathcal{R} + \rho}{\mathcal{R}} \quad \text{numeric } \angle \quad (536)$$

or

$$\text{versh } \theta = \cosh \theta - 1 = \frac{\rho}{\mathcal{R}} = \rho\mathbf{g} \quad \text{numeric } \angle \quad (536a)$$

Thus, in the case of the  $T$ -section of Fig. 208, with  $\rho = j\frac{\mathcal{L}\omega}{2}$ ,

and  $\mathcal{R} = -j\frac{1}{C\omega}$  we have:

$$\cosh \theta = 1 - \frac{C\mathcal{L}}{2}\omega^2 \quad \text{numeric } \angle \quad (537)$$

$$= 1 - 2\frac{\omega^2}{\omega_0^2} \quad \text{numeric } \angle \quad (538)$$

$$= 1 - 2u^2 \quad \text{numeric } \angle \quad (539)$$

\*The Appl. of Hyp. Functions to Elec. Engg. Problems (106), 1911.

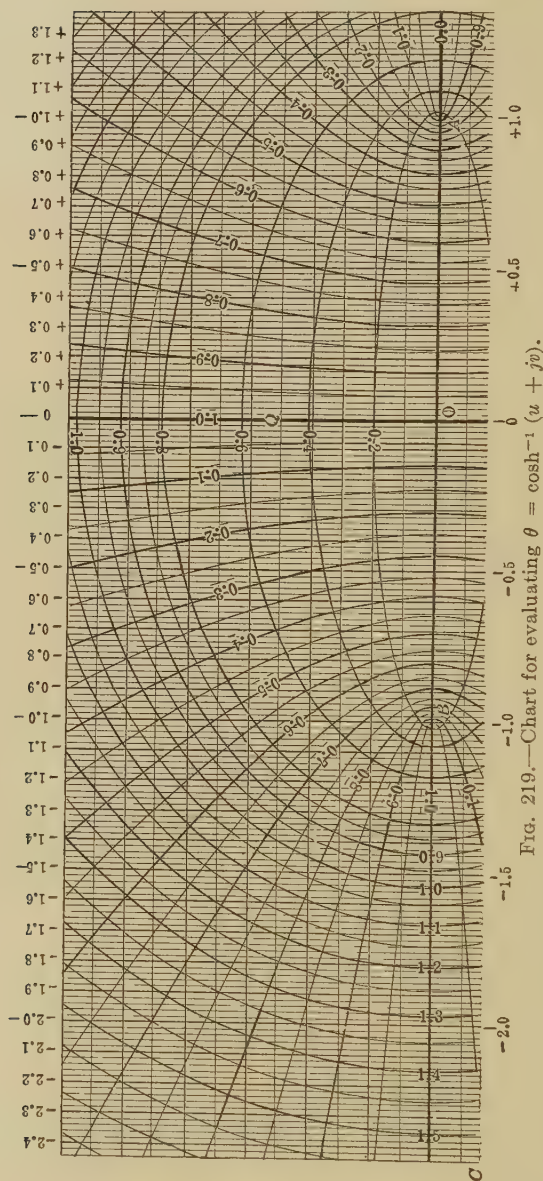


Fig. 219.—Chart for evaluating  $\theta = \cosh^{-1}(u + jv)$ .

As  $u$  increases from 0 to 1,  $\cosh \theta$  diminishes along the axis of reals from 1 to  $-1$ , and  $\theta$  is a pure  $j$  quantity. When  $u$  is increased above 1,  $\theta$  becomes complex.

Figure 219 gives a chart suitable for use with formula (537) or (539). The elliptic axis  $BOA$  is now horizontal. If we wish to find the angle  $\theta$  whose cosine is any real quantity commencing at  $+1$  and passing through  $O$  to any negative value, we enter the diagram at  $A$  and move towards  $B$  to some point  $P$  corresponding to  $\cosh \theta$ , on the rectilinear background. Having found this point,  $\theta$  is read off in the curvilinear coordinates with  $\theta_1$  on the ellipses and  $\theta_2$  on the intersecting hyperbolas.

The hyperbolas in the first quadrant  $AOQ$  are marked 0.1, 0.2 . . . to 1.0. Those in the second quadrant  $QOB$ , similarly marked, should be increased by unity. Thus the point  $P$  on  $OB$  at distance  $-0.707$ , has for its curvilinear coördinates  $0 + j1.5$ . Therefore  $\cosh^{-1} -0.707 = 0 + j1.5$ . The following Table XXXI, taken in conjunction with Table XXIX, will be of assistance in giving familiarity with the use of Fig. 219.

It may be noted that, owing to the limited size of the diagram of Fig. 219, the precision of reading  $\theta$  is somewhat less than with Fig. 210, but the latter may be used as an adjunct to Fig. 219.

TABLE XXXI

Section-angle  $\theta$  for a  $T$ -filter of the type shown in Fig. 208, as a function of the frequency ratio  $u$

$\omega$	$u$	$u^2$	$2u^2$	$1 - 2u^2$	$\theta_1 + jq$ quadrants		$\theta_1 + j\theta_2$ circ. radians	
0	0	0	0	1.0	0	$+j0$	0	$+j0$
1,000	0.1	0.01	0.02	0.98	0	$+j0.13$	0	$+j0.2$
2,000	0.2	0.04	0.08	0.92	0	$+j0.26$	0	$+j0.4$
3,000	0.3	0.09	0.18	0.82	0	$+j0.39$	0	$+j0.61$
4,000	0.4	0.16	0.32	0.68	0	$+j0.52$	0	$+j0.82$
5,000	0.5	0.25	0.5	0.5	0	$+j0.67$	0	$+j1.05$
6,000	0.6	0.36	0.72	0.28	0	$+j0.82$	0	$+j1.29$
7,000	0.7	0.49	0.98	0.02	0	$+j0.99$	0	$+j1.55$
8,000	0.8	0.64	1.28	$-0.28$	0	$+j1.18$	0	$+j1.85$
9,000	0.9	0.81	1.62	$-0.62$	0	$+j1.42$	0	$+j2.24$
10,000	1.0	1.0	2.0	$-1.0$	0	$+j2.0$	0	$+j3.14$
11,000	1.1	1.21	2.42	$-1.42$	0.89	$+j2.0$	0.89	$+j3.14$
12,000	1.2	1.44	2.88	$-1.88$	1.25	$+j2.0$	1.25	$+j3.14$
13,000	1.3	1.69	3.38	$-2.38$	1.51	$+j2.0$	1.51	$+j3.14$

We have assumed hitherto that the condensers and inductors used in filter artificial lines are resistanceless. If, however, the correct resistances belonging to the various elements are inserted in formulas (524), (530), and (539), but little additional difficulty will be experienced. The angles  $\theta$  will always contain some real component  $\theta_1$ , but otherwise the treatment will be the same.

In modern practice, the effective resistance of a good condenser over the range of audio-frequencies (0 to 10,000 cyps.) is relatively small so that it may ordinarily be ignored. The effective resistance of coils containing air cores, at  $\omega = 10,000$  may average about 450 ohms per henry, at  $20^\circ\text{C}$ ., depending upon the construction. With pulverized iron cores as used in filters, the coil effective resistance at  $20^\circ\text{C}$ . and at  $\omega = 10,000$  may be 300 ohms per henry or 3 per cent of the reactance at  $\omega = 10,000$ . With permalloy dust cores the effective resistance at  $\omega = 10,000$  may be as low as 100 ohms per henry, or 1 per cent of the reactance at  $\omega = 10,000$ .

In order to design a low-pass filter of the type shown in Fig. 208, to cutoff at a given impressed angular velocity of  $\omega_0$  when the output apparatus has a mean impedance of  $\sigma$  ohms taken as real, we have to find the section values of  $\mathcal{L}$  and  $C$  appropriate to the case.

One relation between  $\mathcal{L}$  and  $C$  is given by (525) from which

$$\sqrt{\mathcal{L}C} = \frac{2}{\omega_0} \frac{\text{sec.}}{\text{rad.}} \quad (540)$$

The second relation needed relates to the surge impedance of the filter at the frequencies which are to be passed. An examination of Fig. 211 and formula (531) shows that  $\sqrt{\frac{\mathcal{L}}{C}} \cosh \frac{\theta}{2}$  is this surge impedance, where the imaginary part of  $\theta/2$  varies between 0 and 1 quadrant or  $90^\circ$ . There is no single value of  $\theta$  to which  $z_0$  can be referred. It must be regarded as an average value over the range of passed frequencies. We may take as such a value  $\theta_2/2 = 60^\circ$  in which case  $z_0 = 0.5 \sqrt{\mathcal{L}/C}$ , or 100 ohms for the case illustrated in Fig. 213. We then have for this case

$$\sqrt{\frac{\mathcal{L}}{C}} = 2\sigma \quad \text{ohms} \quad (541)$$

Solving (540) and (541) simultaneously,

$$\mathcal{L} = \frac{4\sigma}{\omega_0} \quad \text{henrys} \quad (542)$$



and

$$C = \frac{1}{(\sigma\omega_0)} \quad \text{farads} \quad (543)$$

A similar method can be employed for computing the values of  $\mathfrak{L}$  and  $C$  for a high-pass filter.

**m-Derived Sections.**—It had been shown by Zobel\* that a symmetrical  $T$ - or  $I$ -section can be converted into another  $T$  of the same surge impedance  $z_0$ , but a different angle, by operating on the elements of the former in a definite algebraic manner, involving a coefficient  $m$ . A similar procedure applies also to a  $\Pi$  or  $O$  section. In either case, the original section is called the *prototype*, and the new section an *m-derived type*. The coefficient  $m$  is any number (other than zero), but commonly fractional. By giving successive values of  $m$ , an infinite series of symmetrical derived sections might be produced, with the same  $z_0$ ; but with different attenuation-frequency characteristics.

A particular c.c. case of the proposition is illustrated in Figs. 219A and 219B. The symmetrical  $T$ ,  $A'OB'$ , has  $\rho' = 1,000$  ohms in each branch and 4,000 ohms in the staff. The versed sine of its angle (versh  $\theta$ ) is thus  $1,000/4,000 = 0.25$ , by (536a). Referring to (602b), it will be seen that for real values of versh  $\theta$  less than unity, we have the approximate relation:

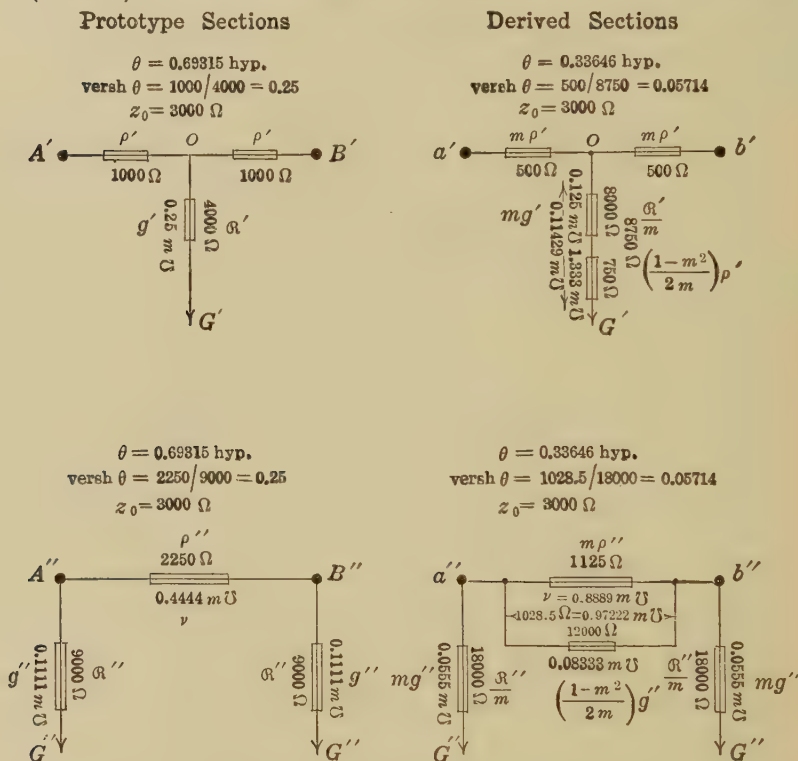
$$\theta \cong \sqrt{2 \text{ versh } \theta} \cong \sqrt{2\rho'/\mathfrak{R}'} \cong \sqrt{2\rho'g'} \cong \sqrt{rg} \quad \text{hyps.} \quad (543a)$$

or in this case  $\theta \cong \sqrt{0.5} \cong 0.707$ , the correct value being  $\theta = 0.69315$  hyp. The surge resistance of the section is also 3,000 ohms, by (180).

If now we make a new  $T$ ,  $a'b'G'$ , in which the arms have  $m\rho'$  ohms or  $m$  times the impedance of the prototype arms, and the staff has also  $mg'$  or  $m$  times the prototype admittance; but with the additionally inserted resistance  $\left(\frac{1-m^2}{2m}\right)\rho'$  ohms  $\angle$ , we obtain for the particular case  $m = 0.5$ , a derived  $T$  symmetrical section, with 500 ohms in each arm, and 8,750 ohms in the staff  $OG'$ . The surge resistance of this derived section is 3,000 ohms, as in the prototype; but its versh  $\theta$  is  $500/8,750 = 0.05714$ , and  $\theta$  is approximately  $\sqrt{0.11428} = 0.338$ , or, by tables, more closely 0.33646 hyp. In an a.c. case, the value of  $m$  might be chosen to suit desired variation of  $\theta$  with  $f$ ; *i.e.* desired cut-off action.

\*O. J. Zobel, *The Bell System Technical Journal*, Vol. 2, No. 1, Jan., 1923.

In Fig. 219B, the symmetrical  $\Pi$ ,  $A''B''G''G''$  is the equivalent of the  $T$ ,  $A'B'G'$  of Fig. 219A. Both have identical values of  $\theta$  and  $z_0$ . The derived  $\Pi$ ,  $a''b''G''G''$  is obtained by applying the coefficient  $m$ , as before, to both series impedance  $\rho''$  and shunt admittance  $g''$ ; but with the addition of a new admittance  $\left(\frac{1-m^2}{2m}\right)g''$  as an element in parallel with  $m\rho''$ . In the case



FIGS. 219A and B.—Examples of  $m$ -derived  $T$  and  $\Pi$  sections for the particular case  $\theta = 0.69315$ ,  $z_0 = 3,000$  and  $m = 0.5$ .

$m = 0.5$ , the added element has 12,000 ohms resistance, or 0.0833 millimho conductance; so that the architrave  $a''b''$  has a total conductance of 0.97222 millimho, or a total resistance of 1,028.5 ohms. The surge impedance of the section remains at 3,000 ohms; but the section angle  $\theta$  is reduced to the same value, 0.33646 hyp., as in the derived  $T$ .

This useful proposition enables a prototype  $T$  or  $\Pi$  in a filter to be replaced by any one of an infinite series of  $T$ 's or  $\Pi$ 's, all having

the same  $z_0$ . By suitably selecting the value of  $m$ , it is possible to make a derived- $T$  staff develop series resonance at some appropriate frequency, thus developing a short circuit in the staff, with  $\theta = \alpha$ . Again, in a  $\Pi$ -derived section, it is possible to produce parallel resonance in the architrave, which, neglecting losses, is equivalent to an open circuit at that frequency, with  $\theta = \alpha$ . By suitably varying the value of  $m$ , the sharpness of cut-off in the filter, can be adjusted.

**Composite Filters.**—It has been pointed out by Johnson\* and Zobel† that composite filters have distinct advantages for many purposes. Certain types of filter section adjusted for a given cutoff frequency differ from others in their behavior beyond the

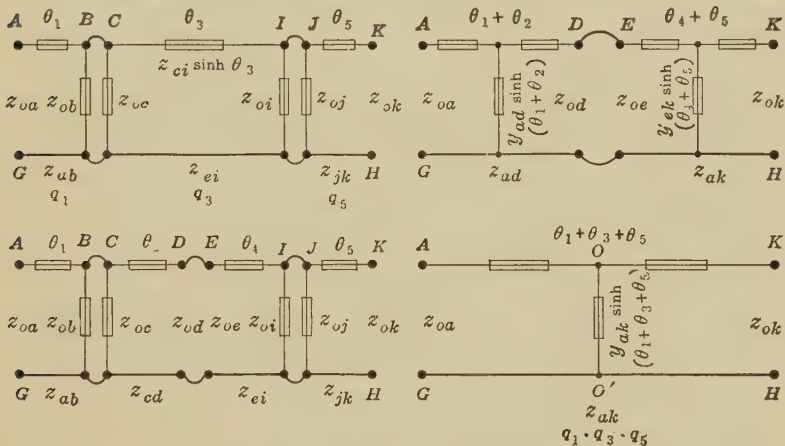


FIG. 220—Composite filter diagram and its resultant  $T$ .

cutoff point. Some may introduce much attenuation after passing the cutoff point, *i.e.*  $m$  types or derived types but may not be so effective further on. Others, *i.e.* prototypes, may not be so effective in building up attenuation at or near the cutoff point, while further on, they may be very effective. By associating such different types in series, a suitable growth of attenuation may be developed, beyond the ability of a uniform-section filter. Moreover, it may be desired to insert the filter between a net of one surge impedance and a receiving circuit of another surge impedance. This may be done without resorting to the use of a special transformer, by suitably grading the surge impedances of the sections of a composite filter.

\* "Transmission Circuits" by K. S. Johnson, Chapters XVI and XVII.

† "Theory and Design of Uniform and Composite Wave Filters" by O. J. Zobel, *Bell System Tech. Jour.*, Jan., 1923, vol. ii, No. 1.

Figure 220 is a diagram of a three-section composite filter. The terminal sections  $AB$  and  $JK$  are cantilevers. The central section is a dissymmetrical  $\Pi$ . Junctions occur at  $BC$  and  $IJ$ .

It is necessary, if the composite filter  $AK$  is to be of the same type as regards cutoff, *i.e.*, entirely low-pass, or entirely high-pass, that each of the three sections shall have the same cutoff frequency  $f_0$ , although the three graphs of attenuation *versus* frequency ( $\theta$  *vs.*  $f$ ) may differ. It is also necessary that there should be conformity between adjacent surge impedances at junctions over the active range of frequencies employed. That is  $z_{ob}$  and  $z_{oc}$  must remain substantially equal, and likewise  $z_{oi}$  and  $z_{oj}$  over the active frequency range, although none of these surge impedances may remain constant. Over the unattenuated portion of the range, each of the three section angles  $\theta_1$ ,  $\theta_3$  and  $\theta_5$  must be wholly circular, or have no hyperbolic component, and their sum will not be equal to the total angle  $\Theta$  of the filter, nor will  $\Theta$  remain, in general, wholly circular, unless the internally connected pairs of surge impedance,  $z_{ob}z_{oc}$ , and  $z_{oi}z_{oj}$ , remain in agreement. On the other hand, the inequality factors  $q_1$ ,  $q_3$  and  $q_5$ , of the three sections are unrestricted.

The central  $\Pi$  is shown as having an angle  $\theta_3$  at the particular frequency considered and surge impedances  $z_{oc}z_{oi}$ . It may be split up into two cantilevers, namely, the gamma  $CD$  and the seven  $EI$ , in such a manner as to retain the external surge impedances  $z_{oc}$  and  $z_{oi}$  unchanged, and two component angles  $\theta_2$  and  $\theta_4$  equal in sum to  $\theta_3$ , and the two internal surge impedances equal ( $z_{od} = z_{oe}$ ) at the point of separation. This can be done in either of two possible ways.

By merging the two parallel-connected leaks at the  $BC$  and  $IJ$  junctions, the system reaches the double  $T$  on the upper right of Fig. 220. Finally, this system may be reduced to the single dissymmetrical  $T$  AOK, GO'H. The total angle  $\Theta$  of the filter remains the sum of the three component angles  $\theta_1$ ,  $\theta_3$ ,  $\theta_5$ , and the total inequality factor is the product of the three constituent factors  $q_1 \cdot q_3 \cdot q_5$ . The external surge impedances  $z_{oa}$  and  $z_{ok}$  remain as before, and the geomean surge impedance  $z_{ak}$  is the same as the geometrical mean of the two original component values of the cantilevers  $AB$  and  $JK$ .

The above process of merging artificial line sections, at any single frequency, is always possible arithmetically. The three final impedances  $AO$ ,  $OK$  and  $OO'$ , may or may not be physically

realisable; but if inductors and condensers can be assigned to the final  $T$  or  $\Pi$  of the resultant net, it is evident that the physical behavior of these three elements, under changes of impressed frequency, will not, in general, duplicate that of the composite system. In other words, a multi-section filter can always be reduced arithmetically, at any one frequency, to an equivalent three-element single section; but this, if physically realisable, cannot be expected to behave, under varied frequency, like the original multi-section filter.

For further particulars on filter design, the reader may be referred to Johnson's "Transmission Circuits." Chapters XVI and XVII.

# Detection of Even-frequency Harmonics in a Generator.—

We have already seen, in Chapter XII, that a quarter-wave line subtends an angle  $\theta_{\frac{1}{4}} = \theta_1 + j1$  hyps. For simplicity, we may assume that a certain smooth line has negligible conductor resistance and dielectric leakance; so that when operated at quarter-wave frequency,  $\theta_1 = 0$ , and  $\theta_{\frac{1}{4}} = j\frac{\pi}{2} = j1$  hyp. The current entering this line at the generator end will be, by (148),

$$I_A = V_A y_0 \coth \delta_A \quad \text{amp.} \quad \angle \quad (544)$$

where  $y_0 = \sqrt{c}/l$  ohms, a real conductance. If now the line is first grounded and then freed at  $B$ , the corresponding values of  $\delta_A$  are  $j1$  and  $j2$  imaginary quadrants, respectively, and the corresponding entering currents will be  $V_A y_0 \coth (j1)$  and  $V_A y_0 \coth (j2)$ . But  $\coth j1 = j0$ , and  $\coth j2 = j\infty$ ; so that with 60 cyps., say, the entering current will be zero with the line grounded at  $B$ , and infinity with the line freed at  $B$ .

Moreover, this state of affairs would be presented for all odd harmonic frequencies. Thus, if a triple-frequency e.m.f. were impressed on the line, still with negligible losses, its angle would be  $j3$  hyps. and  $\coth j3 = \coth j1$ . As in the preceding case, the line would take zero current at  $A$  when grounded at  $B$ , and an infinite current at  $A$  when freed at  $B$ , assuming no losses.

But if an even-harmonic frequency were applied at  $A$ , the lossless line would develop an angle of corresponding even number of imaginary quadrants. In that case, its cotangent would be infinite when the far end was grounded, and zero when the far end was freed. Thus, if the double-harmonic frequency (120~) were impressed at  $A$ , this would be the half-wave frequency,



and the line would develop the half-wave angle  $j2$  hyps. The entering current would now be infinite with  $B$  grounded, and zero with  $B$  freed. The same would be true for any even-harmonic impressed frequency (240~, 360~, 480~, etc.).

If next a 60~ generator is applied at  $A$ , with a complex harmonic e.m.f., or containing a number of harmonic frequencies, and the line is grounded at  $B$ , then the fundamental-frequency current and all the odd-harmonic currents will be zero at  $A$ ; but the even-harmonic currents would be infinite. The line therefore acts as a filter at the  $A$  end, suppressing all the odd-harmonic currents, and increasing indefinitely the even-harmonic currents.

In any actual line, there will necessarily be some conductor resistance and dielectric leakance, so that there will be losses in the line when it carries alternating currents of any frequency and the line angle will not be a pure imaginary. It will contain a real component  $\theta_1$ . In the case, however, of a well-insulated line of large carrying capacity, this real component may be expected to be relatively small. Consequently, when such a line of quarter-wave length at fundamental frequency, is grounded at the far end  $B$ , and has a complex or multi-frequency wave of e.m.f. impressed upon it at  $A$ , the odd-frequency components will not be zero, but may yet be very small, and the even-frequency components will not be infinite, but may yet be very large. Such a quarter-wave line is, therefore, a magnifier of such even-frequency harmonics as exist in the e.m.f. wave, and especially of the first or double-frequency harmonic, since the magnification will be less, the higher the even multiple. A properly constructed a.c. generator is ordinarily supposed to produce no even-harmonic components of e.m.f., and they are admittedly small, but they may be larger than is expected. When the generator is used to excite a quarter-wave line grounded at the distant end  $B$ , and an oscillograph is inserted at  $A$ , the resulting current oscillograph will contain magnified even harmonics, and minified odd harmonics including the fundamental.

For the purposes of such a test, the line may conveniently be a quarter-wave artificial line, with as little linear resistance and linear leakance as is practicable. An oscillogram of the current wave at the generator end, when the distant end is grounded, may be expected to reveal the presence of the magnified even\*

\* "Analyzing Electric Waves for Harmonics," by C. W. Ricker, *Electrical World*, Sept. 18, 1915.

harmonics. If these magnified even harmonics are notably present, they will distort the oscillographed current wave with respect to the zero line, the shape of the positive half-waves being rendered different from that of the negative half-waves.

In the case of the artificial line specified in Table XVIII and tested by Mr. Ricker as a quarter-wave line, the size of the sending-end impedance, with *B* grounded, was found to be 2,799 ohms at 60 cyps., and 42.0 ohms at 120 cyps., a magnification ratio of 66.7 in favor of the double-frequency harmonic.

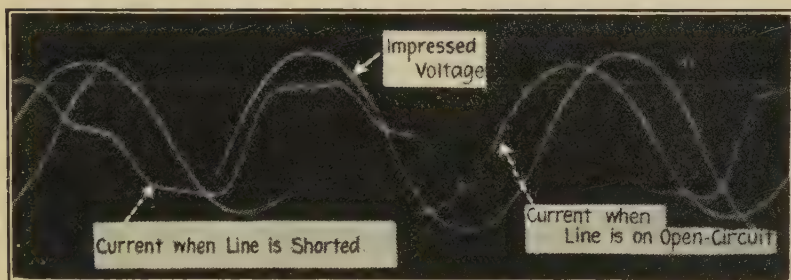


FIG. 221.—Oscillograms of impressed-voltage wave (60~) impressed on a quarter-wave artificial line, and also of the generating-end current with the distant end freed and grounded. The apparent phase relations of these three oscillograms are not significant.

Figure 221 shows the wave forms of the current entering this quarter-wave line, with the distant end *B* freed and grounded respectively, suitable shunts being applied in each case, so as to keep the wave amplitude normal for being photographed. It will be seen that the wave form with *B* on open circuit is substantially a smooth sinusoid. Here the fundamental and odd-harmonic components are favored and the even-harmonic components repressed. In the case of *B* end shorted or grounded, when the even harmonics are magnified and the odds repressed, the wave form not only departs from the sinusoidal, but it is also dissymmetrical on the + and - sides of the mid-line.\* This indicates the presence of even-frequency harmonics in the generated wave, which, from its oscillograph in Fig. 221, might not be suspected.

An artificial line may also be used to magnify some particular harmonic frequency, either odd or even. By shortening a line to the amount necessary for resonance to that particular harmonic, an oscillograph may enable this magnified harmonic to be

\* This mid-line, or zero line, does not appear on the oscillogram.

detected or measured. Thus, Fig. 222 shows the oscillograph of the same impressed e.m.f. as in the last preceding case, and also oscillograms of its third and fifth harmonics, as magnified by this process.

Since in all these cases of harmonic magnification, the magnification factor can be computed to a satisfactory degree of precision, from the constants of the artificial line used, they enable such artificial lines to be used as adjuncts to oscillographic measuring apparatus.

**Artificial Lines as Detectors of Frequency Variations.**—The marked and often objectionably obtrusive influence of variations

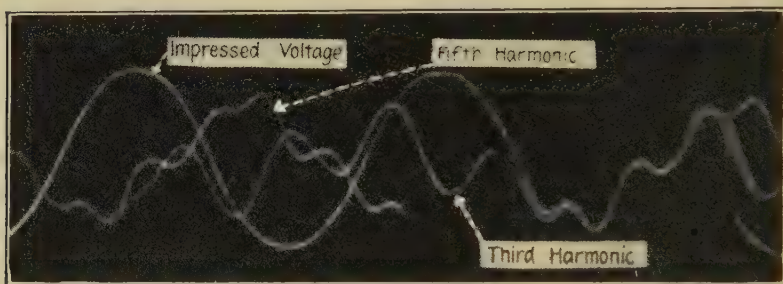


FIG. 222.—Oscillogram of an impressed-voltage wave and of magnified third and fifth harmonics contained in it on successive tests with resonant artificial lines.

in the impressed frequency, on the distributions of potential, current and impedance along an artificial line under tests, naturally suggests the use of such a line for the purpose of detecting and manifesting frequency changes. One such use has already been suggested at the end of Chapter XII, in relation to quarter-wave lines.

**Artificial Lines as Phase Retarders.**—An artificial line having an angle  $\theta = \theta_1 + j\theta_2$  at a certain single frequency, will, as we have seen in Chapter XV, produce a retardation of phase of  $\theta_2$  cir. rad. in voltage and in current between input and output terminals, when the output end is connected to a surge-impedance load. When the load  $\sigma$  differs from the surge-impedance value, the retardation of phase can be computed from the  $A$  and  $B$  position angles. This retardation property may be utilized in electric or acoustic systems where a definite phase retardation is required.

# APPENDIX A

LIST OF IMPORTANT TRIGONOMETRICAL FORMULAS WITH CIRCULAR AND HYPERBOLIC EQUIVALENTS\*

Circular	Hyperbolic
$\sin \beta = \frac{e^{j\beta} - e^{-j\beta}}{j2} = \beta - \frac{\beta^3}{3!} + \frac{\beta^5}{5!} - \frac{\beta^7}{7!} + \dots$	$\sinh \theta = \frac{e^{\theta} - e^{-\theta}}{2} = \theta + \frac{\theta^3}{3!} + \frac{\theta^5}{5!} + \frac{\theta^7}{7!} + \dots \quad (545)$
$\cos \beta = \frac{e^{j\beta} + e^{-j\beta}}{2} = 1 - \frac{\beta^2}{2!} + \frac{\beta^4}{4!} - \frac{\beta^6}{6!} + \dots$	$\cosh \theta = \frac{e^{\theta} + e^{-\theta}}{2} = 1 + \frac{\theta^2}{2!} + \frac{\theta^4}{4!} + \frac{\theta^6}{6!} + \dots \quad (546)$
$\tan \beta = \frac{\sin \beta}{\cos \beta} = \beta + \frac{\beta^3}{3} + \frac{2\beta^5}{15} + \frac{17\beta^7}{315} + \dots$	$\tanh \theta = \frac{\sinh \theta}{\cosh \theta} = \theta - \frac{\theta^3}{3} + \frac{2\theta^5}{15} - \frac{17\theta^7}{315} + \dots \quad (547)$
$\sec \beta = \frac{1}{\cos \beta} = 1 + \frac{\beta^2}{2} + \frac{5\beta^4}{24} + \frac{61\beta^6}{720} + \dots$	$\operatorname{sech} \theta = \frac{1}{\cosh \theta} = \sqrt{1 - \tanh^2 \theta} = 1 - \frac{\theta^2}{2} + \frac{5\theta^4}{24} - \frac{61\theta^6}{720} + \dots \quad (548)$
$\operatorname{cosec} \beta = \frac{1}{\sin \beta} = \sqrt{\cot^2 \beta + 1}$	$\operatorname{cosech} \theta = \frac{1}{\sinh \theta} = \sqrt{\coth^2 \theta - 1} \quad (549)$
$\cot \beta = \frac{1}{\tan \beta} = j \frac{e^{j\beta} + e^{-j\beta}}{e^{j\beta} - e^{-j\beta}} = j \frac{e^{2j\beta} + 1}{e^{2j\beta} - 1}$	$\coth \theta = \frac{1}{\tanh \theta} = \frac{e^{\theta} + e^{-\theta}}{e^{\theta} - e^{-\theta}} = \frac{e^{2\theta} + 1}{e^{2\theta} - 1} \quad (550)$
$e^{\pm j\beta} = \cos \beta \pm j \sin \beta = 1 \pm j\beta - \frac{\beta^2}{2!} \mp j \frac{\beta^3}{3!} + \frac{\beta^4}{4!} \pm \dots$	$e^{\pm \theta} = \cosh \theta \pm \sinh \theta = 1 \pm \theta + \frac{\theta^2}{2!} \pm \frac{\theta^3}{3!} + \frac{\theta^4}{4!} \pm \dots \quad (551)$
$\sin \beta = -j \sinh j\beta = \tanh (jd^{-1}\beta) = -\sin (-\beta)$	$\sinh \theta = -j \sin j\theta = \tanh (gd\theta) = -\sinh (-\theta) \quad (552)$
$\cos \beta = \cosh j\beta = \operatorname{sech} (jd^{-1}\beta) = \cos (-\beta)$	$\cosh \theta = \cos j\theta = \sec (gd\theta) = \cosh (-\theta) \quad (553)$
$\tan \beta = -j \tanh j\beta = \sinh (jd^{-1}\beta) = -\tan (-\beta)$	$\tanh \theta = -j \tan j\theta = \sinh (gd\theta) = -\tanh (-\theta) \quad (554)$
$\sin j\beta = j \sinh \beta$	$\sinh j\theta = j \sin \theta \quad (555)$
$\cos j\beta = \cosh \beta$	$\cosh j\theta = \cos \theta \quad (556)$
$\tan j\beta = j \tan \beta$	$\tanh j\theta = j \tanh \theta \quad (557)$
$\sin 2\beta = 2 \sin \beta \cos \beta = \frac{2 \tan \beta}{1 + \tan^2 \beta}$	$\sinh 2\theta = 2 \sinh \theta \cosh \theta = \frac{2 \tanh \theta}{1 - \tanh^2 \theta} \quad (558)$
$\cos 2\beta = \cos^2 \beta - \sin^2 \beta = 2 \cos^2 \beta - 1$	$\cosh 2\theta = \cosh^2 \theta + \sinh^2 \theta = 2 \cosh^2 \theta - 1 \quad (559)$

\* A more copious list of formulas will be found in "Tables of Complex Hyperbolic and Circular Functions," by A. E. KENNELLY.

## LIST OF IMPORTANT TRIGONOMETRICAL FORMULAS WITH CIRCULAR AND HYPERBOLIC EQUIVALENTS.—(Continued)

Circular	Hyperbolic
$\tan 2\beta = \frac{2 \tan \beta}{1 - \tan^2 \beta} = \frac{2 \cot \beta}{\cot^2 \beta - 1} = \frac{2}{\cot \beta - \tan \beta}$	$\tanh 2\theta = \frac{2 \tanh \theta}{1 + \tanh^2 \theta} = \frac{2 \coth \theta}{\coth^2 \theta + 1} = \frac{2}{\coth \theta + \tanh \theta}$ (560)
$\cot 2\beta = \frac{\cot^2 \beta - 1}{2 \cot \beta} = \frac{2 \tan \beta}{1 - \tan^2 \beta} = \frac{2}{\cot \beta - \tan \beta}$	$\coth 2\theta = \frac{\coth^2 \theta + 1}{2 \coth \theta} = \frac{1 + \tanh^2 \theta}{2 \tanh \theta} = \frac{\coth \theta + \tanh \theta}{2}$ (561)
$\sin \frac{\beta}{2} = \frac{\sin \beta}{2 \cos \frac{\beta}{2}} = \sqrt{\frac{1 - \cos \beta}{2}}$	$\sinh \frac{\theta}{2} = \frac{\sinh \theta}{2 \cosh \frac{\theta}{2}} = \sqrt{\frac{\cosh \theta - 1}{2}}$ (562)
$\cos \frac{\beta}{2} = \frac{\sin \beta}{2 \sin \frac{\beta}{2}} = \sqrt{\frac{1 + \cos \beta}{2}}$	$\cosh \frac{\theta}{2} = \frac{\sinh \theta}{2 \sinh \frac{\theta}{2}} = \sqrt{\frac{\cosh \theta + 1}{2}}$ (563)
$\tan \frac{\beta}{2} = \frac{\sin \beta}{1 + \cos \beta} = \frac{1 - \cos \beta}{\sin \beta} = \sqrt{\frac{1 - \cos \beta}{1 + \cos \beta}}$	$\tanh \frac{\theta}{2} = \frac{\sinh \theta}{1 + \cosh \theta} = \frac{\cosh \theta - 1}{\sinh \theta} = \sqrt{\frac{\cosh \theta - 1}{\cosh \theta + 1}}$ (564)
$\cos^2 \beta + \sin^2 \beta = 1$	$\cosh^2 \theta - \sinh^2 \theta = 1$ (565)
$\operatorname{cosec}^2 \beta - \cot^2 \beta = 1$	$\operatorname{cosech}^2 \theta - \coth^2 \theta = 1$ (566)
$\sec^2 \beta - \tan^2 \beta = 1$	$\operatorname{sech}^2 \theta + \tanh^2 \theta = 1$ (567)
$\cot \beta + \tan \beta = \frac{2}{\sin 2\beta}$	$\coth \theta - \tanh \theta = \frac{2}{\sinh 2\theta}$ (568)
$\sin (\beta_1 \pm \beta_2) = \sin \beta_1 \cos \beta_2 \pm \cos \beta_1 \sin \beta_2$	$\sinh (\theta_1 \pm \theta_2) = \sinh \theta_1 \cosh \theta_2 \pm \cosh \theta_1 \sinh \theta_2$ (569)
$\cos (\beta_1 \pm \beta_2) = \cos \beta_1 \cos \beta_2 \mp \sin \beta_1 \sin \beta_2$	$\cosh (\theta_1 \pm \theta_2) = \cosh \theta_1 \cosh \theta_2 \pm \sinh \theta_1 \sinh \theta_2$ (570)
$\tan (\beta_1 \pm \beta_2) = \frac{\tan \beta_1 \pm \tan \beta_2}{1 \mp \tan \beta_1 \tan \beta_2}$	$\tanh (\theta_1 \pm \theta_2) = \frac{\tanh \theta_1 \pm \tanh \theta_2}{1 \pm \tanh \theta_1 \tanh \theta_2}$ (571)
$\sin \beta_1 + \sin \beta_2 = 2 \sin \frac{\beta_1 + \beta_2}{2} \cdot \cos \frac{\beta_1 - \beta_2}{2}$	$\sinh \theta_1 + \sinh \theta_2 = 2 \sinh \frac{\theta_1 + \theta_2}{2} \cdot \cosh \frac{\theta_1 - \theta_2}{2}$ (572)
$\sin (\beta \pm 2n\pi) = \sin \beta$	$\sinh (\theta \pm 2jn\pi) = \sinh \theta$ (573)



Circular	Hyperbolic
$\cos (\beta \pm 2 n \pi)=\cos \beta$ $\tan (\beta \pm n \pi)=\tan \beta$ $\sin \left(\beta \pm \frac{\pi}{2}\right)=\pm \cos \beta$ $\cos \left(\beta \pm \frac{\pi}{2}\right)=\mp \sin \beta$ $\tan \left(\beta \pm \frac{\pi}{2}\right)=\mp \cot \beta$ $\cot \left(\beta \pm \frac{\pi}{2}\right)=\mp \tan \beta$ $a \cos \beta \pm b \sin \beta=\sqrt{a^2+b^2} \cos \left(\beta \mp \tan ^{-1} \frac{b}{a}\right)$ $a e^{j \beta} \pm b e^{-j \beta}=(a \pm b) \cos \beta+j(a \mp b) \sin \beta$ $\sin \left(\beta_1+\beta_2\right)+\sin \left(\beta_1-\beta_2\right)=2 \sin \beta_1 \cos \beta_2$ $\cos \left(\beta_1+\beta_2\right)+\cos \left(\beta_1-\beta_2\right)=2 \cos \beta_1 \cos \beta_2$ $\sin \left(\beta_1 \pm j \beta_2\right)=\sin \beta_1 \cosh \beta_2 \pm j \cos \beta_1 \sinh \beta_2$ $\cos \left(\beta_1 \pm j \beta_2\right)=\cos \beta_1 \cosh \beta_2 \mp j \sin \beta_1 \sinh \beta_2$	$\cosh (\theta \pm 2 j n \pi)=\cosh \theta$ (574) $\tanh (\theta \pm j n \pi)=\tanh \theta$ (575) $\sinh \left(\theta \pm j \frac{\pi}{2}\right)=\pm j \cosh \theta$ (576) $\cosh \left(\theta \pm j \frac{\pi}{2}\right)=\pm j \sinh \theta$ (577) $\tanh \left(\theta \pm j \frac{\pi}{2}\right)=\coth \theta$ (578) $\coth \left(\theta \pm j \frac{\pi}{2}\right)=\tanh \theta$ (579) $a \cosh \theta \pm b \sinh \theta=\sqrt{a^2-b^2} \cosh \left(\theta \pm \tanh ^{-1} \frac{b}{a}\right)$ $a > b$ (580) $=\sqrt{b^2-a^2} \sinh \left(\theta \pm \tanh ^{-1} \frac{a}{b}\right)$ $b > a$ (581) $a e^{\theta} \pm b e^{-\theta}=(a \pm b) \cosh \theta+(a \mp b) \sinh \theta$ (582) $\sinh \left(\theta_1+\theta_2\right)+\sinh \left(\theta_1-\theta_2\right)=2 \sinh \theta_1 \cosh \theta_2$ (583) $\cosh \left(\theta_1+\theta_2\right)+\cosh \left(\theta_1-\theta_2\right)=2 \cosh \theta_1 \cosh \theta_2$ (584) $\sinh \theta_1 \cos \theta_2 \pm j \cosh \theta_1 \sin \theta_2$ $\sinh \left(\theta_1 \pm j \theta_2\right)=\begin{cases} \sqrt{\sinh ^2 \theta_1+\sin ^2 \theta_2} / \pm \tan ^{-1}(\coth \theta_1 \tan \theta_2) & (585) \\ \sqrt{\cosh ^2 \theta_1-\cos ^2 \theta_2} / \pm \tan ^{-1}(\coth \theta_1 \tan \theta_2) & (586) \\ \cosh \theta_1 \cos \theta_2 \pm j \sinh \theta_1 \sin \theta_2 & (587) \end{cases}$ $\cosh \left(\theta_1 \pm j \theta_2\right)=\begin{cases} \sqrt{\cosh ^2 \theta_1-\sin ^2 \theta_2} / \pm \tan ^{-1}(\tanh \theta_1 \tan \theta_2) & (588) \\ \sqrt{\sinh ^2 \theta_1+\cos ^2 \theta_2} / \pm \tan ^{-1}(\tanh \theta_1 \tan \theta_2) & (589) \end{cases}$

## LIST OF IMPORTANT TRIGONOMETRICAL FORMULAS WITH CIRCULAR AND HYPERBOLIC EQUIVALENTS.—(Continued)

Circular	Hyperbolic
$\tan (\beta_1 \pm j\beta_2) = \frac{\sin \beta_1 \cosh \beta_2 \pm j \cos \beta_1 \sinh \beta_2}{\cos \beta_1 \cosh \beta_2 \mp j \sin \beta_1 \sinh \beta_2}$	$\tanh (\theta_1 \pm j\theta_2) = \frac{\sinh 2\theta_1 \pm j \sin 2\theta_2}{\cosh 2\theta_1 \pm \cos 2\theta_2}$ (590)
$\sin^{-1} (u \pm jv) = \sin^{-1} \left\{ \frac{\sqrt{(1+u)^2 + v^2} - \sqrt{(1-u)^2 + v^2}}{2} \right\}$ $\pm j \cosh^{-1} \left\{ \frac{\sqrt{(1+u)^2 + v^2} + \sqrt{(1-u)^2 + v^2}}{2} \right\}$	$\sinh^{-1} (u \pm jv) = \cosh^{-1} \left\{ \frac{\sqrt{(1+v)^2 + u^2} + \sqrt{(1-v)^2 + u^2}}{2} \right\}$ $\pm j \sin^{-1} \left\{ \frac{\sqrt{(1+v)^2 + u^2} - \sqrt{(1-v)^2 + u^2}}{2} \right\}$ (591)
$\cos^{-1} (u \pm jv) = \cos^{-1} \left\{ \frac{\sqrt{(1+u)^2 + v^2} - \sqrt{(1-u)^2 + v^2}}{2} \right\}$ $\mp j \cosh^{-1} \left\{ \frac{\sqrt{(1+u)^2 + v^2} + \sqrt{(1-u)^2 + v^2}}{2} \right\}$	$\cosh^{-1} (u \pm jv) = \cosh^{-1} \left\{ \frac{\sqrt{(1+u)^2 + v^2} + \sqrt{(1-u)^2 + v^2}}{2} \right\}$ $\pm j \cos^{-1} \left\{ \frac{\sqrt{(1+u)^2 + v^2} - \sqrt{(1-u)^2 + v^2}}{2} \right\}$ (592)
$\tan^{-1} (u \pm jv) = \left\{ \frac{\pi - \tan^{-1} \left( \frac{u}{\pm v - 1} \right) + \tan^{-1} \left( \frac{u}{\pm v + 1} \right)}{2} \right.$ $\left. \pm j \frac{1}{2} \log h \sqrt{\frac{(1 \pm v)^2 + u^2}{(1 \pm v)^2 + u^2}} \right\}$	$\tanh^{-1} (u \pm jv) = \frac{1}{2} \log h \sqrt{\frac{(1+u)^2 + v^2}{(1-u)^2 + v^2}} + \tan^{-1} \left( \frac{u - 1}{\pm v} \right)$ $+ j \left\{ \frac{\pi - \tan^{-1} \left( \frac{u + 1}{\pm v} \right) + \tan^{-1} \left( \frac{u - 1}{\pm v} \right)}{2} \right\}$ (593)
$\sin^{-1} u = -j \sinh^{-1} ju = -j \log h (ju + \sqrt{1 - u^2})$	$\sinh^{-1} u = -j \sin^{-1} ju = \log h (u + \sqrt{1 + u^2})$ (594)
$\cos^{-1} u = \pm j \cosh^{-1} u = \pm j \log h (u + j\sqrt{1 - u^2})$	$\cosh^{-1} u = \pm j \cos^{-1} u = \pm \log h (u + \sqrt{u^2 - 1})$ (595)
$\tan^{-1} u = -j \tanh^{-1} ju = -j \log h \frac{1 + ju}{1 - ju}$	$\tanh^{-1} u = -j \tan^{-1} ju = \frac{1}{2} \log h \frac{1 + u}{1 - u}$ (596)
$\frac{d \sin \beta}{d\beta} = \cos \beta$	$\frac{d \sinh \theta}{d\theta} = \cosh \theta$ (597)

## LIST OF IMPORTANT TRIGONOMETRICAL FORMULAS WITH CIRCULAR AND HYPERBOLIC EQUIVALENTS.—(Continued)

Circular	Hyperbolic
$\frac{d \cos \beta}{d\beta} = -\sin \beta$	$\frac{d \cosh \theta}{d\theta} = \sinh \theta$ (598)
$\frac{d \tan \beta}{d\beta} = \sec^2 \beta$	$\frac{d \tanh \theta}{d\theta} = \operatorname{sech}^2 \theta$ (599)
$\int \sin \beta \, d\beta = -\cos \beta$	$\int \sinh \theta \, d\theta = \cosh \theta$ (600)
$\int \cos \beta \, d\beta = \sin \beta$	$\int \cosh \theta \, d\theta = \sinh \theta$ (601)
$\int \tan \beta \, d\beta = -\log \cos \beta$	$\int \tanh \theta \, d\theta = \log \cosh \theta$ (602)
$\operatorname{vers} \beta = 1 - \cos \beta = \frac{\beta^2}{2!} - \frac{\beta^4}{4!} + \frac{\beta^6}{6!} - \dots$	$\operatorname{vers} \theta = \cosh \theta - 1 = \frac{\theta^2}{2!} + \frac{\theta^4}{4!} + \frac{\theta^6}{6!} + \dots$ (602a)
$\cot \beta - \tan \beta = \frac{2}{\tan 2\beta}$	$\coth \theta + \tanh \theta = \frac{2}{\tanh 2\theta}$ (602b)

## APPENDIX B

### AN ALTERNATIVE METHOD OF DEALING WITH CONTINUOUS-CURRENT LINES IN TERMS OF POSITION ANGLES IN CASES OF SUPER-SURGE-RESISTANCE LOADS

If a line  $AB$ , having a characteristic or surge resistance  $r_0$ , and subtending  $\theta$  hyp. radians, is loaded at  $B$  through  $\sigma$  ohms, the position angle at  $B$  is dependent on  $\sigma$  and  $r_0$ . Three cases present themselves.

(a)  $\sigma < r_0$

(b)  $\sigma = r_0$

(c)  $\sigma > r_0$

The following hyperbolic trigonometric identities will be used in the proof (see Appendix A (580), (549), and (548)).

$$\begin{aligned} a \cosh \theta \pm b \sinh \theta &= \sqrt{a^2 - b^2} \cosh \left( \theta \pm \tanh^{-1} \frac{b}{a} \right) \text{ if } a > b \\ &= \sqrt{b^2 - a^2} \sinh \left( \theta \pm \tanh^{-1} \frac{a}{b} \right) \text{ if } a < b \end{aligned} \quad (603)$$

$$\frac{1}{\sinh \theta} = \sqrt{\coth^2 \theta - 1} \quad (604)$$

$$\frac{1}{\cosh \theta} = \sqrt{1 - \tanh^2 \theta} \quad (605)$$

*Case (a)  $\sigma < r_0$ .*—The load resistance less than the characteristic resistance.

$$V_B = I_B \sigma \quad (605a)$$

From (96)

$$I_P = I_B \cosh \theta_2 + \frac{I_B \sigma}{r_0} \sinh \theta_2 \quad \text{amp.} \quad (606)$$

$$\frac{I_P}{I_B} = \cosh \theta_2 + \frac{\sigma}{r_0} \sinh \theta_2 \quad \text{numeric} \quad (607)$$

The solution of this may be obtained from (603), where  $a = 1$ ,  $b = \sigma/r_0$ .  $a > b$  so we use the first solution.

$$\frac{I_P}{I_B} = \sqrt{1 - \left( \frac{\sigma}{r_0} \right)^2} \cosh \left( \theta_2 + \tanh^{-1} \frac{\sigma}{r_0} \right) \quad \text{numeric} \quad (608)$$

Let  $\delta_B = \tanh^{-1} \frac{\sigma}{r_0}$ , then

$$\frac{I_P}{I_B} = \sqrt{1 - \tanh^2 \delta_B} \cosh (\theta_2 + \delta_B) \quad \text{numeric} \quad (609)$$

If we let  $\delta_P = \theta_2 + \delta_B$  using (605) and (548)

$$\frac{I_P}{I_B} = \frac{\cosh \delta_P}{\cosh \delta_B} \quad \text{numeric} \quad (610)$$

If we let  $P$  move to  $A$  (610) becomes

$$\frac{I_A}{I_B} = \frac{\cosh \delta_A}{\cosh \delta_B} \quad \text{numeric} \quad (611)$$

Dividing (610) by (611) we obtain  $I_P$  in terms of  $I_A$

$$\frac{I_P}{I_A} = \frac{\cosh \delta_P}{\cosh \delta_A} \quad \text{numeric} \quad (612)$$

In a similar manner we obtain the voltage ratio in terms of position angles.

$$V_P = V_B \cosh \theta_2 + I_B r_0 \sinh \theta_2 \quad \text{volts} \quad (613)$$

Using the value of  $I_B$  given by (605a)

$$V_P = V_B \cosh \theta_2 + V_B \frac{r_0}{\sigma} \sinh \theta_2 \quad \text{volts} \quad (614)$$

$$\frac{V_P}{V_B} = \cosh \theta_2 + \coth \delta_B \sinh \theta_2 \quad \text{numeric} \quad (615)$$

This solution also may be obtained from (603) and (580) where  $a = 1$ ,  $b = r_0/\sigma$ .  $a < b$  so we use the second solution.

$$\frac{V_P}{V_B} = (\sqrt{\coth^2 \delta_B - 1}) \sinh \left\{ \theta_2 + \tanh^{-1} \frac{1}{(r_0/\sigma)} \right\} \quad \text{numeric} \quad (616)$$

$$= \frac{\sinh (\theta_2 + \delta_B)}{\sinh \delta_B} \quad (\text{by 604}) \quad \text{numeric} \quad (617)$$

$$= \frac{\sinh \delta_P}{\sinh \delta_B} \quad \text{numeric} \quad (618)$$

If we let  $P$  move to  $A$

$$\frac{V_A}{V_B} = \frac{\sinh \delta_A}{\sinh \delta_B} \quad \text{numeric} \quad (619)$$

Dividing (618) by (619), we obtain  $V_P$  in terms of  $V_A$

$$\frac{V_P}{V_A} = \frac{\sinh \delta_P}{\sinh \delta_A} \quad \text{numeric} \quad (620)$$

Case (b)  $\sigma = r_0$ .—The load resistance equal to the characteristic resistance (see page 47 *et seq.*).

$$V_P = V_B e^{\theta_2} \quad \text{volts} \quad (621)$$

$$I_P = I_B e^{\theta_2} \quad \text{amp.} \quad (622)$$

Case (c)  $\sigma > r_0$ .—The load resistance greater than the characteristic resistance.



Using the equations obtained in case (a), we find  $\tanh \delta_B = \sigma/r_0 > 1$  which gives an imaginary  $\delta_B$ .

This equation does not hold, since it was derived for the condition  $\sigma/r_0 < 1$ . Rewriting the equations as in case (a), we obtain

$$I_P = I_B \cosh \theta_2 + I_B \frac{\sigma}{r_0} \sinh \theta_2 \quad \text{amp.} \quad (623)$$

$$\frac{I_P}{I_B} = \cosh \theta_2 + \frac{\sigma}{r_0} \sinh \theta_2 \quad \text{numeric} \quad (624)$$

The solution of this may be obtained from (580),  $a = 1$ ,  $b = \sigma/r_0$ .  $a < b$  so we use the second solution.

$$\frac{I_P}{I_B} = \left\{ \sqrt{\left(\frac{\sigma}{r_0}\right)^2 - 1} \right\} \sinh \left\{ \theta_2 + \tanh^{-1} \frac{1}{(\sigma/r_0)} \right\} \quad \text{numeric} \quad (625)$$

Let

$$\delta'_B = \tanh^{-1} \frac{r_0}{\sigma}, \quad \text{hyps.} \quad (626)$$

then

$$\frac{I_P}{I_B} = (\sqrt{\coth^2 \delta'_B - 1}) \sinh (\theta_2 + \delta'_B) \quad \text{numeric} \quad (627)$$

$$\frac{I_P}{I_B} = \frac{\sinh \delta'_P}{\sinh \delta'_B} \quad \text{numeric} \quad (628)$$

By the same method as in case (a),

$$\frac{I_P}{I_A} = \frac{\sinh \delta'_P}{\sinh \delta'_A} \quad \text{numeric} \quad (629)$$

Hence we see that if a line is loaded by an infra-surge-resistance load, the current varies as the hyperbolic cosine of the position angle, while if the line is loaded by a super-surge-resistance load, the current varies as the hyperbolic sine of the position angle. In this latter case,  $\delta'_B$  is computed from a reciprocal anti-hyperbolic tangent. For the special case where the load just equals the characteristic resistance, the current varies exponentially.

In a similar manner, we obtain the voltage ratio in terms of position angles.

$$V_P = V_B \cosh \theta_2 + I_B r_0 \sinh \theta_2 \quad \text{volts} \quad (630)$$

$$\frac{V_P}{V_B} = \cosh \theta_2 + \frac{r_0}{\sigma} \sinh \theta_2 \quad \text{numeric} \quad (631)$$

The solution may be obtained from (580)  $a = 1$ ,  $b = r_0/\sigma$ .  $a > b$ , so we use the first solution.

$$\frac{V_P}{V_B} = \left( \sqrt{1 - \left(\frac{r_0}{\sigma}\right)^2} \right) \cosh \left( \theta_2 + \tanh^{-1} \frac{r_0}{\sigma} \right) \quad \text{numeric} \quad (632)$$

$$= \sqrt{1 - \tanh^2 \delta_B} \cosh (\theta_2 + \delta_B') \quad \text{numeric} \quad (633)$$

$$= \frac{\cosh \delta_P'}{\cosh \delta_B'} \quad \text{numeric} \quad (634)$$

and

$$\frac{V_P}{V_A} = \frac{\cosh \delta_P'}{\cosh \delta_A'} \quad \text{numeric} \quad (635)$$

Hence we see that along a line loaded by an infra-surge-resistance load, the voltage varies as the hyperbolic sine of the position angle, while in the case of a super-surge-resistance load, the voltage varies as the cosine of the substitute position angle. In this latter case  $\delta_B'$  is computed from a reciprocal anti-hyperbolic tangent. For the special case where the load just equals the characteristic resistance, the current varies exponentially.

If we are to use this method of computing position angles, the resistance ratio for case (c) becomes

$$\begin{aligned} \frac{R_P}{R_A} &= \frac{V_P}{V_A} \times \frac{I_A}{I_P} = \frac{\cosh \delta_P'}{\cosh \delta_A'} \cdot \frac{\sinh \delta_A'}{\sinh \delta_P'} \\ &= \frac{\coth \delta_P'}{\coth \delta_A'} \quad \text{numeric} \quad (636) \end{aligned}$$

The power ratio is the same as determined in Chapter V.

A table of current, voltage, resistance, and power ratios follows for different values of the ratio  $\sigma/r_0$ .

TABLE XXXII

Ratios of current, voltage, resistance, and power over d.c. lines for various values of the load resistance  $\sigma$

Ratio	$\frac{\sigma}{r_0} < 1$	$\frac{\sigma}{r_0} = 1$	$\frac{\sigma}{r_0} > 1$
$\frac{I_P}{I_B}$	$\frac{\cosh \delta_P}{\cosh \delta_B}$	$e^{\theta_2}$	$\frac{\sinh \delta_P}{\sinh \delta_B} \quad (637)$
$\frac{V_P}{V_B}$	$\frac{\sinh \delta_P}{\sinh \delta_B}$	$e^{\theta_2}$	$\frac{\cosh \delta_P}{\cosh \delta_B} \quad (638)$
$\frac{R_P}{R_B}$	$\tanh \delta_P$	1	$\coth \delta_P \quad (639)$
$\frac{P_P}{P_B}$	$\frac{\sinh 2\delta_P}{\sinh 2\delta_B}$	$e^{2\theta_2}$	$\frac{\sinh 2\delta_P}{\sinh 2\delta_B} \quad (640)$

In any a.c. case, since we can always find the value of  $\tanh^{-1} (\sigma/z_0)$ , the necessity for this alternative method of finding position angles with case (c) entirely disappears.

## APPENDIX C

### DERIVATION OF THE ELEMENTS OF EQUIVALENT T AND II STRUCTURES. CORRECTING FACTORS TO OBTAIN EQUIVALENT T AND II FROM NOMINAL T AND II

**The Equivalent T.**—We can construct a  $T$ -section with series elements  $\rho'$  and a shunt element  $g'$  such that the section will replace the line exactly at its terminals. To determine the values of  $\rho'$  and  $g'$  in terms of  $\theta$  and  $z_0$ , let the equivalent  $T$  of Fig. 22, be grounded at  $b'$ . Then

$$R_{ag} = z_0 \tanh \theta = \rho' + \frac{\frac{\rho'}{g'}}{\rho' + \frac{1}{g'}} \quad \text{ohms } \angle \quad (641)$$

Also if we free  $b'$ ,

$$R_{af} = z_0 \coth \theta = \rho' + \frac{1}{g'} \quad \text{ohms } \angle \quad (642)$$

$$\rho' = z_0 \coth \theta - \frac{1}{g'} \quad \text{ohms } \angle \quad (643)$$

Substituting in (641)

$$z_0 \coth \theta - \frac{1}{g'} + \frac{\frac{z_0 \coth \theta}{g'} - \frac{1}{(g')^2}}{z_0 \coth \theta - \frac{1}{g'} + \frac{1}{g'}} = z_0 \tanh \theta \quad \text{ohms } \angle \quad (644)$$

Multiplying through by  $z_0 \coth \theta$ , we have

$$z_0^2 \coth^2 \theta - \frac{z_0 \coth \theta}{g'} + \frac{z_0 \coth \theta}{g'} - \frac{1}{(g')^2} = z_0^2$$

$$z_0^2 (\coth^2 \theta - 1) = \frac{1}{(g')^2} \quad \text{ohms}^2 \angle \quad (645)$$

$$g' = \frac{1}{\sqrt{(\coth^2 \theta - 1)z_0}}$$

and by (549)

$$= \frac{\sinh \theta}{z_0} = y_0 \sinh \theta \quad \text{mhos } \angle \quad (646)$$

Substituting in (643)

$$\rho' = z_0 \coth \theta - \frac{z_0}{\sinh \theta} = z_0 \frac{(\cosh \theta - 1)}{\sinh \theta}$$

and by (564)

$$= z_0 \tanh \frac{\theta}{2} \quad \text{ohms } \angle \quad (647)$$

We shall next determine  $k_{\rho}$ , and  $k_g$ , the correcting factors by which we multiply  $R/2$  and  $G$ , respectively, of the nominal  $T$ -line to determine  $\rho'$  and  $g'$ .

By the definition given above

$$\rho' = \frac{R}{2} k_{\rho} = z_0 \tanh \frac{\theta}{2} \quad \text{ohms } \angle \quad (648)$$

$$k_{\rho} = \frac{z_0 \tanh \frac{\theta}{2}}{R/2} \quad \text{numeric } \angle \quad (649)$$

but by (52),  $R = \theta z_0$ , so that

$$k_{\rho} = \frac{\tanh \frac{\theta}{2}}{\theta/2} \quad \text{numeric } \angle \quad (650)$$

In like manner,

$$g' = G k_g = \frac{\sinh \theta}{z_0} \quad \text{mhos } \angle \quad (651)$$

$$k_g = \frac{\sinh \theta}{G z_0} \quad \text{numeric } \angle \quad (652)$$

but by (53),  $G = \theta/z_0 = \theta y_0$

$$k_g = \frac{\sinh \theta}{\theta} \quad \text{numeric } \angle \quad (653)$$

Tables of these correcting factors are tabulated and plotted as functions of the angle  $\theta$  in the tables and chart atlas of these functions.

**The Equivalent II.**—We can construct a  $\Pi$ -section with a series element  $\rho''$  and shunt elements  $g''$  such that the section will replace the line exactly at its terminals. To determine the values of  $\rho''$  and  $g''$  in terms of  $\theta$  and  $z_0$ , we let the equivalent  $\Pi$  of Fig. 22 be grounded at  $b''$ . Then

$$R_{ag} = z_0 \tanh \theta = \frac{\rho''/g''}{\rho'' + \frac{1}{g''}} \quad \text{ohms } \angle \quad (654)$$

Also if we let  $b''$  be free

$$R_{Af} = z_0 \coth \theta = \frac{\left(\rho'' + \frac{1}{g''}\right) \frac{1}{g''}}{\rho'' + \frac{2}{g''}} \text{ ohms } \angle \quad (655)$$

Solving (654) for  $\rho''$

$$\begin{aligned} \rho'' &= z_0 \tanh \theta \left( \rho'' + \frac{1}{g''} \right) g'' \\ &= z_0 \tanh \theta (\rho'' g'' + 1) \end{aligned} \quad \text{ohms } \angle \quad (656)$$

$$\rho''(1 - g'' z_0 \tanh \theta) = z_0 \tanh \theta \quad \text{ohms } \angle \quad (657)$$

$$\rho'' = \frac{z_0 \tanh \theta}{1 - g'' z_0 \tanh \theta} \quad \text{ohms } \angle \quad (658)$$

Substituting this value in (655)

$$z_0 \coth \theta = \frac{\left( \frac{z_0 \tanh \theta}{1 - g'' z_0 \tanh \theta} + \frac{1}{g''} \right) \frac{1}{g''}}{\frac{z_0 \tanh \theta}{1 - g'' z_0 \tanh \theta} + \frac{2}{g''}} \quad \text{ohms } \angle \quad (659)$$

$$= \frac{(z_0 g'' \tanh \theta + 1 - g'' z_0 \tanh \theta) \frac{1}{g''}}{z_0 g'' \tanh \theta + 2 - 2g'' z_0 \tanh \theta} \quad \text{ohms } \angle \quad (660)$$

or

$$= \frac{1/g''}{2 - z_0 g'' \tanh \theta} \quad \text{ohms } \angle \quad (661)$$

or

$$2z_0 \coth \theta - z_0^2 g'' = \frac{1}{g''} \quad \text{ohms } \angle \quad (662)$$

$$z_0^2 (g'')^2 - 2z_0 g'' \coth \theta + 1 = 0$$

$$g'' = \frac{2z_0 \coth \theta \pm \sqrt{4z_0^2 \coth^2 \theta - 4z_0^2}}{2z_0^2} \quad \text{mhos } \angle \quad (663)$$

We take the minus value in the above equation, since the plus value gives a negative value for  $\rho''$  which is impossible.

$$g'' = (\coth \theta - \sqrt{\coth^2 \theta - 1}) \frac{1}{z_0} \quad \text{mhos } \angle \quad (664)$$

$$= \left( \coth \theta - \frac{1}{\sinh \theta} \right) \frac{1}{z_0} \quad \text{mhos } \angle \quad (665)$$

$$= \left( \frac{\cosh \theta - 1}{\sinh \theta} \right) \frac{1}{z_0} = \frac{\tanh \frac{\theta}{2}}{z_0} \quad \text{mhos } \angle \quad (666)$$

Substituting in (658)

$$\begin{aligned} \rho'' &= \frac{z_0 \tanh \theta}{\tanh \frac{\theta}{2} z_0 \tanh \theta} \\ &= \frac{1}{z_0} \end{aligned} \quad \text{ohms } \angle \quad (667)$$



$$= \frac{z_0 \frac{\sinh \theta}{\cosh \theta}}{1 - \frac{(\cosh \theta - 1) \sinh \theta}{\sinh \theta \cosh \theta}} \quad \text{ohms } \angle \quad (668)$$

$$= \frac{z_0 \sinh \theta}{\cosh \theta - (\cosh \theta - 1)} = z_0 \sinh \theta \quad \text{ohms } \angle \quad (669)$$

We shall next determine  $k_{\rho''}$  and  $k_{g''}$ , the correcting factors by which we multiply  $R$  and  $G/2$ , respectively, of the nominal  $\Pi$  line to determine  $\rho''$  and  $g''$ .

By the definition given above

$$\rho'' = Rk_{\rho''} = z_0 \sinh \theta \quad \text{ohms } \angle \quad (670)$$

$$k_{\rho''} = \frac{z_0 \sinh \theta}{R} = \frac{z_0 \sinh \theta}{\theta z_0} \quad \text{numeric } \angle \quad (671)$$

$$= \frac{\sinh \theta}{\theta} \quad \text{numeric } \angle \quad (672)$$

In like manner,

$$g'' = \frac{G}{2} k_{g''} = \frac{\tanh \frac{\theta}{2}}{z_0} \quad \text{mhos } \angle \quad (673)$$

$$k_{g''} = \frac{\tanh (\theta/2)}{Gz_0/2} \quad \text{numeric } \angle \quad (674)$$

$$k_{g''} = \frac{\tanh (\theta/2)}{\theta z_0/2z_0} = \frac{\tanh (\theta/2)}{\theta/2} \quad \text{numeric } \angle \quad (675)$$

It is evident that the correcting factors which convert the nominal  $\Pi$  into the equivalent  $\Pi$  of the conjugate smooth line, are the same as those which convert the nominal  $T$  into the equivalent  $T$ , but in inverse order; so that  $k_{\rho''} = k_{g'}$  and  $k_{g''} = k_{\rho'}$ .

## APPENDIX D

### DEVELOPMENT OF VECTOR TRANSMISSION AND REFLECTION COEFFICIENTS OF VOLTAGE AND CURRENT

Formulas (342) to (345), taken with Tables VIII and IX express the relations of the coefficients of transmission and reflection to the surge impedances on each side of a junction. These equations may be briefly developed.

Consider the single uniform line  $AB$  in Fig. 86, grounded at  $B$  through a load  $\sigma$ , or through a terminal section of line having a surge impedance  $z_o = \sigma$ , and energized at  $A$  by a sinusoidal generator, from which an initial outgoing wave is started, without splash, along the line. Attention is directed to the phenomena at junction  $B$ , when the wave arrives there. The load may have any fixed vector value between 0 and  $\infty$ . Let  $z_o$  be the surge impedance of the line  $AB$ .

Let  $V_1$  and  $I_1$  be the potential and current arriving at  $B$ .

Let  $V_2$  and  $I_2$  be the potential and current reflected from  $B$ .

Let  $V_3$  and  $I_3$  be the potential and current transmitted to  $\sigma$ .

Let  $m_c$  be the transmission coefficient for current, and  $m_v$  be the transmission coefficient for voltage.

Let currents flowing in the direction  $AB$  be taken as positive. Then

$$I_3 = m_c I_1 \quad \text{amp. } \angle \quad (676)$$

$$-I_2 = (1 - m_c) I_1 \quad \text{amp. } \angle \quad (677)$$

or

$$I_2 = -(1 - m_c) I_1 = (m_c - 1) I_1 \quad \text{amp. } \angle \quad (678)$$

Thus

$$I_1 + I_2 = I_3 \quad \text{amp. } \angle \quad (679)$$

The potential  $V_3$  due to the passage of current  $I_3$  through the impedance  $\sigma$  is

$$V_3 = I_3 \sigma \quad \text{volts } \angle \quad (680)$$

Similarly

$$V_1 = I_1 z_o \quad \text{volts } \angle \quad (681)$$

The potential  $V_2$  is that produced at  $B$  by the reflected current  $-I_2$  passing through the surge impedance  $z_o$ ,

or

$$V_2 = -I_2 z_o \quad \text{volts } \angle \quad (682)$$

and

$$V_1 + V_2 = V_3 \quad \text{volts } \angle \quad (683)$$

Substituting (680), (681), and (682) in this last equation,

$$I_1 z_o - I_2 z_o = I_3 \sigma \quad \text{volts } \angle \quad (684)$$

substituting (678) and (676),

$$I_1 z_o - (m_c - 1)I_1 z_o = m_c I_1 \sigma \quad \text{volts } \angle \quad (685)$$

whence

$$m_c(\sigma + z_o) = 2z_o \quad \text{ohms } \angle \quad (686)$$

or

$$m_c = \frac{2z_o}{z_o + \sigma} \quad \text{numeric } \angle \quad (687)$$

The reflection coefficient for a current wave from the junction  $B$  is

$$-(1 - m_c) = m_c - 1 = \frac{z_o - \sigma}{z_o + \sigma} \quad \text{numeric } \angle \quad (688)$$

Again if  $V_1$  is the incoming potential at  $B$ ,

$$V_3 = m_v V_1 \quad \text{volts } \angle \quad (689)$$

and by (683)

$$V_2 = V_3 - V_1 = V_1(m_v - 1) = -V_1(1 - m_v) \quad \text{volts } \angle \quad (690)$$

Starting with (679)

$$I_1 + I_2 = I_3 \quad \text{amp. } \angle \quad (691)$$

by (682) and (680)

$$\frac{V_1}{z_o} - \frac{V_2}{z_o} = \frac{V_3}{\sigma} \quad \text{amp. } \angle \quad (692)$$

or by (690)

$$\frac{V_1}{z_o} - \frac{V_1(m_v - 1)}{z_o} = \frac{m_v V_1}{\sigma} \quad \text{amp. } \angle \quad (693)$$

$$\therefore \frac{2 - m_v}{z_o} = \frac{m_v}{\sigma} \quad \text{mhos } \angle \quad (694)$$

or

$$2\sigma - m_v \sigma = m_v z_o \quad \text{ohms } \angle \quad (695)$$

and

$$m_v = \frac{2\sigma}{z_o + \sigma} \quad \text{numeric } \angle \quad (696)$$

The reflection coefficient for a voltage wave from the junction *B* is:

$$-(1 - m_v) = m_v - 1 = \frac{\sigma - z_0}{z_0 + \sigma} \quad \text{numeric } \angle \quad (697)$$

The following table gives a few simple examples of these coefficients.

TABLE XXXIII

Table of transmission and reflection coefficients for a junction between a line of surge impedance  $z_0$  on the *A* side and a line of surge impedance  $\sigma$  on the *B* side, for different values of  $\sigma$ .

Case	$\sigma$ ohms	Current		Voltage	
		Transmitted	Reflected	Transmitted	Reflected
		$\frac{m_c}{2z_0}$ $\frac{2z_0}{z_0 + \sigma}$	$\frac{m_c - 1}{z_0 - \sigma}$ $\frac{z_0 - \sigma}{z_0 + \sigma}$	$\frac{m_v}{2\sigma}$ $\frac{2\sigma}{z_0 + \sigma}$	$\frac{m_v - 1}{\sigma - z_0}$ $\frac{\sigma - z_0}{z_0 + \sigma}$
1	0	2	1	0	-1
2	$\frac{z_0}{2}$	$\frac{4}{3}$	$\frac{1}{3}$	$\frac{2}{3}$	$-\frac{1}{3}$
3	$z_0$	1	0	1	0
4	$2z_0$	$\frac{2}{3}$	$-\frac{1}{3}$	$\frac{4}{3}$	$\frac{1}{3}$
5	$\infty$	0	-1	2	1

It is to be noted that the sum of the transmission coefficients is constant in all cases, or

$$m_c + m_v = 2 \quad \text{numeric} \quad (698)$$

Also the reflection coefficients  $(m_c - 1)$  and  $(m_v - 1)$  are equal and opposite, or

$$(m_c - 1) = -(m_v - 1) \quad \text{numeric } \angle \quad (699)$$

## APPENDIX E

### DERIVATION OF THE ARCHITRAVE IMPEDANCE OF A COMPOSITE LINE

Assume the three-section composite line of Fig. 171, page 298, and that voltage is applied at  $A$ , we desire to show that the architrave impedance, when the line is grounded at  $F$ , is

$$\rho'' = z_1 \sinh \delta_A \frac{\cosh \delta_C \cosh \delta_E}{\cosh \delta_B \cosh \delta_D} \text{ ohms } \angle \quad (700)$$

where the position angles are measured from the  $F$  end.

$$\rho'' = \frac{V_A}{I_F} = \frac{V_F}{I_A} \text{ ohms } \angle \quad (701)$$

according to the end which is assumed grounded. In this case we have assumed the  $F$  end grounded.

$$\frac{I_A}{I_B} = \frac{\cosh \delta_A}{\cosh \delta_B} \text{ numeric } \angle \quad (702)$$

$$\frac{I_C}{I_D} = \frac{\cosh \delta_C}{\cosh \delta_D} \text{ numeric } \angle \quad (703)$$

$$\frac{I_E}{I_F} = \frac{\cosh \delta_E}{\cosh \delta_F} \text{ numeric } \angle \quad (704)$$

But since  $B$  and  $C$  are connected at a junction,

$$I_B = I_C \text{ amp. } \angle \quad (705)$$

and since  $D$  and  $E$  are connected

$$I_D = I_E \text{ amp. } \angle \quad (706)$$

Making use in turn of (704), (706), (703), (705), and (702) we have

$$I_F = \frac{\cosh \delta_F}{\cosh \delta_E} \times I_E \text{ amp. } \angle \quad (707)$$

$$= \frac{\cosh \delta_F}{\cosh \delta_E} \times I_D \text{ amp. } \angle \quad (708)$$

$$= \frac{\cosh \delta_F}{\cosh \delta_E} \times \frac{\cosh \delta_D}{\cosh \delta_C} \times I_C \quad (709)$$

$$= \frac{\cosh \delta_F}{\cosh \delta_E} \times \frac{\cosh \delta_D}{\cosh \delta_C} \times I_B \quad (710)$$

$$= \frac{\cosh \delta_F}{\cosh \delta_E} \times \frac{\cosh \delta_D}{\cosh \delta_C} \times \frac{\cosh \delta_B}{\cosh \delta_A} \times I_A \text{ amp. } \angle \quad (711)$$



$$\frac{V_A}{I_A} = z_1 \tanh \delta_A \quad \text{ohms } \angle \quad (712)$$

$$\rho'' = \frac{V_A}{I_F} = \frac{V_A}{I_A} \frac{\cosh \delta_E}{\cosh \delta_F} \times \frac{\cosh \delta_C}{\cosh \delta_D} \times \frac{\cosh \delta_A}{\cosh \delta_B} \quad \text{ohms } \angle \quad (713)$$

Substituting the value  $V_A/I_A$  from (712)

$$\rho'' = z_1 \frac{\sinh \delta_A}{\cosh \delta_A} \times \frac{\cosh \delta_E}{\cosh \delta_F} \times \frac{\cosh \delta_C}{\cosh \delta_D} \times \frac{\cosh \delta_A}{\cosh \delta_B} \quad \text{ohms } \angle \quad (714)$$

Since  $\delta_F = 0$  for the case in question (714) becomes

$$\rho'' = z_1 \sinh \delta_A \times \frac{\cosh \delta_E}{\cosh \delta_D} \times \frac{\cosh \delta_C}{\cosh \delta_B} \quad \text{ohms } \angle \quad (715)$$

Since we usually desire the  $\Pi$ -network of the composite line only, we are not interested in determining the value of the architrave impedance for the case when  $\delta_F$  is other than zero. The impedance of the load may be subsequently combined with that of the end leak in order to determine the  $\Pi$ -network of the terminally loaded system.

If, in computing through the position angles for a d-c. case, the load caused by the line or lines beyond is greater than the characteristic impedance of the line in question, we may look up the hyperbolic cotangent, and add  $j_2^\pi$  to the angle, or we may use formula (626), Appendix B, to compute the position angle and change cosh to sinh, and sinh to cosh, wherever they occur back to the supply. The method of adding  $j_2^\pi$  to the angle is, however, to be preferred, since the imaginary quadrant is a reminder of this change.

If the position angles are computed for the  $A$  end grounded, we can show in a similar manner that

$$\rho'' = z_3 \sinh \delta_F \frac{\cosh \delta_D}{\cosh \delta_E} \times \frac{\cosh \delta_B}{\cosh \delta_C} \quad \text{ohms } \angle \quad (716)$$

## APPENDIX F

### PROBLEMS FOR SOLUTION

#### Problems on Chapter I

**Problem 1.**—Lay off the hyperbolic angle  $\theta = 2$  on the hyperbola  $xy = 1$ , and divide into four equal parts.

**Problem 2.**—Substituting exponentials for the hyperbolic functions where they occur, determine the right-hand side of the following equations, and express the results finally in terms of hyperbolic functions.

(a)  $\cosh \theta \cosh \phi - \sinh \theta \sinh \phi =$

(b)  $\operatorname{sech}^2 \theta + \tanh^2 \theta =$

(c)  $\frac{\sinh \theta}{2 \cosh \frac{\theta}{2}} =$

**Problem 3.**—Find the hyperbolic equivalents to the following circular trigonometric identities:

(a)  $\sin \frac{\beta}{2} = \frac{\sin \beta}{2 \cos \frac{\beta}{2}} = \sqrt{\frac{1 - \cos \beta}{2}}$

(b)  $\cos \frac{\beta}{2} = \frac{\sin \beta}{2 \sin \frac{\beta}{2}} = \sqrt{\frac{1 + \cos \beta}{2}}$

(c)  $\tan \frac{\beta}{2} = \frac{\sin \beta}{1 + \cos \beta} = \frac{1 - \cos \beta}{\sin \beta} = \sqrt{\frac{1 - \cos \beta}{1 + \cos \beta}}$

(d)  $\cos^2 \beta - \sin^2 \beta = \cos 2\beta = 2 \cos^2 \beta - 1$

(e)  $\sin 2\beta = 2 \sin \beta \cdot \cos \beta = \frac{2 \tan \beta}{1 + \tan^2 \beta}$

(f)  $\sec^2 \beta - \tan^2 \beta = 1$

#### Problems on Chapter IV

**Problem 4.**—A No. 12 N.B.S. copper-wire circuit is 1,000 miles long.  $r = 10.4$  ohms per loop mile.  $g = 5 \times 10^{-8}$  mhos per loop mile.

The impressed voltage at the sending end is 24.0 volts. The  $B$  end is open and the entering current  $I_A$  is  $1.03 \times 10^{-3}$  amp.

Find current and voltage at 200-mile intervals using line equations and plot each *versus* distance from sending end.

**Problem 5.**—The No. 12 N.B.S. circuit of problem 4 is 1,000 miles long. The impressed voltage at the sending end is 24.0 volts. The  $B$  end is short-circuited. The entering current is  $2.70 \times 10^{-3}$  amp. Find current and voltage at 200-mile intervals, using line equations, and plot each *versus* distance from sending end.

**Problem 6.**—A No. 14 N.B.S. copper-wire line 320 miles in length is used for a single-wire telegraph line having the following constants:  $r = 8.56$  ohms per wire mile, and  $g = 2.40 \times 10^{-6}$  mhos per wire mile.

A potential of 120 volts is applied at  $A$ . The line is grounded at  $B$  through 550 ohms. Find  $I_A$ ,  $I_B$ , and  $V_B$  also  $I_P$  and  $V_P$  at 80-mile intervals. Plot current and voltage distribution along the line.

**Problem 7.**—Take the same line grounded through 1,880 ohms at  $B$ , and obtain  $I_A$ ,  $I_B$ , and  $V_B$ , as well as  $I_P$  and  $V_P$  at 80-mile intervals. Plot current and voltage distribution along the line.

**Problem 8.**—Take the same line grounded through 6,000 ohms at  $B$ , and obtain  $I_A$ ,  $I_B$ , and  $V_B$ , as well as  $I_P$  and  $V_P$  at 80-mile intervals. Plot current and voltage distribution along the line.

### Problems on Chapter V

**Problem 9.**—A No. 12 N.B.S. copper-wire telephone line is 400 miles long. Its constants are:  $r = 10.4$  ohms per loop mile,  $g = 5 \times 10^{-8}$  mhos per loop mile and  $V_A = 100$  volts.

- Assuming  $\sigma = 3,000$  ohms, find  $R_P$  and  $P_P$  at 100-mile intervals.
- Repeat (a) for  $\sigma = r_0$ .
- Repeat (a) for  $\sigma = 70,000$  ohms.
- Assume line is 4,000 miles long. Find  $R_A$  when  $\sigma = 0$  and when  $\sigma = \infty$ . Explain.

**Problem 10.**—A certain telephone line is 570 miles long. When shorted at the far end  $R_A$  measures 2,300 ohms. When open at the far end  $R_A$  measures 36,000 ohms. Find  $\theta$ ,  $\alpha$ ,  $r_0$ ,  $r$ , and  $g$ .

**Problem 11.**—With a given line of  $\theta$  hyperbolic radians and  $r_0$  characteristic resistance, find:

- The value of  $\sigma$  for the maximum power at the load terminals.
- The value of  $\sigma$  for the maximum transmission efficiency.

### Problem on Chapter VI

**Problem 12.**—Find the equivalent  $T$  and  $\Pi$  of 400 miles of No. 12 N.B.S. copper-wire telephone line. Its constants are:  $r = 10.4$  ohms per loop mile, and  $g = 5 \times 10^{-8}$  mhos per loop mile.

Assuming  $\sigma = 1,000$  ohms, calculate  $I_A$ ,  $I_B$ , and  $V_B$  from line constants, check through the network and see if it simulates the real line exactly at its terminals, assuming  $V_A$  is 48 volts.

### Problems on Chapter IX

**Problem 13.**—Expand the following:

- $\sinh(\theta + j\phi)$ .
- $\cosh(\theta + j\phi)$ .
- $\tanh(\theta + j\phi)$ .
- $\sinh(\theta - j\phi)$ .
- $\cosh(\theta - j\phi)$ .
- $\tanh(\theta - j\phi)$ .

**Problem 14.**—Find  $\sinh$ ,  $\cosh$ , and  $\tanh$  of:

(a)  $0.3324 + j0.2199$ .

(b)  $1.171 + j2.785$ .

(c)  $1.641 + j1.988$ .

(d) Show that  $\sinh \left\{ x + j \left( y + \frac{\pi}{2} \right) \right\} = j \cosh (x + jy)$ .

(e) Show that  $\sinh \{ x + j(z + 2n\pi) \} = \sinh (x + jz)$ .

**Problem 15.**—Find  $\sinh$ ,  $\cosh$ , and  $\tanh$  of:

(a)  $0.725 + j0.357$ .

(b)  $1.752 + j2.55$ .

(c)  $3.51 + j1.53$ .

(d) Show that  $\cosh (x + jy) = -j \sinh \left\{ x + j \left( y + \frac{\pi}{2} \right) \right\}$ .

(e) Show that  $\cosh \{ x + j(z + \pi) \} = -\cosh (x + jz)$ .

### Problems on Chapter X

**Problem 16.**—A single-wire submarine telegraph cable is operated at a frequency of 20 cycles per second at 50 volts. It is 300 nautical miles in length.

The constants per wire naut. are:  $r = 10$  ohms,  $l = 0$  henry,  $g = 0$  mhos, and  $c = 0.333 \times 10^{-6}$  farads.

(a) Find  $I_A$  and  $I_B$  if line is grounded at the far end.

(b) Find  $I_A$ ,  $I_B$ , and  $V_B$  if line is grounded at  $B$  through  $250 \angle 25^\circ$  ohms.

**Problem 17.**—A certain submarine telephone cable is 19.3 miles long and has the following constants:

Pairs

Phantoms

$t = 22$  ohms per loop mile

$r = 11$  ohms per loop mile

$l = 0$

$l = 0$

$g = 0$

$g = 0$

$c = 0.086$   $\mu$ f. per loop mile.

$c = 0.017$   $\mu$ f. per loop mile.

(a) Assuming 1 volt at 800 cycles per sec. to be applied to a pair at  $A$ , find  $I_A$ ,  $I_B$ , and the ratio  $I_B/I_A$  if the load  $\sigma$  is  $520 \angle 44^\circ$ .

(b) Assuming the same voltage and frequency as in (a) to be applied to the phantom, find  $I_A$ ,  $I_B$ , and  $I_B/I_A$  for the same load applied at  $B$ .

(c) Repeat (a) for the following frequencies and plot current ratio against frequency: 400, 1,200, 1,600, 2,000, 2,500, 3,000 cycles per sec.

**Problem 18.**—A No. 8 B.W.G. telephone pair is 1,000 miles long. Its constants are:

$r = 4.14$  ohms per loop mile.

$g = 80 \times 10^{-8}$  mhos per loop mile.

$l = 3.37 \times 10^{-3}$  henrys per loop mile.

$c = 9.14 \times 10^{-9}$  farads per loop mile.

Assume the applied voltage to be  $1 \angle 0$  volts at  $A$ , and  $\sigma = 0$ , find  $I_P/V_P$  at 200-mile intervals, and make a polar plot. Plot real and imaginary components of volt-amperes *versus* distance.

**Problem 19.**—Repeat problem 18, using  $\sigma = 610 \angle 5^\circ$ .

**Problem 20.**—Repeat problem 18, using  $\sigma = \infty$ .

**Problem 21.**—Number 13 A.W.G. gage cable has the following constants.

$r = 21.4$  ohms per loop mile.

$c = 0.062 \mu\text{f. per loop mile.}$

$l = 1 \times 10^{-3} \text{ henrys per loop mile.}$

$g = 0.$

Plot  $\alpha_1$ ,  $\alpha_2$ , also the resistance component and reactance component of  $z_0$  as a function of frequency, from 0 to 2,000 cycles per sec. by 400-cyp. intervals.

**Problem 22.**—A submarine cable was laid on August 29, 1924, from Aldeburgh, Suffolk, England, to Dombert, Walcheren, on the Dutch coast. Its constants are:

$r = 16.12 \text{ ohms per nautical mile of loop.}$

$g = 2.8 \text{ microhos per nautical mile of loop.}$

$l = 19.3 \text{ millihenrys per nautical mile of loop.}$

$c = 0.11 \mu\text{f. per nautical mile of loop.}$

The length is 86 nautical miles.

(a) Assume 90 volts (ringing) is applied at 16 cycles per sec. Calculate  $I_A$ ,  $I_B$ , and  $V_B$  for the line closed at the far end through a ringer of 1,000-ohm resistance and 1.305-henry inductance.

(b) Assume 20 volts at 800 cycles per sec. is applied. Calculate  $I_A$ ,  $I_B$ , and  $V_B$  for the line closed at  $B$  through a receiver of  $175 \angle 40.4^\circ$  ohms impedance.

(c) Calculate  $\alpha_1$  at 200-cyp. intervals up to 2,200 cycles per sec.

(d) Calculate  $\alpha_2$  and the velocity of propagation at 200-cyp. intervals up 2,200 cycles per sec.

### Problem on Chapter XI

**Problem 23.**—A line 70 km. long has  $\theta = 0.25 + j0.75 \text{ hyp.}$ ,  $V_A = 1\angle 0^\circ \text{ volt}$ , and is open at  $B$ .

(a) Take 10 runs over the line and determine the magnitude of each voltage wave arrival at  $B$ .

(b) Plot these voltages and get the vector sum.

(c) Compare with solution by hyperbolic functions.

(d) If the frequency is 800 cycles per sec. compute the apparent velocity of transmission and the time of propagation of one wave.

### Problems on Chapter XIII

**Problem 24.**—Number 12 N.B.S. copper-wire telephone line has the following constants:  $r = 10.4 \text{ ohms per loop mile}$ , and  $g = 5 \times 10^{-8} \text{ mhos per loop mile}$ .

It is series loaded with loads of 15 ohms per wire every 7.88 miles. Find  $\alpha$  and  $r_0$  before and after loading.

**Problem 25.**—Number 12 N.B.S. copper telephone wire of problem 24, is loaded with leaks of  $2 \times 10^{-8} \text{ mhos between wires every 7.88 miles}$ . Find  $\alpha$  and  $r_0$  before and after loading.

Note: This is not standard practice.

**Problem 26.**—(a) If the inductance of a heavy-weight loading coil is 0.250 henry and its resistance is 6.0 ohms, find the transmission equivalent of No. 19 gage cable, whose linear resistance is 88 ohms per loop mile, and



whose linear capacitance is  $0.062 \mu\text{f.}$  per loop mile, when the coils are spaced 1.14 miles apart. Express in terms of T.U.

(b) Find the velocity of propagation over this circuit.

**Problem 27.**—A side circuit of No. 12 N.B.S. gage open wire has the following constants:

$r = 10.4$  ohms per loop mile.

$l = 3.67 \times 10^{-3}$  henry per loop mile.

$g = 8 \times 10^{-7}$  mho per loop mile.

$c = 8.35 \times 10^{-9}$  farad per loop mile.

(a) Compute and plot: (1)  $\alpha_1$  the attenuation constant; (2)  $\alpha_2$  the wavelength constant; (3) the real part of  $z_0$ ; and (4) the imaginary part of  $z_0$  as a function of added inductance for each of the following values: 0, 10, 20, 30, 40, 50 millihenrys per loop mile. Assume 39.4 ohms per henry for resistance of coils.

(b) Which is the correct weight of loading to insure a distortionless circuit? (Take value from curves.)

(c) For a fixed inductance added (31.2 millihenrys per loop mile) determine the effect of spacing on  $\alpha_1$ ,  $\alpha_2$ , the real part of  $z_0$ , and the imaginary part of  $z_0$  and plot for each of the following spacings:

(1) Uniformly distributed (obtain from part a).

(2) 125-mh. coils at 4-mile intervals.

(3) 246-mh. coils at 7.88-mile intervals.

The above is the standard loading.

(4) 375-mh. coils at 12-mile intervals.

(5) 500-mh. coils at 16-mile intervals.

Assume 39.4 ohms per henry for resistance of coils.

(d) Find the *cutoff* frequency for the conditions of (c, 3).

### Problem on Chapter XV

**Problem 28.**—Find the equivalent  $T$  and  $\Pi$  of 300 miles of No. 12 N.B.S. copper wire telephone line, whose constants at 800 cycles per sec. are:

$r = 10.40$  ohms per loop mile.

$g = 80 \times 10^{-8}$  mhos per loop mile.

$l = 3.67 \times 10^{-3}$  henrys per loop mile.

$c = 8.35 \times 10^{-3} \mu\text{f.}$  per loop mile.

### Problems on Chapter XVII

**Problem 29.**—One of the circuits from Wakefield, Mass., to Portland Me., consists of the following:

1.36 mile No. 14 A.W.G. cable at Wakefield.

20.6 mile No. 12 N.B.S. gage open-wire copper.

0.25 mile No. 13 A.W.G. cable at Groveland Bridge.

93.5 mile No. 12 N.B.S. open-wire copper.

2.26 mile No. 13 A.W.G. cable at Portland.

For No. 14 A.W.G.  $r = 26.7$  ohms per loop mile,  $g = 0.87 \times 10^{-6}$  mho per loop mile.

For No. 13 A.W.G.,  $r = 21.3$  ohms per loop mile,  $g = 0.87 \times 10^{-6}$  mho per loop mile.

For No. 12 N.B.S.,  $r = 10.4$  ohms per loop mile,  $g = 0.8 \times 10^{-6}$  mho per loop mile.

Find:

(a) Distribution of position angles from Portland to Wakefield, with Portland end grounded.

(b) Distribution of position angles from Wakefield to Portland, with Wakefield end grounded.

(c) Hyperbolic II of the system.

(d) What would be the effect on the architrave resistance of replacing the cable at Groveland with aerial No. 4 B.W.G. double-galvanized plow-steel river-crossing wire, whose resistance per loop mile is 19.7 ohms, and whose leakance may be neglected, since there are no insulators except at the ends where the iron line wire joins the copper? (Treat like a casual resistance load.)

**Problem 30.**—A composite line is made up of 5 mile of standard cable and 250 miles of 150-lb. aerial copper wire.

Standard Cable	150-lb. aerial copper wire
$r = 88 \frac{\text{ohms}}{\text{loop mile}}$	$r = 11.73 \frac{\text{ohms}}{\text{loop mile}}$
$l = 10^{-3} \frac{\text{henry}}{\text{loop mile}}$	$l = 3.76 \times 10^{-3} \frac{\text{henry}}{\text{loop mile}}$
$g = 10^{-6} \frac{\text{mho}}{\text{loop mile}}$	$g = 10^{-6} \frac{\text{mho}}{\text{loop mile}}$
$c = 0.054 \times 10^{-6} \frac{\text{farad}}{\text{loop mile}}$	$c = 0.0084 \times 10^{-6} \frac{\text{farad}}{\text{loop mile}}$

(a) Calculate distribution of position angles from each end, at 800 cycles per sec.

(b) Determine the hyperbolic II of the whole combination.

(c) Compute the transmission equivalent, in terms miles of standard cable, by finding the transmission equivalent of each section, and the reflection loss in m.s.c. at the junction and adding these.

(d) Compute the transmission equivalent in terms of miles of standard cable, by finding the architrave impedance, and determine how many miles of standard cable would have an equivalent architrave impedance.

# APPENDIX G

## CONSTANTS OF TELEPHONE LINES—ENGLISH UNITS

Loop-mile constants of telephone lines at a frequency of 796 cycles per sec.

Gage	Construction	$r$ ohms per loop mile	$g$ mho per loop mile	$l$ henry per loop mi'e	$c$ farad per loop mile	$\alpha$ hyp's. $\angle$ per loop mile	$\alpha_1$ hyp's. per loop mile	$\alpha_2$ radians per loop mile	$z_0$ $\angle$ ohms $\angle$	$\lambda$ miles	$v$ miles per sec.
8 B.W.G.	{ Open wire 12-in. spacing	4.14	$0.8 \times 10^{-6}$	$3.37 \times 10^{-3}$	$9.14 \times 10^{-9}$	$0.0299 \angle 82.7^\circ$	0.00380	0.0297	$617 \angle 6.35^\circ$	212	169,000
9 B. & S.	{ Open wire 10½-in. spacing	8.76	$0.8 \times 10^{-6}$	$3.59 \times 10^{-3}$	$8.38 \times 10^{-9}$	$0.0290 \angle 76.5^\circ$	0.00675	0.0282	$692 \angle 12.5^\circ$	222	177,000
12 N.B.S.	{ Open wire 12-in. spacing	10.4	$0.8 \times 10^{-6}$	$3.67 \times 10^{-3}$	$8.35 \times 10^{-9}$	$0.0297 \angle 74.7^\circ$	0.00785	0.0288	$711 \angle 14.2^\circ$	218	174,000
10 B. & S.	Cable	10.5	$0.87 \times 10^{-6}$	$1 \times 10^{-3}$	$62 \times 10^{-9}$	$0.0600 \angle 57.6^\circ$	0.0322	0.0506	$185 \angle 32.2^\circ$	124	98,900
13 B. & S.	Cable	21.4	$0.87 \times 10^{-6}$	$1 \times 10^{-3}$	$62 \times 10^{-9}$	$0.0827 \angle 51.5^\circ$	0.0515	0.0648	$266 \angle 38.3^\circ$	97.0	77,400
16 B. & S.	Cable	42.2	$0.87 \times 10^{-6}$	$1 \times 10^{-3}$	$62 \times 10^{-9}$	$0.115 \angle 48.3^\circ$	0.0765	0.0860	$370 \angle 41.5^\circ$	73.0	58,100
19 B. & S.	Cable	88	$0.87 \times 10^{-6}$	$1 \times 10^{-3}$	$54 \times 10^{-9}$	$0.154 \angle 46.6^\circ$	0.106	0.112	$571 \angle 43.3^\circ$	56.0	44,500
19 B. & S.	Cable	88	$0.87 \times 10^{-6}$	$1 \times 10^{-3}$	$62 \times 10^{-9}$	$0.165 \angle 46.6^\circ$	0.113	0.120	$531 \angle 43.3^\circ$	52.3	41,700
22 B. & S.	Cable	171	$1.75 \times 10^{-6}$	$1 \times 10^{-3}$	$73 \times 10^{-9}$	$0.250 \angle 45.7^\circ$	0.175	0.179	$685 \angle 44.0^\circ$	35.0	27,900
24 B. & S.	Cable	271	$1.75 \times 10^{-6}$	$1 \times 10^{-3}$	$73 \times 10^{-9}$	$0.314 \angle 45.4^\circ$	0.220	0.224	$862 \angle 44.3^\circ$	28.0	22,300

CONSTANTS OF TELEPHONE LINES—METRIC UNITS  
Loop kilometer constants of telephone lines at a frequency of 796 cycles per sec.

Gage	Construction	$r$ ohms per loop km.	$g$ mho per loop km.	$l$ henry per loop km.	$c$ farad per loop km.	$\alpha$ hypos. $\angle$ per loop km.	$\alpha_1$ hypos per loop km.	$\alpha_2$ radians per loop km.	$z_0$ ohms $\angle$	$\lambda$ km.	$v$ km. per sec.
8 B.W.G.	{ Open wire 30.4-cm. spacing	2.57	$0.498 \times 10^{-6}$	$2.10 \times 10^{-3}$	$5.69 \times 10^{-9}$	$0.0186 \angle 82.7^\circ$	0.00236	0.0185	$617 \angle 6.35^\circ$	132	272,000
9 B. & S.	{ Open wire 26.7-cm. spacing	5.45	$0.498 \times 10^{-6}$	$2.23 \times 10^{-3}$	$5.21 \times 10^{-9}$	$0.0180 \angle 76.5^\circ$	0.00420	0.0175	$692 \angle 12.5^\circ$	138	284,000
12 N.B.S.	{ Open wire 30.4-cm. spacing	6.46	$0.498 \times 10^{-6}$	$2.28 \times 10^{-3}$	$5.20 \times 10^{-9}$	$0.0185 \angle 74.7^\circ$	0.00489	0.0179	$711 \angle 14.2^\circ$	136	280,000
10 B. & S.	Cable	6.53	$0.541 \times 10^{-6}$	$0.622 \times 10^{-3}$	$38.6 \times 10^{-9}$	$0.0374 \angle 57.6^\circ$	0.0200	0.0315	$185 \angle 32.2^\circ$	77.1	159,000
13 B. & S.	Cable	13.3	$0.541 \times 10^{-6}$	$0.622 \times 10^{-3}$	$38.6 \times 10^{-9}$	$0.0515 \angle 51.5^\circ$	0.0320	0.0404	$266 \angle 38.3^\circ$	60.4	124,000
16 B. & S.	Cable	26.3	$0.541 \times 10^{-6}$	$0.622 \times 10^{-3}$	$38.6 \times 10^{-9}$	$0.0715 \angle 48.3^\circ$	0.0476	0.0535	$370 \angle 41.5^\circ$	45.5	93,500
19 B. & S.	Cable	51.8	$0.541 \times 10^{-6}$	$0.622 \times 10^{-3}$	$33.6 \times 10^{-9}$	$0.0958 \angle 46.6^\circ$	0.0660	0.0696	$571 \angle 43.3^\circ$	34.8	71,500
19 B. & S.	Cable	51.8	$0.541 \times 10^{-6}$	$0.622 \times 10^{-3}$	$38.6 \times 10^{-9}$	$0.103 \angle 46.6^\circ$	0.0704	0.0745	$531 \angle 43.3^\circ$	32.6	67,000
22 B. & S.	Cable	106	$1.09 \times 10^{-6}$	$0.622 \times 10^{-3}$	$45.4 \times 10^{-9}$	$0.156 \angle 45.7^\circ$	0.109	0.111	$685 \angle 44.0^\circ$	21.8	44,900
24 B. & S.	Cable	169	$1.09 \times 10^{-6}$	$0.622 \times 10^{-3}$	$45.4 \times 10^{-9}$	$0.195 \angle 45.4^\circ$	0.137	0.139	$862 \angle 44.3^\circ$	17.4	35,800

## LIST OF SYMBOLS EMPLOYED

- $A, B$  sizes of complex numbers (numeric); also resistances of a pair of bridge arms (ohms).
- $A_v, A'_v, A''_v$  arbitrary constants in solution of line differential equations (volts  $\angle$ ).
- $A_i, A'_i, A''_i$  arbitrary constants in solution of line differential equations (amperes  $\angle$ ).
- $a$  a hyperbolic angular velocity (hyps. per sec.).
- $\alpha$  linear hyperbolic angle (hyps. per km.  $\angle$ ).
- $\alpha_0 = \sqrt{-j4\pi\gamma\mu\omega} = \alpha_2 - j\alpha_2 = \sqrt{2\pi\gamma\mu\omega} - j\sqrt{2\pi\gamma\mu\omega}$  (cm.<sup>-1</sup> $\angle$ ).
- $\alpha, \alpha,$  linear hyperbolic angle per wire km. and per loop km. respectively (hyps./km.  $\angle$ ).
- $\alpha_1, \alpha_2$  real and imaginary components of linear hyperbolic angle (numeric/km.).
- $B_v$  arbitrary constant in solution of line differential equations (volts  $\angle$ ).
- $B_i$  arbitrary constant in solution of line differential equations (amperes  $\angle$ ).
- $B$  susceptance of an a.c. line (mhos).
- $b = c\omega$  linear susceptance of an a.c. line (mhos/wire km.).
- $\beta, \beta_1, \beta_2$  circular angles (radians or degrees); also slopes of complex quantities (degrees).
- $C$  capacitance of a condenser or of a section conductor (farads).
- $c_0$  linear capacitance of pair of round parallel wires (stat-farads/loop cm.).
- $c,$  linear capacitance of pair of round parallel wires (farads/loop km.).
- $c$  linear capacitance of pair of round parallel wires (farads/wire km.) (numeric  $\angle$ ).
- $\gamma$  admittance of a leak (mhos  $\angle$ ).
- $\gamma = 1/\rho$  conductivity of a substance (abmhos per cm.); also the slope of the radius vector of an equiangular spiral (degrees).
- $\Gamma = 2\gamma$  admittance of a leak load (mhos  $\angle$ ).
- $D$  interaxial distance between two parallel cylindrical conductors (cm.); also pot. or current at a midpoint.
- $d = v/V$  depression factor of a leak applied to a line (numeric  $\angle$ ).
- $\Delta', \Delta''$  auxiliary hyperbolic angles (hyps.  $\angle$ ).
- $\delta_A, \delta_B, \delta_C, \delta_P$  position angles at generator end  $A$ , at motor end  $B$  and at points  $C$  and  $P$ , on a line (hyps.  $\angle$ ).



$\delta'_A, \delta'_B, \delta'_C, \delta'_P$ , substitute position angles on a c.c. line for the case of a super-surge-resistance load (hypos).

$\delta_N, \delta_N$  position angle of junction  $N$  or leak  $N$  of an artificial line (hypos.  $\angle$ ).

$E$  electromotive force (r.m.s. volts).

$e = 2.71828$  . . . Napierian base.

$f$  impressed frequency (cycles/sec.).

$G$  total dielectric admittance of a line (mhos  $\angle$ ); in the d.c. case total dielectric conductance.

$G_1, G_2, G_3$  line admittances to ground on each side of a leak respectively, and their sum (mhos  $\angle$ ).

$G_P, G_C$  line admittance beyond any point  $P$  and a reference point  $C$  of a line (mhos  $\angle$ ).

$g$  linear dielectric admittance of a line (mhos/wire km.  $\angle$ ), in the d.c. case linear dielectric conductance.

$g_1, g_2$  linear dielectric admittance per wire km. and per loop km. respectively (mhos/km.  $\angle$ ).

$g_1, g_2$  pillar leak admittances of an equivalent  $\Pi$  (mhos  $\angle$ ).

$g_0 = 1/r_0$  surge admittance of a line, in the d.c. case surge conductance (mhos  $\angle$ ).

$g'_0 = \sqrt{g/r}$  apparent surge admittance of a  $\Pi$  section, uncorrected for lumpiness (mhos  $\angle$ ).

$g$  leak admittance per section of artificial line (mhos  $\angle$ ).

$g'$  admittance in the staff of an equivalent  $T$  (mhos  $\angle$ ).

$g''$  admittance in the pillar of an equivalent  $\Pi$  (mhos  $\angle$ ).

$\Theta$  angle subtended by a line comprising a plurality of sections (hypos.  $\angle$ ).

$\theta_a$  apparent angle subtended by a  $T$  or  $\Pi$  section, uncorrected for lumpiness (hypos.  $\angle$ ).

$\theta_1, \theta_2, \theta_3$  hyperbolic angles (hyp. radians or hypos.  $\angle$ ), angles subtended by successive sections of a composite line (hypos.  $\angle$ ).

$\theta_1, \theta_2$  real and imaginary components of a hyperbolic angle (numerics).

$\theta, d\theta$  hyperbolic angle and element (hypos. radians  $\angle$ ).

$\theta$  angle subtended by a line (hypos.  $\angle$ ).

$\theta_1, \theta_2$  hyperbolic angle per wire and per loop (hypos.  $\angle$ ).

$\theta'$  angle subtended by a terminal impedance load at motor end of line (hypos.  $\angle$ ).

$\theta_1$  section angle after regular loading (hypos.  $\angle$ ).

$\theta''$  auxiliary hyperbolic angle of a sending-end impedance.

$h$  axial height of a horizontal wire above the level ground assumed as zero-potential surface (meters).

$I$  line current at any point of a smooth line (amperes  $\angle$ ).

$I_1, I_2, I_3$  initial, reflected, and transmitted transient current waves at a junction (amperes  $\angle$ ).

$I_1$  line current at a point 1 km. beyond the reference point (amperes  $\angle$ ).

$I_A$  line current at generator end  $A$  of a line (amperes  $\angle$ ).

- $I_B$  line current at motor end  $B$  of a line (amperes  $\angle$ ).  
 $I_C$  line current at point  $C$  on a line, where the electrical conditions are known (amperes  $\angle$ ).  
 $I_P$  line current at point  $P$  on a line, where the electrical conditions are known (amperes  $\angle$ ).  
 $I_m$  maximum cyclic current strength (amperes).  
 $i_1, i_2$  changes in line current on each side of a leak due to its admittance (amperes  $\angle$ ).  
 $I_a, I_x$  active and reactive components of a stationary vector current  $I$  (r.m.s. amp.).  
 $J_0(\alpha_0 x)$  Bessel function of  $(\alpha_0 x)$  of zeroth order (numeric  $\angle$ ).  
 $J_1(\alpha_0 x)$  Bessel function of  $(\alpha_0 x)$  of first order (numeric  $\angle$ ).  
 $j = \sqrt{-1}$ .  
 $k = V/v$  correcting factor for a leak applied to a line (numeric  $\angle$ ); also the ratio  $\sigma/r_0$  of a terminal load to the surge impedance (numeric); also number of complete  $AB$  waves passing over a line in the initial transient state (integer); also a coupling coefficient (numeric).  
 $k_p$ , correcting factor for line branches of a nominal  $T$  (numeric  $\angle$ ).  
 $k_g$ , correcting factor for staff leak of a nominal  $T$  (numeric  $\angle$ ).  
 $k_{p,,}$  correcting factor for architrave of a nominal  $II$  (numeric  $\angle$ ).  
 $k_{g,,}$  correcting factor for pillar leaks of a nominal  $II$  (numeric  $\angle$ ).  
 $\kappa$  permittivity of a dielectric (nominal numeric).  
 $L$  length of a line (km.).  
 $L_1, L_2$  distances of a point on a line from the generator and motor ends respectively (km.).  
 $\mathcal{L}$  inductance of a coil or of a line (henrys).  
 $L_1, L_2$  inductances of two transformer windings (henrys).  
 $l$  linear inductance of a line (henrys/wire km.).  
 $l_0$  linear inductance of a pair of parallel wires (abhenrys/loop cm.).  
 $l_{,,}$  linear inductance of a pair of parallel wires (henrys/loop km.).  
 $\lambda$  wave length on an a.c. line (km.).  
 $M$  complex multiplier of  $z_1 \sinh \delta_A$  in the theory of composite line equivalent  $II$  architrave (numeric  $\angle$ ); also mutual reactance  $j\mu\omega$  in a transformer (ohms  $\angle$ ).  
 $M_a M_b M_c$  coefficients of linear mutual inductance between a three phase group of wires and a parallel pair of wires (abhenries/linear cm.).  
 $m$  coefficient for developing derived sections in filter design (numeric)  $m_1, m_2$ , roots of a differential equation (numeric/km.).  
 $m_v$  transmission coefficient of voltage wave at transition from  $z_1$  to  $z_2$  (numeric  $\angle$ ).

- $m_c$  transmission coefficient of current wave at transition from  $z_1$  to  $z_2$  (numeric  $\angle$ ).
- $\mu$  internal permeability of a wire (gausses/gilberts per cm.); also mutual inductance of a transformer (henrys).
- $N, \mathbf{N}$  number of a junction and of a leak, respectively, in an artificial line, starting from the motor end (numeric).
- $n$  number of sections in multi-section line (numeric); also exponent of a number (numeric); also ratio of voltage transformation in a transformer (numeric); also number of complete wave lengths included in a line.
- $\nu = 1/\rho''$  admittance of a  $\Pi$  architrave (mhos  $\angle$ ).
- $\nu_1, \nu_2$  architrave admittances on each side of a leak load (mhos  $\angle$ ).
- $P_a$  active component or real component of complex power (watts).
- $P_x$  reactive component or imaginary component of complex power ( $j$  watts).
- $P_P, P_C$  volt-amperes or size of complex power at selected point  $P$ , and at reference point  $C$  of a line (volt-amperes); volt-amperes or size of complex power.
- $P_{cN}, P_{c\mathbf{N}}$  volt-amperes at position of junction  $N$  or leak  $\mathbf{N}$  on a conjugate smooth line (volt-amperes).
- $\Pi$  a delta connection of three impedances simulating a line or net at an assigned frequency. Also the product of three impedances forming a delta (ohms<sup>3</sup>  $\angle$ ).
- $\pi = 3.14159 \dots$
- $Q = \frac{(q \cosh \theta - 1)}{\sin \theta}$  branch factor of a net  $T'$  at  $A$  end (numeric  $\angle$ ).
- $Q = \frac{\left(\frac{1}{q} \cosh \theta - 1\right)}{\sinh \theta}$  branch factor of a net  $T'$  at  $B$  end (numeric  $\angle$ ).
- $q$  the imaginary component of a complex hyperbolic angle expressed in quadrants instead of in radians; also inequality factor  $\sqrt{z_{oa}/z_{ob}}$  of a net (numeric  $\angle$ ).
- $R_N$  impedance at junction  $N$ , especially in c.c. case (ohms  $\angle$ ).
- $R_{\mathbf{N}}, R_{\mathbf{N}}'$  impedance at leak  $\mathbf{N}$ , excluding and including that leak respectively (ohms  $\angle$ ) especially in c.c. case.
- $R_{af}, R_{ao}$  impedances of a line or net at end  $A$ , when respectively freed and grounded at  $B$  end (ohms  $\angle$ ).
- $R_{bf}, R_{bo}$  impedances of a line or net at end  $B$ , when respectively freed and grounded at  $A$  end (ohms  $\angle$ ).
- $R_{fN}, R_{oN}$  corresponding line impedances at and beyond junction  $N$  (ohms  $\angle$ ).
- $R_f, R_g$  impedance offered by a line when freed and grounded respectively at the distant end (ohms  $\angle$ ).
- $R' = 1/G$  impedance equivalent of a total line leakance  $G$  (ohms  $\angle$ ).
- $R_l$  receiving-end impedance of a line, in c.c. case receiving-end resistance (ohms  $\angle$ ).

- $R$  total conductor impedance of a line (ohms  $\angle$ ); in the d.c. case, total conductor resistance.
- $R_{,,}$ ,  $R_{,,}$  total conductor impedance per wire and per loop respectively (ohms  $\angle$ ).
- $R'_N$  line impedance at junction  $N$  of a  $\Pi$  line, including a half-leak only (ohms  $\angle$ ).
- $R_A$ ,  $R_B$ ,  $R_C$ ,  $R_P$  line resistance beyond a generator end  $A$ , a motor end  $B$ , a reference point  $C$  and a selected point  $P$  (ohms  $\angle$ ).
- $R'' = 1/g''$  impedance in pillar leak of an equivalent  $\Pi$  (ohms  $\angle$ ).
- $R_{cN}$ ,  $R_{cN}$  line impedances at positions of a junction  $N$  and leak  $N$ , respectively, on a conjugate smooth line (ohms  $\angle$ ).
- $r$  linear conductor impedance of a line (ohms/wire km.  $\angle$ ); in the c.c. case linear conductor resistance; also radius of a circle (cm.).
- $r'$  linear resistance of a round wire as influenced by skin effect (ohms/wire km.).
- $r$ , linear resistance per wire km. (ohms/w. km.).
- $r_{,,}$  linear resistance per loop km. (ohms/l. km.).
- $r_0 = \sqrt{r/g}$  surge impedance of a line (ohms  $\angle$ ).
- $r_0'$ ,  $r_0''$  surge impedance of wire line and of loop line, respectively (ohms  $\angle$ ).
- $r_0'$  apparent surge impedance  $\sqrt{r/g}$ , uncorrected for lumpiness (ohms  $\angle$ ).
- $r$  line impedance per section of an artificial line (ohms  $\angle$ ).
- $r_{a1}$ ,  $r_{a2}$  interaxial distances between an active wire and two neighboring parallel wires (cm.).
- $r'$   $r$  interaxial distances of a horizontal wire from an inducing wire and its image below the ground (meters).
- $\rho$  length of a radius vector in polar coördinates (cm.); also size of a complex quantity (numeric); also radius of a wire (cm. or meters); also virtual internal resistance of a condenser (ohms); also resistivity of a substance (abohm-cm.).
- $\rho'$  resistance in branch of an equivalent  $T$  (ohms  $\angle$ ).
- $\rho''$  resistance in architrave of an equivalent  $\Pi$  (ohms  $\angle$ ).
- $s$  area of a circle (sq. cm.).
- $s$ ,  $ds$  arc and arc element (cm. or circular radians).
- $\sigma$  impedance load to ground or zero potential at motor end of a line (ohms  $\angle$ ).
- $\Sigma = 2\sigma$  regular impedance load (ohms  $\angle$ ); also the sum of three impedance forming a delta (ohms  $\angle$ ).
- $T$  a star connection of three impedances simulating a line at an assigned frequency; also the time of single transit of a voltage or current wave over a line (sec.).
- $t$  elapsed time (seconds).
- $v = \theta/2$  semi-section angle (hyps.); also apparent velocity of propagation along a line (km./sec.); also the static potential induced on a horizontal wire (volts  $\angle$ ).

- $v_a$  apparent semi-section angle of a  $T$  section, uncorrected for lumpiness (hyps.  $\angle$ ).  
 $V$  potential at any point on a line (volts  $\angle$ ).  
 $V_1$  potential at a point 1 km. beyond the reference point (volts  $\angle$ ).  
 $V_1, V_2, V_3$  initial, reflected and transmitted waves of voltage at a junction, in initial transient state (volts  $\angle$ ).  
 $V_A$  potential at generator end  $A$  of a line (volts  $\angle$ ).  
 $V_B$  potential at motor end  $B$  of a line (volts  $\angle$ ).  
 $V_C$  potential at a point  $C$  of a line, where the electrical conditions are known (volts  $\angle$ ).  
 $V_P$  potential at a point  $P$  on a line (volts  $\angle$ ).  
 $V_X$  potential at an unknown point  $X$  on a line fed from both ends (volts  $\angle$ ).  
 $V_N$  potential at junction  $N$  of an artificial line (volts  $\angle$ ).  
 $V_{cN}$  potential at position of junction  $N$  on a conjugate smooth line (volts  $\angle$ ).  
 $v$  potential at a leak in the presence of its admittance (volts); also velocity of propagation (km./sec.)  
 $V'_1, V'_2, V'_3 \dots$  Fourier sine component amplitudes of a complex harmonic voltage wave (volts).  
 $V''_1, V''_2, V''_3 \dots$  Fourier cosine component amplitudes of a complex harmonic voltage wave (volts).  
 $V_{r1}, V_{r2}, V_{r3} \dots$  Fourier resultant component amplitudes of a complex harmonic voltage wave (volts).  
 $V_0, V_1, V_2, V_3 \dots$  Fourier resultant r.m.s. component amplitudes of a complex harmonic voltage wave (volts).  
 $\varphi$  phase angle of a condenser (defect from  $90^\circ$ ) (degrees).  
 $W$  maximum cyclic energy in a.c. circuit or conductor (joules).  
 $W_a$  active or real component of  $W$  (joules).  
 $W_x$  reactive or imaginary component of  $W$  (joules).  
 $W_m = 2W_x$  maximum cyclic magnetic energy in a.c. circuit or conductor (joules).  
 $X$  reactance of a coil or of a line (ohms); also in the theory of skin effect, the radius of a conducting wire (cm.).  
 $x$  Cartesian coördinate on  $X$  axis; also distance along a line from a reference point in a down-energy direction (km.); also radius of a point in the cross-section of a wire (cm.); also linear reactance (ohms per km.).  
 $Y$  dielectric admittance of a line (mhos  $\angle$ ).  
 $Y_{fA}, Y_{gA}$  line admittance at  $A$ , with motor end freed and grounded (mhos  $\angle$ ).  
 $y$  Cartesian coördinate on  $Y$  axis.  
 $y_0 = 1/z_0$  surge admittance of a line (mhos  $\angle$ ).  
 $y_0'$  surge admittance of a line after regular leak loading (mhos  $\angle$ ).  
 $y = g + jb$  linear dielectric admittance of a line (mhos/wire km.  $\angle$ ).



- $y''$  linear dielectric admittance of a line (mhos/loop km.  $\angle$ ).  
 $y_{00} = 1/z_{00}$  limiting value of surge admittance of a line neglecting losses (mhos).  
 $Z = R + jX$  impedance of a coil or of a line conductor (ohms  $\angle$ ).  
 $Z_{af}, Z_{ag}$  line impedance at  $A$  with motor end freed and grounded (ohms  $\angle$ ).  
 $z'$  linear impedance of a round wire due to skin effect (ohms/wire km.  $\angle$ ).  
 $z_{ab} = \sqrt{z_{oa} \cdot z_{ob}}$  geometric mean surge impedance of a net (ohms  $\angle$ ).  
 $z_0$  surge impedance of a line (ohms  $\angle$ ).  
 $z_{0'}$  surge impedance of a two-wire line (loop ohms  $\angle$ ).  
 $z_{0'}$  apparent surge impedance  $\sqrt{r/g}$  of a  $T$  line (ohms  $\angle$ ).  
 $z_{0''}$  apparent surge impedance  $\sqrt{r/g}$  of a  $\Pi$  line (ohms  $\angle$ ).  
 $z = r + jx$  linear conductor impedance of a line (ohms/wire km.  $\angle$ ).  
 $z_{,,} = r_{,,} + jx_{,,}$  linear conductor impedance of a line (ohms/loop km.  $\angle$ ).  
 $z_r$  impedance of a motor-end load (ohms  $\angle$ ).  
 $\omega = 2\pi f$  angular velocity or angular frequency (radians per sec.).  
 $z_{oa}, z_{ob}$  surge impedances of a net from  $A$  and  $B$  terminals, respectively (ohms  $\angle$ ).  
 $\omega_g = 4f$  angular velocity or angular frequency (quadrants per sec.).  
 $z_{00} = \sqrt{l/c}$  limiting value of surge impedance ignoring losses (ohms).  
 $z_1, z_2, z_3$  in theory of composite lines, surge impedance of successive sections (ohms  $\angle$ ).  
 $z_0$ , surge impedance of a line section after loading (ohms).  
 $\propto$  sign of infinity.  
 $\angle$  sign of a complex quantity or of the slope of a complex quantity.  
 $|\alpha|$  size of the complex quantity  $\alpha$  (numeric).  
 $\bar{\alpha}$  slope of the complex quantity  $\alpha$  (degrees or radians).  
 $\sim$  sign for "cycles per second, or cyps."  
 $\Omega$  sign for ohms impedance.  
 $\mathcal{U}$  sign for mhos admittance.  
 $\cong$  sign for "nearly equals," or approximate equality.  
 $f$  sign for farads capacitance.  
 $\mu f$  sign for microfarads capacitance.  
 $m\mu f$  sign for millimicrofarads.  
 $\mu\mu f$  sign for micromicrofarads.  
 $\log h$  hyperbolic logarithm to base  $e$ .  
 $\log$  common logarithm to base 10.  
 $\text{hyp.}$  contraction for "hyperbolic radian."  
 $\text{r.m.s.}$  contraction for "root mean square."  
 $\text{a.c.}$  contraction for "alternating-current."  
 $\text{c.c.}$  contraction for "continuous-current."  
 $\text{cyps.}$  contraction for  $\text{cy.p.s.}$  or "cycles per second."  
 $\text{T.U.}$  contraction for "transmission units."



## INDEX

### A

$A$  and  $B$  arrival waves, 168  
 $AB$  successive arrival waves, 168  
 Acoustic tonometer, 289  
 Active, reactive, and vector power, 125  
 Actual linear attenuation factor, 20  
 Addition of vectors, 109  
 Admittance function of position angle, 51  
 Ahlborn, G. H., 224  
 Alternating current artificial lines as filters, 358  
     attenuation constant, 151  
     example of composite line, 304  
     surge admittance, 163  
 Alternative  $T$  and  $\Pi$  of transformer, 347  
 Ambiguous impedance diagrams, 280  
 Angle hyperbolic, in exponentials, 113  
     of a line defined, 18  
     of a net defined, 325  
     of terminal load, 40  
 Angles, complex hyperbolic, 112  
     position, defined, 40  
     admittance function of, 51  
     pure cable, 153  
     real circular, 4  
     hyperbolic, 4  
 Angular frequency, 304  
     quadrant measure, 9  
 Apparent velocity of propagation, 290  
 Approximation to  $\theta$  and  $z_0$  for an artificial line, 74  
 Architrave impedance of composite line, 401  
     of a  $\Pi$ , 69

Argument or slope of complex number, 107  
 Arithmetical equivalent circuits, 63  
 Artificial lines, definition of, 1  
     of double  $z_0$ , 273  
     lumpy, 71  
     submarine cable, 228  
     telephone lines, 226  
 Attenuation constant of continuous current line, 18  
 Attenuation expressed in T.U., 204  
     factor, 20  
     actual, 20  
     normal, 20  
     linear, 20  
     normal (see *Normal Attenuation*).  
 Attenuators, distortionless, 228  
 Ayrton, W. E. and Whitehead, C. S., 345

### B

Balanced artificial lines, 272  
 Becker, G. F., "The Gudermannian Complement and Imaginary Geometry," 112  
 Berg, E. J., "The Transmission of Electrical Energy," 143  
 Bessel functions, semi-imaginary, 140  
 Bouton, C. L., formulas, 118  
 Bracket lines, 233  
 Brackets, 233  
 Branch factors of a net, 330

### C

Cable, artificial submarine, 228  
 Campbell, G. A., 102, 195, 354  
 Cantilever nets, 232  
     terminal, 303  
 Casper, W. L., "Telephone Transformers," 349

- Characteristic constants of net, 328  
   impedances of net, 324  
   resistance continuous current line, 21  
 Chart atlas of complex functions, 118  
 Circuit, distortionless, 154  
 Circuits, physical equivalent, 63  
 Circular and hyperbolic equivalents, 14  
 Circular angles, real, 4  
   radians, real, 4  
 Clarke, Edith, "Frequency limits," 290  
 Classification of artificial lines, 230  
 Clerk-Maxwell, "Electricity and Magnetism," 134  
 Coefficient of current transmission, 167  
   of voltage transmission, 167  
 Cohen, B. S. and Shepherd, G. M., 250  
 Common properties of circular and hyperbolic real angles, 5  
 Comparative circular and hyperbolic formulas, 385  
 Complex harmonic potentials, 274  
   hyperbolic angles, 112  
   quantities, 105  
   quantity denoted by sign, 18  
 Composite line, defined, 17  
   second method for, 300  
   tests in laboratory, 314  
   transformer in, 312  
   with terminal load, 298  
 lines, 231, 292  
   admittance and current distribution, 297  
   general case, 295  
   leak admittances, 302  
   potential distribution, 297  
   power distribution, 298  
 Condensive susceptance, 124  
 Conjugate smooth line, 59  
   reversion to, 63  
 Constants, linear, 2  
   of line, defined, 2  
   of telephone lines, 409  
 Continuous-current artificial lines, 93  
 Correcting factor for nominal  $T$  or  $\Pi$ , 61  
   of a leak, 103  
 Cosine formulas for complex angles, 117  
 Crab addition or perpendicular, 276  
 Crystal's "Algebra," 118  
 Cunningham, J. H., 210  
 Current-carrying properties of lines, 2  
   distribution at ends of net, 336  
   in terms of position angle, 42  
   tests on alternating-current line, 288  
 Cutoff frequency of filter, 360  
 Cycloid energy diagram of reactanceless alternating-current circuit, 132  
 Cyps. explained and defined, 120
- ### D
- Definition of line angle, 98  
   of surge resistance, 22  
 Degradation of hyp. functions to Ohm's law, 39  
 Dellenbaugh, F. S., 212  
 Depression factor of a leak, 103  
 Design of continuous-current artificial lines, 93  
 Detection of even-frequency harmonics, 381  
 Derivation of  $T$  and  $\Pi$  correcting factors, 394  
 Direct and reverse nets of transformer, 347  
 Dissymmetrical nets, 232  
    $\Pi$  of a composite line, 302  
 Distortionless attenuators, 228  
   circuit, 154  
 Distribution of tests among observers, 288  
 Disturbances of potential due to volt box, 100  
 Douglas, J. F. H., experimental tests, 185  
 Drainage coil, 147  
 Drysdale, C. V., 158, 250

## E

- Effect of transition at junction, 167
- Eighth-wave line in transient state, 174
- Electrical energy, 143
  - degrees per second, 166
  - length of line, 1
  - separation of net ends, 328
- Electromotive force, induced linear, 148
- Electron-tube voltmeters, 281
- Electrostatic voltmeters, 281
- Electrostatically induced potentials, 142
- Energy, electrical, 143
  - reactive, 124
  - wheel of alternating-current circuit, 131
- Enveloping spiral, 173
- Epsilonic distance on alternating-current lines, 157
- Equiangular spiral polygons, 170
- Equivalent circuits, arithmetical, 63
  - of smooth line, 59
  - physical, 63
  - $T$  of smooth line, 60
  - $\Pi$  of smooth line, 61
- Equivalents, circular, 14
- hyperbolic, 14
- Estwick, C. F., 225
- Evaluation of hyp. angle in exponentials, 11
- Exponentials, evaluation of hyp. angle in, 11
- External linear inductance, 134

## F

- Factor, actual linear attenuation, 20
- Feldmann and Herzog, "Conducting Nets," 62
- Ferric and non-ferric reactors, 213
- Fictitious impedance diagrams, 133
- Filter, cutoff, frequency of, 360
  - frequency ratio, 360
  - high-pass, 371
  - section angle, 359
  - sections,  $m$ -derived, 377
  - total angle, 365

## Filters, 358

- Final sending-end impedance, 163
- Fleming, J. A., 107, 129
- Fore brackets and end brackets, 233
- Four-terminal nets, 232
- Frequency limits of artificial lines, 290
  - measurements, 289
  - ratio of filter, 360
- Frequencies, signalling, 120
- Fundamental constants of a line, 24
  - differential equation of lines in steady state, 26

## G

- Generator and motor ends of line, 32
- Geomean surge impedance of net, 324
- Gray, A., "Absolute Measurements in Electricity and Magnetism," 102
- Greenhill, G., "Differential and Integral Calculus," 131, 158
- Group velocity of propagation, 152
- Growth factor of successive waves, 168
- Gudermannian complement, 112

## H

- Half-wave lines in steady state, 184
- Harden, W. H., 201
- Heaviside, O., "Electrical Papers," 26, 32, 154, 166
- High-pass filter, 371
- Huxley, R. D., 219
- Hyp. angle of a line defined, 18
- Hyp., definition of, 5
- Hyperbolic angle in exponentials, 13
  - linear, of line, 18
  - angles, real, defined, 4
  - radian measure, 9
  - radians defined, 5
  - trigonometric identities, 14

## I

- Identical nets in series, 354
- Inequality factor  $q$  of a net, 329



- Image impedances of a net, 337
    - wire, 142
  - Imaginary circular angles, *i.e.*, real hyperbolic angles, 15
  - Impedance distribution over alternating-current artificial, lines, 251
    - function of position angle, 51
    - loads at both ends, 310
    - method of locating faults, 201
    - model of conjugate line, 287
    - receiving-end, 56
    - sending-end, 55
  - Induced potential, resultant static, 145
  - Inductance, linear, 134
  - Inductive reactance defined, 120
    - susceptance, 124
  - Infra-surge-impedance load, 54
  - Initial current at sending end, 162
    - sending-end impedance, 163
    - transient state, 165
  - Intermediate loads, 311
    - point properties, 90
  - Internal linear inductance, 134
    - impedance of wire due to skin effect, 141
  - Involution of vectors, 111
  - Iterative impedances of a net, 324
    - resistance of continuous current line 21
- J
- Jahnke and Emde, "Functionentafeln," 140
  - Johnson, K. S., 206, 326, 337, 342, 379
- L
- Laboratory tests of composite line, 314
    - on quarter-wave line, 182
  - Lawrence, R. R., "Principles of Alternating Currents," 136, 143
  - Laws, F. A., skin effect, 289
  - Leak, correcting factor for a, 103
    - depression factor of, 103
  - Leakance, linear, 17
  - Length of line, electrical, 1
  - Lewis, L. V., 225
  - Lieberknecht, F. W., line tests, 286
  - Line constants defined, 2
    - hyperbolic angle of, defined, 18
    - rendered virtually infinite, 48
    - resistance in transient state, 54
    - voltaged at both ends, 68
  - Linear attenuation factor, 20
    - capacitance of lines, 135
    - constants, 138
      - defined, 2
      - of smooth line, 17
    - hyperbolic angle, 18
      - and unit of length, 155
      - computed by rectangular and polar methods, 150
      - for single- and two-wire lines, 155
      - significance of, 19
    - induced e.m.f., 148
    - inductance, 134
    - leakance of line defined, 17
    - loop and wire admittance, 149
      - impedance, 149
      - capacitance, 136
      - inductance, 134
      - reactance, 138
    - mutual inductance of wires, 147
    - phase attenuation, 151
    - resistance of line, defined, 17
    - wire capacitance, 136
      - impedance, 140
      - reactance, 138
      - susceptance, 138
    - loop susceptance, 140
  - Lines, artificial, 1, 71, 272, 273
    - bracket, 223
    - classification of artificial, 230
    - real, 1
    - regularly loaded, 193
    - smooth, 17, 59
    - composite (see *Composite lines*).
      - definition of, 1
  - Load, infra-surge-impedance, 54
    - normal-attenuation, 48
    - super-surge-impedance, 45
    - surge impedance, 47
    - terminal, angle of, 40

Loads, intermediate, 311  
 Location of the pole of a spiral polygon, 173  
 Log. polar ratio of inducing wires, 143  
 Loop and wire surge impedances, 162  
   capacitance, linear, 136  
   inductance, linear, 134  
   *km.* and wire-*km.*, 22  
 Losses in miles of standard cable, 206  
   in napiers, 206  
   in transmission units, 206  
 Lossless line under reactive load, 266  
 Lumpiness correction factors, 61  
   correction factors for artificial line, 76  
   error of nominal  $T$  or  $\Pi$ , 61  
   of real lines, 31  
 Lumpy alternating-current artificial lines, 208  
   artificial lines, 71

## M

Magnetically induced voltages, 147  
 Magnusson and Burbank, 184  
 Magnusson, C. E., 219  
 Martin, W. H., 206  
 Maximum power output of a net, 340  
 McCready, H. A. C, "Signalling," 224  
 McKown, F. W., tests of composite lines, 314  
 $M$ -derived filter sections, 377  
 Mean-to-mid interpolation, 92  
   ratio, 91  
 Mechanical construction of lines, 2  
 Merger and hyperbolic equivalent, 294  
 Model for projection of complex cosines and sines, 114  
 Modulus or size of a complex number, 107  
 Motor and generator ends of line, 32  
 Muirhead, A., 208  
 Multiple-section equivalents of line, 70  
 Multiplication of vectors, 109

Mutual admittance of a net, 330  
 impedance of a net, 329

## N

Napiers power loss, 205  
 Natural impedance of net, 324  
 Negative position angle of a load, 69  
 Net, angle of, 325  
   branch factors of, 330  
   characteristic constants of, 328  
   impedances of, 324  
   current distribution over, 336  
   equalized by image impedances, 338  
   geomean surge impedance of, 324  
   image impedances of, 337  
   iterative impedances of, 324  
   inequality factor of, 329  
   maximum power output of, 330  
   mutual admittance of, 330  
     impedance of, 329  
   natural impedance of, 324  
   normal attenuation over, 336  
   position angles on, 333  
   power distribution over, 336  
   receiving-end impedance of, 334  
   rectangular, 323  
   sending-end impedances of, 332  
    $T$  or  $\Pi$  of composite line, 295  
   voltage distribution over, 335  
 Nets, cantilever, 232  
   identical in series, 354  
   symmetrical and dissymmetrical, 231  
   three-terminal, 350  
 Networks or nets, 323  
   defined, 2  
 Nominal  $T$  of smooth line, 60  
    $\Pi$  of smooth line, 61  
 Normal attenuation, continuous  
   current defined, 19  
   equiangular spiral, 158  
   polygons, 237  
   factor, 20  
     alternating-current lines, 157  
     of line, 49  
   load, 48  
   on alternating-current lines, 156

- Normal attenuation, over a net, 336  
     over lossless line, 269  
     polar graph, 158  
     phase attenuation, 242
- Notation, slope, 108
- Number of conductors in a line, 1
- Numerical values of circular, and  
     hyperbolic real functions, 7
- P
- Pender, H., 219  
     and Osborne H. S., 137
- Perunitage defined, 20
- Phase advance rate of alternating-  
     current generator, 166  
     separation of net ends, 328
- Physical equivalent circuits, 63
- Pierce, G. W., linear hyp. angles, 154
- Pierce, P. H., "Skin Effect," 289
- Plane-vector sign defined, 18
- Plane vectors, 105
- Plural frequencies over lines, 274
- Polar and rectangular vectors, 109  
     axes of two inducing wires, 143  
     ratio of two inducing wires, 143
- Polygons, equiangular spiral, 170  
     location of pole of spiral, 173
- Position-angle distributions over  
     composite lines, 296
- Position angles and their functions,  
     164  
     defined, 40  
     at junctions of artificial line, 77  
     on a net, 333
- Potential and current spirals, 159  
     in terms of position angle, 41  
     induced, 145
- Potentials, complex harmonic, 274
- Potentiometer and voltmeter  
     methods, 286  
     tests of artificial lines, 95
- Power, active, reactive, and vector,  
     125  
     distribution over alternating-cur-  
         rent artificial lines, 257  
     under surge-impedance loads,  
         264  
     -transmission ratio, 204
- Problems, 403
- Product, versine of a  $T$  or  $\Pi$ , 63
- Prolate trochoid energy diagram, 132
- Propagation, apparent velocity of,  
     290
- Properties of intermediate points, 90
- Pupin, M. I., 209 and 210
- Pure cable semi-imaginary angles,  
     153
- $\Pi$ -network equivalent of a line, 59  
     with double surge resistance, 225
- Q
- Quadrant measure for circular  
     angles, 119  
     for real circular angles, 9
- Quadrantal imaginaries underscored,  
     119
- Quadranting the imaginary, 119
- Quarter-wave lines, steady-state, 181  
     transient state, 177
- R
- Radian distance on alternating-cur-  
     rent lines, 157
- Radians, real circular, 4
- Range of signalling frequencies, 120
- Ratio of mean to mid, 91
- Rayleigh bridge balance, 278  
     formula for skin effect, 141
- Reactance, inductive, defined, 120  
     loop and wire, 138
- Reactive energy, 124
- Reactors, 213
- Real circular angles, 4  
     and hyperbolic angles com-  
         pared, 4  
     hyperbolic angles, 134  
         defined, 4  
     lines, definition of, 1  
     quantities, 105
- Receiving-end impedance, 56  
     of a net, 334
- Reciprocals of vectors, 111
- Rectangular and polar vectors, 109  
     net, 323
- Reduction from circular to hyper-  
     bolic identities, 16

Reference phase, 122  
 Reflection vector coefficients, 167  
 Regular leak loading, 197  
   series loading, 193  
 Regularly loaded lines, 193  
 Relations between equivalent  $T$  and  $\Pi$ , 62  
 Relative merits of  $T$  and  $\Pi$  sections, 222  
 Resistance of load, joulean and motional, 345  
 Resistivity and conductivity of wire, 140  
 Resultant sine harmonics, 275  
   static induced potential, 145  
 Reversion to conjugate smooth line, 63  
 Ricker, C. W., 382  
 Robertson, D., "The Stroboscope," 289  
 Rotary vector diagrams of  $E$ ,  $I$ , and  $P$ , 128  
 Rotor exponential, 10  
 Russell, A., "Alternating Currents," 137  
   formula for skin effect, 141

## S

Secondary constants of a line, 25  
 Sending-end impedance, 55  
   of a net, 332  
 Seven-lines and gamma-lines, 232  
 Shepherd, G. M. B., 214  
 Short-separation linear loop capacitance, 136  
 Signalling frequencies, range of, 120  
 Silsbee, F. B., inductance of wires, 136  
 Simple alternating-current circuit defined, 120  
 Sine and cosine series of harmonics, 275  
   formulas for complex angles, 118  
 Single-wire and two-wire lines, 22  
 Sixteenth-wave line, transient state, 174  
 Skin effect defined, 120  
   formulas for round wires, 140

Slepian, A., 371  
 Slope notation, 108  
   of complex quantity defined, 10  
 Smooth artificial lines, 208  
 Smooth line, conjugate to  $T$  or  $\Pi$ , 59  
   equivalent circuits of, 59  
   lines defined, 17  
 Solutions of fundamental differential equations of lines, 28  
 Spiral, enveloping, 173  
 Splash transient wave, 162  
 Steady state of lines, fundamental differential equation of, 26  
 Stearns, J. B., 208  
 Steinmetz, C. P., 313  
 Straight-line polygon, 179  
 Substitutibility of star and delta, 62  
 Super-surge-impedance load, 45  
   resistance loads, 490  
 Surge admittance limiting value, 163  
   of alternating current line, 25  
   conductance of continuous current line, 25  
   impedance alternating-current loads, 262  
   in alternating-current lines, 161  
   load, 47  
   of a net, 324  
   resistance of continuous current line, 21  
   of line defined, 22  
 Susceptance inductive or condensive, 124  
 Synchronous-motor effects imitated, 287

## T

$T$  and  $\Pi$  sections, relative advantages, 222  
 $T$ ,  $\Pi$ ,  $I$ ,  $O$ ,  $U$ , and anchor lines, 231  
 Tables of complex functions, 118  
 Taylor, H. A., 208  
 Telephone-line constants, 409, 410  
 Terminal load, angle of, 40  
   cantilevers, 303  
 Three-terminal nets, 332, 350  
 Time interval of a line, 318  
 $T$ -network equivalent of a line, 59  
 Tonometer, acoustic, 289

- Total angle of a filter, 365
  - of multiple-section line, 74
- Track-signalling circuits, 223
- Transformer, equivalent circuits of, 345
  - in composite line, 312
- Transient state, resistance of line, 54
- Transition, effect of at junction, 167
- Transmission Unit, 204
  - vector coefficients, 167
- Transposition of telephone wires, 146
- Trigonometrical properties of real continuous current lines, 17
- Trochoid, prolate, of alternating-current energy diagram, 132
- $T$  with double surge resistance, 225
- Two-dimensional potentiometers, 281
- Two-wire and single-wire lines, 22

## U

- Underscoring quadranted imaginaries, 119
- Unequally spaced three-phase wires, linear constants of, 138
- Unrealizable artificial lines, 236

## V

- Varley, C. F., 208
- Vector Bessel functions, 140
  - cyclic energy, 124
  - electromotive force, 122
  - hyperbolic radian defined, 18
  - impedance, 122
  - linear wire constants, 148
  - power at ends of a net, 336
    - to current phase, 123
  - transmission and reflection coefficients, 398
  - watts, 123

- Vectors, addition of, 109
  - involution of, 111
  - multiplication of, 109
- Velander, Edy, 354
- Velocity of propagation, 152
  - apparent, 290
- Versed-sine produce of a  $T$  or  $\pi$ , 63
- Versors, 108
- Virtual extra-linear resistance of skin effect, 141
- Virtual resistance of e.m.f. load, 69
- Virtually infinite line, 48
- Voltage and current ratios on lines, 185
  - distribution at ends of net, 335
  - reflection coefficient, 167
  - triangles, 282
- Voltages, 147
- Voltmeters, electron-tube, 281

## W

- Wave-length constant, 152
- Wave, splash transient, 162
- Waves, arrival, 168
  - successive, growth factor of, 168
- Wheatstone-bridge tests of continuous current artificial lines, 97
- Whitall, C. W., "Tests of Lines," 314
- Whiting, S. E., "Stroboscopic Fork," 289
- Wire conductivity, 140
  - resistivity, 140
- Wire-km. and loop-km., 22

## Z

- Zero instant of instantaneous e.m.f., 166
  - potential ground surface, 147
- Zobel, O. J., 377, 379



















a39001



007328944b

68859



